NICKEL/COPPER CATALYZED C-C AND C-N BOND FORMATION REACTIONS TO FORGE SP3 CARBON LINKAGES

Xinyang Lyu

UNIVERSITAT ROVIRA i VIRGILI

Nickel/Copper Catalyzed C-C and C-N bond Formation Reactions to Forge sp^3 Carbon Linkages

Xinyang Lyu

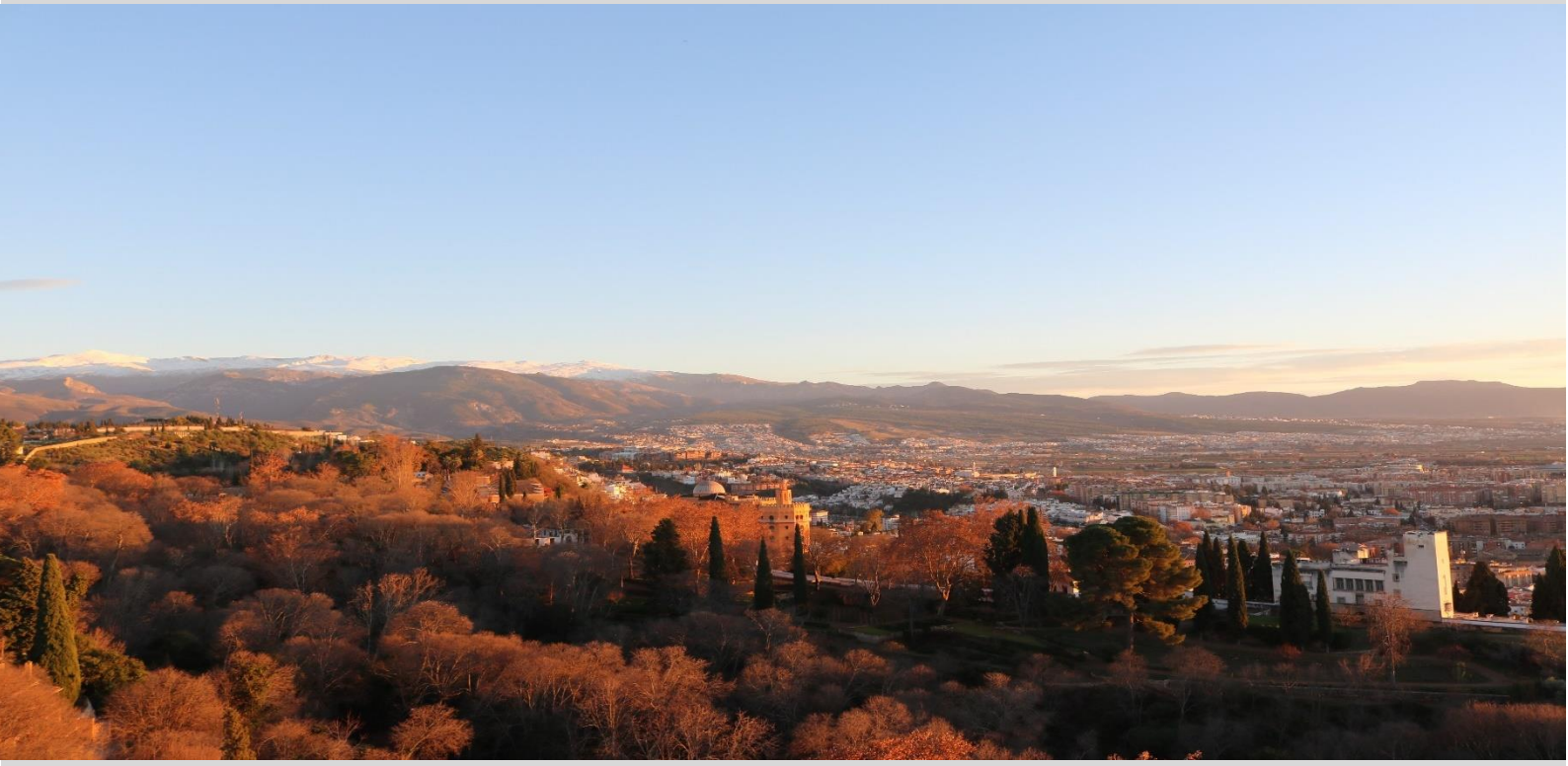

DOCTORAL THESIS

2023

UNIVERSITAT ROVIRA I VIRGILI
NICKEL/COPPER CATALYZED C-C AND C-N BOND FORMATION REACTIONS TO FORGE SP3 CARBON LINKAGES
Xinyang Lyu

UNIVERSITAT ROVIRA I VIRGILI
NICKEL/COPPER CATALYZED C-C AND C-N BOND FORMATION REACTIONS TO FORGE SP3 CARBON LINKAGES
Xinyang Lyu

UNIVERSITAT ROVIRA I VIRGILI
NICKEL/COPPER CATALYZED C-C AND C-N BOND FORMATION REACTIONS TO FORGE SP3 CARBON LINKAGES
Xinyang Lyu

Nickel/Copper Catalyzed C-C and C-N bond Formation Reactions to Forge sp^3 Carbon Linkages

Xinyang Lyu

Doctoral Thesis

Supervised by Prof. Ruben Martin Romo

Institute of Chemical Research of Catalonia (ICIQ)

Universitat Rovira i Virgili (URV)
Department of Analytical Chemistry & Organic Chemistry

Tarragona, 2023

UNIVERSITAT ROVIRA I VIRGILI
NICKEL/COPPER CATALYZED C-C AND C-N BOND FORMATION REACTIONS TO FORGE SP3 CARBON LINKAGES
Xinyang Lyu

Prof. Dr. Ruben Martin Romo, Group Leader at the Institute of Chemical Research of Catalonia (ICIQ) and Research Professor at the Catalan Institution for Research and Advanced Studies (ICREA),

STATES that the present study, entitled "Nickel/copper catalyzed C–C and C–N bond formation reactions to forge sp^3 carbon linkages", presented by Xinyang Lyu for the award of the degree of doctor, has been carried out under his supervision at the Institute of Chemical Research of Catalonia (ICIQ).

Tarragona, August 2023

Doctoral Thesis Supervisor

Prof. Dr. Ruben Martin Romo

UNIVERSITAT ROVIRA I VIRGILI
NICKEL/COPPER CATALYZED C-C AND C-N BOND FORMATION REACTIONS TO FORGE SP3 CARBON LINKAGES
Xinyang Lyu

List of Publications

At the time of printing, the results reported herein have been published as:

1. **Xin-Yang Lv**, Roman Abrams, Ruben Martin. Dihydroquinazolinones as Adaptative C(sp^3) Handles in Arylations and Alkylations via Dual Catalytic C–C Bond-Functionalization. *Nat Commun* **2022**, *13*, 2394–2402.
2. **Xin-Yang Lv**, Roman Abrams, Ruben Martin. Copper-Catalyzed C(sp^3)-Amination of Ketone-Derived Dihydroquinazolinones by Aromatization-Driven C–C Bond Scission. *Angew. Chem. Int. Ed*. **2023**, e202217386.
3. **Xin-Yang Lv**, Ruben Martin. Cu-Catalyzed C(sp^3) Amination of Unactivated Secondary Alkyl Iodides Promoted by Diaryliodonium Salts. *Org. Lett*. **2023**, 25, 3750–3754.

The author has also contributed to the following:

4. Fei Cong, **Xin-Yang Lv**, Craig S. Day, Ruben Martin. Dual Catalytic Strategy for Forging sp^2–sp^3 and sp^3–sp^3 Architectures via β-Scission of Aliphatic Alcohol Derivatives. *J. Am. Chem. Soc*. **2020**, *142*, 20594–20599.

UNIVERSITAT ROVIRA I VIRGILI
NICKEL/COPPER CATALYZED C-C AND C-N BOND FORMATION REACTIONS TO FORGE SP3 CARBON LINKAGES
Xinyang Lyu

UNIVERSITAT ROVIRA I VIRGILI
NICKEL/COPPER CATALYZED C-C AND C-N BOND FORMATION REACTIONS TO FORGE SP3 CARBON LINKAGES
Xinyang Lyu

Table Contents

UNIVERSITAT ROVIRA I VIRGILI
NICKEL/COPPER CATALYZED C-C AND C-N BOND FORMATION REACTIONS TO FORGE SP3 CARBON LINKAGES
Xinyang Lyu

Acknowledgements

Firstly, I would like to express my sincere thanks to **Prof. Ruben Martin** for accepting me as a PhD student in his research group and for his guidance along the four years. Ruben is one of the most patient professors that I've met during my short but fantastic research career. His encouragement and support, broad foundation of knowledge and profound insight have helped me to become a better researcher.

A special thank is dedicated to **Ingrid Mateu** for her administrative work and **David Sadaba** for the technical support to make the group run effectively. I would also like to thank **ICIQ Research Support Units** for the experimental support and **China Scholarship Council** for the financial support.

The four years of PhD pursuing is an incredible journey, and I would like to thank all the current and past members of the Martin group. **Tiago**, **Raúl**, **Andreu**, **Rosie**, **Yiting** and thank you for the help when I joined the group. **Hongfei**, **Yaya**, **Shangzheng**, **Craig** and **Jessica**, thanks for organizing the party and the support at the beginning. **Basudev, Juzeng**, **Yangyang**, **Bradley**, **Riccardo** and **Robert**, thanks for the academic discussions, from which I learned a lot. **Santosh, Matt**, **Jocob** and **Chris**, you guys are very nice, it's really been a pleasure to work with you. **Prof. Liang**, my guider to the group. Hope you are doing well whenever you are.

Roman, an incredible postdoc I have ever met! A deepest appreciation for numerous discussions on chemistry, being critical with the projects which we worked on and generating amazing ideas all the time. Your experience, persistence, altitude and support have been gold to me. Thanks **Jesus**, **Tomas**, **Alvaro**, **Ciro** and **Franz** for the constructive discussions and valuable suggestions for my projects. **Liangliang**, it's been great to meet you, and thank you for helping me with the SFC and sharing the interesting stories in Germany. Good luck with your project! **Zhong**, thanks for the suggestion on the thesis. Hopefully you can find the position that you want!

Dmitry, you are really funny and we spent many happy time together! Good luck for the rest of PhD! **Victoria**, I really enjoyed the spicy Mexican food you brought. Hope all is well with you! **Carlotta**, my Spanish teacher. You are a really kind person! I appreciate your help and good luck with your future career. **Laura**, an industry chemist, you are very nice and friendly. It's been a pleasure to have you around!

Julien, thanks for the help with LCMS, you are an awesome role model. **Julia** and **Adrian**, you guys are very nice, it's been enjoyable to work with you. **Jinhong**, thank you for throw some amazing parties. **Hao**, a pharmaceutical master. thank you sharing the biological knowledge and the LCMS guidance. **Huihui**, a happy PhD, keep going with the laughing gas chemistry!

Filip, **Yubiao**, **Wei** and **Shuai**, the young hardworking PhD students. Hopefully

your projects will work out and enable you to get where you want to go. Thank you also to the visiting members, **Clarence**, thanks for sharing the travel stories all the time. **Joan**, it's been a pleasure to meet you. **Alessandro**, **Mikkel**, **Philipp**, **Pascal**, **Jonas**, **Yutaka**, **Mara**, **Nahury**, **Ha** and **Paula**. It's been nice to get to know you guys.

Finally, I would like to thank my parents and friends for their support and caring.

Preface

The work presented in this thesis has been performed at the Institute of Chemical Research of Catalonia (ICIQ) under the supervision of Professor Rubén Martin. The thesis is divided into five chapters: a general introduction, three research chapters, and a summary of the overall conclusions. Each of the research chapters include an introduction and an aim of the presented project, followed by a discussion of experimental results, conclusions, and an experimental section.

In Chapter 1, background information on the development and current state-of-the-art of transition metal-catalyzed cross-coupling reactions is delineated.

Chapter 2, "Dihydroquinazolinones as adaptative C(sp^3) handles in arylations and alkylations via dual catalytic C–C bond-functionalization." describes a photoredox/nickel dual catalytic strategy that utilizes dihydroquinazolinones derived from aliphatic ketone for forging C(sp^3) architectures via α C–C cleavage with aryl and alkyl bromides. Preliminary mechanistic experiments indicated that a reductive quenching photoredox cycle that was based on an initial single-electron oxidation of dihydroquinazolinone by the excited state of the photocatalyst. This work was carried out in collaboration with Dr. Roman Abrams. This work has been published in *Nat Commun* **2022**, *13*, 2394–2402. DOI: 10.1038/s41467-022-29984-0.

Chapter 3, "Copper-Catalyzed C(sp^3)-Amination of Ketone-Derived Dihydroquinazolinones by Aromatization-Driven C–C Bond Scission." describes the development of a copper catalyzed C(sp^3)-amination of dihydroquinazolinones, enabled by the intermediacy of alkyl radical species arising from homolytic C–C bond-cleavage. Preliminary mechanistic studies indicated that *tert*-butoxyl radical might be key for the activation of the dihydroquinazolinone. This work was carried out in collaboration with Dr. Roman Abrams. This work has been published in *Angew. Chem. Int. Ed*. **2023**, e202217386. DOI: 10.1002/anie.202217386.

Chapter 4, "Cu-Catalyzed C(sp^3) Amination of Unactivated Secondary Alkyl Iodides Promoted by Diaryliodonium Salts." describes the development of a copper-catalyzed C(sp^3) amination of unactivated secondary alkyl iodides mediated by diaryliodonium salts. This reaction is enabled by a cooperative interplay of SET and XAT, allowing for the generation of alkyl radical intermediates that can be intercepted by nitrogen nucleophile-bound copper complex. This work has been published in *Org. Lett*. **2023**, *25*, 3750−3754. DOI: 10.1021/acs.orglett.3c01216.

General conclusions of this Doctoral Thesis are presented in Chapter 5.

Abbreviations & Acronyms

4-CzIPN = 2,4,5,6-Tetra(9H-carbazol-9-yl)isophthalonitrile
Ad = Adamantane
aq = Aqueous
AIBN = Azobisisobutyronitrile
bpy = 2,2′-Bipyridine
BDE = Bond dissociation energy
Boc = *tert*-Butyloxycarbonyl
BTMG = 2-*tert*-Butyl-1,1,3,3-tetramethylguanidine
Cat. = Catalyst
CFL = Compact fluorescent lamp
COD = 1,5-Cyclooctadiene
diglyme = Diglycol methyl ether
dMebpy = 4,4'-Dimethyl-2,2'-bipyridyl
dtbppy = 4,4′-Di-*tert*-butyl-2,2′-dipyridyl
dppe = 1,2-Bis(diphenylphosphino)ethane
DCC = Dicyclohexylcarbodiimide
DCE = 1,2-Dichloroethane
DCM = Dichloromethane
DFT = Density functional theory
DG = Directing group
DIPEA = N,N-Diisopropylethylamine
DMA = Dimethylacetamide
DMAP = 4-Dimethylaminopyridine
DME = Ethylene glycol dimethyl ether
DMF = *N,N*-Dimethylformamide
DMPU = *N*,*N*′-Dimethylpropyleneurea
DMSO = Dimethyl sulfoxide
DTBP = Di-*tert*-butyl peroxide
equiv = Equivalent
EA = Ethyl acetate
EnT = Energy transfer
HAT = Hydrogen atom transfer
HOMO = Highest occupied molecular orbital
IC = Internal conversion
LED = Light-emitting diode
LMCT = Ligand-to-metal charge transfer

LUMO = Lowest unoccupied molecular orbital
m = *meta*
Mes = Mesityl
MLCT = Metal-to-ligand charge transfer
MTBE = Methyl tert-butyl ether
NHC = *N*-heterocyclic carbene
NHPI = *N*-(acyloxy)phthalimides
NMP = *N*-Methyl-2-pyrrolidone
o = *ortho*
p = *para*
PC = Photocatalyst
PCET = Proton-coupled electron transfer
Phen = 1,10-Phenanthroline
rt (RT) = Room temperature
SCE = Saturated calomel electrode
SET = Single electron transfer
SOMO = Singly occupied molecular orbital
t = *tert*
TBAB = Tetrabutylammonium bromide
TBS = *tert*-butyldimethylsilyl
TDAE = Tetrakis(dimethylamino)ethylene
TEMPO = 2,2,6,6-Tetramethyl-1-piperidinyloxy
THF = Tetrahydrofuran
TMG = 1,1,3,3-Tetramethylguanidine
TMHD = 2,2,6,6-Tetramethyl-3,5-heptanedione
TMS = Tetramethylsilane
Tp = Trispyrazolylborate
Tf = triflate
Ts = Tosyl
TTMSS = Tris(trimethylsilyl)silane
UV = Ultraviolet
XAT = Halogen atom transfer

Abstract of This Doctoral Thesis

Transition metal-catalyzed cross-coupling reactions have become indispensable tools for forging carbon-carbon and carbon-heteroatom bonds. These approaches have been widely applied to the preparation of biologically-relevant molecules and functional materials in both academic and industrial laboratories. Aimed at improving the applicability and practicality of these venerable reactions even further, chemists have been challenged to come up with new cross-coupling synthons that operate under ambient conditions, thus increasing the flexibility in synthetic design when accessing densely functionalized molecules. This Doctoral Thesis focuses on the development of new techniques to use ketones and unactivated halides in cross-coupling reactions.

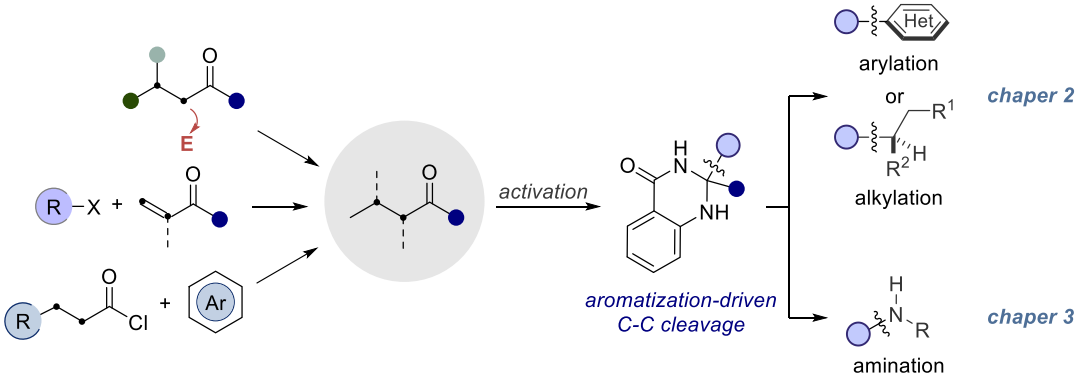

Scheme 1. Ketone as adaptative coupling handles for arylation, alkylation and amination events.

The first section focuses on the development of a photoredox/nickel dual catalytic strategy for forging C(sp^2)–C(sp^3) and C(sp^3)–C(sp^3) architectures from dihyquinazolinones. At the outset of this work, transition metal catalyzed ketone α C–C bond activation was particularly limited to strained structures, utilization of directing groups, high-temperatures, or a combination of the preceding. This methodology takes advantage of ketone derived dihyquinazolinones as adaptive one electron handles in combination with the flexibility and modularity of nickel catalysis, allowing for abundant ketones to be formally used as cross-coupling synthons with aryl and alkyl bromide electrophiles. Preliminary mechanistic experiments suggest a reductive quenching photoredox cycle, initiated by single electron oxidation of the dihyquinazolinones by the excited state of the photocatalyst.

The following chapter focuses on the use of dihyquinazolinones in copper catalyzed C(sp^3) amination reactions as a *de novo* strategy for accesing aliphatic amine architectures from simple ketone derivatives. This protocol is distinguished by its mild reaction conditions, wide substrate scope and controllable regioselectivity, thus setting the basis to apply this technique in advanced building blocks. Preliminary mechanistic investigations indicate the presence of radical intermediates and a mode of action by

which *tert*-butoxyl radical is involved in the activation of the dihyquinazolinone.

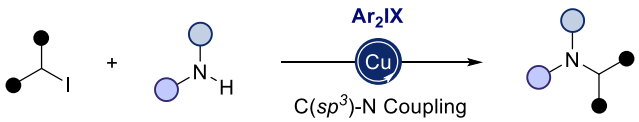

Scheme 2. Copper-catalyzed C(sp^3) amination of unactivated secondary alkyl iodides promoted by diaryliodonium salts.

The last research section deals with a copper-catalyzed C(sp^3) amination of unactivated secondary alkyl iodides promoted by diaryliodonium salts. This technique takes advantage of diaryliodonium salts to generate aryl radicals in the presence of amido-Cu(I) complexes, resulting in halogen atom abstraction of an alkyl iodide prior to sp^3 C–N reductive elimination. This method is characterized by its mild reaction conditions and excellent chemoselectivity while offering a complementary protocol to the preparation of aliphatic amines.

Chapter 1

General Introduction

1.1 Transition Metal-Catalyzed Cross-Coupling Reactions

1.1.1 A Brief History

"Our pursuit in whatever we do must always be for excellence, and if we accomplish excellence, it is its own reward and recognition will follow."

—Ei-ichi Negish

With the 2010 Nobel Prize in Chemistry awarded to Richard Heck, Ei-ichi Negishi, and Akira Suzuki, transition metal-catalyzed cross-coupling reactions have become indispensable tools in organic synthesis.[1] Historically, these reactions can be traced back from the work of Glaser in 1869 when describing the homocoupling of acetylides using stochiometric amount of copper salts (Scheme 1.1).[2] The discovery of cross-coupling reactions was facilitated by the observation in the 1940s that first-row transition metal salts, such as $FeCl_3$, $CoCl_2$, $NiCl_2$, $CuCl_2$, or $CrCl_2$, act as catalysts for the homocoupling of Grignard reagents using alkyl or aryl halides as oxidants.[3] In 1957, Cadiot and Chodkiewicz disclosed a copper-catalyzed cross-coupling protocol of alkynes with bromoalkynes, which is believed to be the first example of transition metal-catalyzed C–C bond cross-coupling reactions.[4] Later on, studies reported by Kochi in the 1970s described the utilization of iron complexes for the cross-coupling of alkenyl halides with Grignard reagents.[5] The 1970s also witnessed the birth of nickel-catalyzed cross-coupling — Corriu and Kumada independently reported nickel-catalyzed cross-coupling reactions of aryl and alkenyl halides with Grignard reagents in 1972.[6] Although the utilization of iron or nickel complexes predates the utilization of palladium for similar purposes, the high reactivity and predictable outcome of the latter gradually overshadowed the utilization of other transition metals, making palladium in most instances the catalyst of choice for a myriad of cross-coupling reactions. Indeed, our portfolio now includes a series of classical palladium-catalyzed

[1] Seechurn, C. C. C. J.; Kitching, M. O.; Colacot, T. J.; Snieckus, V. Palladium-Catalyzed Cross-Coupling: A Historical Contextual Perspective to the 2010 Nobel Prize. *Angew. Chem. Int. Ed*. **2012**, *51*, 5062–5085.
[2] Glaser, C. Beiträge zur Kenntniss des Acetenylbenzols. *Ber. Dtsch. Chem. Ges*. **1869**, *2*, 422–424.
[3] Kharasch, M. S; Reinmuth, O. *Grignard Reactions of Nonmetallic Substances*; Constable: London, 1954.
[4] Chodkiewicz, W. *Ann. Chim. Paris*. **1957**, *2*, 819–869.
[5] Tamura, M.; Kochi, J. K. Vinylation of Grignard Reagents. Catalysis by Iron. *J. Am. Chem. Soc*. **1971**, *93*, 1487–1489.
[6] (a) Corriu, R. J. P. Masse, J. P. Activation of Grignard Reagents by Transition-Metal Complexes. A New and Simple Synthesis of Trans-Stilbenes and Polyphenyls. *J. Chem. Soc. Chem. Commun.* 1972, 144a. (b) Tamao, K.; Kiso, Y.; Sumitani, K.; Kumada, M. Alkyl Group Isomerization in the Cross-Coupling Reaction of Secondary Alkyl Grignard Reagents with Organic Halides in the Presence of Nickel-Phosphine Complexes as Catalysts. *J. Am. Chem. Soc*. **1972**, *94*, 9268–9269.

transformations such as Sonogashira-Hagihara coupling,[7] Negishi coupling,[8] Stille coupling,[9] Suzuki-Miyaura coupling,[10] Hiyama coupling[11] and Buchwald-Hartwig coupling,[12] among others.

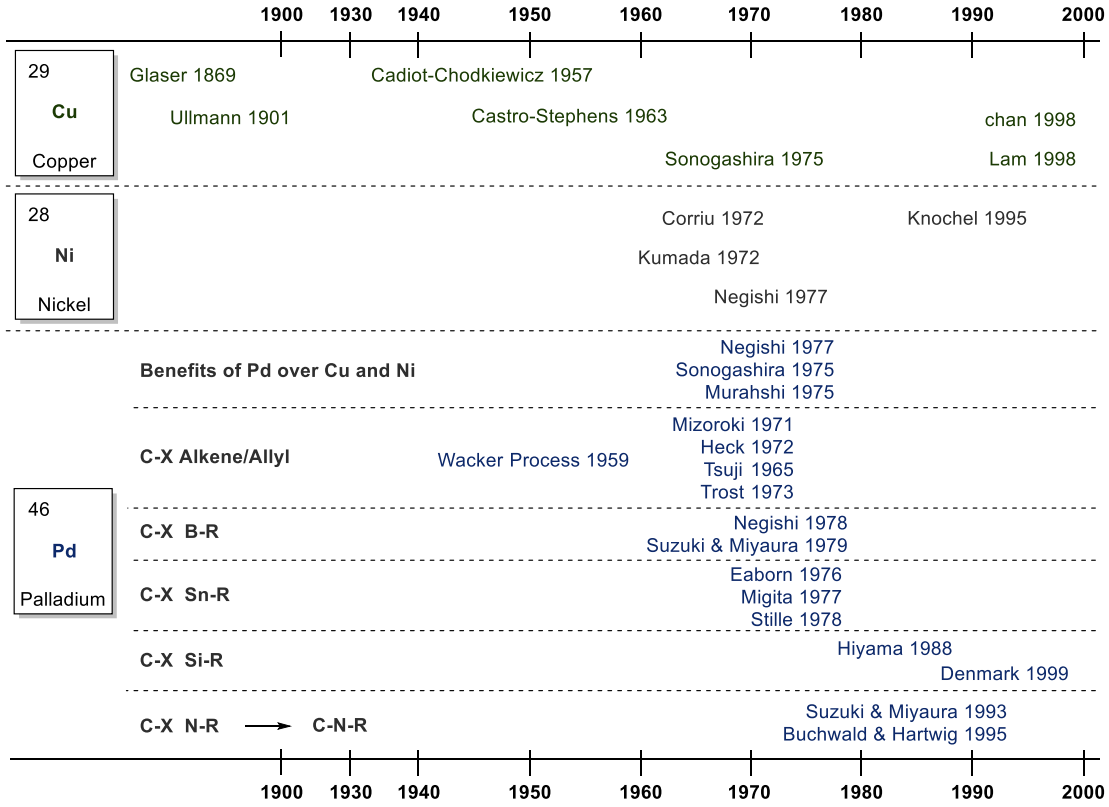

Scheme 1.1 Timeline of the discovery and development of metal-catalyzed cross-coupling reactions.

[7] Chinchilla, R.; Nájera, C. Recent advances in Sonogashira reactions. *Chem. Soc. Rev.* **2011**, *40,* 5084–5121.
[8] Haas, D.; Hammann, J. M.; Greiner, R.; Knochel, P. Recent Developments in Negishi Cross-Coupling Reactions. *ACS Catal*. **2016**, *6*, 1540–1552.
[9] Cordovilla, C.; Bartolomé, C.; Martínez-Ilarduya, J. M.; Espinet, P. The Stille Reaction, 38 Years Later. *ACS Catal*. **2015**, *5*, 3040–3053.
[10] Farhang, M.; Akbarzadeh, A. R.; Rabbani, M.; Ghadiri, A. M. A Retrospective-Prospective Review of Suzuki–Miyaura Reaction: From Cross-Coupling Reaction to Pharmaceutical Industry Applications. *Polyhedron*. **2022**, *227*, 116124–116147.
[11] Noor, R.; Zahoor, A. F.; Irfan, M.; Hussain, S. M.; Ahmad, S.; Irfan, A.; Kotwica-Mojzych, K.; Mojzych, M. Transition Metal Catalyzed Hiyama Cross-Coupling: Recent Methodology Developments and Synthetic Applications. *Molecules* 2022, *27*, 5654–5707.
[12] Ruiz-Castillo, P.; Buchwald, S. L. Applications of Palladium-Catalyzed C–N Cross-Coupling Reactions. *Chem. Rev*. **2016**, *116*, 12564–12649.

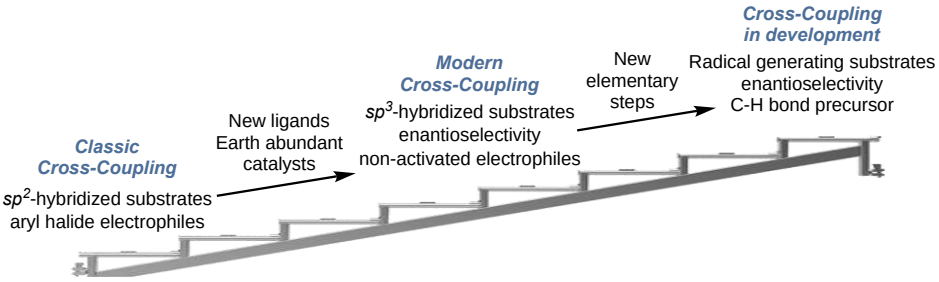

Scheme 1.2 Development of cross-coupling reactions.

For a long time cross-coupling reactions remained confined predominantly to the utilization of aryl or vinyl halides. However, the recent years have witnessed the development of cross-coupling reactions with less-activated sp^2-hybridized electrophiles, such as esters and amides,[13] as well as sp^3-hybridized electrophiles.[14] It is worth noting that the utilization of either phenol derivatives or sp^3-hybridized electrophiles have proven to be particularly efficient with nickel catalysts due to its lower electronegativity and the low propensity for enabling parasitic β-hydride elimination pathways. On the other hand, the success of metal-catalyzed cross-coupling reactions is closely linked to the discovery and development of novel ligands.[15] An illustrative example is the seminal work from Buchwald who showed the importance of sterically bulky dialkylbiarylphosphine ligands for accelerating elementary steps such as oxidative addition and reductive elimination within the catalytic cycle.[16]

Although it has been in development for more than 50 years, transition metal-catalyzed cross-coupling reactions nowadays still represent one of the most important research topics (Scheme 1.2).[17] Undoubtedly, the study of the mechanisms by which these reactions operate has been critical for designing future endeavors within the general area of cross-coupling reactions. Illustrative examples are the development of reductive cross-electrophile couplings, oxidative cross-nucleophile couplings or the development of techniques that result from the merger of multiple disciplines such as metallaphotoredox scenarios. In addition, the recent years have witnessed the design of powerful transformations arising from C–H and C–C functionalization, including traditional coupling events aided by directing groups, chain-walking techniques or hydrogen-atom transfer processes, among others.

---

[13] Takise, R.; Muto, K.; Yamaguchi, J. Cross-Coupling of Aromatic Esters and Amides. *Chem. Soc. Rev*. **2017**, *46*, 5864–5888.
[14] Kranthikumar, R. Recent Advances in C(sp^3)–C(sp^3) Cross-Coupling Chemistry: A Dominant Performance of Nickel Catalysts. *Organometallics* **2022**, *41*, 667–679.
[15] Meijere, A. D.; Diederich, F. *Metal-Catalyzed Cross-Coupling Reactions*; Wiley: Hoboken, 2008.
[16] Surry, D. S.; Buchwald, S. L. Biaryl Phosphane Ligands in Palladium-Catalyzed Amination. *Angew. Chem. Int. Ed*. **2008**, *47*, 6338–6361.
[17] Campeau, L.-C.; Hazari, N. Cross-Coupling and Related Reactions: Connecting Past Success to the Development of New Reactions for the Future. *Organometallics* **2019**, *38*, 3–35.

1.1.2 Palladium-Catalyzed Cross-Coupling Reactions

Some of the most prominent and promising catalysts in organic synthesis for the requisite construction of C–C and C–N bonds are palladium catalysts, which plays a pivotal role in pharmaceutical and medicinal chemistry.[18] In particular, the Suzuki-Miyaura C–C bond cross-coupling reaction has been one of the most investigated cross-coupling reactions in organic synthesis since its discovery in 1979 by Akira Suzuki (Scheme 1.3).[19] The mechanism of palladium-catalyzed cross-coupling is proposed to involve a Pd(0)/Pd(II) cycle, with the elementary steps being oxidative addition of the electrophile to the coordinatively unsaturated palladium(0) catalyst, transmetalation of the nucleophile, and reductive elimination to form the product and regenerate the palladium(0) catalyst.[20] In addition, to further enhance the practicability of the reaction, a number of well-defined bench-stable palladium(II) precatalysts have been developed, thus insuring the cross-coupling reproducibility in various transformations.[21]

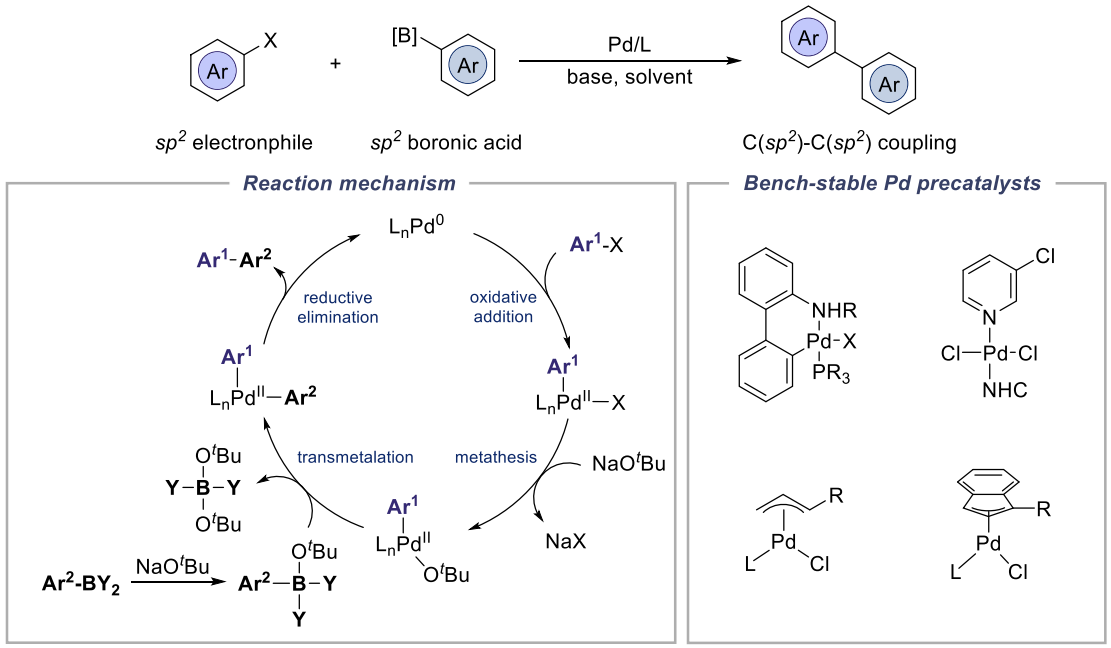

Scheme 1.3 Palladium-catalyzed Suzuki-Miyaura cross-coupling.

Another significant advance in palladium-catalyzed cross-coupling methodology

[18] Rayadurgam, J.; Sana, S.; Sasikumarc, M.; Gu, Q. Palladium Catalyzed C–C and C–N Bond Forming Reactions: An Update on the Synthesis of Pharmaceuticals from 2015–2020. *Org. Chem. Front.* **2021**, *8*, 384–414.
[19] Miyaura, N.; Suzuki, A. Palladium-Catalyzed Cross-Coupling Reactions of Organoboron Compounds, *Chem. Rev*. **1995**, *95*, 2457−2483.
[20] D'Alterio, D. C.; Casals-Cruañas, E.; Tzouras, N. V.; Talarico, G.; Nolan, S. P.; Poater, A. Mechanistic Aspects of the Palladium-Catalyzed Suzuki-Miyaura Cross-Coupling Reaction. *Chem. Eur. J.* **2021**, *27*, 13481–13493.
[21] Li, H.; Johansson Seechurn, C. C. C.; Colacot, T. J. Development of Preformed Pd Catalysts for Cross-Coupling Reactions, Beyond the 2010 Nobel Prize. *ACS Catal*. **2012**, *2*, 1147−1164.

over the last 20 years has been the development of specialized ligands that enhance the rates of the elementary steps in catalysis, such as oxidative addition and reductive elimination.[22] Initially simple triarylphosphine ligands were used in cross-coupling reactions,[23] but seminal work from the Buchwald group showed that sterically bulky dialkylbiarylphosphine ligands generated catalytic systems provide increased scope and efficiency. The development of these ligands was partially responsible for the discovery of catalytic systems capable of room-temperature Suzuki-Miyaura reactions involving unactivated aryl chloride substrates and has been crucial to improvements in the scope of Buchwald-Hartwig reactions (Scheme 1.4).[24] Currently the general design principles for promoting both the elementary steps in catalysis and the formation of the active monoligated palladium(0) species are well-understood. For instance it has been found the electron donating alkyl phosphine effectively promote oxidative addition and second aryl ring bulkiness promotes reductive elimination and increases air stability of the ligand.

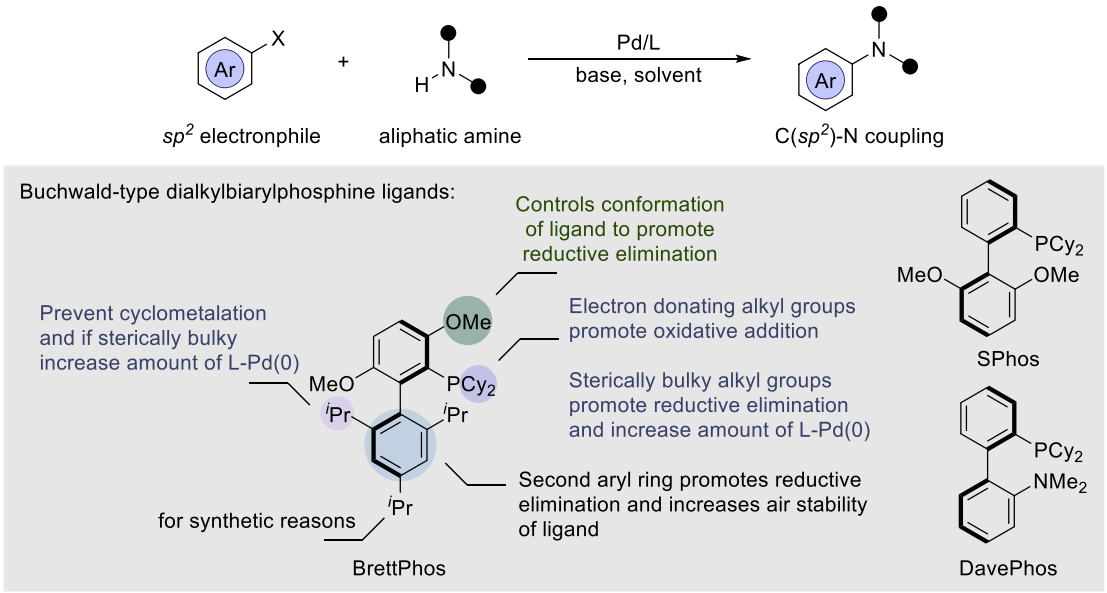

Scheme 1.4 Palladium-catalyzed C–N bond cross-coupling.

[22] (a) Littke, A. F.; Dai, C.; Fu, G. C. Versatile Catalysts for the Suzuki Cross-Coupling of Arylboronic Acids with Aryl and Vinyl Halides and Triflates under Mild Conditions. *J. Am. Chem. Soc*. **2000**, *122*, 4020−4028. (b) Shelby, Q.; Kataoka, N.; Mann, G.; Hartwig, J. Unusual in situ Ligand Modification to Generate a Catalyst for Room Temperature Aromatic C−O Bond Formation. *J. Am. Chem. Soc*. **2000**, *122*, 10718−10719. (c) Martin, R.; Buchwald, S. L. Palladium-Catalyzed Suzuki-Miyaura Cross-Coupling Reactions Employing Dialkylbiaryl Phosphine Ligands. *Acc. Chem. Res*. **2008**, *41*, 1461−1473.

[23] Elschenbroich, C.; Salzer, A. *Organometallics: A Concise Introduction* (2nd ed.); Wiley: Weinheim, 1992.

[24] Ruiz-Castillo, P.; Buchwald, S. L. Applications of Palladium-Catalyzed C−N Cross-Coupling Reactions. *Chem. Rev*. **2016**, *116*, 12564−12649.

1.1.3 Nickel-Catalyzed Cross-Coupling Reactions

The reactivity of nickel in catalyzing cross-coupling reactions was discovered in the early 1970s, but it has been only recently that its potential could be fully exploited as a platform for rapidly and reliably increasing molecular complexity. As shown in Scheme 1.5, nickel has a smaller nucleus and lower electronegativity than palladium, thus facilitating particularly uphill oxidative addition processes. Nickel readily donates *d*-electrons to π-acceptors, making olefin bonding generally stronger than palladium.[25] This property leads nickel to become a privileged catalyst for the functionalization of olefins, even in the context of polymerization events.[26] In addition, alkyl-nickel complexes are particularly resistant to undergo β-hydride elimination. This is largely due to the observation that the main contribution for the agostic interaction is the σ donation of the proximal C–H bond to the nickel center. In the case of nickel, there is a vacant *d* orbital which is higher in energy than the corresponding palladium analogue. This situation makes the orbital overlap with nickel not particularly facile thus causing an elongation of the agostic interaction that is required for β-hydride elimination. Overall, these observations makes nickel particularly suited for C(sp^3) coupling reactions by minimizing the rate of destructive β-hydride elimination. Note, however, that ligand design has been critical to reverse this trend, resulting in chain-walking techniques that enable functionalization at remote C(sp^3)–H sites within the alkyl side chain.[27] In particular, nickel has shown to be suited for electron-transfer events, thus populating manifolds that are beyond reach in canonical Pd-catalyzed reactions. This observation has been turned into a strategic advantage when merging nickel with photoredox catalysis or electrochemical settings.

[25] Tamaru, Y. *Modern Organonickel Chemistry*; Wiley: Weinheim, 2005.
[26] Mitchell, N. E.; Long, B. K. Recent Advances in Thermally Robust, Late Transition Metal-Catalyzed Olefin Polymerization. *Polym Int.* **2019**, *68*, 14–26.
[27] Janssen-Müller, D.; Sahoo, B.; Sun, S.-Z.; Martin, R. Tackling Remote sp^3 C−H Functionalization via Ni-Catalyzed "chain-walking" Reactions. *Isr. J. Chem.* **2020**, *60*, 195–206.

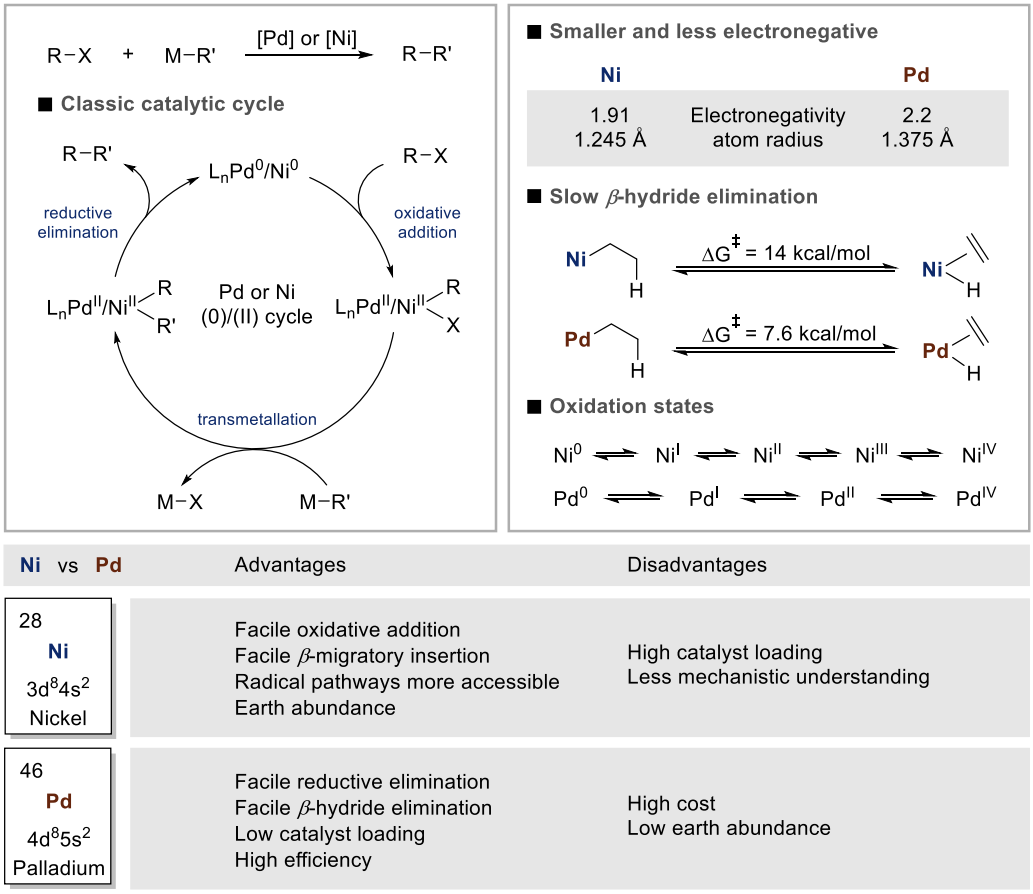

Ni vs Pd	Advantages	Disadvantages
28 Ni $3d^8 4s^2$ Nickel	Facile oxidative addition Facile β-migratory insertion Radical pathways more accessible Earth abundance	High catalyst loading Less mechanistic understanding
46 Pd $4d^8 5s^2$ Palladium	Facile reductive elimination Facile β-hydride elimination Low catalyst loading High efficiency	High cost Low earth abundance

Scheme 1.5 General characteristics of Ni and Pd catalysis.

As indicated before, the recent years have witnessed the development of cross-coupling reactions of phenol derivatives as alternatives to the utilization of organic halide counterparts. Due to the facile oxidative addition power of nickel over palladium, nickel has been found to be particularly effective for the coupling of ethers, esters, carbamates or carbonates, among others (Scheme 1.6).[28]

[28] (a) Cornella, J.; Zarate, C.; Martin, R. Metal-Catalyzed Activation of Ethers via C–O Bond Cleavage: A New Strategy for Molecular Diversity. *Chem. Soc. Rev.* **2014**, *43*, 8081−8097. (b) Tobisu, M.; Chatani, N. Cross-Couplings Using Aryl Ethers via C−O Bond Activation Enabled by Nickel Catalysts. *Acc. Chem. Res.* **2015**, *48*, 1717−1726.

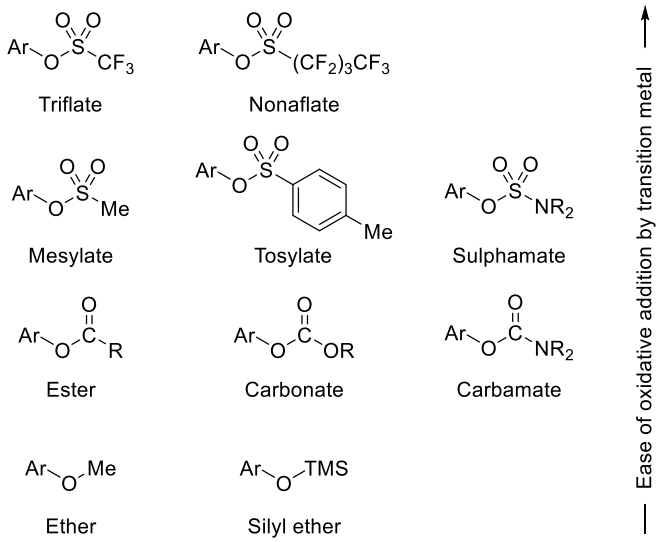

Scheme 1.6 Phenol derivatives as modern electrophiles in cross-coupling reactions.

While the majority of nickel-catalyzed cross-coupling reactions are focusing on C–C bond-forming reactions, the discovery of new ligand backbones has been critical for enabling C–N bond-formations. This is probably associated to the inherent difficulty of nickel catalysis in enabling reductive elimination of C–heteroatom bonds. That being set, a number of bisphosphines, bipyridines, 1,10-phenanthrolines and NHCs have been found to effectively promote nickel-catalyzed Buchwald-Hartwig reaction.[29] Despite different types of ligand used, a conclusive reaction is shown in Scheme 1.7 where two catalytic cycles might a priori be conceivable based on Ni(0)/Ni(II) or Ni(I)/Ni(III).[30] A Ni(0)/Ni(II) cycle involves oxidative addition, amine binding and deprotonation, and product forming C–N reductive elimination. A mechanism involving a Ni(I)/Ni(III) cycle could alternatively be initiated by amine binding and HX loss, followed by aryl halide oxidative addition to the resulting Ni(I)-amido intermediate, and product forming C–N reductive elimination. Recent advances by Stradiotto have demonstrated that DalPhos ligands are particularly prone to enable C–N reductive elimination within a presumptive Ni(0)/Ni(II) catalytic cycle.[31]

[29] Marin, M.; Rama, R. J.; Nicasio, M. C. Ni-Catalyzed Amination Reactions: An Overview. *Chem. Rec*. **2016**, *16*, 1819–1832.

[30] (a) Lavoie, C. M.; Stradiotto, M. Bisphosphines: A Prominent Ancillary Ligand Class for Application in Nickel-Catalyzed C−N Cross-Coupling. *ACS Catal*. **2018**, *8*, 7228−7250. (b) Ritleng, V.; Henrion, M.; Chetcuti, M. J.; Nickel N-Heterocyclic Carbene-Catalyzed C−Heteroatom Bond Formation, Reduction, and Oxidation: Reactions and Mechanistic Aspects. *ACS Catal*. **2016**, *6*, 890−906.

[31] (a) Lavoie, C., MacQueen, P., Rotta-Loria, N.; Sawatzky, R. S.; Borzenko, A.; Chisholm, A. J.; Hargreaves, B. K. V.; McDonal, R.; Ferguson, M. J.; Stradiotto, M. Challenging Nickel-Catalysed Amine Arylations Enabled by Tailored Ancillary Ligand Design. *Nat Commun*. **2016**, *7*, 11073−11084. (b) McGuire, R. T.; Paffile, J. F. J.; Zhou, Y.; Stradiotto, M. Nickel-Catalyzed C−N Cross-Coupling of Ammonia, (Hetero)Anilines, and Indoles with Activated (Hetero)aryl Chlorides Enabled by Ligand Design. *ACS Catal*. **2019**, *9*, 9292−9297.

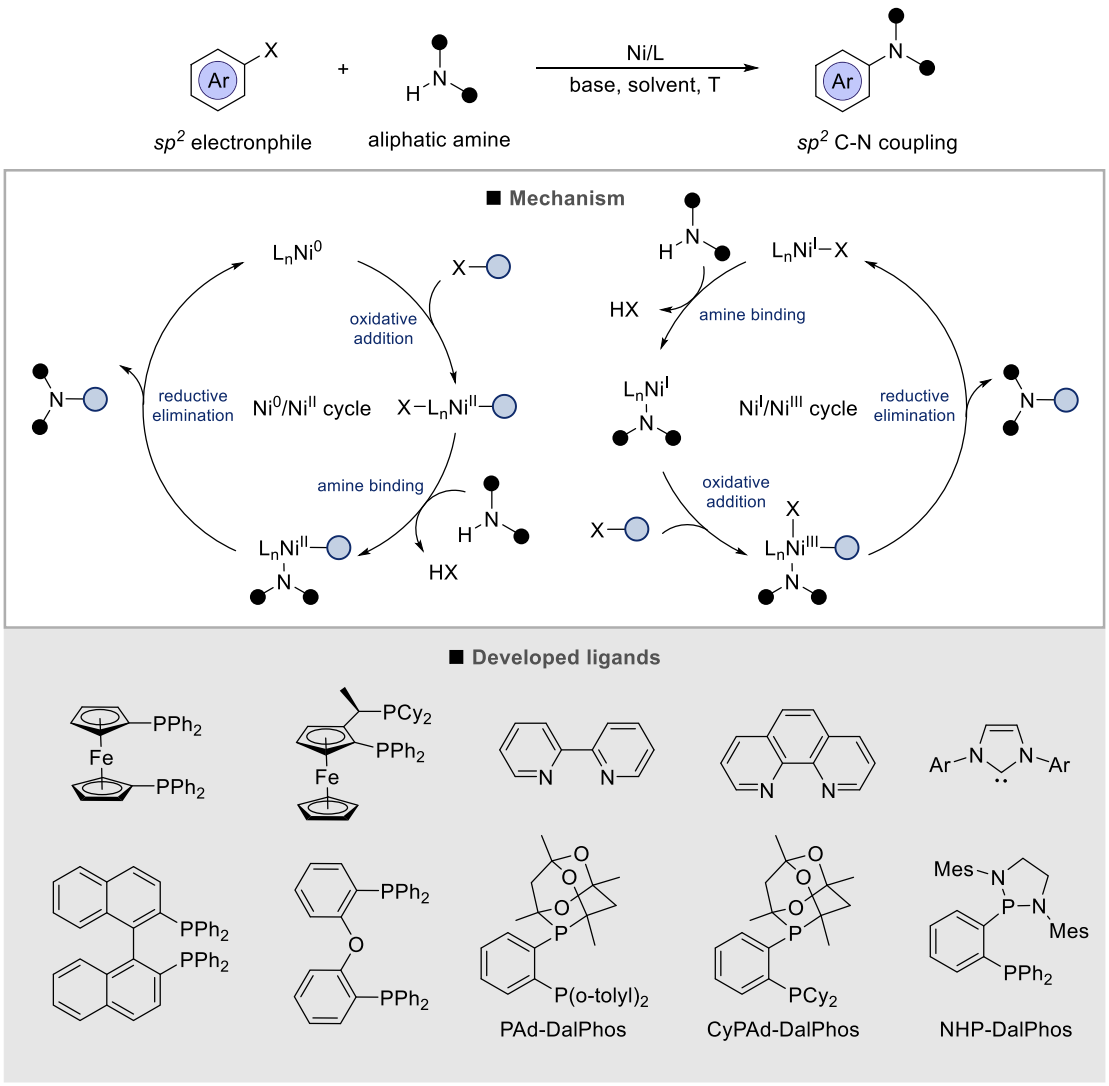

Scheme 1.7 Ligand enabled nickel-catalyzed C–N bond cross-coupling reactions.

Recently, Nocera and co-workers reported the nickel-catalyzed C–N bond and C–O bond cross-coupling reactions under mild conditions (Scheme 1.8)[32] The key to success is attributed to a Ni(I)/Ni(III) redox cycle enabled by addition of catalytic amount of zinc powder.[33] The reduction of Ni(II) precatalyst by zinc gives access to a Ni(I) intermediate which subsequently reacts with aryl bromide through oxidative addition to provide an aryl-Ni(III) intermediate. The resulting Ni(III) intermediate undergoes ligand exchange with nucleophile assisted by base to form an aryl-Ni(III)-Nuc complex, followed by reductive elimination to deliver the coupling product while regenerating the propagating Ni(I) intermediate.

[32] Sun, R.; Qin, Y.; Nocera, D. G. General Paradigm in Photoredox Nickel-Catalyzed Cross-Coupling Allows for Light-Free Access to Reactivity. *Angew. Chem. Int. Ed*. **2020**, *59*, 9527–9533.
[33] Zhu, C.; Yue, H.; Jia, J.; Rueping, M. Nickel-Catalyzed C-Heteroatom Cross-Coupling Reactions under Mild Conditions via Facilitated Reductive Elimination. *Angew. Chem. Int. Ed*. **2021**, *60*, 17810–17831.

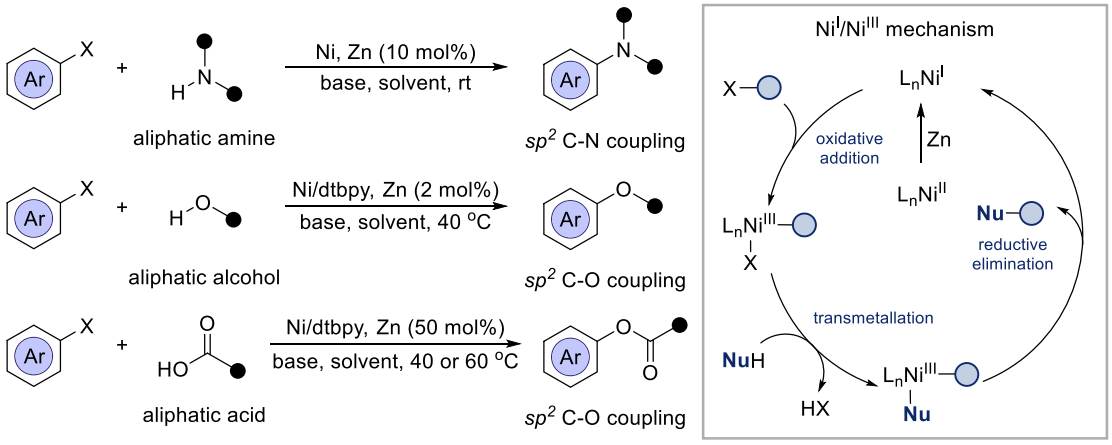

Scheme 1.8 Nickel-catalyzed C–N/C–O bond cross-coupling reactions.

The recent popularity of nickel catalysis is partially ascribed to the ability to couple sp^3 hybridized carbons with exceptional ease, a matter of utmost relevance in industrial settings due to the importance of such motifs in medicinal chemistry settings.[34] One of the initial reports aimed at such a goal was described by Knochel, showing that nickel was particularly suited for the coupling of primary alkyl iodides with organozinc reagents using either an intramolecularly pending alkene[35] or exogenous electron-poor alkene[36] to facilitate reductive elimination. Fu and co-workers in 2003 reported the nickel-catalyzed cross-coupling of secondary alkyl bromides and organozinc reagents (Scheme 1.9).[37] Based on the mechanistic studies, they proposed the reaction is initiated by transmetalation of Ni(I) with alkyl zinc reagent to afford an alkyl-Ni(I) intermediate. Oxidative addition of alkyl halides to alkyl-Ni(I) species gives rise to alkyl-Ni(III)-alkyl entity, thus setting the basis for C(sp^3)–C(sp^3) construction via reductive elimination. The oxidative addition process is thought to proceed through a stepwise mechanism involving halogen-atom abstraction and radical rebound.[38] The chelating tridentate redox active PyBOX ligand was found to be essential, probably for stabilizing the Ni(I) intermediate and slowing the rate of β-hydride elimination, which otherwise requires a vacant coordination site.

[34] Netherton, M. R.; Fu, G. C. Nickel-Catalyzed Cross-Couplings of Unactivated Alkyl Halides and Pseudohalides with Organometallic Compound. *Adv. Synth. Catal*. **2004**, *346*, 1525–1532.
[35] Devasagayaraj, A.; Studemann, T.; Knochel, P. A New Nickel-Catalyzed Cross-Coupling Reaction between sp^3 Carbon Centers. *Angew. Chem. Int. Ed. Engl*. **1996**, *34*, 2723–2725.
[36] Giovannini, R.; Knochel, P. Ni(II)-Catalyzed Cross-Coupling between Polyfunctionalized Arylzinc Derivatives and Primary Alkyl Iodides. *J. Am. Chem. Soc*. **1998**, *120*, 11186–11187.
[37] Zhou, J.; Fu, G. C. Cross-couplings of Unactivated Secondary Alkyl Halides: Room-Temperature Nickel-Catalyzed Negishi Reactions of Alkyl Bromides and Iodides. *J. Am. Chem. Soc*. **2003**, *125*, 14726–14727.
[38] (a) Diccianni, J. B.; Diao, T. Mechanisms of Nickel-Catalyzed Cross-Coupling Reactions. *Trends Chem*. **2019**, *1*, 830–844. (b) Diccianni, J. B.; Katigbak, J.; Hu, C.; Diao, T. Mechanistic Characterization of (Xantphos)Ni(I)-Mediated Alkyl Bromide Activation: Oxidative Addition, Electron Transfer, or Halogen-Atom Abstraction. *J. Am. Chem. Soc*. **2019**, *141*, 1788−1796.

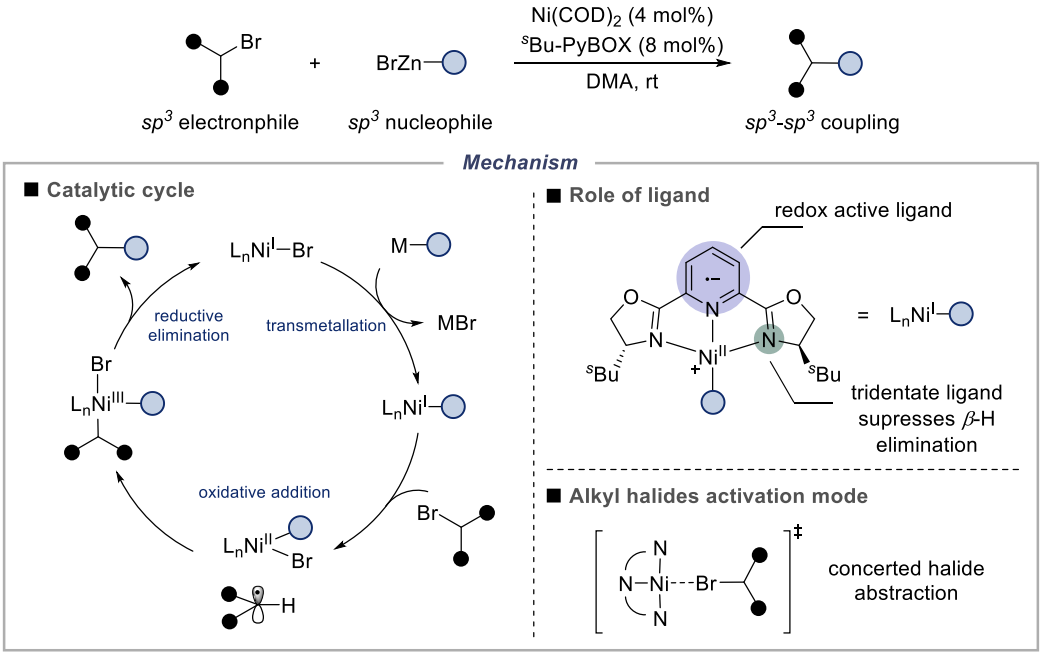

Scheme 1.9 Nickel-catalyzed C(sp^3)–C(sp^3) cross-coupling.

Later on, Hu and co-workers developed a nickel pincer complex (Scheme 1.10) which was shown to be catalytically active for C(sp^3)–C(sp^3) Kumada cross-couplings[39]. A mechanistic study revealed a different mechanism where transmetalation of the nucleophile occurs prior to electrophile activation via bimolecular oxidative addition.[40] Specifically, transmetalation of Ni(II) complex **1.10b** with RMgCl gives a Ni(II)-alkyl species **1.10c**. Halogen-atom abstraction of alkyl bromide by **1.10c** generates Ni(III) complex **1.10e** and an alkyl radical **1.10d** that combines with another molecule of **1.10c** to give Ni(III) species **1.10f**. Reductive elimination delivers the product and Ni(I) complex **1.10g**. Comproportionation of **1.10g** and Ni(III) entity **1.10e** regenerates **1.10b**.

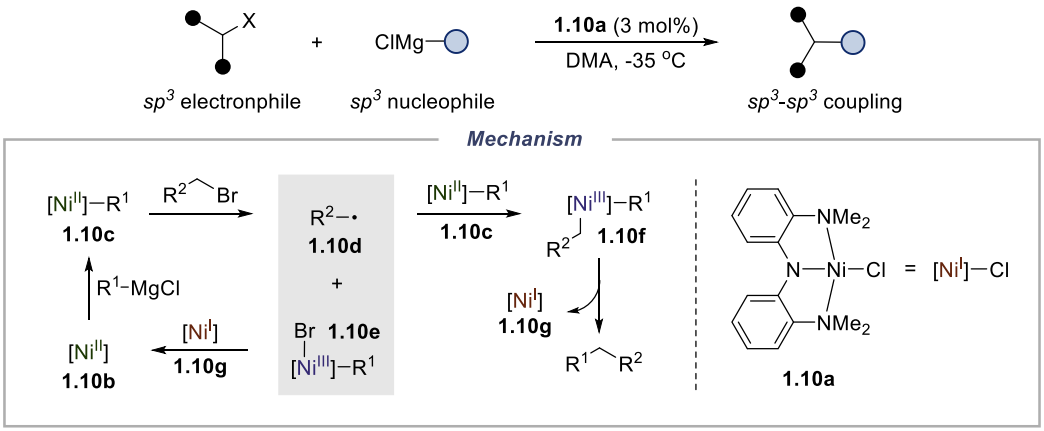

[39] Vechorkin, O.; Hu, X. Nickel-Catalyzed Cross-Coupling of Non-Activated and Functionalized Alkyl Halides with Alkyl Grignard Reagents. *Angew. Chem. Int. Ed*. **2009**, *48*, 2937–2940.
[40] Breitenfeld, J.; Ruiz, J.; Wodrich, M. D.; Hu, X. Bimetallic Oxidative Addition Involving Radical Intermediates in Nickel-Catalyzed Alkyl−Alkyl Kumada Coupling Reactions. *J. Am. Chem. Soc*. **2013**, *135*, 12004–12012.

Scheme 1.10 Nickel-catalyzed C(sp^3)−C(sp^3) Kumada cross-coupling.

Reductive cross-electrophile coupling reactions under reducing conditions have offered an innovative pathway for the coupling of C(sp^3) electrophiles without the need for utilizing air-sensitive organometallic coupling reagents (Scheme 1.11).[41] Key for success was the utilization of a suitable reductant such as Zn, Mn or organic reductants such as tetrakis(dimethylamino)ethylene (TDAE). The origin of these protocols can be traced back to the groundbreaking research conducted by the group of Weix, who demonstrated a nickel-catalyzed reductive coupling reaction of aryl iodide and alkyl iodide.[42] Mechanistic investigations on C(sp^3)-C(sp^2) cross-electrophile coupling reactions with (bpy)$NiBr_2$ as the catalyst and Mn as the reductant suggest a radical chain mechanism. In this mechanism, Ni(I) species **1.11d** initiates radical formation from the C(sp^3) electrophile to form Ni(II) **1.11e**. Upon reduction, Ni(0) complex **1.11a** undergoes oxidative addition to the C(sp^2) electrophile to form Ni(II) intermediate **1.11b**, which combines with the organic radical to form Ni(III) entity **1.11c**, followed by reductive elimination to give rise to the product and Ni(I).[43] An alternative mechanism, namely sequential reduction pathway,[44] involves oxidative addition of the C(sp^2) electrophile by Ni(0) intermediate **1.11f** occurring prior to reduction of Ni(II) to Ni(I). Activation of the C(sp^3) electrophile forms a radical that rebinds to nickel to provide Ni(III) species **1.11i**, followed by reductive elimination to give the product and Ni(I) intermediate **1.11j**. Catalytic turnover is realized by a final reduction of Ni(I) to Ni(0).

[41] (a) Knappke, C. E. I.; Grupe, S.; Gärtner, D.; Corpet, M.; Gosmini, C.; Wangelin, A. J. Reductive Cross-Coupling Reactions between Two Electrophiles. *Chem. Eur. J.* **2014**, *20*, 6828–6842. (b) Weix, D. J. Methods and Mechanisms for Cross-Electrophile Coupling of Csp^2 Halides with Alkyl Electrophiles. *Acc. Chem. Res.* **2015**, *48*, 1767−1775. (c) Poremba, K. E.; Dibrell, S. E.; Reisman, S. E. Nickel-Catalyzed Enantioselective Reductive Cross-Coupling Reactions. *ACS Catal.* **2020**, *10*, 8237−8246. (d) Pang, X.; Su, P.-F.; Shu, X.-Z. Reductive Cross-Coupling of Unreactive Electrophiles. *Acc. Chem. Res.* **2022**, *55*, 2491–2509.

[42] Everson, D. A.; Shrestha, R.; Weix, D. J. Nickel-Catalyzed Reductive Cross-Coupling of Aryl Halides with Alkyl Halides. *J. Am. Chem. Soc.* **2010**, *132*, 920–921.

[43] Biswas, S.; Weix, D. J. Mechanism and Selectivity in Nickel-Catalyzed Cross-Electrophile Coupling of Aryl Halides with Alkyl Halides. *J. Am. Chem. Soc.* **2013**, *135*, 16192–16197.

[44] Wang, K.; Ding, Z.; Zhou, Z.; Kong, W. Ni-Catalyzed Enantioselective Reductive Diarylation of Activated Alkenes by Domino Cyclization/Cross-Coupling. *J. Am. Chem. Soc.* **2018**, *140*, 12364−12368.

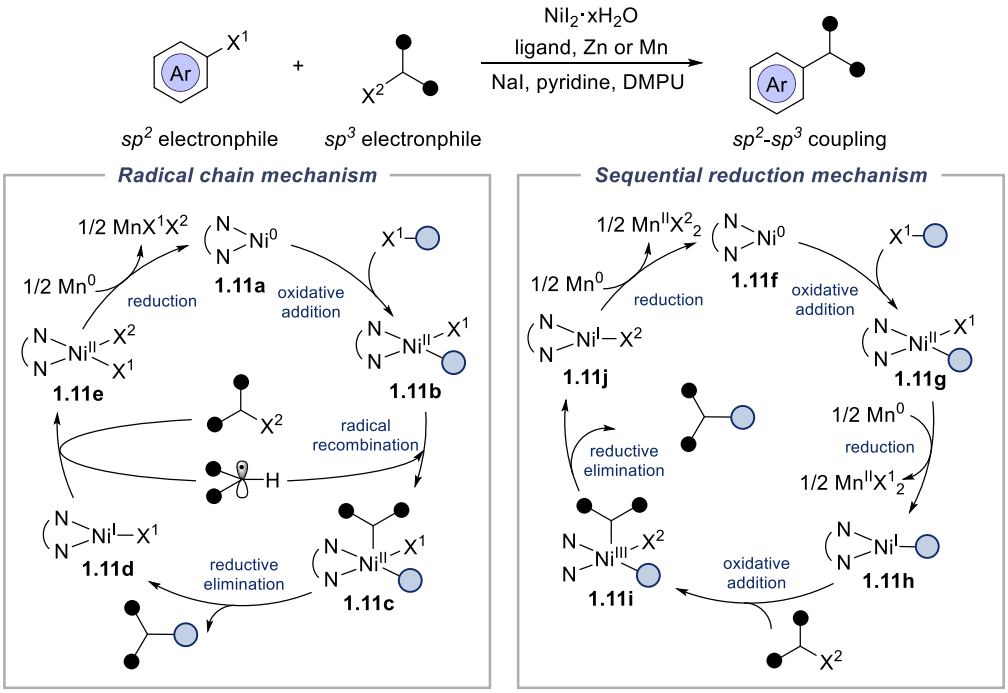

Scheme 1.11 Nickel-catalyzed reductive cross-coupling.

As demonstrated above, probably due to superior oxidative addition power towards phenol derivatives as well as the ability to couple sp^3 hybridized carbons, the recent years have witnessed the rise of nickel catalysis in cross-coupling reactions. In particular, the mechanistic studies of sp^3 hybridized electrophile coupling reaction disclosed the unconventional one-electron pathways and radical intermediates involvement. These observations had been critical for designing new reactivity patterns within the general area of cross-coupling reactions, in which cross electrophile coupling reaction is included. Consequently, as an emerging technique of producing free radicals, photocatalysis no suspense has played an important role in nickel-catalyzed cross-coupling reaction. Aiming at revealing the function of photochemistry in transition metal-catalyzed cross-coupling reactions, the following chapter will focus on the fundamentals of photocatalysis and the merger of photochemistry and transition metal catalysis.

1.2 Merging Photocatalysis with Transition Metal Catalysis

1.2.1 Fundamentals of Photocatalysis

In the past few decades, photochemistry and especially photocatalysis has been embraced by organic chemists as a tool to enable previously elusive synthetic methods. While the conventional catalysts accelerate reactions by means of decreasing the Gibbs energy of activation (Scheme 1.12, A), photocatalysis takes advantage of the light

irradiation, providing a high energy starting point to promote reactions (Scheme 1.12, B). In these transformations, light energy is harvested by organic molecules or photocatalysts to reach an excited state, enabling the formation of new chemical bonds under mild reaction conditions (i.e., at room temperature, use of visible light).

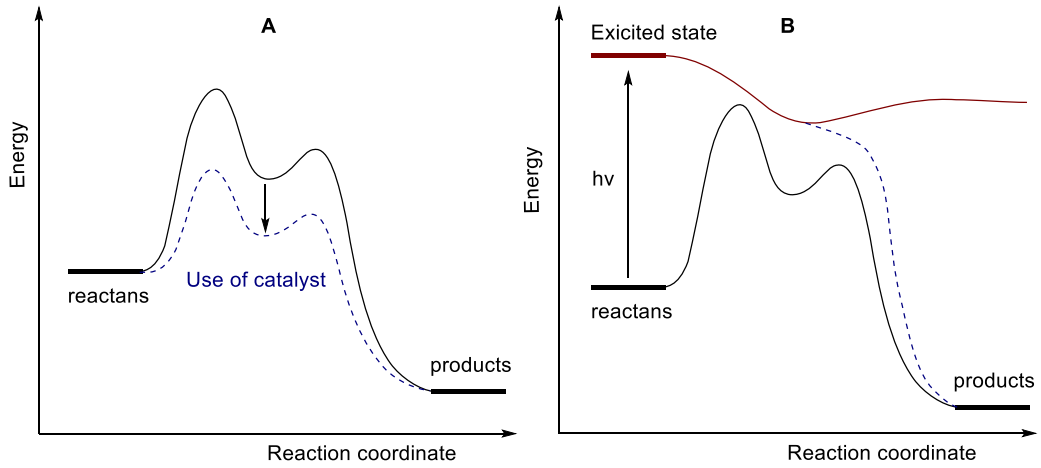

Scheme 1.12 Thermochemical (A) versus photochemical (B) activation.

Known as the first law of photochemistry, Grotthuss-Draper law states that radiation must be absorbed by a chemical substance for a photochemical reaction to take place. For each photon of light absorbed by a chemical system, no more than one molecule is activated for subsequent reaction — known as the Stark-Einstein law, which is defined as the second law of photochemistry. Indicated by Jablonski diagram, when a photosensitizer in ground state (S_0) absorbs photon from light irradiation, one electron is excited to higher orbital level, causing the molecule to be in singlet excited states (S_n) (Scheme 1.13). According to Kasha's rule, higher singlet states would quickly relax to the lowest vibrational level of the lowest singlet excited state (S_1) via internal conversion (IC). The excited state S_1 can relax to ground state by radiative processes — emission of light at a lower frequency (fluorescence) or non-radiative processes — internal conversion (IC) by vibrational relaxation, in which the energy is dissipated as heat. Alternatively, it is also possible for the excited state S1 to undergo intersystem crossing (ISC) and internal conversion (IC) to generate the lowest triplet excited state (T_1). T_1 state has two unpaired electrons with the same spin and according to Hund's rule of maximum multiplicity this state would be more stable than S_1.

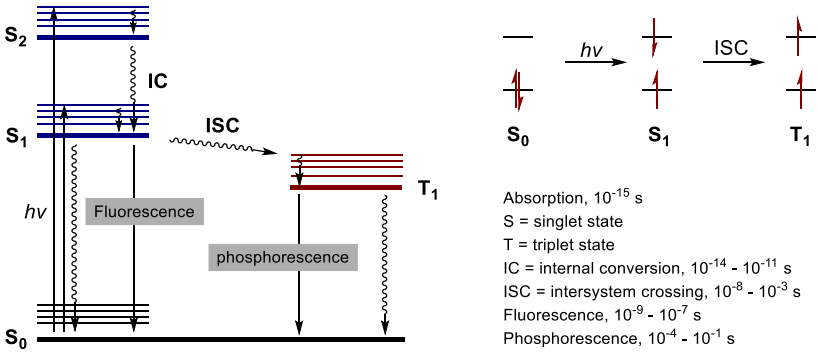

Scheme 1.13 Generalized Jablonski diagram and the spin arrangement in the depicted states.

T_1 can relax to the ground state S_0 by radiationless IC or by emissive pathway — phosphorescence. Phosphorescence process involves a change of electronic spin, which is forbidden by spin selection rules, making phosphorescence much slower than fluorescence. In addition, the relatively long lifetime of T_1 compared to S_1 would allow the excited photosensitizer/photocatalyst to undergo the intermolecular relaxation process, transferring its energy to a suitable molecule — quencher, either through energy transfer (EnT) or single electron transfer (SET) event (Scheme 1.14). Noted that singlet sensitizer could also be quenched, but it's more realistic from triplet state due to its longer lifetime. EnT is used to describe the scenario that excited state of the photosensitizer transfers energy to the ground state of quencher, after which the photosensitizer returns to ground state. EnT consists of Dexter EnT and Forster EnT. Dexter EnT is defined as the direct exchange of the electrons and will produce a triplet Q*. Forster EnT is a coulombic interaction that induces excitation through dipole oscillation and can only produce a singlet Q*. While SET occurs when photosensitizer gets or loses one electron from the quencher to form a radical ion pair ($Q^{\bullet\pm}$ $PS^{\bullet\mp}$).

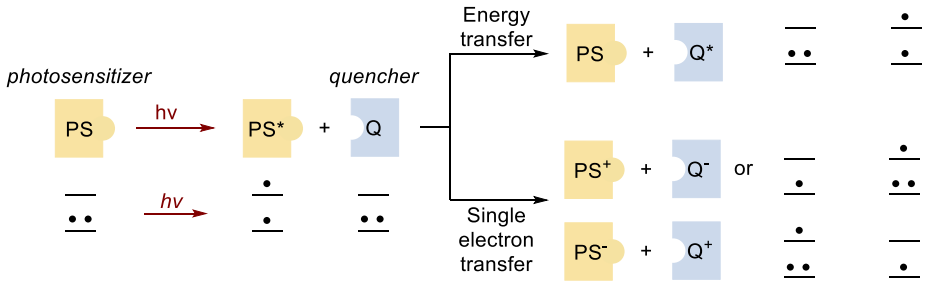

Scheme 1.14 Photosensitizer transfers energy to a molecule through EnT or SET pathway.

To identify whether photosensitizer is quenched by a substrate, Stern-Volmer fluorescence quenching studies are commonly employed. The excited photosensitizer would emit fluorescence in the absence quencher exciting, giving emission intensity marked as I_0. While in the presence of quencher, the intensity of observed emission (I)

decreases as concentration of the quencher increases as shown in Equation 1.1. k_q represents the quenching rate constant, τ_0 is the excited state lifetime and [Q] is the concentration of the quencher. Plotting the ratio of I_0/I against the quencher concentration would give a positive linear relationship in ideal scenario. Noted that this technique cannot distinguish the EnT and SET quenching pathway.

$$\boldsymbol{I_0/I = 1 + k_q\tau_0[Q]}$$

Equation 1.1 Stern-Volmer equation.

1.2.2 Catalytic Functions of Photocatalyst

1.2.2.1 Photoredox Catalyst

Over the last four decades, photoredox catalysis has found widespread application in the fields of water splitting,[45] carbon dioxide reduction,[46] and the development of novel solar cell materials;[47] however, it was only recently that the potential of this catalytic platform in organic synthesis begun to be fully realized.[48] A key factor in the recent yet rapid growth of this activation platform has been the recognition that readily accessible metal polypyridyl complexes and organic dyes can facilitate the conversion of visible light into chemical energy under mild conditions.

Taking $[Ru(bpy)_3]^{2+}$ as a model, photo-irradiation of the photocatalyst under visible-light causes a metal-to-ligand charge transfer (MLCT) process, leading to electron transfer from the Ru(II) metal-centered t_{2g} orbital to a ligand-centered π^* orbital (Scheme 1.15). Due to spin forbidden transition of the triplet state to singlet state, *Ru(II) has a rather long-lived triplet state (1100 ns in MeCN). The photo-induced unpaired nature of the excited state makes the photocatalyst a reductant (E[Ru(III)/*Ru(II)] = -0.81 V vs SCE) as well as an oxidant (E[*Ru(II)/Ru(I)] = +0.77 V vs SCE). In an oxidative quenching cycle, *Ru(II) serves as reductant by donating an electron to an electron accepter, subsequentially affording the oxidized Ru(III) species. Ru(III) is prone to reduction from an appropriate electron donor (E[Ru(III)/Ru(II)] = +1.29 V vs

[45] (a) Gratzel, M. Artificial Photosynthesis: Water Cleavage into Hydrogen and Oxygen by Visible Light. *Acc. Chem. Res*. **1981**, *14*, 376−384. (b) Meyer, T. J. Chemical Approaches to Artificial Photosynthesis. *Acc. Chem. Res*. **1989**, *22*, 163−170.
[46] Takeda, H.; Ishitani, O. Development of Efficient Photocatalytic Systems for CO_2 Reduction using Mononuclear and Multinuclear Metal Complexes based on Mechanistic Studies. *Coord. Chem. Rev*. **2010**, *254*, 346−354.
[47] Kalyanasundaram, K.; Gratzel, M. Applications of Functionalized Transition Metal Complexes in Photonic and Optoelectronic Devices. *Coord. Chem. Rev*. **1998**, *177*, 347−414.
[48] (a) Shaw, M. H.; Twilton, J.; MacMillan, D. W. C. Photoredox Catalysis in Organic Chemistry. *J. Org. Chem*. **2016**, *81*, 6898−6926. (b) Narayanama, J. M. R.; Stephenson, C. R. J. Visible Light Photoredox Catalysis: Applications in Organic Synthesis. *Chem. Soc. Rev*. **2011**, *40*, 102−113. (c) Yoon, T. P.; Ischay, M. A.; Du, J. Visible Light Photocatalysis as a Greener Approach to Photochemical Synthesis. *Nature Chem* **2010**, *2*, 527–532.

SCE), regenerating the ground state. If a reductive quenching cycle operates, *Ru(II) functions as an oxidant by accepting one electron from an electron donor, thus forming the reduced Ru(I) species. Ru(I) then behaves as a reductant to give an electron to an oxidant to recover back the ground state (E[Ru(II)/Ru(I)] = -1.33 V vs SCE).[49]

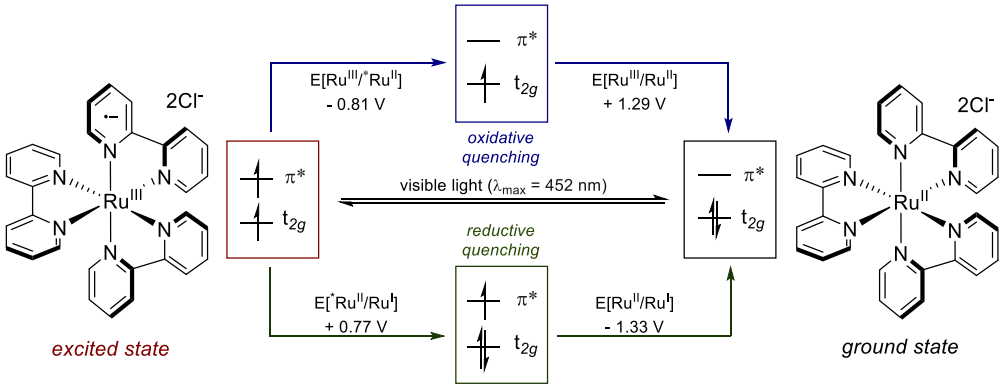

Scheme 1.15 Simplified molecular orbital and redox potential of four possible single electron transfers.

A variety of photocatalyst have been discovered and put into practice. Some of the commonly employed photocatalysts with selected photophysical properties are listed in Scheme 1.16 and Table 1.1. The ability to tune the properties of photocatalysts through structural modifications has allowed for significant improvements in the physical and redox properties of photoredox catalysts.[50] The unique reactivity of photocatalysts such as $Ru(bpy)_3^{2+}$ has led chemists to discover a variety of reactions, including employment of photocatalysis in established radical chemistries, one of which was the merger of photocatalysis with transition metal catalysis.

[49] Prier, C. K.; Rankic, D. A. MacMillan, D. W. C. Visible Light Photoredox Catalysis with Transition Metal Complexes: Applications in Organic Synthesis. *Chem. Rev*. **2013**, *113*, 5322–5363.
[50] Speckmeier, E.; Fischer, T. G.; Zeitler, K. A Toolbox Approach To Construct Broadly Applicable Metal-Free Catalysts for Photoredox Chemistry: Deliberate Tuning of Redox Potentials and Importance of Halogens in Donor−Acceptor Cyanoarenes. *J. Am. Chem. Soc*. **2018**, *140*, 15353−15365.

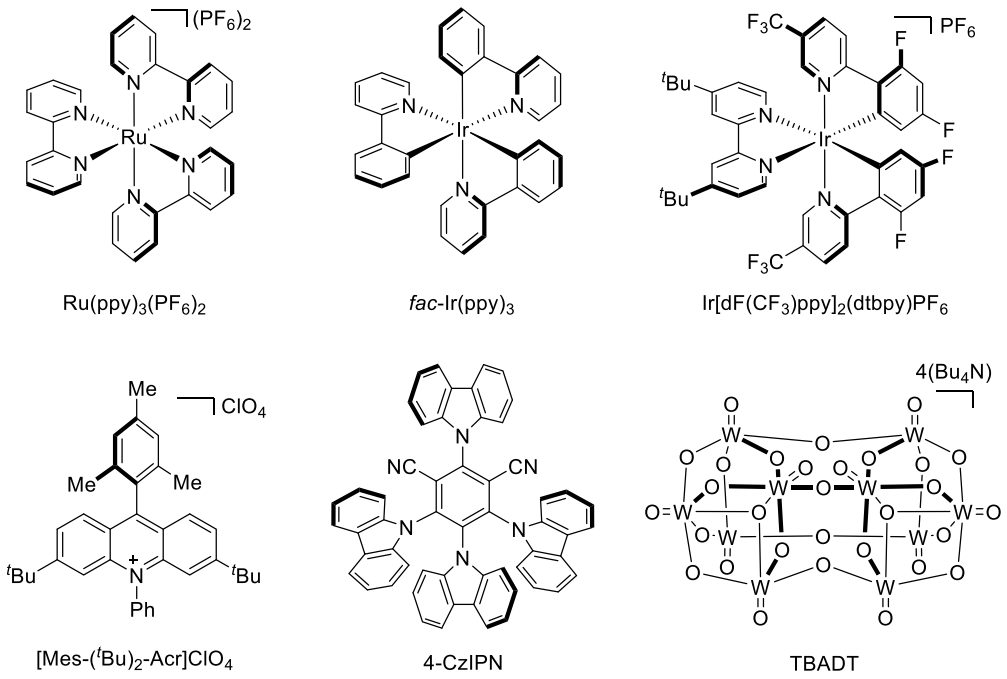

Scheme 1.16 Examples of commonly utilized photoredox catalysts.

Photocatalyst	E (V) (M^+/M^*)	E (V) (M^*/M^-)	E (V) (M^+/M)	E (V) (M/M^-)	Excitaion λ_{max} (nm)	Emission λ_{max} (nm)	Excited state lifetime τ (ns)
$Ru(ppy)_3(PF_6)_2$	-0.81	+0.77	+1.29	-1.33	452	615	1100
fac-$Ir(ppy)_3$	-1.73	+0.31	+0.77	-2.19	375	494	1900
$Ir[dF(CF_3)ppy]_2(dtbpy)PF_6$	-0.89	+1.21	+1.69	-1.37	380	470	2300
$[Mes\text{-}(^tBu)_2\text{-}Acr]BF_4$	—	+2.08	—	-0.59	420	517	14.4
4-CzIPN	-1.04	+1.35	+1.52	-1.21	435	530	5100
TBADT	—	+2.44	—	-0.97	375	—	58

Table 1.1 Redox potential and selected photophysical properties.

1.2.2.2 Energy Transfer Catalyst

Apart from enabling single electron transfer events, the commonly used metal polypyridyl complexes are capable of triggering energy transfer scenarios. Energy transfer is formally defined as "the photophysical process in which an excited state of one molecular entity relaxes to a lower-lying state by transferring energy to a second molecular entity, which is thereby excited to a higher energy state."[51] As shown in scheme 1.17, upon photoexcitation to an excited singlet state, the photosensitizer undergoes intersystem crossing to its triplet state. The latter typically possess longer

[51] Strieth-Kalthoff, F.; James, M. J.; Teders, M.; Pitzera, L.; Glorius, F. Energy transfer catalysis mediated by visible light: principles, applications, directions. *Chem. Soc. Rev.* **2018**, *47*, 7190–7202.

lifetimes, allowing its interaction with a substrate in a bimolecular quenching process. As a result, excited-state energy and spin multiplicity are transferred, and the excited triplet state of the substrate is formed, while simultaneously regenerating the ground state photosensitizer.

As an illustration, some commonly used triplet energy transfer photocatalyst are listed in Scheme 1.18. While early research of energy transfer catalyst from Bach,[52] Yoon [53] and Gilmour [54] mainly focused on thermal forbidden cyclizations and photoisomerizations, the use of EnT to accelerate or enable reaction limiting steps in transition metal catalysis has emerged as a powerful strategy with great synthetic potential.[55]

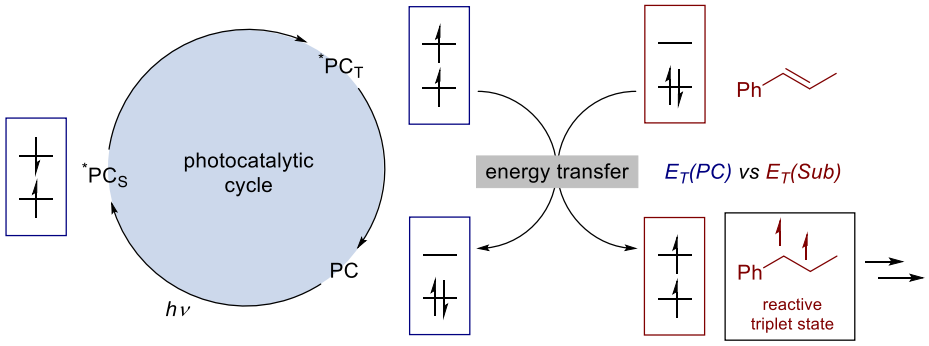

Scheme 1.17 Simplified molecular orbital and energy transfer photocatalysis for the Generation of excited substrate.

[52] Poplata, S.; Tröster, A.; Zou, Y.-Q.; Bach, T. Recent Advances in the Synthesis of Cyclobutanes by Olefin [2 + 2] Photocycloaddition Reactions. *Chem. Rev*. **2016**, *116*, 9748–9815.
[53] Ischay, M. A.; Anzovino, M. E.; Du, J.; Yoon, T. P. Efficient Visible Light Photocatalysis of [2+2] Enone Cycloadditions. *J. Am. Chem. Soc*. **2008**, *130*, 12886–12887.
[54] Metternich, J. B.; Gilmour, R. Photocatalytic E → Z Isomerization of Alkenes. *Synlett* **2016**; *27*, 2541–2552.
[55] Strieth-Kalthoff, F.; Glorius, F. Triplet Energy Transfer Photocatalysis: Unlocking the Next Level. *Chem* **2020**, *6*, 1888–1903.

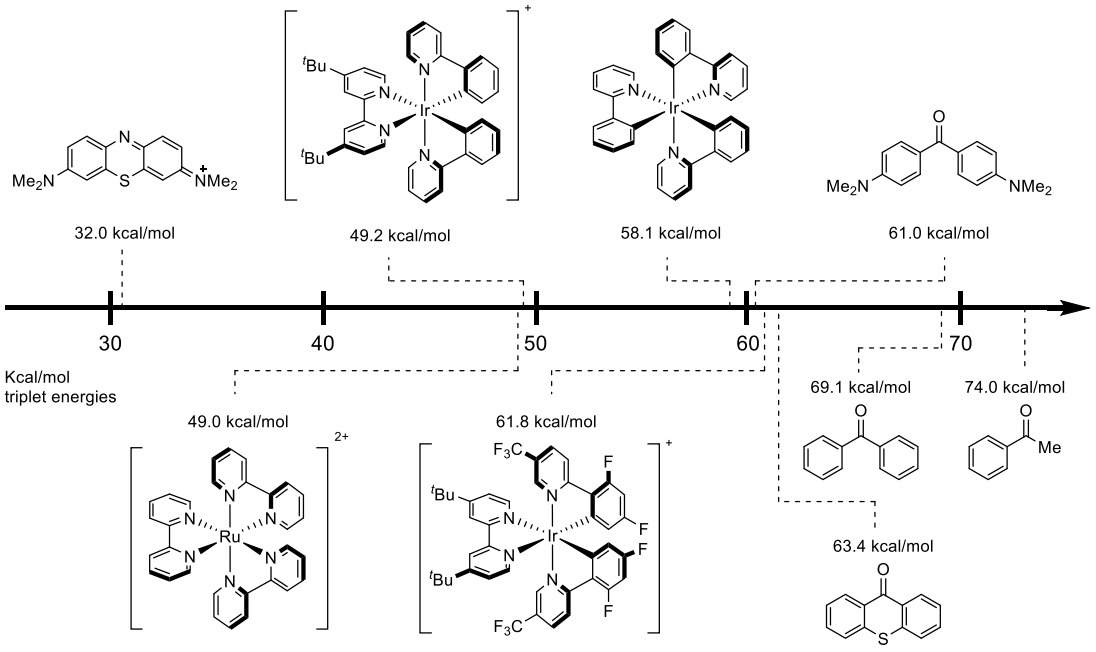

Scheme 1.18 Examples of triplet energy transfer photocatalyst.

1.2.3 Merging Photocatalysis with Transition Metal Catalysis for Cross-Coupling Reactions

In 2007, Osawa and co-workers realized a palladium-catalyzed Sonogashira cross-coupling reaction using $Ru(bpy)_3Cl_2$ photocatalyst in the absence of copper co-catalyst (Scheme 1.19).[56] Following the pioneering research by the group of Osawa, the interception of transition metal-mediated substrate activation with the excited-state chemistry of photocatalysis has emerged as a powerful platform with unique, yet complementary, reactivity in the cross-coupling arena.[57]

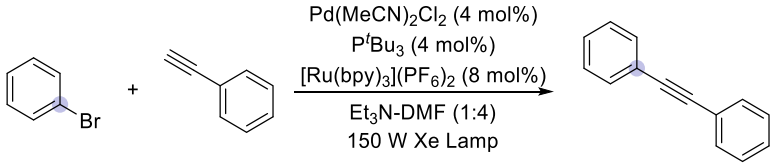

Scheme 1.19 Dual photo palladium-catalyzed Sonogashira cross-coupling.

[56] Osawa, M.; Nagai, H.; Akita, M. Photo-Activation of Pd-Catalyzed Sonogashira Coupling using a Ru/Bipyridine Complex as Energy Transfer Agent. *Dalton Trans.* **2007**, 827–829.

[57] (a) Twilton, J.; Le, C.; Zhang, P.; Shaw, M. H.; Evans, R. W.; MacMillan, D. W. C. The Merger of Transition Metal and Photocatalysis. *Nat Rev Chem* **2017**, *1*, 0052. (b) Chan, A. Y.; Perry, I. B.; Bissonnette, N. B;. Buksh, B. F.; Edwards, G. A.; Frye, L. I.; Garry, O. L.; Lavagnino, M. N.; Li, B. X.; Liang, Y.; Mao, E.; Millet, A.; Oakley, J. V.; Reed, N. L.; Sakai, H. A.; Seath, C. P.; MacMillan, D. W. C. Metallaphotoredox: The Merger of Photoredox and Transition Metal Catalysis. *Chem. Rev.* **2022**, *122*, 1485–1542.

1.2.3.1 Nickel Photocatalysis Mediated Cross-Coupling Reactions

Nickel is known to access Ni(I) and Ni(III) states, which makes it an ideal candidate to be used in conjunction with a SET photoredox platform. Additionally, the low lying *d* orbitals of nickel make electronic transitions relatively easy, which allows for its direct photoexcitation with higher energy visible light or triplet photosensitizer enabled energy transfer.

In 2014, MacMillan, Doyle and co-workers realized the merger of nickel catalysis with photocatalysis to enable aliphatic carboxylic acids as one-electron nucleophilic handles in C(sp^2)–C(sp^3) cross-couplings. Independent research by Molander and co-workers realized a mechanically similar transformation using alkyl potassium trifluoroborate salts as one-electron coupling precursor (scheme 1.20).[58]

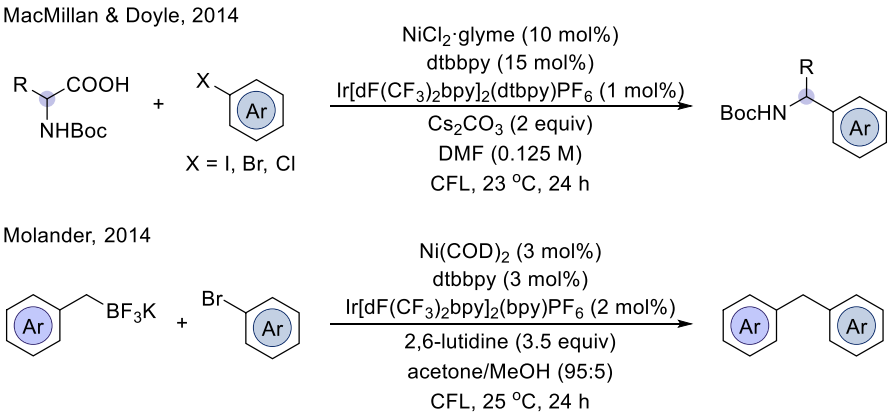

Scheme 1.20 Nickel metallaphotoredox catalyzed arylation reactions.

A mechanistic picture of the transformation is shown in scheme 1.21. Upon excitation by visible light, the excited highly oxidizing $^*Ir^{III}$ ($E[^*Ir(III)/Ir(II)]$ = +1.21 V vs SCE) removes an electron from carboxylic acid (E_{ox} = +1.11 V vs SCE), affording the carbon-centered radical **1.21e**. The alkyl-centered radical was subsequently captured by aryl-Ni(II) complex **1.21b** derived from oxidative addition of aryl halide to nickel(0) **1.21a**, leading to the generation of aryl-Ni(III)-alkyl species **1.21c**. Reductive elimination of **1.21c** provides cross-coupling product and Ni(I) intermediate **1.21d**, which is further reduced by the reduced form of the photocatalyst Ir(II) (E[Ir(III)/Ir(II)] = -1.37 V vs SCE) to recover back Ni(0) (E[Ni(I)/Ni(0)] ≈ -1.11 V vs SCE), thus closing the two catalytic cycles.[59] However, several off-cycle pathways may exist in the dual

[58] (a) Zuo, Z.; Ahneman, D. T.; Chu, L.; Terrett, J. A.; Doyle, A. G.; MacMillan, D. W. C. Merging Photoredox with Nickel Catalysis: Coupling of α-Carboxyl sp^3-Carbons with Aryl Halides. *Science* **2014**, *345*, 437–440. (b) Tellis, J. C.; Primer, D. N.; Molander, G. A. Single-Electron Transmetalation in Organoboron Cross-Coupling by Photoredox/Nickel Dual Catalysis. *Science* **2014**, *345*, 433–436.

[59] (a) Yan, M.; Lo, J. C.; Edwards, J. T.; Baran, P. S. Radicals: Reactive Intermediates with Translational Potential. *J. Am. Chem. Soc.* **2016**, *138*, 12692−12714. (b) Lin, Q.; Spielvogel, E. H.;

catalytic system, which leads to the generation of side products, indicating that judicious choice of reaction parameters is crucial for success. First, direct photolysis of the aryl-nickel complex **1.21b** may result in the generation of aryl radicals.[60] Second, kinetics mismatch would lead to the generation of nickel-black — an issue that can be overcome by decreasing the rate of reductive elimination and increasing the rate of oxidative addition and stabilizing low-valent nickel intermediates with a suitable additive.[61]

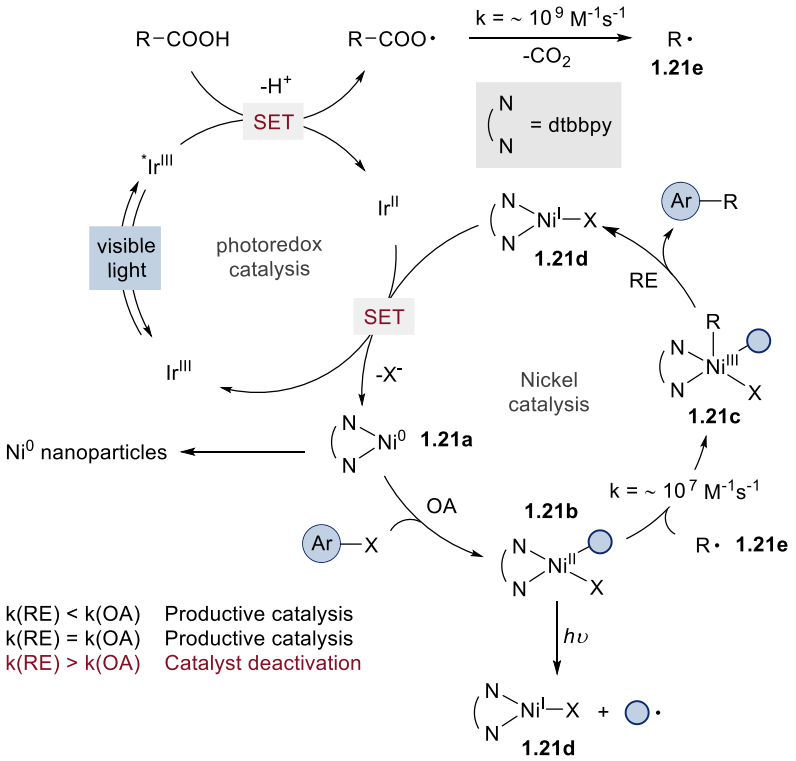

Scheme 1.21 Proposed mechanism for decarboxylative arylation.

Compared to two-electron manifolds, the utilization of carboxylic acids as one-electron coupling handle has inspired chemists to activate a variety of bench-stable and otherwise inert functionalities through radical pathways to forge chemical complexity. Ultimately, this has resulted in significant expansion of the pool of available fragments from preformed organometallic reagents to adaptive functional entities such as

Diao, T. Carbon-Centered Radical Capture at Nickel(II) Complexes: Spectroscopic Evidence, Rates, and Selectivity. *Chem*. **2023**, *9*, 1−14.

[60] (a) Shields, B. J.; Kudisch, B.; Scholes, G. D.; Doyle, A. G. Long-Lived Charge-Transfer States of Nickel(II) Aryl Halide Complexes Facilitate Bimolecular Photoinduced Electron Transfer. *J. Am. Chem. Soc*. **2018**, *140*, 3035−3039. (b) Goldschmid, S. L.; Tay, N. E. S.; Joe, C. L.; Lainhart, B. C.; Sherwood, T. C.; Simmons, E. M.; Sezen-Edmonds, M.; Rovis, T. Overcoming Photochemical Limitations in Metallaphotoredox Catalysis: Red-Light-Driven C–N Cross-Coupling. *J. Am. Chem. Soc*. **2022**, *144*, 22409–22415.

[61] Gisbertz, S.; Reischauer, S.; Pieber, B. Overcoming Limitations in Dual Photoredox/Nickel-Catalysed C–N Cross-Couplings due to Catalyst Deactivation. *Nat Catal* **2020**, *3*, 611–620.

silicates,[62] aldehydes,[63] amines,[64] alcohols,[65] and even simple alkanes (Scheme 1.22).[66] On the other hand, while many early achievements in C–C bond formation reactions involved sp^2-hybridized electrophiles, metallaphotoredox catalysis has allowed the implementation of a series of powerful manifolds for forging C(sp^3)–C(sp^3) linkages.[67] These metallaphotoredox-catalyzed alkylation protocols — making use of reagents that are stable to air and moisture, exhibit good functional group compatibility and cross-coupling efficiencies, complementary to traditional alkyl-alkyl coupling techniques.

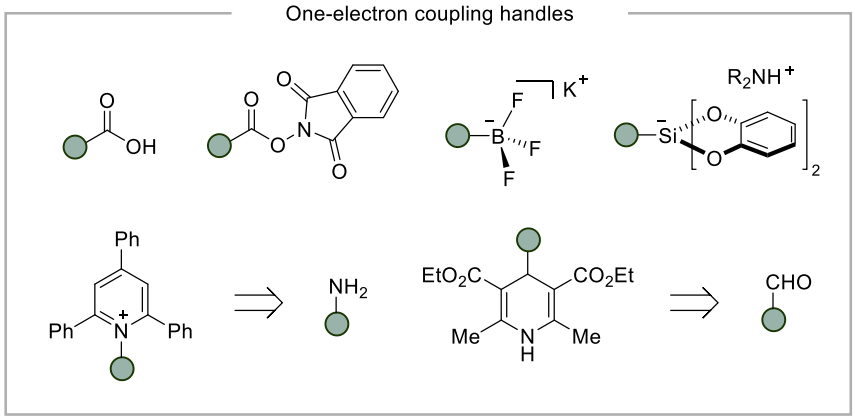

Scheme 1.22 Examples of one-electron coupling handles.

Nickel metallaphotocatalysis has also been utilized for solving historically challenging nickel-catalyzed C–heteroatom bond-forming reactions. Mechanistically, the catalytic, photoinduced shuttling of electron to and from organometallic intermediates has allowed for the formation high-valent nickel species. Alternatively, excited state of organonickel species can be accessed by either direct photoexcitation or energy transfer from a photosensitizer. These transient nickel species enables construction of conventional challenging C–heteroatom bonds via reductive

[62] Leveque, C.; Chenneberg, L.; Corce, V.; Ollivier, C.; Fensterbank, L. Organic Photoredox Catalysis for the Oxidation of Silicates: Applications in Radical Synthesis and Dual Catalysis. *Chem. Commun*. **2016**, *52*, 9877–9880.
[63] Matsui, J. K.; Lang, S. B.; Heitz, D. R.; Molander, G. A. Photoredox-Mediated Routes to Radicals: The Value of Catalytic Radical Generation in Synthetic Methods Development. *ACS Catal*. **2017**, *7*, 2563−2575.
[64] Basch, C. H.; Liao, J.; Xu, J.; Piane, J. J.; Watson, M. P. Harnessing Alkyl Amines as Electrophiles for Nickel-Catalyzed Cross Couplings via C–N Bond Activation. *J. Am. Chem. Soc*. **2017**, *139*, 5313–5316.
[65] Dong, Z.; MacMillan, D. W. C. Metallaphotoredox-Enabled Deoxygenative Arylation of Alcohols. *Nature* **2021**, *598*, 451–456.
[66] Shaw, M. H.; Shurtleff, V. W.; Terrett, J. A.; Cuthbertson, J. D.; MacMillan, D. W. C. Native Functionality in Triple Catalytic Cross-Coupling: sp^3 C–H Bonds as Latent Nucleophiles. *Science* **2016**, *352*, 1304–1308.
[67] Zheng, S.; Hu, Y.; Yuan, W. Recent Advances in C(sp^3)–C(sp^3) Cross-Coupling via Metallaphotoredox Strategies. *Synthesis* **2021**, *53*, 1719–1733.

elimination (Scheme 1.23).[68]

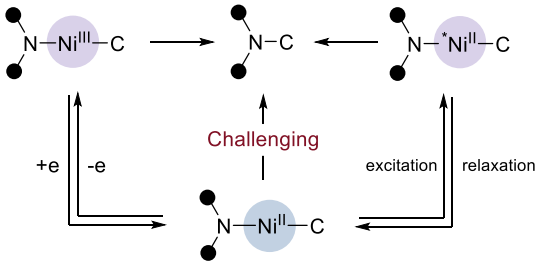

Scheme 1.23 Nickel photocatalysis mediated C–heteroatom bond-forming reactions.

One of the early example was introduced by MacMillan and co-workers, who unlocked a C(sp^2)–N coupling platform using aliphatic amine via dual nickel and photoredox catalysis (Scheme 1.24).[69] Subsequent mechanistic studies pointed out that the majority of product formation resulted from a dark Ni(I)/Ni(III) cycle. The role of photocatalyst was not only to initiate the reaction through Ni(II) reduction by Ir(II) — generated from reductive quenching of the excited state by DABCO (E[DABCO$^{\bullet+}$/DABCO] = +0.71 V vs SCE), but also to ensure reactivity perpetuates through continually reducing the resting-state Ni(II) catalyst to its active, low-valent Ni(I) form.[70]

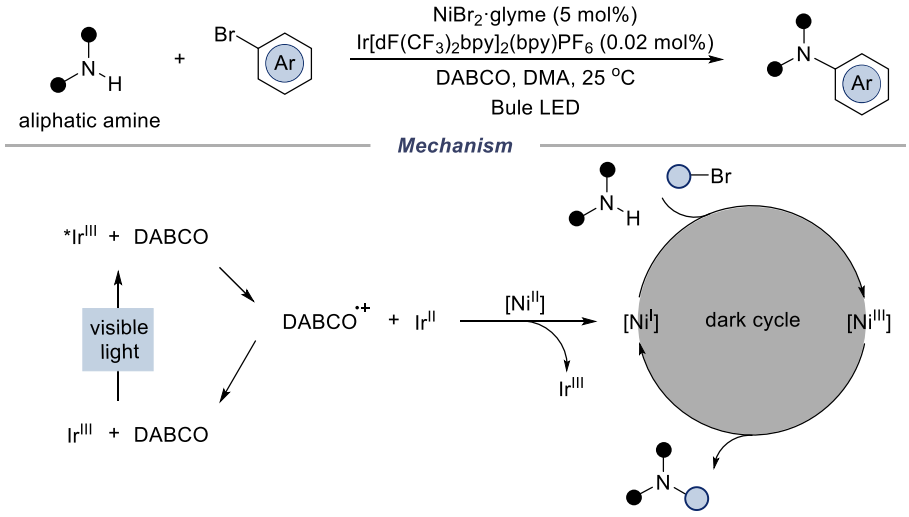

Scheme 1.24 Nickel metallaphotoredox-catalyzed amination.

---

[68] Zhu, C.; Yue, H.; Jia, J.; Rueping, M. Nickel-Catalyzed C-Heteroatom Cross-Coupling Reactions under Mild Conditions via Facilitated Reductive Elimination. *Angew. Chem. Int. Ed*. **2021**, *60*, 17810–17831.

[69] Corcoran, E. B.; Pirnot, M. T.; Lin, S.; Dreher, S. D.; DiRocco, D. A.; Davies, I. W.; Buchwald, S. L.; MacMillan, D. W. C. Aryl Amination Using Ligand-Free Ni(II) Salts and Photoredox Catalysis. *Science* **2016**, *353*, 279–283.

[70] Till, N. A.; Tian, L.; Dong, Z.; Scholes, G. D. MacMillan, D. W. C. Mechanistic Analysis of Metallaphotoredox C−N Coupling: Photocatalysis Initiates and Perpetuates Ni(I)/Ni(III) Coupling Activity. *J. Am. Chem. Soc*. **2020**, *142*, 15830−15841.

Following up their interest in nickel metallaphotoredox catalyzed C–heteroatom bond formations, MacMillan and co-workers reported an esterification protocol utilizing aryl bromides **1.25b** and carboxylic acids **1.25a**.[71] As shown in Scheme 1.25, the yield of the esterification product **1.25d** was found to have a positive correlation with the triplet energy of the photocatalysts but a negative relationship with the oxidizing power of the photocatalysts. Subsequent transient absorption spectroscopic studies in collaboration with Scholes and co-workers confirmed an energy-transfer pathway, demonstrating the mechanism of the reductive elimination is unimolecular process that occurs on the long-lived excited state of the Ni(II) complex **1.25h** via diffusion-controlled energy transfer from the iridium photocatalyst.[72]

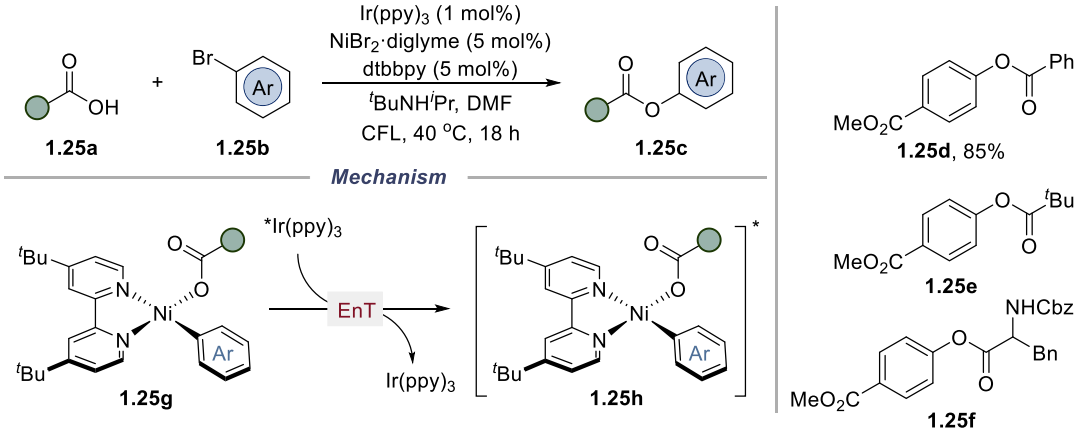

Ir[(ppy)$_2$Ligand](PF$_6$)$_n$	Yield of **1.25d**	Et(kcal)	E[*Ir^{III}/Ir^{II}] (V)	E[Ir^{IV}/Ir^{III}] (V)
ppy	85%	53.6	0.13	0.77
5,5'-dMebpy	80%	49.0	0.61	1.26
4,4'-dMeObpy	70%	47.7	0.58	1.22
4,4'-dMebpy	65%	47.6	0.59	1.25
bpy	50%	46.3	0.61	1.28
4,4'-dClbpy	3%	42.6	0.72	1.32

yield of **P-1** ↑ triplet energy ↑ oxidizing power ↓

Scheme 1.25 Nickel metallaphotoredox catalyzed esterification enabled by energy transfer.

As mentioned before, accessing excited state of organometallic intermediates could also be operative by direct photoexcitation. Doyle and co-workers studied the

[71] Welin, E. R.; Le, C. C.; Arias-Rotondo, D. M.; McCusker, J. K.; MacMillan, D. W. C. Photosensitized, Energy Transfer-Mediated Organometallic Catalysis Through Electronically Excited Nickel(II). *Science* **2017**, *355*, 380–385.
[72] Tian, L.; Till, N. A.; Kudisch, B.; MacMillan, D. W. C.; Scholes, G. D. Transient Absorption Spectroscopy Offers Mechanistic Insights for an Iridium/Nickel-Catalyzed C-O Coupling. *J. Am. Chem. Soc*. **2020**, *142*, 4555−4559.

photoexcitation of nickel (II) aryl halide complexes in 2018,[73] while the utilization of this technique in cross-coupling reaction was initially disclosed by the group of Miyake. In 2018, Miyake and co-workers described a UV light-driven nickel catalyzed C(sp^2)-amination reaction utilizing aryl halides **1.26b** together with aliphatic amines **1.26a** (Scheme 1.26).[74] This amination reaction proceeded via direct 365 nm photoexcitation of nickel-amine complexes, allowing the coupling of a variety of secondary, primary alkyl, or primary (hetero)aryl amines and aryl halides with diverse electronics at room temperature. Preliminary mechanistic studies based on the DFT calculations, UV vis spectra analysis and KIE experiments suggested that photoinduced electron transfer from electron-rich morpholine to the electron-poor Ni(II) metal center results in the reduced Ni(I) species and oxidized morpholine radical cation, which could subsequently dissociate into the corresponding ion pairs. Ion pairs intermediate **1.26f** underwent rate-determining deprotonation step with excess morpholine, followed by interception with aryl bromide either through atom bromine atom displacement (*path I*) or oxidatively displacement (*path II*) to close the catalytic cycle.

[73] Shields, B. J.; Kudisch, B.; Scholes, G. D.; Doyle, A. G. Long-Lived Charge-Transfer States of Nickel(II) Aryl Halide Complexes Facilitate Bimolecular Photoinduced Electron Transfer. *J. Am. Chem. Soc*. **2018**, *140*, 3035−3039.
[74] Lim, C.-H.; Kudisch, M.; Liu, B.; Miyake, G. M. C–N Cross-Coupling via Photoexcitation of Nickel–Amine Complexes. *J. Am. Chem. Soc*. **2018**, *140*, 7667−7673.

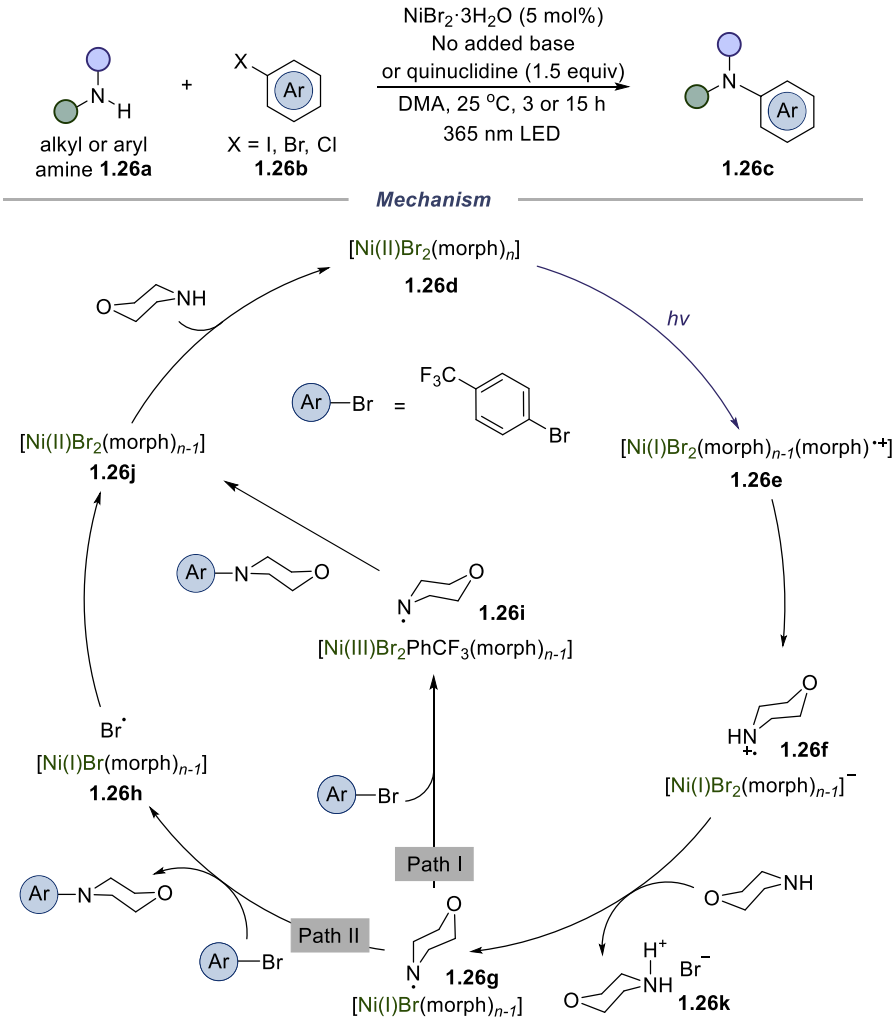

Scheme 1.26 C(sp^2)–N formation via photoexcitation of nickel–amine complex.

The advancement achieved in nickel metallaphotoredox catalyzed C–heteroatom formation reaction has inspired chemists to couple a series of historically challenging functionalities such as sulfonamides,[75] amides,[76] phenols,[77] alcohols,[78] phosphine oxides,[79] or thiols[80] et al. In addition, valence control of metal centers by exogenous

[75] Kim, T.; McCarver, S. J.; Lee, C.; MacMillan, D. W. C. Sulfonamidation of Aryl and Heteroaryl Halides through Photosensitized Nickel Catalysis. *Angew. Chem. Int. Ed*. **2018**, *57*, 3488−3492.
[76] Song, G.; Li, Q.; Nong, D.-Z.; Song, J.; Li, G.; Wang, C.; Xiao, J.; Xue, D. Ni-Catalyzed Photochemical C−N Coupling of Amides with (Hetero)aryl Chlorides. *Chem. Eur. J*. **2023**, *29*, e20230045.
[77] Luo, H.; Wang, G.; Feng, Y.; Zheng, W.; Kong, L.; Ma, Y.; Matsunaga, S.; Lin, L. Photoinduced Nickel-Catalyzed Carbon–Heteroatom Coupling. *Chem. Eur. J*. **2023**, *29*, e202202385.
[78] Terrett, J. A.; Cuthbertson, J. D.; Shurtleff, V. W. MacMillan, D. W. C. Switching on Elusive Organometallic Mechanisms with Photoredox Catalysis. *Nature* **2015**, *524*, 330−334.
[79] Zhu, D.-L.; Jiang, S.; Wu, Q.; Wang, H.; Chai, L.-L.; Li, H.-Y.; Li, H.-X. Visible-Light-Induced Nickel-Catalyzed P(O)−C(sp^2) Coupling Using Thioxanthen-9-one as a Photoredox Catalysis. *Org. Lett*. **2021**, *23*, 160−165.
[80] Oderinde, M. S.; Frenette, M.; Robbins, D. W.; Aquila, B.; Johannes, J. W. Photoredox Mediated Nickel Catalyzed Cross-Coupling of Thiols With Aryl and Heteroaryl Iodides via Thiyl Radicals. *J. Am. Chem. Soc*. **2016**, *138*, 1760–1763.

factors has been recognized as a feasible strategy to create new pathways in transition metal catalysis.

1.2.3.2 Copper Metallaphotocatalysis Mediated Cross-Coupling Reactions

The merger of photocatalysis with copper catalysis was initially disclosed by Fu and Peters, who described a photoinduced copper-catalyzed C(sp^2)–N coupling reaction in 2012 (Scheme 1.27).[81] One year later, they further expanded the Ullmann type C–N coupling protocol to alkyl halides based on the same strategy.[82] Mechanistic studied indicated the UV light excitation of the amido-copper complex might be the key enabling the whole transformation. Specifically, UV light irradiation of Li[Cu(carbazolide)$_2$] **1.27g** led to the generation of excited Cu(I) complex **1.27h**, followed by a SET event of alkyl halide to generate carbon centered radical, which could be intercepted by amido-Cu(II) species to provide the C(sp^3)–N coupling product.

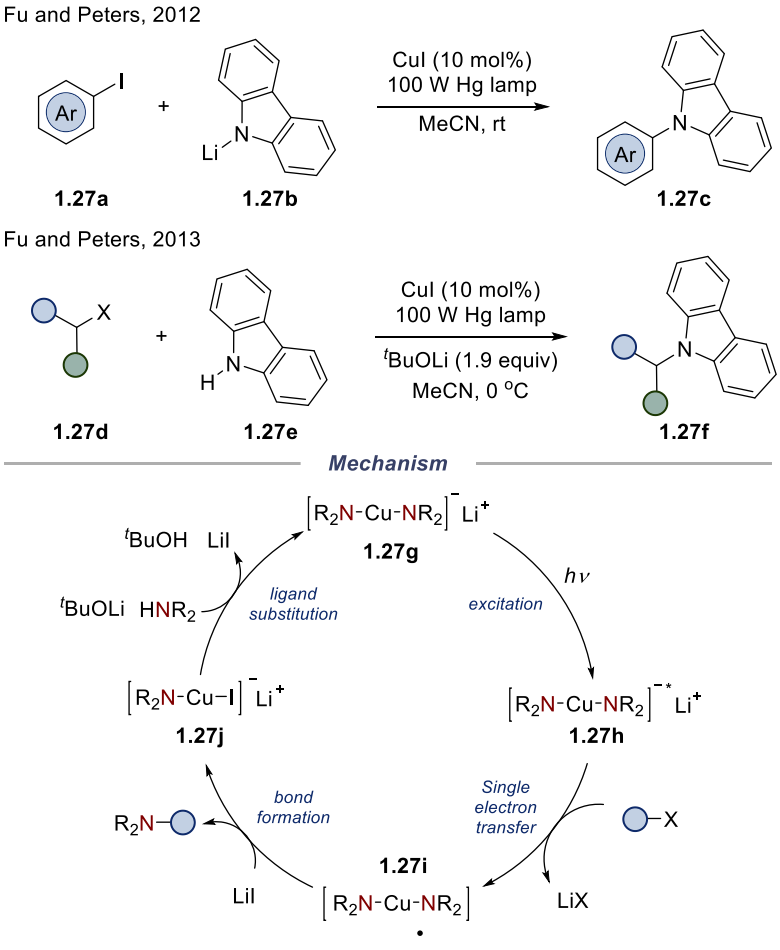

[81] Creutz, S. E.;. Lotito, K. J.; Fu, G. C.; Peters, J. C. Photoinduced Ullmann C–N Coupling: Demonstrating the Viability of a Radical Pathway. *Science* **2012**, *338*, 647–651.
[82] Bissember, A. C.; Lundgren, R. J.; Creutz, S. E.; Peters, J. C.; Fu, G. C. Transition-Metal-Catalyzed Alkylations of Amines with Alkyl Halides: Photoinduced, Copper-Catalyzed Couplings of Carbazoles. *Angew. Chem. Int. Ed*. **2013**, *52*, 5129–5133.

Scheme 1.27 UV light induced copper-catalyzed C–N formation via photoexcitation of copper-amido complex.

Despite its potential for C–heteroatom bond construction, copper catalysis has been less successful than palladium or nickel with respect to diverse applications in cross-coupling chemistry, largely attributed to its low reducing ability.[83] Fu and Peters' pioneer research opened a new avenue to activate alkyl halides with low valent copper species, which would be challenging through classical two-electron oxidative additions elementary step. Indeed, one of the biggest benefit of combining copper catalysis with photochemistry is that it makes up the inherent poor reducibility of low-valent Cu(I) intermediate and allows for the generation of high-valent Cu(III) intermediate at room temperature (Scheme 1.28).[84]

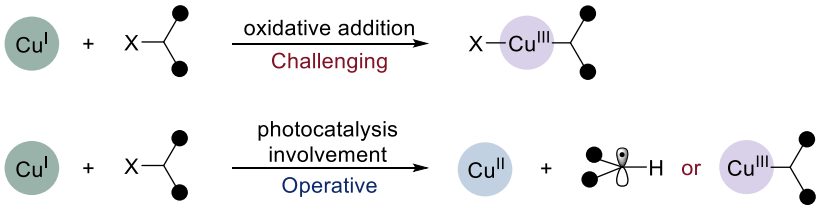

Scheme 1.28 Benefits of copper photocatalysis mediated reactions.

Fu and Peters sought to further expand the scope of available nucleophiles by separating the roles of photocatalyst from bond-forming catalyst. With an idea that an appropriate ligand on copper would provide an organometallic complex, which could absorb visible light as a potent photoreductant, even in the absence of nucleophiles, they designed a carbazole-based PNP pincer-type ligand **1.29c** (Scheme 1.29).[85] Upon coordination with Cu(I), this in situ-generated photocatalyst **1.29b** was competent in the facile reduction of secondary alkyl bromides to carbon-centered radicals, irrespective of nucleophile structure or conjugation. A number of carbamates were competent nucleophiles, providing the corresponding protected amines from alkyl bromides in good yields. The transformation was proposed to operate in an analogous manner to previous transformations, with the remaining unligated copper serving to facilitate bond formation between nucleophile and radicals generated via SET from complex in a dual-copper catalyst system.

[83] Beletskaya, I. P.; Cheprakov, A. V. Copper in Cross-Coupling Reactions: The Post-Ullmann Chemistry. *Coord Chem Rev*. **2004**, *248*, 2337–2364.
[84] Levin, M. D.; Kim, S.; Toste, F. D. Photoredox Catalysis Unlocks Single-Electron Elementary Steps in Transition Metal Catalyzed Cross-Coupling. *ACS Cent. Sci*. **2016**, *2*, 293−301.
[85] Ahn, J. M.; Peters, J. C.; Fu, G. C. Design of a Photoredox Catalyst That Enables the Direct Synthesis of Carbamate-Protected Primary Amines via Photoinduced, Copper-Catalyzed N-Alkylation Reactions of Unactivated Secondary Halides. *J. Am. Chem. Soc*. **2017**, *139*, 18101−18106.

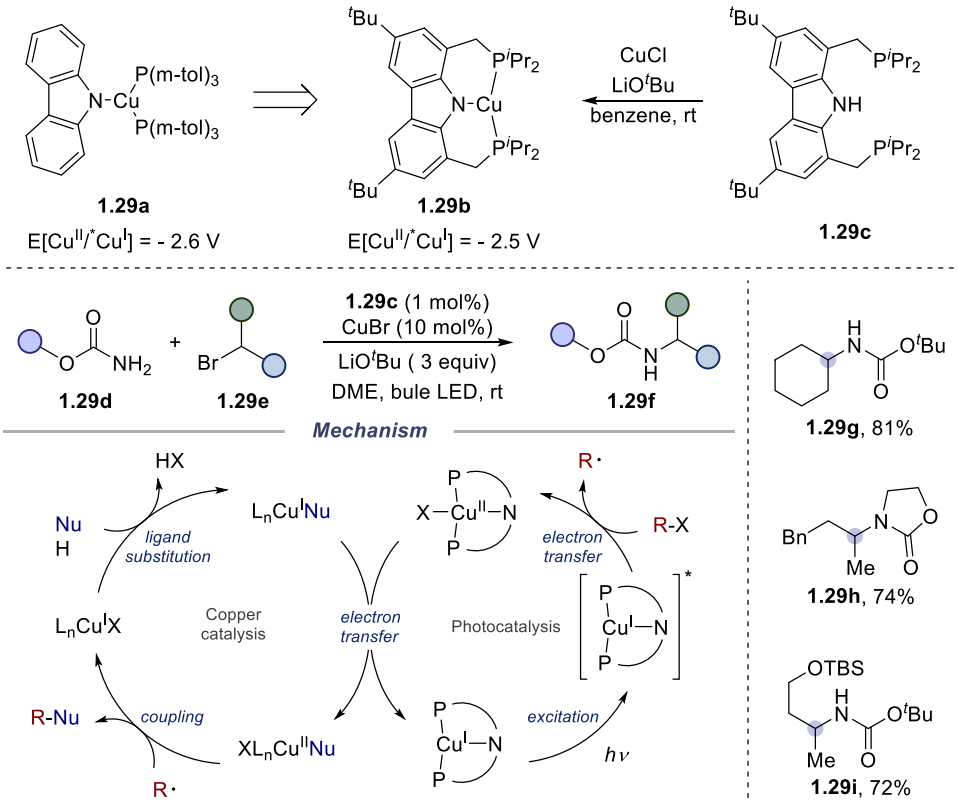

Scheme 1.29 Carbamate alkylation with dual copper catalytic system.

Following on the work in the field of photoredox palladium catalysis, the Sanford laboratory demonstrated the copper metallaphotoredox-catalyzed trifluoromethylation reaction of aryl boronic acids (Scheme 1.30).[86] The reaction was proposed to go through a reductive quenching cycle of the photocatalyst, beginning with a SET oxidation event of the Cu(I) intermediate **1.30d** by photoexcited Ru(I) complex. A trifluoromethyl radical **1.30h** is then generated via reduction of CF_3I by Ru(I) photocatalyst, while recovering back the ground state Ru(II). Cu(II) complex **1.30e** sequentially underwent interception with the trifluoromethyl radical **1.30h**, transmetalation with aryl boronic acid and reductive elimination to afford the trifluoromethyl product.

[86] Ye, Y.; Sanford, M. S. Merging Visible-Light Photocatalysis and Transition-Metal Catalysis in the Copper-Catalyzed Trifluoromethylation of Boronic Acids with CF_3I. *J. Am. Chem. Soc*. **2012**, *134*, 9034–9037.

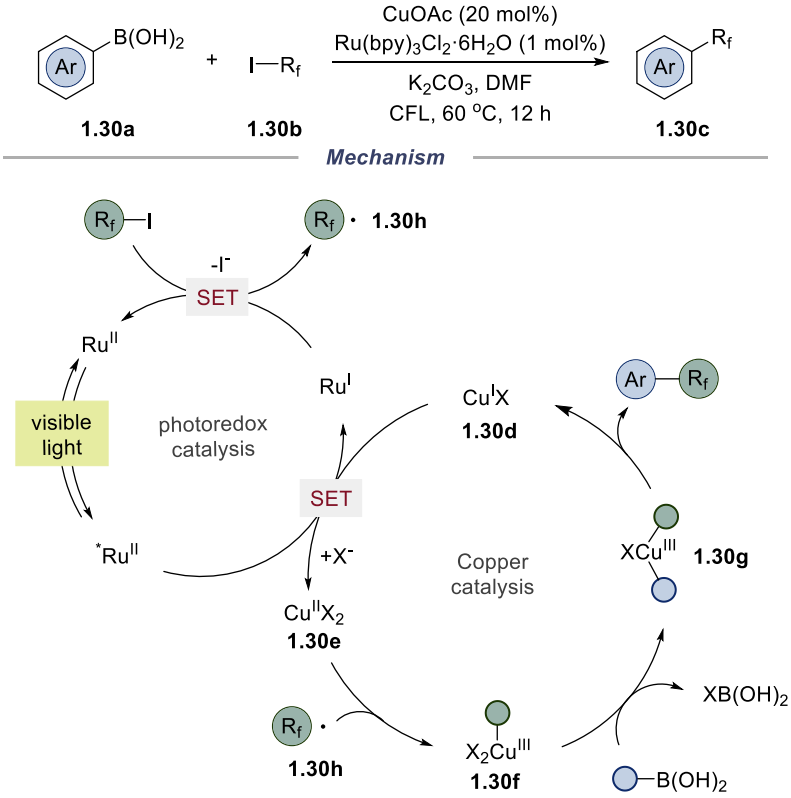

Scheme 1.30 Copper metallaphotoredox catalyzed trifluoromethylation of boronic acids.

MacMillan and co-workers recently reported a copper photoredox dual catalyzed decarboxylative amination of alkyl carboxylic acids with a broad scope of *N*-nucleophiles.[87] As shown in scheme 1.31, *in situ* generated Cu(I)-amido complex **1.31e** (from coordination of the nitrogen nucleophile followed by deprotonation) is oxidized by excited *Ir(III) photocatalyst ($E[^{*}Ir(III)/Ir(II)]$ = +0.94 V vs SCE) ($E[Cu^{II}(BPhen)_2/Cu^{I}(BPhen)_2]$ = +0.08 V vs SCE BPhen = Bathophenanthroline) to generate the corresponding copper(II)-amido species **1.31f** and the reduced photocatalyst Ir(II). At this stage the iodomesitylene dicarboxylate **1.31d**, which is preformed via the mixing of carboxylic acid **1.31b** and iodomesitylene diacetate is readily reduced by the Ir(II) (E[Ir(III)/Ir(II)] = -1.50 V versus SCE, E[**1.31d**/**1.31d**$^{\bullet-}$] = -1.14 V vs SCE) to generate alkyl radical **1.31i**, while reconstituting the ground-state photocatalyst. Copper(II)-amido complex **1.31f** captures alkyl radical **1.31i** to form copper(III) complex **1.31g**, which upon reductive elimination yields the desired sp^3 C–N coupling product **1.31c** and regenerate copper(I) catalyst **1.31e**.

[87] Liang, Y.; Zhang, X.; MacMillan, D. W. C. Decarboxylative sp^3 C–N Coupling via Dual Copper and Photoredox Catalysis. *Nature* **2018**, *559*, 83–88.

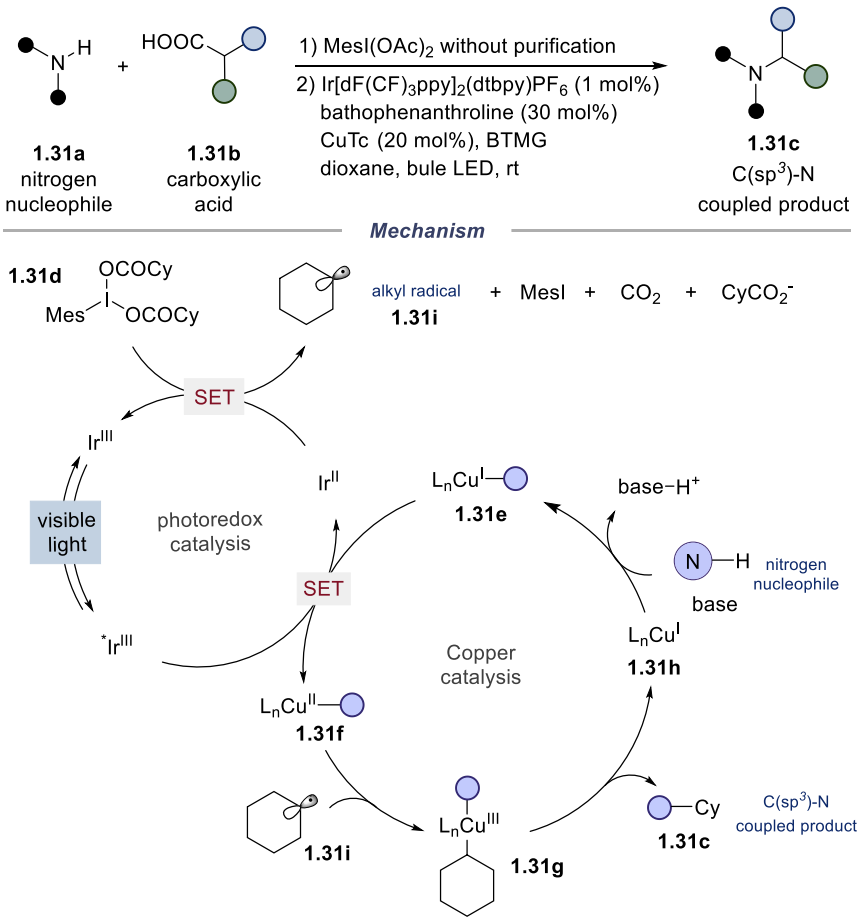

Scheme 1.31 Copper metallaphotoredox catalyzed decarboxylative amination.

1.3 Summary

Cross-coupling reactions continue to offer new grounds for research in multiple disciplines, becoming an indispensable tool to rapidly and reliably generate molecular complexity from simple precursors. This chapter briefly describes the evolution and the state-of-the-art in cross-coupling reactions, with a particular emphasis on the recent developments in nickel catalysis as well as copper metallaphotocatalysis. While early achievements in cross-coupling reactions relied primarily on the utilization of specialized ligands, the recent advances in merging photoredox catalysis with transition metal catalysis has opened up new avenues that would otherwise be difficult to access in ground state reactivity (Scheme 1.32).

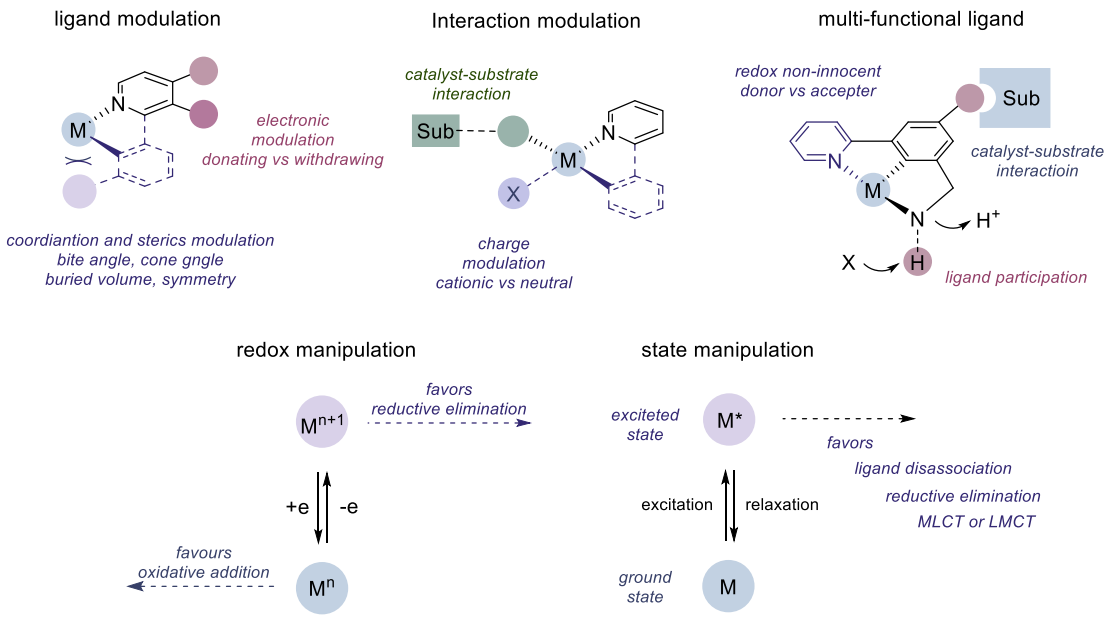

Scheme 1.32 Manipulation of transition metal catalysis.

Despite numerous advances realized, there are still some aspects that will be worth to develop within the general area of cross-coupling reactions. Among these, particularly attractive would be the following: (1) design and implementation of new activation model for promoting the functionalization of particularly inert functionalities such as site-selective functionalization of alkanes at either C–H or C–C linkages; (2) exploration of new techniques that allow for the coupling of functional groups as nucleophilic or electrophilic handles for either C–C or C–heteroatom bond-formations.

1.4 General Objective of the Doctoral Thesis

The past few decades have witnessed the rapid development of transition metal-catalyzed cross-coupling reactions, aiming at designing more efficient catalysts with broader substrate scope. Despite the numerous advances realized, there are still a number of functionalities that remain particularly problematic in cross-coupling reactions such as abundant, yet particularly strong, α C–C bonds. Based on Martin group's expertise in transition metal catalysis as well as photocatalysis, the following thesis is heading for making use of abundant and readily available feedstocks, unlocking new activation model to prepare value-added products that would otherwise be beyond reach using classical cross-coupling toolbox. To this end, the following objectives will be taken into consideration:

1. To develop a nickel photoredox dual catalyzed C(sp^2)–C(sp^3) and C(sp^3)–C(sp^3) cross coupling protocol utilizing aliphatic ketones as nucleophilic handles under mild conditions.

2. To develop a general platform to access C(sp^3)–N bond formation via ketone C–C bond cleavage, creating a new use for carbonyl compounds in retrosynthetic analysis when accessing aliphatic amine backbones.

3. To realize a practical copper-catalyzed C(sp^3) amination technique of unactivated secondary alkyl iodides, constructing valuable substituted aliphatic amines under mild reaction conditions with wide substrate scope.

Chapter 2

Dihydroquinazolinones as adaptative C(sp^3) handles in arylations and alkylations via dual catalytic C–C bond-functionalization

2.1 Introduction

Carbon-carbon bonds are ubiquitous in organic molecules, including biomolecules, polymers, pharmaceuticals, and petroleum feedstocks. The functionalization of molecules through the cleavage of C–C bonds holds promise to access unusual transformations and new retrosynthetic disconnections. However, compared to the vast progress made in C–H bond functionalization, the related processes involving activating C–C bonds has received less attention.

Nevertheless, C–C bond functionalization reactions are routinely used, for instance in the steam cracking process of crude oil at high temperatures and pressures in the petroleum industry.[88] Additionally, classical reactions such as sigmatropic rearrangements,[89] Beckmann rearrangement,[90] Bayer-Villiger oxidation,[91] retro-Aldol[92] have been broadly applied in organic synthesis (Scheme 2.1). In recent years, transition metal catalyzed C–C bond activation as well as radical induced C–C bond cleavage have emerged as powerful methods capable of functionalizing C–C bonds, thus adding new possibilities to this field.

[88] Negi, H.; Verma, P.; Singh, R. K. A Comprehensive Review on the Applications of Functionalized Chitosan in Petroleum Industry. *Carbohydrate Polymers*. **2021**, *266*, 118125–118142.
[89] Ilardi, E. A.; Stivala, C. E.; Zakarian, A. [3,3]-Sigmatropic Rearrangements: Recent Applications in the Total Synthesis of Natural Products. *Chem. Soc. Rev*. **2009**, *38*, 3133–3148.
[90] Kaur, K.; Srivastava, S. Beckmann Rearrangement Catalysis: A Review of Recent Advances. *New J. Chem*. **2020**, *44*, 18530–18572.
[91] Ten Brink, G.-J.; Arends, I. W. C. E.; Sheldon, R. A. The Baeyer−Villiger Reaction: New Developments toward Greener Procedures. *Chem. Rev*. **2004**, *104*, 4105–4124.
[92] Dzhafarov, M. K. Retro-Aldol Processes in Steroid Chemistry. *Russ. Chem. Rev*. **1992**, *61*, 363.

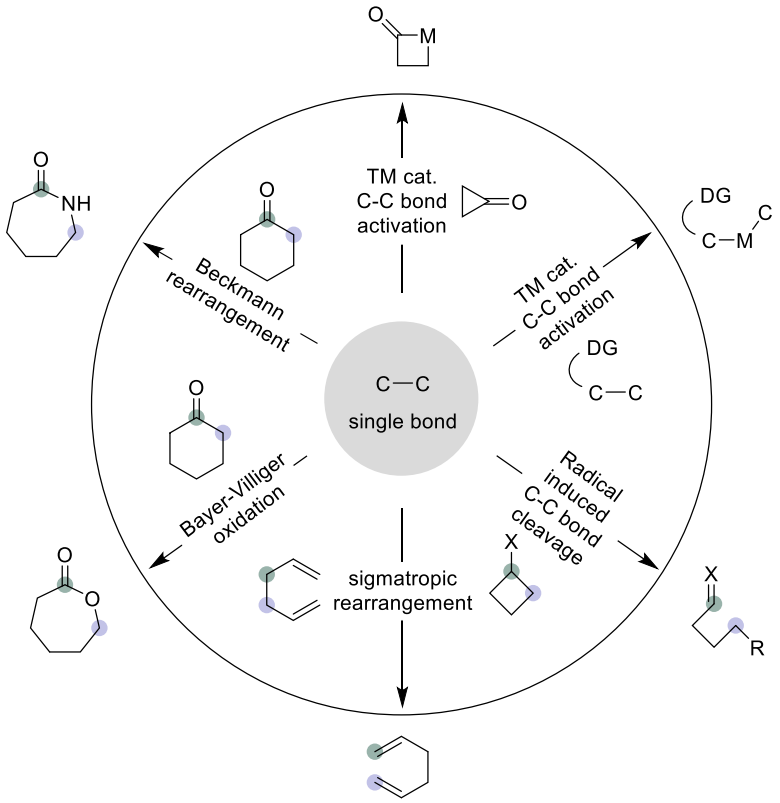

Scheme 2.1 C–C bond functionalization reactions.

2.1.1 Transition Metal-Catalyzed C–C Bond Cleavage

Transition metal-catalyzed C–C bond cleavage has been one of the main method for C–C bond functionalization, despite several challenges. Relatively high stability of the C–C bond [C–C BDE(alkane) ≈ 90 kcal/mol].[93] The accessibility of the transition metal center to C–C bonds is generally difficult due to the steric hindrance. Substituents on both ends can prevent the approach of the metal through steric effects. This makes the activation of C–C bonds difficult from a kinetic perspective as well. C–H bond activation is a competitive process of C–C activation, which is kinetically more favorable. There is no inherent polarization between the C–C bond, and neither atom possesses appropriate orbitals that significantly overlap with the transition metal. The relevant orbital interactions between C–C, C=C and C–H bonds and transition metal are compared in Scheme 2.2. In the case of a C=C bond (Scheme 2.2, *a*), favorable interactions between the *σ*-orbitals of the olefin and the metal *d*-orbitals are possible, allowing for facile coordination and activation of the bond. In contrast, a C–H bond is oriented perpendicular to the metal orbitals, however the spherical nature of the hydrogen allows for good overlap with the metal orbitals (Scheme 2.2, *b*). The highly

[93] Luo, Y.-R. *Handbook of Bond Dissociation Energies in Organic Compounds*; CRC Press: Boca Raton, 2002.

directional *σ*-bonding orbital of a C–C bond does not allow for significant overlap with the *d*-orbitals of transition metals unless they are heavily distorted by the metal (Scheme 2.2, *c*).

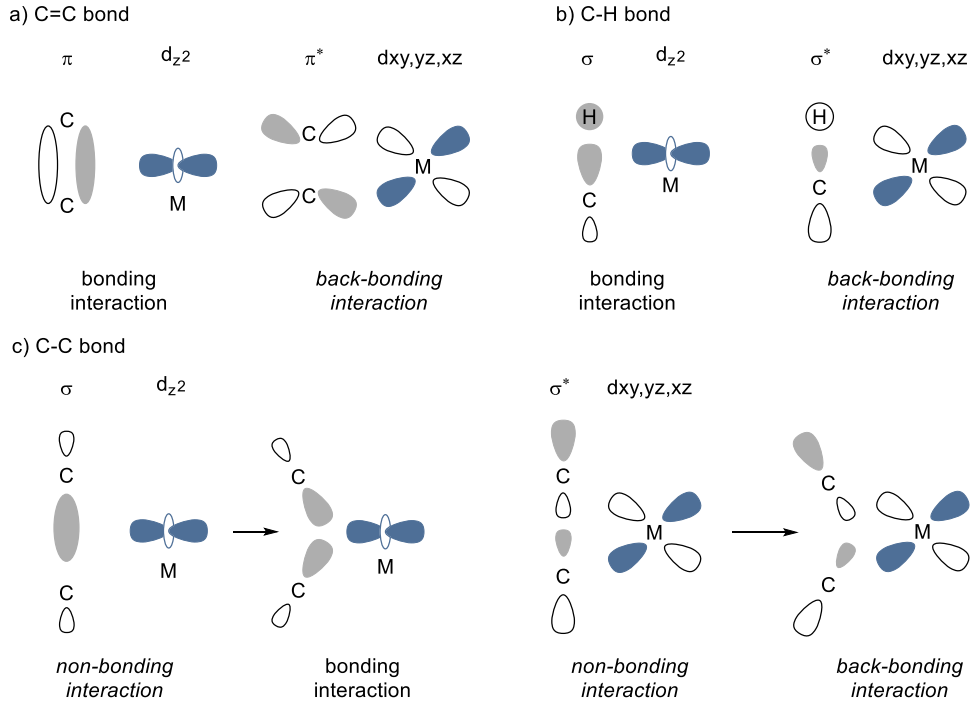

Scheme 2.2 Interaction of metal orbitals with a (a) C=C bond; (b) C–H bond; (c) C–C bond.

Despite these challenges, various chemical transformations of C–C bonds by homogenous transition metal catalysts have been realized in the past few decades.[94] Broadly speaking, two basic strategies that have been employed to facilitate C–C bond cleavage are: (1) the use of reactive starting materials, (2) the generation of highly stabilized products. The first strategy is exemplified by the reactions of substrates containing strained ring systems such as cyclopropanes and cyclobutanes. The second strategy includes the aromatization of pro-aromatic compounds and the formation of cyclometallated products through chelation-assistance.

[94] (a) Jun, C.-H. Transition Metal-Catalyzed Carbon–Carbon Bond Activation. *Chem. Soc. Rev.* **2004**, *33*, 610–618. (b) Dong, G. *C−C bond activation of Topics in Current Chemistry*; Springer, 2014. (c) Murakami, M.; Ishida, N. Potential of Metal-Catalyzed C-C Single Bond Cleavage for Organic Synthesis. *J. Am. Chem. Soc.* **2016**, *138*, 13759−13769. (d) Souillart, L.; Cramer, N. Catalytic C-C Bond Activations *via* Oxidative Addition to Transition Metals. *Chem. Rev.* **2015**, *115*, 9410−9464. (e) Chen, F.; Wang, T.; Jiao, N. Recent Advances in Transition-Metal-Catalyzed Functionalization of Unstrained Carbon-Carbon Bonds. *Chem. Rev.* **2014**, *114*, 8613−8661. (f) Song, F.; Gou, T.; Wang, B.-Q.; Shi, Z.-J. Catalytic Activations of Unstrained C-C Bond Involving Organometallic Intermediates. *Chem. Soc. Rev.* **2018**, *47*, 7078−7115. (g) Kim, D.-S.; Park, W.-J.; Jun, C.-H. Metal−Organic Cooperative Catalysis in C−H and C−C Bond Activation. *Chem. Rev.* **2017**, *117*, 8977−9015.

2.1.1.1 Strained Motif Enabled C–C Bond Activation

As shown in Scheme 2.3, strained 3- or 4-membered ring compounds have inherently greater strain energy compared to the 5- or 6-membered ring. Hence the relief of this strain energy through metal insertion compensates for the thermodynamic disadvantage of C–C bond activation by forming ring-expanded metallacyclic complexes. Also, the distorted *σ*-bonding orbital of a C–C bond in small ring system allows for overlap with the *d*-orbitals of transition metals. These factors make small rings ideal substrates for metal-catalyzed C–C bond activation methodologies.[95]

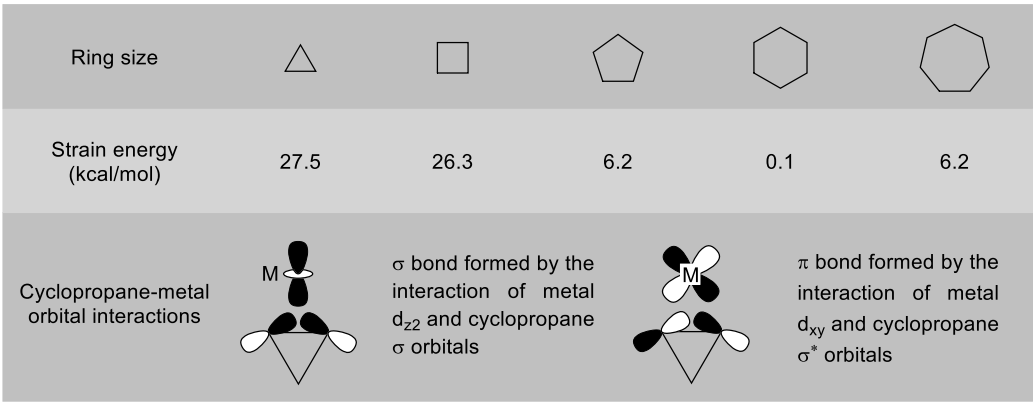

Scheme 2.3 Ring size and strain energy.

[95] Fumagalli, G.; Stanton, S.; Bower, J. F. Recent Methodologies That Exploit C−C Single-Bond Cleavage of Strained Ring Systems by Transition Metal Complexes. *Chem. Rev*. **2017**, *117*, 9404−9432.

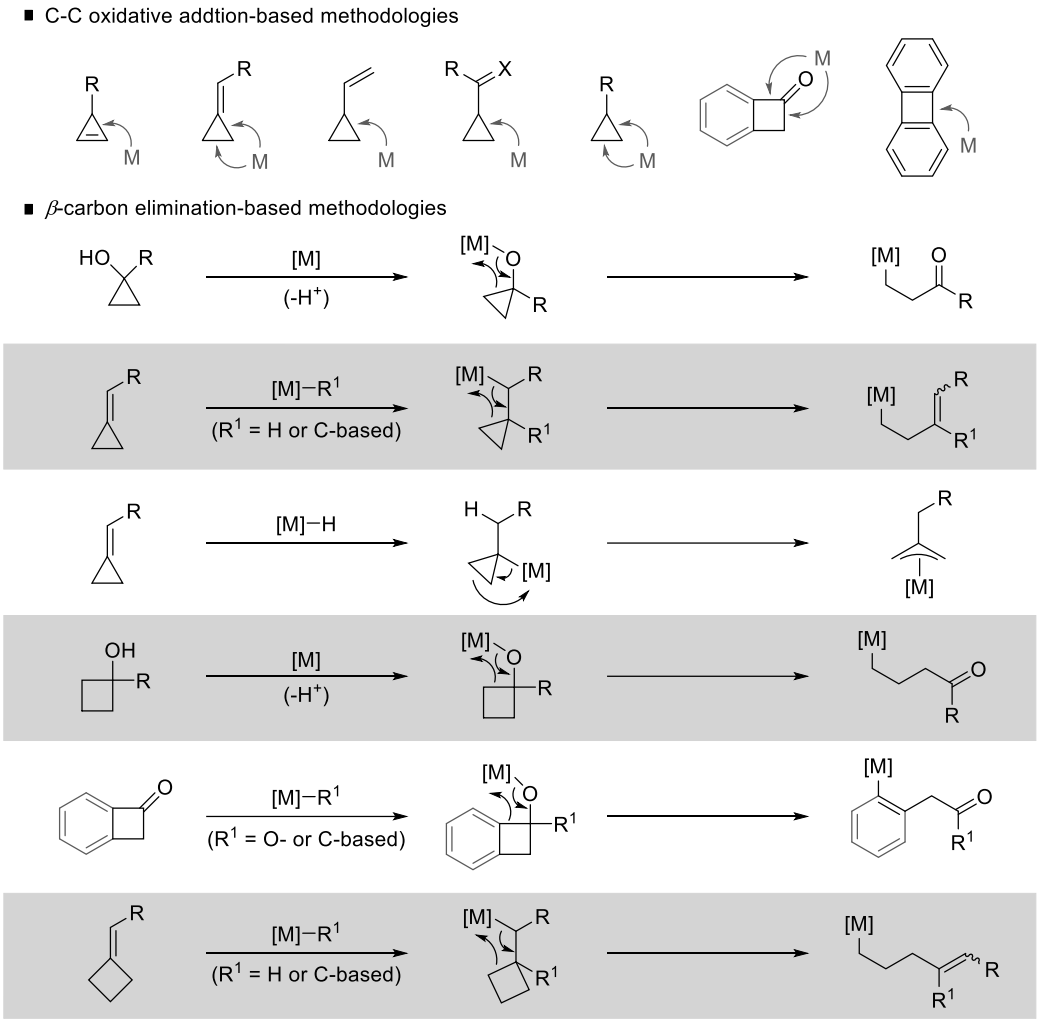

Scheme 2.4 C-C activation of small rings via oxidative addition and *β*-carbon elimination.

The first example of a metal-mediated cleavage of C–C bond dates back to Tipper's 1955 report of the reaction between $PtCl_2$ and cyclopropane.[96] Since then, many advances have been made in the discovery of C–C bond cleavage reactions. As summarized in Scheme 2.4, many established C–C activation protocols were based on oxidative addition and *β*-carbon elimination mechanism.

As an early example, the direct insertion of late transition-metals (Fe, Ni, Ir, Pt, Pd, etc.) into the strained C–C *σ*-bond of biphenylene has been investigated extensively.[97] Biphenylenes can undergo a variety of insertion reactions with small molecules in the presence of metal catalysts, leading to the formation of various functionalized aromatic compounds (Scheme 2.5). For instance, Jones reported the

[96] Tipper, C. F. H. Some Reactions of Cyclopropane, and a Comparison with the Lower Olefins. Part II. Some Platinum-Cyclopropane Complexes. *J. Chem. Soc*. **1955**, 2045–2046.
[97] Perthuisot, C.; Edelbach, B. L.; Zubris, D. L.; Simhai, N.; Iverson, C. N.; Muller, C.; Satoh, T.; Jones, W. D. Cleavage of the Carbon–Carbon Bond in Biphenylene Using Transition Metals. *J. Mol. Catal. A* **2002**, *189*, 157–168.

nickel-catalyzed coupling of biphenylene with alkynes, carbon monoxide, and isocyanides to form phenanthrenes (**2.5d**), fluorenone (**2.5e**), and fluorenimines (**2.5f**), respectively.[98] Biphenylene has also been used in various palladium-catalyzed cross-coupling reactions to generate substituted biphenyls (**2.5g**–**2.5i**).[99]

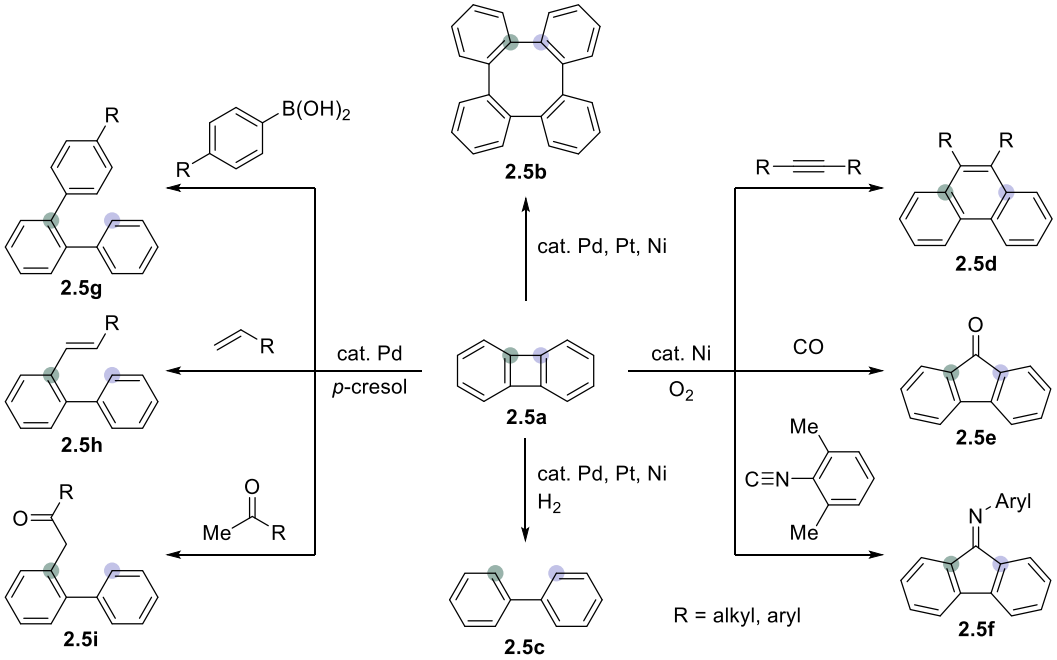

Scheme 2.5 Transition metal catalyzed C–C activation of biphenylenes.

Cyclobutanone derivative is another commonly used substrate for C–C bond activation, as demonstrated by Murakami and co-workers.[100] In 1994, they described Rh(I) complex could undergo oxidative addition into cyclobutanone derivatives **2.6a** regioselectively and stereoselectively affording ring-expanded Rh(III) intermediate **2.6b**, which transforms into alcohol **2.6c** upon hydrogenolysis under the high pressure of H_2.

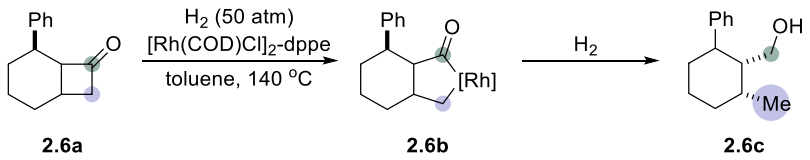

Scheme 2.6 Rhodium catalyzed C−C activation of cyclobutanone via oxidative addition.

[98] Edelbach, B. L.; Lachicotte, R. J.; Jones, W. D. Catalytic Carbon−Carbon Bond Activation and Functionalization by Nickel Complexes. *Organometallics* **1999**, *18*, 4040–4049.
[99] Satoh, T.; Jones, W. D. Palladium-Catalyzed Coupling Reactions of Biphenylene with Olefins, Arylboronic Acids, and Ketones Involving C−C Bond Cleavage. *Organometallics* **2001**, *20*, 2916–2919.
[100] Murakami, M.; Amii, H.; Ito, Y. Selective Activation of Carbon–Carbon Bonds Next to a Carbonyl Group. *Nature* **1994**, *370*, 540–541.

In 1999, Uemura reported the palladium catalyzed arylation of *tert*-cyclobutanols with aryl bromides via palladium *β*-carbon elimination.[101] In this reaction, the key step is the *β*-carbon elimination of Pd(II) alkoxide complex formed *in situ*. The strain relief associated with the C–C bond-cleavage makes this step irreversible, resulting in an alkyl Pd(II) intermediate **2.7d**. Reductive elimination of intermediate **2.7d** forms the arylated product **2.7b** and regenerates the Pd(0) catalyst.

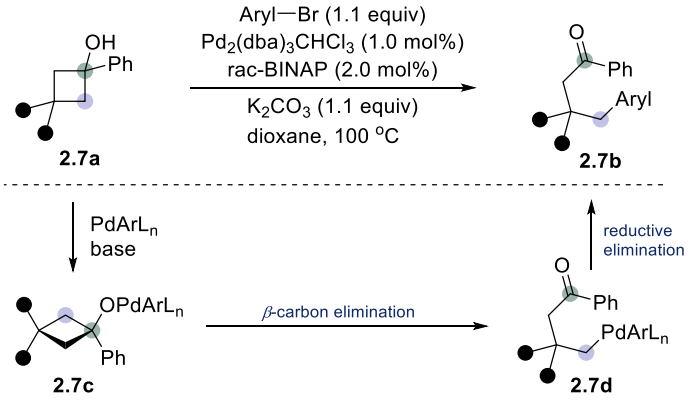

Scheme 2.7 Palladium-catalyzed C–C activation of cyclobutanol via *β*-carbon elimination.

2.1.1.2 Chelation Assisted C–C Bond Activation

For the C–C bond activation of unstrained molecules, directed cleavage by chelation-assistance is one of the most prominent methods.[102] This strategy requires a coordinating functional group on the substrate that can direct the metal to the bond to be cleaved, resulting in the formation of a stable five-membered metallocycle. In 1993, Milstein used a pincer-type bis-phosphine ligand with rhodium pre-catalyst, for selective C–C bond cleavage of an unactivated methyl group.[103] This discovery was later adapted into a catalytic protocol with $[Rh(C_8H_{14})_2Cl]_2$ in dioxane at 180 °C under H_2 pressure or with an excess of $HSi(OEt)_3$ as hydrogen source (Scheme 2.8).[104] The transformation was proposed to begin with a C–C bond activation to give pincer Rh(III) complex **2.8c**, which subsequently reacts with H_2 to release methane along with pincer Rh(III) hydride species **2.8d**.

---

[101] Nishimura, T.; Uemura, S. Palladium-Catalyzed Arylation of tert-Cyclobutanols with Aryl Bromide via C−C Bond Cleavage: New Approach for the γ-Arylated Ketones. *J. Am. Chem. Soc*. **1999**, *121*, 11010–11011.

[102] (a) Xia, Y.; Dong, G. Temporary or Removable Directing Groups Enable Activation of Unstrained C–C Bonds. *Nat Rev Chem*. **2020**, *4*, 600–614. (b) Dreis, A. M.; Douglas, C. J. *Carbon–Carbon Bond Activation with 8-Acylquinolines.* Springer: **2014**.

[103] Gozin, M.; Weisman, A.; Ben-David, Y.; Milstein, D. Activation of a Carbon−Carbon Bond in solution by Transition-Metal Insertion. *Nature* **1993**, *364*, 699−701.

[104] Liou, S.-Y.; Boom, M. E. Milstein, D. Catalytic Selective Cleavage of a Strong C−C Single Bond by Rhodium in Solution. *Chem. Commun*. **1998**, 687−688.

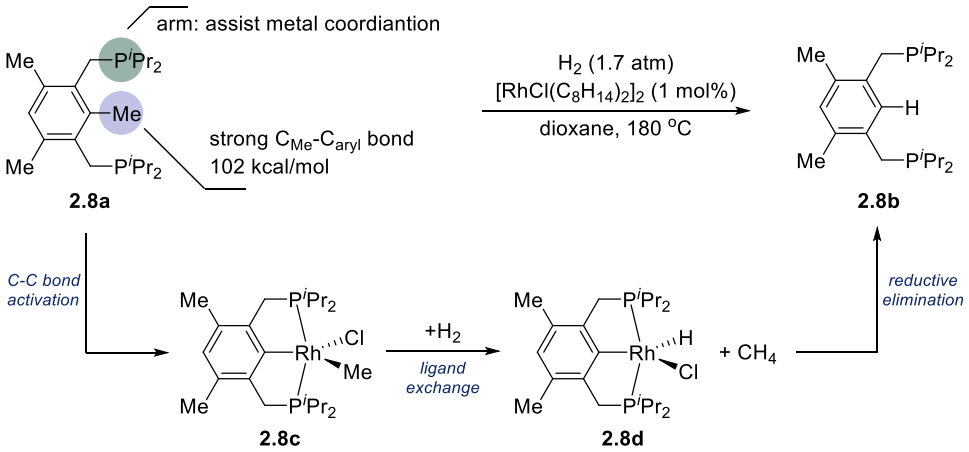

Scheme 2.8 C–C bond activation by PCP system.

In 1985, Jun and Suggs reported the use of 8-quinolinyl phenyl ketone **2.9a** for directing rhodium(I) complex to the *α*-keto C–C bond, resulting in selective activation (Scheme 2.9).[105] In the presence of excess ethylene, phenyl is expelled through a sequential migratory insertion and *β*-hydrogen elimination process. This is followed by a final ethylene insertion to Rh(III) hydride complex **2.9e** and reductive elimination to access ethyl ketone **2.9b**.

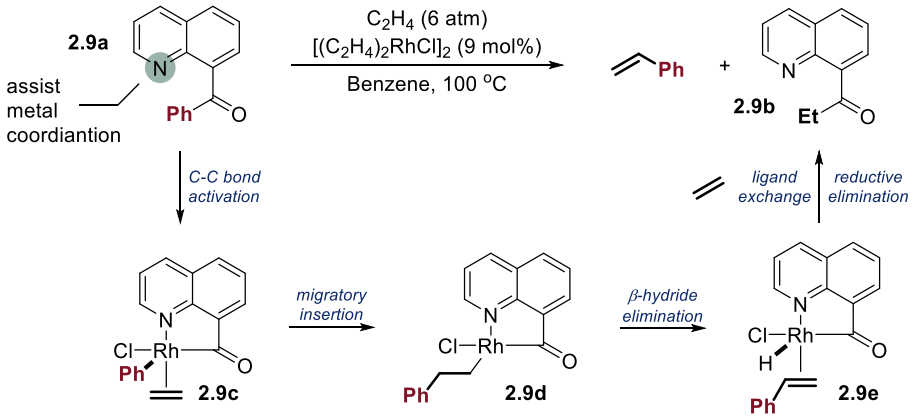

Scheme 2.9 Rh(I)-catalyzed alkyl transfer with 8-quinolinyl alkyl ketone.

Although directing group enabled C–C bond activation had emerged as a powerful technique for functionalization of unstrained C–C bond, the removal of the DG from the product limits the synthetic utility of such a process. Jun addressed this shortcoming with a temporary chelating auxiliary 2-amino-3-picoline, which can be easily removed from the product by hydrolysis.[106] As shown in Scheme 2.10, initially ketimine **2.10e** is formed from benzylacetone **2.10a** and 2-amino-3-picoline. Ketimine **2.10e** then

[105] Jun, C. H.; Suggs, J. W. Metal-Catalyzed Alkyl Ketone to Ethyl Ketone Conversions in Chelating Ketones via Carbon–Carbon Bond Cleavage. *J chem. Soc. Chem. Commun*. **1985**, 92−93.
[106] Jun, C.-H.; Lee, H. Catalytic Carbon−Carbon Bond Activation of Unstrained Ketone by Soluble Transition-Metal Complex. *J. Am. Chem. Soc*. **1999**, *121*, 880−881.

undergoes C–C bond activation to form intermediate **2.10f**. Intermediate **2.10f** undergoes *β*-hydrogen elimination releasing styrene and forming intermediate **2.10g** upon hydrometalation. Reductive elimination of intermediate **2.10g** produced ketimine **2.10h**, which upon hydrolysis affords **2.10d**. Since the transformation is in thermodynamic equilibrium the removal of styrene through polymerization and the addition of excess olefin are crucial to drive the reaction forward.

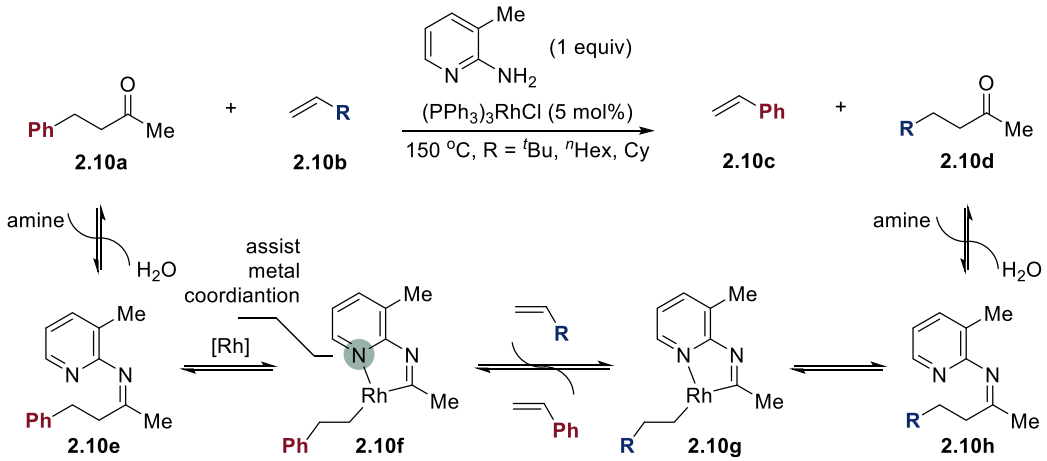

Scheme 2.10 Rh(I)-catalyzed alkyl group transfer using 2-amino-3-picoline.

2.1.1.3 Other Methods

Transition metal-catalyzed C–CN bond cleavage also offers innovative opportunities within the realm of C–C bond-functionalization.[107] The cyano group is considered an "active" functional group due to its ability to coordinate to transition metals in an η^1-fashion or η^2-fashion.[108] In particular, η^2-coordination is known to trigger the activation of a C–CN bond via oxidative addition (Scheme 2.11, *path A*) or via formation of silylisonitrile complexes when a Lewis acidic silyl group is ligated on the metal (Scheme 2.11, *path B*). Transition metal complexes that have been reported to cleave the C–CN bond through an oxidative addition mechanism mainly involve Group 10 transition metals (Ni, Pd, Pt). Cleavage through deinsertion of silyl isocyanide is often demonstrated by Rh, Ir, and Fe complexes.

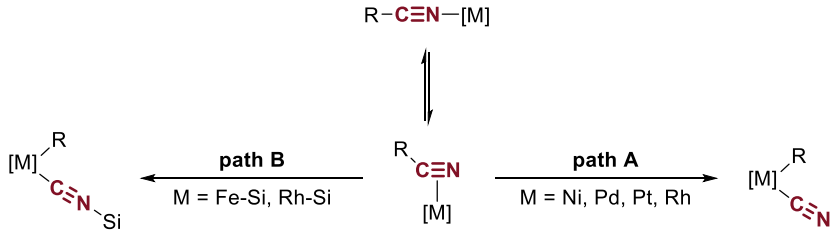

[107] Wen, Q.; Lu, P.; Wang, Y. Recent Advances in Transition-Metal-Catalyzed C−CN Bond Activations. *RSC Adv*. **2014**, *4*, 47806−47826.
[108] Storhoff, B. N.; Lewis, H. C. Organonitrile Complexes of Transition Metals. Jr. *Coord. Chem. Rev*. **1977**, *23*, 1−29.

Scheme 2.11 Transition metal catalyzed C–CN bond activation.

Both processes have been successfully applied in the catalytic reactions.[109] Examples of these reactions include: hydrodecyanation of nitriles,[110] cross-coupling using nitriles as electrophiles,[111] cyanation of aryl halides and arenes using organic nitriles as cyanating agents,[112] and carbocyanation of unsaturated compounds.[113] As an early example, Maiti and co-workers developed a nickel-catalyzed hydrodecyanation of various aromatic and aliphatic nitriles proceeds with tetramethyldisiloxane as a hydride donor (Scheme 2.12).[114] This reaction was proposed to proceed through oxidative addition of C–CN bonds to nickel(0), followed by transmetalation with tetramethyldisiloxane **2.12b** to form nickel hydride species which forms product **2.12c** upon reductive elimination.

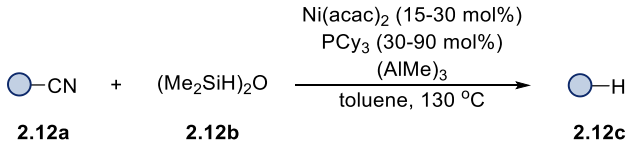

Scheme 2.12 Nickel catalyzed hydrodecyanantion of nitriles with hydrosilanes.

Another main pathway for C–C bond activation in unstrained structures often involves relief of steric congestion.[115] In 2001, Miura and co-workers reported a palladium-catalyzed coupling reaction of *tert*-benzyl alcohol **2.13b** with bromobenzene **2.13a** via C–C bond cleavage (Scheme 2.13).[116] The reaction proceeded through oxidative addition of bromobenzene (**2.13a**) onto Pd(0). Subsequent exchange of the bromide ligand on Pd(II) oxidative addition complex with the alkoxide ligand forms intermediate **2.13d**. *β*-carbon elimination of intermediate **2.13d** gave an aryl-Pd(II)-aryl species **2.13e** with extrusion of acetone followed by reductive elimination to afford the

[109] Nakao, Y. Metal-Mediated C–CN Bond Activation in Organic Synthesis. *Chem. Rev*. **2021**, *121*, 327–344.
[110] Paul, N.; Patra, T.; Maiti, D. Recent Developments in Hydrodecyanation and Decyanative Functionalization Reactions. *Asian J. Org. Chem*. **2022**, e202100591.
[111] Sun, M.; Zhang, H.-Y.; Han, Q.; Yang, K.; Yang, S.-D. Nickel-Catalyzed C–P Cross-Coupling by C–CN Bond Cleavage. *Chem. Eur. J*. **2011**, *17*, 9566–9570.
[112] Mills, L. R.; Graham, J. M.; Patel, P.; Rousseaux, S. A. L. Ni-Catalyzed Reductive Cyanation of Aryl Halides and Phenol Derivatives via Transnitrilation. *J. Am. Chem. Soc*. **2019**, *141*, 19257–19262.
[113] Nakao, Y.; Hiyama, T. Nickel-Catalyzed Carbocyanation of Alkynes. *Pure and Applied Chemistry*. **2008**, *80*, 1097–1107.
[114] Patra, T.; Agasti, S.; Akanksha; Maiti, D. Nickel-Catalyzed Decyanation of Inert Carbon-Cyano Bonds. *Chem. Commun*. **2013**, *43*, 69−71.
[115] Lutz, M .D .R.; Morandi, B. Metal-Catalyzed Carbon−Carbon Bond Cleavage of Unstrained Alcohols. *Chem. Rev*. **2021**, *121*, 300−326.
[116] Terao, Y.; Wakui, H.; Satoh, T.; Miura, M.; Nomura, M. Palladium-Catalyzed Arylative Carbon-Carbon Bond Cleavage of α, α-Disubstituted Arylmethanols. *J. Am. Chem. Soc*. **2001**, *123*, 10407−10408.

2.13c. The ortho methyl group on the alcohol **2.13b** is key for success of the reaction, indicating that relief of steric congestion plays a key role in this C–C bond cleavage.

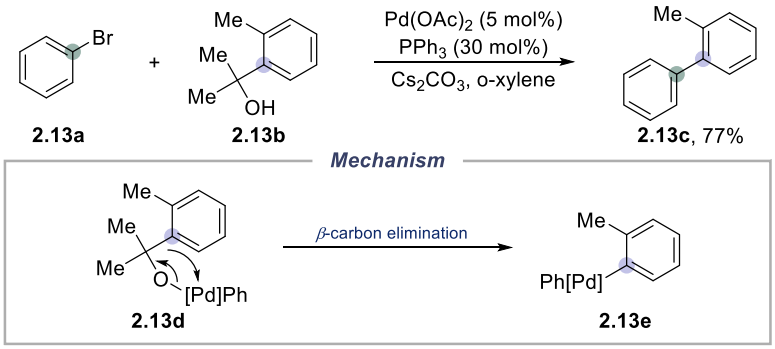

Scheme 2.13 *β*-carbon elimination enabled C–C bond activation of unstrained molecules.

The advances made in the C–C bond activation arena provide ample examples of elegant strategies for overcoming the thermodynamic and kinetic barriers to C–C bond activation. The examples shown mainly serve as "proof of concept" reactions demonstrating C–C bonds may be used as functional handles, in spite of the inherent limitations in substrate breadth/compatibility and functional group tolerance. These limitations arise from the substrate engineering and harsh reaction conditions (e.g. relief of ring strain in small rings and chelating functional groups). However, the ingenuity and increased understanding provided by the examples shown leave ample room for other further developments.

2.1.2 Radical Mediated C-C Bond Cleavage

Discovered in 1936 and 1937, Norrish type I and type II reactions represent early methods for radical mediated carbon-carbon bond cleavage (Scheme 2.14).[117] The type I Norrish reaction is the photoinduced homolysis of aldehydes and ketones into two free radical intermediates. The Norrish type II reaction involves intramolecular abstraction of a *γ*-hydrogen by a triplet state carbonyl compound. The HAT step is followed by either *β*-scission to form an alkene and an enol or intramolecular radical recombination to form cyclobutanol structure. Despite Norrish reactions representing the early examples of C–C bond cleavage, the reaction's synthetic utility is limited by the use of UV light. Since a number of functional groups are able to absorb UV light (Figure 2.1), leading to undesired side reactions.

[117] (a) Norrish, R. G. W.; Bamford, C. H. Photodecomposition of Aldehydes and Ketones. *Nature* **1936**, *138*, 1016. (b) Norrish, R. G. W.; Bamford, C. H. Photo-decomposition of Aldehydes and Ketones. *Nature* **1937**, *140*, 195–196.

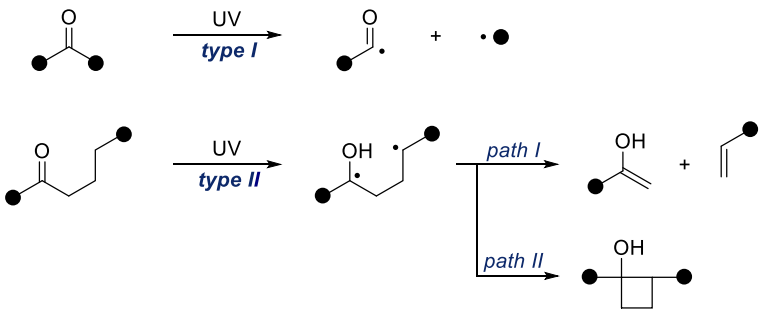

Scheme 2.14 Norrish reactions.

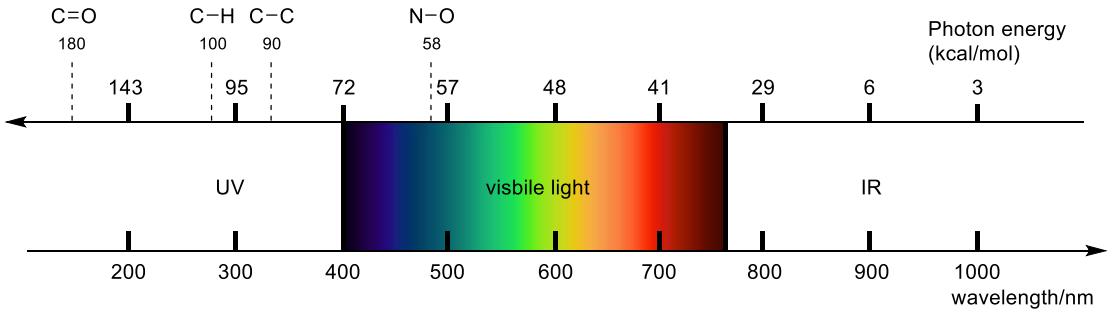

Figure 2.1 Electromagnetic spectrum.

Although examples had been shown, Barton's nitrite reaction was the first broadly applied method making use of radical induced C–C bond cleavage. In 1961, Barton and co-workers published an elegant solution for generating alkoxy radicals through photolysis of alkyl nitrites formed *in situ* from the corresponding alcohol and nitrosyl chloride (or nitrosylsulfuric acid).[118] This strategy was used in the synthesis of steroid derivatives (Scheme 2.15). The mechanism relies on photolysis of nitrite **2.15a** to form nitric oxide and an alkoxy radical **2.15c**, followed by *β*-scission. The resulting tertiary alkyl radical **2.15d** then combines with nitric oxide to form the nitroso aldehyde **2.15e**, leading to hydroxamic acid **2.15b** after cyclization.

[118] Robinson, C. H.; Gnoj, O.; Mitchell, A.; Wayne, R.; Townley, E.; Kabasakalian, P.; Oliveto, E. P.; Barton, D. H. R. The Photolysis of Organic Nitrites. II. Synthesis of Steroidal Hydroxamic Acids. *J. Am. Chem. Soc.* **1961**, *83*, 1771–1772.

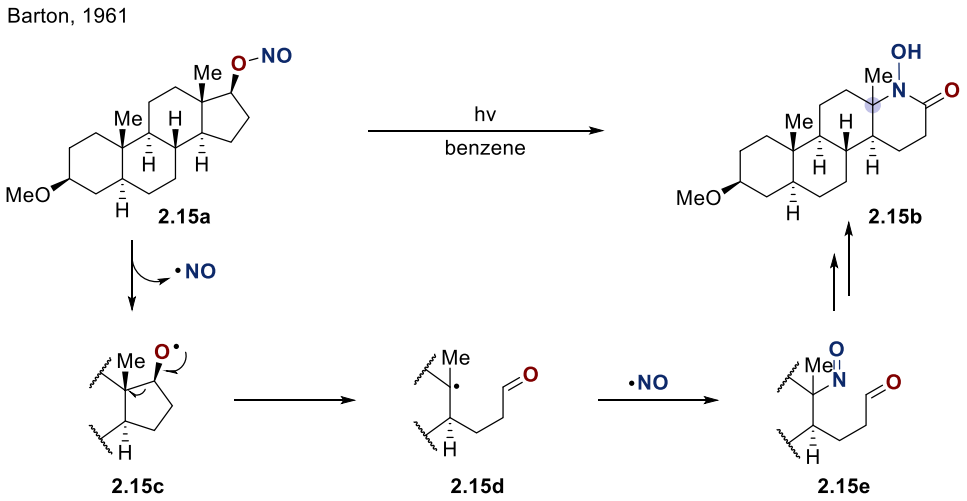

Scheme 2.15 oxygen radical initiated C–C bond cleavage.

As a highly reactive species, radical generation and its fragmentation behavior hold promise for C–C bond functionalization. Historically, generation of radical species relied on the use of toxic metals such as tin/mercury, stoichiometric oxidants/reductants, and the use of UV light. However, recent developments in photoredox catalysis, photochemistry (e.g. EDA complexes etc), and electrochemistry have allowed for the broad application of radicals species in a controllable and predictable manner,[119] making the radical fragmentation also emerged as an attractive strategy for C–C bond functionalization.[120]

2.1.2.1 Nitrogen Radical in C−C Bond Cleavage

Nitrogen-centered radicals, such as iminyl, aminyl, amidyl and aminyl radicals are important and synthetically versatile class of radical intermediates that have been extensively used in various C–N bond-forming reactions (Scheme 2.16).[121] Specifically, iminyl radicals are considered to be ambiphilic. Amidyl and aminium radicals both possessing a π-type configuration as the unpaired electron resides in a *p*-orbital, are electrophilic. Aminyl radicals are nucleophilic.

[119] Crespi, S.; Fagnoni, M. Generation of Alkyl Radicals: From the Tyranny of Tin to the Photon Democracy. *Chem. Rev*. **2020**, *120*, 9790−9833.
[120] (a) Yu, X.-Y.; Chen, J.-R.; Xiao, W.-J. Visible Light-Driven Radical-Mediated C–C Bond Cleavage/Functionalization in Organic Synthesis. (b) Morcillo, S. P. Radical-Promoted C–C Bond Cleavage: A Deconstructive Approach for Selective Functionalization. *Angew. Chem. Int. Ed*. **2019**, *58*, 14044–14054.
[121] Xiong, T.; Zhang, Q. New Amination Strategies Based on Nitrogen-Centered Radical Chemistry. *Chem. Soc. Rev*. **2016**, *45*, 3069–3087.

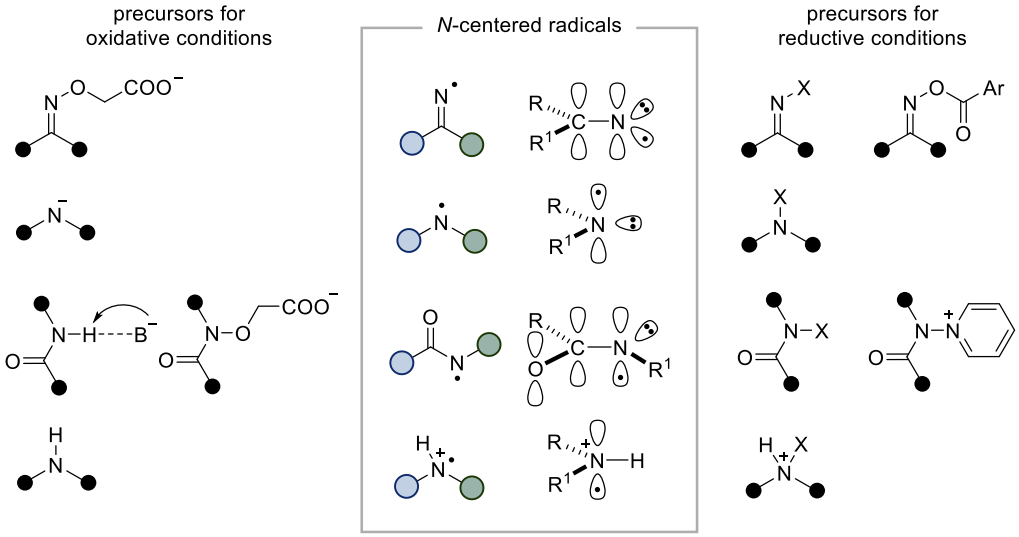

Scheme 2.16 *N*-centered radicals and their generation.

Nitrogen-centered radicals can be formed by oxidative, reductive and homolytic pathways (Scheme 2.16).[122] Oxidative pathways use photocatalysts or oxidants (for example, hypervalent iodine reagents or *tert*-butyl hypochlorite) to take an electron from N–H bonds or oxime esters. Hydrogen-bonding activation is needed for N–H bond oxidation in some cases, for the photocatalyst itself cannot efficiently oxidize the substrates.[123] Reductive conditions commonly use SET pathways with low valent transition metals or photocatalysts to cleave N–X, N–O or N–N bonds. Homolytic pathway is often induced by UV light or triplet photosensitizer for the homolysis of N–X, N–O or N–N bonds.

[122] (a) Kwon, K.; Simons, R. T.; Nandakumar, M.; Roizen, J. L. Strategies to Generate Nitrogen-centered Radicals That May Rely on Photoredox Catalysis: Development in Reaction Methodology and Applications in Organic Synthesis. *Chem. Rev*. **2022**, *122*, 2353–2428. (b) Zard, S. Z. Recent Progress in the Generation and Use of Nitrogen-Centred Radicals. *Chem. Soc. Rev*. **2008**, *37*, 1603–1618. (c) Jiang, H.; Studer, A. Chemistry With N-Centered Radicals Generated by Single-Electron Transfer-Oxidation Using Photoredox Catalysis. *CCS Chem*. **2019**, *1*, 38–49. (d) Xiong, P.; Xu, H.-C. Chemistry with Electrochemically Generated N-Centered Radicals. *Acc. Chem. Res*. **2019**, *52*, 3339–3350. (e) Kärkäs, M. D. Photochemical Generation of Nitrogen-Centered Amidyl, Hydrazonyl, and Imidyl Radicals: Methodology Developments and Catalytic Applications. ACS Catal. 2017, 7, 4999–5022.

[123] Murray, P. R. D.; Cox, J. H.; Chiappini, N. D.; Roos, C. B.; McLoughlin, E. A.; Hejna, B. G.; Nguyen, S. T.; Ripberger, H. H.; Ganley, J. M.; Tsui, E.; Shin, N. Y.; Koronkiewicz, B.; Qiu, G.; Knowles, R. R. Photochemical and Electrochemical Applications of Proton-Coupled Electron Transfer in Organic Synthesis. *Chem. Rev*. **2022**, *122*, 2017−2291.

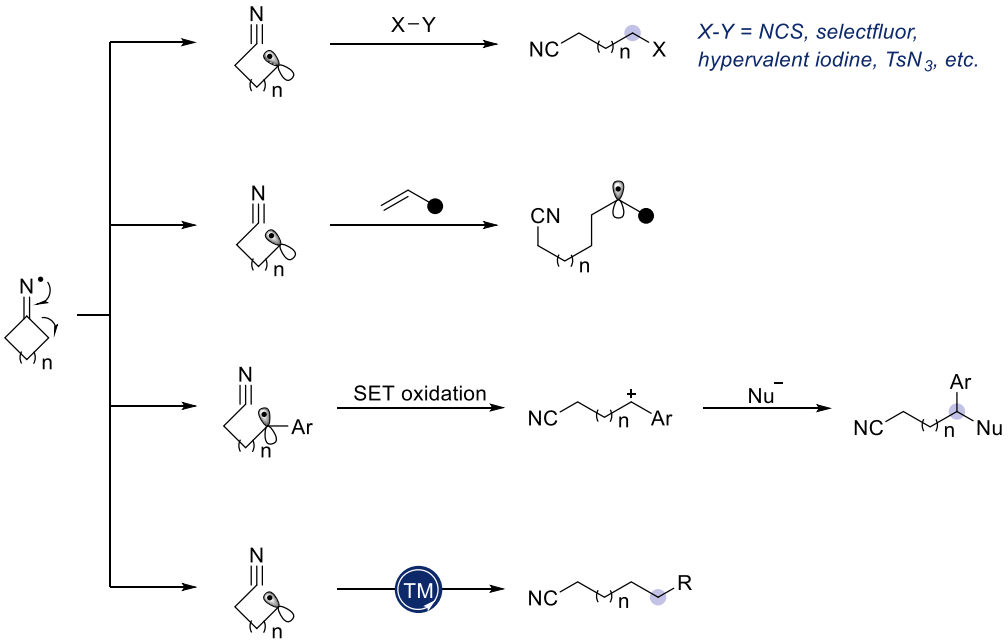

Scheme 2.17 Imine radical induced C–C bond cleavage.

During the past few years, the group of Shi,[124] Xiao,[125] Leonori[126] and others have reported a number of studies on the fragmentation of cyclic oxime esters, constituting the majority of *N*-centered radical induced C–C bond functionalization reactions.[127] Upon iminyl radical generation, the *β*-fragmentation process occurs driven by the relief of ring strain, formation of a cyano group or a stable radical intermediate (e.g. benzylic, tertiary or acyl radical etc). As shown in Scheme 2.17, the resulting alkyl radical can undergo: (1) interception by SOMOphiles (e.g. NCS, TsN_3, unsaturated moieties etc); (2) radical polar cross over (RPCO), for instance oxidation of the benzylic position to form a carbocation which can trap nucleophiles; (3) interception by organometallic complexes.

For instance, in 2018 Wang and co-workers developed a nickel-catalyzed cross-electrophile coupling reaction of cyclic oxime esters and acyl chlorides (Scheme 2.18).[128] In this approach, a *in situ* generated Ni(I) complex, reduced the oxime esters **2.18a** to afford a Ni(II) complex as well as a iminyl radical **2.18d**, which would undergo

[124] Zhao, B.; Shi, Z. Copper-Catalyzed Intermolecular Heck-Like Coupling of Cyclobutanone Oximes Initiated by Selective C−C Bond Cleavage. *Angew. Chem. Int. Ed*. **2017**, *56*, 12727–12731.
[125] Yu, X,-Y.; Zhou, Q,-Q.; Chen, J; Chen, J,-R.; Xiao, W.-J. Copper-Catalyzed Radical Cross-Coupling of Redox-Active Oxime Esters, Styrenes and Boronic Acids. *Angew. Chem. Int. Ed*. **2018**, *57*, 15505–15509.
[126] Dauncey, E. M.; Dighe, S. U.; Douglas, J. J.; Leonori, D. A Dual Photoredox-Nickel Strategy for Remote Functionalization *via* Iminyl Radicals: Radical Ring-Opening-Arylation, -Vinylation and -Alkylation Cascades. *Chem. Sci*. **2019**, *10*, 7728–7733.
[127] Chen, P.; Huang, H.; Tan, Q.; Ji, X.; Zhao, F. Recent Advances in Molecule Synthesis Involving C-C Bond Cleavage of Ketoxime Esters. *Molecules* **2023**, *28*, 2667−2700.
[128] Ding, D.; Wang, C. Nickel-Catalyzed Reductive Electrophilic Ring Opening of Cycloketone Oxime Esters with Aroyl Chlorides. *ACS Catal*. **2018**, *8*, 11324–11329.

β-scission to form an alkyl radical. The generated Ni(II) complex could recombine with the alkyl radical to give the Ni(III) intermediate **2.18e**. In the presence of Mn, the Ni(III) intermediate is reduced to Ni(I), and is thus able to provide an oxidative addition to aroyl chlorides. The resulting Ni(III) complex **2.18g** undergoes reductive elimination to form cyanoketones **2.18c** and Ni(I) catalyst.

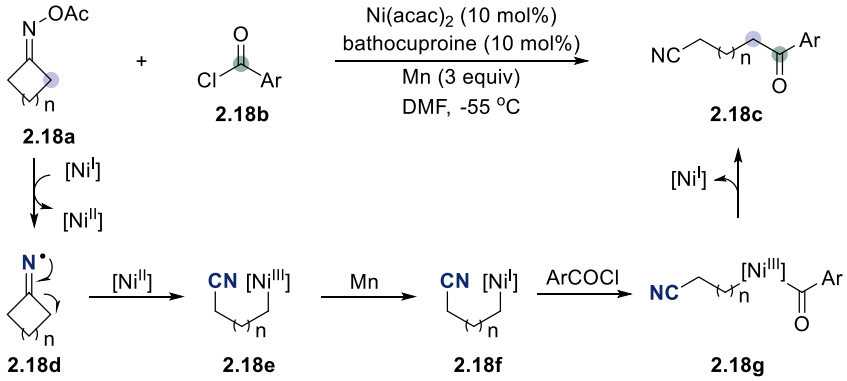

Scheme 2.18 Ni-catalyzed C–C bond cleavage/cross-electrophile coupling.

In many photoredox-catalyzed reactions, amines have been frequently used as sacrificial reductants due to their low oxidation potential and widely availability.[129] In most of the cases, aminium radicals lose a proton to generate aminyl radicals. However, aminium radicals could also undergo *β*-scission to form an alkyl radical which can be used in further reactions. The Zheng group made the major contributions in secondary amine radical cation-mediated C–C bond cleavage. For instance, they reported that aminium radical cations generated by SET oxidation undergoes irreversible *β*-scission to form an alkyl radical with an iminium ion. This process is driven by strain release of the cyclopropyl ring, and the resulting species was used in intermolecular [3+2] or [4+2] cycloadditions with unsaturated hydrocarbons (Scheme 2.19, *top*).[130] The similar strategy was reported by the Waser group with amide substrate, who captured the alkyl radical with SOMOphiles and imine ion with nucleophile (Scheme 2.19, *bottom*).[131]

[129] Nakajima, M.; Fava, E.; Loescher, S.; Jiang, Z.; Rueping, M. Photoredox-Catalyzed Reductive Coupling of Aldehydes, Ketones, and Imines with Visible Light. *Angew. Chem. Int. Ed*. **2015**, *54*, 8828–8832.
[130] Wang, J.; Zheng, N. The Cleavage of a C−C Bond in Cyclobutylanilines by Visible-Light Photoredox Catalysis: Development of a [4+2] Annulation Method. *Angew. Chem. Int. Ed*. **2015**, *54*, 11424–11427.
[131] Wang, M.-M.; Waser, J. Oxidative Fluorination of Cyclopropylamides through Organic Photoredox Catalysis. *Angew. Chem. Int. Ed*. **2020**, *59*, 16420–16424.

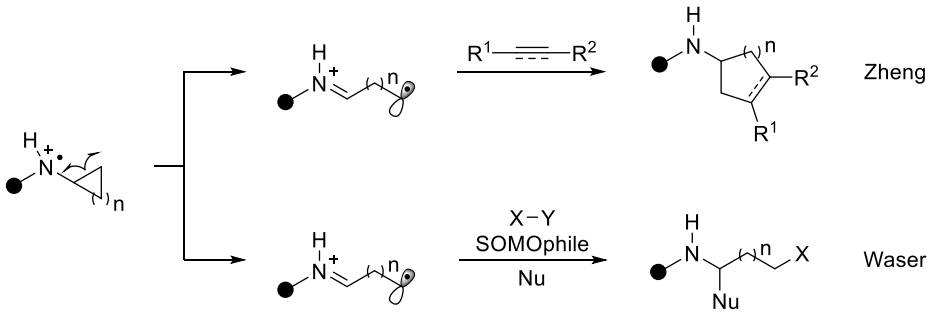

Scheme 2.19 Aminium radical and amidyl radical induced C–C bond cleavage.

The Stephenson group used aminium radical triggered C–C bond cleavage for the modification of amine substrates **2.20a** (Scheme 2.20).[132] In this reaction, photochemically generated radical cation **2.20f** undergoes C–C bond fragmentation to give ring-opened radical cation **2.20g**. This protocol was also applied in the semisynthesis of (−)-pseudotabersonine (**2.20c**), (−)-pseudovincadifformine (**2.20d**), and (+)-coronaridine (**2.20e**) in good yields.

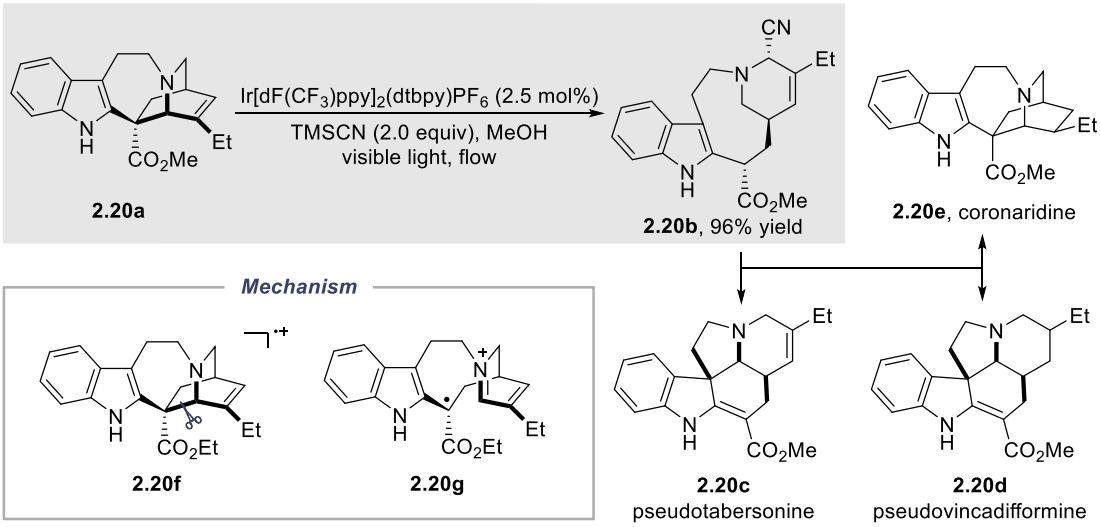

Scheme 2.20 Visible light-induced, amino cation-mediated C–C bond cleavage for the synthesis and modification of alkaloids.

2.1.2.2 Oxygen Radicals in C−C Bond Cleavage

Oxygen centered radicals — typically considered to be electrophilic, also exhibit great potential in inducing *β*-C–C bond fragmentation.[133] Given the high BDE value of O–H bonds (≈ 105 kcal/mol), the direct homolysis of alcoholic O–H bonds is

[132] Beatty, J. W.; Stephenson, C. R. J. Synthesis of (−)-Pseudotabersonine, (−)-Pseudovincadifformine, and (+)-Coronaridine Enabled by Photoredox Catalysis in Flow. *J. Am. Chem. Soc*. **2014**, *136*, 10270−10273.
[133] Bietti, M.; Lanzalunga, O.; Salamone, M. Structural Effects on the β-Scission Reaction of Alkoxyl Radicals. Direct Measurement of the Absolute Rate Constants for Ring Opening of Benzocycloalken-1-oxyl Radicals. *J. Org. Chem*. **2005**, *70*, 1417–1422.

problematic.[134] Consequently, at the early stage the generation of oxygen-centered radicals was mainly based on light or heating induced homolysis of relatively weak O–X, O–NO, or O–O bonds (Scheme 2.21).[135] Later on, conditions that involved using stoichiometric amounts of strong oxidants, along with a catalytic amount of Ag, Mn, or Cu catalysts were employed to produce alkoxy radicals. In recent years, photoredox catalysis has served as reductant to generate oxygen-centered radicals under mild conditions. Radical precursors containing O–N and O–I bonds such as *N*-alkoxyphthalimides were put into practice. Alternatively, advances in photochemistry have opened new avenues for alkoxy radical generation either through proton-coupled electron transfer (PCET) [136] or photoinduced metal-to-ligand charge transfer (MLCT)[137] directly from O–H bond providing catalytic access to alkoxy radicals.

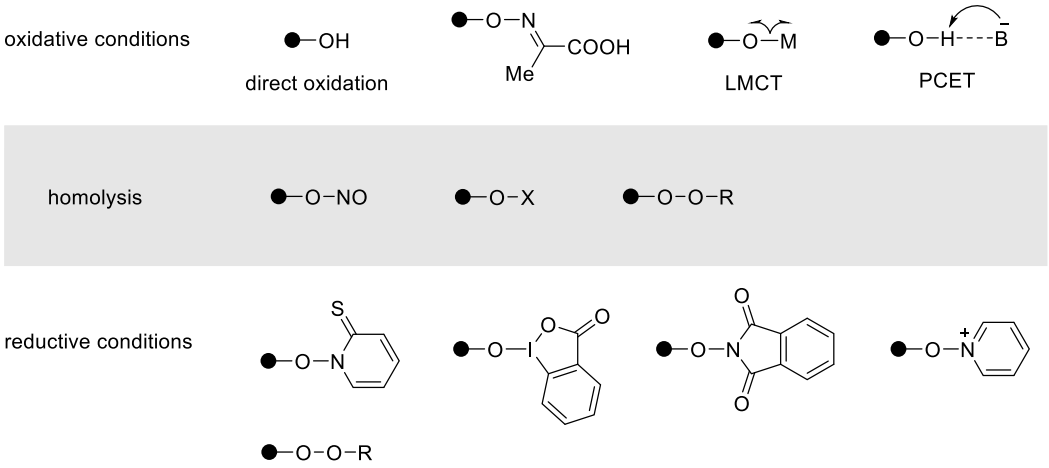

Scheme 2.21 Approaches for oxygen centered radicals generation.

Similarly to nitrogen centered radicals, C–C bond cleavage from oxygen-centered radical has also been driven by similar factors. For example, ring strain release (Scheme 2.22, *top*), the formation of conjugated system (carbonyl), or the generation of alkyl radicals (which are more stable than oxyl radicals).[138] Once generated, a cycloalkoxy

[134] (a) Tsui, E.; Wang, H.; Knowles, R. R. Catalytic Generation of Alkoxy Radicals from Unfunctionalized Alcohols. *Chem. Sci*. **2020**, *11*, 11124−11141. (b) El Gehani, A. A. M. A.; Maashi, H.; Harnedy, J.; Morrill, L. C. Electrochemical Generation and Utilization of Alkoxy Radicals. *Chem. Commun*. **2023**, *59*, 3655−3664. (c) Chang, L.; An, Q.; Duan, L.; Feng, K.; Zuo, Z. Alkoxy Radicals See the Light: New Paradigms of Photochemical Synthesis. *Chem. Rev*. **2022**, *122*, 2429−2486.

[135] Sheldon, R. A. *Synthesis and Uses of Alkyl Hydroperoxides and Dialkyl Peroxides*; Wiley, 1983.

[136] Yayla, H. G..; Wang, H.; Tarantino, K .T.; Orbe, H. S.; Knowles, R. R. Catalytic Ring-Opening of Cyclic Alcohols Enabled by PCET Activation of Strong O−H Bonds. *J. Am. Chem. Soc*. **2016**, *138*, 10794−10797.

[137] Guo, J.-J.; Hu, A.; Chen, Y.; Sun, J.; Tang, H.; Zuo, Z. Photocatalytic C−C Bond Cleavage and Amination of Cycloalkanols by Cerium(III) Chloride Complex. *Angew. Chem. Int. Ed*. **2016**, *55*, 15319–15322.

[138] (a) Wu, X.; Zhu, C. Recent Advances in Alkoxy Radical-Promoted C–C and C–H Bond Functionalization Starting from Free Alcohols. *Chem. Commun*. **2019**, *55*, 9747−9756. (b) Jia, K.; Chen, Y. Visible-Light-Induced Alkoxyl Radical Generation for Inert Chemical Bond

radical undergoes *β*-scission to form carbonyl group along with an alkyl radical, which could be intercepted by (1) SOMOphiles (e.g. DEAD, RSH, selectfluor etc); (2) Ag, Mn or Cu mediated C–X bond formation; (3) organometallic species for cross-coupling reactions (Scheme 2.22, *middle*). In the second scenario, stoichiometric amount of oxidant would push the M^n–X species to the high valent state (Ag^{III}–X, Mn^{V}–X, Cu^{III}–X). After SET oxidation an alkoxy radical is formed at the same time as the release of M^{n-1}–X. Reactions combining metal catalysts, X–Y reagents, and oxidants have enabled the groups of Narasaka,[139] Murakami,[140] Zhu,[141] Loh,[142] Duan,[143] Zhang,[144] and Lopp,[145] to achieve a wide range of deconstructive functionalization of cycloalkanols. Cross coupling reactions have been developed by Rueping and Yu,[146] who used metallaphotoredox in tandem with a nickel catalyst for C–C, and later copper for C–N forming reactions. Notably, acyclic alkoxyl radicals could also undergo *β*-scission to form alkyl radicals, though this process does not proceed as efficient as stained-ring containing substrates (Scheme 2.22, *bottom*).

Cleavage/Functionalization. *Chem. Commun*. **2018**, *54*, 6105−6112. (c) Murakami, M.; Ishida, N. *β*-Scission of Alkoxy Radicals in Synthetic Transformations. *Chem. Lett*. **2017**, *46*, 1692–1700.

[139] (a) Chiba, S.; Cao, Z.; El Bialy, S. A. A.; Narasaka, K. Generation of β-Keto Radicals from Cyclopropanols Catalyzed by $AgNO_3$. *Chem. Lett*. **2006**, *35*, 18–19. (b) Chiba, S.; Kitamura, M.; Narasaka, K. Synthesis of (−)-Sordarin. *J. Am. Chem. Soc*. **2006**, *128*, 6931–6937.

[140] Ishida, N.; Okumura, S.; Nakanishi, Y.; Murakami, M. Ring-opening Fluorination of Cyclobutanols and Cyclopropanols Catalyzed by Silver. *Chem. Lett*. **2015**, *44*, 821–823.

[141] (a) Zhao, H.; Fan, X.; Yu, J.; Zhu, C. Silver-Catalyzed Ring-Opening Strategy for the Synthesis of β- and γ-Fluorinated Ketones. *J. Am. Chem. Soc*. **2015**, *137*, 3490–3493. (b) Ren, R.; Zhao, H.; Huan, L.; Zhu, C. Manganese-Catalyzed Oxidative Azidation of Cyclobutanols: Regiospecific Synthesis of Alkyl Azides by C–C Bond Cleavage. *Angew. Chem. Int. Ed*. **2015**, *54*, 12692–12696. (c) Ren, R.; Wu, Z.; Xu, Y.; Zhu, C. C−C Bond-Forming Strategy by Manganese-Catalyzed Oxidative Ring-Opening Cyanation and Ethynylation of Cyclobutanol Derivatives. *Angew. Chem. Int. Ed*. **2016**, *55*, 2866–2869. (d) Fan, X.; Zhao, H.; Yu, J.; Bao, X.; Zhu, C. Regiospecific Synthesis of Distally Chlorinated Ketones via C–C bond Cleavage of Cycloalkanols. *Org. Chem. Front*. **2016**, *3*, 227–232. (e) Ren, R.; Wu, Z.; Zhu, C. Manganese-Catalyzed Regiospecific sp^3 C–S Bond Formation through C–C Bond Cleavage of Cyclobutanols. *Chem. Commun*. **2016**, *52*, 8160–8163.

[142] Ren, S.; Feng, C.; Loh, T.-P. Iron- or Silver-Catalyzed Oxidative Fluorination of Cyclopropanols for the Synthesis of β-Fluoroketones. *Org. Biomol. Chem*. **2015**, *13*, 5105–5109.

[143] Lu, S.-C.; Li, H.-S.; Xu, S.; Duan, G.-Y. Silver-Catalyzed C2-Selective Direct Alkylation of Heteroarenes with Tertiary Cycloalkanols. *Org. Biomol. Chem*. **2017**, *15*, 324–327.

[144] Huang, F.-Q.; Xie, J.; Sun, J.-G.; Wang, Y.-W.; Dong, X.; Qi, L.-W. Zhang, B. Regioselective Synthesis of Carbonyl-Containing Alkyl Chlorides via Silver-Catalyzed Ring-Opening Chlorination of Cycloalkanols. *Org. Lett*. **2016**, *18*, 684–687.

[145] Kananovich, D. G.; Konik, Y. A.; Zubrytski, D. M.; Jarvinga, I.; Lopp, M. Simple Access to β-Trifluoromethyl-Substituted Ketones *via* Copper-Catalyzed Ring-Opening Trifluoromethylation of Substituted Cyclopropanols. *Chem. Commun*. **2015**, *51*, 8349–8352.

[146] (a) Huang, L.; Ji, T.; Rueping, M. Remote Nickel-Catalyzed Cross-Coupling Arylation via Proton-Coupled Electron Transfer-Enabled C–C Bond Cleavage. *J. Am. Chem. Soc*. **2020**, *142*, 3532–3539. (b) Ge, Y.; Shao, Y.; Wu, S.; Liu, P.; Li, J.; Qin, H.; Zhang, Y.; Xue, X.; Chen, Y. Distal Amidoketone Synthesis Enabled by Dimethyl Benziodoxoles via Dual Copper/Photoredox Catalysis. *ACS Catal*. **2023**, *13*, 3749−3756.

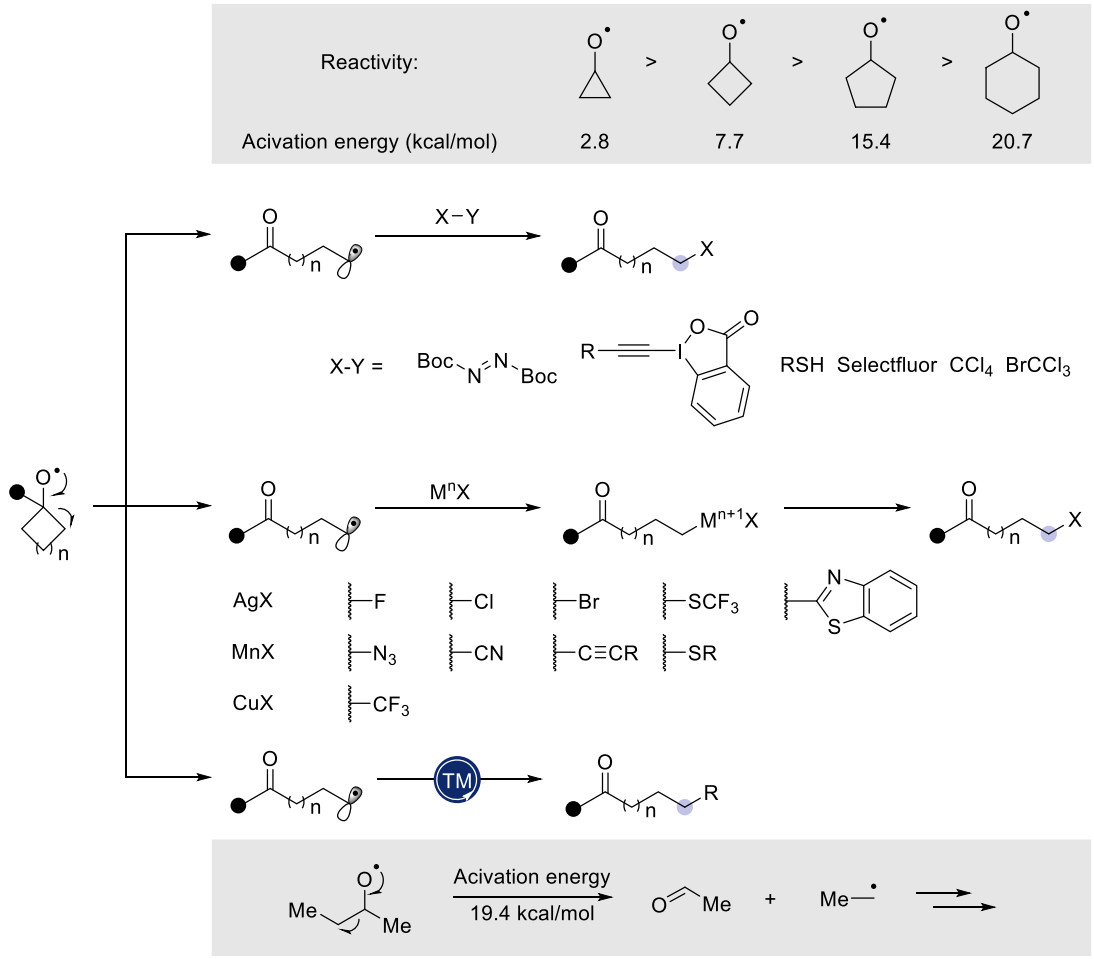

Scheme 2.22 oxygen centered radical induced C–C bond cleavage.

Zuo and co-workers reported an example of LMCT enabled oxygen centered radical generation involving a C(sp^2)–C(sp^3) cross-coupling reaction via oxygen radical induced C–C bond cleavage (Scheme 2.23).[147] The combination of cerium catalysis with nickel catalyst exhibited a wide range of substrate applicability, including numerous alcohols and aromatic halides. The author proposed that the coordination of the alcohol with a cerium benzoate complex is followed by photoinduced electron transfer with DPA ($E[^*\text{DPA}/\text{DPA}^{\bullet-}]$) = +1.19 V vs SCE in DMSO) generating a photoactive Ce(IV) alkoxide species **2.23j**. Under light irradiation, one electron of the higher lying alkoxide ligand orbital will be promoted to the empty *4f* orbital of cerium, resulting in the homolysis of the Ce–O bond. Homolysis of the Ce–O bond leads to the generation of Ce(III) benzoate **2.23i** and alkoxy radical, which undergoes *β*-scission to form alkyl radicals **2.23k**. The oxidative addition complex of nickel **2.23m** captures the alkyl radical forming a Ni(III) complex **2.23n**. This complex undergoes reductive

147 Chen, Y.; Wang, X.; He, X.; An, Q.; Zuo, Z. Photocatalytic Dehydroxymethylative Arylation by Synergistic Cerium and Nickel Catalysis. *J. Am. Chem. Soc*. **2021**, *143*, 4896–4902.

elimination to deliver the dehydroxymethylative arylation product **2.23c** along with the Ni(I) **2.23o**, which is SET reduced by DPA anion afterwards.

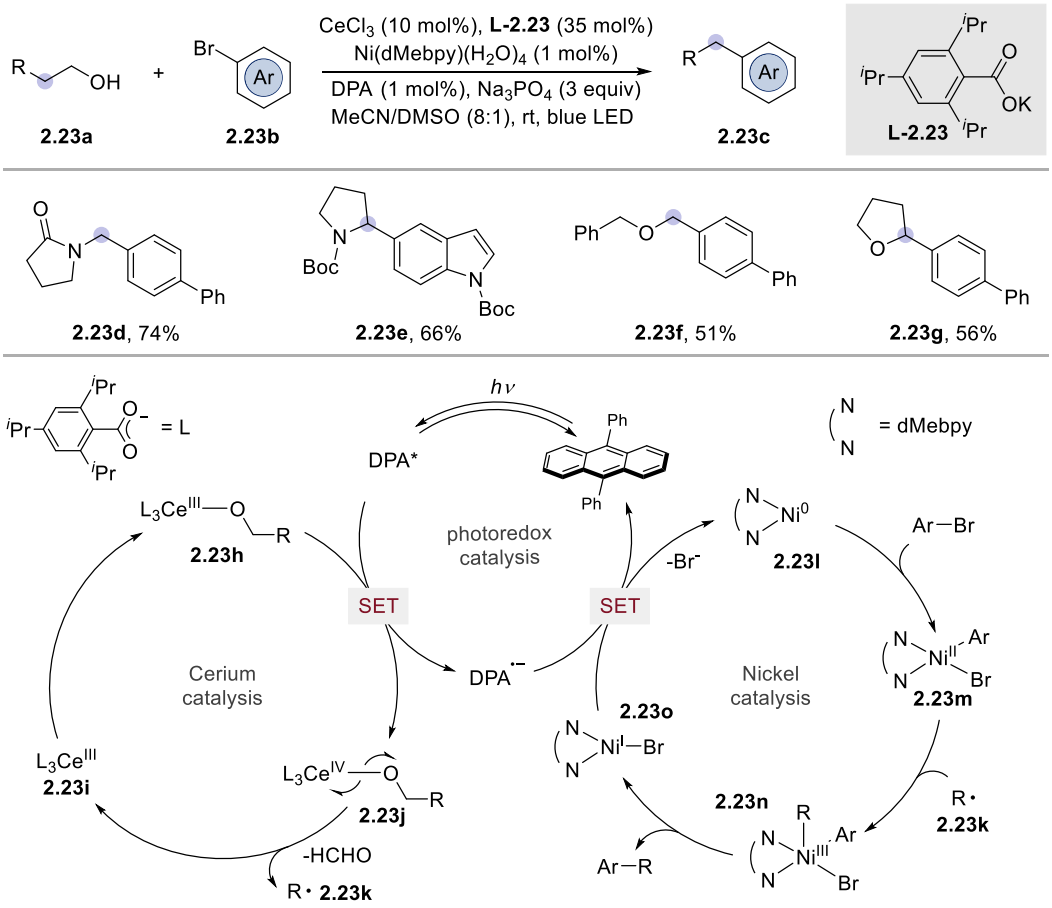

Scheme 2.23 Nickel-catalyzed dehydroxymethylarylation via LMCT.

2.1.2.3 C−C Bond Cleavage Using Pro-aromatic Substrates

As discussed before, radical induced C–C bond fragmentation process often requires driving forces such as ring strain relief or the formation of conjugated systems. As one of the most stable conjugated structures, aromatic molecules are commonly used in group transfer reactions as a driving force in organic synthesis not only in radical type transformations but also in polar reactions.[148] However, the strategy of using pro-aromatic compounds as reagents for group transfer reactions is not new and its roots can be found in nature. In biological transformations, reduced nicotinamide adenine dinucleotide (NADH) and the nicotinamide adenine dinucleotide phosphate (NAD^+) act as hydride donor/acceptor cofactors (scheme 2.24).[149]

[148] Walker, J. C. L.; Oestreich, M. Ionic Transfer Reactions with Cyclohexadiene-Based Surrogates. *Synlett* **2019**, *30*, 2216–2232.
[149] Walsh, C.T.; Tu, B. P.; Tang, Y. Eight Kinetically Stable but Thermodynamically Activated Molecules that Power Cell Metabolism. *Chem. Rev*. **2018**, *118*, 1460–1494.

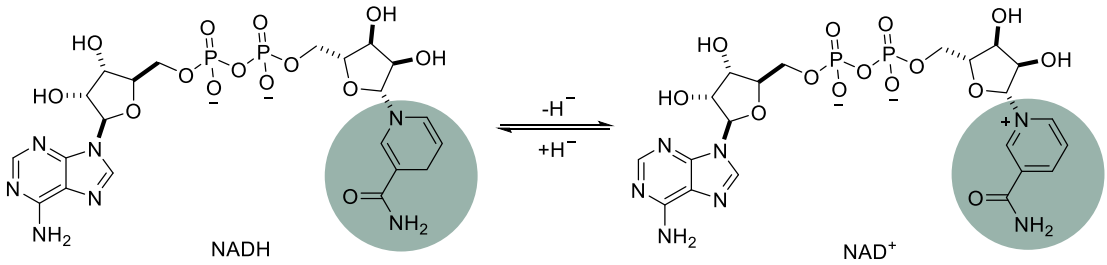

Scheme 2.24 Hydride shuttle system in biological systems.

4-Substituted Hantzsch esters, which could be easily prepared from aldehydes in a single step, could act as alkyl, acyl, and amidyl radical precursors driven by the pyridine byproduct generation and were successfully used a series of radical type transformations (Scheme 2.25).[150] In 2014, Tang and co-workers utilized 4-substituted Hantzsch esters as alkyl radical precursor for Giese-type reactions.[151] This was followed up by Nishibayashi,[152] Molander,[153] Yu[154] and others who used Hantzsch esters as radical precursors in metallaphotoredox catalyzed cross-coupling reactions and allylic substitution reactions.

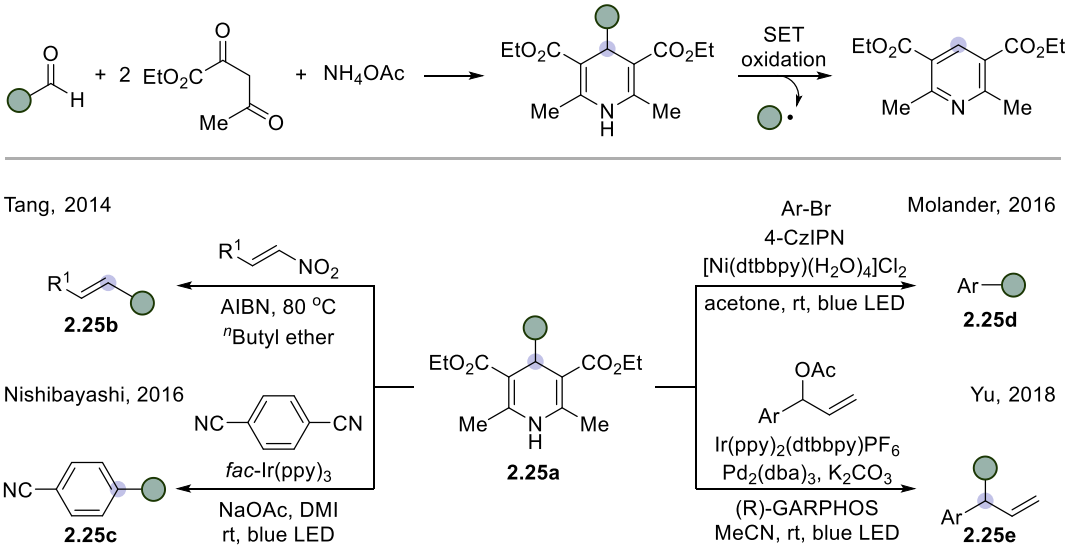

[150] Ye, S.; Wu, J. 4-Substituted Hantzsch Esters as Alkylation Reagents in Organic Synthesis. *Acta Chimica Sinica*. **2019**, *77*, 814–831.
[151] Li, G.; Wu, L.; Lv, G.; Liu, H.; Fu, Q.; Zhang, X.; Tang, Z. Alkyl Transfer from C–C Cleavage: Replacing the Nitro Group of Nitro-Olefins. *Chem. Commun*. **2014**, *50*, 6246–6248.
[152] Nakajima, K.; Nojima, S.; Sakata, K.; Nishibayashi, Y. Visible-Light-Mediated Aromatic Substitution Reactions of Cyanoarenes with 4-Alkyl-1,4-dihydropyridines through Double Carbon–Carbon Bond Cleavage. *ChemCatChem* **2016**, *8*, 1028–1032.
[153] Gutiérrez-Bonet, Á.; Tellis, J. C.; Matsui, J. K.; Vara, B. A. Molander, G. A. 1,4-Dihydropyridines as Alkyl Radical Precursors: Introducing the Aldehyde Feedstock to Nickel/Photoredox Dual Catalysis. *ACS Catal*. **2016**, *6*, 8004–8008.
[154] Zhang, H.-H.; Zhao, J.-J.; Yu, S. Enantioselective Allylic Alkylation with 4-Alkyl-1,4-dihydropyridines Enabled by Photoredox/Palladium Cocatalysis. *J. Am. Chem. Soc*. **2018**, *140*, 16914–16919.

Scheme 2.25 Visible light-induced, amino cation-mediated C−C bond cleavage for the synthesis and modification of alkaloids.

In 2021, Luo's group disclosed an nickel-catalyzed dealkenylative cross-coupling reactions enabled by the formation of 4-alkyl-1,4-dihydropyridazine, which can be obtained by the Hetero-Diels-Alder reaction of alkene and tetrazine (Scheme 2.26).[155] According to the proposed mechanism, upon 390 nm photoexcitation, the 4-alkyl-1,4-dihydropyridazine **2.26a** undergoes homolysis to generate an alkyl radical **2.26e** and intermediate **2.26d**. Subsequently, the alkyl radical **2.26e** can be intercepted by Ni(I) complex **2.26h** to afford Ni(II) species **2.26i**. This is followed by SET reduction by intermediate **2.26c** to form akyl Ni(I) complex **2.26f**. Species **2.26f** reacts with aryl halides to form aryl-Ni(III)-alkyl complex **2.26g**, which sequentially undergoes reductive elimination to provide cross-coupling product and reforms the Ni(I) catalyst **2.26h**.

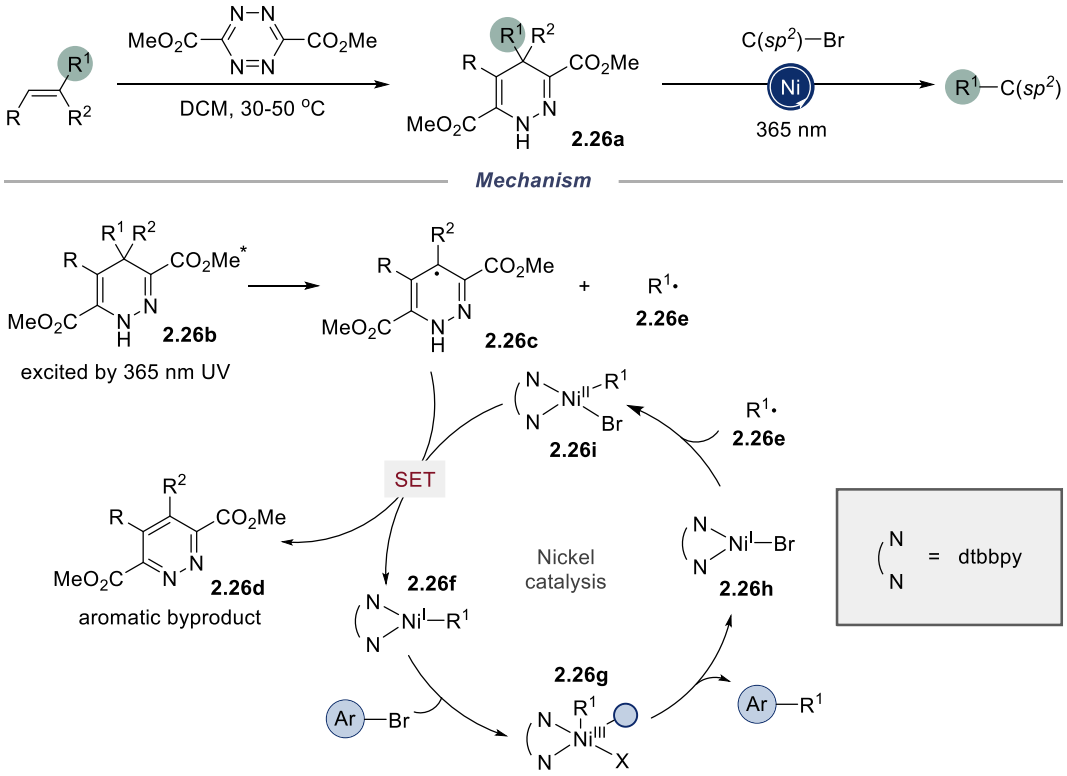

Scheme 2.26 Dealkenylative Ni-catalyzed cross-coupling enabled by 4-alkyl-1,4-dihydropyridazine and photoexcitation.

Ketones are one of the most abundant feedstocks in organic synthesis, while the C–C bond activation of ketones typically relied on transition metal catalysis under harsh

[155] Chen, S.-C.; Zhu, Q.; Cao, Y.; Li, C.; Guo, Y.; Kong, L.; Che, J.; Guo, Z.; Chen, H.; Zhang, N.; Fang, X.; Lu, J.-T.; Luo, T. Dealkenylative Ni-Catalyzed Cross-Coupling Enabled by Tetrazineand Photoexcitation. *J. Am. Chem. Soc*. **2021**, *143*, 14046–14052.

conditions (section 2.1.1). In recent years, C–C bond activation enabled by aromatization of a pro-aromatic intermediate has emerged as an effective approach to functionalize ketone under mild conditions (Scheme 2.27).[156] In 2019 Aliyama and co-workers demonstrated the substituted benzothiazolines could be used as alkyl radical transfer reagents under photoredox catalysis.[157] Dong and co-workers transferred aliphatic ketones into pyrazoles and triazoles, and realized a series of deacylative transformations, which otherwise would be challenging with conventional transition metal catalyzed C–C bond activation techniques.[158] Zhu and co-workers demonstrated that dihydroquinazolinone derivatives acted as alkyl radical precursors for Geise type reaction.[159] Dihydroquinazolinone derivatives could be prepared by one step condensation from ketone and 2-aminobenzamide.

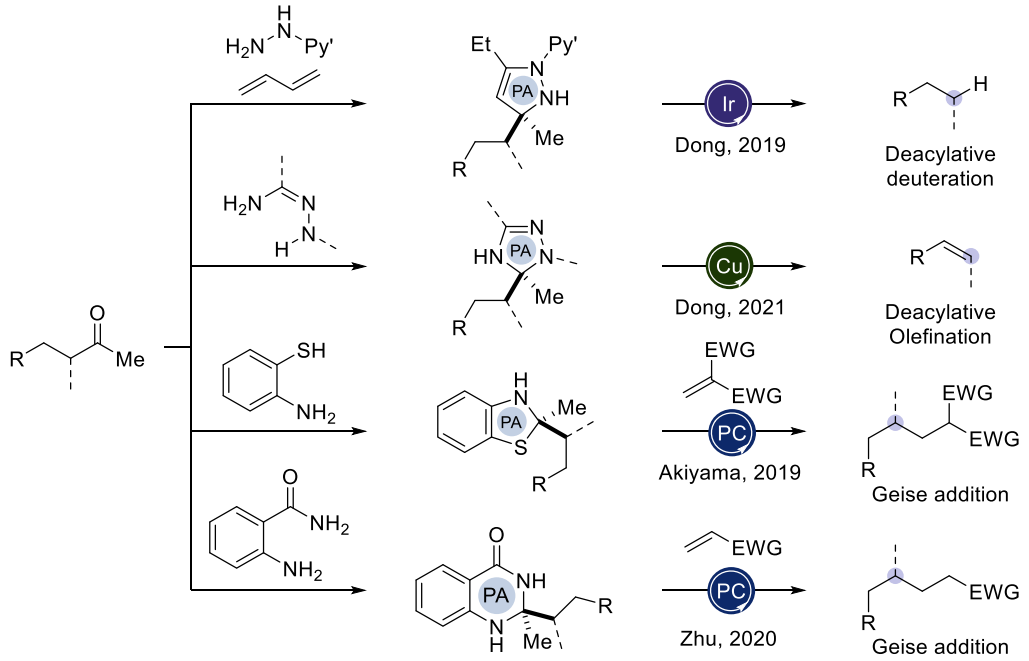

[156] Bhunia, A.; Studer, A. Recent Advances in Radical Chemistry Proceeding through Pro-aromatic Radicals. *Chem* **2021**, *7*, 1–14.

[157] Uchikura, T.; Moriyama, K.; Toda, M.; Mouri, T.; Ibanez, L.; Akiyama, T. Benzothiazolines as Radical Transfer Reagents: Hydroalkylation and Hydroacylation of Alkenes by Radical Generation under Photoirradiation Conditions. *Chem. Commun*. **2019**, *55*, 11171–11174.

[158] (a) Xu, Y.; Qi, X.; Zheng, P.; Berti, C. C.; Liu, P.; Dong, G. Deacylative Transformations of Ketones via Aromatization-Promoted C–C Bond Activation. *Nature* **2019**, *567*, 373–378. (b) Zhou, X.; Xu, Y.; Dong, G. Deacylation-Aided C–H Alkylative Annulation through C–C Cleavage of Unstrained Ketones. *Nat Catal* **2021**, *4*, 703–710. (c) Zhou, X.; Xu, Y.; Dong, G. Olefination via Cu-mediated Dehydroacylation of Unstrained Ketones. *J. Am. Chem. Soc*. **2021**, *143*, 20042–20048. (d) Zhou, X.; Yu, T.; Dong, G. Site-Specific and Degree-Controlled Alkyl Deuteration via Cu-Catalyzed Redox-Neutral Deacylation. *J. Am. Chem. Soc*. **2022**, *144*, 9570–9575. (e) Zhou, X.; Pyle, D.; Zhang, Z.; Dong, G. Deacylative Thiolation by Redox-Neutral Aromatization-Driven C−C Fragmentation of Ketones. *Angew. Chem. Int. Ed*. **2023**, *62*, e202213691.

[159] Li, L.; Fang, L.; Wu, W.; Zhu, J. Visible-Light-Mediated Intermolecular Radical Conjugate Addition for the Construction of Vicinal Quaternary Carbon Centers. *Org. Lett*. **2020**, 22, 5401–5406.

Scheme 2.27 Activation of unstrained aliphatic ketone enabled by proaromatic precursors.

C–C bond fragmentation could also be triggered by carbon-centered radicals and other transient species. However, these examples will not be discussed here due to their limited relevance to the work described in the thesis.

2.1.3 Metallaphotoredox Catalyzed C(sp^3)–C(sp^3) Cross-Coupling Reactions

The development of photoredox catalysis has allowed chemists to access alkyl radicals from various radical precursors. Transition metal catalysts have been instrumental to expanding the reactivity of radicals beyond classical reactions such as the Giese, Minisci additions. In 2016, MacMillan and co-workers described the first Ni/photoredox dual-catalyzed C(sp^3)–C(sp^3) cross-coupling of carboxylic acids with alkyl halides.[160] Further examples of metallaphotoredox catalyzed C(sp^3)–C(sp^3) cross-coupling reactions have been demonstrated by Fensterbank,[161] Martin,[162] Rovis,[163] Leonori[164], Konig[165] and others[166] (scheme 2.28). This mechanistically distinct strategy allows the cross-coupling reactions to be performed under mild conditions with broad functional group tolerance. Although the alkyl radical used in such cross-coupling reactions can be generated from many different functional groups, these protocols proceed with similar mechanism. Specifically, Ni(0) undergoes oxidative addition with alkyl/aryl halides and the resulting oxidative addition complex captures an alkyl radical to form a Ni(III) complex. Reductive elimination of the Ni(III) complex forms the cross coupling product and Ni(I). Ni(0) is recovered through

[160] Johnston, C. P.; Smith, R. T.; Allmendinger, S.; McMillan, D. W. C. Metallaphotoredox-Catalysed sp^3–sp^3 Cross-Coupling of Carboxylic Acids with Alkyl Halides. *Nature* **2016**, *536*, 322–325.

[161] Lévêque, C.; Corcé, V.; Chenneberg, L.; Ollivier, C.; Fensterbank, L. Photoredox/Nickel Dual Catalysis for the C(sp^3)–C(sp^3) Cross-Coupling of Alkylsilicates with Alkyl Halides. *Eur. J. Org. Chem*. **2017**, 2118–2121.

[162] Shen, Y.; Gu, Y. sp^3 C–H Arylation and Alkylation Enabled by the Synergy of Triplet Excited Ketones and Nickel Catalysts. *J. Am. Chem. Soc*. **2018**, *140*, 12200–12209.

[163] Ashley, M.; Rovis, T. Photoredox-Catalyzed Deaminative Alkylation via C–N Bond Activation of Primary Amines. *J. Am. Chem. Soc*. **2020**, *142*, 18310–18316.

[164] Dauncey, E. D.; Dighe, S. U.; Douglas, J. J.; Leonori. D. A Dual Photoredox-Nickel Strategy for Remote Functionalization via Iminyl Radicals: Radical Ring-Opening-Arylation, -Vinylation and -Alkylation Cascades. *Chem. Sci*. **2019**, *10*, 7728-7733.

[165] Santos, M. S.; Corrêa, A. G.; Paixão, M. W.; König, B. C(sp^3)–C(sp^3) Cross-Coupling of Alkyl Bromides and Ethers Mediated by Metal and Visible Light Photoredox Catalysis. *Adv. Synth. Catal*. **2020**, *362*, 2367.

[166] Zheng, S.; Hu, Y.; Yuan, W. Recent Advances in C(sp^3)–C(sp^3) Cross-Coupling via Metallaphotoredox Strategies. *Synthesis* **2021**, *53*, 1719–1733.

reduction with a photocatalyst.

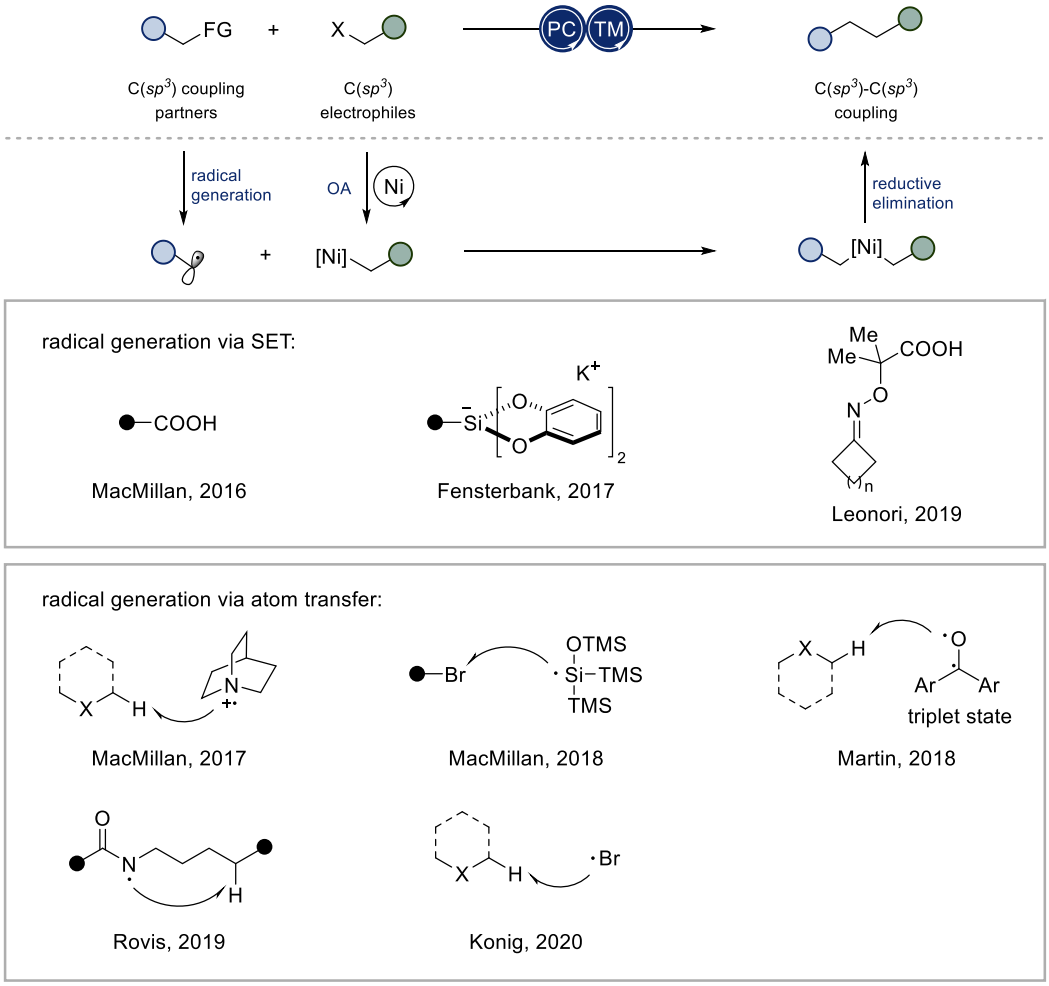

Scheme 2.28 Metallaphotoredox catalyzed C(sp^3)–C(sp^3) cross-coupling reactions.

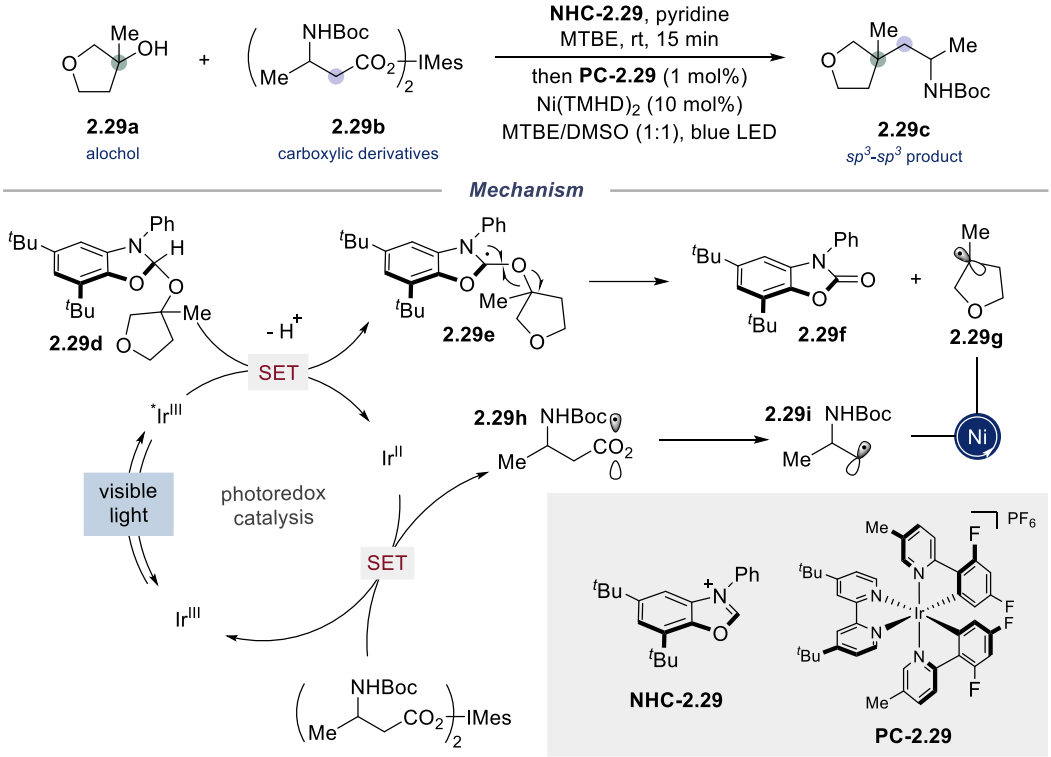

Scheme 2.29 Nickel metallaphotoredox catalyzed C(sp^3)–C(sp^3) cross-coupling of alcohols and carboxylic acids.

An alternative approach was disclosed by MacMillan and co-workers, who realized a nickel metallaphotoredox catalyzed C(sp^3)–C(sp^3) formation utilizing alcohols and carboxylic acids.[167] First, the carboxylic acid is premixed with iodomesitylene diacetate to afford the activated iodonium dicarboxylate **2.29b**, which could be used directly without additional purification.[168] The condensation of alcohol **2.29a** with benzoxazolium salt **NHC-2.29** to form a proaromatic NHC-alcohol adduct **2.29d** under basic conditions.[169] The excited-state Ir complex (E[*Ir(III)/Ir(II)] = +0.77 V vs. SCE) oxidizes the nitrogen atom of aniline via a SET mechanism. The C–H bond adjacent to the resulting nitrogen radical cation is significantly weakened and more acidic (pka ≈ 10).[170] Hence, it can be deprotonated with a base to yield an α-amino radical **2.29e**. The carbon-centered radical **2.29e** undergoes rapid β-scission to give carbamate **2.29f**, and deoxygenated alkyl radical **2.29g**. The aromatized carbamate

[167] Sakai, H. A.; MacMillan, D. W. C. Nontraditional Fragment Couplings of Alcohols and Carboxylic Acids: C(sp^3)–C(sp^3) Cross-Coupling via Radical Sorting. *J. Am. Chem. Soc*. **2022**, *144*, 6185–6192.
[168] Zhang, X.; Smith, R. T.; Le, C.; McCarver, S. J.; Shireman, B. T.; Carruthers, N. I.; MacMillan, D. W. C. Copper-Mediated Synthesis of Drug-Like Bicyclopentanes. *Nature* **2020**, *580*, 220−226.
[169] Dong, Z.; MacMillan, D. W. C. Metallaphotoredox-Nnabled Deoxygenative Arylation of Alcohols. *Nature* **2021**, *598*, 451−456.
[170] Dinnocenzo, J.P.; Banach, T. E. Deprotonation of Tertiary Amine Cation Radicals. A Direct Experimental Approach. *J. Am. Chem. Soc*. **1989**, *111*, 8646–8653.

byproduct possessing a strong C=O double bond provides the thermodynamic driving force for alcohol C–O bond homolysis. Concurrently, reduction of the preformed iodonium dicarboxylate **2.29b** affords the acid-derived radical **2.29i** along with the Ir(III) photocatalyst. The alkyl radical **2.29g** and **2.29i** coupling is mediated by nickel catalysis by means of sequential radical capture, however the exact mechanism is unclear.

2.2 General Aim of the Project

Ketones are one of most widely used synthetic feedstocks in organic synthesis due to their extensive availability, high reactivity, and relative stability. Early synthetic manipulation of aliphatic ketones generally relies on the electrophilicity of the carbonyl carbon or the nucleophilicity of the enolate. As demonstrated in introduction section, the cleavage of ketone α C–C bonds by means of transition metal catalyzed C–C bond activation or radical induced C–C bond scission to forge new functionalities had made significant progress. While a general protocol for using unstrained ketones as cross-coupling partner is still in need.

Convinced by the feasibility and modulability of transferring aliphatic ketones into proaromatic structures, we wondered if we could develop a metallaphotoredox catalyzed platform to enable ketones derived dihydroquinazolinones as adaptive C(sp^3) coupling handles in the C(sp^2)–C(sp^3) and C(sp^3)–C(sp^3) cross-coupling reactions. Such a technique would hold promise to provide a practical pathway to harness ketones for diverse transition metal catalyzed-functionalization reactions, offering a referential sample for designing radical induced C–C bond functionalization reactions.

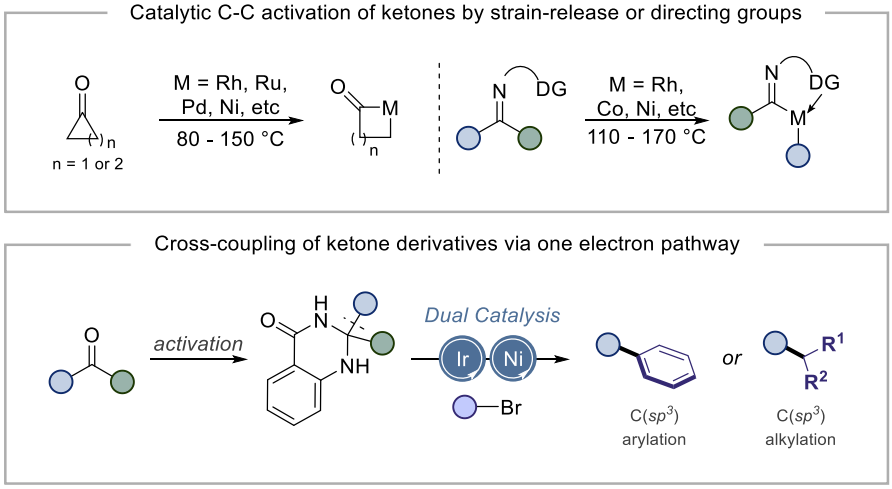

Scheme 2.30 Ketone as adaptive sp^3 handles in metallaphotoredox catalyzed arylation and alkylation events.

2.3 Optimization

A detailed description of our proposal for harnessing ketone as cross-coupling partner in nickel metallaphotoredox catalyzed arylations and alkylations event is outlined in Scheme 2.31. We anticipated that the excited photocatalyst could SET oxidize dihydroquinazolinone **2.31a**, generating a nitrogen centered radical, followed by C–C bond cleavage to provide a carbon centered radical **2.31c**. The overall process is driven forward by the formation of aromatic byproduct **2.31b**. The alkyl radical **2.31c** would be captured by aryl-Ni(II) complex **2.31f**, derived from oxidative addition of aryl halides to Ni(0) **2.31e**, leading to aryl-Ni(III)-alkyl species **2.31g**. Reductive elimination of Ni(III) **2.31g** would release cross-coupling product along with Ni(I) **2.31d**, which would be further reduced by photocatalyst to close both catalytic cycles.

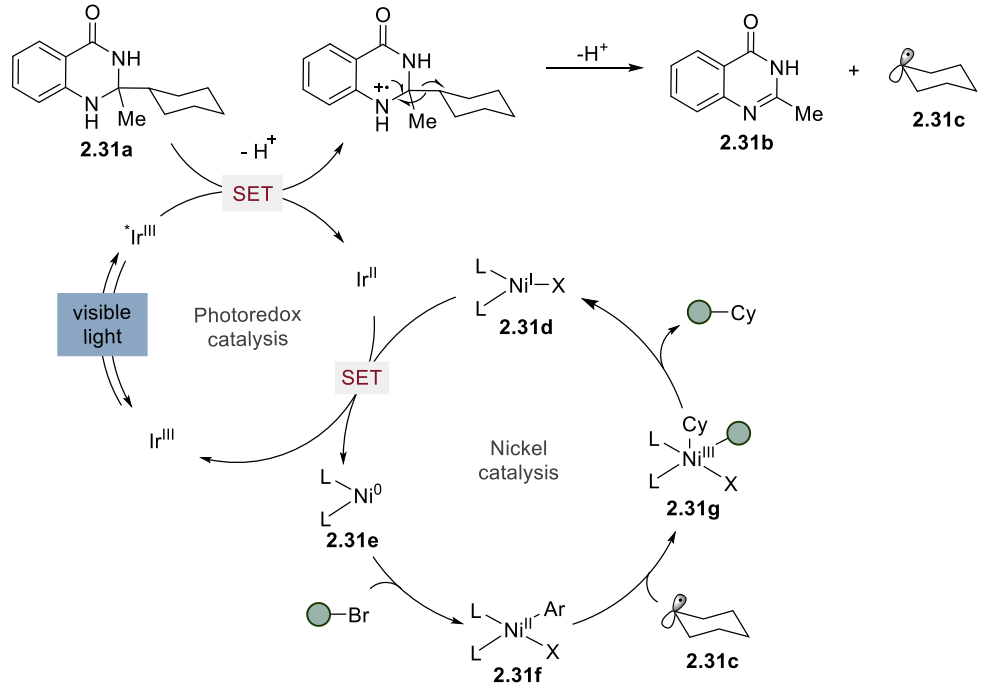

Scheme 2.31 Ketone as cross-coupling handles: reaction proposal.

We started our study by choosing dihydroquinazolinone 2a as the standard substrate. This substrate was formed through one step condensation from methyl cyclohexyl ketone with 2-aminobenzamide. The initial optimization studies focused on screening a variety of ligands, as the ligand plays crucial role in modulating the properties of the metal catalyst. As judged by the knowledge acquired in the field, redox non-innocent nitrogen ligands are commonly employed in metallaphotoredox catalyzed reactions, as these ligands might modulate the multiple oxidation state of the nickel center, promoting radical involvement in catalytic processes.[171] As shown in Table 2.1,

[171] Hu, X. Nickel-Catalyzed Cross Coupling of Non-activated Alkyl Halides: A Mechanistic

a series of bidentate nitrogen ligands were tested in the reactions (**L1**–**L8**), resulting in the product formation in low yields. Specifically, we found that terpyridine ligand was particularly effective for this transformation (**L9**–**L13**). In the terpyridine series, inferior results were obtained for terpyridine ligands having electro-withdrawing group on the pyridine backbone or substitutes adjacent to the coordinating nitrogen. Among all the terpyridine ligands series, *tert*-butyl substituted **L11** provided the best result, affording the cross-coupling product **3a** in 86% yield. The better performance of **L11** over **L13** might result from blocking some side reactions (homodimerization, etc.) initiated by radicals at the terpyridine backbone.[172] The use of other tridentate nitrogen ligand (**L14**–**L16**) or even tetradentate nitrogen ligand **L17** bearing different substitutes led to lower yields. Under limited number of detections, no methylation product derived from **1a** was detected, probably due to thermodynamic stability of cyclohexyl radical over methyl radical in reaction system.

Perspective. *Chem. Sci*. **2011**, *2*, 1867–1886.

[172] Dugan, T. R.; Bill, E.; MacLeod, K. C.; Christian, G. J.; Cowley, R. E.; Brennessel, W. W.; Ye, S.; Neese, F.; Holland, P. L. Reversible C–C Bond Formation Between Redox-Active Pyridine Ligands in Iron Complexes. *J. Am. Chem. Soc.* **2012**, *134*, 20352–20364.

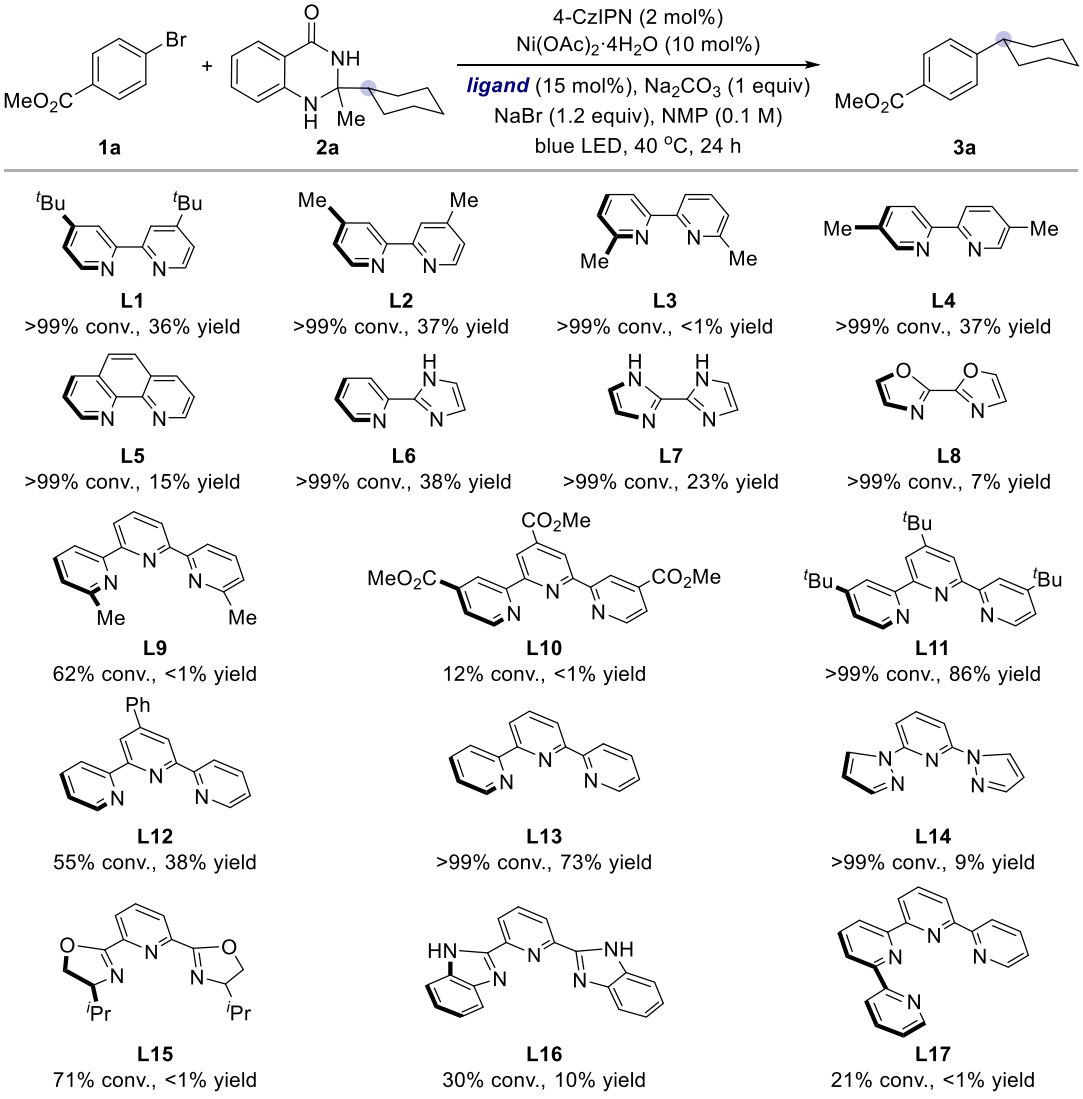

[a] Conditions: **1a** (0.10 mmol), **2a** (0.12 mmol), $Ni(OAc)_2·4H_2O$ (10 mol%), ligand (15 mol%), 4-CzIPN (2 mol%), NaBr (0.12 mmol), Na_2CO_3 (0.10 mmol) in NMP (0.10 M) under blue LED irradiation at 40 °C for 24 h. [b] GC yield and conversion using dodecane as internal standard.

Table 2.1 Screening of ligands.

With terpyridine **L11** as the optimal ligand, we next examined the effect of photocatalyst. As shown in Table 2.2, the utilization of a series of iridium-based photocatalysts proved to be effective for turning over the catalytic cycle, giving the rise to **3a** in excellent yields (69–99% yield). While good yields were obtained with organic photocatalyst, ruthenium-based photocatalyst $[Ru(bpy)_3]PF_6$ failed to provide any targeted product. Although it has not been completely clear what photophysical properties and redox potential were sufficient to drive the catalytic cycle, a suitable redox potential of photocatalyst to reduce Ni(I) might be crucial for success ($E[Ni(I)/Ni(0)] \approx -1.11$ V vs SCE). 4-CzIPN was chosen as the optimal photocatalyst for the following optimization, due to the availability of photocatalyst and reproducibility of the reactions.

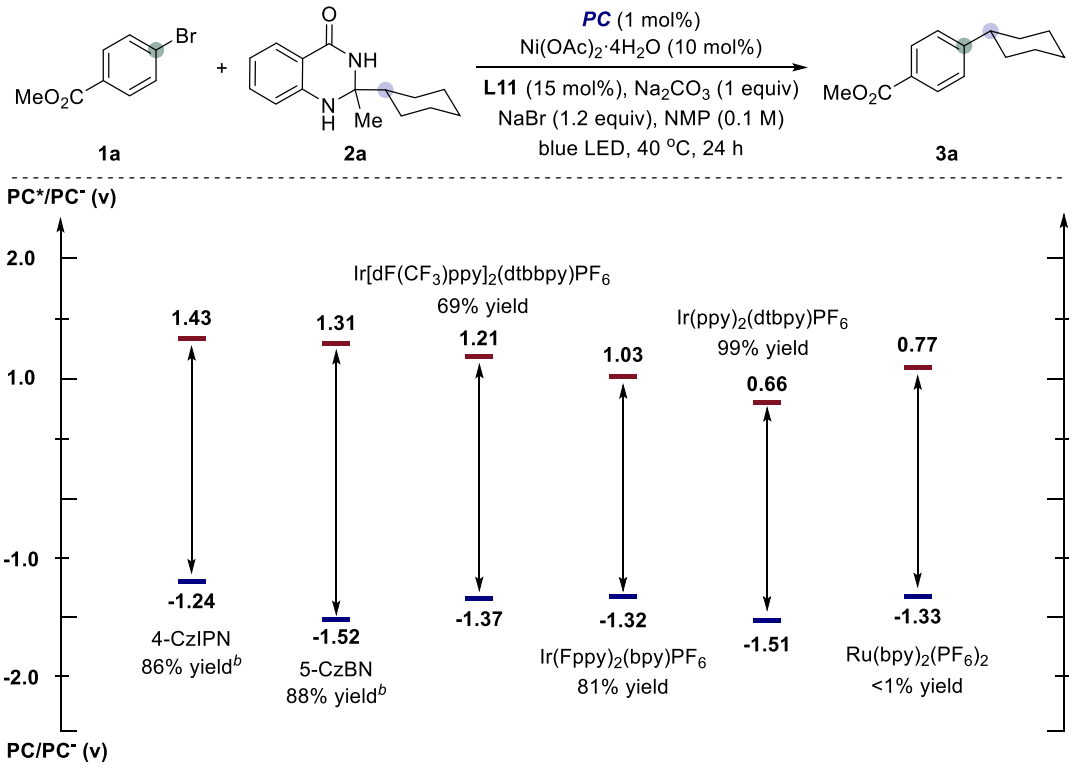

[a] Conditions: **1a** (0.10 mmol), **2a** (0.12 mmol), $Ni(OAc)_2·4H_2O$ (10 mol%), **L11** (15 mol%), PC (1 mol%), NaBr (0.12 mmol), Na_2CO_3 (0.10 mmol) in NMP (0.10 M) under blue LED irradiation at 40 °C for 24 h. [b] 2 mol% PC was used. [c] GC yield and conversion using dodecane as internal standard.

Table 2.2 Screening of photocatalysts.

Utilizing 4-CzIPN as photocatalyst, the influence of nickel precatalyst was investigated afterwards. Indicated by Table 2.3, the reaction worked better with Ni(II) precatalysts instead of $Ni(COD)_2$, as a series of Ni(II) precatalysts could provide **3a** in good yields (>78%). $Ni(COD)_2$ provided the product in lower yield (61%), might due to the competition binding risen from COD or its sensitivity to moisture. Considering the involvement of Ni(0) in the catalytic cycle, the Ni(0) species may be generated *in situ* by reduction with the photocatalyst and **2a** as sacrificial reductant. $Ni(OAc)_2·4H_2O$ was chosen as the nickel precatalyst for the following optimization studies, for its commercial availability and the reaction efficiency it could promote. During the screening of the optimized reaction conditions, dehalogenation product **1a'** was identified as the major side product, which may be rationalized by light induced aryl radical generation.[173]

[173] Shields, B. J.; Kudisch, B.; Scholes, G. D.; Doyle, A. G. Long-Lived Charge-Transfer States of Nickel(II) Aryl Halide Complexes Facilitate Bimolecular Photoinduced Electron Transfer. *J. Am. Chem. Soc.* **2018**, *140*, 3035–3039.

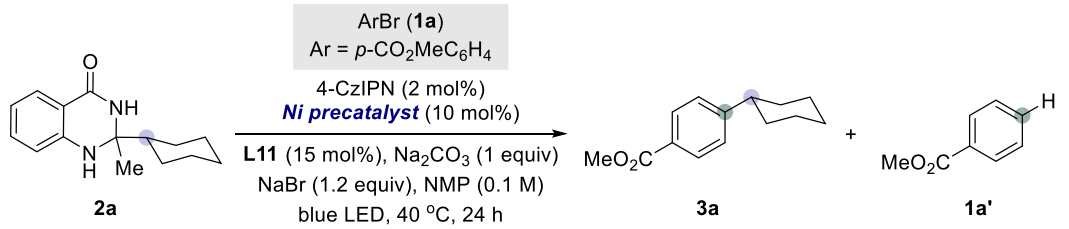

entry	Ni precatalyst	conversion (%)[a]	**3a** (%)[b]	**1a'** (%)[b]
1	$Ni(acac)_2$	>99	78	18
2	$NiBr_2$·diglyme	>99	83	6
3	$NiBr_2$·DME	>99	82	5
4	$NiCl_2$·DME	>99	92	6
5	$Ni(COD)_2$	79	61	7
6	$Ni(OAc)_2·4H_2O$	>99	88	9
7	$NiCl_2·6H_2O$	>99	86	8
8	$Ni(BF_4)_2·6H_2O$	>99	80	9
9	$Ni(NO_3)_2·6H_2O$	>99	83	6
10	$Ni(ClO_4)_2·6H_2O$	>99	88	6

[a] Conditions: **1a** (0.10 mmol), **2a** (0.12 mmol), Ni precatalyst (10 mol%), **L11** (15 mol%), 4-CzIPN (2 mol%), NaBr (0.12 mmol), Na_2CO_3 (0.10 mmol) in NMP (0.10 M) under blue LED irradiation at 40 °C for 24 h. [b] GC yield and conversion using dodecane as internal standard.

Table 2.3 Screening of nickel precatalysts.

Next we assessed the role exerted by the base. A screening of commonly used bases showed that the use of sodium carbonate was more effective than others (entry 2), giving **3a** in 83% yield. Stronger base including sodium methoxide (entry 8) and potassium *tert*-butoxide (entry 9) gave high conversions but lower yields of **3a** due to unidentified side reactions.

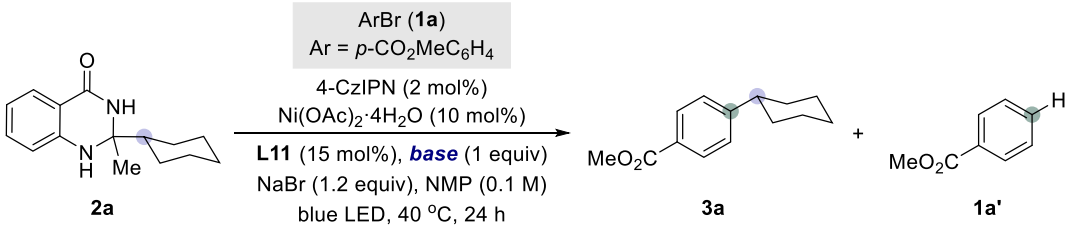

entry	base	conversion (%)[a]	**3a** (%)[b]	**1a'** (%)[b]
1	Cs_2CO_3	>99	78	12
2	Na_2CO_3	>99	83	8
3	$NaHCO_3$	>99	81	10
4	K_3PO_4	>99	81	16
5	Na_2HPO_4	>99	69	20
6	NaH_2PO_4	>99	63	31
7	NaOAc	>99	84	13
8	NaOMe	90	2	42
9	^{t}BuOK	>99	<1	28

[a] Conditions: **1a** (0.10 mmol), **2a** (0.12 mmol), $Ni(OAc)_2·4H_2O$ (10 mol%), **L11** (15 mol%), 4-CzIPN (2 mol%), NaBr (0.12 mmol), base (0.10 mmol) in NMP (0.10 M) under blue LED irradiation at 40 °C for 24 h. [b] GC yield and conversion using dodecane as internal standard.

Table 2.4 Screening of bases.

As shown in Table 2.5, good yields were obtained when utilizing polar aprotic solvents including NMP, DMF, DMA or MeCN (entries 1-3, 5), with NMP and DMA yielding the best results. Interestingly, less polar solvents such as dioxane, $PhCF_3$ and DCE almost shut down the reactivities (entries 4, 6, 7), leading to low conversions of **2a**. The better performance of polar solvent over others led to the hypothesis that a better solubility of **2a** would be beneficial to this reaction system.

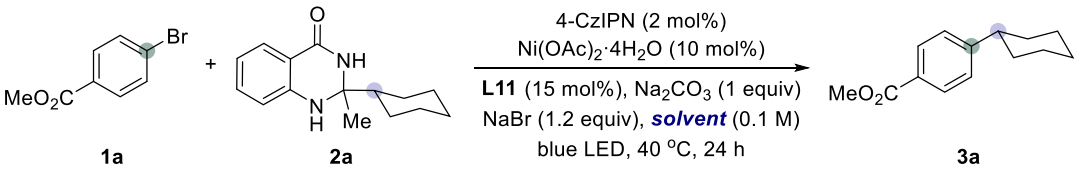

1a **2a** **3a**

entry	solvent	conversion (%)[b]	**3a** (%)[b]
1	NMP	>99	96
2	DMF	>99	88
3	DMA	>99	96
4	Dioxane	8	<1
5	MeCN	76	63
6	$PhCF_3$	<1	<1
7	DCE	12	<1

[a] Conditions: **1a** (0.10 mmol), **2a** (0.12 mmol), $Ni(OAc)_2{\cdot}4H_2O$ (10 mol%), **L11** (15 mol%), 4-CzIPN (2 mol%), NaBr (0.12 mmol), Na_2CO_3 (0.10 mmol) in solvent (0.10 M) under blue LED irradiation at 40 °C for 24 h. [b] GC yield and conversion using dodecane as internal standard.

Table 2.5 Screening of solvents.

The inorganic additives had an important effect on the reaction outcome. As shown in Table 2.6, addition of sodium bromide performed better than bromide salts (entries 1–4). In the sodium salt series, the use of chloride salt had a positive effect (entry 5) whereas related iodide salt had a deleterious effect on the reactivity (entry 6).

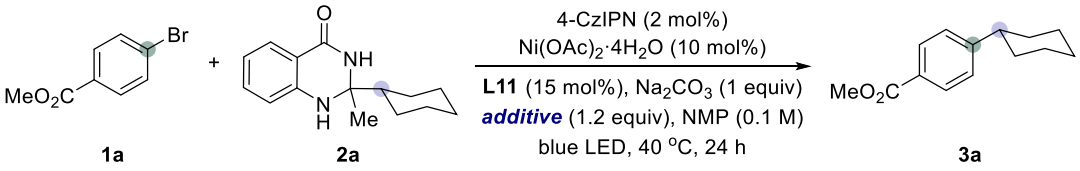

1a **2a** **3a**

entry	additive	conversion (%)[b]	**3a** (%)[b]
1	NaBr	>99	99
2	TBAB	>99	87
3	KBr	>99	94
4	LiBr	>99	99
5	NaCl	>99	93
6	NaI	>99	<1

[a] Conditions: **1a** (0.10 mmol), **2a** (0.12 mmol), $Ni(OAc)_2{\cdot}4H_2O$ (10 mol%), **L11** (15 mol%), 4-CzIPN (2 mol%), additive (0.12 mmol), Na_2CO_3 (0.10 mmol) in NMP (0.10 M) under blue LED irradiation at 40 °C for 24 h. [b] GC yield and conversion using dodecane as internal standard.

Table 2.6 Screening of additives.

In the end, control experiment were conducted to ensure that all the reaction parameters were necessary for obtaining high yield. Indeed, listed in Table 2.7, no

targeted product was formed in the absence of photocatalyst, irradiation, nickel precatalyst or ligand (entries 2–5). Although 90% of **3a** was obtained without NaBr (entry 6), the presence of NaBr in the reaction mixture would inhibit the dehalogenation product formation, bring additional benefits for isolation.

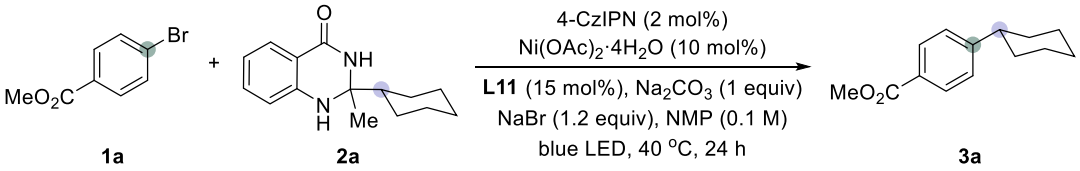

1a **2a** **3a**

entry	deviation standard conditions	**3a** (%)[b]
1	none	99 (93)[c]
2	no PC	<1
3	no light	<1
4	no $Ni(OAc)_2·4H_2O$	<1
5	no **L11**	<1
6	no NaBr	90

[a] Conditions: **1a** (0.10 mmol), **2a** (0.12 mmol), $Ni(OAc)_2·4H_2O$ (10 mol%), **L11** (15 mol%), 4-CzIPN (2 mol%), NaBr (0.12 mmol), Na_2CO_3 (0.10 mmol) in NMP (0.10 M) under blue LED irradiation at 40 °C for 24 h. [b] GC yield and conversion using dodecane as internal standard. [c] isolated yield.

Table 2.7 Control experiments.

2.4 Substrate Scope

2.4.1 Scope of Ketone Derived Dihydroquinazolinones

Utilizing the established reaction conditions shown in Table 2.7 (entry 1), the generality of the arylation protocol of dihydroquinazolinones via C–C bond cleavage was investigated. As shown in Scheme 2.32, the site-selectivity can be dictated and modulated by an appropriate selection of the substituents on the dihydroquinazolinone core. Specifically, the coupling of secondary alkyl radicals (**3a**–**3f**), secondary oxygen-stabilized radicals (**3g**, **3h**) or oxygen- or nitrogen-stabilized primary radical congeners (**3i**–**3l**) could be within reach for Me-substituted analogues. Additionally, it is worth noting that ethyl-substituted dihydroquinazolinones were applicable without deviation in cross-coupling productivity from their methyl-congeners (**3a**, **3l**). The arylation of a primary butyl residue to form **3m** was found to operate with dihydroquinazolinone cores decorated with methyl groups. However, superior yields were afforded when using aryl-substituted analogues. As such, primary alkyl residues were transferred using dihydroquinazolinone cores containing phenyl groups (**3n**–**r**). It is worth noting this preference for alkyl bond scission over C(sp^3)-aromatic cleavage provides an alternative selectivity to transition-metal-catalyzed C–C activations of ketones, which

generally give the more stable metal-aryl complex over alkyl species.[174] In addition, the chemoselectivity and tolerance of functional groups in this part were good as well, which was indicated by the employment of biotin (**3q**) or ciprofloxacin (**3r**) containing structures for cross-coupling reactions, thus showing the prospective potential that this method might have when derivatizing advanced synthetic intermediates.

[174] (a) Okumura, S.; Sun, F.; Ishida, N.; Murakami, M. Palladium-Catalyzed Intermolecular Exchange Between C–C and C–Si σ-bonds. *J. Am. Chem. Soc*. **2017**, *139*, 12414–12417. (b) Jiang, C.; Zheng, Z.-J.; Yu, T.-Y.; Wei, H. Suzuki–Miyaura Coupling of Unstrained Ketones via Chelation-Assisted C–C Bond Cleavage. *Org. Biomol. Chem*. **2018**, *16*, 7174–7177. (c) Xia, Y.; Ochi, S.; Dong, G. Two-Carbon Ring Expansion of 1-Indanones via Insertion of Ethylene into Carbon–Carbon Bonds. *J. Am. Chem. Soc*. **2019**, *141*, 13038–13042. (d) Li, H.; Ma, B.; Liu, Q.-S.; Wang, M.-L.; Wang, Z. -Y.; Xu, H.; Li, L.-J.; Wang, X.; Dai, H.-X. Transformations of Aryl Ketones via Ligand-Promoted C−C Bond Activation. *Angew. Chem. Int. Ed*. **2020**, *59*, 14388–14393.

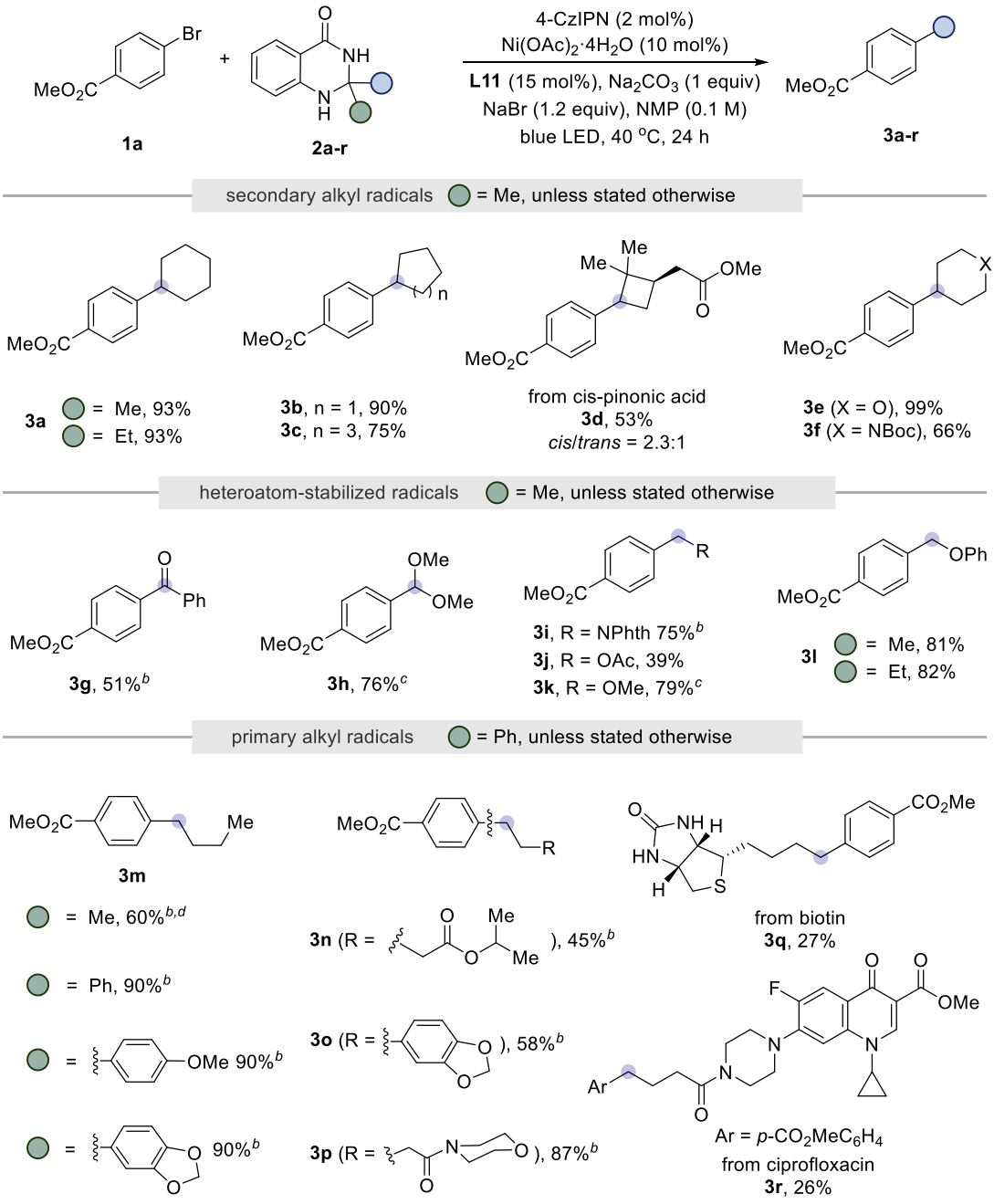

[a] Conditions: **1a** (0.20 mmol), **2** (0.24 mmol), $Ni(OAC)_2{\cdot}4H_2O$ (10 mol%), **L11** (15 mol%), 4-CzIPN (2 mol%), NaBr (1.2 equiv), Na_2CO_3 (1.0 equiv) in NMP (0.1 M) under blue LED irradiation at 40 °C for 24 h; yields of isolated product, average of two independent runs. [b] Using $NiCl_2{\cdot}DME$ as Ni source in NMP (0.2 M). [c] Using 5-CzBN (2 mol%) as photocatalyst, LiBr (1.2 equiv) as additive. [d] ^1H NMR yield using CH_2Br_2 as standard.

Scheme 2.32 Scope of dihydroquinazolinones.

2.4.2 Scope of Aryl Bromides and Vinyl Bromides.

This dual catalytic platform was found to be widely applicable for an array of aryl bromides regardless of their electronic and steric environment (**5a**–**5p**). As evident from the results compiled in Scheme 2.33, the catalytic system displays an excellent chemoselectivity profile, including accommodation of structures containing aldehyde

(**5a**), nitrile (**5b**), ketone (**5c**), sulfonamide (**5g**). As shown for cross-coupling products **5h**, the reaction could also be extended to vinyl bromides. Notably, oxygen- and nitrogen containing heterocycles were compatible in this cross-coupling protocol (**5i**–**5n**), including pyridine, quinoline, oxadiazole and dibenzofuran scaffolds. For electron-rich or sterically encumbered aryl bromides use of terpyridine ligand **L11** failed to give synthetic useful yield of product. For these examples a brief re-optimization found that the use of 2,2'-bipyridine ligand **L1** was effective in exacting the desired transformation (**5e**, **5m**, **5n**). In addition, C(sp^3) arylation could be affected in the presence of aryl chlorides (**5f**), leaving ample room for further derivatization by other approaches.[175] Importantly, our protocol could be employed for accessing glucose (**5o**) containing cross-coupling products, thus demonstrating the synthetic potential of this method in the biologically intermediates derivatizations.

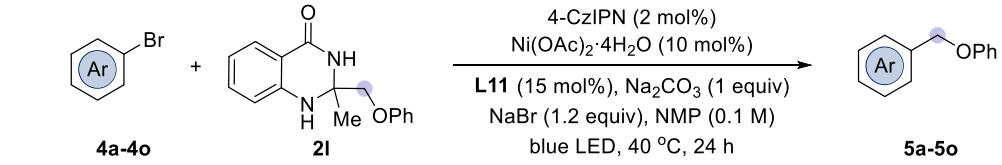

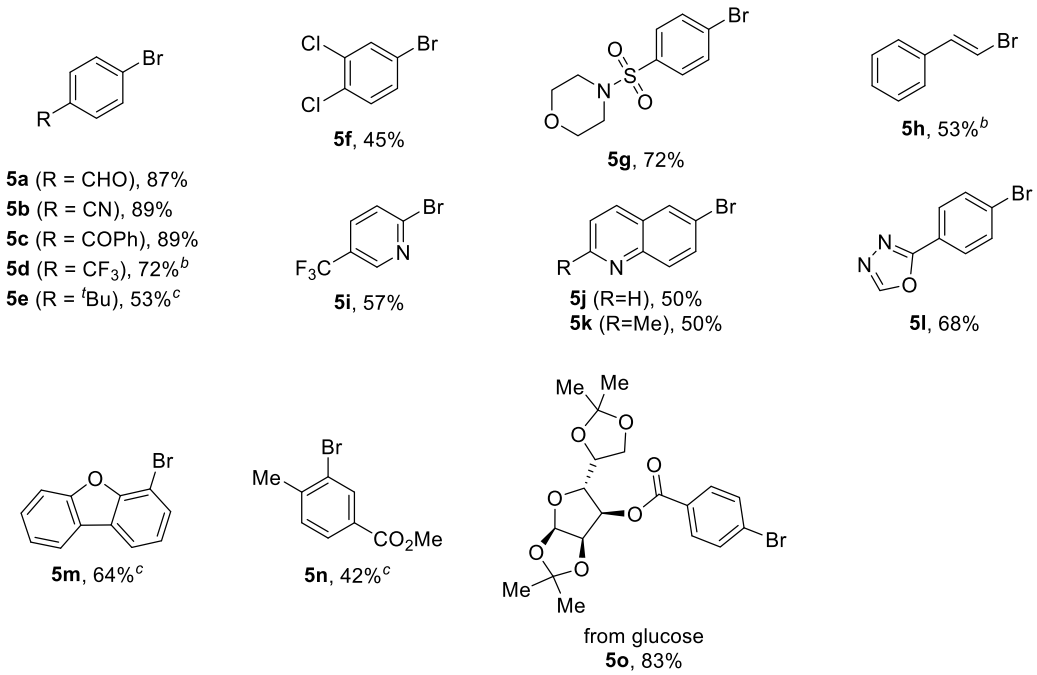

[a] Conditions: **1a** (0.20 mmol), **2** (0.24 mmol), $Ni(OAC)_2{\cdot}4H_2O$ (10 mol%), **L11** (15 mol%), 4-CzIPN (2 mol%), NaBr (1.2 equiv), Na_2CO_3 (1.0 equiv) in NMP (0.1 M) under blue LED irradiation at 40 °C for 24 h; yields of isolated product, average of two independent runs. [b] Using $NiCl_2{\cdot}$DME as Ni source in NMP (0.2 M). [c] Conditions: **1** (0.20 mmol), **2** (0.30 mmol), 4-CzIPN (2 mol%), $NiBr_2{\cdot}$diglyme (10 mol%), **L1** (15 mol%), LiHMDS (1.5 equiv), in dioxane (0.1 M) under blue LED irradiation at 40 °C for 24 h; yields of isolated product, average of two independent runs.

175 (a) Kim, S.; Goldfogel, M. J.; Gilbert, M. M.; Weix, D. J. Nickel-Catalyzed Cross Electrophile Coupling of Aryl Chlorides with Primary Alkyl Chlorides. *J. Am. Chem. Soc*. **2020**, *142*, 9902–9907. (b) Bedford, R. B.; Cazin, C. S. J.; Holder, D. The Development of Palladium Catalysts for C–C and C–Heteroatom Bond Forming Reactions of Aryl Chloride Substrates. *Coord. Chem. Rev*. **2004**, *248*, 2283–2321.

Scheme 2.33 Scope of aryl bromides.

2.4.3 Scope of Alkyl Halides

Next, we focused our attention on the utilization of unactivated alkyl halides as counterparts to forge C(sp^3)–C(sp^3) architectures. What could be anticipated was the transformation would be more problematic than utilizing sp^2 electrophiles, for alkyl nickel complex is known for undergoing beta-hydrogen elimination and are significantly less stable than their corresponding aryl nickel counterparts.[176] Exposure of alkyl bromide **6a** to dihydroquinazolinone **2e** under the Ni/**L11** regime used in Scheme 2.32 failed to provide satisfactory levels of C(sp^3)–C(sp^3) bond-formation (**7a**). Nevertheless, after a brief re-optimization a protocol based on the Ni/**L14** regime turned out to be particularly applicable for the coupling of unactivated alkyl bromides (Scheme 2.34). As shown, our method was suited not only for the formation of C(sp^3)–C(sp^3) linkages arising from the coupling of primary unactivated alkyl halides with secondary alkyl radicals (**7a**–**i**), but also the coupling of primary alkyl halides with primary alkyl radical species (**7j**, **7k**). As part of the latter, we used this approach to synthesize the ethyl-ester of gemfibrozil (**7m**), a medication for dyslipidemia, providing an unconventional disconnection towards this target. In addition, the coupling of secondary alkyl halides with primary alkyl radical intermediates could also be realized, delivering cross-coupling products **7l**. Furthermore, alkyl bromides bearing oxygen-, sulfur- and nitrogen-containing heterocycles all successfully participated (**7g**–**7i**) in the intended C(sp^3)–C(sp^3) cross-coupling reaction. More importantly, cross-coupling products **7n**, **7o** and **7p** arising from the conjoining of estrone, oxaprozin or cholesterol containing alkyl bromide derivatives posed no problems, thus holding promise for the application of our protocol when coupling advanced intermediates. Although in comparatively lower yields than those shown in Scheme 2.33, these results should be benchmarked against the challenge of catalytic C(sp^3)–C(sp^3) cross-coupling by offering a complementary technique to existing approaches.

[176] Sommer, H.; Juliá-Hernández, F.; Martin, R.; Marek, L. Walking Metals for Remote Functionalization. *ACS Cent. Sci.* **2018**, *4*, 153–165.

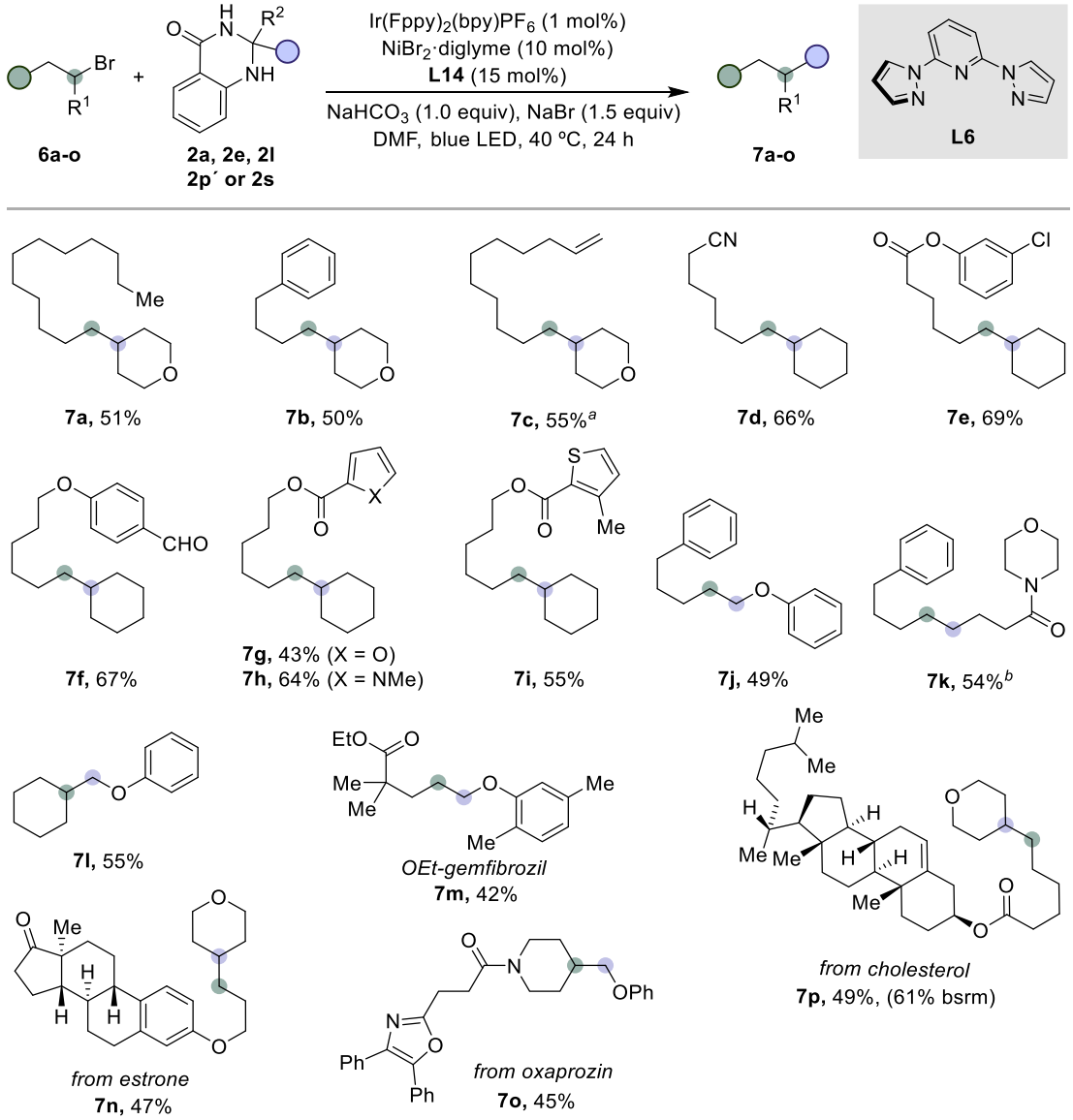

[a] Conditions: **7** (0.20 mmol), **2** (0.24 mmol), $NiBr_2$·diglyme (10 mol%), **L6** (15 mol%), $Ir(Fppy)_2(bpy)PF_6$ (2 mol%), $NaHCO_3$ (1.0 equiv), NaBr (1.5 equiv) in DMF (0.1 M) under blue LED irradiation at 40 °C for 24 h; yields of isolated product, average of two independent runs. [b] DMF (0.2 M).

Scheme 2.34 Scope of C(sp^3)–C(sp^3) cross-coupling.

2.4.4 Telescoping the Formation of Dihydroquinazolinones en route to sp^3 Architectures

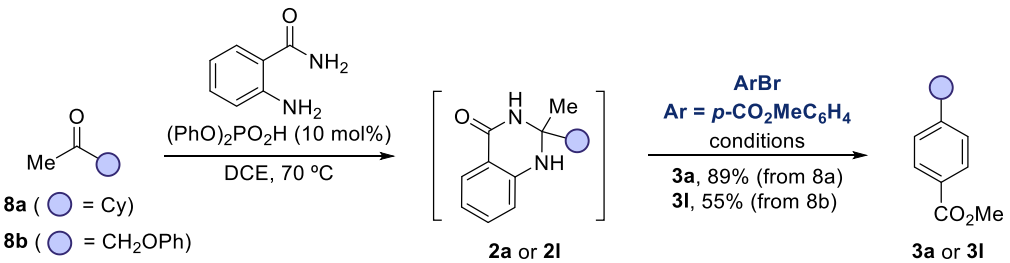

Scheme 2.35 Telescoping the formation of dihydroquinazolinones from ketone congeners.

In the interest of providing a bonus from an operational standpoint, we wondered whether we could telescope the formation of dihydroquinazolinones from their corresponding ketones. This was successful with cross-coupling products **3a** and **3l** being obtained in one-pot from ketones **8a** and **8b** in synthetically useful yields via their respective dihydroquinazolinone alkyl radical precursors (**2a**, **2l**) (Scheme 2.35).

2.4.5 Unsuccessful Substrates

While exploring the substrate scope of this cross-coupling method some substrates were found to afford low yields of the targeted products. As shown in Scheme 2.36, a series of dihydroquinazolinones cannot be utilized in this protocol, thus providing the some important information: (1) methyl radical and trifluoromethyl radical exclusion might be problematic due to the lacking thermodynamic driving force (**9a**, **9b**); (2) steric hindrance factor should be taken into consideration when applying this cross-coupling technique, since the coupling of tertiary radical led to low yields (**9c**); (3) benzylic radicals might not be suitable for this transformation, which furnish large amount of the benzylic homologation side product (**9e**); (4) Alkyne containing structures and attempt to coupling sulfur stabilized radicals would lead to messy reaction system.

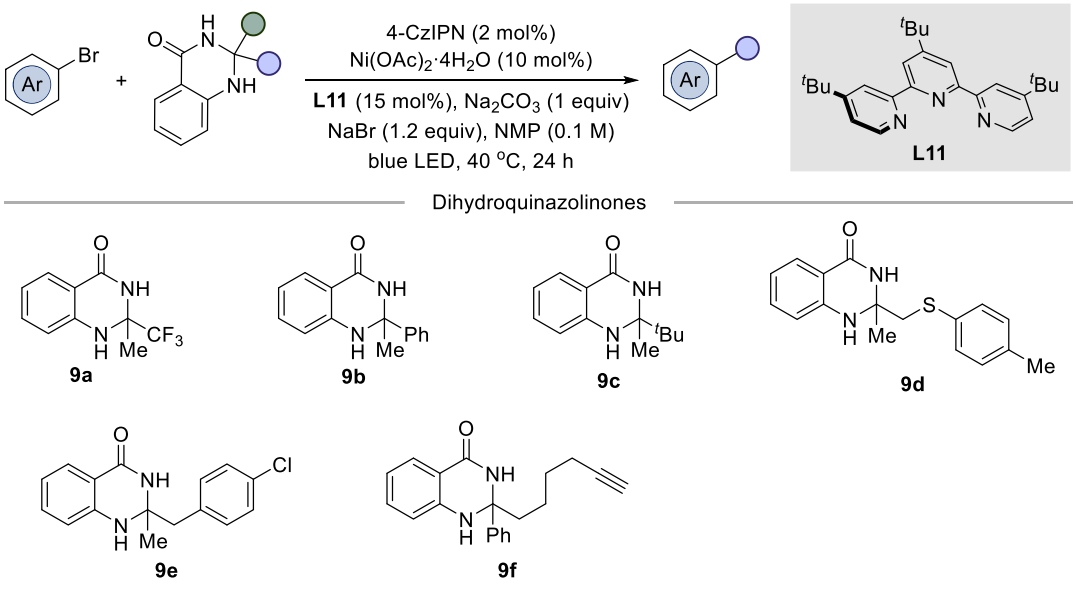

Scheme 2.36 Unsuccessful substrates regarding to dihydroquinazolinones.

A series of sp^2 hybridized electrophiles failed to provide satisfactory amount of the product, as demonstrated in scheme 2.37. Aryl bromides bearing electro-donating group typically resulted in low conversion (**9k**), probably due to the low efficiency of

the oxidative addition arising from low valent nickel species. while aryl bromides and vinyl bromides gave good yields, the analogous iodides failed to give cross-coupling product (**9i**, **9j**) and chlorides gave a diminished yields (**9g**, **9h**). Some certain chemical functionalities seemed to be incompatible, including unprotected alcohols and phenols (**9l**, **9m**). Furthermore, 3-bromopyridine failed to give satisfactory cross-coupling products might resulting from the pyridine competing bonding to nickel center (**9n**, **9o**).

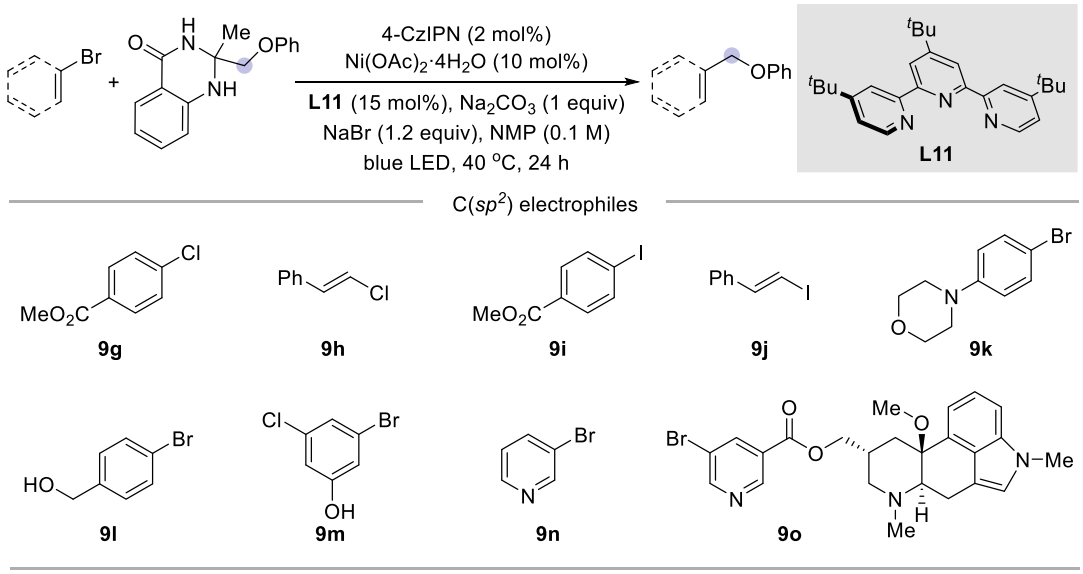

Scheme 2.37 Unsuccessful substrates regarding to C(sp^2) electrophiles.

Although we demonstrated that the C(sp^3)–C(sp^3) cross-coupling of unactivated alkyl bromides occurred with a wide substrate scope, a number of examples failed to provide the desired product or gave lower yield (<30%) (Scheme 2.38). For example, alkyne containing structure and alkyl chloride containing substrate **9q** and **9r** would lead to the complicated spectral analysis probably due to their participation. Alkyl bromide bearing thiol ether caused the reaction low conversion, as demonstrated by example **9p**. Biologically relevant substrate **9s** and **9t** afforded mostly dehalogenation product, giving trace amount of the targeted coupling product.

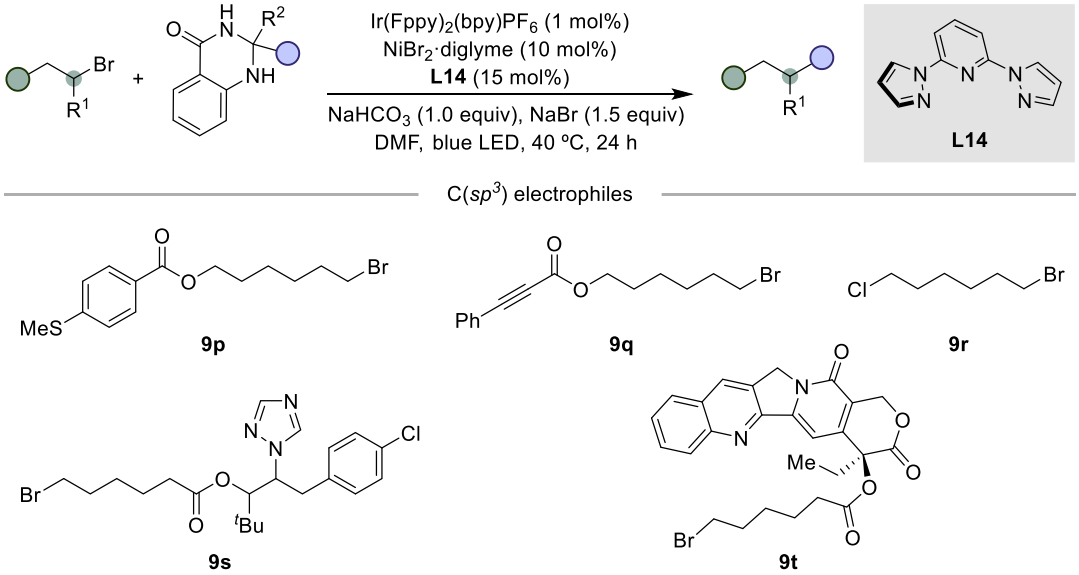

Scheme 2.38 Unsuccessful substrates regarding to C(sp^3) electrophiles.

2.5 Mechanistic Studies

2.5.1 Experiments with Radical Probes

To support our initial hypothesis that a radical fragmentation was generated during the reaction process, TEMPO inhabitation experiments and radical clock experiments were conducted. Firstly, the cross-coupling of aryl bromide **1a** with dihydroquinazolinone **2e** was completely inhibited in the presence of a stoichiometric amount of TEMPO as radical scavenger, with only the TEMPO tetrahydropyran adduct (**10**) being observed (Scheme 2.39, *top*). Subjection of our metallaphotoredox reaction conditions to a cyclopropane containing dihydroquinazolinone (**2t**) yielded only the ring opened cross-coupling product (**11**) along with aromatization by-product (**2t'**) (Scheme 2.39, *bottom*). These results indirectly proved the existence of radical intermediate arising from dihydroquinazolinones.

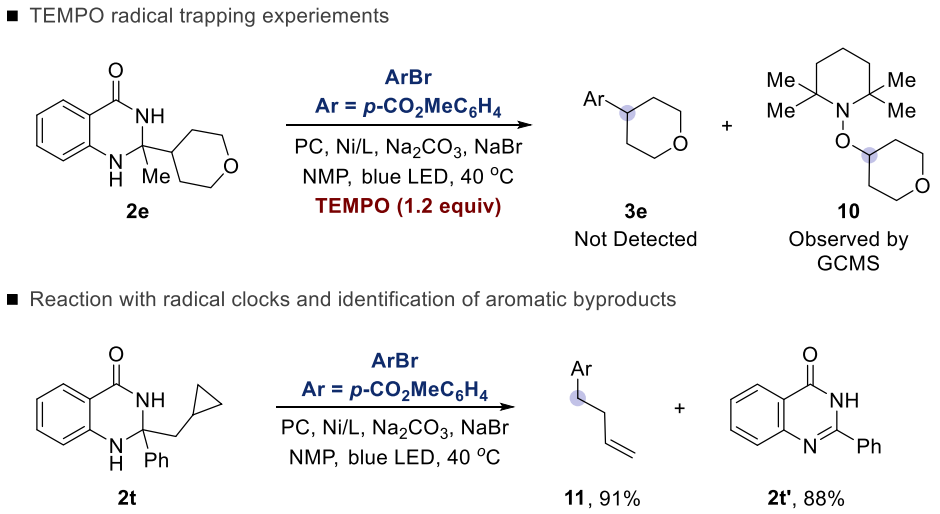

Scheme 2.39 Indirect evidence for aromatization-driven radical generation.

2.5.2 Stern-Volmer Fluorescence Quenching Experiment

To further confirm the interaction between excited photocatalyst and dihydroquinazolinones, Stern-Volmer quenching experiments were performed. As shown in Figure 2.2 and Figure 2.3, the intensity of the 4-CzIPN fluorescence decreased as adding increasing amounts of dihydroquinazolinones **2e.** By using the excited-state lifetime of 4-CzIPN (2.15 μs)[177] and the Stern-Volmer equation (Equation 2.1), the fluorescence quenching rate constant was calculated to be 3.32 x 10^7 $M^{-1}.s^{-1}$.

$$\boldsymbol{I_0/I = 1 + k_q \tau_0 [Q]}$$

Equation 2.1 Stern-Volmer equation.

In addition, the oxidation potential of dihydroquinazolinone **2e** ($E_{1/2}^{ox}$ = +1.07 V vs SCE in NMP) was measured using cyclic voltammetry and was shown to be within the oxidizing power of 4-CzIPN (+1.43 V vs SCE). These observations suggest a canonical reductive quenching scenario where single electron transfer from dihydroquinazolinone to photoexcited 4-CzIPN occurs, initiating formal C–C cleavage en route to alkyl radical driven by the formation of an aromatic by-product.

[177] Takeda, H.; Takeda, M.; Yoshioka, H.; Minamide, H.; Oki, Y.; Adachi, C. Fluorescence Lifetime Elongation of Thermally Activated Delayed Fluorescence 4CzIPN Molecules with Encapsulation into Zeolitic Imidazole Frameworks ZIF-11. *Opt. Mater. Express* **2019**, *9*, 1150.

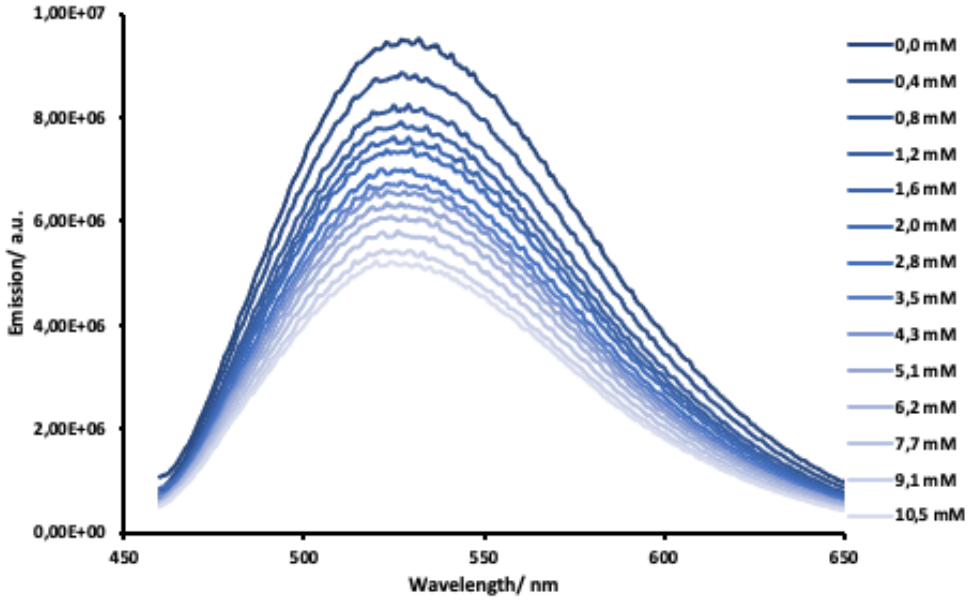

Figure 2.2 Emission spectra of a 7.0 x 10^{-6} M solution of 4-CzIPN in NMP containing varying amounts of 2-methyl-2-(tetrahydro-2H-pyran-4-yl)-2,3-dihydroquinazolin-4(1H)-one (**2e**) quencher.

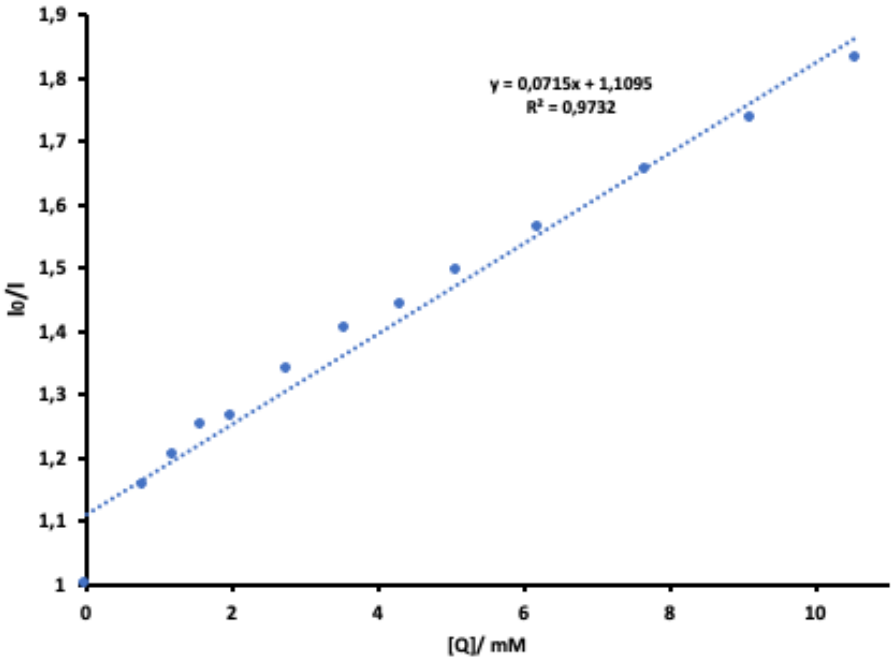

Figure 2.3 Emission intensities observed at 530 nm plotted against 2-methyl-2-(tetrahydro-2*H*-pyran-4-yl)-2,3-dihydroquinazolin-4(1*H*)-one (**2e**) concentration.

2.5.3 Experiments with Well-Defined Oxidative Addition Species Ni-I

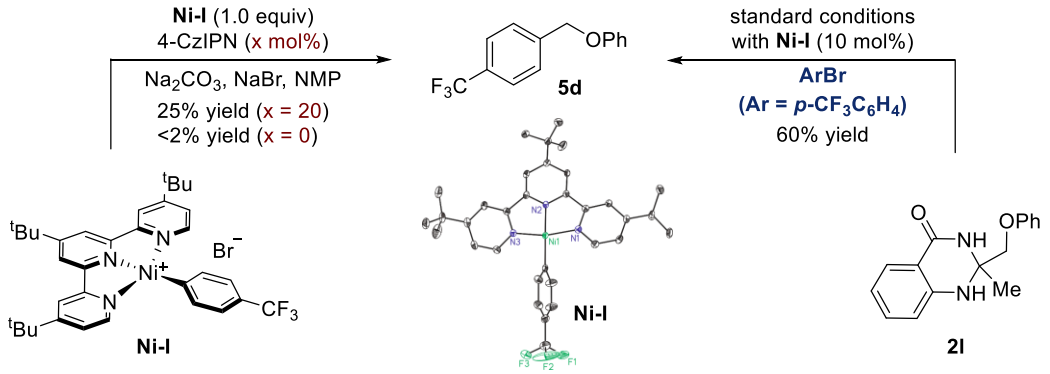

Scheme 2.40 Cross-coupling competence of well-defined oxidative addition species **Ni-I**.

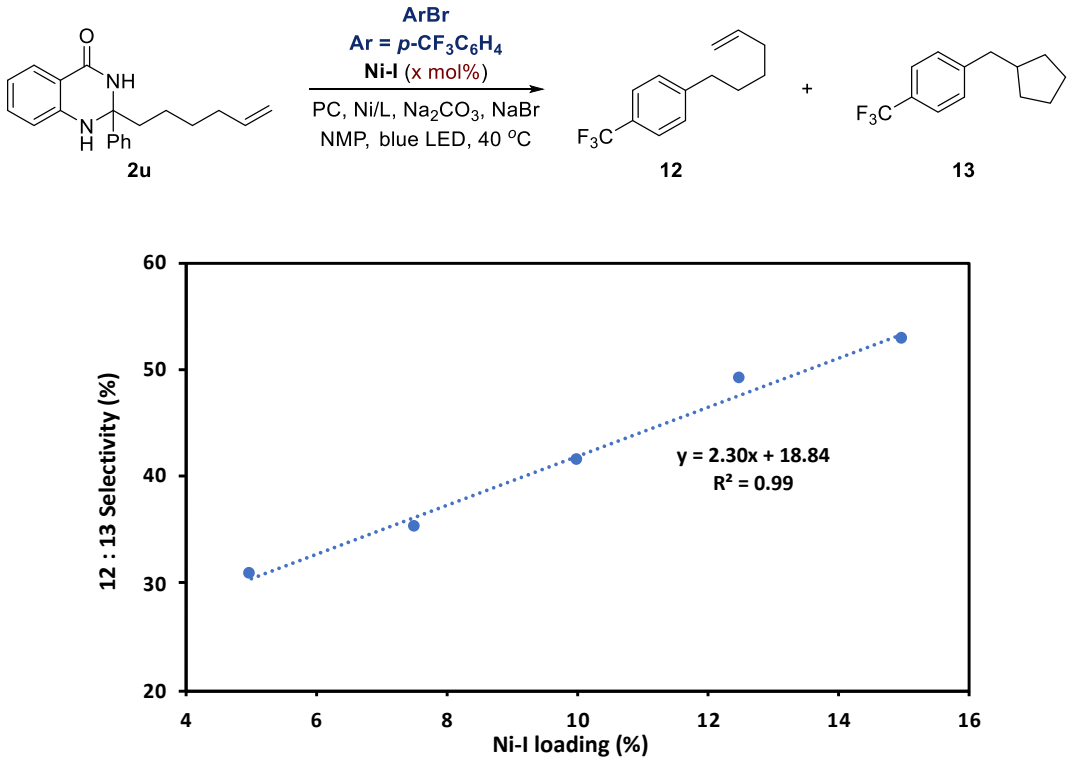

Scheme 2.41 Radical cyclization as a function of catalyst loading.

Terpyridine ligated nickel complex (**Ni-I**) was obtained by exposure of $Ni(COD)_2/PPh_3$ to aryl bromide **4d** followed by ligand exchange with terpyridine **L11**,[178] with the structure of this complex confirmed by X-ray diffraction. As anticipated, isolated complex **Ni-I** was found to be catalytically competent in the cross-coupling of dihydroquinazolinone **2l** with aryl bromide **4d** (Scheme 2.40, right). Next, we performed the stoichiometric reaction between dihydroquinazolinone **2l** and isolated complex **Ni-I** affording the cross-coupling product **5d** in 25% yield. This

[178] Klein, A.; Feth, M. P.; Bertagnolli, H.; Záliš, S. On the Electronic Structure of Mesitylnickel Complexes of α-Diimines – Combining Structural Data, Spectroscopy and Calculations. *Eur. J. Inorg. Chem*. **2004**, 2784–2796.

suggests that **Ni-I** and similar nickel complexes can capture radicals and undergo reductive elimination under our established conditions (Scheme 2.40, *left*). A positive linear relationship between **Ni-I** catalyst concentration and linear selectivity in the cross-coupling of dihydroquinazolinone **2u** with **4d** was observed (Scheme 2.41). This is consistent with the formation of C(sp^3)-centered hex-1-enyl radical from dihydroquinazolinone **2u**, which is captured by **Ni-I**. Higher concentrations of **Ni-I** shortens the lifetime of the alkyl radical in solution resulting in diminished cyclization product **13** formation and greater selectivity for the linear product (**12**).

Taken together, these mechanistic experiments suggested to a catalytic cycle starting with SET oxidation of dihydroquinazolinone by excited 4-CzIPN give an aromatic by-product and alkyl radical. The latter could be intercepted by a aryl-Ni(II) complex, which upon reductive elimination from aryl-Ni(III)-alkyl species affords the desired cross coupling product and Ni(I). The reduced-state 4-CzIPN ultimately promotes a SET reduction to recover back the propagating Ni(0) intermediates and ground-state 4-CzIPN.

2.6 Conclusions

This chapter summarizes the efforts towards the development of a nickel photoredox dual catalytic platform enabled C(sp^3)–C(sp^2) and C(sp^3)–C(sp^3) bonds formation by using ketone derived dihydroquinazolinones as one-electron C(sp^3) handles via α C–C bond cleavage. This technology offers an unconventional disconnection within the retrosynthetic planning phase of synthesis by enabling C(sp^3)-arylations and C(sp^3)-alkylations with an excellent chemoselectivity profile while operating under ambient temperature. In addition, a judicious choice of the starting precursor allows to control the site-selectivity of C–C bond-cleavage.

This method is distinguished by its wide scope and broad application profile — including chemical diversification of advanced intermediates — providing a catalytic technique complementary to existing C(sp^3) cross-coupling reactions that operates within the C–C bond-functionalization arena. Mechanistic experiments were conducted, all of which are consistent with the operation of a reductive quenching photoredox cycle, beginning with oxidative single-electron transfer of dihydroquinazolinone radical precursor by excited-state photocatalyst resulting in radical fragmentation driven by formation of an aromatic by-product.

2.7 Experimental Section

2.7.1 General Considerations

Reagents. Commercially available aryl bromides and alkyl bromides were used as received without further purification. $Ni(OAc)_2 \cdot 4H_2O$ (98% purity) was purchased from Aldrich. $NiBr_2 \cdot$diglyme (97% purity) was purchased from Aldrich. 4,4',4"-Tri-tert-Butyl-2,2':6',2"-terpyridine (95 % purity) was purchased from Aldrich. 2,6-Di(1-pyrazolyl)pyridine (>98% purity) was purchased from TCI. Anhydrous Na_2CO_3 (99.5 % purity) was purchased from PanReac. NaBr (>99 % purity) was purchased from Across. $NaHCO_3$ (>99% purity) was purchased from Fisher. Anhydrous 1-Methyl-2-pyrrolidinone (NMP, 99.5% purity) and DMF (99.8% purity) were purchased from Across.

Analytical methods. ^1H and ^{13}C NMR spectra were recorded on Bruker 300 MHz, Bruker 400 MHz and Bruker 500 MHz at 20 °C. All ^1H NMR spectra are reported in parts per million (ppm) downfield of TMS and were calibrated using the residual solvent peak of $CHCl_3$ (7.26 ppm), unless otherwise indicated. All ^{13}C NMR spectra are reported in ppm relative to TMS, were calibrated using the signal of residual $CHCl_3$ (77.16 ppm), ^{11}B NMR and ^{19}F NMR were obtained with ^1H decoupling unless otherwise indicated. Coupling constants, *J*, are reported in Hertz. Melting points were measured using open glass capillaries in a Büchi B540 apparatus. Gas chromatographic analyses were performed on Hewlett-Packard 6890 gas chromatography instrument with a FID detector. Flash chromatography was performed with EM Science silica gel 60 (230-400 mesh). Thin layer chromatography was used to monitor reaction progress and analyze fractions from column chromatography. To this purpose TLC Silica gel 60 F_{254} aluminium sheets from Merck were used and visualization was achieved using UV irradiation and/or staining with Cerium Molybdate solution. The yields reported in Scheme 3.26-3.29 refer to isolated yields and represent an average of at least two independent runs. The procedures described in this section are representative. Thus, the yields may differ slightly from those given in the Schemes of the manuscript. In the cases the High-Resolution Mass Spectra of the molecular ion could not be obtained using ESI and APCI ionization modes the GC-MS of the compound was given.

Photoreactor. Arylation and alkylation reactions were performed with 451 nm LEDs (OSRAM Oslon® SSL 80 royal- blue LEDs), which were installed at the bottom of a custom-made 8 flat-bottom Schlenk tubes holder (the distance between the flat-bottom Schlenk tube and the light source was measured to be ~7 mm), equipped with chiller cooling system (the thermostat was set at 40 °C) and a magnetic stirrer (1000 rpm).

Figure S2.1 Photo reaction setting up.

2.7.2 Synthesis of Starting Materials

General procedure 1 (GP1): Synthesis of aryl bromides and alkyl bromides

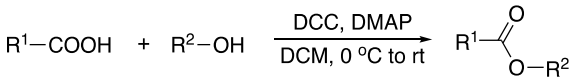

To a stirred solution of carboxylic acid (1.2 equiv) and alcohol (1.0 equiv) in DCM (0.5 M) was added DMAP (0.8 equiv) and DCC (1.5 equiv) at 0 ºC. The reaction mixture was allowed to stir at 20 °C for 20 hours. The reaction mixture was filtered through silica gel and the precipitate was washed with DCM. The received crude material was concentrated under reduced pressure and purified by silica gel chromatography to yield the desired product.

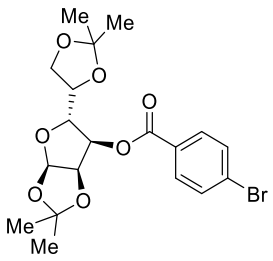

(3a*R*,5*R*,6*R*,6a*R*)-5-((*R*)-2,2-Dimethyl-1,3-dioxolan-4-yl)-2,2 dimethyltetrahydrofuro[2,3-*d*][1,3]dioxol-6-yl 4-bromobenzoate (4o). Following GP1, using 4-bromobenzoic acid (1.21 g, 6.0 mmol) and 1,2:5,6-di-o-isopropylidene-α-D-allofuranose (1.30 g, 5.0 mmol) were used, affording the title compound as an amorphous white solid (1.63 g, 74% yield), by using hexane/EtOAc (20:1) as chromatography eluent. **IR (neat, cm^{-1}):** 2987, 1724, 1590, 1372, 1268, 1011, 845, 756. **^{1}H NMR (400 MHz, CDCl$_3$)** δ 7.95 – 7.87 (m, 2H), 7.64 – 7.56 (m, 2H), 5.89 (d, *J* = 3.8 Hz, 1H), 5.06 (dd, *J* = 8.1, 5.1 Hz, 1H), 4.95 (dd, *J* = 5.1, 3.9 Hz, 1H), 4.37 – 4.26 (m, 2H), 4.11 (dd, *J* = 8.6, 6.6 Hz, 1H), 3.96 (dd, *J* = 8.6, 5.3 Hz, 1H), 1.54 (s, 3H), 1.39 (s, 3H), 1.33 (s, 3H), 1.33 (s, 3H) ppm. **^{13}C NMR (101 MHz, CDCl$_3$)** δ 165.1, 132.0, 131.5, 128.7, 128.5, 113.4, 110.2, 104.5, 78.0, 78.0, 75.4, 73.7, 66.1, 26.9, 26.8, 26.5, 25.1 ppm. **HRMS** [ESI$^+$] *calcd*. for ($C_{19}H_{23}BrNaO_7$) [M+Na]$^+$: 465.0525, *found*: 465.0521.

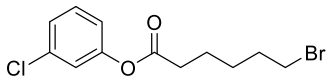

3-Chlorophenyl 6-bromohexanoate (6e). Following GP1, using 6-bromohexanoic acid (0.94 g, 4.8 mmol) and 3-chlorophenol (0.52 g, 4.0 mmol) were used, affording the title compound as a colourless liquid (0.93 g, 77% yield), by using hexane/EtOAc (20:1) as chromatography eluent. **^{1}H NMR (400 MHz, CDCl$_3$)** δ 7.30 (t, *J* = 8.1 Hz, 1H), 7.22 (ddd, *J* = 8.1, 2.0, 1.0 Hz, 1H), 7.12 (t, *J* = 2.1 Hz, 1H), 6.99 (ddd, *J* = 8.1, 2.2, 1.0 Hz, 1H), 3.44 (t, *J* = 6.7 Hz, 2H), 2.58 (t, *J* = 7.4 Hz, 2H), 1.98 – 1.88 (m, 2H), 1.84 – 1.72 (m, 2H), 1.63 – 1.52 (m, 2H) ppm. **^{13}C NMR (101 MHz, CDCl$_3$)** δ 171.6, 151.3, 134.8, 130.3, 126.2, 122.4, 120.1, 34.2, 33.5, 32.5, 27.7, 24.1 ppm. Spectral data in agreement with literature.[179]

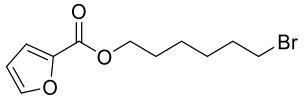

6-Bromohexyl furan-2-carboxylate (6g). Following GP1, using furan-2-carboxylic acid (0.54 g, 4.8 mmol) and 6-bromohexan-1-ol (0.72 g, 4.0 mmol) were used, affording the title compound as a colourless liquid (0.55g, 50% yield), by using hexane/EtOAc (20:1) as chromatography eluent. **^{1}H NMR (400 MHz, CDCl$_3$)** δ 8.00 (dd, *J* = 1.5, 0.7 Hz, 1H), 7.42 (t, *J* = 1.7 Hz, 1H), 6.73 (dd, *J* = 1.9, 0.7 Hz, 1H), 4.25 (t, *J* = 6.6 Hz, 2H), 3.41 (t, *J* = 6.8 Hz, 2H), 1.94 – 1.82 (m, 2H), 1.79 – 1.68 (m, 2H), 1.55 – 1.39 (m, 4H) ppm. **^{13}C NMR (101 MHz, CDCl$_3$)** δ 163.3, 147.7, 143.8, 119.7, 110.0, 64.5, 33.8, 32.7, 28.7, 27.9, 25.4 ppm. Spectral data was in agreement with the literature.[180]

[179] Ding, D.; Dong, H.; Wang, C. Nickel-Catalyzed Asymmetric Domino Ring Opening/Cross-Coupling Reaction of Cyclobutanones via a Reductive Strategy. *Iscience*. **2000**, *23,* 101017.
[180] Bam, R.; Alexandros S. Pollatos, A. S.; Moser, A. J. West. J. G. Mild Olefin Formation via Bio-Inspired Vitamin B12 Photocatalysis. *Chem. Sci*. **2021**, *12*, 1736–1744.

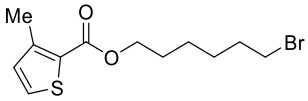

6-Bromohexyl 3-methylthiophene-2-carboxylate (6i). Following GP1, using 3-methylthiophene-2-carboxylic acid (0.68 g, 4.8 mmol) and 6-bromohexan-1-ol (0.72 g, 4.0 mmol) were used, affording the title compound as a colourless liquid (0.55g, 45% yield) by using hexane/EtOAc (20:1) as chromatography eluent. **IR (neat, cm^{-1}):** 2935, 1703, 1414, 1255, 1102, 1071, 767, 725, 609. **^{1}H NMR (400 MHz, $CDCl_3$)** δ 7.38 (d, *J* = 5.0 Hz, 1H), 6.91 (d, *J* = 5.0 Hz, 1H), 4.27 (t, *J* = 6.6 Hz, 2H), 3.41 (t, *J* = 6.8 Hz, 2H), 2.55 (s, 3H), 1.94 – 1.83 (m, 2H), 1.81 – 1.71 (m, 2H), 1.56 – 1.41 (m, 4H) ppm. **^{13}C NMR (101 MHz, $CDCl_3$)** δ 163.0, 146.2, 131.9, 130.1, 127.1, 64.7, 33.8, 32.8, 28.7, 27.9, 25.4, 16.1 ppm. **HRMS** [ESI$^+$] *calcd*. for ($C_{12}H_{17}BrNaO_2S$) [M+Na]$^+$: 327.0030, *found*: 327.0028.

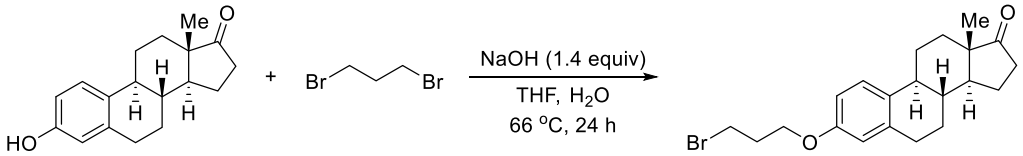

Synthesis of (8*R*,9*S*,13*S*,14*S*)-3-(3-Bromopropoxy)-13-methyl-6,7,8,9,11,12,13,14,15,16-decahydro-17*H*-cyclopenta[*a*]phenanthren-17-one (6n). A 50 mL RBF was charged with a stirrer bar, estrone (1.0 g, 3.7 mmol), sodium hydroxide (200 mg, 5.0 mmol), THF (20 mL) and water (5 mL). 1,3-Dibromopropane (0.508 mL, 5.0 mmol) was added to the reaction mixture, which was stirred for 24 hours at 66 °C. The reaction mixture was quenched with 2.7 M HCl (aq., 75 mL) and extracted with EtOAc (2 x 75 mL). The combined organic extracts were dried over $MgSO_4$ and concentrated under reduced giving a light brown oil as crude material, which was purified by silica gel chromatography (0 to 10% Et_2O in hexane) and then recrystallization (MeOH), affording the title compound (186 mg, 12%) as white feathered crystals. **M.p.**: 103 °C. **^{1}H NMR (400 MHz, $CDCl_3$)** δ 7.20 (d, *J* = 8.5 Hz, 1H), 6.72 (dd, *J* = 8.5, 2.8 Hz, 1H), 6.66 (d, *J* = 2.6 Hz, 1H), 4.08 (t, *J* = 5.8 Hz, 2H), 3.60 (t, *J* = 6.5 Hz, 2H), 2.94 – 2.87 (m, 2H), 2.50 (dd, *J* = 18.6, 8.7 Hz, 1H), 2.43 – 2.37 (m, 1H), 2.35 – 2.22 (m, 3H), 2.20 – 1.93 (m, 4H), 1.68 – 1.40 (m, 6H), 0.91 (s, 3H) ppm. **^{13}C NMR (126 MHz, $CDCl_3$)** δ 220.9, 156.9, 138.0, 132.5, 126.5, 114.7, 112.3, 65.4, 50.6, 48.2, 44.1, 38.5, 36.0, 32.6, 31.7, 30.2, 29.8, 26.7, 26.1, 27.7, 14.0 ppm. Spectral data was in agreement with the literature.[181]

[181] Jadhav, V. H.; Kim, J. G.; Jeong, H. J.; Kim, D. W. Nucleophilic Hydroxylation in Water Media Promoted by a Hexa-Ethylene Glycol-Bridged Dicationic Ionic Liquid. *J. Org. Chem*. **2015**, *80*, 7275–7280.

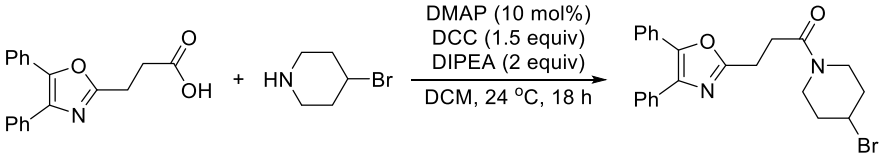

Synthesis of 1-(4-bromopiperidin-1-yl)-3-(4,5-diphenyloxazol-2-yl)propan-1-one (6o). A 27 mL vial was charged with a stirrer bar, 4-bromopiperidine hydrobromide (486 mg, 2.0 mmol), *N*,*N*'-dicyclohexylmethanediimine (619 mg, 3.0 mmol) and DMAP (24.4 mg, 0.2 mmol), then equipped with a rubber septum with an argon inlet. The contents of the reaction vessel were flushed with argon, then charged with DCM (4 mL, anhydrous) and DIPEA (0.70 mL, 4.0 mmol). A solution of oxaprozin (486 mg, 2.0 mmol) in DCM (1 mL, anhydrous) was prepared under an inert atmosphere, which was added to the reaction mixture over 5 minutes. The reaction mixture was stirred for 18 hours at 24 °C then concentrated under reduced pressure yielding a white residue, which was suspended in 2 M NaOH (aq, 50 mL) and extracted with EtOAc (3 x 40 mL). The combined organic extracts were washed with 1 M HCl (aq, 50 mL), dried ($MgSO_4$) and concentrated under reduced pressure giving a white solid as crude material, which was purified by silica gel chromatography (0 to 50% EtOAc in hexane), affording the title compound (475 mg, 54%) as a colourless oil.**^{1}H NMR (500 MHz, $CDCl_3$)** δ 7.64 – 7.60 (m, 2H), 7.58 – 7.55 (m, 2H), 7.39 – 7.28 (m, 6H), 4.40 (sep., *J* = 3.6 Hz, 1H), 3.83 (ddd, 13.5, 7.7, 3.6 Hz, 1H), 3.76 (ddd, *J* = 13.9, 7.7, 3.4 Hz, 1H), 3.63 (ddd, *J* = 13.6, 7.1, 3.8 Hz, 1H), 3.47 (ddd, *J* = 13.9, 7.3, 3.6 Hz, 1H), 3.22 (dd, *J* = 8.5, 6.8 Hz, 2H), 2.94 (dd, *J* = 8.0, 6.8 Hz, 2H), 2.18 – 2.06 (m, 2H), 2.04 – 1.91 (m, 2H) ppm. **^{13}C NMR (126 MHz, $CDCl_3$)** δ 169.6, 162.8, 145.5, 135.1, 132.5, 130.0, 129.2, 129.0, 128.8, 128.7, 128.6, 128.2, 128.1, 126.6, 49.0, 43.7, 40.1, 36.0, 35.4, 29.9, 23.9 ppm. Spectral data was in agreement with the literature.[182]

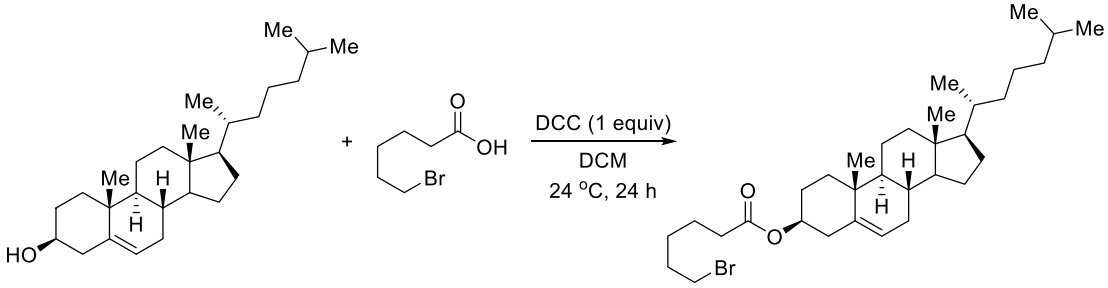

Synthesis of (3*S*,8*S*,9*S*,10*R*,13*R*,14*S*,17*R*)-10,13-Dimethyl-17-((*R*)-6-methylheptan-2-yl)-2,3,4,7,8,9,10,11,12,13,14,15,16,17-tetradecahydro-1*H*-cyclopenta[a]phenanthren-3-yl 6-bromohexanoate (6p). To a 100 mL RBF was sequentially added cholesterol (3.0 g, 7.7 mmol), *N*,*N*'-dicyclohexylmethanediimine (1.6 g, 7.7 mmol), DMAP (40 mg) and DCM (40 mL). The reaction mixture was stirred

[182] Wang, G.-W.; Wheatley, M.; Simonetti, M.; Cannas, D. M.; Larrosa, I. Cyclometalated Ruthenium Catalyst Enables Ortho-Selective C–H Alkylation with Secondary Alkyl Bromides. *Chem* **2020**, *6*, 1459–1468.

for 2 minutes at 24 °C, then 6-bromohexanoic acid (1.5 g, 7.7 mmol) was added and the reaction was stirred for another 18 hours at 24 °C during which a white precipitate formed. The reaction mixture was filtered and the collected organic filtrate was concentrated under reduced pressure affording a white solid as crude product, which was purified by recrystallization (EtOH) yielding the title compound (2.65 g, 61%) as white crystals. **M.p.**: 122 °C. **^{1}H NMR (400 MHz, $CDCl_3$)** δ 5.37 (br. d, *J* = 4.7 Hz, 1H), 4.67 – 4.56 (m, 1H), 3.40 (t, *J* = 6.8 Hz, 1H), 2.35 – 2.25 (m, 4H), 2.04 – 1.93 (m, 2H), 1.91 – 1.78 (m, 5H), 1.69 – 1.28 (m, 15H), 1.19 – 0.94 (m, 13H), 0.91 (d, *J* = 6.5 Hz, 3H), 0.87 (d, *J* = 1.8, Hz, 3H), 0.87 (d, *J* = 1.8, Hz, 3H), 0.67 (s, 3H) ppm. **^{13}C NMR (126 MHz, $CDCl_3$)** δ 173.0, 139.8, 122.8, 74.0, 56.8, 56.3, 50.2, 42.5, 39.9, 39.7, 38.3, 37.1, 36.7, 36.3, 35.9, 34.6, 33.6, 32.6, 32.0, 32.0, 28.4, 28.2, 28.0, 27.8, 24.4, 24.3, 24.0, 23.0, 22.7, 21.2, 19.5, 18.9, 12.0 ppm. Spectral data was in agreement with the literature.[183]

General procedure 2 (GP2): Synthesis of 2,2-disubstituted dihydroquinazolinones

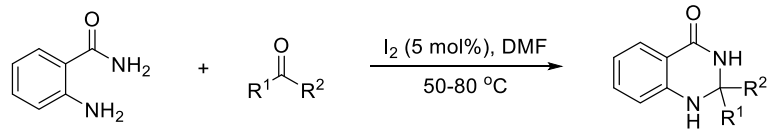

A 100 mL flask containing a stirring bar was charged with 2-aminobenzamide (1.0 equiv.), ketone (1.05 equiv), iodine (5 mol%) and DMF (0.67 M). The reaction mixture was stirred at 50–80 °C for 24 hours. The reaction was cooled to 20 °C and water (50 mL) was added to the reaction generating precipitate that was collected as crude product by suction filtration. The crude material was washed with water and purified by recrystallization (EtOH) to give targeted product.

General procedure 3 (GP3): Alternative synthesis of 2,2-disubstituted dihydroquinazolinones

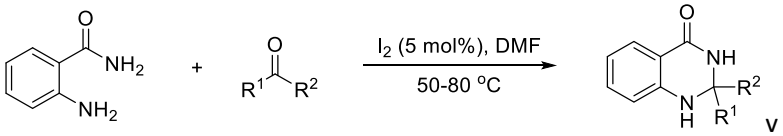

v

A 100 mL flask containing a stirring bar was charged with 2-aminobenzamide (1.0 equiv.), ketone (1.05 equiv.), iodine (5 mol%) and DMF (0.67 M). The reaction mixture was stirred at 50–80 °C for 24 hours. The reaction was cooled to 20 °C, quenched with 10% $Na_2S_2O_3$(aq.) (50 mL) and extracted using EtOAc (2 x 50 mL). The combined organic extracts were dried (Na_2SO_4) and concentrated under reduced pressure affording crude material, which was purified by silica gel chromatography yielding the desired product.

[183] Theis, A.; Ritter, H. Synthesis and Kinetic Studies on the Photochemical Behavior of Polymeric Mesoions from Novel Methacrylic Monomers and of Mesoionic Copolymers with Liquid Crystalline Properties. *Macromolecules* **2003**, *36*, 7552–7559.

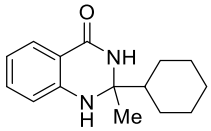

2-Cyclohexyl-2-methyl-2,3-dihydroquinazolin-4(1*H*)-one (2a). Following GP2, using 2-aminobenzamide (1.36 g, 10.0 mmol), 1-cyclohexylethan-1-one (1.32 g, 10.5 mmol) and iodine (0.13 g, 0.5 mmol) in DMF (15 mL) at 80 ºC for 24 hours. The product was obtained as a white solid (1.61 g, 66% yield). **M.p.**: 215 °C. **^{1}H NMR (400 MHz, DMSO-*d*$_6$)** δ 7.87 (s, 1H), 7.52 (dd, *J* = 7.7, 1.6 Hz, 1H), 7.18 (ddd, *J* = 8.2, 7.1, 1.7 Hz, 1H), 6.66 (d, *J* = 8.1, 1H), 6.59 (s, 1H), 6.55 (ddd, *J* = 7.9, 7.2, 1.1 Hz, 1H), 1.83 – 1.66 (m, 4H), 1.63 – 1.49 (m, 2H), 1.30 (s, 3H), 1.14 – 0.95 (m, 5H) ppm. **^{13}C NMR (101 MHz, DMSO-*d*$_6$)** δ 162.8, 147.0, 133.2, 127.0, 115.7, 113.6, 113.5, 71.2, 47.8, 26.6, 26.3, 26.0, 25.9, 25.9, 24.8 ppm. Spectroscopic data was in agreement with the literature.[159]

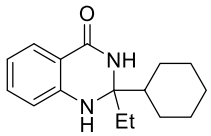

2-Cyclohexyl-2-ethyl-2,3-dihydroquinazolin-4(1*H*)-one (2a´). Following GP2, using 2-aminobenzamide (1.36 g, 10.0 mmol), 1-cyclohexylpropan-1-one (1.47 g, 10.5 mmol) and iodine (0.13 g, 0.5 mmol) in DMF (15 mL) at 80 ºC for 24 hours. The product was obtained as a white solid (1.68 g, 60% yield). **M.p.**: 172 °C. **IR (neat, cm^{-1}):** 3370, 3184, 2934, 2858, 1636, 1611, 743. **^{1}H NMR (500 MHz, DMSO-*d*$_6$)** δ 7.67 (s, 1H), 7.49 (dd, *J* = 7.7, 1.5 Hz, 1H), 7.13 (ddd, *J* = 8.6, 7.2, 1.6 Hz, 1H), 6.64 (d, *J* = 8.2 Hz, 1H), 6.48 (td, *J* = 7.4, 1.0 Hz, 1H), 6.43 (s, 1H), 1.77 – 1.67 (m, 4H), 1.58 (q, *J* = 7.3, 2H), 1.54 – 1.47 (m, 1H), 1.19 – 0.97 (m, 6H), 0.87 (t, *J* = 7.2 Hz, 3H). **^{13}C NMR (126 MHz, DMSO-*d*$_6$)** δ 163.6, 148.2, 133.6, 127.4, 115.5, 113.6, 113.1, 74.4, 48.4, 26.8, 26.5, 26.5, 26.5, 8.3. **HRMS** [ESI$^+$] *calcd*. for ($C_{16}H_{23}N_2O$) $[M+H]^+$: 259.1805, *found*: 259.1798.

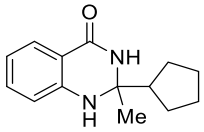

2-Cyclopentyl-2-methyl-2,3-dihydroquinazolin-4(1*H*)-one (2b). Following GP2, using 2-aminobenzamide (1.16 g, 8.5 mmol), 1-cyclopentylethan-1-one (1.00 g, 8.9 mmol) and iodine (0.11 g, 0.4 mmol) in DMF (12 mL) at 80 ºC for 24 hours. The product was obtained as a white solid (0.91 g, 46% yield). **M.p.**: 190 °C. **IR (neat, cm^{-1}):** 3308, 3179, 2951, 2868, 1632, 1482, 1150, 754. **^{1}H NMR (400 MHz, DMSO-*d*$_6$)** δ 7.85 (s, 1H), 7.52 (dd, *J* = 7.7, 1.7 Hz, 1H), 7.17 (ddd, *J* = 8.1, 7.1, 1.7 Hz, 1H), 6.65 (dd, *J* = 8.2, 0.7 Hz, 1H), 6.58 – 6.52 (m, 1H), 6.51 (s, 1H), 2.25 – 2.13 (m, 1H), 1.61 – 1.37 (m, 8H), 1.33 (s, 3H) ppm. **^{13}C NMR (101 MHz, DMSO-*d*$_6$)** δ 162.9, 147.3,

133.1, 126.9, 115.7, 113.6, 113.4, 70.8, 50.8, 26.8, 26.6, 26.5, 25.5, 25.2 ppm. **HRMS** [ESI$^+$] *calcd*. for ($C_{14}H_{18}N_2NaO$) [M+Na]$^+$: 253.1317, *found*: 253.1317.

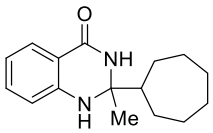

2-Cycloheptyl-2-methyl-2,3-dihydroquinazolin-4(1*H*)-one (2c). Following GP2, using 2-aminobenzamide (1.36 g, 10.0 mmol), 1-cycloheptylethan-1-one (1.47 g, 10.5 mmol) and iodine (0.13 g, 0.5 mmol) in DMF (15 mL) at 80 ºC for 24 hours. The product was obtained as a white solid (1.54 g, 60% yield). **M.p.**: 198 °C. **IR (neat, cm^{-1}):** 3309, 3177, 2915, 2851, 1630, 1516, 1279, 1150, 749. **^{1}H NMR (400 MHz, DMSO-*d*$_6$)** δ 7.97 (s, 1H), 7.54 (dd, *J* = 7.7, 1.7 Hz, 1H), 7.19 (ddd, *J* = 8.1, 7.2, 1.7 Hz, 1H), 6.70 – 6.63 (m, 2H), 6.61 – 6.53 (m, 1H), 1.86 – 1.71 (m, 3H), 1.72 – 1.55 (m, 2H), 1.54 – 1.38 (m, 4H), 1.36 – 1.18 (m, 7H) ppm. **^{13}C NMR (101 MHz, DMSO-*d*$_6$)** δ 162.8, 146.8, 133.1, 127.0, 115.8, 113.9, 113.8, 71.8, 47.9, 28.1, 27.7, 27.7, 27.5, 26.9, 26.7, 23.8 ppm. **HRMS** [ESI$^+$] *calcd*. for ($C_{16}H_{22}N_2NaO$) [M+Na]$^+$: 281.1630, *found*: 281.1627.

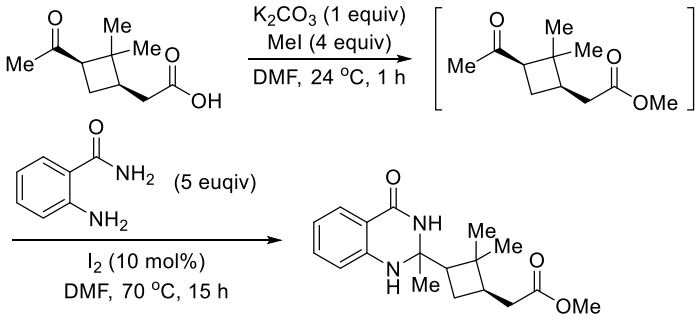

Synthesis of Methyl 2-((1*R*)-2,2-dimethyl-3-(2-methyl-4-oxo-1,2,3,4-tetrahydroquinazolin-2-yl)cyclobutyl)acetate (2d). A 50 mL RBF was charged with *cis*-pinonic acid (500 mg, 2.7 mmol) and potassium carbonate (380 mg, 2.7 mmol), then equipped with a rubber septum with argon inlet. The reaction vessel was flushed with argon and then charged DMF (40 mL, anhydrous). The reaction mixture was stirred for an hour at 24 °C, after which iodomethane (0.67 mL, 10.8 mmol) was added and the reaction mixture was stirred for an additional 16 hours at 24 °C. The reaction mixture was quenched with saturated Na_2CO_3 (aq., 50 mL) and extracted with ethyl acetate (2 x 50 mL). The combined organic extracted were dried ($MgSO_4$) and concentrated under reduced pressure affording crude product as a a yellow oil. The crude material was filtered through a plug of silica (loaded using hexane, released using 20% EtOAc in Hexane) to afford a colourless oil as crude material (522 mg), which was used without further purification. A 10 mL RBF was containing a stirring bar was charged with the crude material of the previous step (552 mg), DMF (4 mL), 2-aminobenzamide (338 mg, 2.5 mmol) and iodine (30.4 mg, 0.12 mmol). The reaction mixture was stirred at 70 °C for 15 hours. Additional iodine (30.4 mg, 0.12 mmol) was added and the reaction

mixture was stirred at 70 °C for 5 hours and then heated to 95 °C and stirred for 25 hours. The reaction mixture was cooled to 20 °C, quenched with 10% $Na_2S_2O_3$ (aq., 30 mL) and extracted using EtOAc (3 x 30 mL). The combined organic extracts were dried (Na_2SO_4) and concentrated under reduced pressure affording crude material, which was purified by silica gel chromatography (0 to 6% MeOH in DCM) yielding the title compound (224 mg, 28% over 2 step) as a colourless oil. **IR (film, cm^{-1})** = 3297, 2952, 1723, 1651, 1612, 1486. **^{1}H NMR (500 MHz, $CDCl_3$, mixture of diasteromers A:B:C:D in a 0.41:0.34:0.13:0.12 ratio)** δ 7.85 – 7.78 (m, 1H), 7.29 – 7.21 (m, 1H), 6.62 (s, 0.34H), 6.60 – 6.49 (m, 1.25H), 6.29 (s, 0.41H), 3.65 – 3.58 (m, 3H), 2.50 – 2.41 (m, 0.25H), 2.37 – 2.27 (m, 1.16H), 2.26 – 1.91 (m, 3.65H), 1.77 – 1.69 (m, 0.13H), 1.65 – 1.53 (m, 0.87H), 1.48–1.42 (m, 3H), 1.28 (s, 0.36H), 1.27 (s, 0.39H), 1.16 (s, 1.15H), 1.13 (s, 1.32H), 1.12 (s, 2.18H), 1.03 (s, 0.39H), 1.02 (s, 0.36H) ppm. **^{13}C NMR (126 MHz, $CDCl_3$)** δ 173.6, 173.6, 173.4, 173.4, 164.3, 164.2, 164.2, 146.1, 146.0, 146.0, 145.9, 134.2, 134.2, 134.1, 134.1, 128.3, 128.3, 128.2, 118.4, 118.4, 118.4, 118.4, 114.2, 114.1, 114.1, 114.1, 71.4, 71.3, 71.0, 70.9, 53.9, 53.1, 51.7, 51.6, 51.6, 51.4, 42.5, 42.4, 40.3, 40.2, 38.6, 38.3, 38.2, 37.9, 35.5, 35.4, 34.7, 34.6, 31.3, 31.2, 28.3, 28.3, 28.1, 28.1, 26.2, 26.1, 25.6, 25.0, 24.9, 24.5, 24.1, 17.8, 17.7 ppm. **HRMS** [ESI$^+$] *calcd*. for ($C_{18}H_{24}N_2NaO_3$) [M+Na]$^+$: 339.1679, *found* 339.1690.

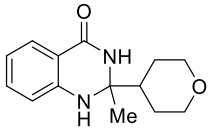

2-Methyl-2-(tetrahydro-2*H*-pyran-4-yl)-2,3-dihydroquinazolin-4(1*H*)-one (2e). Following GP2, using 2-aminobenzamide (1.36 g, 10.0 mmol), 1-(tetrahydro-2*H*-pyran-4-yl)ethan-1-one (1.35 g, 10.5 mmol) and iodine (0.13 g, 0.5 mmol) in DMF (15 mL) at 80 ºC for 24 hours. The product was obtained as a white solid (1.00 g, 41% yield). **M.p.**: 196 °C. **IR (neat, cm^{-1}):** 3355, 3170, 2968, 2840, 1631, 1504, 1271, 1149, 1095, 753. **^{1}H NMR (400 MHz, DMSO-*d*$_6$)** δ 7.92 (s, 1H), 7.53 (dd, *J* = 7.7, 1.6 Hz, 1H), 7.18 (ddd, *J* = 8.2, 7.1, 1.7 Hz, 1H), 6.66 (d, *J* = 8.0 Hz, 1H), 6.63 (s, 1H), 6.59 – 6.52 (m, 1H), 3.92 – 3.81 (m, 2H), 3.21 – 3.08 (m, 2H), 1.83 – 1.71 (m, 1H), 1.61 – 1.47 (m, 2H), 1.42 – 1.25 (m, 5H) ppm. **^{13}C NMR (101 MHz, DMSO-*d*$_6$)** δ 162.9, 147.0, 133.3, 127.0, 115.9, 113.6, 113.4, 70.7, 67.1, 67.0, 45.5, 26.8, 26.6, 24.9 ppm. **HRMS** [ESI$^+$] *calcd*. for ($C_{14}H_{18}N_2NaO_2$) [M+Na]$^+$: 269.1266, *found*: 269.1269.

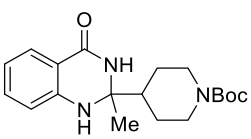

***tert*-Butyl 4-(2-methyl-4-oxo-1,2,3,4-tetrahydroquinazolin-2-yl)piperidine-1-carboxylate (2f).** Following GP2, using 2-aminobenzamide (1.36 g, 10.0 mmol), *tert*-butyl 4-acetylpiperidine-1-carboxylate (2.38 g, 10.5 mmol) and iodine (0.13 g, 0.5 mmol) in DMF (15 mL) at 80 ºC for 24 hours. The product was obtained as a white

solid (1.95 g, 56% yield). **M.p.**: 206 °C. **IR (neat, cm^{-1}):** 3297, 3175, 2951, 1688, 1632, 1425, 1239, 1161, 1209, 755. **^{1}H NMR (400 MHz, DMSO-*d*$_6$)** δ 7.92 (s, 1H), 7.52 (dd, *J* = 7.7, 1.5 Hz, 1H), 7.17 (ddd, *J* = 8.1, 7.2, 1.6 Hz, 1H), 6.64 (d, *J* = 7.7 Hz, 1H), 6.61 (s, 1H), 6.58 – 6.52 (m, 1H), 4.13 – 3.84 (m, 2H), 2.65 – 2.39 (m, 2H), 1.75 – 1.57 (m, 3H), 1.36 (s, 9H), 1.30 (s, 3H), 1.22 – 1.08 (m, 2H) ppm. **^{13}C NMR (101 MHz, DMSO-*d*$_6$)** δ 162.8, 153.7, 146.9, 133.3, 127.0, 115.9, 113.6, 113.3, 78.5, 70.8, 46.5, 28.1, 26.0, 25.8, 25.2 ppm. **HRMS** [ESI$^+$] *calcd*. for ($C_{19}H_{27}N_3NaO_3$) [M+Na]$^+$: 368.1950, *found*: 368.1944.

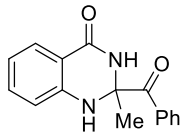

2-Benzoyl-2-methyl-2,3-dihydroquinazolin-4(1*H*)-one (2g). Following GP2, using 2-aminobenzamide (1.36 g, 10.0 mmol), 1-phenylpropane-1,2-dione (1.55 g, 10.5 mmol) and iodine (0.13 g, 0.5 mmol) in DMF (15 mL) at 80 ºC for 24 hours. The product was obtained as a white solid (0.90 g, 34% yield). **M.p.**: 168 °C. **^{1}H NMR (400 MHz, DMSO-*d*$_6$)** δ 8.63 (s, 1H), 7.95 – 7.89 (m, 2H), 7.61 – 7.51 (m, 3H), 7.50 – 7.43 (m, 2H), 7.24 (ddd, *J* = 8.2, 7.2, 1.6 Hz, 1H), 6.77 – 6.72 (m, 1H), 6.69 – 6.63 (m, 1H), 1.67 (s, 3H) ppm. **^{13}C NMR (101 MHz, DMSO-*d*$_6$)** δ 200.7, 163.2, 146.6, 134.8, 133.5, 132.4, 128.9, 128.4, 127.3, 117.6, 114.5, 114.4, 73.8, 24.5 ppm. Spectral data was in agreement with the literature.[184]

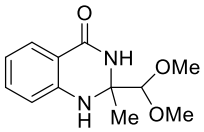

2-(Dimethoxymethyl)-2-methyl-2,3-dihydroquinazolin-4(1*H*)-one (2h). Following GP2, using 2-aminobenzamide (2.72 g, 20.0 mmol), 1,1-dimethoxypropan-2-one (2.48 g, 21.0 mmol) and iodine (0.25 g, 1.0 mmol) in DMF (30 mL) at 80 ºC for 24 hours. The product was obtained as a pale-yellow solid (1.56 g, 33% yield). **M.p.**: 169 °C. **IR (neat, cm^{-1}):** 3300, 2935, 1649, 1517, 1483, 1331, 1272, 1070, 982, 740. **^{1}H NMR (400 MHz, DMSO-*d*$_6$)** δ 7.87 (s, 1H), 7.55 (dd, *J* = 7.7, 1.7 Hz, 1H), 7.19 (ddd, *J* = 8.2, 7.1, 1.6 Hz, 1H), 6.75 – 6.68 (m, 2H), 6.62 – 6.55 (m, 1H), 4.13 (s, 1H), 3.35 (s, 3H), 3.35 (s, 3H), 1.28 (s, 3H) ppm. **^{13}C NMR (101 MHz, DMSO-*d*$_6$)** δ 162.9, 146.9, 133.2, 126.9, 116.2, 113.8, 113.5, 107.9, 70.3, 57.6, 57.5, 21.4 ppm. **HRMS** [ESI$^+$] *calcd*. for ($C_{12}H_{16}N_2NaO_3$) [M+Na]$^+$: 259.1059, *found*: 259.1055.

[184] Wang, J.; Zhang, M,-M.; Wang, X.-S. Structurally Diversified Synthesis of 2,3-Dihydroquinazolin-4-(1H)-ones from 2-Aminobenzamides and 1,2-Dicarbonyl Compounds in Ionic Liquids Catalyzed by Iodine. *Res Chem Intermed*. **2017**, *43*, 2985–3005.

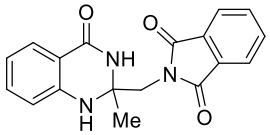

2-((2-Methyl-4-oxo-1,2,3,4-tetrahydroquinazolin-2-yl)methyl)isoindoline-1,3-dione (2i). Following GP2, using 2-aminobenzamide (1.36 g, 10.0 mmol), 2-(2-oxopropyl)isoindoline-1,3-dione (2.13 g, 10.5 mmol) and iodine (0.13 g, 0.5 mmol) in DMF (15 mL) at 80 ºC for 24 hours. The product was obtained as a pale-yellow solid (2.34 g, 73% yield). **M.p.**: 215 °C. **IR (neat, cm^{-1}):** 3371, 3335, 1699, 1661, 1613, 1516, 1425, 1391, 1150, 1076, 761, 532. **^{1}H NMR (400 MHz, DMSO-*d*$_6$)** δ 8.02 (s, 1H), 7.87 – 7.79 (m, 4H), 7.54 (dd, *J* = 7.7, 1.5 Hz, 1H), 7.21 (ddd, *J* = 8.2, 7.2, 1.6 Hz, 1H), 6.81 (s, 1H), 6.64 – 6.54 (m, 2H), 3.76 – 3.66 (m, 2H), 1.39 (s, 3H) ppm. **^{13}C NMR (101 MHz, DMSO-*d*$_6$)** δ 167.9, 162.6, 146.6, 134.2, 133.1, 131.8, 127.0, 123.0, 116.6, 114.5, 113.8, 69.2, 45.4, 26.3 ppm. **HRMS** [ESI$^+$] *calcd*. for ($C_{18}H_{15}N_3NaO_3$) [M+Na]$^+$: 344.1011, *found*: 344.1009.

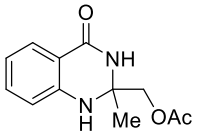

(2-Methyl-4-oxo-1,2,3,4-tetrahydroquinazolin-2-yl)methyl acetate (2j). Following GP3, using 2-aminobenzamide (1.36 g, 10.0 mmol), 2-oxopropyl acetate (1.22 g, 10.5 mmol) and iodine (0.13 g, 0.5 mmol) in DMF (15 mL) at 80 ºC for 24 hours. The product was obtained as a white solid (1.57 g, 67% yield), by using hexane/EtOAc (1:1) as chromatography eluent. **M.p.**: 138 °C. **^{1}H NMR (400 MHz, DMSO-*d*$_6$)** δ 7.96 (s, 1H), 7.49 (dd, *J* = 7.9, 1.5 Hz, 1H), 7.18 – 7.09 (m, 1H), 6.72 (s, 1H), 6.60 – 6.50 (m, 2H), 3.96 (d, *J* = 10.9 Hz, 1H), 3.87 (d, *J* = 10.9 Hz, 1H), 1.80 (s, 3H), 1.30 (s, 3H) ppm. **^{13}C NMR (101 MHz, DMSO-*d*$_6$)** δ 170.1, 163.1, 146.8, 133.4, 127.1, 116.7, 114.0, 113.7, 68.0, 67.9, 24.8, 20.5 ppm. Spectroscopic data was in agreement with the literature.[185]

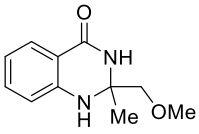

2-(Methoxymethyl)-2-methyl-2,3-dihydroquinazolin-4(1*H*)-one (2k). Following GP2, using 2-aminobenzamide (1.36 g, 10.0 mmol), 1-methoxypropan-2-one (0.92 g, 10.5 mmol) and iodine (0.13 g, 0.5 mmol) in DMF (15 mL) at 80 ºC for 24 hours. The product was obtained as a white solid (0.61 g, 30% yield). **M.p.**: 210 °C. **^{1}H NMR (400 MHz, DMSO-*d*$_6$)** δ 7.91 (s, 1H), 7.54 (dd, *J* = 7.7, 1.6 Hz, 1H), 7.20 (ddd, *J* = 8.2, 7.2,

[185] Soural, M.; Funk, P.; Kvapil, L.; Hradil, P.; Hlaváč, J.; Bertolasi, V. Study of Anthranilate Cyclisation to 2-Hydroxymethyl-2,3-Dihydro-quinazolin-4(1H)-ones and an Alternative Synthetic Route. *ARKIVOC,* **2010**, *10,* 255–265.

1.6 Hz, 1H), 6.71 (s, 1H), 6.69 – 6.64 (m, 1H), 6.63 – 6.57 (m, 1H), 3.36 (d, *J* = 9.4 Hz, 1H), 3.24 (s, 3H), 3.21 (d, *J* = 9.4 Hz, 1H), 1.35 (s, 3H) ppm. **^{13}C NMR (101 MHz, DMSO-*d*$_6$)** δ 163.0, 146.9, 133.3, 127.1, 116.4, 114.0, 113.7, 77.4, 68.3, 58.9, 24.8 ppm. Spectroscopic data was in agreement with the literature.[159]

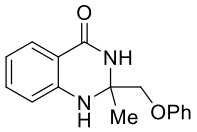

2-Methyl-2-(phenoxymethyl)-2,3-dihydroquinazolin-4(1*H*)-one (2l). Following GP2, using 2-aminobenzamide (1.36 g, 10.0 mmol), 1-phenoxypropan-2-one (1.58 g, 10.5 mmol) and iodine (0.13 g, 0.5 mmol) in DMF (15 mL) at 80 ºC for 24 hours. The product was obtained as a white solid (1.59 g, 59% yield). **M.p.**: 163 °C. **^{1}H NMR (400 MHz, DMSO-*d*$_6$)** δ 8.08 (s, 1H), 7.57 (dd, *J* = 7.7, 1.8 Hz, 1H), 7.26 – 7.16 (m, 3H), 6.93 – 6.86 (m, 2H), 6.86 – 6.80 (m, 2H), 6.70 – 6.58 (m, 2H), 3.94 (d, *J* = 9.4 Hz, 1H), 3.81 (d, *J* = 9.4 Hz, 1H), 1.48 (s, 3H) ppm. **^{13}C NMR (101 MHz, DMSO-*d*$_6$)** δ 163.1, 158.4, 146.8, 133.3, 129.5, 127.0, 120.9, 116.5, 114.8, 113.9, 113.8, 73.0, 68.2, 24.9 ppm. Spectroscopic data was in agreement with the literature.[159]

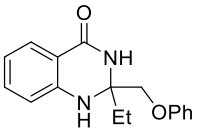

2-Ethyl-2-(phenoxymethyl)-2,3-dihydroquinazolin-4(1*H*)-one (2l′). Following GP2, using 2-aminobenzamide (1.36 g, 10.0 mmol), 1-phenoxybutan-2-one (1.72 g, 10.5 mmol) and iodine (0.13 g, 0.5 mmol) in DMF (15 mL) at 80 ºC for 24 hours. The product was obtained as a pale-yellow solid (1.68 g, 60% yield). **M.p.**: 167 °C. **IR (neat, cm^{-1}):** 3381, 2979, 2935, 1660, 1597, 1484, 1237, 746. **^{1}H NMR (500 MHz, DMSO-*d*$_6$)** δ 7.95 (s, 1H), 7.57 (dd, *J* = 7.7, 1.4 Hz, 1H), 7.23 (t, *J* = 7.9 Hz, 2H), 7.21 – 7.16 (m, 1H), 6.90 (t, *J* = 7.3 Hz, 1H), 6.84 (d, *J* = 7.9, 2H), 6.74 (s, 1H), 6.68 (d, *J* = 7.9 Hz, 1H), 6.59 (t, *J* = 7.4 Hz, 1H), 3.93 (d, *J* = 9.4 Hz, C*H*$_a$CH$_b$, 1H), 3.81 (d, *J* = 9.4 Hz, CH$_a$C*H*$_b$, 1H), 1.84 – 1.71 (m, 2H), 0.98 (t, *J* = 7.2 Hz, 3H). **^{13}C NMR (126 MHz, DMSO-*d*$_6$)** δ 163.5, 158.5, 147.3, 133.2, 129.5, 127.0, 120.9, 116.1, 114.8, 113.8, 113.3, 73.1, 71.0, 29.1, 7.5. **HRMS** [ESI$^+$] *calcd*. for ($C_{17}H_{18}N_2NaO_2$) [M+Na]$^+$: 305.1260, *found*: 305.1259.

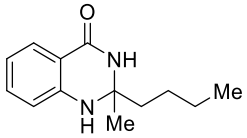

2-Butyl-2-methyl-2,3-dihydroquinazolin-4(1*H*)-one (2m). Following GP2, using 2-aminobenzamide (1.36 g, 10.0 mmol), hexan-2-one (1.20 g, 10.5 mmol) and iodine (0.13 g, 0.5 mmol) in DMF (15 mL) at 80 ºC for 24 hours. The product was obtained as a white solid (816 mg, 37% yield). **M.p.**: 181 °C. **IR (neat, cm^{-1}):** 3326, 3166, 2952,

1636, 1611, 754. **^{1}H NMR (500 MHz, DMSO-*d*$_6$)** δ 7.85 (s, 1H), 7.54 (dd, *J* = 7.7, 1.6 Hz, 1H), 7.19 (ddd, *J* = 8.6, 7.2, 1.7 Hz, 1H), 6.63 (d, *J* = 8.1 Hz, 1H), 6.60 – 6.55 (m, 2H), 1.67 – 1.56 (m, 2H), 1.38 – 1.28 (m, 5H), 1.23 (h, *J* = 7.2, 2H), 0.84 (t, *J* = 7.2, 1.0 Hz, 3H). **^{13}C NMR (126 MHz, DMSO-*d*$_6$)** δ 163.1, 147.2, 133.2, 127.1, 116.0, 114.0, 113.5, 69.1, 41.1, 27.9, 25.6, 22.5, 14.0. **HRMS** [ESI$^+$] *calcd*. for ($C_{13}H_{18}N_2NaO$) [M+Na]$^+$: 241.1311, *found*: 241.1310.

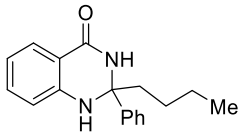

2-Butyl-2-phenyl-2,3-dihydroquinazolin-4(1*H*)-one (2m´). Following GP3, using 2-aminobenzamide (1.36 g, 10.0 mmol), 1-phenylpentan-1-one (1.70 g, 10.5 mmol) and iodine (0.13 g, 0.5 mmol) in DMF (15 mL) at 80 ºC for 24 hours. The product was obtained as a white solid (1.67 g, 60% yield), by using hexane/EtOAc (1:1) as eluent. **M.p.**: 143 °C. **IR (neat, cm^{-1}):** 3270, 2945, 1610, 1482, 1378, 1149, 746, 697. **^{1}H NMR (400 MHz, CDCl$_3$)** δ 7.74 (dd, *J* = 7.8, 1.3 Hz, 1H), 7.44 (s, 1H), 7.40 – 7.33 (m, 2H), 7.24 – 7.10 (m, 4H), 6.71 – 6.61 (m, 2H), 1.97 (t, *J* = 8.2 Hz, 2H), 1.39 – 1.16 (m, 4H), 0.77 (t, *J* = 7.1 Hz, 2H) ppm. **^{13}C NMR (101 MHz, CDCl$_3$)** δ 165.3, 146.1, 145.1, 134.1, 128.6, 128.5, 127.9, 125.5, 119.0, 115.8, 115.0, 73.6, 42.7, 26.0, 22.7, 14.0 ppm. **HRMS** [ESI$^+$] *calcd*. for ($C_{18}H_{20}N_2NaO$) [M+Na]$^+$: 303.1473, *found*: 303.1474.

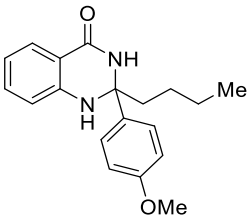

2-Butyl-2-(4-methoxyphenyl)-2,3-dihydroquinazolin-4(1*H*)-one (2m´´) Following GP3, using 2-aminobenzamide (1.36 g, 10.0 mmol), 1-(4-methoxyphenyl)pentan-1-one (2.02 g, 10.5 mmol) and iodine (0.13 g, 0.5 mmol) in DMF (15 mL) at 80 ºC for 24 hours. The product was obtained as a white solid (1.90 g, 61% yield), by using hexane/EtOAc (3:1) as eluent. **M.p.**: 163 °C. **IR (neat, cm^{-1}):** 3255, 3178, 2957, 1644, 1611, 1255, 752. **^{1}H NMR (500 MHz, DMSO-*d*$_6$)** δ 8.57 (s, 1H), 7.46 (dd, *J* = 7.7, 1.5 Hz, 1H), 7.39 (s, 1H), 7.36 (d, *J* = 8.9 Hz, 2H), 7.18 (ddd, *J* = 8.2, 7.2, 1.6 Hz, 1H), 6.82 (d, *J* = 8.9 Hz, 2H), 6.80 (d, *J* = 8.1 Hz, 1H), 6.54 (d, *J* = 7.6 Hz, 1H), 3.67 (s, 3H), 1.83 – 1.71 (m, 2H), 1.43 (quint., *J* = 7.9 Hz, 2H), 1.32 – 1.22 (m, 2H), 0.87 (t, *J* = 7.3 Hz, 3H).**^{13}C NMR (126 MHz, DMSO-*d*$_6$)** δ 164.1, 158.1, 147.5, 139.7, 133.1, 127.1, 126.6, 116.5, 114.8, 114.4, 113.2, 72.6, 55.0, 42.3, 26.0, 22.2, 14.0. **HRMS** [ESI$^+$] *calcd*. for ($C_{19}H_{23}N_2O_2$) [M+H]$^+$: 311.1754, *found*: 311.1750.

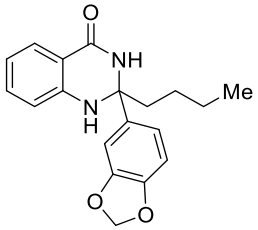

2-(Benzo[d][1,3]dioxol-5-yl)-2-butyl-2,3-dihydroquinazolin-4(1*H*)-one (2m´´´). Following GP3, using 2-aminobenzamide (1.36 g, 10.0 mmol), 1-(benzo[*d*][1,3]dioxol-5-yl)pentan-1-one (2.16 g, 10.5 mmol) and iodine (0.13 g, 0.5 mmol) in DMF (15 mL) at 80 ºC for 24 hours. The product was obtained as a white solid (1.84 g, 57% yield), by using hexane/EtOAc (3:1) as eluent. **M.p.**: 85 °C. **IR (neat, cm^{-1}):** 3257, 2957, 1646, 1611, 1484, 1242. **^{1}H NMR (500 MHz, DMSO-*d*$_6$)** δ 8.57 (s, 1H), 7.46 (d, *J* = 7.7 Hz, 1H), 7.38 (s, 1H), 7.22 – 7.17 (m, 1H), 7.03 (d, *J* = 1.7 Hz, 1H), 6.89 (dd, *J* = 8.1, 1.7 Hz, 1H), 6.79 (d, *J* = 8.2 Hz, 1H), 6.78 (d, *J* = 8.1 Hz, 1H), 6.56 (t, *J* = 7.6 Hz, 1H), 5.94 (s, C*H*$_a$CH$_b$, 1H), 5.93 (s, CH$_a$C*H*$_b$, 1H), 1.79 – 1.70 (m, 2H), 1.42 (quint., *J* = 7.8 Hz, 2H), 1.27 (h, *J* = 7.3 Hz, 2H), 0.87 (t, *J* = 7.3 Hz, 3H). **^{13}C NMR (126 MHz, DMSO-*d*$_6$)** δ 164.5, 147.9, 147.6, 146.6, 142.5, 133.7, 127.6, 119.1, 117.1, 115.3, 114.9, 107.8, 106.6, 101.4, 73.3, 42.7, 26.4, 22.7, 14.5. **HRMS** [ESI$^+$] *calcd*. for ($C_{19}H_{20}N_2NaO_3$) [M+Na]$^+$: 347.1366, *found*: 347.1360.

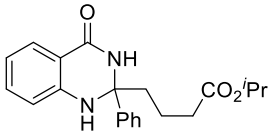

Isopropyl 4-(4-oxo-2-phenyl-1,2,3,4-tetrahydroquinazolin-2-yl)butanoate (2n). Following GP3, using 2-aminobenzamide (1.36 g, 10.0 mmol), isopropyl 5-oxo-5-phenylpentanoate (2.46 g, 10.5 mmol) and iodine (0.13 g, 0.5 mmol) in DMF (15 mL) at 80 ºC for 24 hours. The product was obtained as a white solid (2.71 g, 49% yield), by using hexane/EtOAc (2:1) as chromatography eluent. **M.p.**: 165 °C. **IR (neat, cm^{-1}):** 3326, 2977, 1712, 1643, 1485, 1371, 1285, 1201, 1109, 757, 698. **^{1}H NMR (400 MHz, DMSO-*d*$_6$)** δ 8.67 (s, 1H), 7.49 (s, 1H), 7.47 – 7.42 (m, 3H), 7.27 (t, *J* = 7.6 Hz, 2H), 7.22 – 7.13 (m, 2H), 6.82 (d, *J* = 7.7 Hz, 1H), 6.58 – 6.52 (m, 1H), 4.86 (hept., *J* = 6.3 Hz, 1H), 2.28 – 2.20 (m, 2H), 1.83 – 1.68 (m, 4H), 1.15 (d, *J* = 6.2, Hz, 6H) ppm. **^{13}C NMR (101 MHz, DMSO-*d*$_6$)** δ 172.2, 164.0, 147.5, 147.4, 133.3, 128.0, 127.2, 127.1, 125.3, 116.7, 114.7, 114.4, 72.8, 67.0, 41.4, 33.8, 21.6, 19.8 ppm. **HRMS** [ESI$^+$] *calcd*. for ($C_{21}H_{24}N_2NaO_3$) [M+Na]$^+$: 375.1685, *found*: 375.1677.

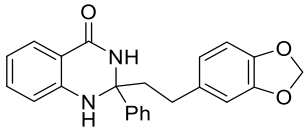

2-(2-(Benzo[*d*][1,3]dioxol-5-yl)ethyl)-2-phenyl-2,3-dihydroquinazolin-4(1*H*)-one (2o). Following GP3, using 2-aminobenzamide (1.36 g, 10.0 mmol), 3-

(benzo[*d*][1,3]dioxol-5-yl)-1-phenylpropan-1-one (2.67 g, 10.5 mmol) and iodine (0.13 g, 0.5 mmol) in DMF (15 mL) at 80 ºC for 24 hours. The product was obtained as a white solid (2.83 g, 76% yield), by using hexane/EtOAc (2:1) as chromatography eluent. **M.p.**: 95 °C. **IR (neat, cm^{-1}):** 3293, 1647, 1609, 1482, 1443, 1244, 1035, 925, 752, 697. **^{1}H NMR (400 MHz, $CDCl_3$)** δ 7.99 (s, 1H), 7.77 (dd, *J* = 7.8, 1.3 Hz, 1H), 7.44 – 7.36 (m, 2H), 7.27 – 7.10 (m, 4H), 6.73 – 6.67 (m, 1H), 6.63 – 6.58 (m, 3H), 6.54 – 6.50 (m, 1H), 5.83 – 5.81 (m, 2H), 2.74 – 2.55 (m, 2H), 2.33 – 2.16 (m, 2H) ppm. **^{13}C NMR (101 MHz, $CDCl_3$)** δ 165.5, 147.9, 146.1, 146.0, 145.0, 134.9, 134.2, 128.8, 128.6, 128.1, 125.4, 121.3, 119.2, 115.7, 115.0, 109.1, 108.4, 101.0, 73.6, 44.8, 30.4 ppm. **HRMS** [ESI$^+$] *calcd*. for ($C_{23}H_{20}N_2NaO_3$) [M+Na]$^+$: 395.1372, *found*: 395.1371.

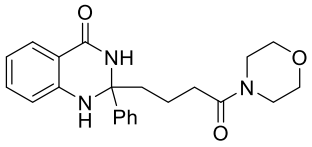

2-Methyl-2-(4-morpholino-4-oxobutyl)-2,3-dihydroquinazolin-4(1*H*)-one (2p). Following GP2, using 2-aminobenzamide (1.36 g, 10.0 mmol), 1-morpholino-5-phenylpentane-1,5-dione (2.74 g, 10.5 mmol) and iodine (0.13 g, 0.5 mmol) in DMF (15 mL) at 80 ºC for 24 hours. The product was obtained as a white solid (2.21 g, 70% yield). **M.p.**: 254 °C. **IR (neat, cm^{-1}):** 3322, 3232, 1627, 1510, 1363, 1276, 1226, 1112, 1027, 757, 705. **^{1}H NMR (400 MHz, DMSO-d_6)** δ 8.67 (s, 1H), 7.49 (s, 1H), 7.47 – 7.42 (m, 3H), 7.31 – 7.24 (m, 2H), 7.22 – 7.13 (m, 2H), 6.82 (d, *J* = 7.7 Hz, 1H), 6.58 – 6.52 (m, 1H), 3.56 – 3.48 (m, 4H), 3.44 – 3.36 (m, 4H), 2.32 – 2.24 (m, 2H), 1.87 – 1.76 (m, 2H), 1.74 – 1.62 (m, 2H) ppm. **^{13}C NMR (101 MHz, DMSO-d_6)** δ 170.7, 164.0, 147.6, 147.5, 133.3, 127.9, 127.2, 127.0, 125.4, 116.6, 114.7, 114.5, 72.9, 66.1, 45.5, 41.8, 41.4, 32.2, 19.8 ppm. **HRMS** [ESI$^+$] *calcd*. for ($C_{22}H_{25}N_3NaO_3$) [M+Na]$^+$: 402.1794, *found*: 402.1784.

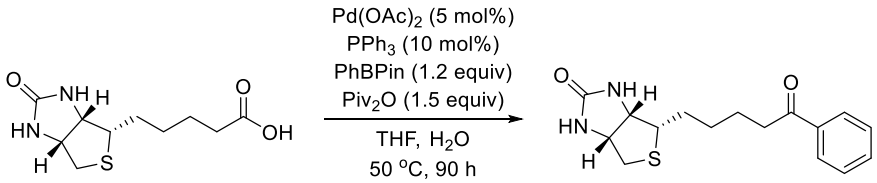

Synthesis of (3a*S*,4*S*,6a*R*)-4-(5-oxo-5-phenylpentyl)tetrahydro-1*H*-thieno[3,4-*d*]imidazol-2(3*H*)-one (S1). A 27 mL glass screw-cap vial was charged with a stirrer bar, palladium acetate (12.5 mg, 0.06 mmol, trimer), triphenylphosphine (31.7 mg, 0.12 mmol), D-(+)-biotin (266 mg, 1.09 mmol) and phenylboronic acid (161 mg, 1.32 mmol). The reaction vessel was equipped with a rubber septum with an argon inlet. The contents of the reaction vessel were flushed with argon, then charged with THF (5 mL), pivalic anhydride (0.32 mL, 1.64 mmol) and water (47 mL). The rubber septum and argon inlet were quickly removed and replaced with a screw cap. The reaction mixture was stirred for 90 hours at 50 °C, after which the reaction mixture was concentrated

under reduced pressure yielding crude material, which was purified by silica gel chromatography (0 to 3% MeOH in DCM), yielding the title compound (68.4 mg, 21%) as a white solid. **M.p.** 171 °C. **IR (film, cm^{-1})** = 3210, 2922, 1698. **^{1}H NMR (500 MHz, CDCl3)** δ 7.98 – 7.93 (m, 2H), 7.55 (tt, *J* = 7.4, 1.2 Hz, 1H), 7.46 (tt, *J* = 7.4 Hz, 2H), 4.52 (dd, *J* = 7.8, 5.0 Hz, 1H), 4.33 (dd, *J* = 7.8, 4.6 Hz, 1H), 3.19 (ddd, *J* = 8.5, 6.5, 4.6 Hz, 1H), 3.00 (t, *J* = 7.3 Hz, 2H), 2.92 (dd, *J* = 12.9, 5.0 Hz, 1H), 2.74 (d, *J* = 12.9 Hz, 1H), 1.85 – 1.67 (m, 4H), 1.57 – 1.46 (m, 2H) ppm. **^{13}C NMR (126 MHz, $CDCl_3$)** δ. 200.5, 163.5, 137.0, 133.2, 128.8, 128.2, 62.2, 60.4, 55.5, 40.7, 38.3, 28.7, 28.6, 24.2 ppm. **HRMS** [ESI$^+$] *calcd*. for ($C_{16}H_{20}N_2NaO_2S$) [M+Na]$^+$: 327.1138, *found* 327.1130.

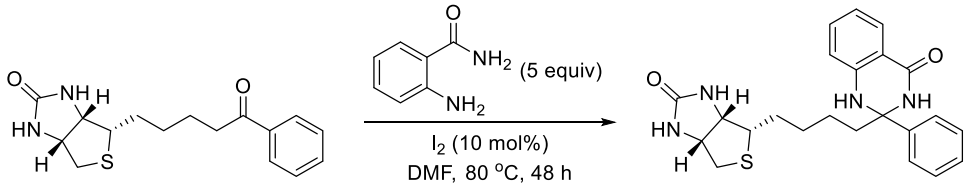

Synthesis of (3a*S*,4*S*,6a*R*)-4-(4-(4-Oxo-2-phenyl-1,2,3,4-tetrahydroquinazolin-2-yl)butyl)tetrahydro-1*H*-thieno[3,4-*d*]imidazol-2(3*H*)-one (2q). A 25 mL flask containing a stirring bar was charged with 2-aminobenzamide (558 mg, 4.1 mmol), (3a*S*,4*S*,6a*R*)-4-(5-oxo-5-phenylpentyl)tetrahydro-1*H*-thieno[3,4-*d*]imidazol-2(3*H*)-one (251 mg, 0.82 mmol), iodine (20.3 mg, 0.08 mmol) and DMF (10 mL). The reaction mixture was stirred at 70 °C for 68 hours. The reaction was cooled to 20 °C, quenched with 10% $Na_2S_2O_3$ (aq., 20 mL) and extracted using EtOAc (3 x 30 mL). The combined organic extracts were dried (Na_2SO_4) and concentrated under reduced pressure affording crude material, which was purified by silica gel chromatography (0 to 6% MeOH in DCM) yielding the title compound (44.3 mg, 10%) as a white solid. **M.p.** 170 °C. **IR (film, cm^{-1})** = 3245, 2923, 1687, 1687, 1611, 1483. **^{1}H NMR (500 MHz, DMSO-*d*6)** δ 8.65 (s, 1H), 7.50 – 7.43 (m, 4H), 7.27 (t, *J* = 7.6 Hz, 2H), 7.21 – 7.15 (m, 2H), 6.81 (d, *J* = 8.2 Hz, 1H), 6.55 (t, *J* = 7.4 Hz, 1H), 6.40 (br. s, 1H), 6.36 (br. s, 1H), 4.32 – 4.28 (m, 1H), 4.14 – 4.10 (m, 1H), 3.11 (tt, *J* = 10.0, 5.5 Hz, 1H), 2.81 (ddd, *J* = 12.5, 5.1, 2.7 Hz, 1H), 2.57 (d, *J* = 12.4 Hz, 1H), 1.85 – 1.70 (m, 2H), 1.66 – 1.57 (dt, *J* = 17.7, 6.0 Hz, 1H), 1.55 – 1.43 (m, 3H), 1.39 – 1.26 (m, 2H) ppm. **^{13}C NMR (126 MHz, DMSO-*d*6)** δ 164.6, 163.2, 148.3, 148.0, 133.7, 128.4, 127.6, 127.4, 125.8, 117.1, 115.2, 114.9, 73.4, 61.6, 59.7, 55.8, 42.6, 40.2, 29.0, 28.7, 24.2 ppm. **HRMS** [ESI$^+$] *calcd*. for ($C_{23}H_{26}N_4NaO_2S$) [M+Na]$^+$: 445.1669, *found* 445.1662.

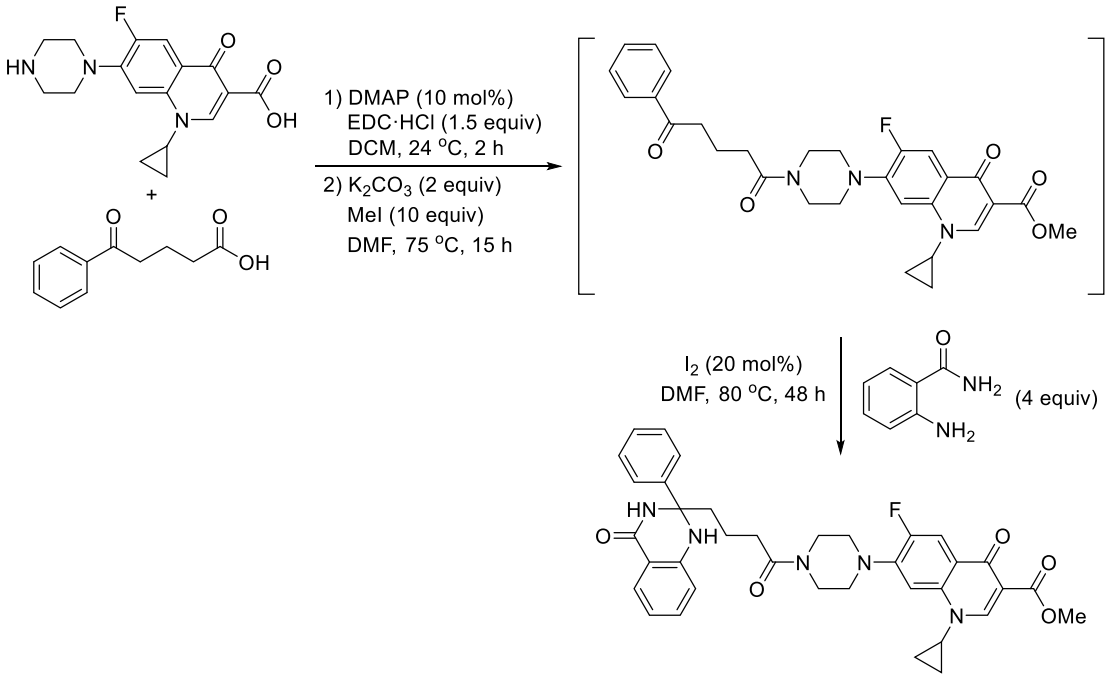

Synthesis of methyl 1-cyclopropyl-6-fluoro-4-oxo-7-(4-(4-(4-oxo-2-phenyl-1,2,3,4-tetrahydroquinazolin-2-yl)butanoyl)piperazin-1-yl)-1,4-dihydroquinoline-3-carboxylate (2r). A 27 mL screw cap vial equipped with a stirrer bar was charged with ciprofloxacin (900 mg, 2.72 mmol) and DCM (15 mL). The mixture was cooled to 0 °C, then 5-oxo-5-phenylpentanoic acid (782 mg, 4.07 mmol), *N*-(3-Dimethylaminopropyl)-*N*′-ethylcarbodiimide hydrochloride (780 mg, 4.07 mmol) and DMAP (33 mg, 0.27 mmol) were sequentially added forming a white suspension in solution. The reaction mixture was warmed to 24 °C and stirred for 2 hours, during which the white suspension dissolved forming a yellow solution. The reaction was quenched with 1 M HCl (aq., 40 mL) and extracted with DCM (2 x 75 mL). The combined organic extracts were dried ($MgSO_4$) and concentrated under reduced pressure affording crude material (1.50 g) as a white solid, which was used without further purification. A 27 mL glass vial equipped with a stirrer bar was charged with the crude material (1.50 g) of the previous step and potassium carbonate (752 mg, 5.44 mmol). The reaction vessel was equipped with a rubber septum and an argon inlet. Contents of the reaction vessel were flushed with argon, then charged with DMF (20 mL, anhydrous) and stirred for 30 minutes at 60 °C. The reaction mixture was cooled to 24 °C and charged with iodomethane (0.68 mL, 10.9 mmol). The reaction vessel was sealed with a screw cap and the contents were stirred at 70 °C for 16 hours. The reaction mixture was cooled to 24 °C then quenched with saturated Na_2CO_3 (aq., 150 mL) and extracted with DCM (3 x 100 mL). The combined organic extracts were dried ($MgSO_4$) and concentrated under reduced pressure yielding crude material as a brown residue, which was filtered through a plug of silica (loaded with DCM, released with 3% MeOH in DCM) affording crude material (1.15 g) as a white solid that was used without further purification. A 27 mL glass vial

equipped with a stirring bar was charged with the crude material (1.15 mg) of the previous step, 2-aminobenzamide (1.37 g, 10.1 mmol), iodine (66 mg, 0.26 mmol) and DMF (10 mL). The reaction mixture was stirred for 5 hours at 80 °C, then an extra aliquot of iodine (33 mg, 0.13 mmol) was added and the reaction was stirred for an additional 3 hours at 80 °C. The reaction mixture was cooled to 20 °C, quenched with water (60 mL) and filtered affording a brown residue as crude material. A 500 mL RBF was charged with the crude material and while heating at 90 °C ethanol (125 mL) was added forming a white suspension. While still hot the white suspension was filtered yielding a white solid, which was sequentially washed with methanol (30 mL) and diethyl ether (30 mL), yielding the title compound (963 mg, 56%) as a white solid. **M.p.** 292 °C. **IR (film, cm^{-1}) =** 3300, 1686, 1660, 1618, 1446, 1242. **^{1}H NMR (500 MHz, DMSO-*d*$_6$)** δ 8.71 (s, 1H), 8.43 (s, 1H), 7.76 (d, *J* = 13.1 Hz, 1H), 7.56 –7.40 (m, 5 H), 7.29 (t, *J* = 7.7 Hz, 2H), 7.24 – 7.14 (m, 2H), 6.84 (d, *J* = 8.1 Hz, 1H), 6.56 (d, *J* = 8.1 Hz, 1H), 3.73 (s, 3H), 3.70 – 3.59 (m, 5H), 3.23 (br.s, 2H), 3.19 (br.s, 2H), 2.41 – 2.32 (m, 2H), 1.91 – 1.80 (m, 2H), 1.80 – 1.67 (m, 2H), 1.29 – 1.23 (m, 2H), 1.14 – 1.04 (m, 2H) ppm. **^{13}C NMR (126 MHz, DMSO-*d*$_6$)** δ 171.5, 170.6, 164.9, 164.0, 152.5 (d, *J* = 246.5 Hz), 148.30, 147.6, 147.5, 143.6 (d, *J* = 10.2 Hz), 138.0, 133.3, 127.9, 127.1, 127.0, 125.4, 122.1 (d, *J* = 6.2 Hz), 116.6, 114.7, 114.4, 111.6 (d, *J* = 22.6 Hz), 109.0, 106.6, 72.9, 51.3, 49.9, 49.4, 44.8, 41.8, 40.7, 34.8, 32.4, 19.9, 7.6 ppm. **^{19}F NMR (376 MHz, DMSO-*d*$_6$)** δ -124.7 (dd, *J* = 13.3, 7.5 Hz). **HRMS** [ESI$^+$] *calcd*. for ($C_{36}H_{37}FN_5O_5$) $[M+H]^+$: 638.2773, *found* 638.2767.

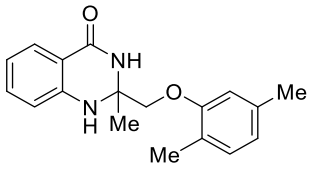

2-((2,5-Dimethylphenoxy)methyl)-2-methyl-2,3-dihydroquinazolin-4(1*H*)-one (2s). Following GP3, using 2-aminobenzamide (3.81 g, 28.0 mmol), 1-phenylpentan-1-one (2.52 g, 14.1 mmol) and iodine (0.36 g, 1.4 mmol) in DMF (20 mL) at 80 ºC for 48 hours. The product was obtained as a pale-yellow solid (2.69 g, 64% yield), by using 0% to 20% acetone in hexane as eluent. **M.p.**: 159 °C. **IR (neat, cm^{-1}):** 3249, 3172, 3016, 1639, 1614, 1261, 752. **^{1}H NMR (500 MHz, DMSO-*d*$_6$)** δ 8.05 (s, 1H), 7.58 (dd, *J* = 7.7, 1.4 Hz, 1H), 7.19 (ddd, *J* = 8.6, 7.2, 1.6 Hz, 1H), 6.91 (d, *J* = 7.5 Hz, 1H), 6.81 (s, 1H), 6.66 – 6.63 (m, 2H), 6.62 – 6.58 (m, 2H), 3.90 (d, *J* = 9.3 Hz, C*H*$_a$CH$_b$, 1H), 3.80 (d, *J* = 9.3 Hz, CH$_a$C*H*$_b$, 1H), 2.19 (s, 3H), 1.85 (s, 3H), 1.52 (s, 3H). **^{13}C NMR (126 MHz, DMSO-*d*$_6$)** δ 163.3, 156.2, 147.1, 136.1, 133.2, 130.0, 127.1, 122.8, 120.9, 116.2, 113.8, 113.6, 112.0, 73.9, 68.3, 25.2, 20.9, 15.2. **HRMS** [ESI$^+$] *calcd*. for ($C_{18}H_{20}N_2NaO_2$) $[M+Na]^+$: 319.1417, *found*: 319.1418.

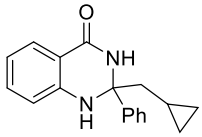

2-(Cyclopropylmethyl)-2-phenyl-2,3-dihydroquinazolin-4(1*H*)-one (2t). Following GP3, using 2-aminobenzamide (787 mg, 5.8 mmol), 2-cyclopropyl-1-phenylethan-1-one (926 mg, 5.8 mmol) and iodine (74 mg, 0.3 mmol) in DMF (8.5 mL) at 80 ºC for 24 hours. The product was obtained as a white solid (1.24 g, 77% yield), by using hexane/EtOAc (3:1) as chromatography eluent. **M.p.**: 154 °C. **IR (neat, cm^{-1}):** 3438, 3011, 1657, 1611, 1488, 1373, 1268, 1155, 1028, 762, 699. **^{1}H NMR (400 MHz, DMSO-*d*$_6$)** δ 8.61 (s, 1H), 7.53 – 7.42 (m, 4H), 7.30 – 7.22 (m, 2H), 7.21 – 7.11 (m, 2H), 6.86 – 6.79 (m, 1H), 6.58 – 6.50 (m, 1H), 1.81 – 1.65 (m, 2H), 1.02 – 0.90 (m, 1H), 0.43 – 0.28 (m, 2H), 0.24 – 0.15 (m, 1H), 0.07 – -0.03 (m, 1H) ppm. **^{13}C NMR (101 MHz, DMSO-*d*$_6$)** δ 164.1, 147.6, 147.5, 133.2, 127.8, 127.2, 127.0, 125.5, 116.6, 114.7, 114.4, 73.5, 46.9, 6.2, 4.3, 4.1 ppm. **HRMS** [ESI$^+$] *calcd*. for ($C_{18}H_{18}N_2NaO$) [M+Na]$^+$: 301.1317, *found*: 301.1319.

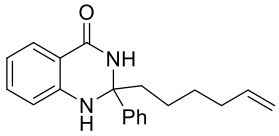

2-(Hex-5-en-1-yl)-2-phenyl-2,3-dihydroquinazolin-4(1*H*)-one (2u). Following GP3, using 2-aminobenzamide (680 mg, 5.0 mmol), 1-phenylhept-6-en-1-one (987 mg, 5.3 mmol) and iodine (64 mg, 0.3 mmol) in DMF (8 mL) at 80 ºC for 24 hours. The product was obtained as a white solid (1.18 g, 77% yield), by using hexane/EtOAc (3:1) as eluent. **M.p.**: 111 °C. **IR (neat, cm^{-1}):** 3274, 2930, 1639, 1608, 1487. **^{1}H NMR (500 MHz, DMSO-*d*$_6$)** δ 8.67 (s, 1H), 7.49 – 7.44 (m, 4H), 7.27 (t, *J* = 7.6 Hz, 2H), 7.21 – 7.14 (m, 2H), 6.81 (d, *J* = 8.1 Hz, 1H), 6.55 (t, *J* = 7.5 Hz, 1H), 5.79 (ddt, *J* = 17.0, 10.1, 6.7 Hz, 1H), 5.00 (dq, *J* = 17.0, 1.7 Hz, 1H), 4.93 (ddt, *J* = 10.1, 2.3, 1.2 Hz, 1H), 2.02 (q, *J* = 7.1 Hz, 2H), 1.84 – 1.73 (m, 2H), 1.51 (quint., *J* = 7.9 Hz, 2H), 1.39 – 1.30 (m, 2H). **^{13}C NMR (126 MHz, DMSO-*d*$_6$)** δ 164.1, 147.9, 147.5, 138.7, 133.2, 127.9, 127.1, 126.9, 125.3, 116.5, 114.8, 114.7, 114.4, 72.9, 42.2, 33.3, 28.4, 23.4. **HRMS** [ESI$^+$] *calcd*. for ($C_{20}H_{22}N_2NaO$) [M+Na]$^+$: 329.1624, *found*: 329.1619.

2.7.3 Synthesis of Product

General procedure 4 (GP4): Nickel-catalyzed coupling with aryl bromides

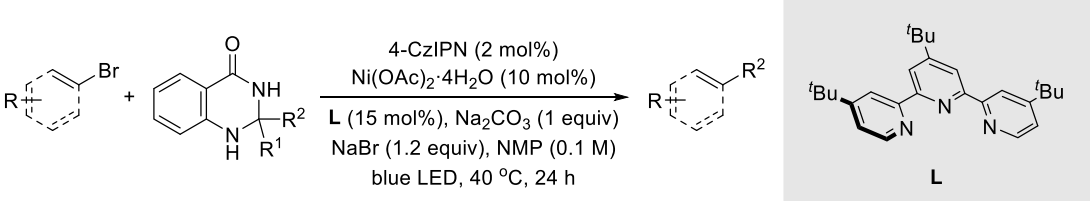

An oven-dried 8 mL screw-cap test tube containing a stirring bar was charged with 4-CzIPN (3.2 mg, 2 mol%), $Ni(OAc)_2 \cdot 4H_2O$ (5.0 mg, 10 mol%), 4,4',4"-tri-tert-butyl-2,2':6'2"- terpyridine (12.1 mg, 15 mol%), NaBr (24.7 mg, 1.2 equiv), aryl bromide (if solid, 1.0 equiv, 0.2 mmol) and ketone derivative (1.2 equiv). The test tube was introduced in a nitrogen-filled glovebox where Na_2CO_3 (21.2 mg, 1.0 equiv) was added. The reaction vessel was sealed with a screw cap and removed from the glovebox. Afterwards, aryl bromide (if liquid) or vinyl bromide and NMP (2 mL, 0.1 M) were added by syringe. Parafilm was used to reseal the pierced cap. The reaction mixture was stirred at rt for 1 minute, then exposed to blue LED irradiation at 40 °C for 24 hours. The reaction mixture was quenched with water/brine (10 mL) and extracted with ethyl acetate (3 x 10 mL). The combined organic extracts were dried (Na_2SO_4), concentrated under reduced pressure and purified by silica gel chromatography.

General procedure 5 (GP5): Alternative nickel-catalyzed coupling with aryl bromides

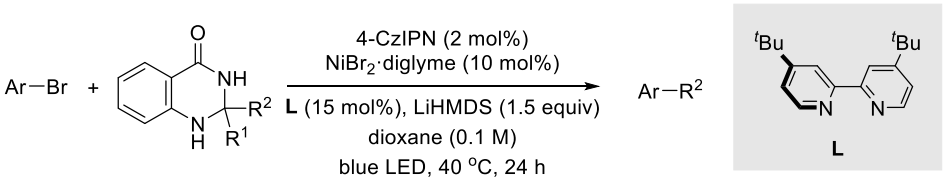

An oven-dried 8 mL screw-cap test tube containing a stirring bar was charged with 4-CzIPN (3.2 mg, 2 mol%), 4,4'-di-*tert*-butyl-2,2'-bipyridine (8.0 mg, 15 mol%), aryl bromide (if solid, 1.0 equiv, 0.2 mmol) and ketone derivative (1.5 equiv). The test tube was taken into a nitrogen-filled glovebox where $NiBr_2 \cdot$diglyme (7.1 mg, 10 mol%) and LiHMDS (50.1 mg, 1.5 equiv) were added to the reaction vessel. The reaction tube was sealed with a screw cap and removed from the glovebox. Afterwards, aryl bromide (if liquid) and dioxane (2 mL, 0.1 M) were added by syringe. Parafilm was used to reseal the pierced cap. The reaction mixture was stirred at rt for 1 minute, then exposed to blue LED irradiation at 40 °C for 24 hours. The reaction mixture was quenched with water/brine (10 mL) and extracted with ethyl acetate (3 x 10 mL). The combined organic extracts were dried (Na_2SO_4), concentrated under reduced pressure and purified by silica gel chromatography.

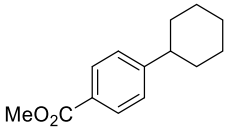

Methyl 4-cyclohexylbenzoate (3a). Following GP4, methyl 4-bromobenzoate (43.0 mg, 0.20 mmol) and 2-cyclohexyl-2-methyl-2,3-dihydroquinazolin-4(1*H*)-one (**2a**) (58.6 mg, 0.24 mmol) were used, affording the title compound as a colourless liquid (41.0 mg, 94% yield), by using hexane/EtOAc (100:1) as chromatography eluent. In a

second independent experiment, 40.7 mg (93%) were obtained, giving an average of 93% yield. **^{1}H NMR (400 MHz, $CDCl_3$)** δ 7.98 – 7.93 (m, 2H), 7.30 – 7.24 (m, 2H), 3.89 (s, 3H), 2.62 – 2.49 (m, 1H), 1.93 – 1.80 (m, 4H), 1.80 – 1.71 (m, 1H), 1.49 – 1.33 (m, 4H), 1.32 – 1.19 (m, 1H) ppm. **^{13}C NMR (101 MHz, $CDCl_3$)** δ 167.3, 153.6, 129.8, 127.9, 127.0, 52.1, 44.8, 34.3, 26.9, 26.2 ppm. Spectral data was in agreement with the literature.[186]

Following GP4, methyl 4-bromobenzoate (43.0 mg, 0.20 mmol) and 2-cyclohexyl-2-ethyl-2,3-dihydroquinazolin-4(1*H*)-one (**2a´**) (61.9 mg, 0.24 mmol) were used, affording the title compound as a colourless liquid (40.8 mg, 94% yield), by using hexane/EtOAc (100:1) as chromatography eluent. In a second independent experiment, 40.6 mg (93%) were obtained, giving an average of 93% yield. **^{1}H NMR (400 MHz, $CDCl_3$)** δ 8.00 – 7.93 (m, 2H), 7.31 – 7.24 (m, 2H), 3.90 (s, 3H), 2.62 – 2.50 (m, 1H), 1.95 – 1.81 (m, 4H), 1.81 – 1.72 (m, 1H), 1.51 – 1.34 (m, 4H), 1.32 – 1.20 (m, 1H) ppm. **^{13}C NMR (101 MHz, $CDCl_3$)** δ 167.3, 153.6, 129.8, 127.9, 127.0, 52.1, 44.8, 34.3, 26.9, 26.2 ppm.

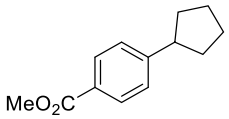

Methyl 4-cyclopentylbenzoate (3b). Following GP4, methyl 4-bromobenzoate (43.0 mg, 0.20 mmol) and 2-cyclopentyl-2-methyl-2,3-dihydroquinazolin-4(1*H*)-one (55.2 mg, 0.24 mmol) were used, affording the title compound as a colourless liquid (36.4 mg, 89% yield) by using hexane/EtOAc (100:1) as eluent. In a second independent experiment, 37.3 mg (91%) were obtained, giving an average of 90% yield. **^{1}H NMR (400 MHz, $CDCl_3$)** δ 7.98 – 7.92 (m, 2H), 7.32 – 7.27 (m, 2H), 3.90 (s, 3H), 3.04 (tt, *J* = 9.6, 7.5 Hz, 1H), 2.14 – 2.04 (m, 2H), 1.89 – 1.53 (m, 6H) ppm. **^{13}C NMR (101 MHz, $CDCl_3$)** δ 167.3, 152.4, 129.7, 127.8, 127.3, 52.1, 46.1, 34.6, 25.7 ppm. Spectral data was in agreement with the literature.[186]

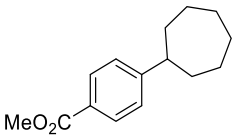

Methyl 4-cycloheptylbenzoate (3c). Following GP4, methyl 4-bromobenzoate (43.0 mg, 0.20 mmol) and 2-cycloheptyl-2-methyl-2,3-dihydroquinazolin-4(1*H*)-one (61.9 mg, 0.24 mmol) were used, affording the title compound as a colourless liquid (35.0 mg, 75% yield), by using hexane/EtOAc (100:1) as chromatography eluent. In a second independent experiment, 34.5 mg (74%) were obtained, giving an average of 75% yield. **^{1}H NMR (400 MHz, $CDCl_3$)** δ 7.98 – 7.90 (m, 2H), 7.29 – 7.21 (m, 2H), 3.89 (s, 3H),

[186] Zhang, X.; MacMillan. D. W. C. Alcohols as Latent Coupling Fragments for Metallaphotoredox Catalysis: sp^3–sp^2 Cross-Coupling of Oxalates with Aryl Halides. *J. Am. Chem. Soc.* **2016**, *138*, 13862–13865.

2.71 (tt, *J* = 10.5, 3.6 Hz, 1H), 1.97 – 1.85 (m, 2H), 1.85 – 1.76 (m, 2H), 1.75 – 1.48 (m, 8H) ppm. **^{13}C NMR (101 MHz, $CDCl_3$)** δ 167.3, 155.5, 129.9, 127.6, 126.8, 52.0, 47.2, 36.6, 28.0, 27.4 ppm. Spectral data was in agreement with the literature.[187]

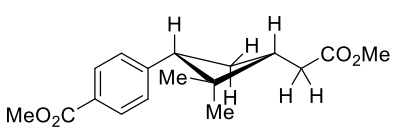

Maj.

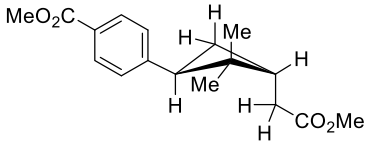

Min.

Methyl 4-((3*S*)-3-(2-methoxy-2-oxoethyl)-2,2-dimethylcyclobutyl)benzoate (3d) Following GP4, methyl 4-bromobenzoate (43.0 mg, 0.20 mmol) and methyl 2-((1*R*)-2,2-dimethyl-3-(2-methyl-4-oxo-1,2,3,4-tetrahydroquinazolin-2-yl)cyclobutyl)acetate (75.8 mg, 0.24 mmol) were used, affording the title compound as a colourless oil (30.9 mg, 53% yield, 2.3:1 d.r.), by using hexane/EtOAc (10:1) as chromatography eluent. In a second independent experiment, 30.1 mg (52%, 2.3:1 d.r.) were obtained, giving an average of 53% yield. **IR (film, cm^{-1})** = 2952, 1720, 1435, 1277, 1179, 1110. **^{1}H NMR (500 MHz, $CDCl_3$, mixture of diasteromers A:B in a 0.7:0.3 ratio)** δ 8.01 – 7.69 (m, 2H), 7.23 (d, *J* = 8.1 Hz, 0.6H), 7.18 (d, *J* = 8.1 Hz, 1.4H), 3.93 (s, 0.9H), 3.92 (s, 2.1H), 3.32 (t, *J* = 8.3 Hz, 0.3H), 3.24 (dd, *J* = 11.0, 7.5 Hz, 0.7H), 2.62 (dd, *J* = 15.4, 6.7 Hz, 0.3H), 2.59 – 2.55 (m, 0.3H), 2.54 (d, *J* = 8.9 Hz, 0.3H), 2.50 – 2.44 (m, 0.7H), 2.43 (d, *J* = 7.1 Hz, 0.3H), 2.40 (d, *J* = 7.2 Hz, 0.7H), 2.38 (d, *J* = 7.9 Hz, 0.7H), 2.31 (td, *J* = 7.6, 3.2 Hz, 0.7H), 2.05 – 1.96 (m, 1H), 1.28 (s, 2.1H), 1.17 (s, 0.9H), 0.71 (s, 0.9H), 0.60 (s, 2.1H) ppm. **^{13}C NMR (126 MHz, $CDCl_3$)** δ 173.8 (Min.), 173.6 (Maj.), 167.3 (Maj. + Min.), 147.4 (Min.), 146.5 (Maj.), 129.5 (Min.), 129.5 (Maj.), 128.0 (Maj. + Min.), 127.65 (Min.), 127.4 (Maj.), 76.9 (Maj.), 52.1 (Maj. + Min.), 51.7 (Min.), 51.7 (Maj.), 47.8 (Maj.), 47.2 (Min.), 43.8 (Maj.), 41.8 (Min.), 38.5 (Maj.), 38.1 (Min.), 36.0 (Min.), 35.2 (Maj.), 30.1 (Maj.), 26.8 (Maj.), 26.0 (Min.), 25.1 (Min.), 24.9 (Min.), 17.7 (Maj.) ppm. **HRMS** [ESI$^+$] *calcd.* for ($C_{17}H_{22}NaO_4$) $[M+Na]^+$: 313.1410, *found* 313.1405.

NOESy:

[187] Kawajiri,T.; Kato, M.; Nakata, H.; Goto, R.; Aibara,, S.; Ohta,, R.; Fujioka, H.; Sajiki, H.; Sawama, Y. Chemoselective Nucleophilic Functionalizations of Aromatic Aldehydes and Acetals via Pyridinium Salt Intermediates. *J. Org. Chem.* **2019**, *84*, 3853–3870.

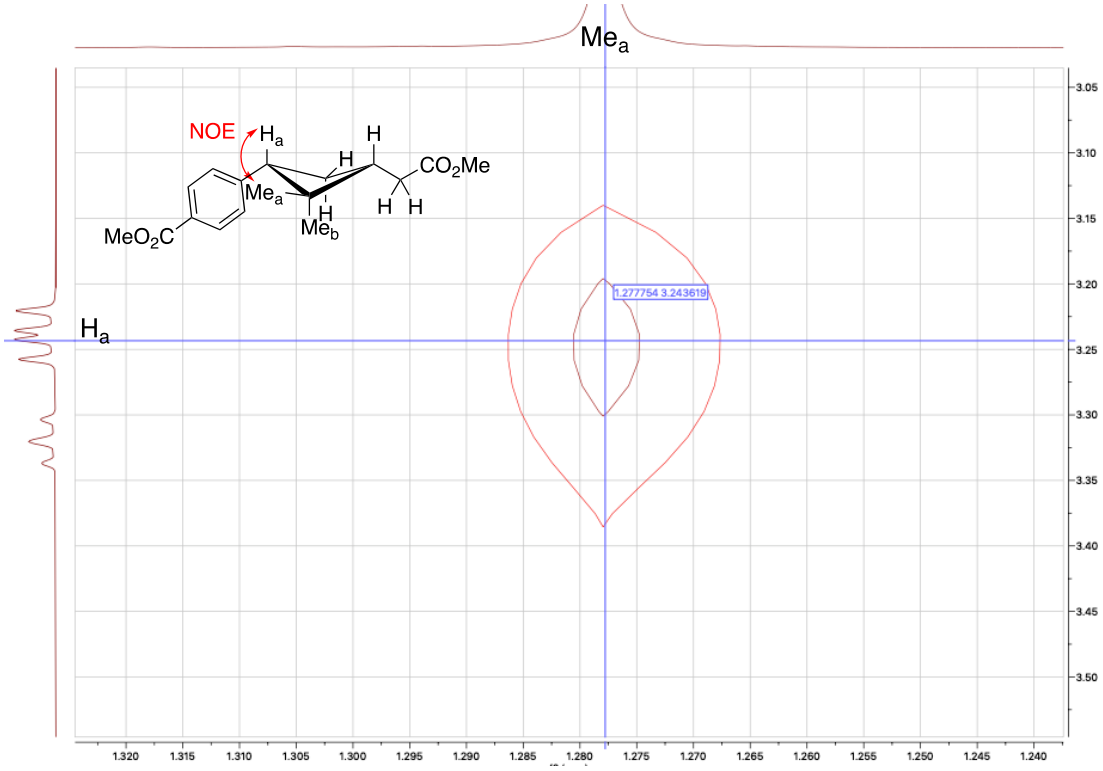
Me$_a$
NOE
H$_a$
H
H
CO$_2$Me
Me$_a$
H
Me$_b$
MeO$_2$C
H H
1.277754 3.243619
H$_a$

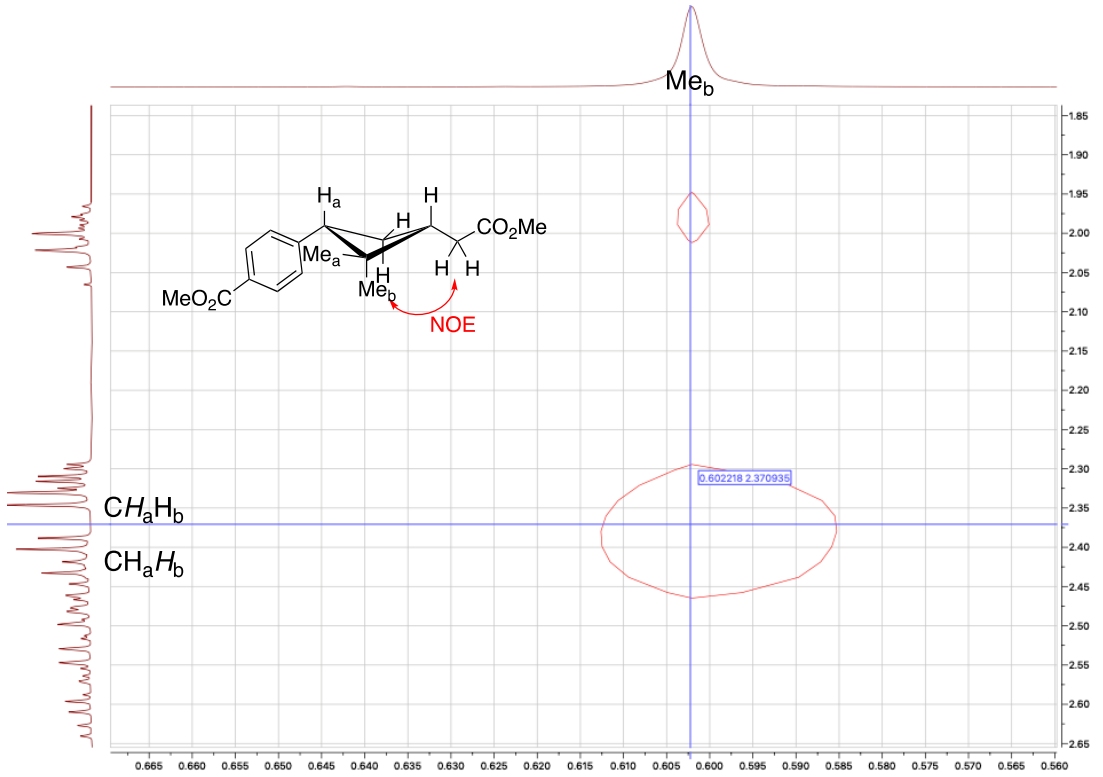
Me$_b$
H$_a$
H
H
CO$_2$Me
Me$_a$
H
Me$_b$
MeO$_2$C
H H
NOE
0.602218 2.370935
CH$_a$H$_b$
CH$_a$H$_b$

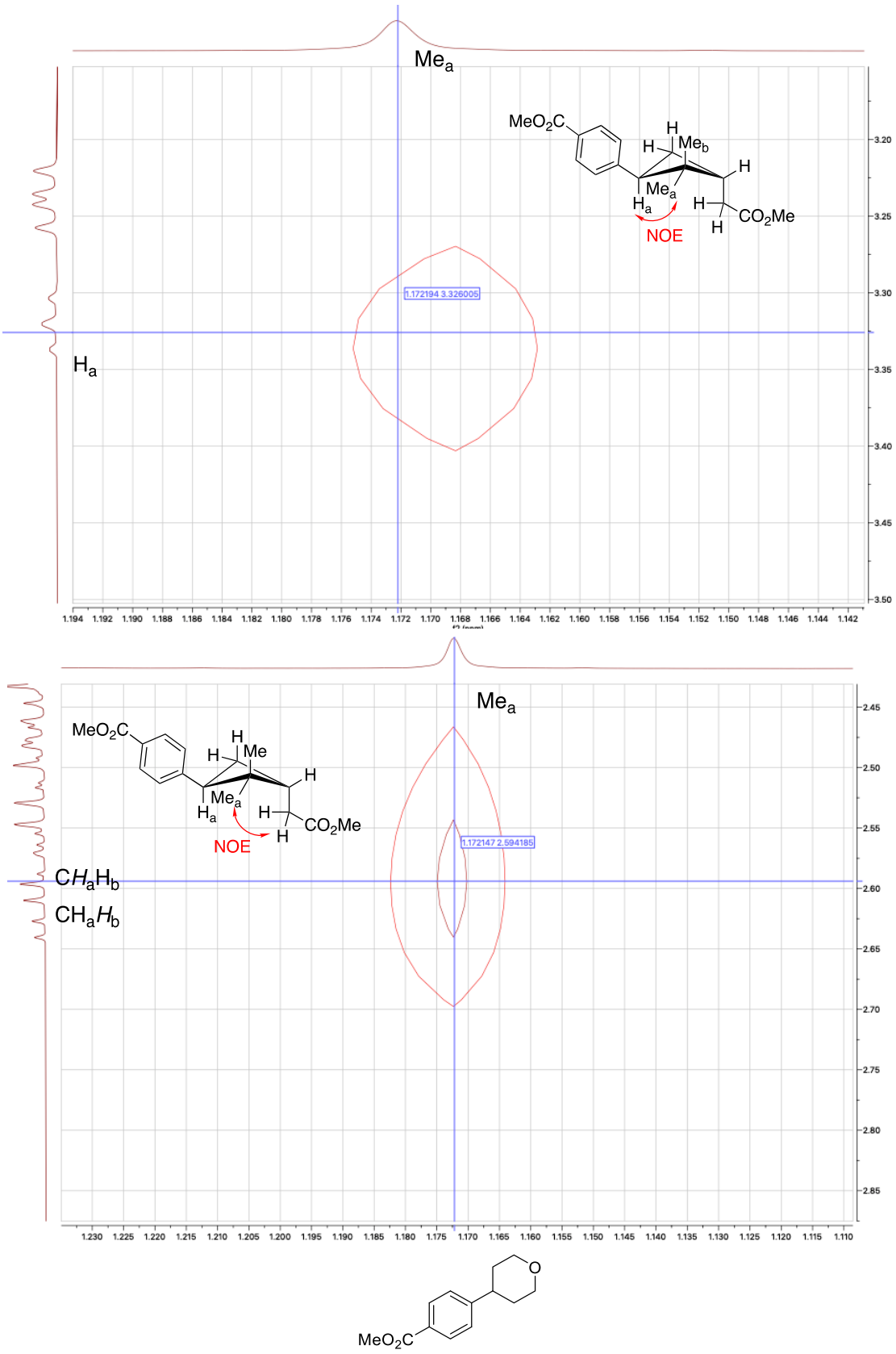

Methyl 4-(tetrahydro-2*H*-pyran-4-yl)benzoate (3e). Following GP4, methyl 4-bromobenzoate (43.0 mg, 0.20 mmol) and 2-methyl-2-(tetrahydro-2*H*-pyran-4-yl)-2,3-dihydroquinazolin-4(1*H*)-one (59.0 mg, 0.24 mmol) were used, affording the title compound as a white solid (44.6 mg, 99% yield), by using hexane/EtOAc (50:1) as

chromatography eluent. In a second independent experiment, 44.3 mg (99%) were obtained, giving an average of 99% yield. **M.p.**: 71 °C. **^{1}H NMR (400 MHz, $CDCl_3$)** δ 8.02 – 7.95 (m, 2H), 7.32 – 7.24 (m, 2H), 4.12 – 4.04 (m, 2H), 3.91 (s, 3H), 3.58 – 3.47 (m, 2H), 2.87 – 2.75 (m, 1H), 1.89 – 1.71 (m, 4H) ppm. **^{13}C NMR (101 MHz, $CDCl_3$)** δ 167.1, 151.2, 130.0, 128.4, 126.9, 68.3, 52.1, 41.8, 33.7 ppm. Spectral data was in agreement with the literature.[187]

Following GP4, methyl 4-(((trifluoromethyl)sulfonyl)oxy)benzoate (56.8 mg, 0.20 mmol) and 2-methyl-2-(tetrahydro-2H-pyran-4-yl)-2,3-dihydroquinazolin-4(1*H*)-one (59.0 mg, 0.24 mmol) were used, affording the title compound as a white solid (21.6 mg, 49% yield), by using hexane/EtOAc (20:1) as chromatography eluent. In a second independent experiment, 23.0 mg (52%) were obtained, giving an average of 51% yield. **^{1}H NMR (400 MHz, $CDCl_3$)** δ 8.02 – 7.95 (m, 2H), 7.32 – 7.29 (m, 2H), 4.14 – 4.04 (m, 2H), 3.90 (s, 3H), 3.53 (m, 2H), 2.88 – 2.76 (m, 1H), 1.90 – 1.71 (m, 4H) ppm. **^{13}C NMR (101 MHz, $CDCl_3$)** δ 167.2, 151.2, 130.0, 128.5, 126.9, 68.4, 52.2, 41.8, 33.7 ppm.

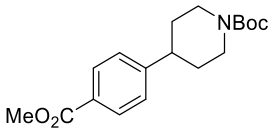

***tert*-Butyl 4-(4-(methoxycarbonyl)phenyl)piperidine-1-carboxylate (3f)**. Following GP4, methyl 4-bromobenzoate (43.0 mg, 0.20 mmol) and *tert*-butyl 4-(2-methyl-4-oxo-1,2,3,4-tetrahydroquinazolin-2-yl)piperidine-1-carboxylate (82.8 mg, 0.24 mmol) were used, affording the title compound as a white solid (44.4 mg, 70% yield), by using hexane/EtOAc (30:1) as chromatography eluent. In an independent experiment, 39.8 mg (62%) were obtained, giving an average of 66% yield. **M.p.**: 79 °C. **^{1}H NMR (400 MHz, $CDCl_3$)** δ 8.00 – 7.95 (m, 2H), 7.29 – 7.25 (m, 2H), 4.26 (d, *J* = 13.2 Hz, 2H), 3.90 (s, 3H), 2.81 (td, *J* = 13.2, 2.5 Hz, 2H), 2.76 – 2.65 (m, 1H), 1.83 (d, *J* = 13.5 Hz, 2H), 1.70 – 1.57 (m, 2H), 1.48 (s, 9H) ppm. **^{13}C NMR (101 MHz, $CDCl_3$)** δ 167.1, 155.0, 151.2, 130.0, 128.5, 127.0, 79.7, 52.2, 44.4, 43.0, 33.0, 28.6 ppm. Spectral data was in agreement with the literature.[187]

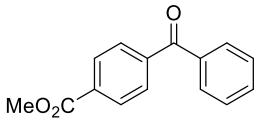

Methyl 4-((1,3-dioxoisoindolin-2-yl)methyl)benzoate (3g). Following GP4, methyl 4-bromobenzoate (43.0 mg, 0.20 mmol) and 2-benzoyl-2-methyl-2,3-dihydroquinazolin-4(1*H*)-one (63.8 mg, 0.24 mmol) were used, affording the title compound as a white solid (24.7 mg, 51% yield) by using hexane/EtOAc (20:1) as chromatography eluent. In a second independent experiment, 24.5 mg (51%) were obtained, giving an average of 51% yield. **M.p.**: 110 °C. **^{1}H NMR (400 MHz, $CDCl_3$)** δ 8.18 – 8.12 (m, 2H), 7.87 – 7.78 (m, 4H), 7.65 – 7.58 (m, 1H), 7.54 – 7.46 (m, 2H),

3.97 (s, 3H) ppm. **^{13}C NMR (101 MHz, $CDCl_3$)** δ 196.2, 166.5, 141.5, 137.1, 133.4, 133.1, 130.3, 129.9, 129.7, 128.6, 52.6 ppm. Spectral data was in agreement with the literature.[188]

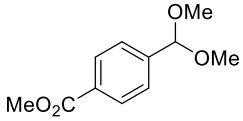

Methyl 4-(dimethoxymethyl)benzoate (3h). Following GP4, methyl 4-bromobenzoate (43.0 mg, 0.20 mmol) and 2-(dimethoxymethyl)-2-methyl-2,3-dihydroquinazolin-4(1*H*)-one (56.6 mg, 0.24 mmol) were used, affording the title compound as a white solid (30.8 mg, 73% yield), by using hexane/EtOAc (20:1) as chromatography eluent. In a second independent experiment, 32.1 mg (76%) were obtained, giving an average of 75% yield. **M.p.**: 206 °C. **^{1}H NMR (400 MHz, $CDCl_3$)** δ 8.07 – 7.97 (m, 2H), 7.52 (d, *J* = 8.7 Hz, 2H), 5.43 (s, 1H), 3.91 (s, 3H), 3.32 (s, 6H) ppm. **^{13}C NMR (101 MHz, $CDCl_3$)** δ 167.0, 143.1, 130.4, 129.7, 126.9, 102.5, 52.8, 52.3 ppm. Spectral data was in agreement with the literature.[187]

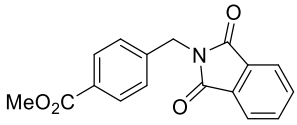

Methyl 4-((1,3-dioxoisoindolin-2-yl)methyl)benzoate (3i). Following GP4, methyl 4-bromobenzoate (43.0 mg, 0.20 mmol) and 2-((2-methyl-4-oxo-1,2,3,4-tetrahydroquinazolin-2-yl)methyl)isoindoline-1,3-dione (77.0 mg, 0.24 mmol) were used, affording the title compound as a white solid (46.1 mg, 78% yield), by using hexane/EtOAc (6:1) as chromatography eluent. In a second independent experiment, 42.1 mg (71%) were obtained, giving an average of 75% yield. **M.p.**: 153 °C. **^{1}H NMR (400 MHz, $CDCl_3$)** δ 8.01 – 7.96 (m, 2H), 7.89 – 7.83 (m, 2H), 7.75 – 7.69 (m, 2H), 7.47 (d, *J* = 8.5 Hz, 2H), 4.89 (s, 2H), 3.89 (s, 3H) ppm. **^{13}C NMR (101 MHz, $CDCl_3$)** δ 168.1, 166.9, 141.4, 134.3, 132.2, 130.2, 129.8, 128.6, 123.6, 52.3, 41.4 ppm. Spectral data was in agreement with the literature.[189]

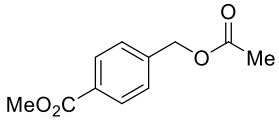

Methyl 4-(acetoxymethyl)benzoate (3j). Following GP4, methyl 4-bromobenzoate (43.0 mg, 0.20 mmol) and (2-methyl-4-oxo-1,2,3,4-tetrahydroquinazolin-2-yl)methyl acetate (56.2 mg, 0.24 mmol) were used, affording the title compound as a colourless liquid (15.5 mg, 37% yield), by using hexane/EtOAc (20:1) as chromatography eluent.

[188] Boudjelel, M.; Sadek, O.; Mallet-Ladeira, S.; García-Rodeja, Y.; Carrizo, E. D. S.; Miqueu, K.; Bouhadir, G.; Bourissou, D. Phosphine–Borane Ligands Induce Chemoselective Activation and Catalytic Coupling of Acyl Chlorides at Palladium. *ACS Catal.* **2021**, *11*, 3822–3829.
[189] Lee, Y. H.; Morandi, B. Metathesis-Active Ligands Enable a Catalytic Functional Group Metathesis between Aroyl Chlorides and Aryl Iodides. *Nature Chem.* **2018**, *10*, 1016–1022.

In a second independent experiment, 17.3 mg (42%) were obtained, giving an average of 39% yield. **^{1}H NMR (400 MHz, $CDCl_3$)** δ 8.05 – 8.01 (m, 2H), 7.44 – 7.39 (m, 2H), 5.15 (s, 2H), 3.92 (s, 3H), 2.13 (s, 3H) ppm. **^{13}C NMR (101 MHz, $CDCl_3$)** δ 170.8, 166.9, 141.1, 130.1, 123.0, 127.8, 65.6, 52.3, 21.1 ppm. Spectral data was in agreement with the literature.[190]

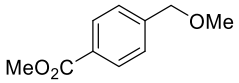

Methyl 4-(methoxymethyl)benzoate (3k). Following GP4, methyl 4-bromobenzoate (43.0 mg, 0.20 mmol) and 2-(methoxymethyl)-2-methyl-2,3-dihydroquinazolin-4(1*H*)-one (49.4 mg, 0.24 mmol) were used, affording the title compound as a colourless liquid (28.5 mg, 79% yield), by using hexane/EtOAc (50:1) as chromatography eluent. In a second independent experiment, 28.3 mg (79%) were obtained, giving an average of 79% yield. **^{1}H NMR (400 MHz, $CDCl_3$)** δ 8.05 – 7.99 (m, 2H), 7.43 – 7.37 (m, 2H), 4.51 (s, 2H), 3.91 (s, 3H), 3.41 (s, 3H) ppm. **^{13}C NMR (101 MHz, $CDCl_3$)** δ 167.1, 143.7, 129.9, 129.5, 127.3, 74.2, 58.5, 52.2 ppm. Spectral data was in agreement with the literature.[191]

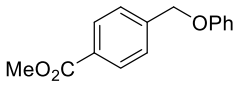

Methyl 4-(phenoxymethyl)benzoate (3l). Following GP4, methyl 4-bromobenzoate (43.0 mg, 0.20 mmol) and 2-methyl-2-(phenoxymethyl)-2,3-dihydroquinazolin-4(1*H*)-one (64.3 mg, 0.24 mmol) were used, affording the title compound as a white solid (39.3 mg, 81% yield), by using hexane/EtOAc (50:1) as chromatography eluent. In a second independent experiment, 39.1 mg (81%) were obtained, giving an average of 81% yield. **M.p.**: 88 °C. **^{1}H NMR (400 MHz, $CDCl_3$)** δ 8.09 – 8.04 (m, 2H), 7.51 (d, *J* = 8.1 Hz, 2H), 7.34 – 7.27 (m, 2H), 7.01 – 6.95 (m, 3H), 5.13 (s, 2H), 3.93 (s, 3H) ppm. **^{13}C NMR (101 MHz, $CDCl_3$)** δ 167.0, 158.6, 142.5, 130.0, 129.8, 129.7, 127.1, 121.4, 115.0, 69.4, 52.2 ppm. Spectral data was in agreement with the literature.[192]

Following GP4, methyl 4-bromobenzoate (43.0 mg, 0.20 mmol) and 2-ethyl-2-(phenoxymethyl)-2,3-dihydroquinazolin-4(1*H*)-one (67.7 mg, 0.24 mmol) were used, affording the title compound as a white solid (39.4 mg, 81% yield), by using hexane/EtOAc (50:1) as chromatography eluent. In a second independent experiment, 39.8 mg (82%) were obtained, giving an average of 82% yield. **^{1}H NMR (400 MHz, $CDCl_3$)** δ 8.10 – 8.03 (m, 2H), 7.55 – 7.48 (m, 2H), 7.34 – 7.27 (m, 2H), 7.02 – 6.94

[190] Chen, J.; Lin, J.-H.; Xiao, J.-C. Dehydroxylation of Alcohols for Nucleophilic Substitution. *Chem. Commun.* **2018**, *54*, 7034–7037.

[191] Zhang, P.; Le, C.; MacMillan, D. W. C. Silyl Radical Activation of Alkyl Halides in Metallaphotoredox Catalysis: A Unique Pathway for Cross-Electrophile Coupling. *J. Am. Chem. Soc.* **2016**, *138*, 8084–8087.

[192] Ming, X.-X.; Tian, Z.-Y.; Zhang, C.-P. Base-Mediated O-Arylation of Alcohols and Phenols by Triarylsulfonium Triflates. *Chem. Asian J.* **2019**, *14*, 3370–3379.

(m, 3H), 5.13 (s, 2H), 3.93 (s, 3H) ppm. **^{13}C NMR (101 MHz, $CDCl_3$)** δ 167.0, 158.6, 142.5, 130.0, 129.8, 129.7, 127.1, 121.4, 115.0, 69.4, 52.3 ppm.

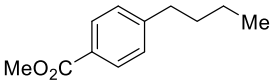

Methyl 4-butylbenzoate (3m). Following GP4, methyl 4-bromobenzoate (43.0 mg, 0.20 mmol) and 2-butyl-2-phenyl-2,3-dihydroquinazolin-4(1*H*)-one (**2m´**) (67.2 mg, 0.24 mmol) were used, affording the title compound as a colourless liquid (33.8 mg, 88% yield), by using hexane/EtOAc (100:1) as chromatography eluent. In a second independent experiment, 35.5 mg (92%) were obtained, giving an average of 90% yield. **^{1}H NMR (400 MHz, $CDCl_3$)** δ 7.97 – 7.91 (m, 2H), 7.25 – 7.21 (m, 2H), 3.90 (s, 3H), 2.66 (t, *J* = 7.7 Hz, 2H), 1.67 – 1.55 (m, 2H), 1.41 – 1.29 (m, 2H), 0.93 (t, *J* = 7.3 Hz, 3H) ppm. **^{13}C NMR (101 MHz, $CDCl_3$)** δ 167.3, 148.6, 129 .8, 128.6, 127.8, 52.1, 35.8, 33.4, 22.4, 14.0 ppm. Spectral data was in agreement with the literature.[193]

Following GP4, methyl 4-bromobenzoate (43.0 mg, 0.20 mmol) and 2-butyl-2-(4-methoxyphenyl)-2,3-dihydroquinazolin-4(1*H*)-one (**2m´´**) (74.4 mg, 0.24 mmol) were used, affording the title compound as a colourless liquid (30.8 mg, 80% yield), by using hexane/EtOAc (100:1) as chromatography eluent. In a second independent experiment, 30.7 mg (80%) were obtained, giving an average of 80% yield. **^{1}H NMR (400 MHz, $CDCl_3$)** δ 7.98 – 7.91 (m, 2H), 7.26 – 7.21 (m, 2H), 3.90 (s, 3H), 2.70 – 2.62 (m, 2H), 1.67 – 1.56 (m, 2H), 1.41 – 1.29 (m, 2H), 0.93 (t, *J* = 7.3 Hz, 3H) ppm. **^{13}C NMR (101 MHz, $CDCl_3$)** δ 167.3, 148.6, 129.8, 128.6, 127.8, 52.1, 35.8, 33.4, 22.4, 14.0 ppm.

Following GP4, methyl 4-bromobenzoate (43.0 mg, 0.20 mmol) and 2-(benzo[d][1,3]dioxol-5-yl)-2-butyl-2,3-dihydroquinazolin-4(1*H*)-one (**2m´´´**) (77.8 mg, 0.24 mmol) were used, affording the title compound as a colourless liquid (30.6 mg, 80% yield), by using hexane/EtOAc (100:1) as chromatography eluent. In a second independent experiment, 29.7 mg (77%) were obtained, giving an average of 79% yield. **^{1}H NMR (400 MHz, $CDCl_3$)** δ 7.97 – 7.92 (m, 2H), 7.26 – 7.21 (m, 2H), 3.90 (s, 3H), 2.70 – 2.62 (m, 2H), 1.66 – 1.56 (m, 2H), 1.41 – 1.30 (m, 2H), 0.93 (t, J = 7.3 Hz, 3H) ppm. **^{13}C NMR (101 MHz, $CDCl_3$)** δ 167.4, 148.6, 129.8, 128.6, 127.8, 52.1, 35.8, 33.4, 22.5, 14.0 ppm.

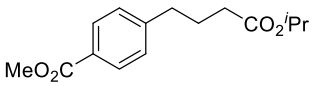

Methyl 4-(4-isopropoxy-4-oxobutyl)benzoate (3n). Following GP4, methyl 4-bromobenzoate (43.0 mg, 0.20 mmol) and isopropyl 4-(4-oxo-2-phenyl-1,2,3,4-tetrahydroquinazolin-2-yl)butanoate (84.5 mg, 0.24 mmol) were used, affording the title compound as a colourless liquid (22.9 mg, 43% yield), by using hexane/EtOAc

[193] Eckert, P.; Organ, M. G. A Path to More Sustainable Catalysis: The Critical Role of LiBr in Avoiding Catalyst Death and its Impact on Cross-Coupling. *Chem. Eur. J.* **2020**, *26*, 4861–4865.

(40:1) as chromatography eluent. In a second independent experiment, 24.2 mg (46%) were obtained, giving an average of 45% yield. **IR (neat, cm^{-1}):** 2980, 1719, 1610, 1435, 1374, 1275, 1178, 1105, 763. **^{1}H NMR (400 MHz, $CDCl_3$)** δ 7.98 – 7.92 (m, 2H), 7.24 (d, *J* = 8.2 Hz, 2H), 5.01 (hept, *J* = 6.3 Hz, 1H), 3.90 (s, 3H), 2.74 – 2.66 (m, 2H), 2.28 (t, *J* = 7.4 Hz, 2H), 2.00 – 1.90 (m, 2H), 1.23 (d, *J* = 6.3 Hz, 6H) ppm. **^{13}C NMR (101 MHz, $CDCl_3$)** δ 172.9, 167.2, 147.2, 129.9, 128.7, 128.2, 67.8, 52.1, 35.3, 34.0, 26.4, 22.0 ppm. **HRMS** [ESI$^+$] *calcd*. for ($C_{15}H_{20}NaO_4$) [M+Na]$^+$: 287.1259, *found*: 287.1252.

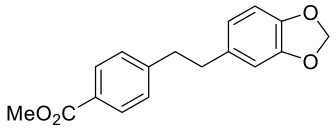

Methyl 4-(2-(benzo[*d*][1,3]dioxol-5-yl)ethyl)benzoate (3o). Following GP4, methyl 4-bromobenzoate (43.0 mg, 0.20 mmol) and 2-(2-(benzo[*d*][1,3]dioxol-5-yl)ethyl)-2-phenyl-2,3-dihydroquinazolin-4(1*H*)-one (89.3 mg, 0.24 mmol) were used, affording the title compound as a white solid (32.0 mg, 56% yield), by using hexane/EtOAc (20:1) as chromatography eluent. In a second independent experiment, 34.3 mg (60%) were obtained, giving an average of 58% yield. **M.p.**: 83 °C. **^{1}H NMR (400 MHz, $CDCl_3$)** δ 7.97 – 7.92 (m, 2H), 7.21 (d, *J* = 8.4 Hz, 2H), 6.71 (d, *J* = 7.9 Hz, 1H), 6.64 (d, *J* = 1.6 Hz, 1H), 6.57 (dd, *J* = 7.9, 1.7 Hz, 1H), 5.92 (s, 2H), 3.90 (s, 3H), 2.97 – 2.89 (m, 2H), 2.89 – 2.82 (m, 2H) ppm. **^{13}C NMR (101 MHz, $CDCl_3$)** δ 167.3, 147.7, 147.2, 145.9, 135.1, 129.8, 128.7, 128.1, 121.4, 109.0, 108.3, 100.9, 52.1, 38.3, 37.3 ppm. Spectral data was in agreement with the literature.[194]

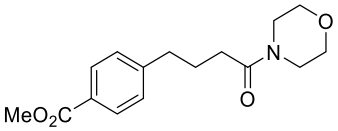

Methyl 4-(4-morpholino-4-oxobutyl)benzoate (3p). Following GP4, methyl 4-bromobenzoate (43.0 mg, 0.20 mmol) and 2-(4-morpholino-4-oxobutyl)-2-phenyl-2,3-dihydroquinazolin-4(1*H*)-one (91.0 mg, 0.24 mmol) were used, affording the title compound as a white solid (52.2 mg, 90% yield), by using hexane/EtOAc (3:1) as chromatography eluent. In a second independent experiment, 49.6 mg (85%) were obtained, giving an average of 87% yield. **M.p.**: 68 °C. **IR (neat, cm^{-1}):** 2956, 2865, 1712, 1639, 1608, 1432, 1275, 1187, 1109, 1028, 961, 833, 762. **^{1}H NMR (400 MHz, $CDCl_3$)** δ 7.92 – 7.86 (m, 2H), 7.19 (d, *J* = 8.1 Hz, 2H), 3.83 (s, 3H), 3.57 (s, 6H), 3.31 (s, 2H), 2.67 (t, *J* = 7.5 Hz, 2H), 2.23 (t, *J* = 7.4 Hz, 2H), 1.99 – 1.88 (m, 2H) ppm. **^{13}C NMR (101 MHz, $CDCl_3$)** δ 171.2, 167.2, 147.3, 129.9, 128.6, 128.2, 67.0, 66.8, 52.1,

[194] Yue, H.; Zhu, C.; Shen, L.; Geng, Q.; Hock, K. J.; Yuan, T.; Cavallo, L.; Rueping, M. Nickel-Catalyzed C–N bond Activation: Activated Primary Amines as Alkylating Reagents in Reductive Cross-Coupling. *Chem. Sci*. **2019**, *10*, 4430–4435.

46.0, 42.0, 35.4, 32.1, 26.3 ppm. **HRMS** [ESI$^+$] *calcd*. for ($C_{16}H_{21}NNaO_4$) [M+Na]$^+$: 314.1368, *found*: 314.1354.

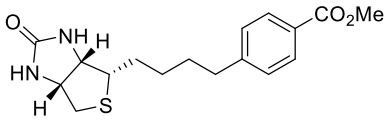

Methyl 4-(4-((3a*R*,4*R*,6a*S*)-2-oxohexahydro-1*H*-thieno[3,4-d]imidazol-4-yl)butyl)benzoate (3q). An oven-dried 8 mL screw-cap test tube containing a stirring bar was charged with (3a*S*,4*S*,6a*R*)-4-(4-(4-oxo-2-phenyl-1,2,3,4-tetrahydroquinazolin-2-yl)butyl)tetrahydro-1*H*-thieno[3,4-*d*]imidazol-2(3*H*)-one (**2r**) (101.4 mg, 0.24 mmol), methyl 4-bromobenzoate (**1a**) (43.0 mg, 0.2 mmol) and NaBr (24.8 mg, 0.24 mmol). The reaction vessel was brough into a nitrogen-filled glove box, then charged with 4-CzIPN (3.2 mg, 2 mol%), $Ni(OAc)_2 \cdot 4H_2O$ (5.0 mg, 10 mol%), 4,4',4''-tri-tert-butyl-2,2':6'2''- terpyridine (12.2 mg, 15 mol%), Na_2CO_3 (22.0 mg, 0.2 mmol) and NMP (2.0 mL, 0.1 M). The reaction mixture was stirred for 3 minutes, then the reaction vessel was sealed with a screw cap and removed from the glovebox. The cap of the reaction vessel was further sealed with Parafilm, and then the reaction mixture was irradiated with blue LEDs at 40 °C for 48 hours. The reaction mixture was quenched with brine (5 mL) and extracted with ethyl acetate (5 x 3 mL). The combined organic extracts were dried ($MgSO_4$), concentrated under reduced pressure, purified by silica gel chromatography (0 to 3% MeOH in DCM) and then purified a second time by silica gel chromatography (EtOAc), affording the title compound (16.1 mg, 24%) as a white solid. In a second independent experiment, 20.1 mg (30%) of the title compound was obtained, giving an average of 27% yield. **M.p.** 192 °C. **IR (film, cm^{-1})** = 3220, 2927, 1698, 1283. **M.p.**: 192 °C. **^{1}H NMR (500 MHz, CD_3OD)** δ 7.94 (d, *J* = 8.3, Hz, 2H), 7.33 (d, *J* = 8.3, Hz, 2H), 4.50 (ddd, *J* = 7.9, 5.0, 0.9 Hz, 1H), 4.30 (dd, *J* = 7.9, 4.5, 0.9 Hz, 1H), 3.24 – 3.19 (m, 1H), 2.94 (dd, *J* = 12.7, 5.0 Hz, 1H), 2.75 – 2.70 (m, 3H), 1.83 – 1.68 (m, 3H), 1.67 – 1.60 (m, 1H), 1.50 (q, *J* = 12.7, 7.5 Hz, 1H) ppm. **^{13}C NMR (126 MHz, CD_3OD)** δ 168.7, 166.1, 149.8, 130.6, 129.7, 128.9, 63.5, 61.6, 57.1, 52.5, 41.0, 36.7, 32.2, 29.9, 29.6 ppm. **HRMS** [ESI$^+$] *calcd*. for ($C_{17}H_{22}N_2NaO_3S$) [M+Na]$^+$: 357.1243, *found* 357.1232.

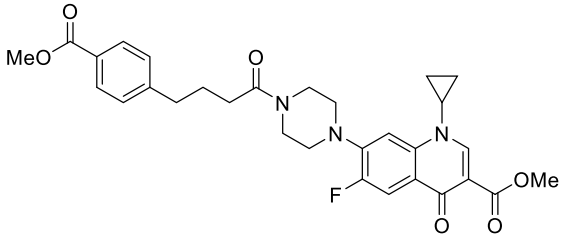

Methyl 1-cyclopropyl-6-fluoro-7-(4-(4-(4-(methoxycarbonyl)phenyl)butanoyl)piperazin-1-yl)-4-oxo-1,4-dihydroquinoline-3-carboxylate (3r). An oven-dried 8 mL screw-cap test tube containing a stirring bar was charged with methyl 1-cyclopropyl-6-fluoro-4-oxo-7-(4-(4-(4-oxo-2-phenyl-

1,2,3,4-tetrahydroquinazolin-2-yl)butanoyl)piperazin-1-yl)-1,4-dihydroquinoline-3-carboxylate (**2q**) (98.1 mg, 0.15 mmol), methyl 4-bromobenzoate (**1a**) (28.0 mg, 0.13 mmol) and NaBr (16.1 mg, 0.15 mmol). The reaction vessel was brough into a nitrogen-filled glove box, then charged with 4-CzIPN (2.1 mg, 2 mol%), $Ni(OAc)_2 \cdot 4H_2O$ (3.2 mg, 10 mol%), 4,4',4"-tri-tert-butyl-2,2':6'2"- terpyridine (7.8 mg, 15 mol%), Na_2CO_3 (13.8 mg, 0.13 mmol) and NMP (1.2 mL, 0.1 M). The reaction mixture was stirred for 3 minutes, then the reaction vessel was sealed with a screw cap and removed from the glovebox. The cap of the reaction vessel was further sealed with Parafilm, and then the reaction mixture was irradiated with blue LEDs at 40 °C for 48 hours. The reaction mixture was quenched with brine (5 mL) and extracted with ethyl acetate (5 x 3 mL). The combined organic extracts were dried ($MgSO_4$), concentrated under reduced pressure and purified twice by silica gel chromatography (0 to 3% MeOH in DCM, then again using 0 to 20% acetone in DCM) , affording the title compound (24.4 mg, 22%) as a colorless film. In a second independent experiment, 30.3 mg (30%) of the title compound was obtained, giving an average of 26% yield. **IR (film, cm^{-1})** = 3488, 2951, 1718, 1618, 1434, 1247. **^{1}H NMR (400 MHz, $CDCl_3$)** δ 8.54 (s, 1H), 8.03 (d, *J* = 8.1 Hz, 13.0, 1H), 7.67 (d, *J* = 8.1 Hz, 8.1, 2H), 7.30 – 7.24 (m, 3H), 3.91 (s, 3H), 3.90 (s, 3H), 3.85 (br. t, *J* = 8.1 Hz, 4.7, 2H), 3.62 (br. t, *J* = 8.1 Hz, 4.7, 2H), 3.43 (tt, *J* = 7.2, 3.9 Hz, 4.7, 1H), 3.25 – 3.18 (m, 4H), 2.77 (t, *J* = 8.1 Hz, 7.4, 2H), 2.38 (t, *J* = 8.1 Hz, 7.4, 2H), 2.04 (p, *J* = 7.5 Hz, 7.4, 2H), 1.33 (p, *J* = 6.8 Hz, 7.4, 2H), 1.17 – 1.11 (m, 2H) ppm. **^{13}C NMR (126 MHz, $CDCl_3$)** δ 173.13, 171.15, 167.20, 166.48, 153.5 (d, *J* = 248.9 Hz), 148.61, 147.22, 144.2 (d, *J* = 10.7 Hz), 138.11, 129.91, 128.66, 128.21, 123.74 (d, *J* = 6.7 Hz), 113.77 (d, *J* = 22.9 Hz), 110.35, 105.22, 52.24, 52.16, 50.60, 49.74, 45.50, 41.42, 35.38, 34.66, 32.18, 26.29, 8.30. **^{19}F NMR (376 MHz, $CDCl_3$)** δ -124.0 (dd, *J* = 13.1, 7.0 Hz) ppm. **HRMS** [ESI$^+$] *calcd*. for ($C_{30}H_{32}FN_3NaO_6$) [M+Na]$^+$: 572.2167, *found* 572.2160.

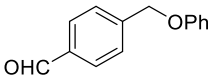

4-(Phenoxymethyl)benzaldehyde (5a). Following GP4, 4-bromobenzaldehyde (37.0 mg, 0.20 mmol) and 2-methyl-2-(phenoxymethyl)-2,3-dihydroquinazolin-4(1*H*)-one (64.3 mg, 0.24 mmol) were used, affording the title compound as a white solid (37.2 mg, 88% yield), by using hexane/EtOAc (40:1) as chromatography eluent. In a second independent experiment, 36.4 mg (86%) were obtained, giving an average of 87% yield. **M.p.**: 78 °C. **IR (neat, cm^{-1}):** 2917, 2852, 1692, 1580, 1486, 1466, 1375, 1230, 1166, 1014, 810, 755, 691, 508. **^{1}H NMR (400 MHz, $CDCl_3$)** δ 10.03 (s, 1H), 7.94 – 7.87 (m, 2H), 7.61 (d, *J* = 8.0 Hz, 2H), 7.34 – 7.27 (m, 2H), 7.02 – 6.95 (m, 3H), 5.16 (s, 2H) ppm. **^{13}C NMR (101 MHz, $CDCl_3$)** δ 192.0, 158.5, 144.3, 136.1, 130.2, 129.7, 127.6, 121.5, 115.0, 69.3 ppm. **HRMS** [ESI$^+$] *calcd*. for ($C_{15}H_{16}NaO_3$) [M+CH_3OH+Na]$^+$: 267.0997, *found*: 267.1005.

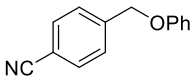

4-(Phenoxymethyl)benzonitrile (5b). Following GP4, 4-bromobenzonitrile (36.4 mg, 0.20 mmol) and 2-methyl-2-(phenoxymethyl)-2,3-dihydroquinazolin-4(1*H*)-one (64.3 mg, 0.24 mmol) were used, affording the title compound as a white solid (37.8 mg, 90% yield), by using hexane/EtOAc (10:1) as chromatography eluent. In a second independent experiment, 36.5 mg (87%) were obtained, giving an average of 89% yield. **M.p.**: 62 °C. **^{1}H NMR (400 MHz, CDCl$_3$)** δ 7.71 – 7.65 (m, 2H), 7.58 – 7.52 (m, 2H), 7.35 – 7.27 (m, 2H), 7.03 – 6.93 (m, 3H), 5.13 (s, 2H) ppm. **^{13}C NMR (101 MHz, CDCl$_3$)** δ 158.3, 142.7, 132.5, 129.8, 127.7, 121.6, 118.8, 114.9, 111.8, 69.0 ppm. Spectral data was in agreement with the literature.[195]

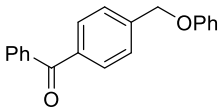

(4-(Phenoxymethyl)phenyl)(phenyl)methanone (5c). Following GP4, (4-bromophenyl)(phenyl)methanone (52.2 mg, 0.20 mmol) and 2-methyl-2-(phenoxymethyl)-2,3-dihydroquinazolin-4(1*H*)-one (64.3 mg, 0.24 mmol) were used, affording the title compound as a white solid (52.2 mg, 91% yield) by using hexane/EtOAc (40:1) as chromatography eluent. In a second independent experiment, 49.8 mg (86%) were obtained, giving an average of 89% yield. **M.p.**: 76 °C. **^{1}H NMR (400 MHz, CDCl$_3$)** δ 7.87 – 7.79 (m, 4H), 7.63 – 7.54 (m, 3H), 7.53 – 7.46 (m, 2H), 7.35 – 7.28 (m, 2H), 7.03 – 6.96 (m, 3H), 5.17 (s, 2H). ppm. **^{13}C NMR (101 MHz, CDCl$_3$)** δ 196.4, 158.6, 142.0, 137.7, 137.2, 132.6, 130.5, 130.2, 129.7, 128.4, 127.1, 121.4, 115.0, 69.4 ppm. Spectral data was in agreement with the literature.[196]

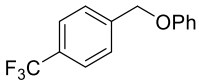

1-(Phenoxymethyl)-4-(trifluoromethyl)benzene (5d). Following GP4, 1-bromo-4-(trifluoromethyl)benzene (45.0 mg, 0.20 mmol) and 2-methyl-2-(phenoxymethyl)-2,3-dihydroquinazolin-4(1*H*)-one (64.3 mg, 0.24 mmol) were used, affording the title compound as a white solid (35.1 mg, 70% yield), by using hexane/EtOAc (100:1) as chromatography eluent. In a second independent experiment, 37.8 mg (75%) were obtained, giving an average of 72% yield. **M.p.**: 77 °C. **^{1}H NMR (400 MHz, CDCl$_3$)** δ 7.65 (d, J = 8.1 Hz, 2H), 7.56 (d, J = 8.0 Hz, 2H), 7.36 – 7.28 (m, 2H), 7.03 – 6.94 (m, 3H), 5.14 (s, 2H) ppm. **^{13}C NMR (126 MHz, CDCl$_3$)** δ 158.5, 141.3, 130.2 (q, $J_{C,F}$ = 32 Hz), 129.7, 127.5, 125.7 (q, $J_{C,F}$ = 4 Hz), 124.3 (q, $J_{C,F}$ = 272 Hz), 121.5, 115.0,

[195] Molander, G. A.; Canturk. B. Preparation of Potassium Alkoxymethyltrifluoroborates and Their Cross-Coupling with Aryl Chlorides. *Org. Lett*. **2008**, *10*, 2135–2138.
[196] Qin, X.; Ding, G.; Gong, Y.; Jing, C.; Peng, G.; Liu, S.; Niu, L.; Zhang, S.; Luo, Z.; Li, H.; Gao, F. Stilbene-Benzophenone Dyads for Free Radical Initiating Polymerization of Methyl Methacrylate under Visible Light Irradiation. *Dyes and Pigments*. **2016**, *132*, 27–40.

69.2 ppm. **^{19}F NMR (376 MHz, $CDCl_3$)** δ -62.64 ppm. Spectral data was in agreement with the literature.[197]

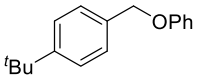

1-(*tert*-Butyl)-4-(phenoxymethyl)benzene (5e). Following GP5, 1-bromo-4-(*tert*-butyl)benzene (42.6 mg, 0.20 mmol) and 2-methyl-2-(phenoxymethyl)-2,3-dihydroquinazolin-4(1*H*)-one (80.4 mg, 0.30 mmol) were used, affording the title compound as a white solid (26.7 mg, 56% yield), by using hexane/EtOAc (100:1) as chromatography eluent. In a second independent experiment, 24.3 mg (51%) were obtained, giving an average of 53% yield. **M.p.**: 100 °C. **^{1}H NMR (400 MHz, $CDCl_3$)** δ 7.45 – 7.36 (m, 4H), 7.34 – 7.27 (m, 2H), 7.03 – 6.93 (m, 3H), 5.04 (s, 2H), 1.34 (s, 9H) ppm. **^{13}C NMR (101 MHz, $CDCl_3$)** δ 159.1, 151.2, 134.2, 129.6, 127.6, 125.7, 121.0, 115.0, 69.9, 34.7, 31.5 ppm. Spectral data was in agreement with the literature.[198]

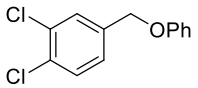

1,2-Dichloro-4-(phenoxymethyl)benzene (5f). Following GP4, 4-bromo-1,2-dichlorobenzene (45.2 mg, 0.20 mmol) and 2-methyl-2-(phenoxymethyl)-2,3-dihydroquinazolin-4(1*H*)-one (64.3 mg, 0.24 mmol) were used, affording the title compound as a colourless liquid (15.5 mg, 31% yield), by using hexane/EtOAc (100:1) as chromatography eluent. In an independent experiment, 29.6 mg (58%) were obtained, giving an average of 45% yield. **IR (neat, cm^{-1}):** 3061, 1598, 1494, 1402, 1235, 1172, 1130, 1030, 880, 808, 751, 689. **^{1}H NMR (400 MHz, $CDCl_3$)** δ 7.57 (d, *J* = 2.0 Hz, 1H), 7.47 (d, *J* = 8.2 Hz, 1H), 7.37 – 7.25 (m, 3H), 7.05 – 6.95 (m, 3H), 5.04 (s, 2H) ppm. **^{13}C NMR (101 MHz, $CDCl_3$)** δ 158.4, 137.6, 132.9, 132.0, 130.7, 129.8, 129.4, 126.7, 121.5, 115.0, 68.6 ppm. Spectral data was in agreement with the literature. **HRMS** [ESI$^+$] *calcd*. for ($C_{15}H_{12}N_2NaO_2$) $[M+Na]^+$: 275.0796, *found*: 275.0800.

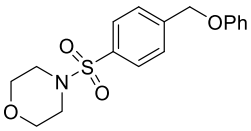

4-((4-(Phenoxymethyl)phenyl)sulfonyl)morpholine (5g). Following GP4, 4-((4-bromophenyl)sulfonyl)morpholine (61.2 mg, 0.20 mmol) and 2-methyl-2-(phenoxymethyl)-2,3-dihydroquinazolin-4(1*H*)-one (64.3 mg, 0.24 mmol) were used, affording the title compound as a white solid (47.2 mg, 71% yield), by using hexane/EtOAc (3:1) as chromatography eluent. In a second independent experiment,

[197] Cong, F.; Lv. X.-Y.; Day, C. S.; Martin, R. Dual Catalytic Strategy for Forging sp^2–sp^3 and sp^3–sp^3 Architectures via β-Scission of Aliphatic Alcohol Derivatives. *J. Am. Chem. Soc*. **2020**, *142*, 20594–20599.

[198] Bering, L.; Jeyakumar, K.; Antonchick, A. P. Metal-Free C–O Bond Functionalization: Catalytic Intramolecular and Intermolecular Benzylation of Arenes. *Org. Lett*. **2018**, *20*, 3911–3914.

48.3 mg (73%) were obtained, giving an average of 72% yield. **M.p.**: 178 °C. **IR (neat, cm^{-1}):** 2860, 1601, 1588, 1491, 1450, 1410, 1345, 1245, 1159, 1109, 941, 815, 733, 531. **^{1}H NMR (400 MHz, CDCl$_3$)** δ 7.81 – 7.74 (m, 2H), 7.63 (d, *J* = 8.6 Hz, 2H), 7.36 – 7.28 (m, 2H), 7.04 – 6.95 (m, 3H), 5.16 (s, 2H), 3.79 – 3.71 (m, 4H), 3.06 – 2.97 (m, 4H) ppm. **^{13}C NMR (101 MHz, CDCl$_3$)** δ 158.4, 142.9, 134.7, 129.8, 128.3, 127.8, 121.6, 114.9, 68.9, 66.2, 46.1 ppm. **HRMS** [ESI$^+$] *calcd*. for ($C_{17}H_{19}NNaO_4S$) [M+Na]$^+$: 356.0932, *found*: 356.0920.

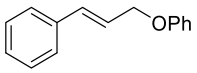

(Cinnamyloxy)benzene (5h). Following GP4, (*E*)-(2-bromovinyl)benzene (36.6 mg, 0.20 mmol) and 2-methyl-2-(phenoxymethyl)-2,3-dihydroquinazolin-4(1*H*)-one (64.3 mg, 0.24 mmol) were used, affording the title compound as a white solid (21.2 mg, 50% yield), by using hexane/EtOAc (100:1) as chromatography eluent. In a second independent experiment, 23.6 mg (56%) were obtained, giving an average of 53% yield. **M.p.**: 66 °C. **^{1}H NMR (400 MHz, CDCl$_3$)** δ 7.49 – 7.41 (m, 2H), 7.39 – 7.25 (m, 5H), 7.04 – 6.96 (m, 3H), 6.77 (d, *J* = 16.0 Hz, 1H), 6.45 (dt, *J* = 16.0, 5.8 Hz, 1H), 4.73 (dd, *J* = 5.8, 1.5 Hz, 2H) ppm. **^{13}C NMR (101 MHz, CDCl$_3$)** δ 158.8, 136.6, 133.1, 129.6, 128.7, 128.0, 126.7, 124.7, 121.1, 114.9, 68.7 ppm. Spectral data was in agreement with the literature.[199]

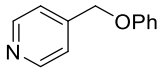

4-(Phenoxymethyl)pyridine (5i). Following GP4, 4-bromopyridine (31.6 mg, 0.20 mmol) and 2-methyl-2-(phenoxymethyl)-2,3-dihydroquinazolin-4(1*H*)-one (64.3 mg, 0.24 mmol) were used, affording the title compound as a colourless oil (25.5 mg, 69% yield), by using hexane/EtOAc (3:1) as chromatography eluent. In a second independent experiment, 20.9 mg (56%) were obtained, giving an average of 63% yield. **IR (neat, cm^{-1}):** 3031, 1597, 1493, 1415, 1240, 1043, 798, 751, 690. **^{1}H NMR (400 MHz, CDCl$_3$)** δ 8.67 – 8.56 (m, 2H), 7.39 – 7.34 (m, 2H), 7.33 – 7.27 (m, 2H), 7.03 – 6.93 (m, 3H), 5.09 (s, 2H) ppm. **^{13}C NMR (101 MHz, CDCl$_3$)** δ 158.3, 150.1, 146.5, 129.8, 121.6, 121.6, 114.9, 68.2 ppm. **HRMS** [ESI$^+$] *calcd*. for ($C_{12}H_{12}NO$) [M+H]$^+$: 186.0919, *found*: 186.0913.

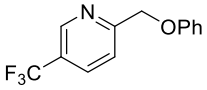

2-(Phenoxymethyl)-5-(trifluoromethyl)pyridine (5j). Following GP4, 2-bromo-5-(trifluoromethyl)pyridine (45.2 mg, 0.20 mmol) and 2-methyl-2-(phenoxymethyl)-2,3-dihydroquinazolin-4(1*H*)-one (64.3 mg, 0.24 mmol) were used, affording the title compound as a white solid (28.9 mg, 57% yield), by using hexane/EtOAc (20:1) as

[199] Zhang, Y.-L.; Yang. L.; Wu, J.; Zhu, C.; Wang, P. Vinyl Sulfonium Salts as the Radical Acceptor for Metal-Free Decarboxylative Alkenylation. *Org. Lett*. **2020**, *22*, 7768–7772.

chromatography eluent. In a second independent experiment, 29.2 mg (58%) were obtained, giving an average of 57% yield. **M.p.**: 57 °C. **IR (neat, cm^{-1}):** 2927, 1604, 1586, 1491, 1448, 1394, 1324, 1244, 1211, 1078, 1014, 848, 755, 691, 568. **^{1}H NMR (400 MHz, $CDCl_3$)** δ 8.89 – 8.84 (m, 1H), 7.96 (dd, *J* = 8.2, 2.0 Hz, 1H), 7.70 (d, *J* = 8.2 Hz, 1H), 7.35 – 7.27 (m, 2H), 7.04 – 6.94 (m, 3H), 5.28 (s, 2H) ppm. **^{13}C NMR (126 MHz, $CDCl_3$)** δ 161.7 (d, $J_{C,F}$ = 1 Hz), 158.1, 146.3 (q, $J_{C,F}$ = 4 Hz), 134.1 (q, $J_{C,F}$ = 4 Hz), 129.8, 125.7 (q, $J_{C,F}$ = 33 Hz), 123.6 (q, $J_{C,F}$ = 273 Hz), 121.7, 120.9, 114.9, 70.1 ppm. **^{19}F NMR** (376 MHz, $CDCl_3$) δ -62.43. **HRMS** [ESI$^+$] *calcd*. for ($C_{13}H_{11}F_3NO$) $[M+H]^+$: 254.0793, *found*: 254.0786.

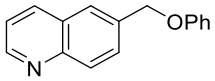

6-(Phenoxymethyl)quinoline (5k). Following GP4, 6-bromoquinoline (41.6 mg, 0.20 mmol) and 2-methyl-2-(phenoxymethyl)-2,3-dihydroquinazolin-4(1*H*)-one (64.3 mg, 0.24 mmol) were used, affording the title compound as a white solid (26.0 mg, 55% yield), by using hexane/EtOAc (3:1) as chromatography eluent. In a second independent experiment, 21.3 mg (45%) were obtained, giving an average of 50% yield. **M.p.**: 81 °C. **IR (neat, cm^{-1}):** 2911, 1586, 1492, 1224, 768. **^{1}H NMR (400 MHz, $CDCl_3$)** δ 8.92 (dd, J = 4.2, 1.7 Hz, 1H), 8.19 – 8.11 (m, 2H), 7.91 – 7.86 (m, 1H), 7.78 (dd, J = 8.7, 1.9 Hz, 1H), 7.41 (dd, J = 8.3, 4.2 Hz, 1H), 7.35 – 7.28 (m, 2H), 7.07 – 6.95 (m, 3H), 5.26 (s, 2H) ppm. **^{13}C NMR (101 MHz, $CDCl_3$)** δ 158.7, 150.6, 148.1, 136.2, 135.7, 123.0, 129.7, 128.9, 128.3, 126.0, 121.5, 121.3, 115.0, 69.7 ppm. **HRMS** [ESI$^+$] *calcd*. for ($C_{16}H_{14}NO$) $[M+Na]^+$: 236.1070, *found*: 236.1068.

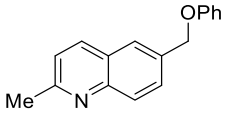

2-Methyl-6-(phenoxymethyl)quinoline (5l). Following GP4, 6-bromo-2-methylquinoline (44.4 mg, 0.20 mmol) and 2-methyl-2-(phenoxymethyl)-2,3-dihydroquinazolin-4(1*H*)-one (64.3 mg, 0.24 mmol) were used, affording the title compound as a white solid (24.7 mg, 50% yield), by using hexane/EtOAc (3:1) as chromatography eluent. In a second independent experiment, 25.4 mg (51%) were obtained, giving an average of 50% yield. **M.p.**: 89 °C. **IR (neat, cm^{-1}):** 2913, 1595, 1489, 1461, 1370, 1230, 1175, 1028, 1009, 895, 817, 770, 699. **^{1}H NMR (400 MHz, $CDCl_3$)** δ 8.05 (dd, *J* = 8.4, 5.6 Hz, 2H), 7.83 (s, 1H), 7.74 (dd, *J* = 8.7, 1.9 Hz, 1H), 7.35 – 7.27 (m, 3H), 7.05 – 6.95 (m, 3H), 5.23 (s, 2H), 2.76 (s, 3H) ppm. **^{13}C NMR (101 MHz, $CDCl_3$)** δ 159.3, 158.8, 147.6, 136.4, 134.7, 129.7, 129.1, 129.0, 126.5, 125.9, 122.5, 121.3, 115.0, 69.8, 25.4 ppm. **HRMS** [ESI$^+$] *calcd*. for ($C_{17}H_{16}NO$) $[M+H]^+$: 250.1232, *found*: 250.1229.

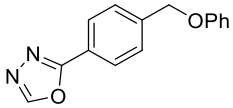

2-(4-(Phenoxymethyl)phenyl)-1,3,4-oxadiazole (5m). Following GP4, 2-(4-bromophenyl)-1,3,4-oxadiazole (45.0 mg, 0.20 mmol) and 2-methyl-2-(phenoxymethyl)-2,3-dihydroquinazolin-4(1*H*)-one (64.3 mg, 0.24 mmol) were used, affording the title compound as a white solid (36.0 mg, 71% yield), by using hexane/EtOAc (3:1) as chromatography eluent. In a second independent experiment, 33.0 mg (65%) were obtained, giving an average of 68% yield. **M.p.**: 134 °C. **IR (neat, cm^{-1}):** 3158, 2917, 1586, 1559, 1486, 1466, 1375, 1230, 1067, 1013, 871, 827, 755, 639. **^{1}H NMR (400 MHz, $CDCl_3$)** δ 8.47 (s, 1H), 8.14 – 8.07 (m, 2H), 7.60 (d, *J* = 8.6 Hz, 2H), 7.34 – 7.27 (m, 2H), 7.02 – 6.95 (m, 3H), 5.15 (s, 2H) ppm. **^{13}C NMR (101 MHz, $CDCl_3$)** δ 164.7, 158.5, 152.7, 141.6, 129.7, 127.9, 127.5, 123.1, 121.5, 115.0, 69.3 ppm. **HRMS** [ESI^+] *calcd*. for ($C_{15}H_{12}N_2NaO_2$) $[M+Na]^+$: 275.0796, *found*: 275.0800.

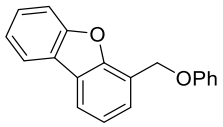

4-(Phenoxymethyl)dibenzo[*b*,*d*]furan (5n). Following GP5, 4-bromodibenzo[*b*,*d*]furan (49.4 mg, 0.20 mmol) and 2-methyl-2-(phenoxymethyl)-2,3-dihydroquinazolin-4(1*H*)-one (80.4 mg, 0.30 mmol) were used, affording the title compound as a white solid (34.2 mg, 62% yield), by using hexane/EtOAc (50:1) as chromatography eluent. In an independent experiment, 36.0 mg (66%) were obtained, giving an average of 64% yield. **M.p.**: 105 °C. **IR (neat, cm^{-1}):** 3038, 1596, 1583, 1489, 1450, 1432, 1386, 1229, 1184, 1080, 1030, 1013, 844, 748, 691. **^{1}H NMR (400 MHz, $CDCl_3$)** δ 8.01 – 7.90 (m, 2H), 7.62 (d, *J* = 8.1 Hz, 2H), 7.52 – 7.46 (m, 1H), 7.42 – 7.28 (m, 4H), 7.12 – 7.06 (m, 2H), 7.03 – 6.95 (m, 1H), 5.49 (s, 2H) ppm. **^{13}C NMR (101 MHz, $CDCl_3$)** δ 158.9, 156.3, 153.9, 129.7, 127.4, 126.7, 124.4, 124.4, 123.1, 123.0, 121.3, 121.2, 120.9, 120.5, 115.1, 111.9, 64.7 ppm. **HRMS** [ESI^+] *calcd*. for ($C_{19}H_{14}NaO_2$) $[M+Na]^+$: 297.0891, *found*: 297.0887.

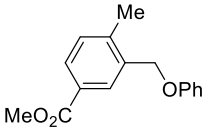

Methyl 4-methyl-3-(phenoxymethyl)benzoate (5o). Following GP5, methyl 3-bromo-4-methylbenzoate (45.8 mg, 0.20 mmol) and 2-methyl-2-(phenoxymethyl)-2,3-dihydroquinazolin-4(1*H*)-one (80.4 mg, 0.30 mmol) were used, affording the title compound as a colourless liquid (24.7 mg, 48% yield), by using hexane/EtOAc (20:1) as chromatography eluent. In a second independent experiment, 18.1 mg (35%) were obtained, giving an average of 42% yield. **IR (neat, cm^{-1}):** 2950, 1716, 1598, 1495, 1435, 1294, 1211, 1101, 1007, 839, 752, 690. **^{1}H NMR (400 MHz, $CDCl_3$)** δ 8.12 (d, *J* = 1.7 Hz, 1H), 7.93 (dd, *J* = 7.9, 1.8 Hz, 1H), 7.36 – 7.27 (m, 3H), 7.04 – 6.96 (m, 3H), 5.06 (s, 2H), 3.91 (s, 3H), 2.44 (s, 3H) ppm. **^{13}C NMR (101 MHz, $CDCl_3$)** δ 167.1,

158.9, 142.6, 135.4, 130.7, 130.0, 129.7, 129.63, 128.3, 121.3, 115.0, 68.4, 52.2, 19.3 ppm. **HRMS** [ESI$^+$] *calcd*. for ($C_{16}H_{16}NaO_3$) [M+Na]$^+$: 279.0997, *found*: 279.0998.

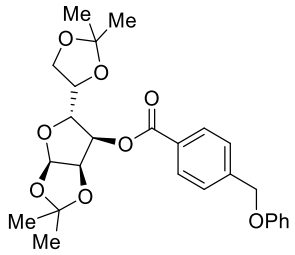

(3a*R*,5*R*,6*R*,6a*R*)-5-((*R*)-2,2-dimethyl-1,3-dioxolan-4-yl)-2,2-dimethyltetrahydrofuro[2,3-*d*][1,3]dioxol-6-yl 4-(phenoxymethyl)benzoate (5p). Following GP4, (3a*R*,5*R*,6*R*,6a*R*)-5-((*R*)-2,2-dimethyl-1,3-dioxolan-4-yl)-2,2-dimethyltetrahydrofuro[2,3-*d*][1,3]dioxol-6-yl 4-bromobenzoate (88.6 mg, 0.20 mmol) and 2-methyl-2-(phenoxymethyl)-2,3-dihydroquinazolin-4(1*H*)-one (64.3 mg, 0.24 mmol) were used, affording the title compound as an amorphous white solid (76.7 mg, 81% yield), by using hexane/EtOAc (5:1) as chromatography eluent. In a second independent experiment, 79.9 mg (85%) were obtained, giving an average of 83% yield. **IR (neat, cm^{-1}):** 3468, 2988, 1712, 1599, 1494, 1382, 1270, 1100, 1015, 841, 750, 690. **^{1}H NMR (400 MHz, $CDCl_3$)** δ 8.10 – 8.04 (m, 2H), 7.53 (d, *J* = 8.5 Hz, 2H), 7.34 – 7.27 (m, 2H), 7.01 – 6.94 (m, 3H), 5.90 (d, *J* = 3.8 Hz, 1H), 5.14 (s, 2H), 5.08 (dd, *J* = 8.1, 5.1 Hz, 1H), 4.97 (dd, *J* = 5.1, 3.9 Hz, 1H), 4.40 – 4.31 (m, 2H), 4.15 – 4.08 (m, 1H), 4.01 – 3.95 (m, 1H), 1.55 (s, 3H), 1.41 (s, 3H), 1.34 (s, 3H), 1.33 (s, 3H) ppm. **^{13}C NMR (101 MHz, $CDCl_3$)** δ 165.5, 158.6, 143.0, 130.3, 129.7, 129.1, 127.2, 121.4, 115.0, 113.3, 110.2, 104.5, 78.0, 78.0, 75.4, 73.4, 69.3, 65.9, 26.9, 26.8, 26.5, 25.2 ppm. **HRMS** [ESI$^+$] *calcd*. for ($C_{26}H_{30}NaO_8$) [M+Na]$^+$: 493.1838, *found*: 493.1830.

General procedure 6 (GP6): Nickel-catalyzed coupling with alkyl bromides

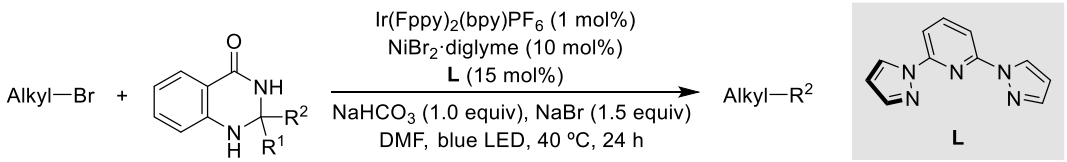

An oven-dried 8 mL screw-cap test tube containing a stirring bar was charged with $Ir(Fppy)_2(bpy)PF_6$ (1.6 mg, 1 mol%), 2,6-di(1-pyrazolyl)pyridine (12.1 mg, 15 mol%), NaBr (30.9 mg, 1.5 equiv), alkyl bromide (if solid, 1.0 equiv, 0.2 mmol) and ketone derivative (1.5 equiv). The test tube was introduced in a nitrogen-filled glovebox where $NiBr_2$·diglyme (7.1 mg, 10 mol%) and $NaHCO_3$ (16.8 mg, 1.0 equiv) were added to the reaction vessel. The reaction tube was sealed with a screw cap and removed from the glovebox. Afterwards, alkyl bromide (if liquid) and DMF (2 mL, 0.1 M) were added by syringe. Parafilm was used to reseal the pierced cap. The reaction mixture was stirred at rt for 1 minute, then exposed to blue LED irradiation at 40 °C for 24 hours. The

reaction mixture was quenched with water/brine (10 mL) and extracted with ethyl acetate (3 x 10 mL). The combined organic extracts were dried (Na_2SO_4), concentrated under reduced pressure and purified by silica gel chromatography.

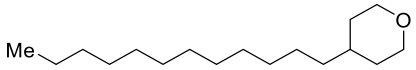

4-Dodecyltetrahydro-2*H*-pyran (7a). Following GP6, 1-bromododecane (49.8 mg, 0.20 mmol) and 2-methyl-2-(tetrahydro-2*H*-pyran-4-yl)-2,3-dihydroquinazolin-4(1*H*)-one (73.8 mg, 0.30 mmol) were used, affording the title compound as a colourless liquid (26.5 mg, 52% yield), by using hexane/EtOAc (100:1) as chromatography eluent. In a second independent experiment, 25.9 mg (51%) were obtained, giving an average of 51% yield. **IR (neat, cm^{-1}):** 2921, 2851, 1465, 1099. **^{1}H NMR (400 MHz, $CDCl_3$)** δ 3.98 – 3.89 (m, 2H), 3.36 (td, *J* = 11.9, 2.1 Hz, 2H), 1.64 – 1.54 (m, 2H), 1.51 – 1.38 (m, 1H), 1.35 – 1.17 (m, 24H), 0.92 – 0.83 (m, 3H) ppm. **^{13}C NMR (101 MHz, $CDCl_3$)** δ 68.4, 37.1, 35.1, 33.4, 32.1, 30.0, 29.8, 29.8, 29.8, 29.8, 29.8, 29.5, 26.5, 22.8, 14.3 ppm. **HRMS** [APCI$^+$] *calcd*. for ($C_{17}H_{35}O$) $[M+H]^+$: 255.2688, *found*: 255.2680.

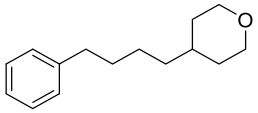

4-(4-Phenylbutyl)tetrahydro-2*H*-pyran (7b). Following GP6, (4-bromobutyl)benzene (42.6 mg, 0.20 mmol) and 2-methyl-2-(tetrahydro-2*H*-pyran-4-yl)-2,3-dihydroquinazolin-4(1*H*)-one (73.8 mg, 0.30 mmol) were used, affording the title compound as a colourless liquid (22.3 mg, 51% yield), by using hexane/EtOAc (100:1) as chromatography eluent. In a second independent experiment, 21.7 mg (50%) were obtained, giving an average of 50% yield. **^{1}H NMR (400 MHz, $CDCl_3$)** δ 7.32 – 7.25 (m, 2H), 7.21 – 7.15 (m, 3H), 4.00 – 3.88 (m, 2H), 3.36 (td, *J* = 11.9, 2.1 Hz, 2H), 2.66 – 2.55 (m, 2H), 1.66 – 1.53 (m, 4H), 1.52 – 1.40 (m, 1H), 1.40 – 1.18 (m, 6H) ppm. **^{13}C NMR (101 MHz, $CDCl_3$)** δ 142.9, 128.5, 128.4, 125.8, 68.3, 36.9, 36.1, 35.1, 33.4, 31.8, 26.2 ppm. Spectral data was in agreement with the literature.[200]

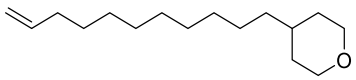

4-(Undec-10-en-1-yl)tetrahydro-2*H*-pyran (7c). Following GP6, 11-bromoundec-1-ene (46.6 mg, 0.20 mmol) and 2-methyl-2-(tetrahydro-2*H*-pyran-4-yl)-2,3-dihydroquinazolin-4(1*H*)-one (73.8 mg, 0.30 mmol) were used, affording the title compound as a colourless liquid (26.5 mg, 56% yield), by using hexane/EtOAc (100:1) as eluent. In a second independent experiment, 25.4 mg (53%) were obtained, giving an average of 55% yield. **IR (neat, cm^{-1}):** 2922, 2852, 1100, 908. **^{1}H NMR (400 MHz,**

[200] Sun, S.-Z.; Romano, C.; Martin, R. Site-Selective Catalytic Deaminative Alkylation of Unactivated Olefins. *J. Am. Chem. Soc.* **2019**, *141*, 16197–16201.

$CDCl_3$) δ 5.81 (ddt, *J* = 16.9, 10.2, 6.7 Hz, 1H), 5.04 – 4.89 (m, 2H), 3.99 – 3.89 (m, 2H), 3.36 (td, *J* = 11.9, 2.1 Hz, 2H), 2.09 – 1.98 (m, 2H), 1.67 – 1.54 (m, 2H), 1.50 – 1.17 (m, 19H) ppm. **^{13}C NMR (101 MHz, $CDCl_3$)** δ 139.4, 114.2, 68.4, 37.1, 35.1, 34.0, 33.4, 30.0, 29.8, 29.7, 29.6, 29.3, 29.1, 26.5 ppm. **HRMS** [APCI$^+$] *calcd*. for ($C_{16}H_{31}O$) [M+H]$^+$: 239.2375, *found*: 239.2365.

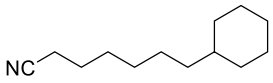

7-Cyclohexylheptanenitrile (7d). Following GP6, 7-bromoheptanenitrile (38.0 mg, 0.20 mmol) and 2-cyclohexyl-2-methyl-2,3-dihydroquinazolin-4(1*H*)-one (73.2 mg, 0.30 mmol) were used, affording the title compound as a colourless liquid (25.6 mg, 67% yield), by using hexane/EtOAc (10:1) as chromatography eluent. In a second independent experiment, 24.6 mg (65%) were obtained, giving an average of 66% yield. **^{1}H NMR (400 MHz, $CDCl_3$)** δ 2.33 (t, *J* = 7.1 Hz, 2H), 1.74 – 1.59 (m, 7H), 1.49 – 1.39 (m, 2H), 1.35 – 1.09 (m, 10H), 0.92 – 0.78 (m, 2H) ppm. **^{13}C NMR (101 MHz, $CDCl_3$)** δ 120.0, 37.7, 37.5, 33.6, 29.2, 28.8, 26.9, 26.7, 26.5, 25.5, 17.3 ppm. Spectral data was in agreement with the literature.[201]

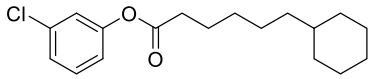

3-Chlorophenyl 6-cyclohexylhexanoate (7e). Following GP6, 3-chlorophenyl 6-bromohexanoate (61.0 mg, 0.20 mmol) and 2-cyclohexyl-2-methyl-2,3-dihydroquinazolin-4(1*H*)-one (73.2 mg, 0.30 mmol) were used, affording the title compound as a colourless liquid (40.8 mg, 66% yield), by using hexane/EtOAc (50:1) as chromatography eluent. In a second independent experiment, 45.8 mg (73%) were obtained, giving an average of 69% yield. **IR (neat, cm^{-1}):** 2920, 2850, 1763, 1590, 1473, 1199, 1114, 873, 778, 676. **^{1}H NMR (400 MHz, $CDCl_3$)** δ 7.30 (t, *J* = 8.1 Hz, 1H), 7.21 (ddd, *J* = 8.1, 2.0, 1.0 Hz, 1H), 7.12 (t, *J* = 2.0 Hz, 1H), 6.99 (ddd, *J* = 8.1, 2.2, 1.0 Hz, 1H), 2.54 (t, *J* = 7.5 Hz, 2H), 1.80 – 1.61 (m, 7H), 1.43 – 1.30 (m, 4H), 1.30 – 1.10 (m, 6H), 0.96 – 0.80 (m, 2H) ppm. **^{13}C NMR (101 MHz, $CDCl_3$)** δ 172.0, 151.4, 134.8, 130.2, 126.1, 122.4, 120.2, 37.8, 37.4, 34.5, 33.6, 29.5, 26.9, 26.6, 26.6, 25.0 ppm. **HRMS** [ESI$^+$] *calcd*. for ($C_{18}H_{25}ClNaO_2$) [M+Na]$^+$: 331.1441, *found*: 331.1439.

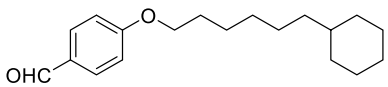

4-((6-Cyclohexylhexyl)oxy)benzaldehyde (7f). Following GP6, 4-((6-bromohexyl)oxy)benzaldehyde (57.0 mg, 0.20 mmol) and 2-cyclohexyl-2-methyl-2,3-dihydroquinazolin-4(1*H*)-one (73.2 mg, 0.30 mmol) were used, affording the title

[201] Bhunia, A.; Bergander, K.; Studer, A. Cooperative Palladium/Lewis Acid-Catalyzed Transfer Hydrocyanation of Alkenes and Alkynes Using 1-Methylcyclohexa-2,5-diene-1-carbonitrile. *J. Am. Chem. Soc*. **2018**, *140*, 16353–16359.

compound as a colourless liquid (37.8 mg, 66% yield), by using hexane/EtOAc (50:1) as chromatography eluent. In a second independent experiment, 39.4 mg (68%) were obtained, giving an average of 67% yield. **IR (neat, cm^{-1}):** 2920, 2850, 1691, 1599, 1577, 1509, 1448, 1311, 1253, 1157, 830, 617. **^{1}H NMR (400 MHz, CDCl$_3$)** δ 9.88 (s, 1H), 7.82 (d, *J* = 8.8 Hz, 2H), 6.99 (d, *J* = 8.7 Hz, 2H), 4.03 (t, *J* = 6.6 Hz, 2H), 1.87 – 1.76 (m, 2H), 1.74 – 1.57 (m, 5H), 1.52 – 1.41 (m, 2H), 1.39 –1.27 (m, 4H), 1.27 – 1.09 (m, 6H), 0.94 – 0.78 (m, 2H) ppm. **^{13}C NMR (126 MHz, CDCl$_3$)** δ 190.9, 164.4, 132.1, 129.9, 114.9, 68.5, 37.8, 37.5, 33.6, 29.8, 29.2, 26.9, 26.6, 26.1 ppm. (two peaks overlap in 26.9) **HRMS** [ESI$^+$] *calcd*. for ($C_{19}H_{28}NaO_2$) [M+Na]$^+$: 311.1987, *found*: 311.1986.

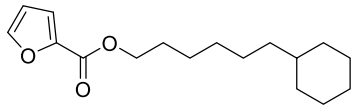

6-Cyclohexylhexyl furan-2-carboxylate (7g). Following GP6, 6-bromohexyl furan-2-carboxylate (55.0 mg, 0.20 mmol) and 2-cyclohexyl-2-methyl-2,3-dihydroquinazolin-4(1*H*)-one (73.2 mg, 0.30 mmol) were used, affording the title compound as a colourless liquid (25.9 mg, 47% yield), by using hexane/EtOAc (50:1) as chromatography eluent. In a second independent experiment, 21.6 mg (39%) were obtained, giving an average of 43% yield. **IR (neat, cm^{-1}):** 2921, 2851, 1723, 1578, 1507, 1448, 1304, 1159, 1075, 974, 874, 761, 603. **^{1}H NMR (400 MHz, CDCl$_3$)** δ 8.00 (dd, *J* = 1.5, 0.8 Hz, 1H), 7.43 – 7.40 (m, 1H), 6.74 (dd, *J* = 1.9, 0.8 Hz, 1H), 4.23 (t, *J* = 6.7 Hz, 2H), 1.77 – 1.60 (m, 7H), 1.45 – 1.09 (m, 12H), 0.92 – 0.79 (m, 2H) ppm. **^{13}C NMR (101 MHz, CDCl$_3$)** δ 163.4, 147.7, 143.8, 119.8, 110.0, 64.8, 37.8, 37.6, 33.6, 29.7, 28.8, 26.9, 26.9, 26.6, 26.2 ppm. **HRMS** [ESI$^+$] *calcd*. for ($C_{17}H_{26}NaO_3$) [M+Na]$^+$: 301.1780, *found*: 301.1770.

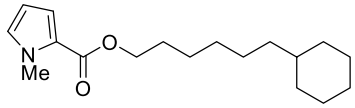

6-Cyclohexylhexyl 1-methyl-1*H*-pyrrole-2-carboxylate (7h). Following GP6, 6-bromohexyl 1-methyl-1*H*-pyrrole-2-carboxylate (57.6 mg, 0.20 mmol) and 2-cyclohexyl-2-methyl-2,3-dihydroquinazolin-4(1*H*)-one (73.2 mg, 0.30 mmol) were used, affording the title compound as a colourless liquid (36.0 mg, 62% yield) by using Hexane/EtOAc (50:1) as eluent. In an independent experiment, 38.7 mg (66%) were obtained, giving an average of 64% yield. **IR (neat, cm^{-1}):** 2920, 2850, 1701, 1531, 1414, 1319, 1243, 1107, 731. **^{1}H NMR (400 MHz, CDCl$_3$)** δ 6.94 (dd, *J* = 4.0, 1.8 Hz, 1H), 6.77 (t, *J* = 2.1 Hz, 1H), 6.11 (dd, *J* = 3.9, 2.5 Hz, 1H), 4.21 (t, *J* = 6.7 Hz, 2H), 3.92 (s, 3H), 1.77 – 1.59 (m, 7H), 1.46 – 1.36 (m, 2H), 1.36 – 1.25 (m, 5H), 1.24 – 1.13 (m, 5H), 0.93 – 0.79 (m, 2H) ppm. **^{13}C NMR (101 MHz, CDCl$_3$)** δ 161.6, 129.4, 122.9, 117.8, 107.9, 64.1, 37.8, 37.6, 36.9, 33.6, 29.7, 29.0, 26.9, 26.9, 26.6, 26.2 ppm. **HRMS** [ESI$^+$] *calcd*. for ($C_{18}H_{29}NNaO_2$) [M+Na]$^+$: 314.2096, *found*: 314.2094.

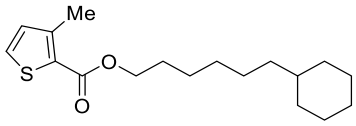

6-Cyclohexylhexyl 3-methylthiophene-2-carboxylate (7i). Following GP6, 6-bromohexyl 3-methylthiophene-2-carboxylate (61.0 mg, 0.20 mmol) and 2-cyclohexyl-2-methyl-2,3-dihydroquinazolin-4(1*H*)-one (73.2 mg, 0.30 mmol) were used, affording the title compound as a colourless liquid (30.8 mg, 50% yield), by using hexane/EtOAc (50:1) as chromatography eluent. In a second independent experiment, 37.1 mg (60%) were obtained, giving an average of 55% yield. **IR (neat, cm^{-1}):** 2920, 2850, 1707, 1541, 1415, 1255, 1101, 1071, 767, 721. **^{1}H NMR (400 MHz, CDCl$_3$)** δ 7.37 (d, *J* = 5.0 Hz, 1H), 6.90 (d, *J* = 5.0 Hz, 1H), 4.26 (t, *J* = 6.7 Hz, 2H), 2.55 (s, 3H), 1.78 – 1.60 (m, 7H), 1.47 – 1.36 (m, 2H), 1.36 – 1.09 (m, 10H), 0.93 – 0.78 (m, 2H) ppm. **^{13}C NMR (101 MHz, CDCl$_3$)** δ 163.1, 146.0, 131.8, 123.0, 127.3, 65.0, 37.8, 37.6, 33.6, 29.7, 28.9, 26.9, 26.9, 26.6, 26.2, 16.1 ppm. **HRMS** [ESI$^+$] *calcd*. for ($C_{18}H_{28}NaO_2S$) [M+Na]$^+$: 331.1708, *found*: 331.1701.

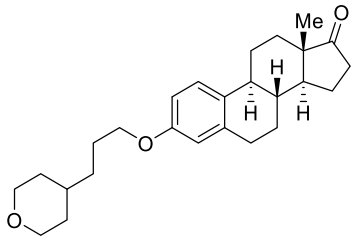

(8*R*,9*S*,13*S*,14*S*)-13-Methyl-3-(3-(tetrahydro-2*H*-pyran-4-yl)propoxy)-6,7,8,9,11,12,13,14,15,16-decahydro-17*H*-cyclopenta[a]phenanthren-17-one (7n). Following GP6 by running the reaction for 50 hours, (8*R*,9*S*,13*S*,14*S*)-3-(3-bromopropoxy)-13-methyl-6,7,8,9,11,12,13,14,15,16-decahydro-17*H*-cyclopenta[*a*]phenanthren-17-one (**6j**) (78.3 mg, 0.20 mmol) and 2-methyl-2-(tetrahydro-2*H*-pyran-4-yl)-2,3-dihydroquinazolin-4(1*H*)-one (**2d**) (73.9 mg, 0.30 mmol) were used. The resulting crude material was purified by silica gel chromatography (0 to 7.5% THF in hexane), affording the title compound as a white solid (40.3 mg, 51%). In a second independent experiment, 33.6 mg (42%) of the title compound was obtained, giving an average of 47% yield. **M.p.** 116 °C. **IR (film, cm^{-1})** = 2925, 2853, 1737, 1499, 1234. **^{1}H NMR (500 MHz, CDCl$_3$)** δ 7.19 (d, *J* = 8.6 Hz, 1H), 6.70 (dd, *J* = 8.6, 2.7 Hz, 1H), 6.64 (d, *J* = 2.7 Hz, 1H), 4.02 – 3.88 (m, 4H), 3.37 (td, *J* = 11.7, 1.8 Hz, 2H), 2.95 – 2.83 (m, 2H), 2.57 – 2.45 (m, 1H), 2.30 – 2.21 (m, 1H), 2.18 – 1.92 (m, 4H), 1.83 – 1.74 (m, 2H), 1.66 – 1.22 (m, 14H), 0.91 (s, 3H) ppm. **^{13}C NMR (126 MHz, CDCl$_3$)** δ 157.2, 137.9, 132.1, 126.4, 114.7, 112.2, 68.22, 68.1, 50.5, 48.2, 44.1, 38.5, 36.0, 34.9, 33.4, 33.3, 31.7, 29.8, 26.7, 26.4, 26.1, 21.7, 14.0 ppm. **HRMS** [ESI$^+$] *calcd*. for ($C_{26}H_{36}NaO_3$) [M+Na]$^+$: 419.2557, *found* 419.2559.

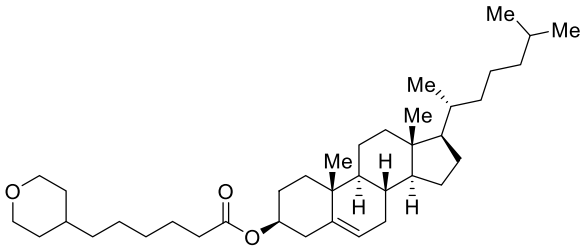

(3*S*,8*S*,9*S*,10*R*,13*R*,14*S*,17*R*)-10,13-Dimethyl-17-((*R*)-6-methylheptan-2-yl)-2,3,4,7,8,9,10,11,12,13,14,15,16,17-tetradecahydro-1*H*-cyclopenta[a]phenanthren-3-yl 6-(tetrahydro-2H-pyran-4-yl)hexanoate (7p). Following GP6 by running the reaction for 72 hours, (3*S*,8*S*,9*S*,10*R*,13*R*,14*S*,17*R*)-10,13-dimethyl-17-((*R*)-6-methylheptan-2-yl)-2,3,4,7,8,9,10,11,12,13,14,15,16,17-tetradecahydro-1*H*-cyclopenta[a]phenanthren-3-yl 6-bromohexanoate (**6k**) (112.7 mg, 0.20 mmol) and 2-methyl-2-(tetrahydro-2*H*-pyran-4-yl)-2,3-dihydroquinazolin-4(1*H*)-one (**2d**) (73.9 mg, 0.30 mmol) were used. The resulting crude material was purified by silica gel chromatography (0 to 4% Et_2O in hexane), affording the title compound as a white solid (53.0 mg, 47%) and recovered (3*S*,8*S*,9*S*,10*R*,13*R*,14*S*,17*R*)-10,13-dimethyl-17-((*R*)-6-methylheptan-2-yl)-2,3,4,7,8,9,10,11,12,13,14,15,16,17-tetradecahydro-1*H*-cyclopenta[a]phenanthren-3-yl 6-bromohexanoate (**6k**) (25.4 mg, 45 mmol). In a second independent experiment, 57.1 mg (50%) of the title compound along with recovered (3*S*,8*S*,9*S*,10*R*,13*R*,14*S*,17*R*)-10,13-dimethyl-17-((*R*)-6-methylheptan-2-yl)-2,3,4,7,8,9,10,11,12,13,14,15,16,17-tetradecahydro-1*H*-cyclopenta[a]phenanthren-3-yl 6-bromohexanoate (**6k**) (21.5 mg, 38 mmol) were obtained, giving an average of 49% yield (61% brsm). **M.p.** 94 °C. **IR (film, cm^{-1})** = 2929, 2849, 1734, 1165. **^{1}H NMR (400 MHz, $CDCl_3$)** δ 5.37 (br. d, *J* = 4.9, Hz, 1H), 4.66 – 4.56 (m, 1H), 3.93 (dd, *J* = 11.5, 3.5 Hz, 2H), 3.35 (td, *J* = 11.5, 1.7 Hz, 2H), 2.31 (d, *J* = 8.1, 3.5 Hz, 2H), 2.27 (t, *J* = 7.5 Hz, 2H), 2.06 – 1.91 (m, 2H), 1.90 – 1.78 (m, 3H), 1.66 – 1.41 (m, 12H), 1.39 – 1.20 (m, 12H), 1.19 – 1.05 (m, 7H), 1.05 – 0.95 (m, 6H), 0.91 (d, *J* = 6.6 Hz, 3H), 0.87 (d, *J* = 1.8 Hz, 3H), 0.85 (d, *J* = 1.8 Hz, 3H), 0.68 (s, 3H) ppm. **^{13}C NMR (126 MHz, $CDCl_3$)** δ 173.2, 139.7, 122.6, 73.7, 68.2, 56.7, 56.1, 50.0, 42.3, 39.7, 39.5, 38.2, 37.0, 36.7, 36.6, 36.2, 35.8, 34.9, 34.7, 33.2, 31.9, 31.9, 29.2, 28.2, 28.0, 27.8, 26.0, 25.0, 24.3, 23.8, 22.8, 22.6, 21.0, 19.3, 18.7, 11.9 ppm. **HRMS** [ESI$^+$] *calcd*. for ($C_{38}H_{64}NaO_3$) $[M+Na]^+$: 591.4748, *found* 591.4734.

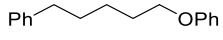

(5-Phenoxypentyl)benzene (7j). Following GP6, (4-bromobutyl)benzene (42.6 mg, 0.20 mmol) and 2-methyl-2-(phenoxymethyl)-2,3-dihydroquinazolin-4(1*H*)-one (80.4 mg, 0.30 mmol) were used, affording the title compound as a colourless liquid (24.0 mg, 50% yield), by using hexane/EtOAc (100:1) as chromatography eluent. In a second independent experiment, 23.0 mg (48%) were obtained, giving an average of 49% yield. **^{1}H NMR (400 MHz, $CDCl_3$)** δ 7.32 – 7.24 (m, 4H), 7.23 – 7.15 (m, 3H), 6.96 – 6.86

(m, 3H), 3.96 (t, *J* = 6.5 Hz, 2H), 2.70 – 2.61 (m, 2H), 1.87 – 1.78 (m, 2H), 1.76 – 1.65 (m, 2H), 1.58 – 1.47 (m, 2H) ppm. **^{13}C NMR (101 MHz, CDCl$_3$)** δ 159.2, 142.7, 129.6, 128.6, 128.4, 125.8, 120.6, 114.7, 67.9, 36.0, 31.4, 29.3, 25.9 ppm. Spectral data was in agreement with the literature.[202]

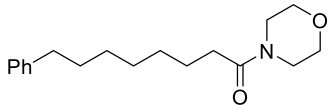

1-Morpholino-8-phenyloctan-1-one (7k). Following GP6, (4-bromobutyl)benzene (42.6 mg, 0.20 mmol) and 2-(4-morpholino-4-oxobutyl)-2-phenyl-2,3-dihydroquinazolin-4(1*H*)-one (113.7 mg, 0.30 mmol) were used, affording the title compound as a colourless liquid (30.3 mg, 52% yield), by using hexane/EtOAc (3:1) as chromatography eluent. In a second independent experiment, 32.1 mg (56%) were obtained, giving an average of 54% yield. **IR (neat, cm^{-1}):** 2924, 2853, 1643, 1427, 1229, 1114, 1036, 699. **^{1}H NMR (400 MHz, CDCl$_3$)** δ 7.32 – 7.26 (m, 2H), 7.22 – 7.16 (m, 3H), 3.73 – 3.56 (m, 6H), 3.48 (s, 2H), 2.67 – 2.58 (m, 2H), 2.37 – 2.28 (m, 2H), 1.70 – 1.57 (m, 4H), 1.44 – 1.32 (m, 6H) ppm. **^{13}C NMR (101 MHz, CDCl$_3$)** δ 172.0, 142.9, 128.5, 128.4, 125.7, 67.1, 66.8, 46.2, 42.0, 36.1, 33.2, 31.6, 29.5, 29.4, 29.3, 25.4 ppm. **HRMS** [ESI$^+$] *calcd*. for ($C_{18}H_{27}NNaO_2$) [M+Na]$^+$: 312.1939, *found*: 312.1942.

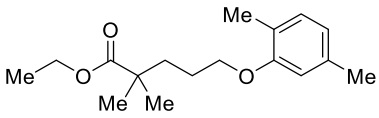

Ethyl 5-(2,5-dimethylphenoxy)-2,2-dimethylpentanoate (7m). Following GP6, ethyl 4-bromo-2,2-dimethylbutanoate (44.6 mg, 0.20 mmol) and 2-((2,5-dimethylphenoxy)methyl)-2-methyl-2,3-dihydroquinazolin-4(1*H*)-one (88.8 mg, 0.30 mmol) were used, affording the title compound as a colourless liquid (25.2 mg, 45% yield), by using hexane/EtOAc (50:1) as chromatography eluent. In a second independent experiment, 21.1 mg (38%) were obtained, giving an average of 42% yield. **IR (neat, cm^{-1}):** 2978, 2930, 1724, 1266, 1140, 1129. **^{1}H NMR (400 MHz, CDCl$_3$)** δ 7.01 (d, J = 7.5 Hz, 1H), 6.66 (d, J = 7.5 Hz, 1H), 6.61 (s, 1H), 4.13 (q, J = 7.1 Hz, 2H), 3.92 (t, J = 5.7 Hz, 2H), 2.31 (s, 3H), 2.18 (s, 3H), 1.79 – 1.69 (m, 4H), 1.25 (t, J = 7.1 Hz, 3H), 1.22 (s, 6H) ppm. **^{13}C NMR (101 MHz, CDCl$_3$)** δ 178.0, 157.1, 136.6, 130.4, 123.7, 120.8, 112.1, 68.1, 60.4, 42.1, 37.2, 25.3, 25.3, 21.5, 15.9, 14.4 ppm. **HRMS** [ESI$^+$] *calcd*. for ($C_{17}H_{26}NaO_3$) [M+Na]$^+$: 301.1774, *found*: 301.1773.

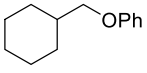

(Cyclohexylmethoxy)benzene (7l). Following GP6, bromocyclohexane (32.6 mg, 0.20 mmol) and 2-methyl-2-(phenoxymethyl)-2,3-dihydroquinazolin-4(1*H*)-one (80.4

[202] Gao, Y.; Yang, C.; Bai, S.; Liu, X.; Wu, Q.; Wang, J.; Jiang, C.; Qi, X. Visible-Light-Induced Nickel-Catalyzed Cross-Coupling with Alkylzirconocenes from Unactivated Alkenes. *Chem*. **2020**, *6*, 675–688.

mg, 0.30 mmol) were used, affording the title compound as a colourless liquid (22.5 mg, 59% yield), by using hexane/EtOAc (100:1) as chromatography eluent. In a second independent experiment, 19.0 mg (50%) were obtained, giving an average of 55% yield. **^{1}H NMR (400 MHz, $CDCl_3$)** δ 7.33 – 7.23 (m, 2H), 6.97 – 6.86 (m, 3H), 3.76 (d, *J* = 6.4 Hz, 2H), 1.93 – 1.84 (m, 2H), 1.84 – 1.67 (m, 4H), 1.38 – 1.15 (m, 3H), 1.12 – 1.00 (m, 2H) ppm. **^{13}C NMR (101 MHz, $CDCl_3$)** δ 159.5, 129.5, 120.5, 114.7, 73.6, 37.9, 30.1, 26.7, 26.0 ppm. Spectral data was in agreement with the literature.[203]

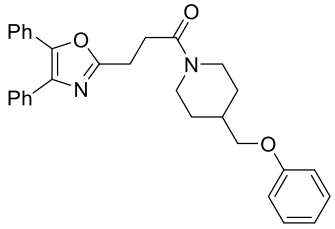

3-(4,5-Diphenyloxazol-2-yl)-1-(4-(phenoxymethyl)piperidin-1-yl)propan-1-one (7o). Following GP6 by running the reaction for 48 hours, 1-(4-bromopiperidin-1-yl)-3-(4,5-diphenyloxazol-2-yl)propan-1-one (**6m**) (87.9 mg, 0.20 mmol) and 2-methyl-2-(phenoxymethyl)-2,3-dihydroquinazolin-4(1*H*)-one (**2l**) (80.5 mg, 0.30 mmol) were used. The resulting crude material was purified by silica gel chromatography (0 to 10% Et_2O in DCM) and then a second time by silica gel chromatography (0 to 40% EtOAc in *n*-pentane), affording the title compound as a colourless oil (37.3 mg, 40%). In a second independent experiment, 46.8 mg (50%) of the title compound was obtained, giving an average of 45% yield. **IR (film, cm^{-1})** = 2921, 1643, 1599, 1497, 1445, 1244. **^{1}H NMR (500 MHz, $CDCl_3$)** δ 7.66 – 7.62 (m, 2 H), 7.59 – 7.55 (m, 2 H), 7.39 – 7.55 (m, 6 H), 7.30 – 7.26 (m, 2 H), 6.94 (tt, *J* = 7.4, 1.0 Hz, 1H), 6.87 (dd, *J* = 8.7, 1.1, 2H), 4.70 (d, *J* = 13.5 Hz, 1H), 4.01 (d, *J* = 13.5 Hz, 1H), 3.84 – 3.73 (m, 2H), 3.29 – 3.21 (m, 2H), 3.10 (td, *J* = 12.9, 2.3, 1H), 2.99 (q, *J* = 7.3, 2H), 2.65 (td, *J* = 12.9, 2.3, 1H), 2.11 – 2.00 (m, 1H), 1.94 (d, *J* = 12.9, 1H), 1.87 (d, *J* = 12.9, 1H), 1.38 – 1.23 (m, 2H) ppm. **^{13}C NMR (126 MHz, $CDCl_3$)** δ 169.4, 163.3, 159.0, 145.5, 134.7, 132.1, 129.6, 128.9, 128.8, 128.8, 128.7, 128.4, 128.2, 126.6, 120.9, 114.6, 72.0, 45.6, 42.0, 36.5, 30.2, 29.7, 28.8, 24.0 ppm. **HRMS** [ESI$^+$] *calcd*. for ($C_{30}H_{30}N_2NaO_3$) [M+Na]$^+$: 489.2149, *found* 489.2140.

2.7.4 Mechanistic Experiments

2.7.4.1 Experiments with a Well-Defined Nickel Complex

Synthesis of nickel toluene complex (Ni-I)

[203] Sugataa, H.; Tsubogoa, T.; Kinoa, Y.; Uchiro, H. Ullmann C–O Coupling of Sterically Hindered Secondary Alcohols Using Excess Amount of Strongly Coordinating Monodentate Ligands. *Tetrahedron Lett.* **2017**, *58*, 1015–1019.

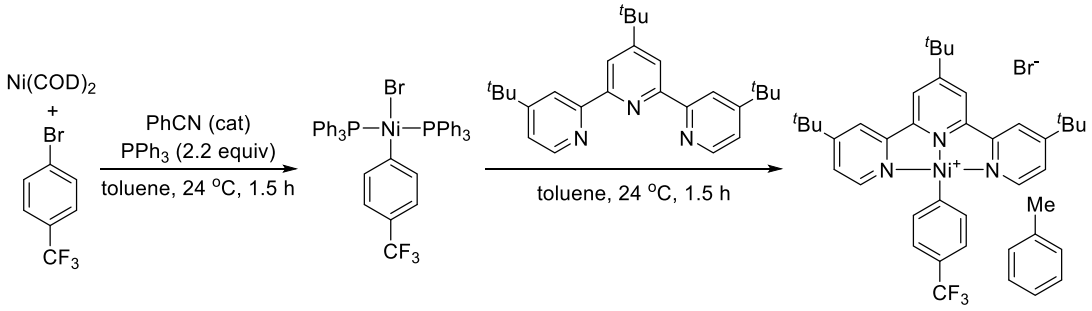

nickel toluene complex (Ni-I). A 27 mL glass vial equipped with a stirrer bar was taken into a nitrogen-filled glovebox, then charged with $Ni(COD)_2$ (128 mg, 0.5 mmol), triphenylphosphine (289 mg, 1.1 mmol) and toluene (3 mL, anhydrous). The reaction mixture was stirred for 1.5 hours at 24 °C, then 1-bromo-4-(trifluoromethyl)benzene (0.35 mL, 2.5 mmol) and benzonitrile (2 drops) were added. Reaction mixture was stirred for 5 minutes at 24 °C, after which the solution produces a thick yellow precipitate. Extra toluene (2 mL, anhydrous) was added, and the reaction mixture was stirred for 10 minutes at 24 °C. The reaction vessel was removed from the glovebox and charged with hexane (20 mL) forming more yellow precipitate. The yellow suspension was filtered yielding a yellow solid, which was sequentially washed with hexane (20 mL) and ice-cold methanol (2 x 4 mL) affording a yellow solid (231 mg) that was used in the next step without further purification. A 27 mL glass vial equipped with a stirrer bar was charged with the yellow solid (220 mg) obtained from the previous step, taken into a nitrogen-filled glovebox, and charged with 4,4′,4″-tri-*tert*-butyl-2,2′:6′,2″-terpyridine (120 mg, 0.30 mmol) and toluene (5 mL, anhydrous). The reaction mixture was stirred for 1.5 hours at 24 °C. The reaction vessel was removed from the glovebox and charged with hexane (20 mL) forming a yellow precipitate. The yellow suspension was filtered yielding a yellow solid, which was washed with hexane (20 mL) affording the desired complex (168 mg, 43%) as a yellow solid. Crystals for analysis by x-ray diffraction were prepared by layering diethyl ether upon a saturated solution of **Ni-I** in DCM. **IR (neat, cm^{-1})** = 2962, 1614, 1582, 1317, 1154, 1115, 1073. **^{1}H NMR (400 MHz, CD_3CN)** δ 8.28 (s, 2H), 8.25 (d, *J* = 2.0 Hz, 2H), 8.03 (d, *J* = 8.0 Hz, 2H), 7.47 (d, *J* = 8.0 Hz, 2H), 7.37 (dd, *J* = 6.1, 2.0 Hz, 2H), 7.28 (d, *J* = 6.1 Hz, 2H), 7.30 – 7.20 (m, 5H, toluene), 2.33 (s, 3H, toluene), 1.53 (s, 9H), 1.38 (s, 18H) ppm. **^{1}H NMR (500 MHz, DMSO-*d*$_6$)** δ 8.63 (br. s, 2H), 8.62 (br. s, 2H), 8.06 (br. d, *J* = 6.1 Hz, 2H), 7.59 (br. s, 2H), 7.46 (br. d, *J* = 8.0 Hz, 2H), 7.31 – 7.07 (m, 2H + toluene 5H), 2.30 (s, 3H, toluene), 1.52 (s, 9H), 1.35 (s, 18H) ppm. **^{13}C NMR (126 MHz, DMSO-*d*$_6$)** δ 166.3, 155.6, 153.3, 151.9, 137.8 (Tol), 137.0, 129.3 (Tol), 128.6 (Tol), 125.8 (Tol), 125.6, 125.5 (q, *J* = 271.4 Hz, CF_3), 125.4, 125.3, 125.1, 122.8, 122.8, 121.6, 37.3, 36.3, 30.8, 30.2, 21.5 (Tol) ppm. **^{19}F NMR (376 MHz, DMSO-*d*$_6$)** δ −60.4.

Catalytic competency of Ni-I

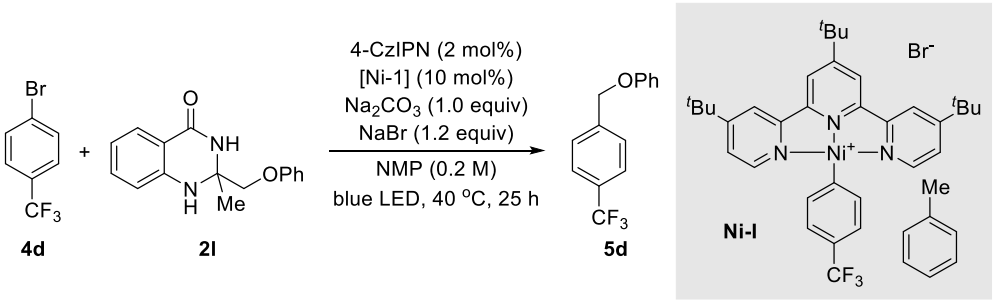

An oven-dried 8 mL screw-cap test tube containing a stirring bar was charged with sodium bromide (24.7 mg, 0.24 mmol), 4-CzIPN (3.2 mg, 2 mol%) and 2-methyl-2-(phenoxymethyl)-2,3-dihydroquinazolin-4(1*H*)-one (64.3 mg, 0.24 mmol). The reaction vessel was taken into a nitrogen-filled glove box, then sequentially charged with nickel complex (15.5 mg, 10 mol%), sodium carbonate (21.2 mg, 0.2 mmol), NMP (1 mL) and 1-bromo-4-(trifluoromethyl)benzene (28 mL, 45.0 mg, 0.2 mmol). The reaction mixture was stirred for 3 minutes, then the reaction vessel was sealed, removed from the glovebox and the screw cap was further sealed with parafilm. The reaction mixture was stirred while exposed to blue LED irradiation for 25 hours at 40 °C. The reaction was quenched with brine (5 mL) and extracted with EtOAc (5 x 3 mL). The combined organic extracts were dried ($MgSO_4$) and concentrated under reduced pressure. The received crude residue was analyzed by ^{19}F NMR using 1-fluoro-3-nitrobenzene (22.0 mL, 0.206 mmol) as an internal standard, showing had 1-(phenoxymethyl)-4-(trifluoromethyl)benzene formed (60%).

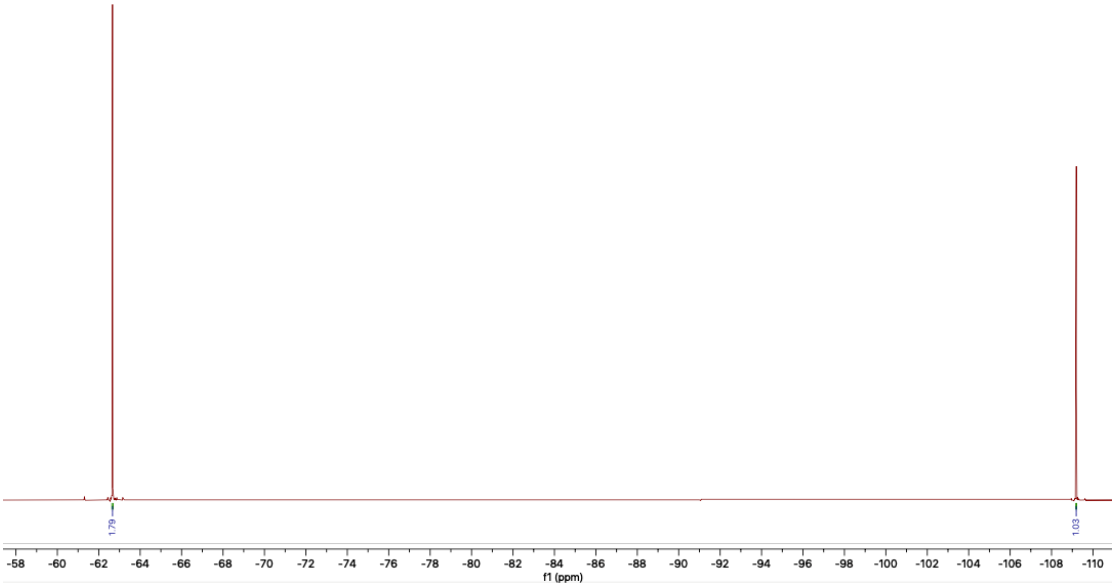

Stoichiometric experiments with Ni-I

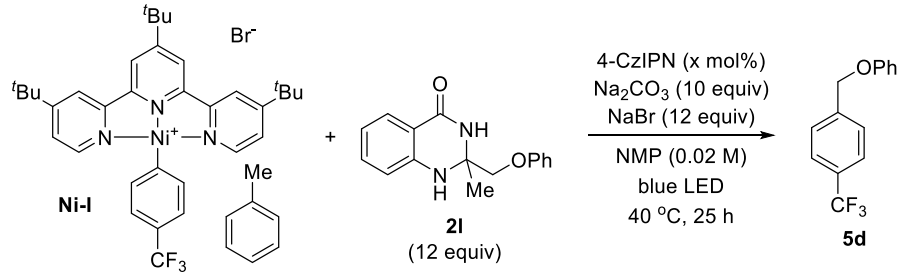

An oven-dried 8 mL screw-cap test tube containing a stirring bar was charged with sodium bromide (61.7 mg, 0.6 mmol). The reaction vessel was taken into a nitrogen-filled glove box, then sequentially charged with 4-CzIPN (8 mg, 20 mol%), nickel complex (38.8 mg, 0.05 mmol), sodium carbonate (53.0 mg, 0.5 mmol), 2-methyl-2-(phenoxymethyl)-2,3-dihydroquinazolin-4(1*H*)-one (161 mg, 0.6 mmol) and NMP (2.5 mL). The reaction mixture was stirred for 3 minutes, then the reaction vessel was sealed, removed from the glovebox and the screw cap was further sealed with parafilm. The reaction mixture was stirred while exposed to blue LED irradiation for 25 hours at 40 °C. The reaction was quenched with brine (5 mL) and extracted with EtOAc (5 x 3 mL). The combined organic extracts were dried ($MgSO_4$) and concentrated under reduced pressure. The received crude residue was analyzed by ^{19}F NMR using 1-fluoro-3-nitrobenzene (6.0 mL, 0.056 mmol) as an internal standard, showing had 1-(phenoxymethyl)-4-(trifluoromethyl)benzene formed (24%).

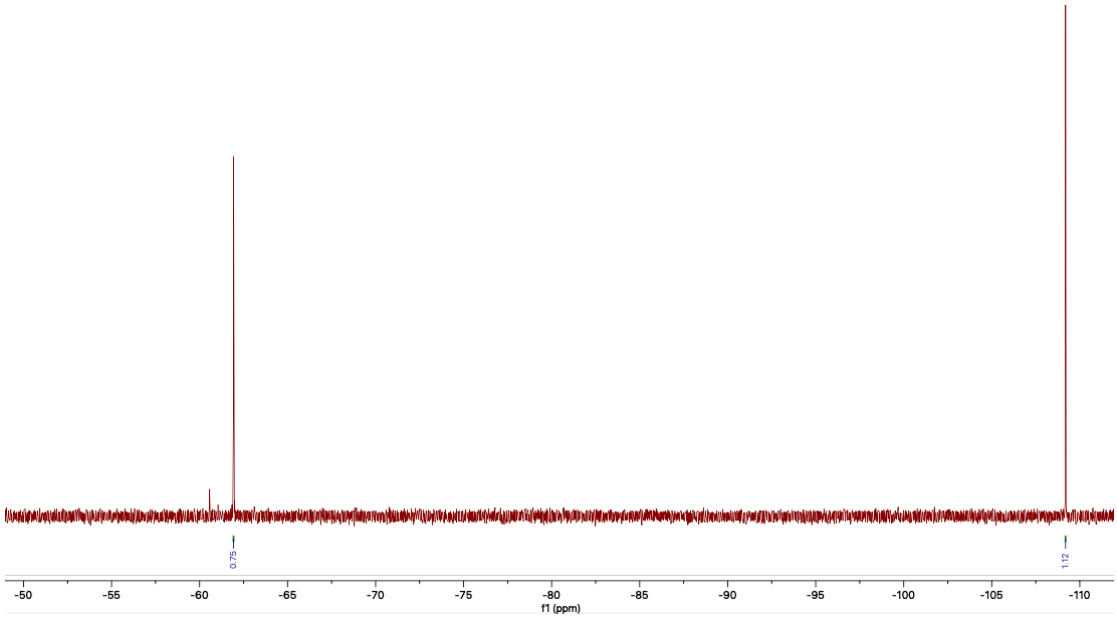

The reaction was repeated in the absence of 4-CzIPN, the resulting crude was analyzed by ^{19}F NMR using 1-fluoro-3-nitrobenzene (6.0 mL, 0.056 mmol) as an internal standard, showing had 1-(phenoxymethyl)-4-(trifluoromethyl)benzene formed (2%).

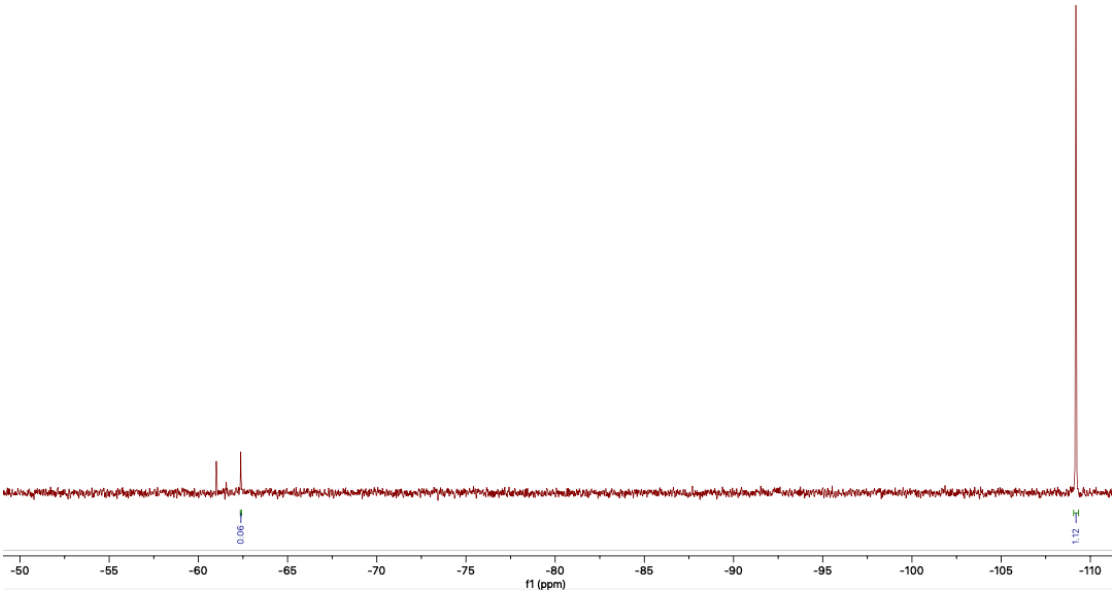

2.7.4.2 UV-Vis. Spectroscopy

Samples for UV-Vis. analysis were prepared in a 4 mL quartz cuvette (path length: l = 1.0 cm) equipped with a rubber septum screwcap under an atmosphere of nitrogen. A 4.4 x 10^{-5} M solution of nickel complex **Ni-I** and a 7.0 x 10^{-6} M solution of 4-CzIPN were prepared in a nitrogen-filled glovebox from dry and degassed NMP.

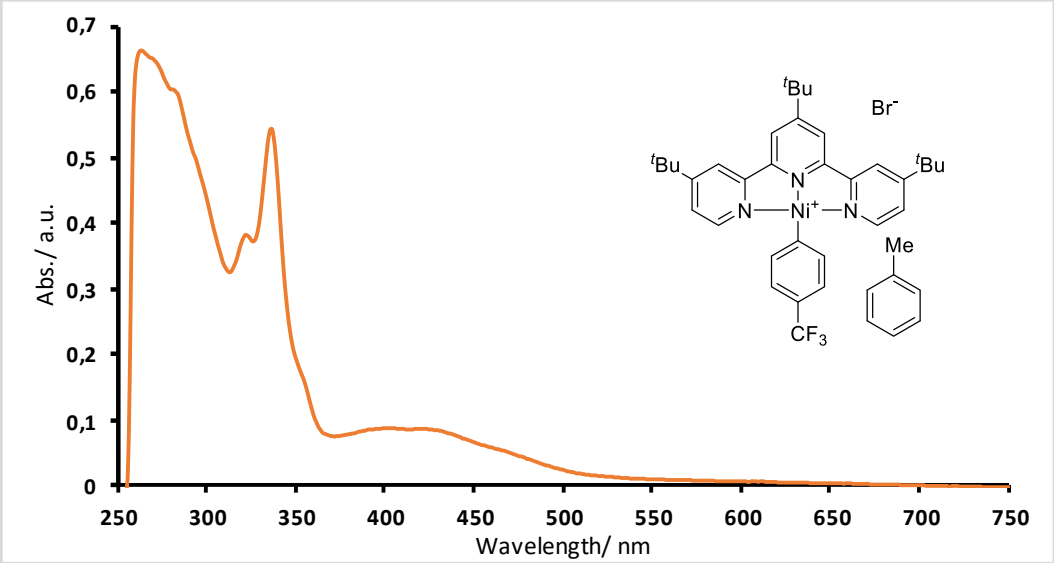

Figure S2.2 UV-Vis. spectrum of a 4.4 x 10^{-5} M solution of **Ni-I** in NMP.

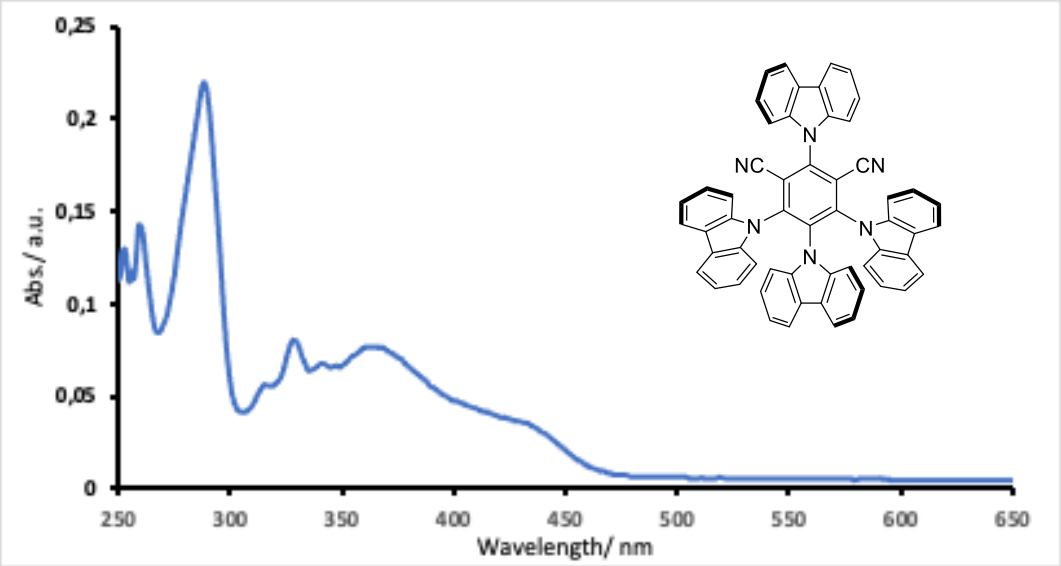

Figure S2.3 UV-Vis. spectrum of a 7.0 x 10^{-6} M solution of 4-CzIPN in NMP.

2.7.4.3 Fluorescence Quenching Studies

A 7.0 x 10^{-6} M solution of 4-CzIPN in anhydrous and degassed NMP was prepared in a nitrogen filled glovebox. 4-CzIPN solution (2.0 mL) was transferred to a 4 mL quartz cuvette (path length: l = 1.0 cm) under an atmosphere of nitrogen, where upon irradiation at 450 nm an emission at maximum at 530 nm was observed. Separate solutions of quenchers 2-methyl-2-(tetrahydro-2*H*-pyran-4-yl)-2,3-dihydroquinazolin-4(1*H*)-one (**2e**, 160 mM) and **Ni-I** (2.9 mM) were prepared from anhydrous and degassed NMP in a nitrogen filled glovebox. Distilled and degassed 1-bromo-4-(trifluoromethyl)benzene (**4d**) was used neat. Aliquots of the quencher solutions were added to the solution of 4-CzIPN contained in a quartz cuvette (path length: l = 1.0 cm) under an atmosphere of nitrogen, followed by recording of the emission spectra (Figure S2.4 and Figure S2.6).

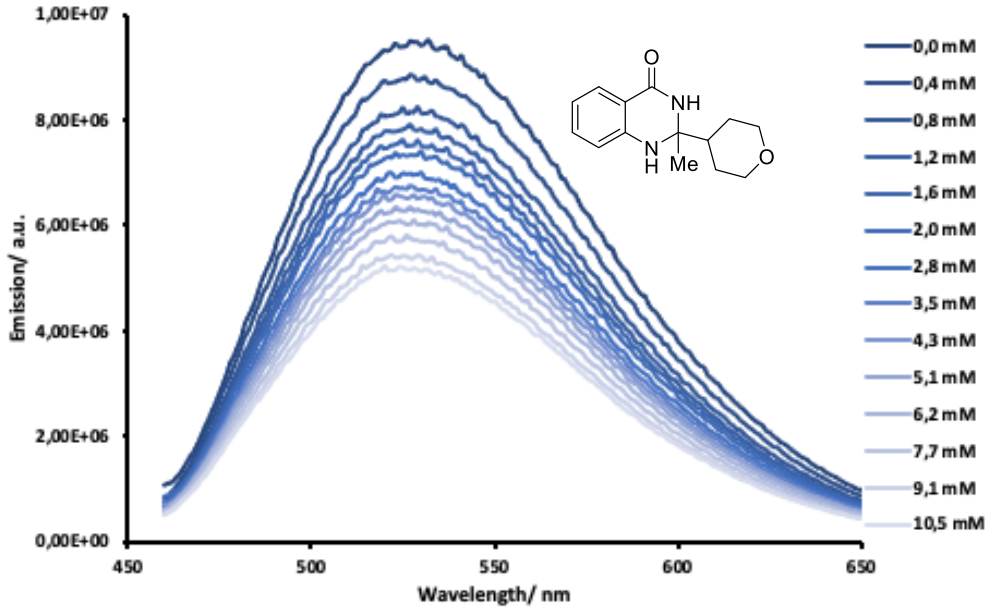

Figure S2.4 Emission spectra of a 7.0 x 10^{-6} M solution of 4-CzIPN in NMP containing varying amounts of 2-methyl-2-(tetrahydro-2*H*-pyran-4-yl)-2,3-dihydroquinazolin-4(1*H*)-one (**2e**) quencher.

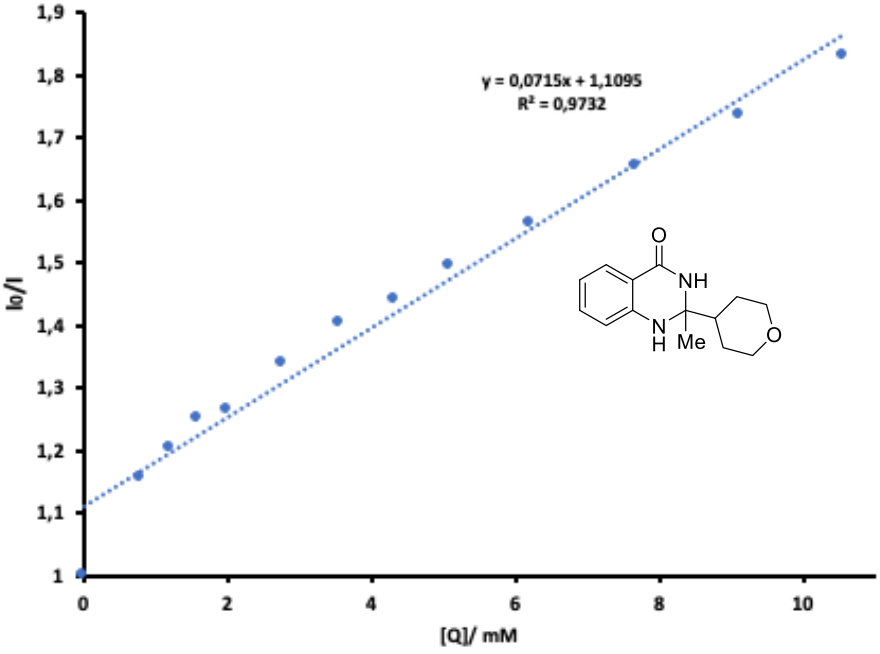

Figure S2.5 Emission intensities observed at 530 nm plotted against 2-methyl-2-(tetrahydro-2*H*-pyran-4-yl)-2,3-dihydroquinazolin-4(1*H*)-one (**2e**) concentration.

By using the gradient of Figure S2.5, the excited-state lifetime of 4-CzIPN (2.15 μs)[141] and the Stern-Volmer equation (Equation 2.1), the fluorescence quenching rate constant was calculated to be 3.32 x 10^{7} $M^{-1}.s^{-1}$.

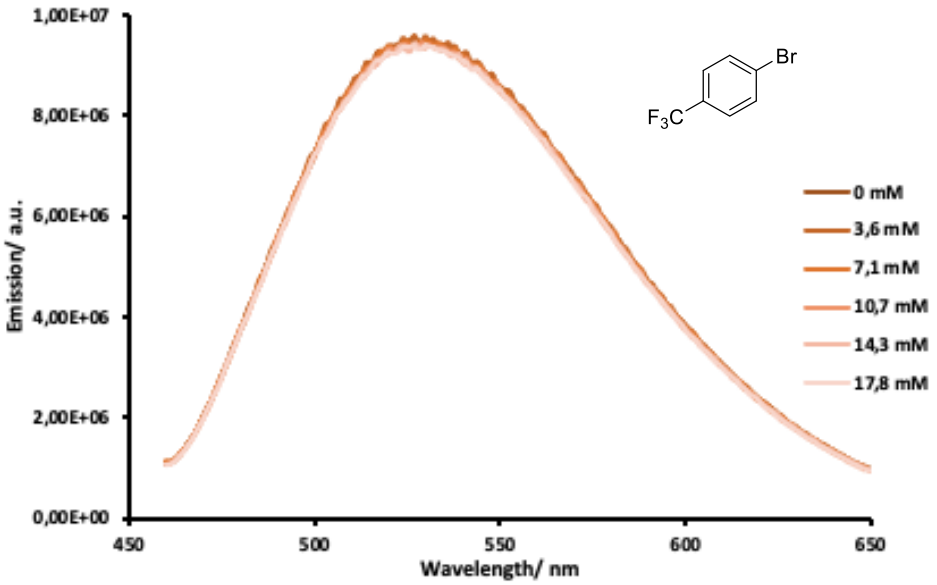

Figure S2.6 Emission spectra of a 7.0 x 10^{-6} M solution of 4-CzIPN in NMP containing varying amounts of 1-bromo-4-(trifluoromethyl)benzene (**4d**) quencher.

No fluorescence quenching of 4-CzIPN was observed in the presence of 1-bromo-4-(trifluoromethyl)benzene.

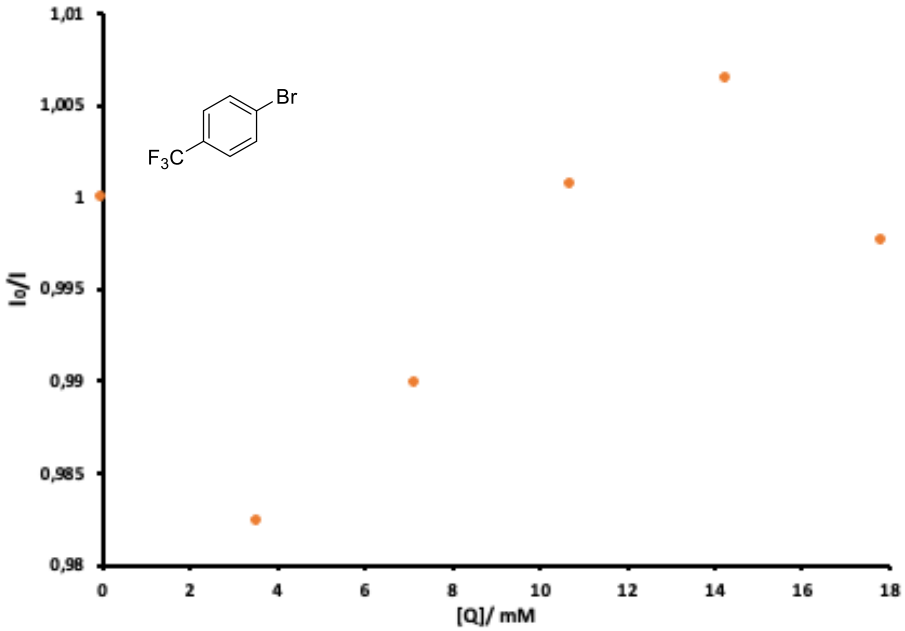

Figure S2.7 Emission intensities observed at 530 nm plotted against 1-bromo-4-(trifluoromethyl)benzene (**4d**) concentration.

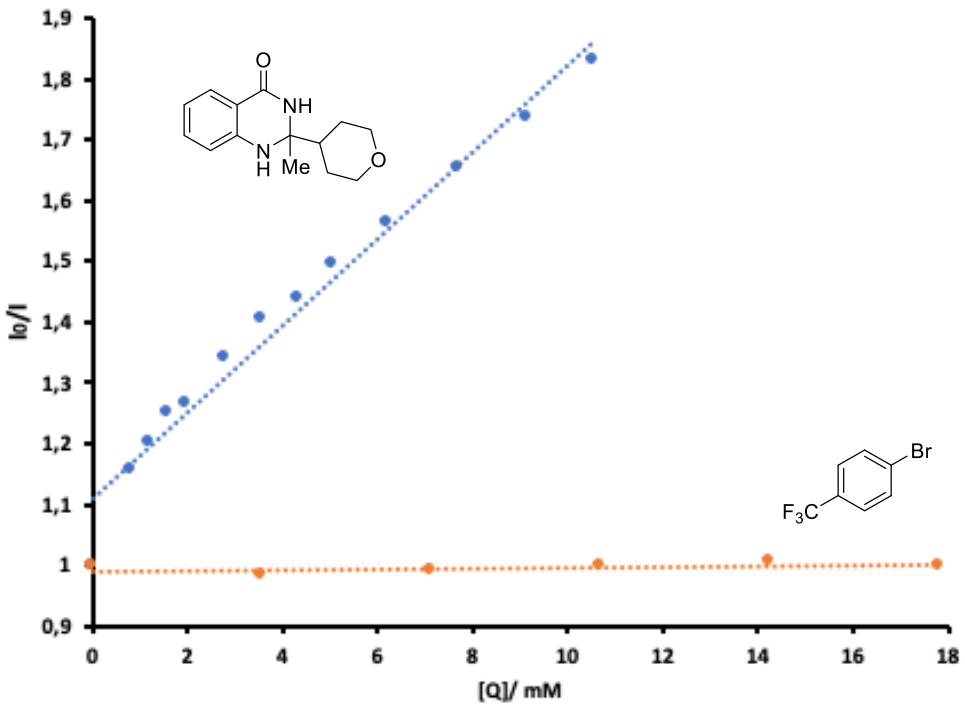

Figure S2.8 Overlay of Figure S2.5 and Figure S2.7.

4-CzIPN fluorescence decay was also observed when a 3.0 mM solution of **Ni-I** in NMP was titrated into a 7.0 x 10^{-6} M solution of 4-CzIPN in NMP (Figure S2.9 and Figure S2.10). However, due to **Ni-**I absorbing light at 450 nm and containing a redox active anion, the degree or if any 4-CzIPN fluorescence quenching is occurring by transfer of photonic energy to the nickel complex cannot be deduced.

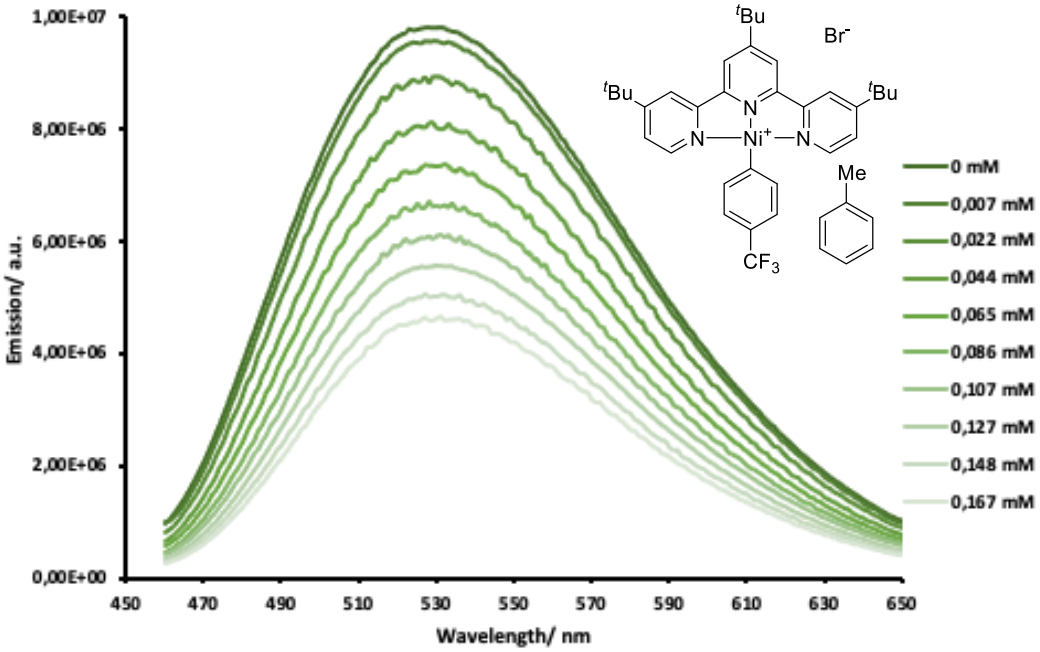

Figure S2.9 Emission intensities observed at 530 nm plotted against **Ni-I**

concentration.

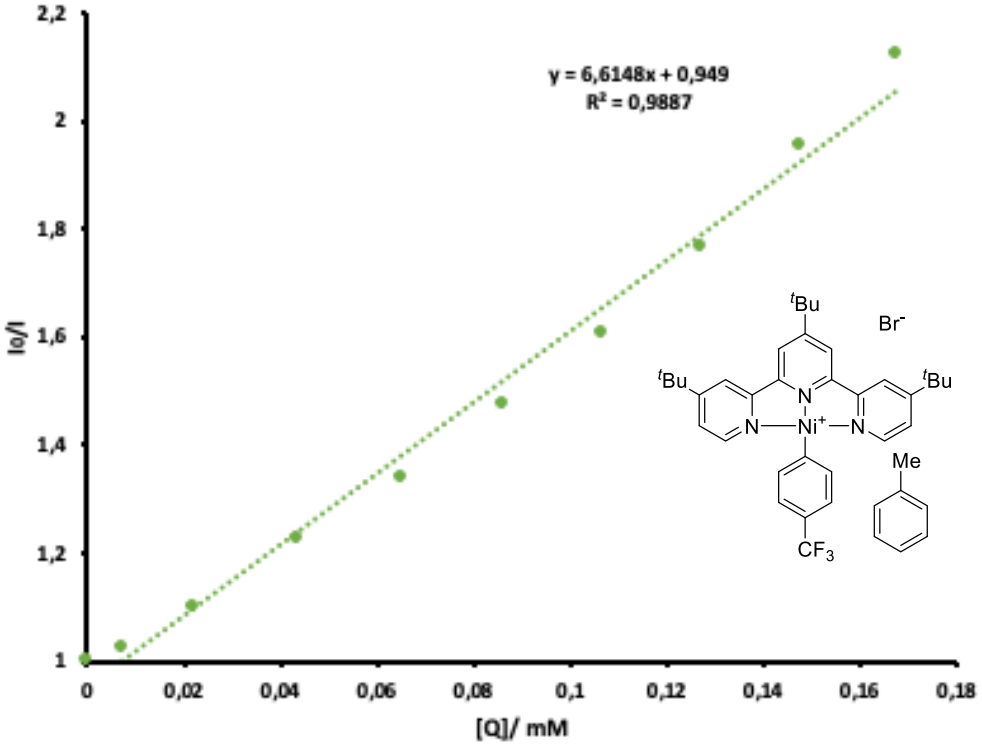

Figure S2.10 Emission intensities observed at 530 nm plotted against **Ni-I** concentration.

2.7.4.4 Cyclic Voltammetry Analysis

Cyclic voltammetry was performed on a CH Instruments Electrochemical Analyzer. Analyte (25 mmol) was added to a 0.1 M solution of tetra-*n*-butylammonium hexafluorophosphate in dry, degassed NMP (5 mL). A glassy carbon working electrode, a platinum flag counter electrode and a silver wire reference electrode were used. Three cycles at a scan rate of 100 or 500 mV/s were applied.

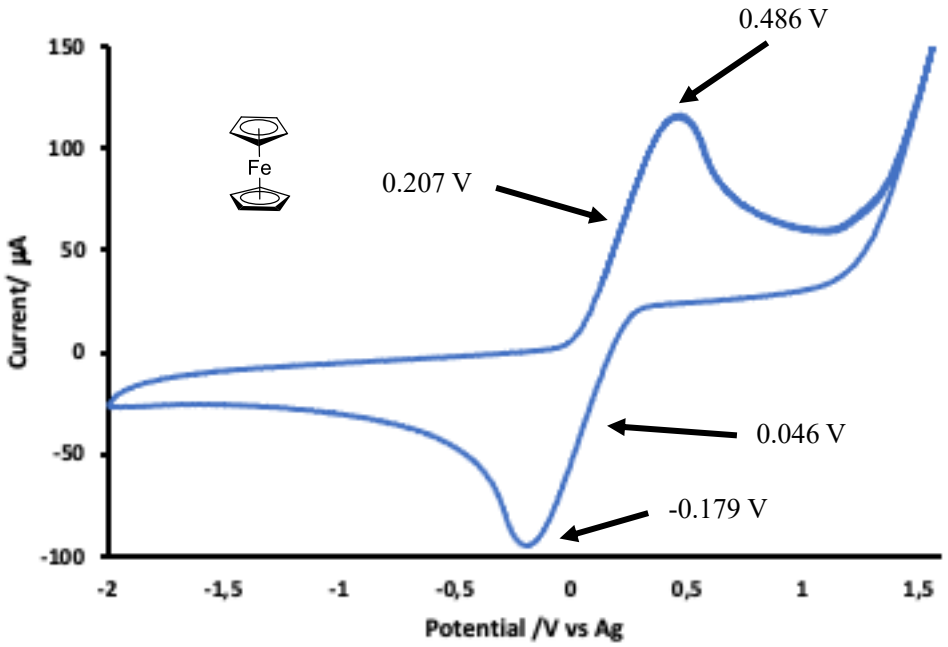

Figure S2.11 Cyclic voltamogram of ferrocene (4.7 mg, 25 mmol) at a scan rate of 500 mV/s.

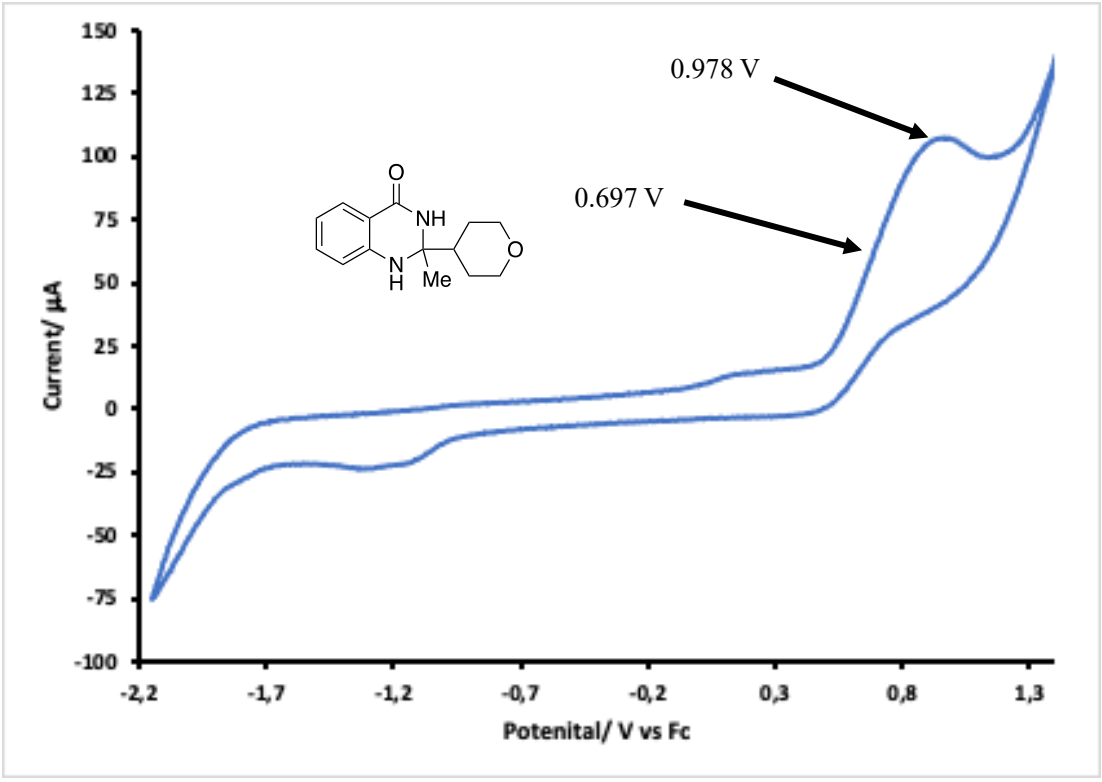

Figure S2.12 Cyclic voltamogram of 2-methyl-2-(tetrahydro-2*H*-pyran-4-yl)-2,3-dihydroquinazolin-4(1*H*)-one (**2e**) (6.2 mg, 25 mmol) at a scan rate of 500 mV/s.

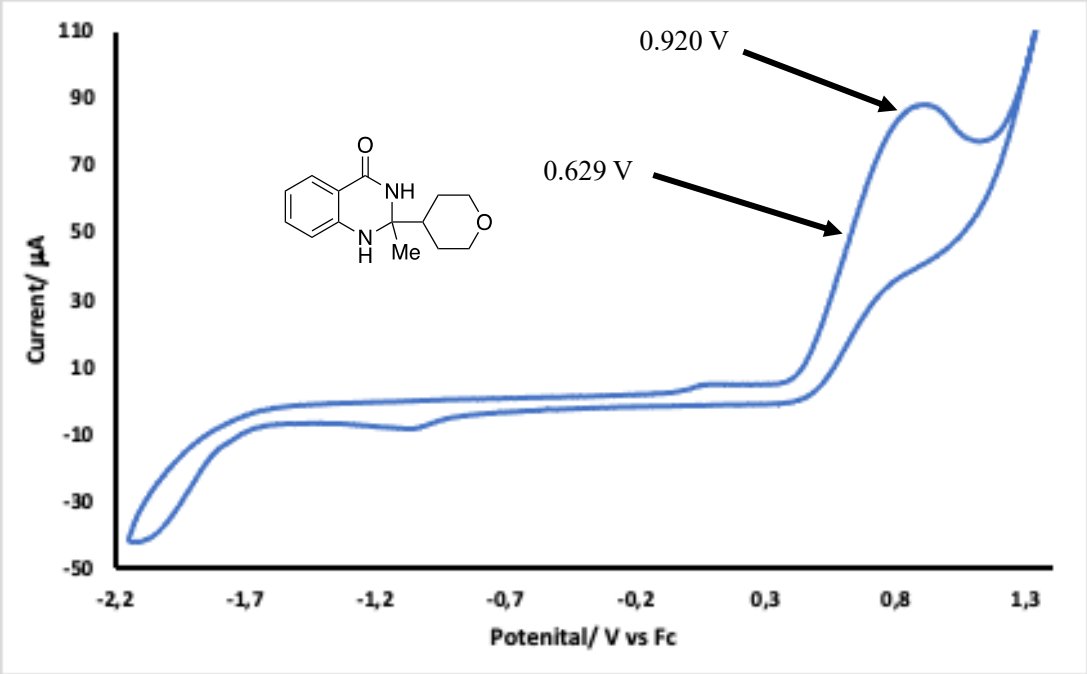

Figure S2.13 Cyclic voltamogram of 2-methyl-2-(tetrahydro-2*H*-pyran-4-yl)-2,3-dihydroquinazolin-4(1*H*)-one (**2e**) (6.2 mg, 25 mmol) at a scan rate of 100 mV/s.

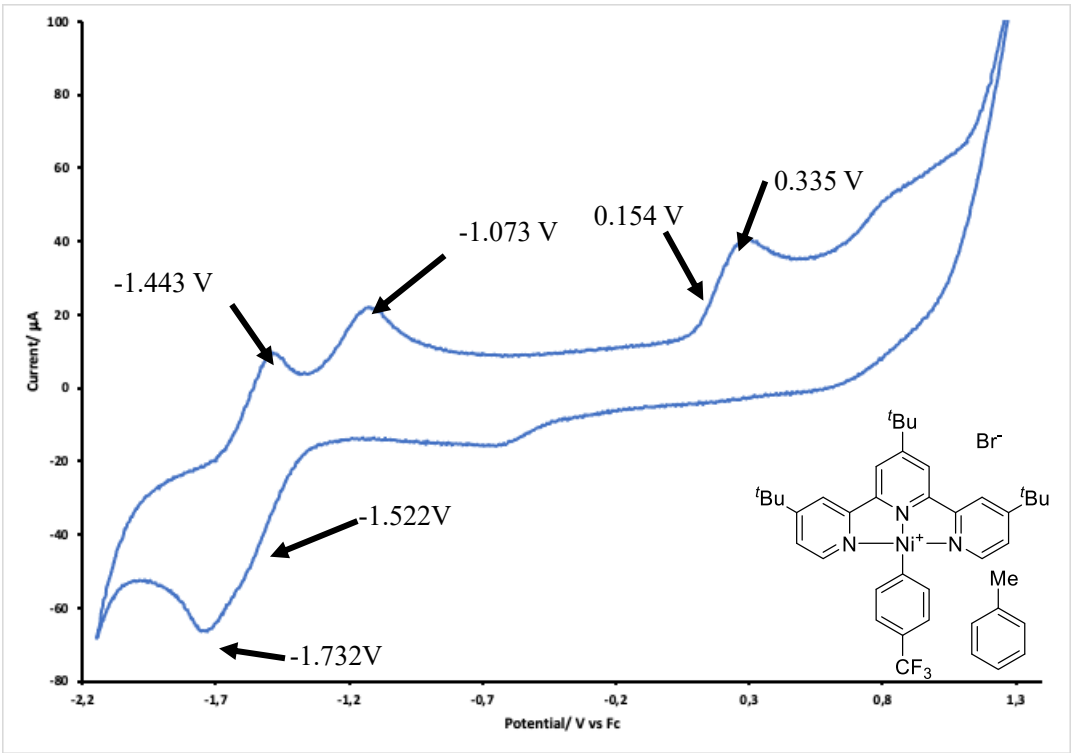

Figure S2.14 Cyclic voltamogram of **Ni-I** (19.4 mg, 25 mmol) at a scan rate of 500 mV/s.

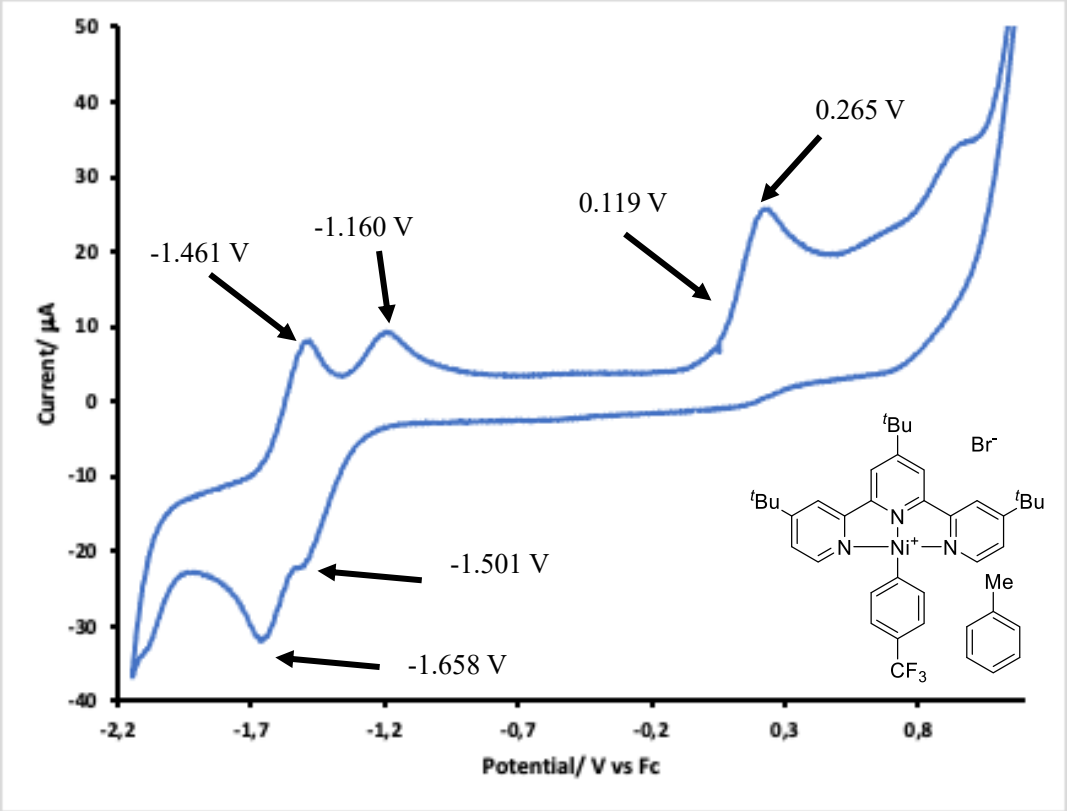

Figure S2.15 Cyclic voltamogram of **Ni-I** (19.4 mg, 25 mmol) at a scan rate of 100 mV/s.

Oxidation peaks observed in the CVs of **Ni-I** (Figure S2.14 and Figure S2.15) are likely due to oxidation of the bromide counter ion of the complex (Figure S2.16 and Figure S2.17).

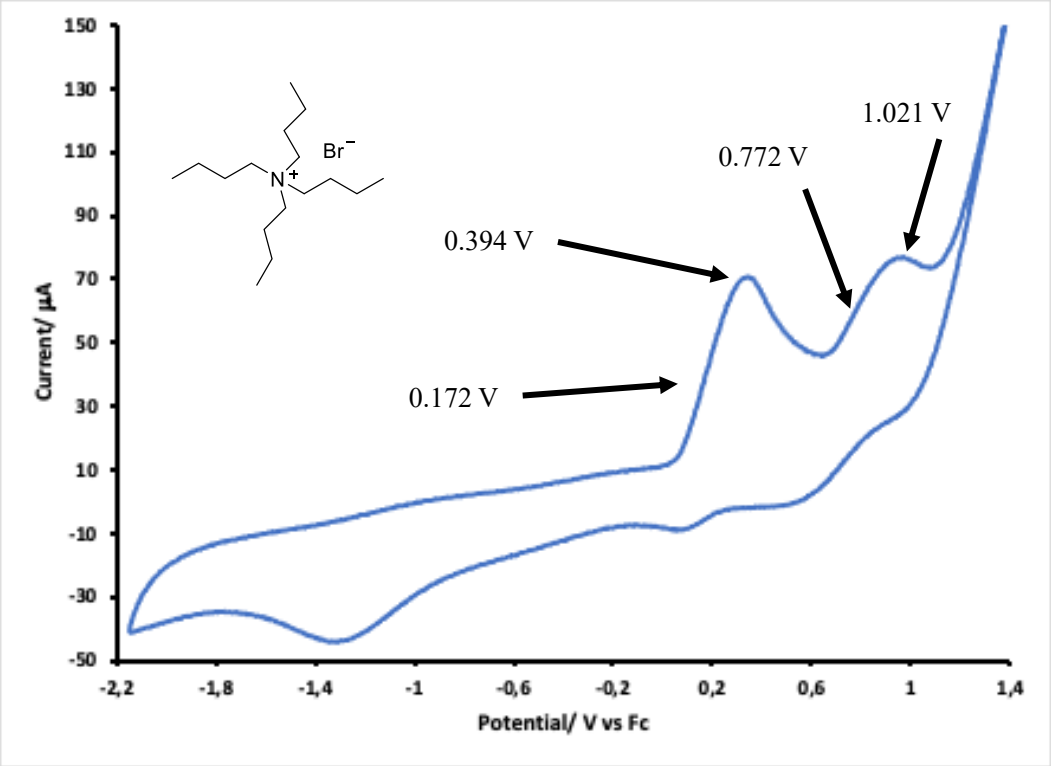

Figure S2.16 Cyclic voltamogram of tetramethylammonium bromide (8.1 mg, 25 mmol) at a scan rate of 500 mV/s.

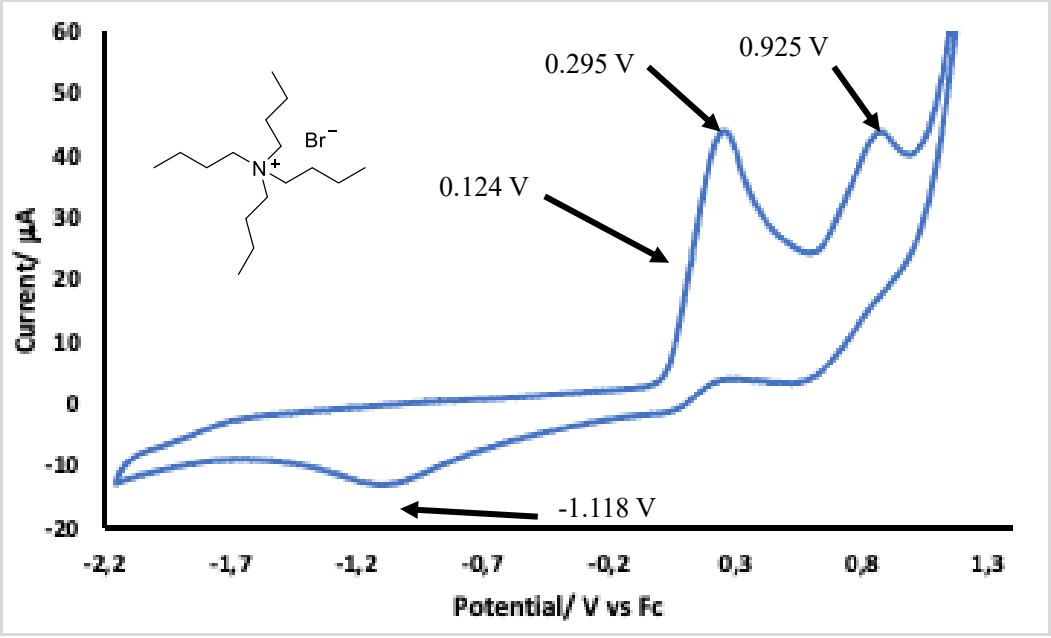

Figure S2.17 Cyclic voltamogram of tetramethylammonium bromide (8.1 mg, 25 mmol) at a scan rate of 100 mV/s.

2.7.4.5 Radical Clock Experiments

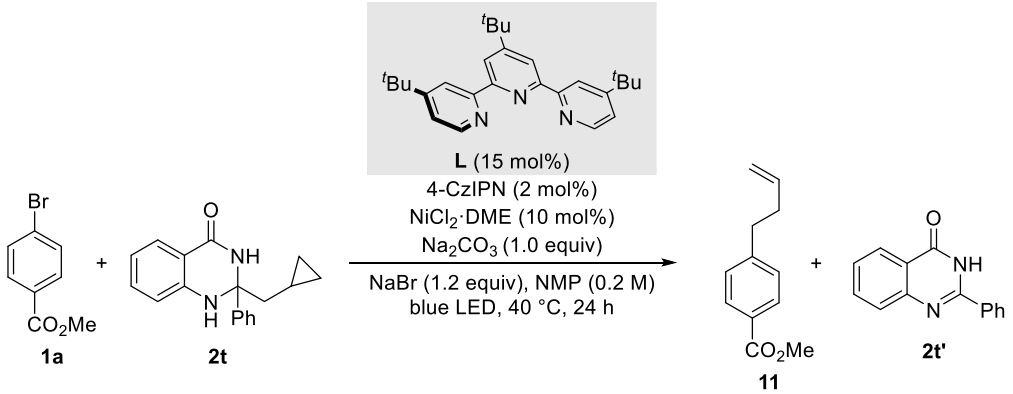

An oven-dried 8 mL screw-cap test tube was charged with a stirring bar, 4-CzIPN (3.2 mg, 2 mol%), $NiCl_2$·DME (4.4 mg, 10 mol%), 4,4',4"-tri-tert-butyl-2,2':6'2"-terpyridine (12.1 mg, 15 mol%), NaBr (24.7 mg, 1.2 equiv), methyl 4-bromobenzoate (43.0 mg, 0.2 mmol) and 2-(cyclopropylmethyl)-2-phenyl-2,3-dihydroquinazolin-4(1*H*)-one (66.7 mg, 1.2 equiv). The test tube was taken into a nitrogen-filled glovebox where Na_2CO_3 (21.2 mg, 1.0 equiv) was added to the reaction vessel. The reaction vessel was sealed with a screw cap and removed from the glovebox. Afterwards, NMP (1.0 mL, 0.2 M) was added by syringe. Parafilm was used to ensure the tightness of the reaction system. The reaction mixture was stirred at rt for 1 min. before exposure to blue LED irradiation at 40 °C for 24 hours. The reaction mixture was quenched with brine (10 mL) and extracted with ethyl acetate (3 x 5 mL). The combined organic extracts were dried (Na_2SO_4) and concentrated under reduced pressure yielding crude material, which was purified by silica gel chromatography (0 to 25% EtOAc in hexane), affording **11** as a colourless liquid (31.3 mg, 91%) and **2t'** as a white solid (47.1 mg, 88%).

Methyl 4-(but-3-en-1-yl)benzoate (11). ^{1}H NMR (400 MHz, $CDCl_3$) δ 7.99 – 7.93 (m, 2H), 7.26 (d, *J* = 8.3 Hz, 2H), 5.84 (ddt, *J* = 16.9, 10.2, 6.6 Hz, 1H), 5.08 – 4.96 (m, 2H), 3.91 (s, 3H), 2.81 – 2.73 (m, 2H), 2.44 – 2.35 (m, 2H) ppm. **^{13}C NMR (101 MHz, $CDCl_3$)** δ 167.3, 147.5, 137.6, 129.8, 128.6, 128.0, 115.5, 52.1, 35.5, 35.2 ppm. Spectral data was in agreement with the literature.[186]

2-Phenylquinazolin-4(3*H*)-one (2t'). M.p.: 233 °C. **^{1}H NMR (400 MHz, DMSO-d_6)** δ 8.22 – 8.09 (m, 3H), 7.84 – 7.75 (m, 1H), 7.74 – 7.68 (m, 1H), 7.59 – 7.44 (m, 4H) ppm. **^{13}C NMR (101 MHz, DMSO)** δ 162.3, 152.3, 148.7, 134.6, 132.7, 131.4, 128.6, 127.8, 127.5, 126.5, 125.9, 121.0 ppm. Spectral data was in agreement with the literature.[204]

[204] Das, S.; Mondal, R.; Chakraborty, G.; Guin, A. K.; Das, A.; Paul, N. D. Zinc Stabilized Azo-anion Radical in Dehydrogenative Synthesis of N-Heterocycles. An Exclusively Ligand Centered Redox Controlled Approach. *ACS Catal*. **2021**, *11*, 7498–7512.

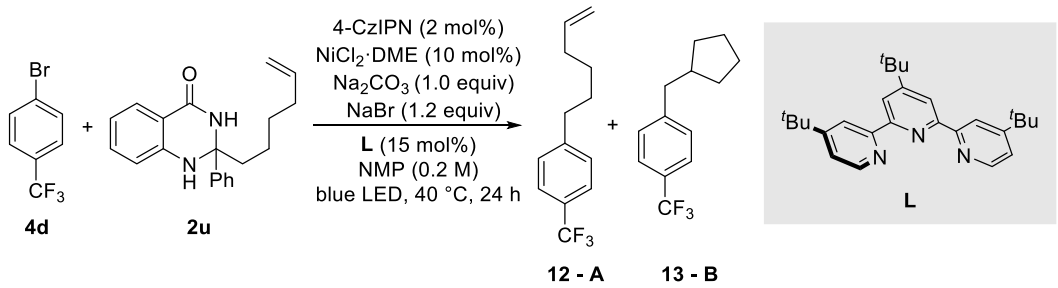

An oven-dried 8 mL screw-cap test tube was charged with a stirring bar, 4-CzIPN (1.6 mg, 2 mol%), $NiCl_2$·DME (2.2 mg, 10 mol%), 4,4',4''-tri-tert-butyl-2,2':6'2''-terpyridine (6.0 mg, 15 mol%), NaBr (12.4 mg, 1.2 equiv), 1-bromo-4-(trifluoromethyl)benzene (22.5 mg, 0.10 mmol), and 2-(hex-5-en-1-yl)-2-phenyl-2,3-dihydroquinazolin-4(1*H*)-one (36.7 mg, 0.12 mmol). The test tube was taken into a nitrogen-filled glovebox where Na_2CO_3 (10.6 mg, 1.0 equiv) was added to the reaction vessel. The reaction vessel was sealed with a screw cap and removed from the glovebox. Afterwards, NMP (0.5 mL, 0.2 M) was added by syringe. Parafilm was used to ensure the tightness of the reaction system. The reaction mixture was stirred at rt for 1 min. before exposure to blue LED irradiation at 40 °C for 24 hours. The reaction mixture was quenched with brine (10 mL) and extracted with ethyl acetate (3 x 5 mL). The combined organic extracts were dried (Na_2SO_4) and concentrated under reduced pressure yielding crude material, which was purified by silica gel chromatography (0 to 1% EtOAc in hexane), affording **12** and **13** as a colourless liquid (13.2 mg, 58%, 0.62:0.38 **12**:**13** ratio).

IR (film, cm^{-1}): 2930, 2855, 1622, 1324, 1166, 1118, 1066. **^{1}H NMR (500 MHz, $CDCl_3$)** δ 7.55 (d, *J* = 8.1 Hz, 0.8H A), 7.54 (d, *J* = 8.1 Hz, 1.2H B), 7.32 – 7.29 (m, 0.8H A + 1.2H B), 5.82 (ddt, *J* = 16.9, 10.2, 6.7 Hz, 0.4H A), 5.03 (dq, *J* = 17.1, 1.7 Hz, 0.4H A), 4.98 (ddt, *J* = 10.2, 2.2, 1.2 Hz, 0.4H A), 2.70 (t, *J* = 7.4 Hz, 0.8H A), 2.69 (d, *J* = 7.5 Hz, 1.2H B), 2.16 – 2.07 (m, 0.8H A + 0.6H B), 1.77 – 1.71 (m, 1.2H B), 1.70 – 1.64 (m, 0.8H A + 1.2H B), 1.58 – 1.54 (m, 1.2H, B), 1.46 (quint., *J* = 7.5 Hz, 0.8H A), 1.24 – 1.17 (m, 1.2H, B). **^{13}C NMR (126 MHz, $CDCl_3$)** δ 146.8 (C_{quat} A), 146.5 (C_{quat} B), 138.6 (*C*H A), 129.0 (2 x Ar*C*H B), 128.7 (2 x Ar*C*H A), 128.0 (C_{quat} A + B , q, J_{CF} = 32.2 Hz), 125.2 (2 x Ar*C*H A, q, J_{CF} = 3.7 Hz), 125.1 (2 x Ar*C*H B, q, J_{CF} = 3.7 Hz), 124.4 (*C*F_3 A + B, q, J_{CF} = 271.8 Hz), 114.6 (*C*H_2 A), 41.9 (*C*H_2 B), 41.8 (*C*H B), 35.6 (*C*H_2 A), 33.5 (*C*H_2 A), 32.4 (2 x CH_2 B), 30.6 (CH_2 A), 28.4 (CH_2 A), 24.9 (2 x CH_2 B). **^{19}F NMR (471 MHz, DMSO-*d*$_6$)** δ -62.43 (B), -62.40 (A). **HRMS** [APCI$^+$] *calcd*. for ($C_{13}H_{15}F_2$) [M-F]$^+$: 209.1136, *found*: 209.1148.

2.7.4.6 Radical Cyclization as a Function of Catalyst Loading

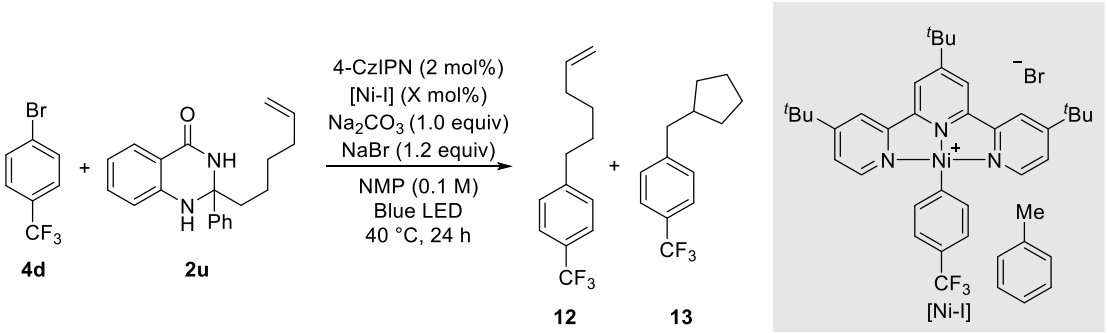

An oven-dried 8 mL screw-cap test tube containing a stirring bar was charged with sodium bromide (12 mg, 0.12 mmol), 4-CzIPN (1.6 mg, 2 mol%) and 2-(hex-5-en-1-yl)-2-phenyl-2,3-dihydroquinazolin-4(1*H*)-one (37 mg, 0.12 mmol). The reaction vessel was taken into a nitrogen-filled glove box, then sequentially charged with nickel complex **Ni-I**, sodium carbonate (11 mg, 0.1 mmol), NMP (1.0 mL) and 1-bromo-4-(trifluoromethyl)benzene (14 mL, 23 mg, 0.1 mmol). The reaction mixture was stirred for 3 minutes, then the reaction vessel was sealed, removed from the glovebox and the screw cap was further sealed with parafilm. The reaction mixture was stirred while exposed to blue LED irradiation for 25 hours at 40 °C. The reaction was quenched with brine (5 mL) and extracted with EtOAc (5 x 3 mL). The combined organic extracts were dried ($MgSO_4$) and concentrated under reduced pressure. The received crude residue was purified by silica gel chromatography using hexane/EtOAc (100:1), giving a mixture of **12** and **13** (50-60%) as a colourless oil. ^{19}F NMR was used to evaluate the ratio of **13** (-62.43 ppm) against **12** (−62.40 ppm).

15 mol% **Ni-I**

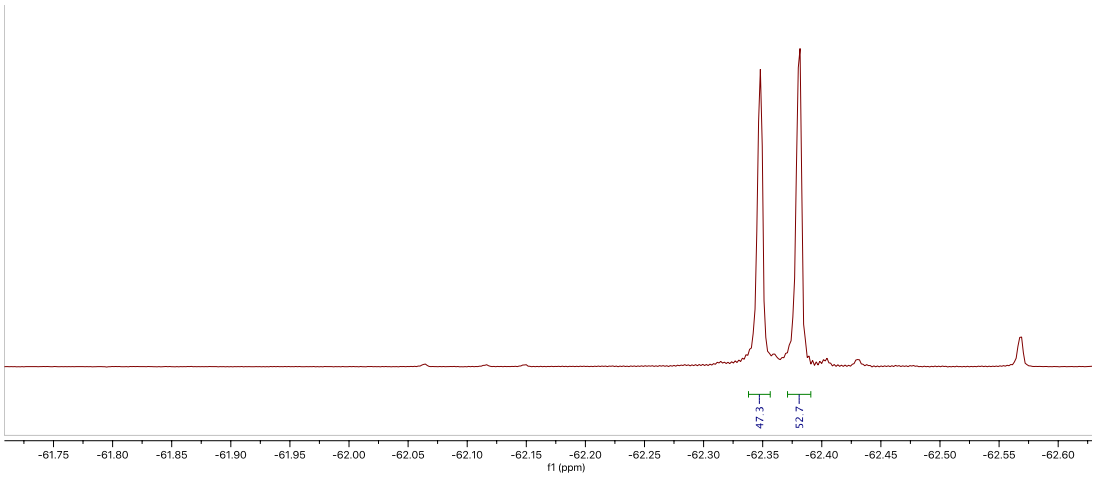

12.5 mol% **Ni-I**

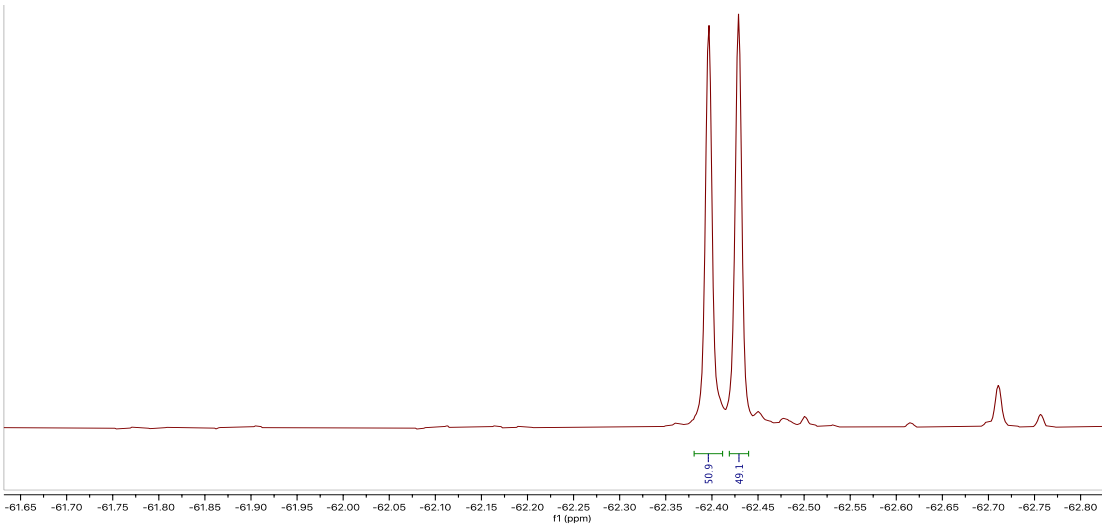

10 mol% **Ni-I**

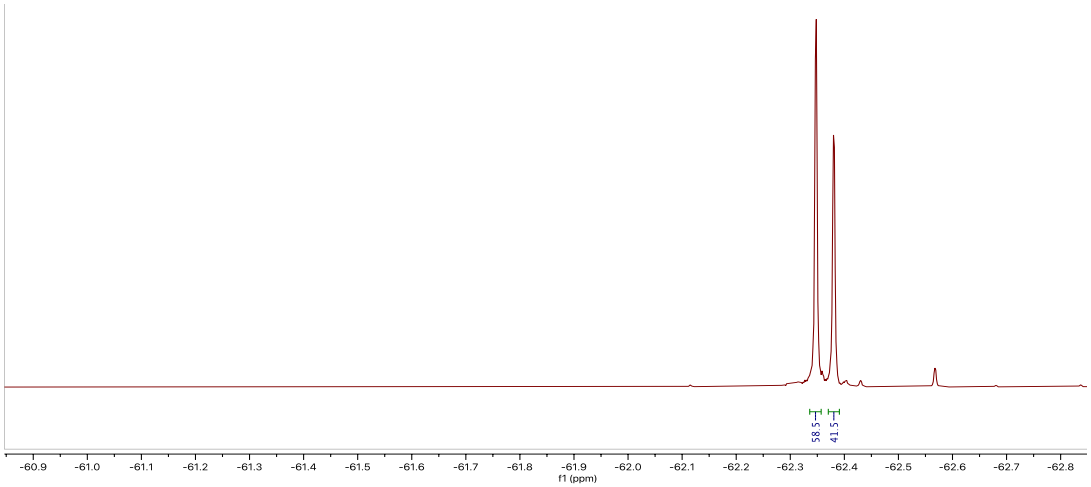

7.5 mol% **Ni-I**

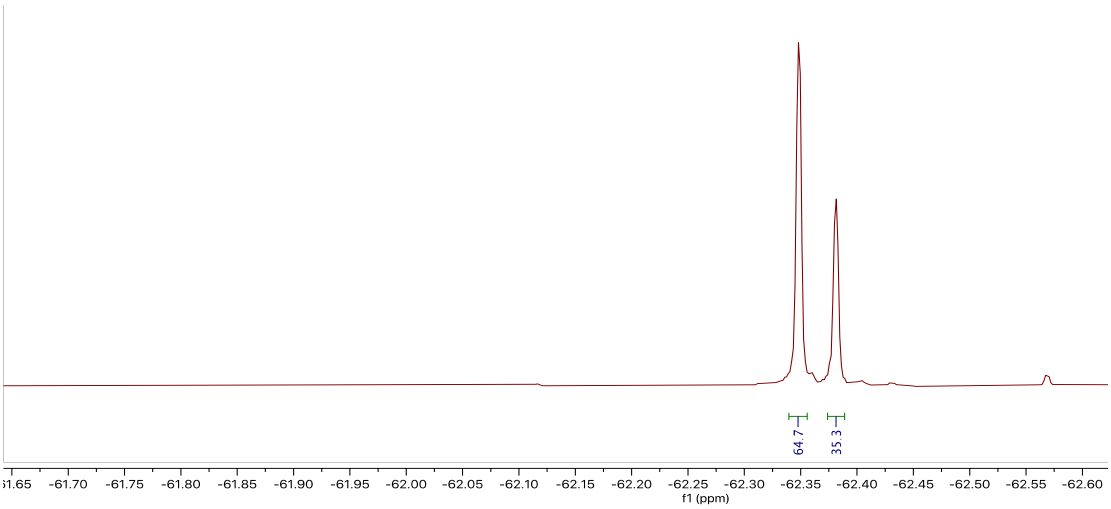

5 mol% **Ni-I**

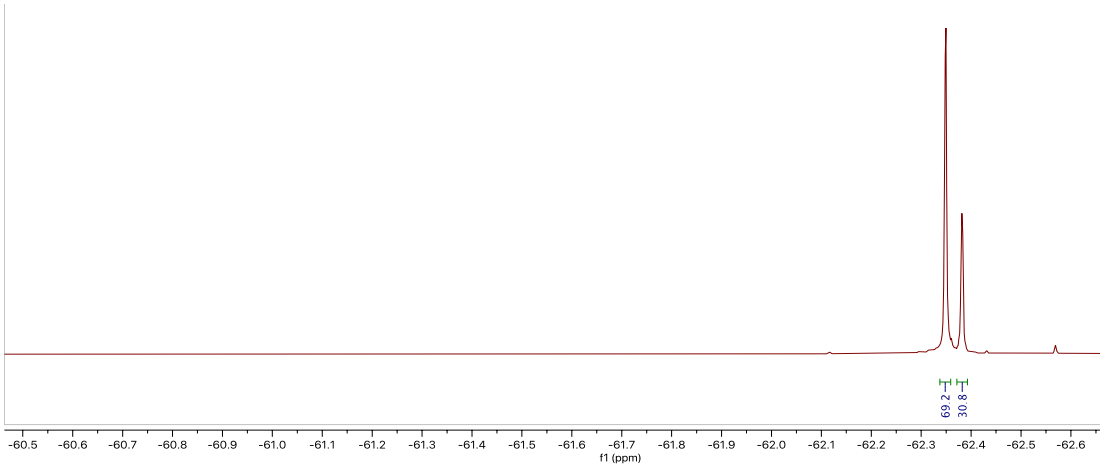

Ni-I mol%	**12** selectivity/%	**13** selectivity/%
15	52.7	47.3
12.5	50.9	49.1
10	41.5	58.5
7.5	35.3	64.7
5	30.8	69.2

Table S2.1 Tabulated ratios of cross-coupling products **12** and **13** at different **Ni-I** catalyst loadings.

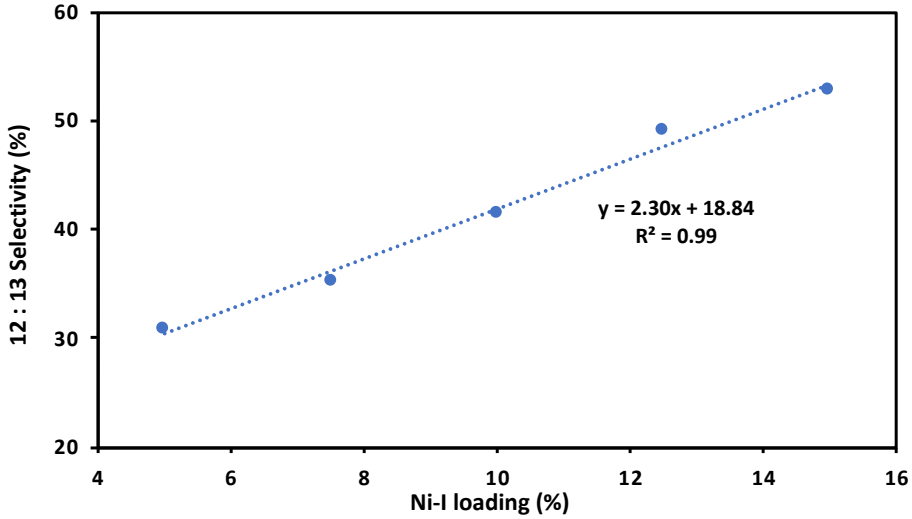

Figure S2.18 Plot ratios of cross-coupling products **12** and **13** at different **Ni-I** catalyst loadings.

2.7.4.7 TEMPO Radical Probe Experiments

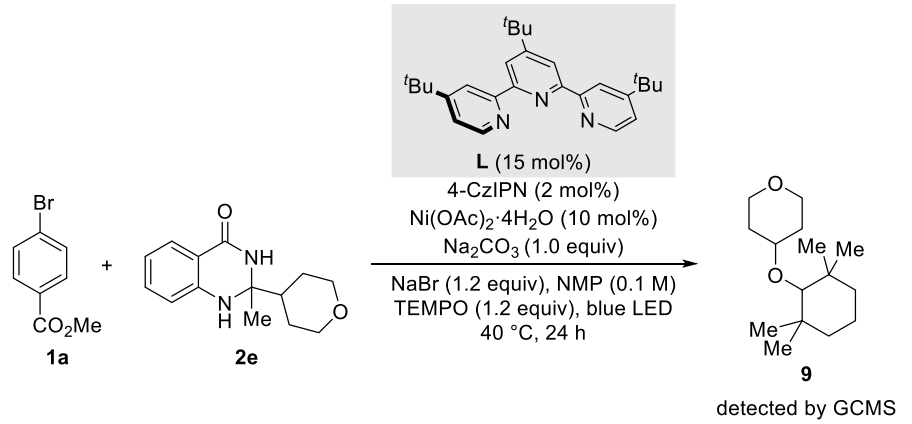

An oven-dried 8 mL screw-cap test tube was charged with a stirring bar, 4-CzIPN (1.6 mg, 2 mol%), $Ni(OAc)_2 \cdot 4H_2O$ (2.5 mg, 10 mol%), 4,4',4"-tri-tert-butyl-2,2':6'2"-terpyridine (6.0 mg, 15 mol%), NaBr (12.4 mg, 1.2 equiv), methyl 4-bromobenzoate (21.5 mg, 0.1 mmol), 2-methyl-2-(tetrahydro-2H-pyran-4-yl)-2,3-dihydroquinazolin-4(1*H*)-one (29.5 mg, 1.2 equiv) and TEMPO (18.7 mg, 1.2 equiv). The test tube was taken into a nitrogen-filled glovebox where Na_2CO_3 (10.6 mg, 1.0 equiv) was added to the reaction vessel. The reaction vessel was sealed with a screw cap and removed from the glovebox. Afterwards, NMP (1.0 mL, 0.1 M) was added by syringe. Parafilm was used to ensure the tightness of the reaction system. The reaction mixture was stirred at rt for 1 min. before exposure to blue LED irradiation at 40 °C for 24 hours. After that, the reaction mixture was analyzed by GC-mass and the corresponding TEMPO-adduct was detected by GC mass spectroscopy.

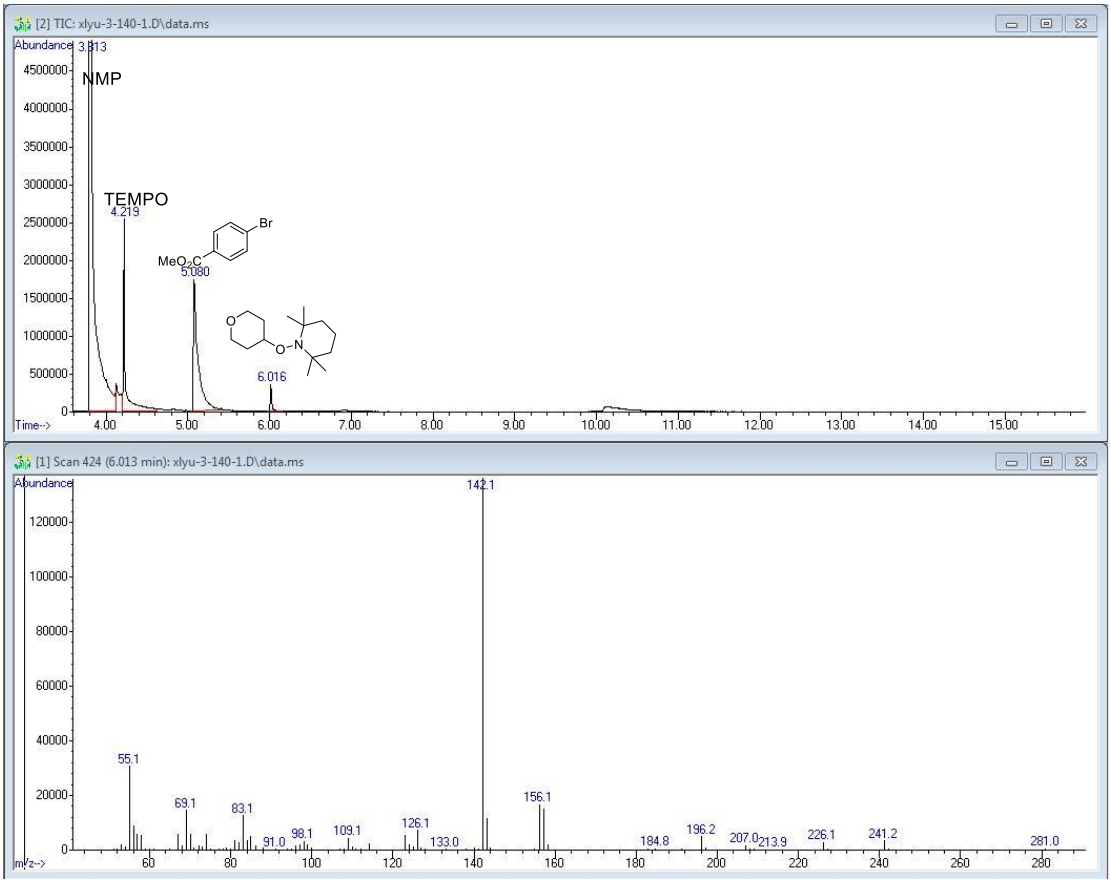

Figure S2.19 GC-MS spectra of radical inhibition reaction mixtures.

2.7.4.8 X-ray diffraction of Ni-I

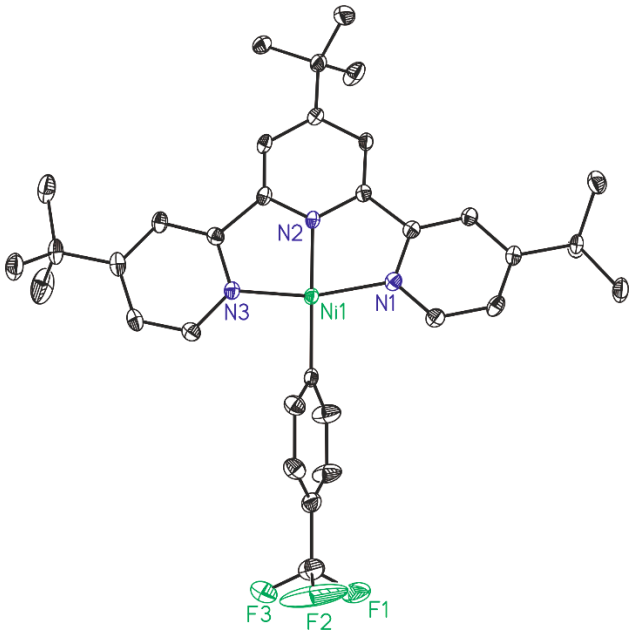

Figure S2.20 ORTEP diagram of **Ni-I**.

Table S2.2 Crystallographic Data.

Empirical formula	C35 H41 Br Cl2 F3 N3 Ni	
Formula weight	770.23	
Temperature	100(2)K	
Wavelength	0.71073 Å	
Crystal system	monoclinic	
Space group	C 2/c	
Unit cell dimensions	a = 17.5031(16)Å	a= 90°.
	b = 22.317(2)Å	b = 91.787(3)°.
	c = 17.5404(16)Å	g = 90°.
Volume	6848.3(11) $Å^3$	
Z	8	
Density (calculated)	1.494 Mg/m^3	
Absorption coefficient	1.935 mm^{-1}	
F(000)	3168	
Crystal size	0.400 x 0.250 x 0.250 mm^3	
Theta range for data collection	1.825 to 26.464°.	
Index ranges	-21<=h<=21, -26<=k<=27, -21<=l<=21	
Reflections collected	33394	
Independent reflections	7029[R(int) = 0.0420]	
Completeness to theta =26.464°	99.5%	
Absorption correction	Multi-scan	
Max. and min. transmission	0.74 and 0.59	
Refinement method	Full-matrix least-squares on F^2	
Data / restraints / parameters	7029/ 46/ 456	
Goodness-of-fit on F^2	0.916	
Final R indices [I>2sigma(I)]	R1 = 0.0350, wR2 = 0.1112	
R indices (all data)	R1 = 0.0482, wR2 = 0.1216	
Largest diff. peak and hole	0.932 and -0.940 $e.Å^{-3}$	

Table S2.3 Bond lengths [Å] and angles [°] for **Ni-I**.

Bond lengths----		
F1	C34	1.320(3)
C1	N1	1.335(3)
C1	C2	1.384(4)
C1	H1	0.9500
N1	C5	1.373(3)

N1	Ni1	1.917(2)
Ni1	N2	1.859(2)
Ni1	C28	1.882(3)
Ni1	N3	1.909(2)
F2	C34	1.315(4)
C2	C3	1.390(4)
C2	H2	0.9500
N2	C10	1.334(3)
N2	C6	1.341(3)
F3	C34	1.335(4)
C3	C4	1.400(3)
C3	C16	1.526(3)
N3	C15	1.345(3)
N3	C11	1.367(3)
C4	C5	1.372(3)
C4	H4	0.9500
C5	C6	1.478(3)
C6	C7	1.383(3)
C7	C8	1.411(3)
C7	H7	0.9500
C8	C9	1.399(3)
C8	C20	1.520(4)
C9	C10	1.377(3)
C9	H9	0.9500
C10	C11	1.482(3)
C11	C12	1.379(3)
C12	C13	1.394(4)
C12	H12	0.9500
C13	C14	1.396(4)
C13	C24	1.524(4)
C14	C15	1.379(4)
C14	H14	0.9500
C15	H15	0.9500
C16	C17	1.524(3)
C16	C18	1.531(4)
C16	C19	1.534(4)
C17	H17A	0.9800
C17	H17B	0.9800
C17	H17C	0.9800

C18	H18A	0.9800
C18	H18B	0.9800
C18	H18C	0.9800
C19	H19A	0.9800
C19	H19B	0.9800
C19	H19C	0.9800
C20	C23	1.527(4)
C20	C21	1.528(4)
C20	C22	1.541(4)
C21	H21A	0.9800
C21	H21B	0.9800
C21	H21C	0.9800
C22	H22A	0.9800
C22	H22B	0.9800
C22	H22C	0.9800
C23	H23A	0.9800
C23	H23B	0.9800
C23	H23C	0.9800
C24	C26	1.523(4)
C24	C27	1.526(4)
C24	C25	1.542(4)
C25	H25A	0.9800
C25	H25B	0.9800
C25	H25C	0.9800
C26	H26A	0.9800
C26	H26B	0.9800
C26	H26C	0.9800
C27	H27A	0.9800
C27	H27B	0.9800
C27	H27C	0.9800
C28	C33	1.391(4)
C28	C29	1.398(4)
C29	C30	1.390(4)
C29	H29	0.9500
C30	C31	1.384(4)
C30	H30	0.9500
C31	C32	1.382(4)
C31	C34	1.482(4)
C32	C33	1.380(4)

C32	H32	0.9500	
C33	H33	0.9500	
C1B	Cl1B	1.753(3)	
C1B	Cl1B#	1.754(3)	2_655
C1B	H1BA	0.9900	
C1B	H1BB	0.9900	
C1C	Cl1C	1.786(7)	
C1C	Cl2C	1.799(8)	
C1C	H1CA	0.9900	
C1C	H1CB	0.9900	
C1D	Cl1D	1.775(9)	
C1D	Cl2D	1.781(9)	
C1D	H1DA	0.9900	
C1D	H1DB	0.9900	

Angles----------

N1	C1	C2	123.4(2)
N1	C1	H1	118.3
C2	C1	H1	118.3
C1	N1	C5	117.2(2)
C1	N1	Ni1	128.63(17)
C5	N1	Ni1	113.84(16)
N2	Ni1	C28	174.43(10)
N2	Ni1	N3	82.66(9)
C28	Ni1	N3	96.84(10)
N2	Ni1	N1	82.33(9)
C28	Ni1	N1	98.00(9)
N3	Ni1	N1	164.97(9)
C1	C2	C3	119.7(2)
C1	C2	H2	120.1
C3	C2	H2	120.1
C10	N2	C6	121.4(2)
C10	N2	Ni1	119.02(17)
C6	N2	Ni1	119.08(17)
C2	C3	C4	116.8(2)
C2	C3	C16	123.5(2)
C4	C3	C16	119.7(2)
C15	N3	C11	117.0(2)
C15	N3	Ni1	128.87(18)

C11	N3	Ni1	114.00(16)
C5	C4	C3	120.5(2)
C5	C4	H4	119.7
C3	C4	H4	119.7
C4	C5	N1	121.9(2)
C4	C5	C6	124.7(2)
N1	C5	C6	113.3(2)
N2	C6	C7	120.5(2)
N2	C6	C5	110.3(2)
C7	C6	C5	129.2(2)
C6	C7	C8	119.4(2)
C6	C7	H7	120.3
C8	C7	H7	120.3
C9	C8	C7	118.1(2)
C9	C8	C20	121.9(2)
C7	C8	C20	120.0(2)
C10	C9	C8	119.4(2)
C10	C9	H9	120.3
C8	C9	H9	120.3
N2	C10	C9	121.2(2)
N2	C10	C11	110.4(2)
C9	C10	C11	128.2(2)
N3	C11	C12	122.9(2)
N3	C11	C10	113.0(2)
C12	C11	C10	124.0(2)
C11	C12	C13	120.0(2)
C11	C12	H12	120.0
C13	C12	H12	120.0
C12	C13	C14	116.5(2)
C12	C13	C24	123.0(2)
C14	C13	C24	120.6(2)
C15	C14	C13	121.0(2)
C15	C14	H14	119.5
C13	C14	H14	119.5
N3	C15	C14	122.4(2)
N3	C15	H15	118.8
C14	C15	H15	118.8
C17	C16	C3	112.1(2)
C17	C16	C18	109.3(2)

C3	C16	C18	109.8(2)
C17	C16	C19	108.6(2)
C3	C16	C19	107.3(2)
C18	C16	C19	109.6(2)
C16	C17	H17A	109.5
C16	C17	H17B	109.5
H17A	C17	H17B	109.5
C16	C17	H17C	109.5
H17A	C17	H17C	109.5
H17B	C17	H17C	109.5
C16	C18	H18A	109.5
C16	C18	H18B	109.5
H18A	C18	H18B	109.5
C16	C18	H18C	109.5
H18A	C18	H18C	109.5
H18B	C18	H18C	109.5
C16	C19	H19A	109.5
C16	C19	H19B	109.5
H19A	C19	H19B	109.5
C16	C19	H19C	109.5
H19A	C19	H19C	109.5
H19B	C19	H19C	109.5
C8	C20	C23	112.4(2)
C8	C20	C21	108.6(2)
C23	C20	C21	109.1(2)
C8	C20	C22	109.0(2)
C23	C20	C22	108.3(2)
C21	C20	C22	109.4(2)
C20	C21	H21A	109.5
C20	C21	H21B	109.5
H21A	C21	H21B	109.5
C20	C21	H21C	109.5
H21A	C21	H21C	109.5
H21B	C21	H21C	109.5
C20	C22	H22A	109.5
C20	C22	H22B	109.5
H22A	C22	H22B	109.5
C20	C22	H22C	109.5
H22A	C22	H22C	109.5

H22B	C22	H22C	109.5
C20	C23	H23A	109.5
C20	C23	H23B	109.5
H23A	C23	H23B	109.5
C20	C23	H23C	109.5
H23A	C23	H23C	109.5
H23B	C23	H23C	109.5
C26	C24	C13	108.5(2)
C26	C24	C27	110.9(3)
C13	C24	C27	109.0(2)
C26	C24	C25	108.5(3)
C13	C24	C25	112.2(2)
C27	C24	C25	107.9(2)
C24	C25	H25A	109.5
C24	C25	H25B	109.5
H25A	C25	H25B	109.5
C24	C25	H25C	109.5
H25A	C25	H25C	109.5
H25B	C25	H25C	109.5
C24	C26	H26A	109.5
C24	C26	H26B	109.5
H26A	C26	H26B	109.5
C24	C26	H26C	109.5
H26A	C26	H26C	109.5
H26B	C26	H26C	109.5
C24	C27	H27A	109.5
C24	C27	H27B	109.5
H27A	C27	H27B	109.5
C24	C27	H27C	109.5
H27A	C27	H27C	109.5
H27B	C27	H27C	109.5
C33	C28	C29	116.7(2)
C33	C28	Ni1	118.5(2)
C29	C28	Ni1	124.78(19)
C30	C29	C28	121.6(2)
C30	C29	H29	119.2
C28	C29	H29	119.2
C31	C30	C29	120.2(2)
C31	C30	H30	119.9

C29	C30	H30	119.9		
C32	C31	C30	119.1(3)		
C32	C31	C34	119.4(3)		
C30	C31	C34	121.5(2)		
C33	C32	C31	120.4(3)		
C33	C32	H32	119.8		
C31	C32	H32	119.8		
C32	C33	C28	122.1(3)		
C32	C33	H33	119.0		
C28	C33	H33	119.0		
F2	C34	F1	105.0(3)		
F2	C34	F3	106.0(3)		
F1	C34	F3	103.8(3)		
F2	C34	C31	114.1(3)		
F1	C34	C31	114.1(2)		
F3	C34	C31	112.9(3)		
Cl1B	C1B	Cl1B#	112.0(2)		2_655
Cl1B	C1B	H1BA	109.2		
Cl1B#	C1B	H1BA	109.2	2_655	
Cl1B	C1B	H1BB	109.2		
Cl1B#	C1B	H1BB	109.2	2_655	
H1BA	C1B	H1BB	107.9		
Cl1C	C1C	Cl2C	105.0(4)		
Cl1C	C1C	H1CA	110.7		
Cl2C	C1C	H1CA	110.7		
Cl1C	C1C	H1CB	110.7		
Cl2C	C1C	H1CB	110.7		
H1CA	C1C	H1CB	108.8		
Cl1D	C1D	Cl2D	118.0(10)		
Cl1D	C1D	H1DA	107.8		
Cl2D	C1D	H1DA	107.8		
Cl1D	C1D	H1DB	107.8		
Cl2D	C1D	H1DB	107.8		
H1DA	C1D	H1DB	107.2		

Table S2.4 Torsion angles [°] for **Ni-I**.

C2	C1	N1	C5	-4.3(4)

C2	C1	N1	Ni1	168.68(19)
N1	C1	C2	C3	-2.4(4)
N3	Ni1	N2	C10	2.72(18)
N1	Ni1	N2	C10	-178.23(19)
N3	Ni1	N2	C6	-169.72(19)
N1	Ni1	N2	C6	9.33(18)
C1	C2	C3	C4	7.0(4)
C1	C2	C3	C16	-170.3(2)
C2	C3	C4	C5	-5.2(4)
C16	C3	C4	C5	172.2(2)
C3	C4	C5	N1	-1.4(4)
C3	C4	C5	C6	-177.6(2)
C1	N1	C5	C4	6.2(3)
Ni1	N1	C5	C4	-167.84(19)
C1	N1	C5	C6	-177.3(2)
Ni1	N1	C5	C6	8.7(2)
C10	N2	C6	C7	-1.7(3)
Ni1	N2	C6	C7	170.59(18)
C10	N2	C6	C5	-178.9(2)
Ni1	N2	C6	C5	-6.7(3)
C4	C5	C6	N2	174.8(2)
N1	C5	C6	N2	-1.7(3)
C4	C5	C6	C7	-2.2(4)
N1	C5	C6	C7	-178.6(2)
N2	C6	C7	C8	2.4(4)
C5	C6	C7	C8	179.1(2)
C6	C7	C8	C9	-0.3(4)
C6	C7	C8	C20	-178.7(2)
C7	C8	C9	C10	-2.3(4)
C20	C8	C9	C10	176.0(2)
C6	N2	C10	C9	-1.1(4)
Ni1	N2	C10	C9	-173.39(18)
C6	N2	C10	C11	174.4(2)
Ni1	N2	C10	C11	2.2(3)
C8	C9	C10	N2	3.1(4)
C8	C9	C10	C11	-171.6(2)
C15	N3	C11	C12	4.4(4)
Ni1	N3	C11	C12	-172.11(19)
C15	N3	C11	C10	-173.0(2)

Ni1	N3	C11	C10	10.5(3)
N2	C10	C11	N3	-8.2(3)
C9	C10	C11	N3	167.0(2)
N2	C10	C11	C12	174.4(2)
C9	C10	C11	C12	-10.4(4)
N3	C11	C12	C13	-3.0(4)
C10	C11	C12	C13	174.1(2)
C11	C12	C13	C14	-1.0(4)
C11	C12	C13	C24	178.3(2)
C12	C13	C14	C15	3.4(4)
C24	C13	C14	C15	-175.9(2)
C11	N3	C15	C14	-1.8(4)
Ni1	N3	C15	C14	174.09(19)
C13	C14	C15	N3	-2.1(4)
C2	C3	C16	C17	-5.6(3)
C4	C3	C16	C17	177.1(2)
C2	C3	C16	C18	-127.3(3)
C4	C3	C16	C18	55.5(3)
C2	C3	C16	C19	113.6(3)
C4	C3	C16	C19	-63.7(3)
C9	C8	C20	C23	-0.8(3)
C7	C8	C20	C23	177.5(2)
C9	C8	C20	C21	120.1(3)
C7	C8	C20	C21	-61.7(3)
C9	C8	C20	C22	-120.8(3)
C7	C8	C20	C22	57.4(3)
C12	C13	C24	C26	121.3(3)
C14	C13	C24	C26	-59.4(3)
C12	C13	C24	C27	-117.9(3)
C14	C13	C24	C27	61.3(3)
C12	C13	C24	C25	1.4(4)
C14	C13	C24	C25	-179.3(2)
N3	Ni1	C28	C33	92.9(2)
N1	Ni1	C28	C33	-84.7(2)
N3	Ni1	C28	C29	-85.7(2)
N1	Ni1	C28	C29	96.7(2)
C33	C28	C29	C30	0.2(4)
Ni1	C28	C29	C30	178.8(2)
C28	C29	C30	C31	0.4(4)

C29	C30	C31	C32	-0.6(4)
C29	C30	C31	C34	-179.7(3)
C30	C31	C32	C33	0.1(5)
C34	C31	C32	C33	179.2(3)
C31	C32	C33	C28	0.5(5)
C29	C28	C33	C32	-0.7(4)
Ni1	C28	C33	C32	-179.4(3)
C32	C31	C34	F2	160.3(3)
C30	C31	C34	F2	-20.7(4)
C32	C31	C34	F1	39.5(4)
C30	C31	C34	F1	-141.4(3)
C32	C31	C34	F3	-78.7(4)
C30	C31	C34	F3	100.4(4)

Symmetry operations

---

1 'x, y, z'
2 '-x, y, -z+1/2'
3 'x+1/2, y+1/2, z'
4 '-x+1/2, y+1/2, -z+1/2'
5 '-x, -y, -z'
6 'x, -y, z-1/2'
7 '-x+1/2, -y+1/2, -z'
8 'x+1/2, -y+1/2, z-1/2'

2.7.5 Representative NMR Spectra

^{1}H NMR of **2a**

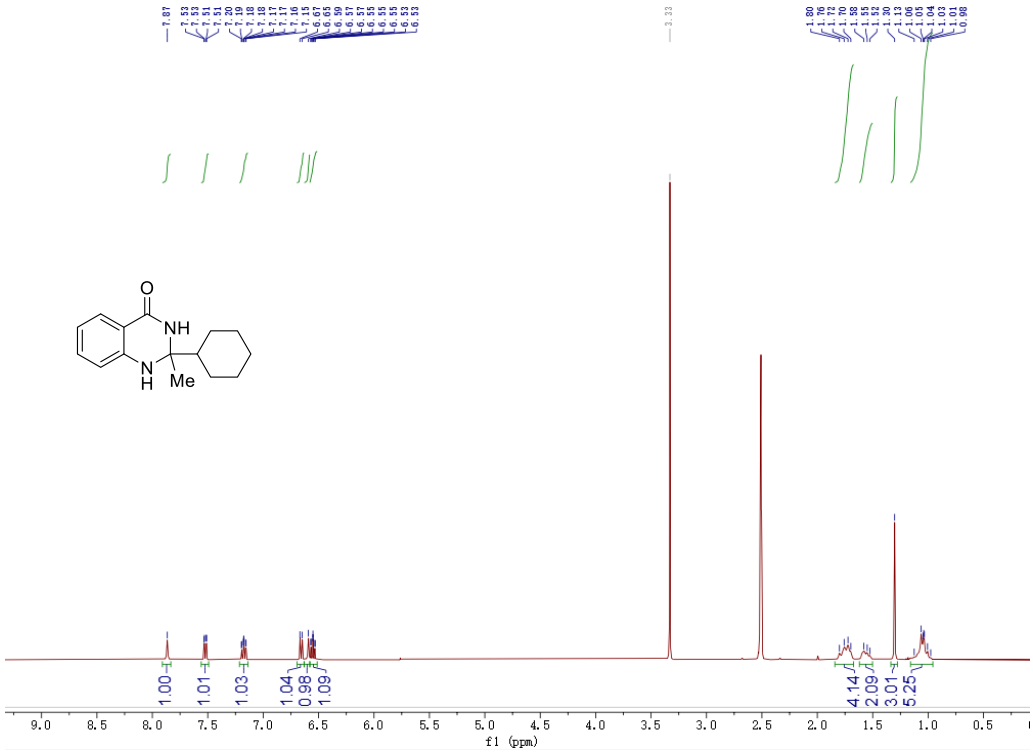

^{13}C NMR of **2a**

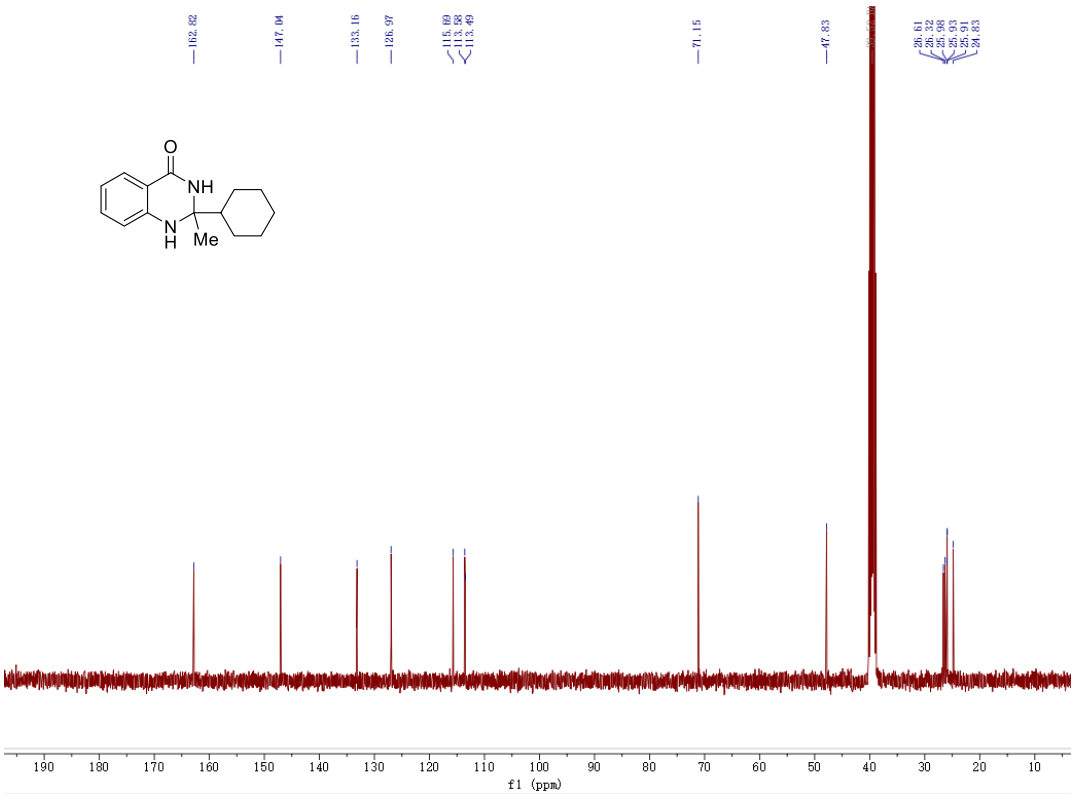

^{1}H NMR of **2m´**

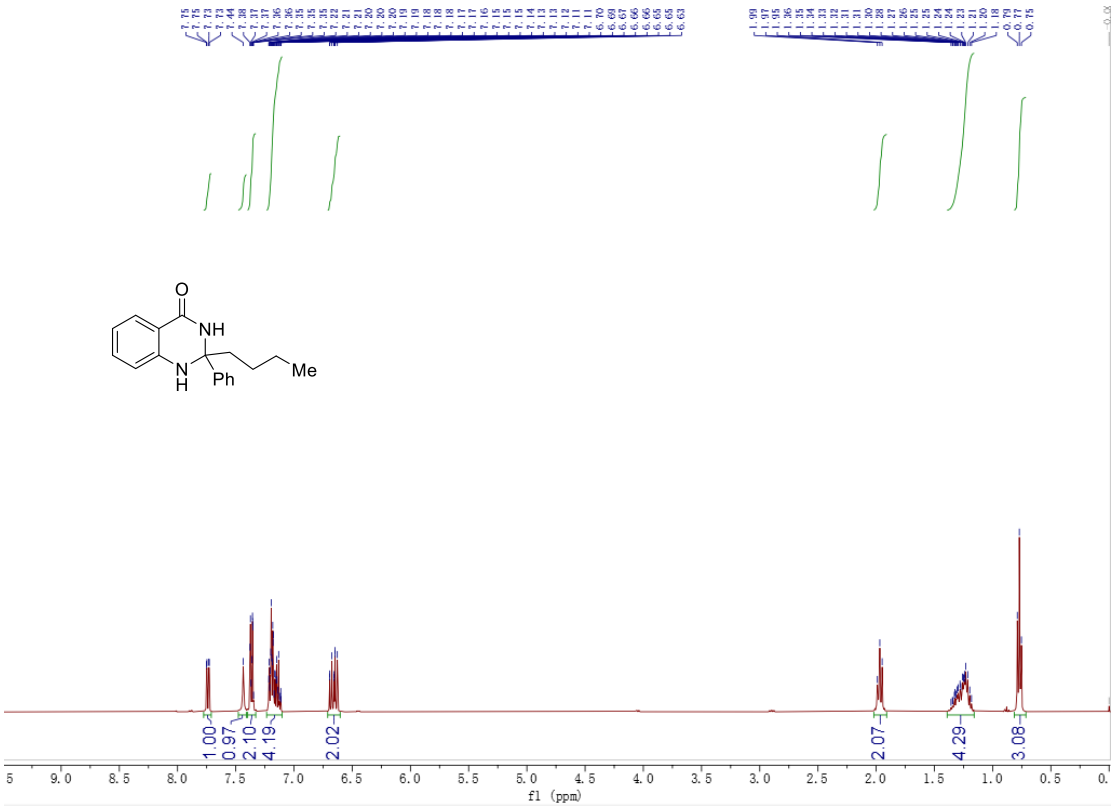

^{13}C NMR of **2m´**

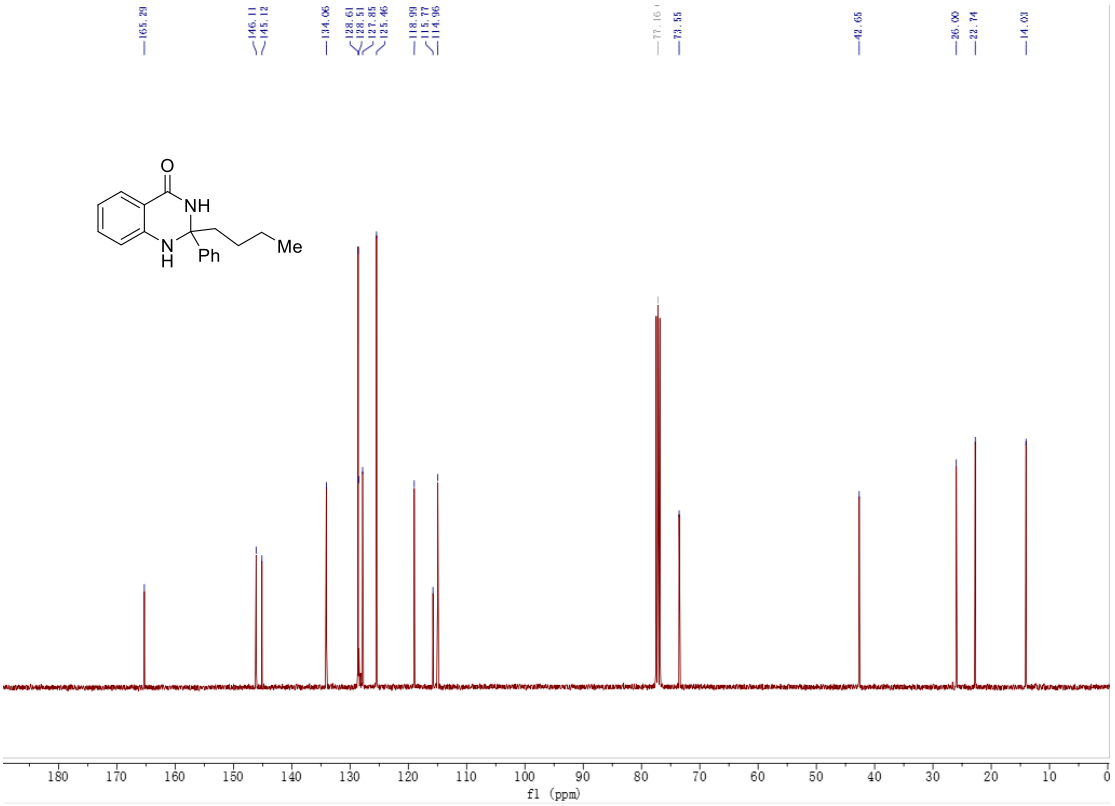

^{1}H NMR of **5p**

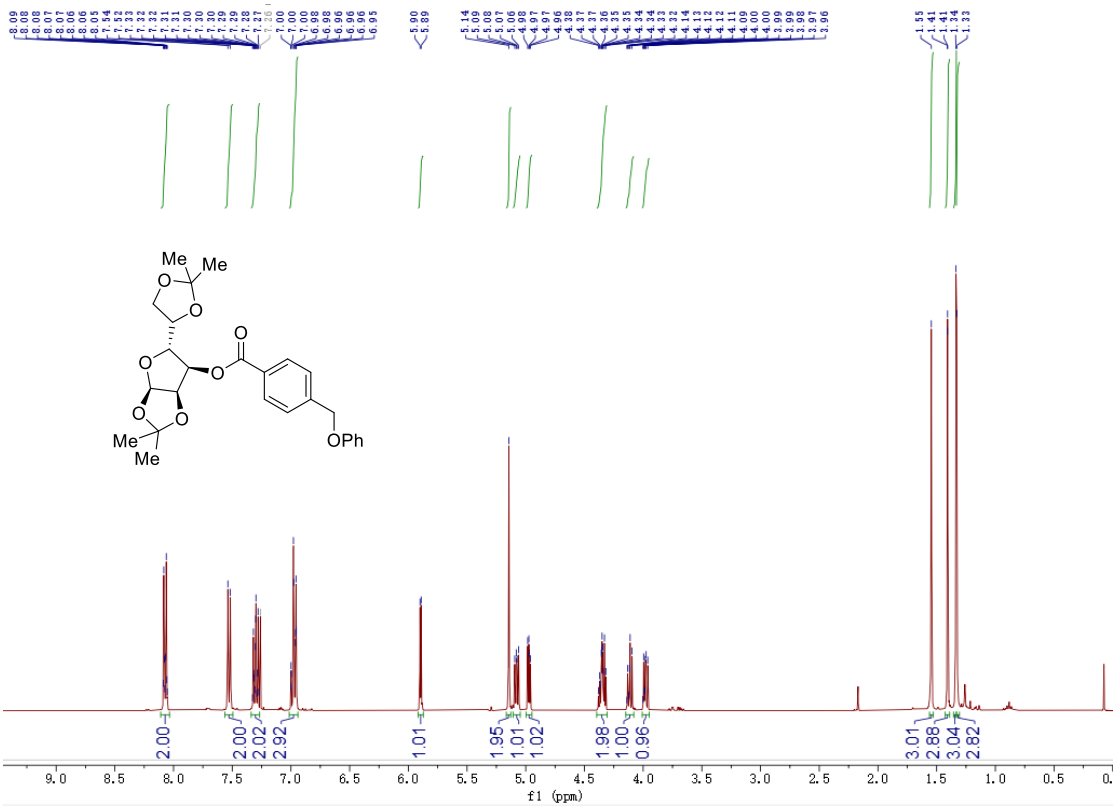

^{13}C NMR of **5p**

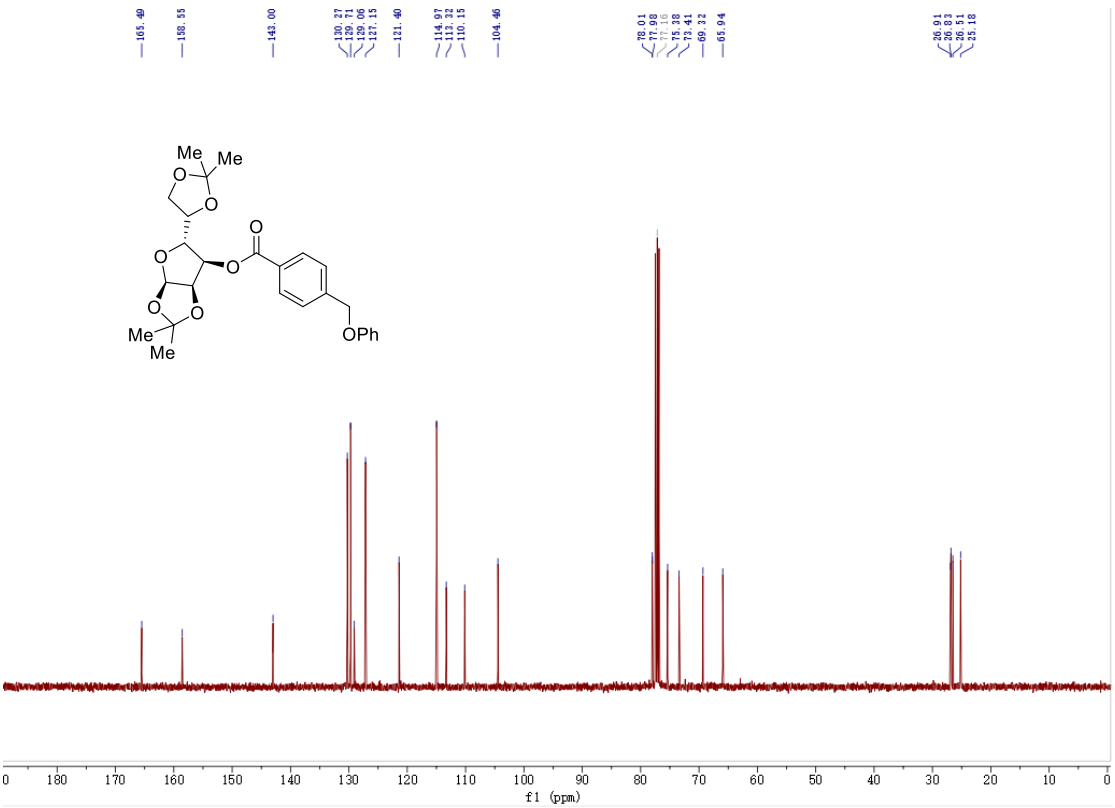

^{1}H NMR of **7e**

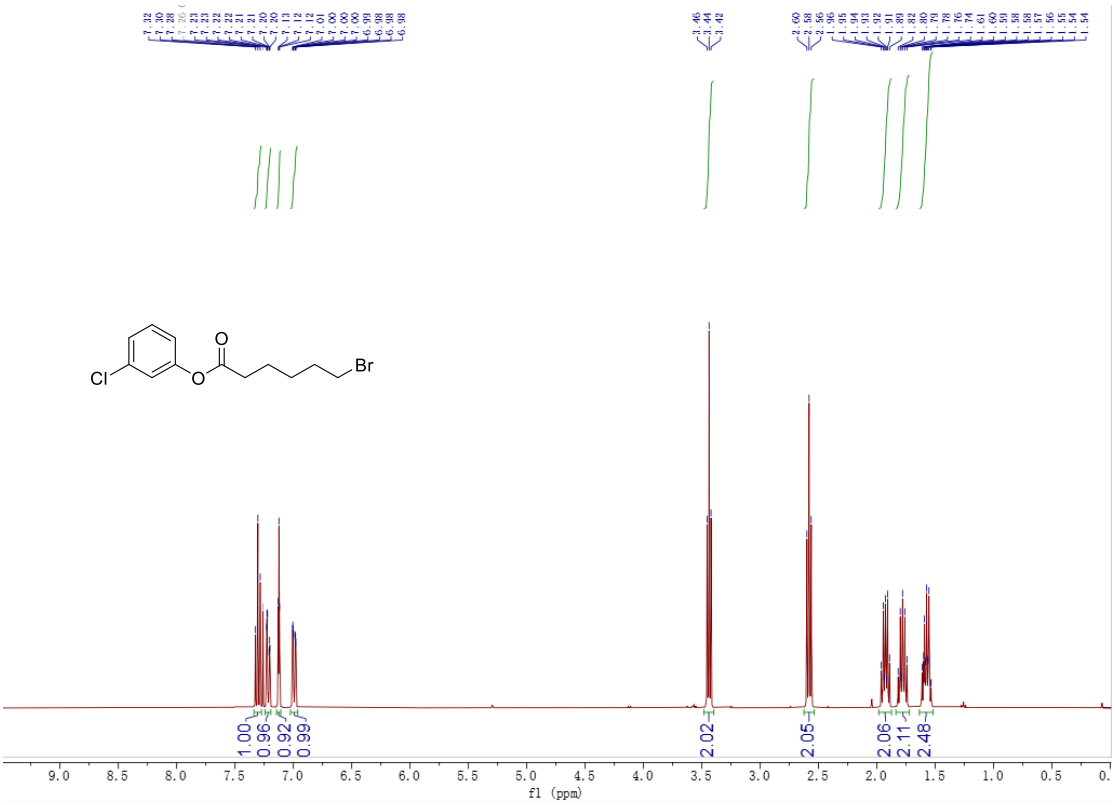

^{13}C NMR of **7e**

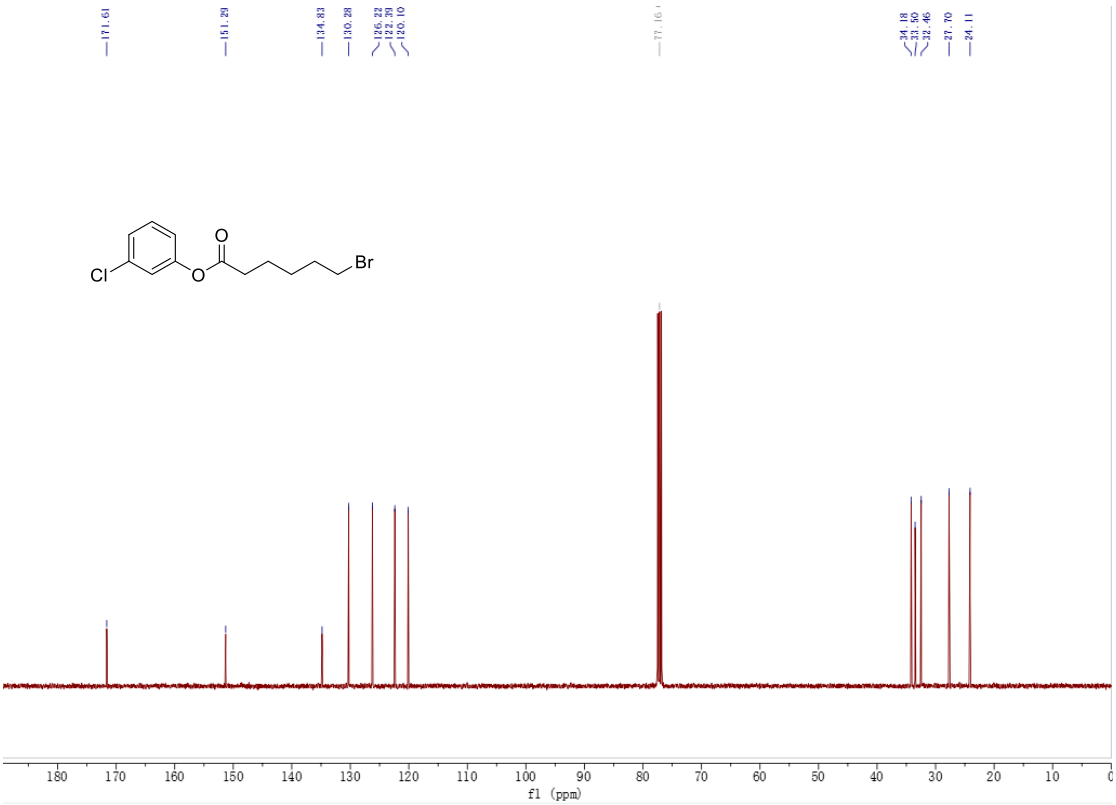

^{1}H NMR of **8n**

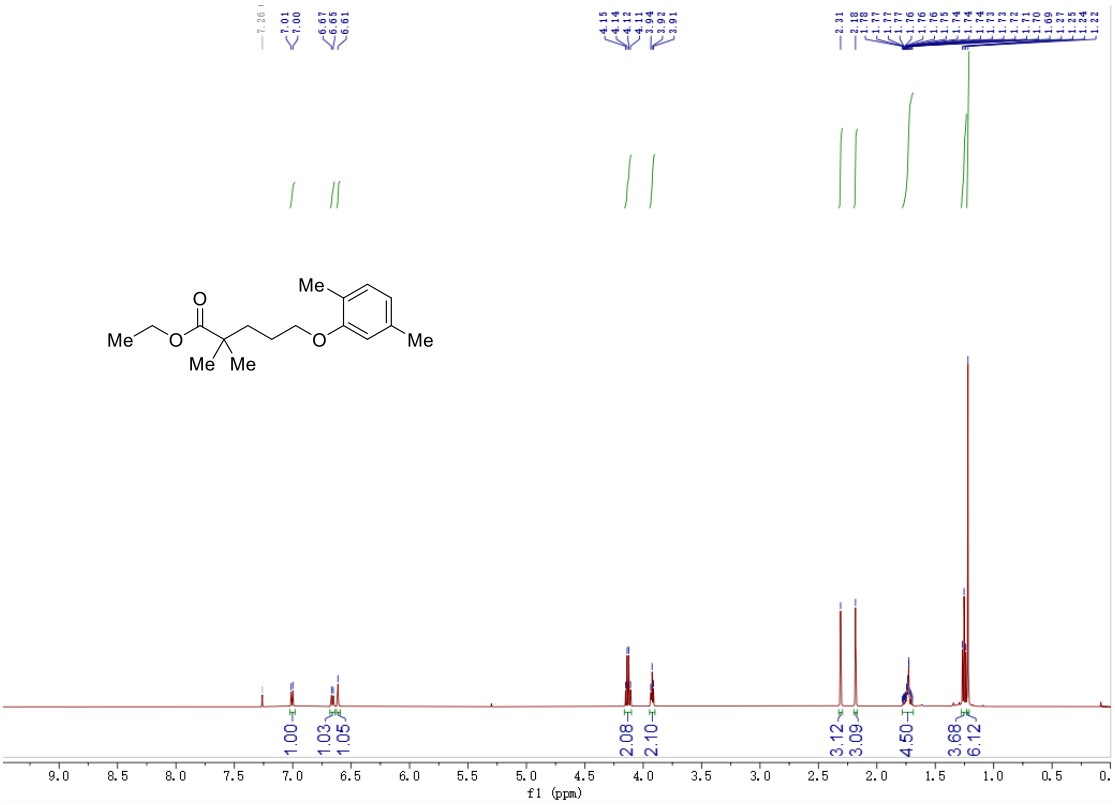

^{13}C NMR of **8n**

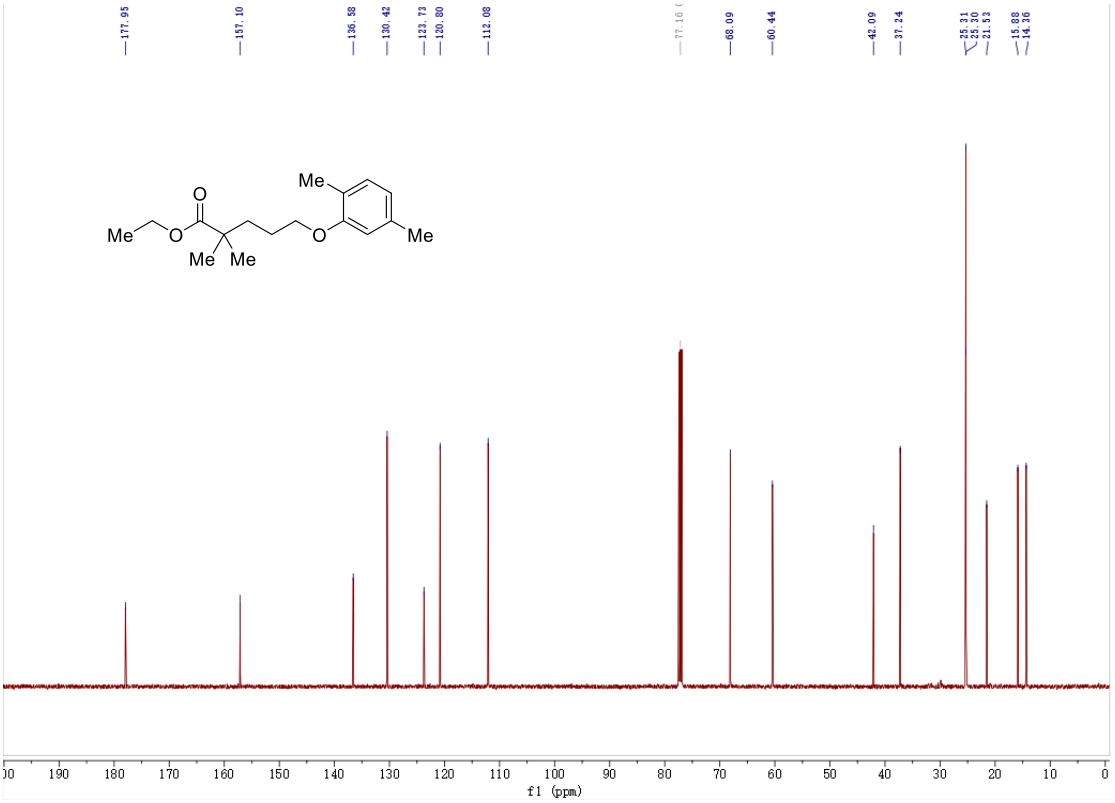

^{1}H NMR of **11**

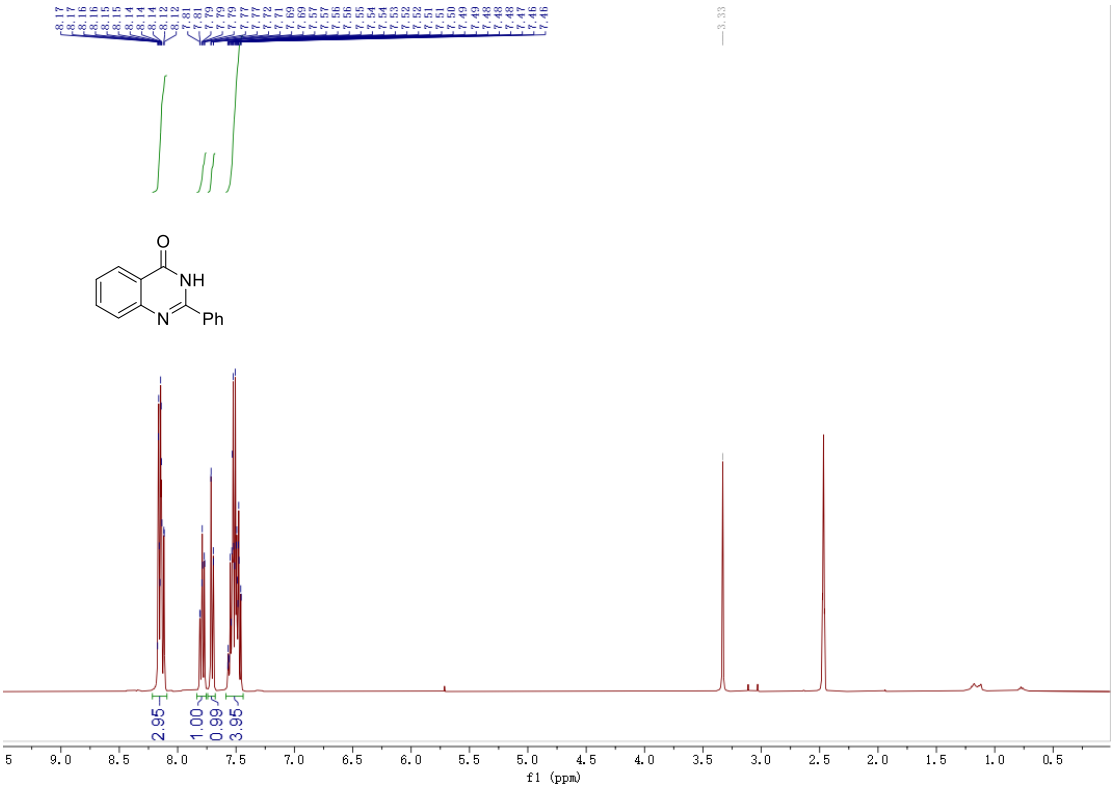

^{13}C NMR of **11**

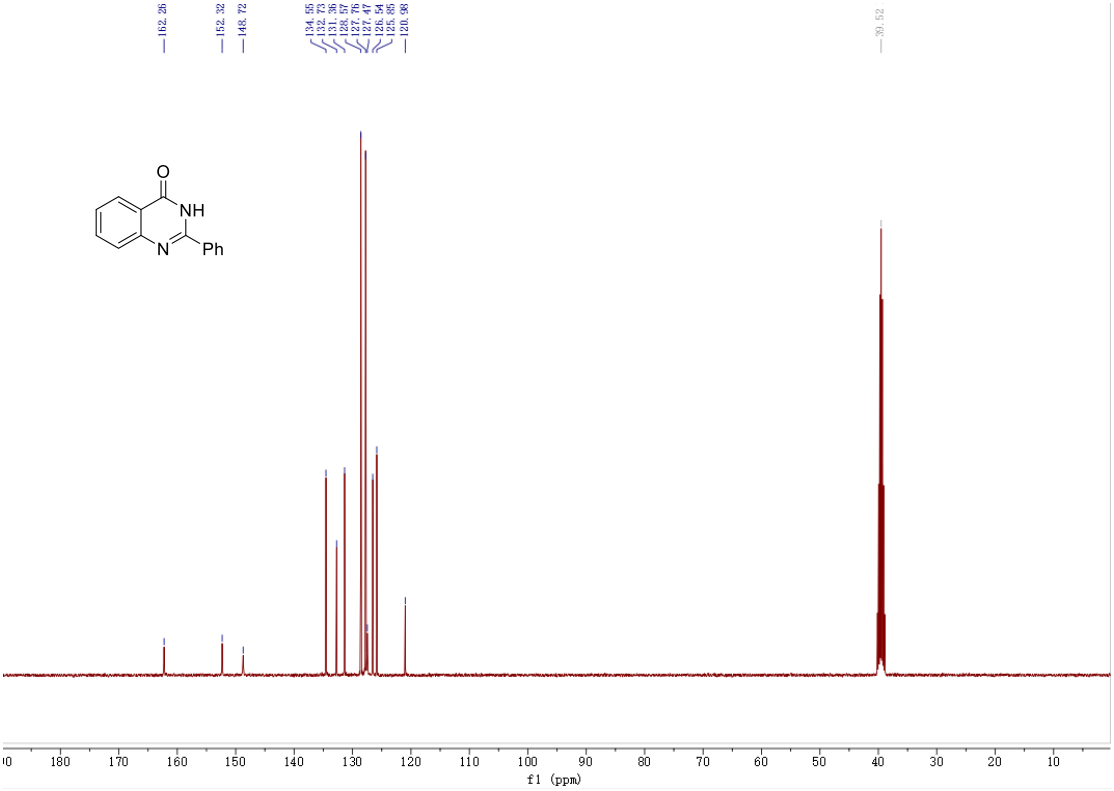

^{1}H NMR of **Ni-I** in MeCN-d_3

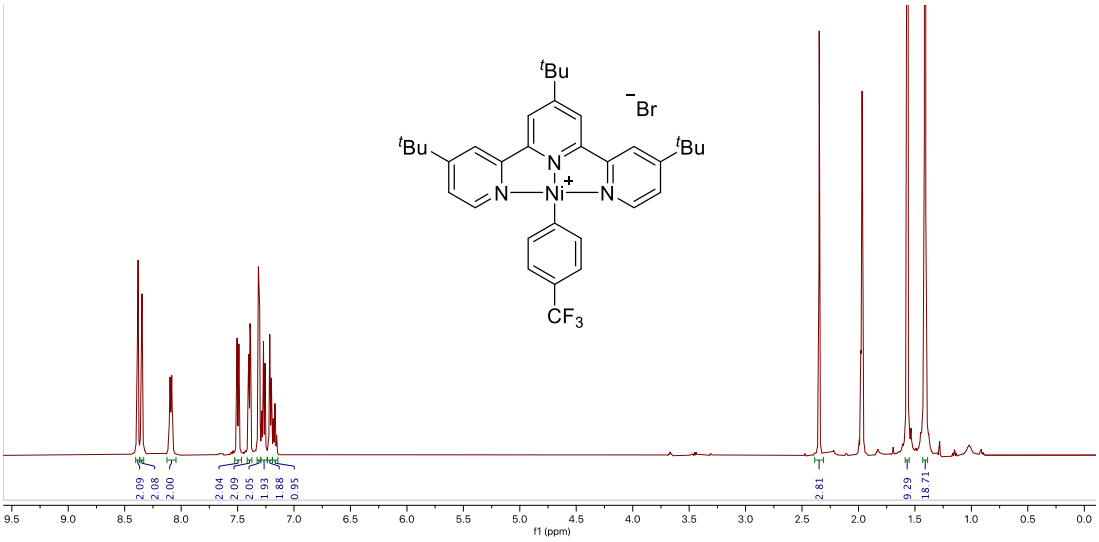

^{1}H NMR of **Ni-I** in DMSO-d_6

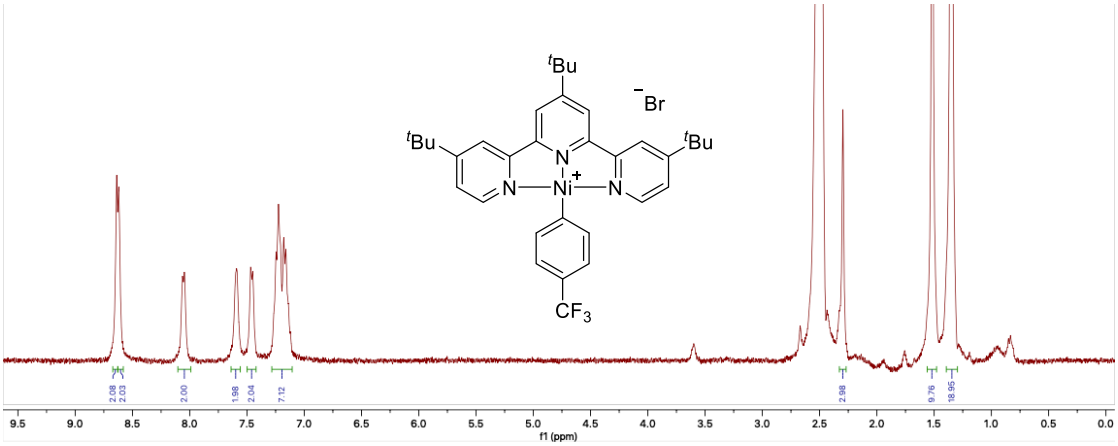

^{19}F NMR of **Ni-I**

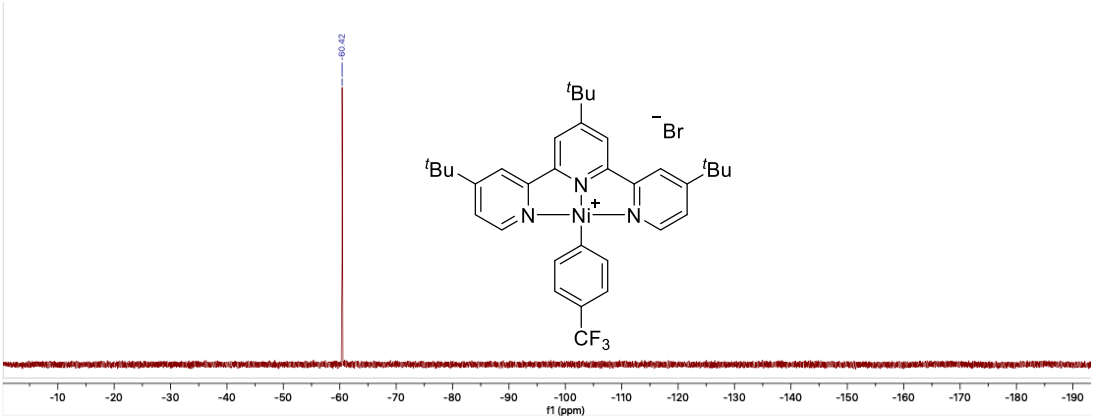

^{13}C NMR of **Ni-I**

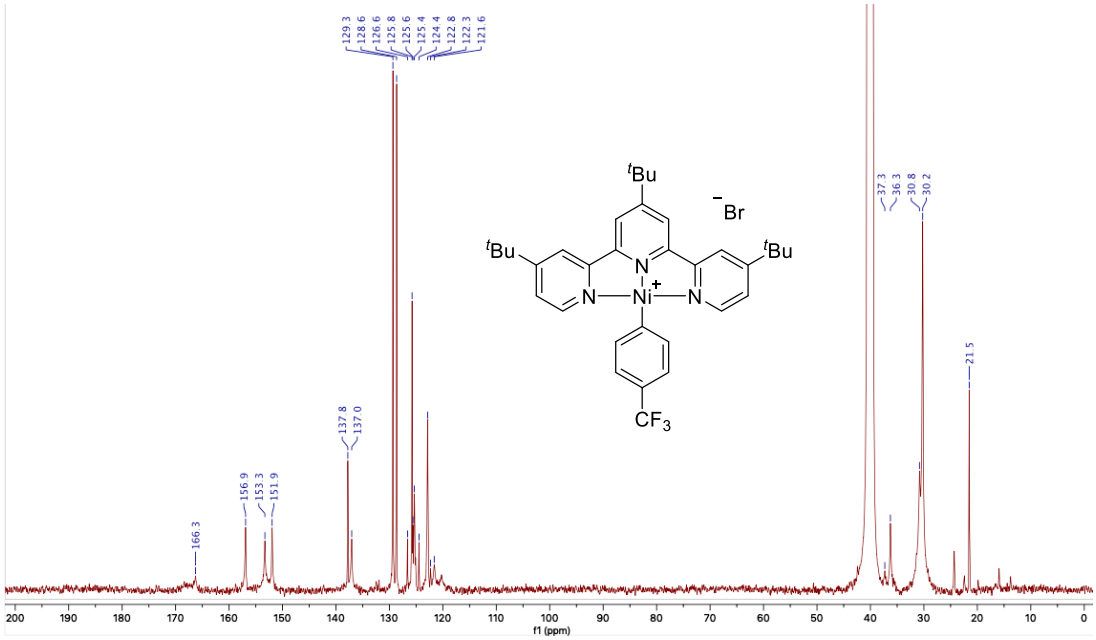
129.3
128.6
126.6
125.8
125.6
125.4
124.4
122.8
122.3
121.6
37.3
36.3
30.8
30.2
21.5
137.8
137.0
156.9
153.3
151.9
166.3
tBu
tBu
tBu
Br
N
N
Ni
N
CF3
200
190
180
170
160
150
140
130
120
110
100
90
80
70
60
50
40
30
20
10
0
f1 (ppm)

Chapter 3

Copper-Catalyzed C(sp^3)-Amination of Ketone-Derived Dihydroquinazolinones by Aromatization-Driven C-C Bond Scission

3.1 Introduction

Nitrogen containing molecules are a structural mainstay for medicinal chemists in optimizing pharmacological properties of lead candidates (Scheme 3.1).[205] Unsurprisingly, chemists have been challenged to develop mild catalytic protocols devoiding toxic reagents for their assembly.[206] Ideally, such modern C(sp^3)–N bond-forming reactions should be broadly applicable and amenable to functionalization of advanced substrates, thus complementing classical approaches, which include Curtius rearrangement,[207] reductive amination,[208] Mitsunobu reaction[209] and amination of alkyl halides,[210] among others.[211]

[205] (a) Vitaku, E.; Smith, D. T.; Njardarson, J. T. Analysis of the Structural Diversity, Substitution Patterns, and Frequency of Nitrogen Heterocycles among U.S. FDA Approved Pharmaceuticals. *J. Med. Chem*. **2014**, *57*, 10257–10274. (b) Kerru, N.; Gummidi, L.; Maddila, S.; Gangu, K. K.; Jonnalagadda, S. B. A Review on Recent Advances in Nitrogen-Containing Molecules and Their Biological Applications. *Molecules* **2020**, *25*, 1909–1951.

[206] (a) Trowbridge, A.; Walton, S. M.; Gaunt, M. J. New Strategies for the Transition-Metal Catalyzed Synthesis of Aliphatic Amines. *Chem. Rev*. **2020**, *120*, 2613–2692. (b) Rivas, M.; Palchykov, V.; Jia, X.; Gevorgyan, V. Recent Advances in Visible Light-Induced C(sp^3)–N Bond Formation. *Nat Rev Chem* **2022**, *6*, 544–561. (c) Park, Y.; Kim, Y.; Chang, S. Transition Metal-Catalyzed C–H Amination: Scope, Mechanism, and Applications. *Chem. Rev*. **2017**, *117*, 9247–9301.

[207](a) Ghosh, A. K.; Brindisi, M.; Sarkar, A. The Curtius Rearrangement: Applications in Modern Drug Discovery and Medicinal Chemistry. *ChemMedChem* **2018**, *13*, 2351–2373. (b) Ghosh, A. K.; Sarkar, A.; Brindisi, M. The Curtius Rearrangement: Mechanistic Insight and Recent Applications in Natural Product Syntheses *Org. Biomol. Chem*. **2018**, *16*, 2006–2027.

[208] (a) Afanasyev, O. I.; Kuchuk, E.; Usanov, D. L.; Chusov, D. Reductive Amination in the Synthesis of Pharmaceuticals. *Chem. Rev*. **2019**, *119*, 11857–11911. (b) Irrgang, T.; Kempe, R. Transition-Metal-Catalyzed Reductive Amination Employing Hydrogen. *Chem. Rev*. **2020**, *120*, 9583–9674. (c) Tian, Y.; Hu, L.; Wang, Y.-Z.; Zhang, X.; Yin, Q. Recent Advances on Transition-Metal-Catalysed Asymmetric Reductive Amination. *Org. Chem. Front*. **2021**, *8*, 2328–2342.

[209] (a) Swamy, K. C. K.; Kumar, N. N. B.; Balaraman, E.; Kumar, K. V. P. P. Mitsunobu and Related Reactions: Advances and Applications. *Chem. Rev*. **2009**, *109*, 2551–2651. (b) Beddoe, R. H.; Sneddon, H. F.; Denton, R. M. The Catalytic Mitsunobu Reaction: A Critical Analysis of the Current State-of-the-art. *Org. Biomol. Chem*. **2018**, *16*, 7774–7781.

[210] (a) Salvatore, R. N.; Nagle, A. S.; Jung, K. W. Cesium Effect: High Chemoselectivity in Direct N-Alkylation of Amines. *J. Org. Chem*. **2002**, *67*, 674–683. (b) Cinelli, M. A.; Li, H.; Chreifi, G.; Martasek, P.; Roman, L. J.; Poulos, T. L.; Silverman, R. B. Simplified 2-Aminoquinoline-Based Scaffold for Potent and Selective Neuronal Nitric Oxide Synthase Inhibition. *J. Med. Chem*. **2014**, *57*, 1513–1530. (c) Okunola-Bakare, O. M.; Cao, J.; Kopajtic, T.; Katz, J. L.; Loland, C. J.; Shi, L.; Newman, A. M. Elucidation of Structural Elements for Selectivity across Monoamine Transporters: Novel 2-[(Diphenylmethyl)sulfinyl]acetamide (Modafinil) Analogues. *J. Med. Chem*. **2014**, *57*, 1000–1013.

[211] (a) Huang, L.; Arndt, M.; Gooßen, K.; Heydt, H.; Gooßen, L. J. Late Transition Metal-Catalyzed Hydroamination and Hydroamidation. *Chem. Rev*. **2015**, *115*, 2596–2697. (b) Müller, P.; Fruit, C. Enantioselective Catalytic Aziridinations and Asymmetric Nitrene Insertions into CH Bonds. *Chem. Rev*. **2003**, *103*, 2905–2920.

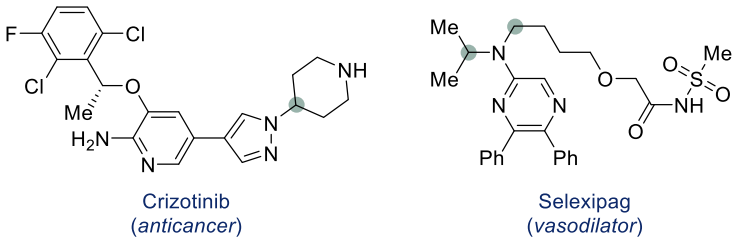

Scheme 3.1 Prevalence of C(sp^3)–N architectures.

The Beckmann rearrangement is an illustrative example of the potential utility of ketones as traceless synthons for accessing C(sp^3)–N motifs (Scheme 3.2, *left*).[212] However, it finds little utility in modern medicinal chemistry, likely due to its limited application within diversity-oriented synthesis. Alternative approach could be transition metal-catalyzed C(sp^3)–N bond formation reaction via catalytic C–C bond activation (Scheme 3.2, *right*). Up to date, this pathway remains unavailable, even when using directing groups (DG) or strained high-energy substrates.

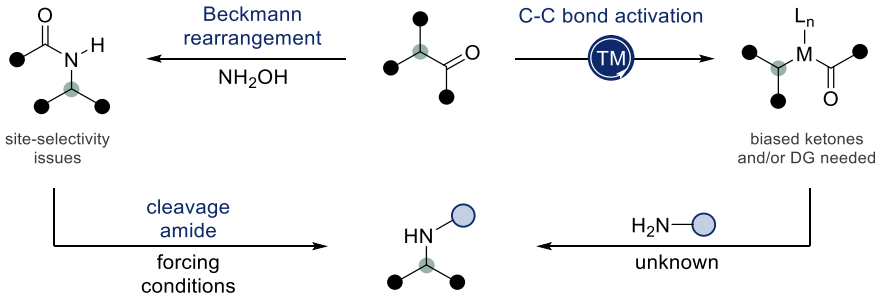

Scheme 3.2 Construction of C(sp^3)–N architectures via ketone C–C bond cleavage.

A recent breakthrough was made by Zuo and co-workers, who developed a formally catalytic C(sp^3)–N formation technique through selective C–C bond cleavage of ketones (Scheme 3.3).[213] A cooperative utilization of Lewis acid catalysis and LMCT catalysis results in selective and effective generation of oxygen-centered radical in cyclic and acyclic ketones. The oxygen-centered radical triggered *β*-scission enables the installation of amino group at the carbon-centered radical position.

[212] (a) Kaur, K.; Srivastava, S. Beckmann Rearrangement Catalysis: A Review of Recent Advances. *New J. Chem*. **2020**, *44*, 18530–18572. (b) Tang, L.; Wang, Z.-L.; Wan, H.-L.; He, Y.-H.; Guan, Z. Visible-Light-Induced Beckmann Rearrangement by Organic Photoredox Catalysis. *Org. Lett*. **2020**, *22*, 6182–6186. (c) Zhang, X.; Rovis, T. Photocatalyzed Triplet Sensitization of Oximes Using Visible Light Provides a Route to Nonclassical Beckmann Rearrangement Products. *J. Am. Chem. Soc*. **2021**, *143*, 21211–21217.

[213] Chen, Y.; Du, J.; Zuo, Z. Selective C-C Bond Scission of Ketones via Visible-Light-Mediated Cerium Catalysis. *Chem* **2020**, *6*, 266–279.

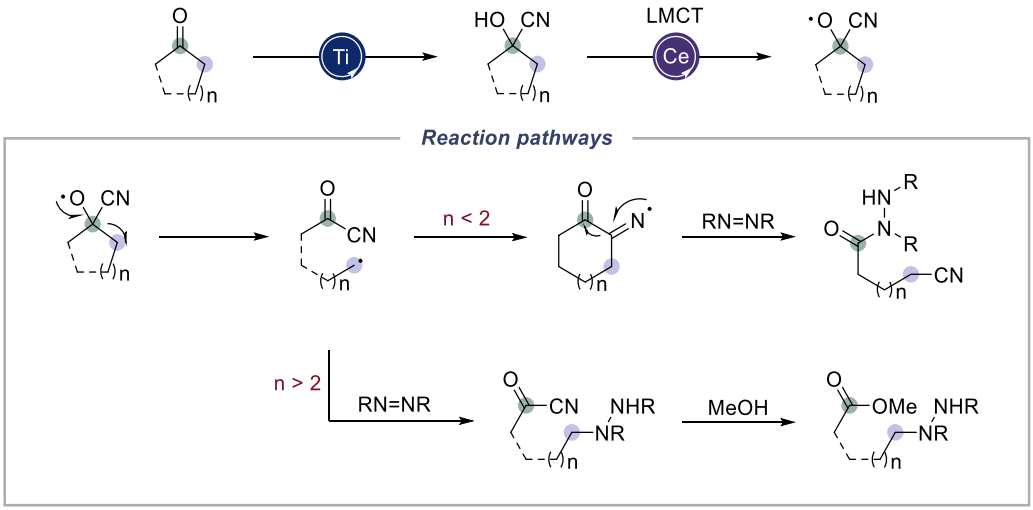

Scheme 3.3 C(sp^3)–N bond formation via selective C–C bond scission of ketones.

The example that existed in the functionalization of the ketone C–C bond demonstrates the synthetic potential that radical induced C–C bond fragmentation process has. In the following part of this chapter, the development of a copper-catalyzed C(sp^3) amination of ketone-derived dihydroquinazolinones methodology, as well as the theoretical foundations of this protocol will be discussed. Additionally, copper-catalyzed nitrene transfer reaction will be briefly discussed as an alternative technique for C(sp^3)–H bond amination.

3.1.1 Copper-Catalyzed Cross-Coupling Reactions

Organocopper chemistry pushed the field of coupling reactions into sight, when Glaser reported the homocoupling of metallic acetylides.[214] Early investigations largely focused on the use of stoichiometric amounts of organocopper species, such as Gilman reagents.[215] The catalytic use of copper catalyst, generally for the coupling of alkyl Grignard reagents with alkyl halides, was disclosed afterwards. In 1997, Burns and co-workers developed a highly active soluble copper precatalyst, which allowed the cross-coupling of alkyl tosylates and mesylates with a number of Grignard reagents (Scheme 3.4).[216] The use of copper catalysis in the formation of C–C bonds has

[214] Thapa, S.; Shrestha, B.; Gurung, S. K.; Giri, R. Copper-Catalysed Cross-Coupling: An Untapped Potential. *Org. Biomol. Chem*. **2015**, *13*, 4816–4827.
[215] Gilman, H.; Jones, R. G.; Woods, L. A. The Preparation of Methylcopper and Some Observations on the Decomposition of Organocopper Compounds. *J. Org. Chem*. **1952**, *17*, 1630–1634.
[216] Burns, D. H.; Miller, J. D.; Chan, H.-K.; Delaney, M. O. Scope and Utility of a New Soluble Copper Catalyst [CuBr−LiSPh−LiBr−THF]: A Comparison with Other Copper Catalysts in Their Ability to Couple One Equivalent of a Grignard Reagent with an Alkyl Sulfonate. *J. Am. Chem. Soc*. **1997**, *119*, 2125–2133.

remained successful not only with traditional organometallic reagents — organozinc,[217] organotin [218] and zirconium, [219] but also with stable organosilicon [220] and organoboron [221] compounds. The reaction mechanism for organocopper (I) intermediates reacting with alkyl halides and pseudohalides is believed to be a traditional S_N2 process, since the product is formed with complete inversion of configuration.[222] On the contrary, reaction of organocopper(I) species with aryl halides has been proposed to proceed via oxidative addition/reductive elimination sequence with the involvement of Cu(III) intermediate.[223]

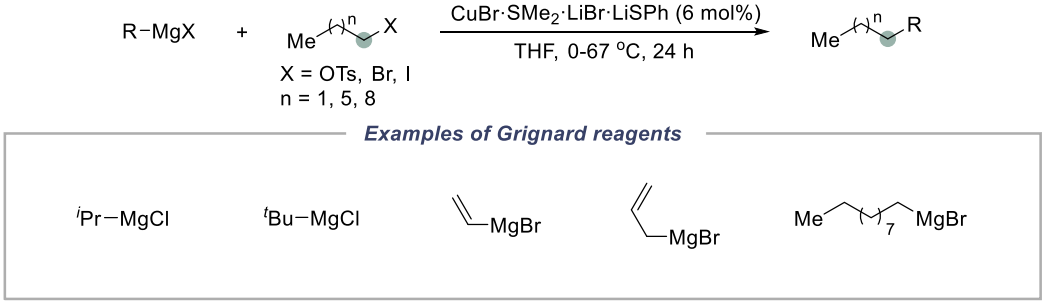

Scheme 3.4 Copper-catalyzed cross-coupling of Grignard reagents with primary alkyl electrophiles.

Unlike the limited employment in C–C bond cross-coupling reaction, catalytic copper promoted C–heteroatom bond construction has found broad applications. Traditional "Ullmann-type" coupling protocols demonstrate limited substrate scope and harsh reaction conditions. Subsequent ligand design for "Ullmann-type" reactions greatly expanded substrate limitations, making this copper-based cross-coupling attractive for both academia and industry.[224] Over the past decades, a decent number

[217] Hofstee, H. K.; Boersma, J.; Van Der Kerk, G. J. M. Reaction of Diarylzinc Compounds with Copper(I) Salts. Synthesis and Characterization of Arylcopper(I) Compounds. *J. Organomet. Chem*. **1978**, *144*, 255–261.
[218] Behling, J. R.; Babiak, K. A.; Ng, J. S.; Campbell, A. L.; Moretti, R.; Koerner, M.; Lipshutz, B. H. In situ Cuprate Formation via Transmetalation between Vinylstannanes and Higher Order Cyanocuprates. *J. Am. Chem. Soc*. **1988**, *110*, 2641–2643.
[219] Takahashi, T.; Hara, R.; Nishihara, Y.; Kotora, M. Copper-Mediated Coupling of Zirconacyclopentadienes with Dihalo Aromatic Compounds. Formation of Fused Aromatic Rings. *J. Am. Chem. Soc*. **1996**, *118*, 5154–5155.
[220] Herron, J. R.; Russo, V.; Valente, E. J; Ball, Z. T. Catalytic Organocopper Chemistry from Organosiloxane Reagents. *Chem. Eur. J*. **2009**, *15*, 8713–8716.
[221] Gurung, S. K.; Thapa, S.; Kafle, A.; Dickie, D. A.; Giri, R. Copper-Catalyzed Suzuki–Miyaura Coupling of Arylboronate Esters: Transmetalation with (PN)CuF and Identification of Intermediates. *Org. Lett*. **2014**, *16*, 1264–1267.
[222] Yang, C.-T.; Zhang, Z.-Q.; Liang, J.; Liu, J.-H.; Lu, X.-Y.; Chen, H.-H.; Liu, L. Copper-Catalyzed Cross-Coupling of Nonactivated Secondary Alkyl Halides and Tosylates with Secondary Alkyl Grignard Reagents. *J. Am. Chem. Soc*. **2012**, *134*, 11124–11127.
[223] Hickman, A. J.; Sanford, M. S. High-Valent Organometallic Copper and Palladium in Catalysis. *Nature* **2012**, *484*, 177–185.
[224] Lin, H.; Sun, D. Recent Synthetic Developments and Applications of the Ullmann Reaction. A Review. *Org. Prep. Proced. Int*. **2013**, *45*, 341–394.

of ligands have been found to effectively promote coupling of aryl halides and nucleophiles, with some distinguished structure shown in Scheme 3.5. They can be divided into: amino acids, 2-picolinic acids, pyrrole2-carboxylic acids, diamines, phenanthroline, 1,3-diketones, (2-pyridyl)acetone, 8-quinolinol, Schiff bases, oxalic diamides and related amides.[225] Mechanistically, a Cu(I)/Cu(III) catalytic cycle has been supported by relevant studies.[226] However, detailed reaction course might vary as it is dependent on the exact reaction parameters. One possibility involves oxidative addition, nucleophiles binding and deprotonation, and product forming reductive elimination (Scheme 3.5, *left*). Complementary mechanisms initiates with nucleophile binding prior to oxidative addition to aryl halides, followed by product-forming reductive elimination from an Cu(III) entity (Scheme 3.5, *right*).

[225] Bhunia, S.; Pawar, G. G.; Kumar, S. V.; Jiang, Y.; Ma, D. Selected Copper-Based Reactions for C–N, C–O, C–S, and C–C Bond Formation. *Angew. Chem. Int. Ed*. **2017**, *56*, 16136–16179.
[226] Sambiagio, C.; Marsden, S. P.; Blacker, A. J.; McGowan, P. C. Copper Catalysed Ullmann Type Chemistry: From Mechanistic Aspects to Modern Development. *Chem. Soc. Rev*. **2014**, *43*, 3525–3550.

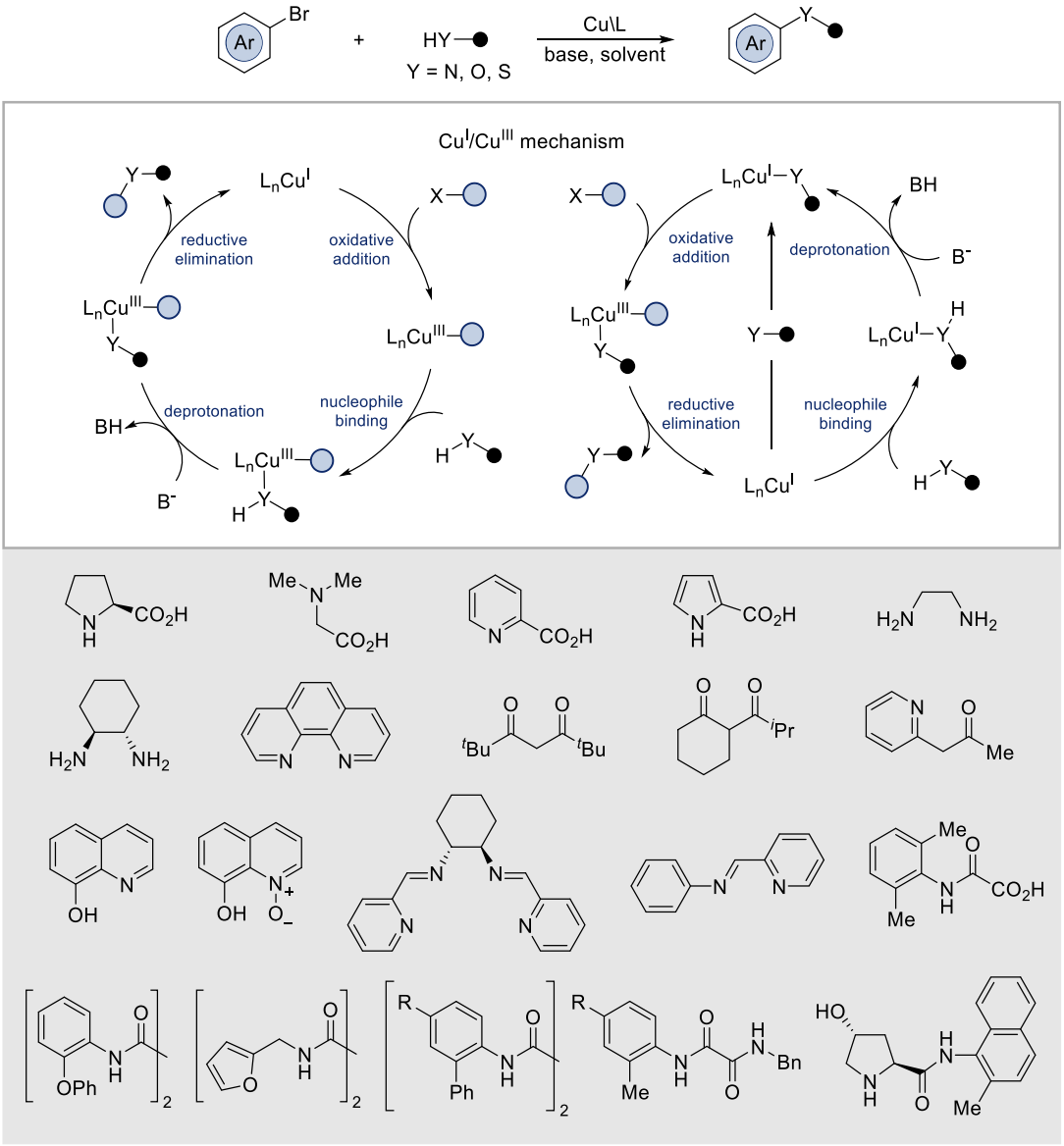

Scheme 3.5 Copper-catalyzed "Ullmann-type" coupling.

As an example of copper-catalyzed "Ullmann-type" reaction for synthetic application, the Ma group utilized Cu/*N,N*-dimethylglycine catalyst system to prepare non-racemic diaryl ethers bearing amino ester moieties from L-tyrosine-derived phenol **3.6a** and L-phenylalanine-derived iodide **3.6b** (Scheme 3.6).[227] The coupling product can be used in the synthesis of ACE inhibitor K-13.

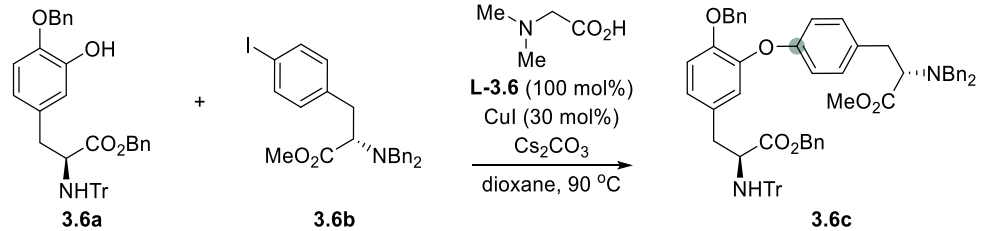

[227] Cai, Q.; He, G.; Ma, D. Mild and Nonracemizing Conditions for Ullmann-type Diaryl Ether Formation between Aryl Iodides and Tyrosine Derivatives. *J. Org. Chem*. **2006**, *71*, 5268–5273.

Scheme 3.6 Copper-catalyzed non-racemizing diaryl ether formation from phenylalanine and tyrosine derivatives.

In 1998, the Chan group[228] and the Lam group[229] independently described the copper-catalyzed coupling of aryl boronic acids with *N*-nucleophiles under air (Scheme 3.7). After these pioneering discoveries, significant progress has been made within the Chan-Lam coupling, using a variety of phenols, amines, anilines, amides, imides, ureas, carbamates and sulfonamides as coupling partners.[230]

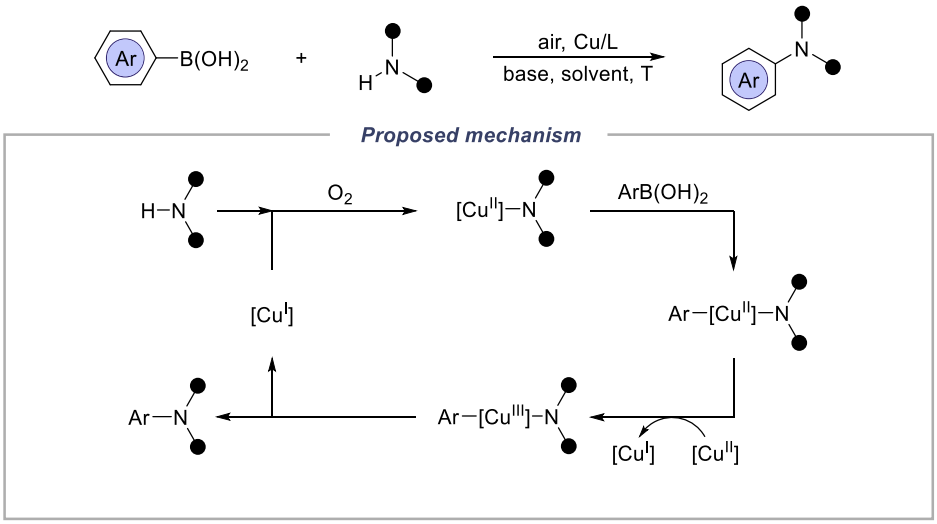

Scheme 3.7 Chan-Lam coupling reaction.

The Chan-Lam oxidative coupling reaction is typically induced by a stoichiometric amount of Cu(II) salts or a catalytic amount of copper precatalyst which is reoxidized by atmospheric oxygen or additional oxidant. Contrary to classical cross-coupling reactions where a pair of nucleophile and electrophile are employed, oxidative coupling refers to the bond construction process between two nucleophiles with the aid of oxidant (Scheme 3.8).[231] As some nucleophiles are abundant chemicals applied in organic synthesis such as hydrocarbons, alcohols and amines, the oxidative coupling reactions could provide an attractive synthetic approach from a step-saving standpoint.[232] Copper catalysis demonstrates low reactivity towards unactivated electrophiles, while many of the Cu-catalyzed oxidative coupling reactions offer

[228] Chan, D. M. T..; Monaco, K. L.; Wang, R.-P.; Winters, M. P. New N- and O-Arylations with Phenylboronic Acids and Cupric Acetate. *Tetrahedron Lett.* **1998**, *39*, 2933–2936.
[229] Lam, P. Y. S.; Clark, C. G.; Saubern, S.; Adams, J.; Winters, M. P.; Chan, D. M. T.; Combs, A. New Aryl/Heteroaryl C–N Bond Cross-Coupling Reactions via Arylboronic Acid/Cupric Acetate Arylation. *Tetrahedron Lett.* **1998**, *39*, 2941–2944.
[230] Chen, J.-Q.; Li, J.-H.; Dong, Z.-B. A Review on the Latest Progress of Chan-Lam Coupling Reaction. *Adv. Synth. Catal.* **2020**, *362*, 3311–3331.
[231] Funes-Ardoiz, I.; Maseras, F. Oxidative Coupling Mechanisms: Current State of Understanding. *ACS Catal.* **2018**, *8*, 1161–1172.
[232] Gulzar, N.; Schweitzer-Chaput, B.; Klussmann, M. Oxidative Coupling Reactions for the Functionalisation of C–H Bonds Using Oxygen. *Catal. Sci. Technol.* **2014**, *4*, 2778–2796

advantages over analogous two-electron oxidation reactions mediated by palladium or other noble metals.

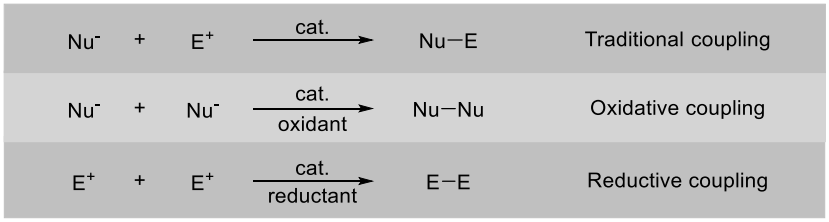

Scheme 3.8 Classification of cross-coupling reactions.

In this aspect, Li and co-workers reported the coupling of *N,N*-dialkylaniline and alkyne and they named the reaction as copper-catalyzed CDC (cross dehydrogenative coupling) reaction.[233] Sequentially they realized the synthesis of *β*-carbonylamine from tetrahydroisoquinolines with malonic acid esters catalyzed in presence of *tert*-butyl hydroperoxide as the oxidant in 2005 (Scheme 3.9).[234] The possible reaction mechanism was proposed: the tertiary amine is oxidized to form an iminium intermediate coordinated with the copper catalyst, meanwhile the malonate ester forms a six-membered ring intermediate coordinated with copper upon enolization. The two intermediates then undergo "Mannich-type" reaction to produce the desired final product and regenerate the copper catalyst. Following the concept of CDC, the Li group developed a series of copper-catalyzed oxidative coupling reactions.[235] Many of CDC coupling reactions rely on the organometallic species nucleophilic attack onto a stabilized carbocation intermediate, which is produced by the oxidative H-removal (Scheme 3.9, *bottom*).[236]

[233] Li, Z.; Li, C.-J. CuBr-Catalyzed Efficient Alkynylation of sp^3 C-H Bonds Adjacent to a Nitrogen Atom. *J. Am. Chem. Soc*. **2004**, *126*, 11810–11811.
[234] Li, Z.; Li, C.-J. Highly Efficient CuBr-Catalyzed Cross-Dehydrogenative Coupling (CDC) between Tetrahydroisoquinolines and Activated Methylene Compounds. *Eur. J. Org. Chem*. **2005**, 3173–3176.
[235] (a) Tian, T.; Li, Z.; Li, C.-J. Cross-Dehydrogenative Coupling: a Sustainable Reaction for C–C Bond Formations. *Green Chem*. **2021**, *23*, 6789–6862. (b) Li, C.-J. Cross-Dehydrogenative Coupling (CDC): Exploring C−C Bond Formations beyond Functional Group Transformations. *Acc. Chem. Res*. **2009**, *42*, 335–344.
[236] Boess, E.; Schmitz, C.; Klussmann, M. A Comparative Mechanistic Study of Cu-Catalyzed Oxidative Coupling Reactions with N-Phenyltetrahydroisoquinoline. *J. Am. Chem. Soc*. **2012**, *134*, 5317–5325.

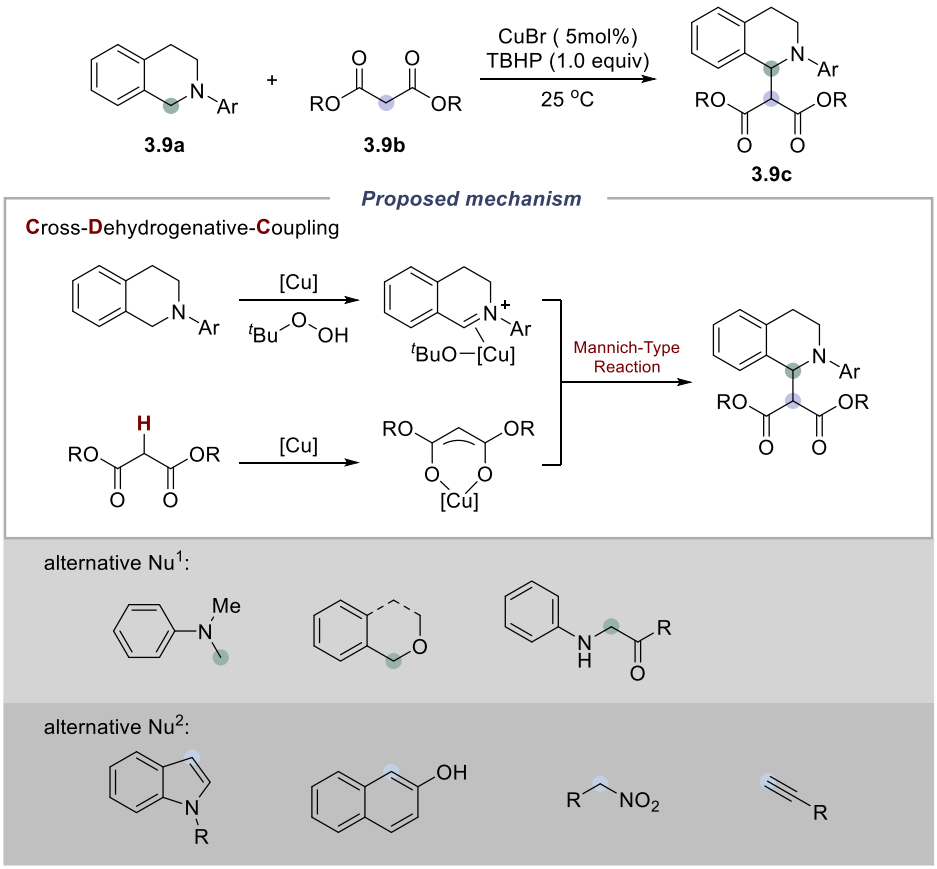

Scheme 3.9 Copper-catalyzed cross-dehydrogenative coupling.

Further exploration of the copper-catalyzed oxidative coupling reactions was focused on intercepting the carbon-centered radical, which is produced by a single-electron oxidation of C–H bond by oxidant or H-abstractor. In 2014, Hartwig and co-workers described the copper-catalyzed amidation and imidation of unactivated alkanes (Scheme 3.10).[237] As shown in the general mechanism (Scheme 3.10), the alkane activation relies on hydrogen atom abstraction mediated by *tert*-butoxy radical. Then alkyl radical **3.10h** is captured by nucleophile bounded copper complex **3.10f**. Final alkane functionalization is realized via reductive elimination from high valent copper complex **3.10g**. The subsequent studies demonstrate the possibility of installing

[237] Tran, B. L.; Li, B. J.; Driess, M.; Hartwig, J. F. Copper-Catalyzed Intermolecular Amidation and Imidation of Unactivated Alkanes. *J. Am. Chem. Soc*. **2014**, *136*, 2555−2563.

cyanide,[238] arene,[239] alkyne,[240] fluoroalkane,[241] amide,[242] alcohol,[243] carboxylic acid moieties[244] on inherent C(sp^3)–H bonds even in an enantioselective manner.[245] In fact, alkyl radical generation via hydrogen atom transfer (HAT) nowadays represents one of the most powerful techniques for unactivated C(sp^3)–H bond functionalization,[246] which exhibits unique profile of reactivity and selectivity compared to transition metal-catalyzed C–H bond activation.[247]

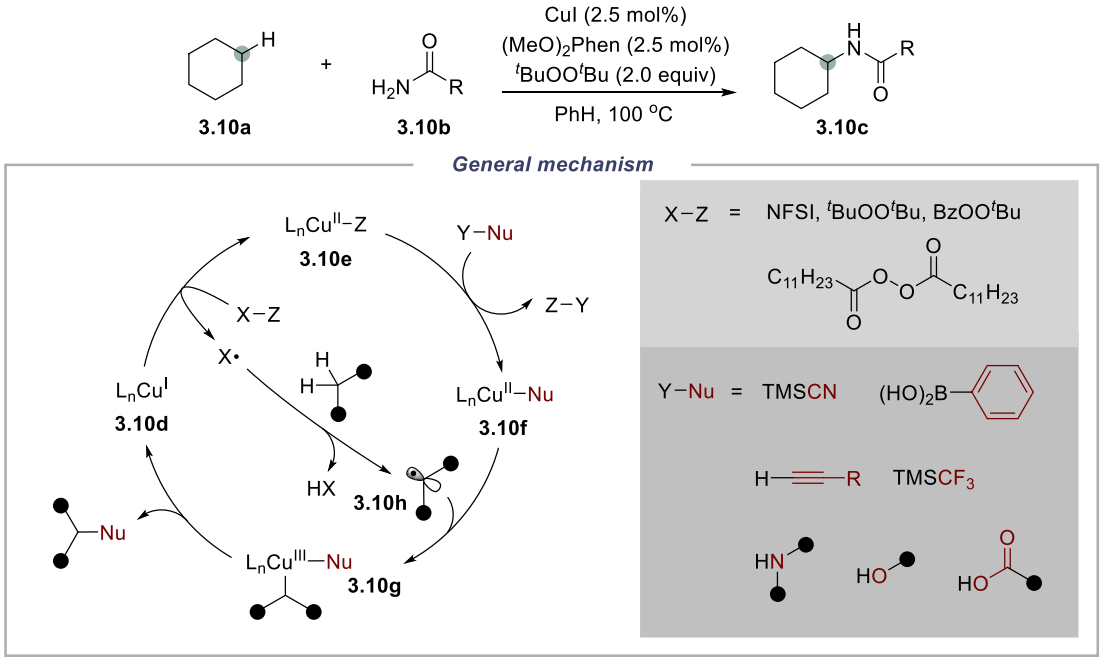

[238] Zhang, W.; Wang, F.; McCann, S. D.; Wang, D.; Chen, P.; Stahl, S. S. Liu, G. Enantioselective cyanation of benzylic C–H bonds via copper-catalyzed radical relay. *Science* **2016**, *353*, 1014–1018.
[239] Zhang, W.; Chen, P.; Liu, G. Copper-Catalyzed Arylation of Benzylic C–H bonds with Alkylarenes as the Limiting Reagents. *J. Am. Chem. Soc*. **2017**, *139*, 7709–7712.
[240] Fu, L.; Zhang, Z.; Chen, P.; Lin, Z.; Liu, G. Enantioselective Copper-Catalyzed Alkynylation of Benzylic C–H Bonds via Radical Relay. *J. Am. Chem. Soc*. **2020**, *142*, 12493–12500.
[241] Xiao, H.; Liu, Z.; Shen, H.; Zhang, B.; Zhu, L.; Li, C. Copper-Catalyzed Late-Stage Benzylic C(sp3)–H Trifluoromethylation. *Chem* **2019**, *4*, 940–949.
[242] Pelletier, G.; Powell, D. A. Copper-Catalyzed Amidation of Allylic and Benzylic CH Bonds. *Org. Lett*. **2006**, *8*, 6031–6034.
[243] Hu, H.; Chen, S.-J.; Mandal, M.; Pratik, S. M.; Buss, J. A.; Krska, S. W.; Cramer, C. J.; Stahl, S. S. Copper-Catalysed Benzylic C–H Coupling with Alcohols via Radical Relay Enabled by Redox Buffering. *Nat Catal* **2020**, *3*, 358–367.
[244] Tran, B. L.; Driess, M.; Hartwig, J. F. Copper-Catalyzed Oxidative Dehydrogenative Carboxylation of Unactivated Alkanes to Allylic Esters via Alkenes. *J. Am. Chem. Soc*. **2014**, *136*, 17292–17301.
[245] (a) Zhang, Z.; Chen, p.; Liu, G. Copper-Catalyzed Radical Relay in C(sp^3)–H Functionalization. *Chem. Soc. Rev*. **2022**, *51*, 1640–1658. (b) Munoz-Molina, J. M.; Belderrain, T. R.; Perez, P. J. Recent Advances in Copper-Catalyzed Radical C-H Bond Activation Using N-F Reagents. *Synthesis* **2021**, *53*, 51–64.
[246] Yi, H.; Zhang, G.; Wang, H.; Huang, Z.; Wang, J.; Singh, A. K.; Lei, A. Recent Advances in Radical C−H Activation/Radical Cross-Coupling. *Chem. Rev*. **2017**, *117*, 9016−9085.
[247] Gandeepan, P.; Müller, T.; Zell, D.; Cera, G.; Warratz, S.; Ackermann, L. 3d Transition Metals for C–H Activation. *Chem. Rev*. **2019**, *119*, 2192–2452.

Scheme 3.10 Copper-catalyzed C(sp^3)–H functionalization.

Inspired by the feasibility of intercepting carbon-centered radicals in copper-catalyzed cross-coupling reactions, a series of research works aiming at interrupting alkyl radicals were developed afterwards. For instance, Zhu and co-workers developed a copper-catalyzed arylation protocol, based on the idea of capturing benzylic radical with aryl copper(II) species (Scheme 3.11). [248] The SET reduction of *N*-fluorosulfonamides **3.11a** by Cu(I) complex provides amidyl radical **3.11d**, thus setting the basis for benzylic radical generation via 1,5-hydrogen atom transfer.

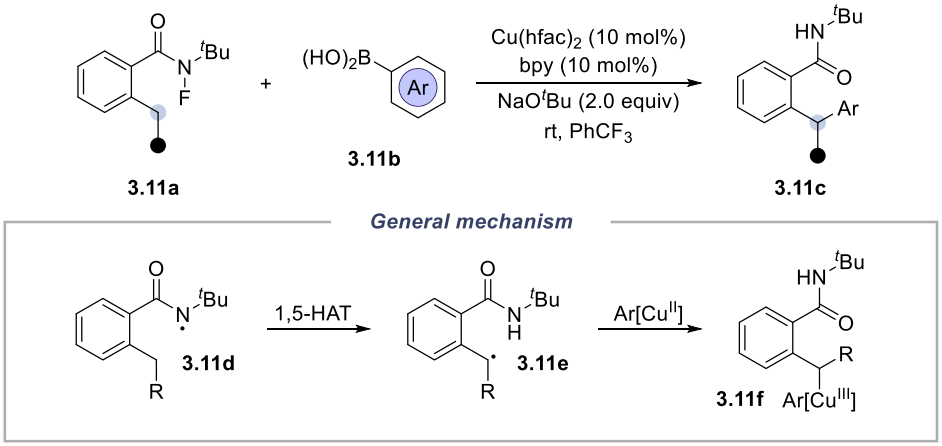

Scheme 3.11 Copper-catalyzed arylation of benzylic C(sp^3)–H bonds via 1,5-HAT.

It is important to note that the introducing of photocatalysis in copper-catalyzed cross-coupling reactions could significantly improve the oxidative addition ability of low-valent copper species. However, this part will no longer be discussed herein, as relevant background has been illustrated in chapter I.

3.1.2 C–H Aminations via Nitrene Transfer

3.1.2.1 Fundamentals of Nitrene

Nitrene is the nitrogen analogue of a carbene. Similar to carbon-centered carbenes, there are two possible spin states of carbenes, depending on the whether the two non-bonding electrons have their spins paired or unpaired (Scheme 3.12). In general, nitrene obeys Hund's rule, which means low energy form of free nitrene is the triplet state with one electron in each of the *p* orbitals. And the high energy form is the singlet state with two electron pairs filling two sp^2 orbitals and other *p* orbital vacant. The energy difference between the singlet and triplet states is estimated to be 145 kJ/mol.

[248] Li, Z.; Wang, Q.; Zhu, J. Copper-Catalyzed Arylation of Remote C(sp^3)–H Bonds in Carboxamides and Sulfonamides. *Angew. Chem. Int. Ed*. **2018**, *57*, 13288–13292.

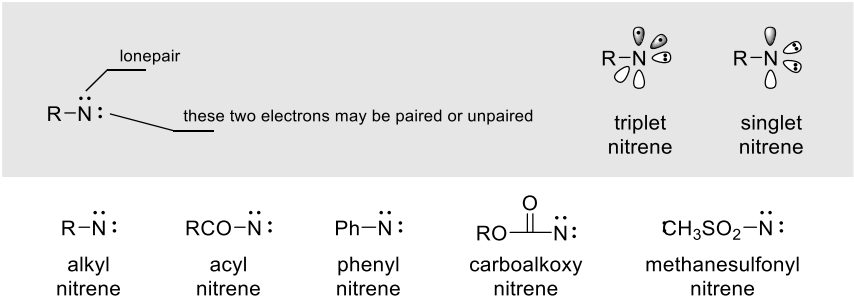

Scheme 3.12 Nitrene electronic structure and category.

Free nitrene is a highly transient species, and a common and effective way to study nitrene chemistry is through a transition metal nitrene complex derived from nitrene precursors (Scheme 3.13). A simplified mechanism of transition-metal-mediated nitrene transfer reaction involves initial reaction of a metal catalyst L_nM with nitrene precursor RN=LG to form metal-nitrene species. There are two major reactivity patterns that have been broadly studied for metal nitrene intermediates — nitrene addition to C=C bond and nitrene insertion into C–H bond. Depending on the electronic structure of the nitrene species, the reaction can occur through either a concerted or a stepwise pathway. Concerted nitrene transfer reactions has been reported for Rh, Ru and Ir complexes. While metals that participate in stepwise nitrene transfer reactions include Fe, Ru, Cu, Co and Ag, among the others.[249]

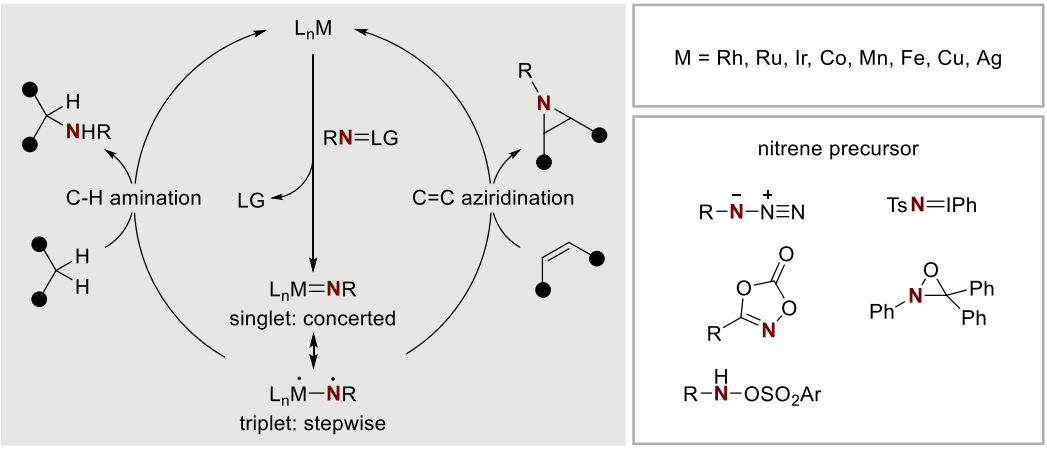

Scheme 3.13 Transition metal-catalyzed nitrene transfer reaction.

Pioneering research from Breslow and co-workers demonstrated the first metal mediated nitrene C–H bond insertion by Mn and Fe porphyrins catalyst, transferring what was known for P-450 oxidations into an artificial system for aminations.[250]

[249] Ju, M.; Schomaker, J. M. Nitrene Transfer Catalysts for Enantioselective C–N Bond Formation. *Nat Rev Chem* **2021**, *5*, 580–594.
[250] Breslow, R.; Gellman, S. H. Tosylamidation of Cyclohexane by a Cytochrome P-450 Model. *J. Chem. Soc., Chem. Commun.* **1982**, 1400–1401.

Stemming from the pioneering breakthroughs, the field of nitrene insertions has matured into reliable methodology, with current efforts being focused on asymmetric intermolecular C–H amination reactions.[251]

3.1.2.2 Copper-Catalyzed C–H Aminations via Nitrene Transfer

With respect to copper catalysis, Pérez and co-workers demonstrated the catalytic nitrene insertion into C–H bonds of cyclohexane, toluene and ethers, giving rise to trisubstituted amines in moderate to high yields (Scheme 3.14).[252] Using PhI=NTs as the nitrene source and TpCu(I) derivatives as catalyst, this reaction was enabled by generating the corresponding copper nitrene species *in situ*.

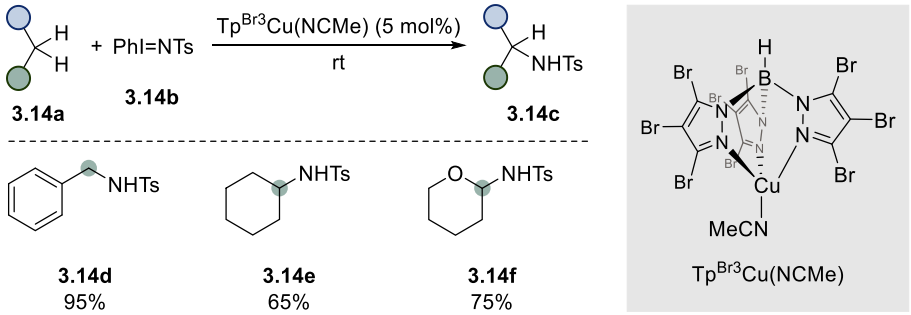

Scheme 3.14 Copper-catalyzed intermolecular nitrene C–H bond insertion.

Warren and co-workers investigated the diketiminato copper complex catalyzed C–H amination reaction with diazo compounds as nitrene precursors (Scheme 3.15).[253] The reaction exhibit excellent regioselectivity, depending on the BDE value of the corresponding C–H bond. Proposed mechanism for the catalytic C–H amination reaction is a stepwise process, starting with a HAT abstraction followed by radical rebound to form the product. A benzylic radical clock experiment with compound **3.15h** supports the stepwise mechanism, as only ring-opened C–H amination product **3.15j** was obtained. In addition, DFT calculations were employed to study the putative copper nitrene intermediate, and the multireference techniques predict the occupations of

[251] Hayashi, H.; Uchida, T. Nitrene Transfer Reactions for Asymmetric C–H Amination: Recent Development. *Eur. J. Org. Chem*. **2020**, 909–916.
[252] (a) Díaz-Requejo, M. M.; Belderraín, T. R.; Nicasio, M. C.; Trofimenko, S.; Pérez, P. J. Cyclohexane and Benzene Amination by Catalytic Nitrene Insertion into C−H Bonds with the Copper-Homoscorpionate Catalyst Tp^{Br3}Cu(NCMe). *J. Am. Chem. Soc*. **2003**, *125*, 12078–12079 (b) Fructos, M. R.; Trofimenko, S.; Diaz-Requejo, M. M.; Pérez, J. P. Facile Amine Formation by Intermolecular Catalytic Amidation of Carbon–Hydrogen Bonds. *J. Am. Chem. Soc*. **2006**, *128*, 11784–11791.
[253] Badiei, Y. M.; Dinescu, A.; Dai, X.; Palomino, R. M.; Heinemann, F. W.; Cundari, T. R.; Warren, T. H. Copper–Nitrene Complexes in Catalytic C–H Amination. *Angew. Chem. Int. Ed*. **2008**, *47*, 9961–9964.

Cu−N π and π^* orbitals are approximately 1.5 e and 0.5 e, respectively.[254]

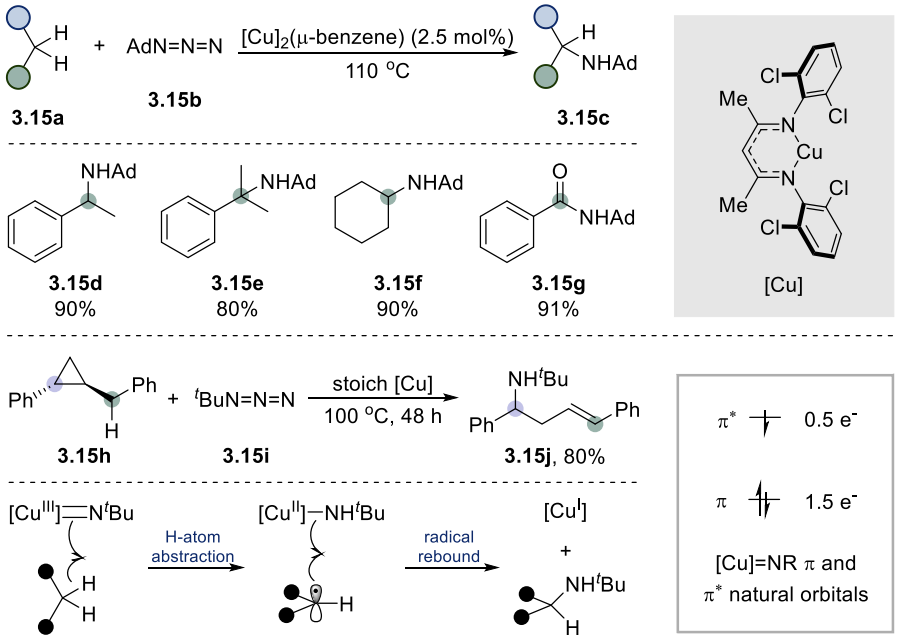

Scheme 3.15 Nitrene C–H bond insertion enabled by *β*-diketiminato copper complex.

3.2 General Aim of the Project

At the outset of our investigation, a general and practical platform that enables C(sp^3)–N bond-formation via catalytic ketone C–C cleavage still remained unavailable. Driven by this observation, we believed a solution to the preceding methodology gap could be achieved through the conversion of ketones into pro-aromatic analogues. These pro-aromatic structures might generate alkyl radical intermediates via site-selective homolytic C–C bond-cleavage under net oxidative conditions. If the latter could be interfaced with the ability of Cu catalysis to enable C(sp^3)–N formation, this transformation would constitute a *de novo* strategy for accessing C(sp^3)–N structures from ketone derivatives (Scheme 3.16). The following part of this chapter will focus on the reaction investigation. This includes establishing reaction conditions and exploring the reaction synthetic potential.

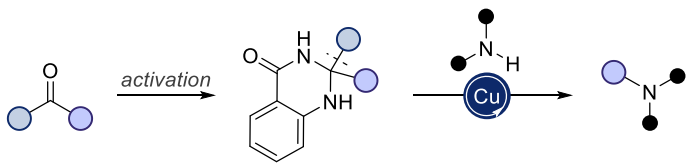

Scheme 3.16 Ketones as traceless synthons for forging C(sp^3)–N linkages.

[254] (a) Aguila, M. J. B.; Badiei, Y. M.; Warren, T. H. Mechanistic Insights into C−H Amination via Dicopper Nitrenes. *J. Am. Chem. Soc.* **2013**, *135*, 9399−9406. (b) Gephart, III, R. T.; Warren, T. H. Copper-Catalyzed sp^3 C−H Amination. *Organometallics* **2012**, *31*, 7728−7752.

3.3 Optimization

A detailed description of our proposal for harnessing ketone as cross-coupling handle in copper catalyzed amination event is outlined in Scheme 3.17. Initial oxidation of an in situ generated Cu(I)-amido intermediate **3.17a** leads to Cu(II) species **3.17b**. Then oxidant activates dihydroquinazolinone and release alkyl radical **3.17e**. Radical **3.17e** is expected to be intercepted by Cu(II) species **3.17b** forming alkyl-Cu(III)-amido entity **3.17c**. Reductive elimination of Cu(III) intermediate **3.17c** results in the targeted C(sp^3)–N coupling product while recovering back the propagating Cu(I)-amido intermediate.

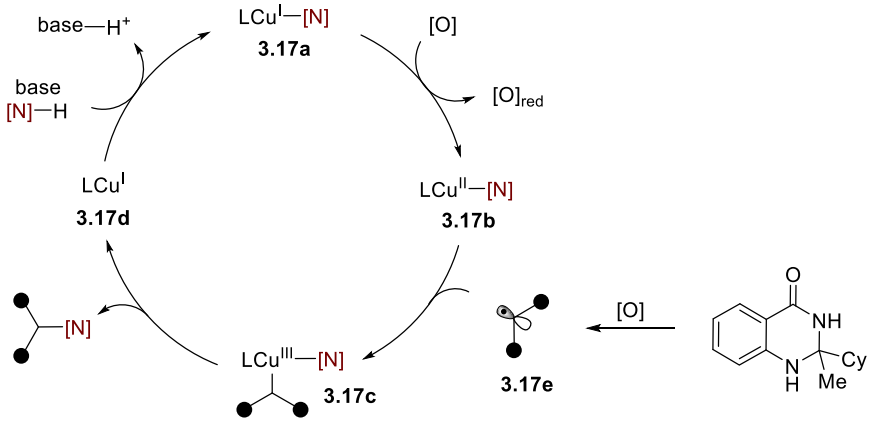

Scheme 3.17 Copper-catalyzed C(sp^3)-amination of ketone-derived dihydroquinazolinones: reaction proposal.

We started our study by choosing indazole **1a** and dihydroquinazolinone **2a** as the model substrate. The initial optimization studies focused on screening a variety of oxidants, as an oxidant plays crucial role in modulating the oxidation state of copper intermediate and activating the dihydroquinazolinones. As shown in Table 2.1, a series of commonly used oxidants were tested. In all cases the C(sp^3)–N coupling product was detected. Among all oxidants tested, it was observed that *tert*-butyl peroxybenzoate was the most effective for this transformation, providing the C(sp^3)–N coupling product in 83% yield (entry 6). Lower yields were obtained when 2.5 or 1.5 equivalent of the *tert*-butyl peroxybenzoate was utilized (entry 10). Interestingly, analogous di-*tert*-butyl peroxide and dicumyl peroxide (entry 7, 8) and benzoyl peroxide (entry 9) failed to provide comparable results. Under limited number of detections, no *N*-methylation product derived from **1a** was detected, probably due to thermodynamic stability of cyclohexyl radical over methyl radical in solution.

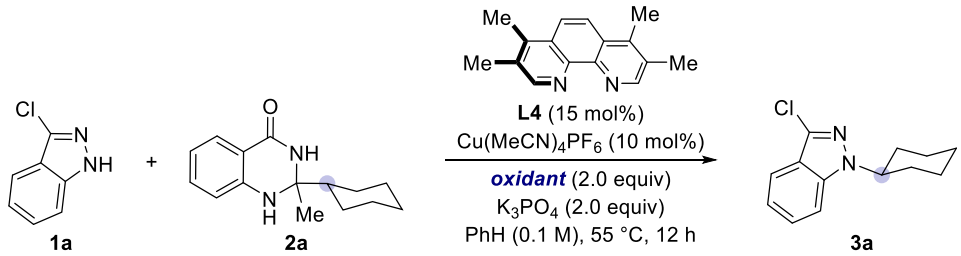

1a + 2a → 3a

entry	oxidant	**3a** (%)[b]
1	NFSI	18
2	selectfluor	25
3	$Na_2S_2O_8$	4
4	oxone	13
5	$PhI(OAc)_2$	2
6	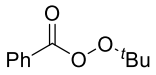	83
7	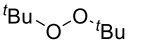	12
8	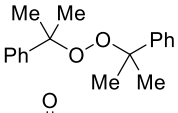	27
9	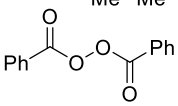	15
10	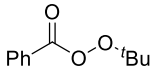	81[c], 63[d]

[a] Conditions: **1a** (0.10 mmol), **2a** (0.12 mmol), $Cu(MeCN)_4PF_6$ (10 mol%), **L1** (15 mol%), $BzOO^tBu$ (2.0 equiv), K_3PO_4 (0.20 mmol) in benzene (0.10 M) at 55 °C for 12 h. [b] GC yield and conversion using dodecane as internal standard. [c] 1.5 equiv of oxidant was used. [d] 2.5 oxidant was used.

Table 3.1 Screening of oxidants.

With *tert*-butyl peroxybenzoate as the optimal oxidant, the effect of ligands on the reaction outcome was investigated. As shown in Table 3.2, a series of bidentate and tridentate nitrogen ligands were tested (**L1**–**L12**), resulting in the product formation in good yields. Specifically, it was observed that in this transformation phenanthroline ligands (**L1**–**L9)** tend to perform better than terpyridine ligand (**L10**) and bipyridine ligand (**L12**). In the phenanthroline series, inferior results were obtained for ligands having electro-donating group (**L5**) or electro-withdrawing group (**L6**) on the phenanthroline backbone or substituents adjacent to the coordinating nitrogen (**L8**, **L9**). Among all the phenanthroline ligands series, tetramethyl substituted **L4** provided the best result, affording the cross-coupling product **3a** in 89% yield. The better performance of **L4** over **L1** might result from blocking some side reactions (homodimerization, etc.) initiated by radicals at the phenanthroline backbone. The use of other bidentate nitrogen ligand (**L11**) led to lower yield.

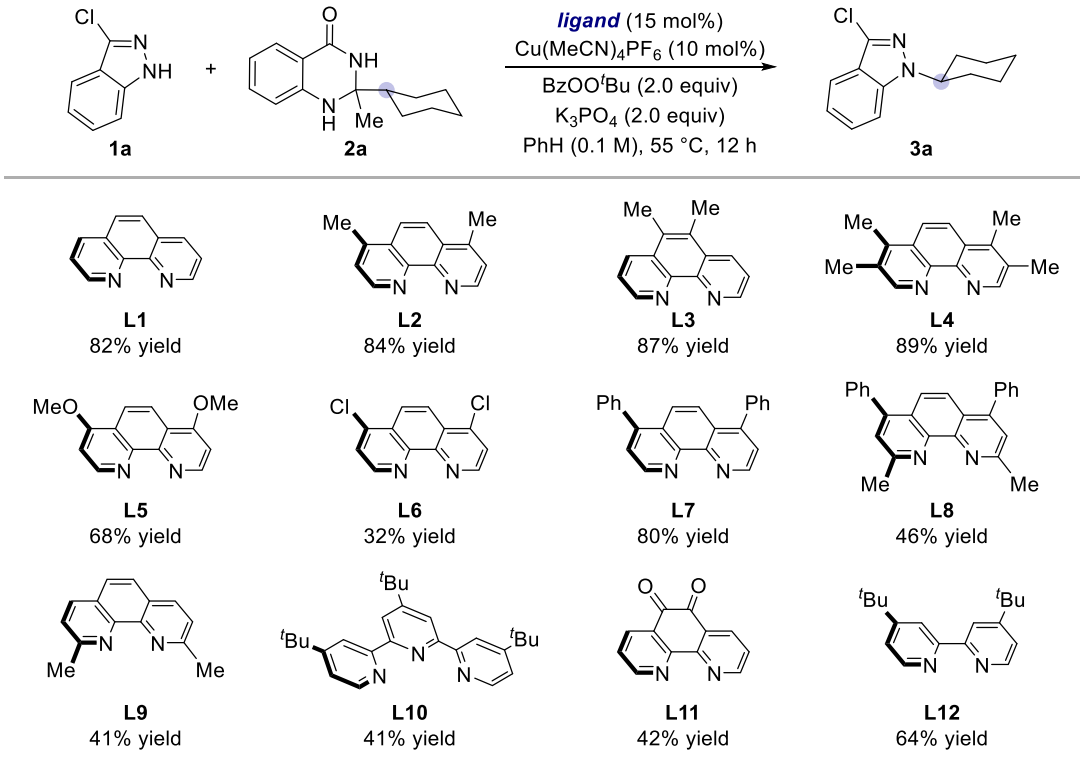

[a] Conditions: **1a** (0.10 mmol), **2a** (0.12 mmol), $Cu(MeCN)_4PF_6$ (10 mol%), ligand (15 mol%), $BzOO^tBu$ (2.0 equiv), K_3PO_4 (0.20 mmol) in benzene (0.10 M) at 55 °C for 12 h. [b] GC yield and conversion using dodecane as internal standard.

Table 3.2 Screening of ligands.

The effect of copper precatalyst was investigated . As shown in Table 3.3, a series of copper(I) and copper (II) precatalysts could provide **3a** in good yields. The best result was found when utilizing $Cu(MeCN)_4PF_6$ (entry 1). Since the reaction is conducted under oxidative conditions, the *in situ* generated Cu(III) species could undergo reductive elimination to provide Cu(I) complex, which might explain TON number greater than one in case of Cu(II) precatalysts (entry 7–10).

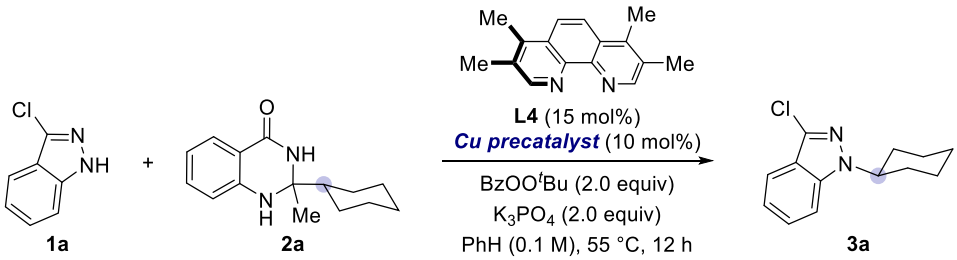

entry	Cu precatalyst	**3a** (%)[b]
1	$Cu(MeCN)_4PF_6$	89
2	$Cu(MeCN)_4BF_4$	81
3	CuTc	83
4	CuCl	62
5	CuBr	80
6	CuI	80
7	$CuCl_2$	75
8	$CuBr_2$	75
9	$Cu(OTf)_2$	76
10	$Cu(TMHD)_2$	62

[a] Conditions: **1a** (0.10 mmol), **2a** (0.12 mmol), Cu precatalyst (10 mol%), **L4** (15 mol%), BzOO^{t}Bu (2.0 equiv), K_3PO_4 (0.20 mmol) in benzene (0.10 M) at 55 °C for 12 h. [b] GC yield and conversion using dodecane as internal standard.

Table 3.3 Screening of copper precatalysts.

The evaluation of different bases was undertaken next. As shown in Table 3.4, inorganic bases (entry 1-7) afforded product **3a** in varying degrees of success. Employment of strong bases gave lower yields (entry 3–7), whereas weaker base K_3PO_4 provided the desired product in 89% yield (entry 2). The investigation of commonly used carbonate base Cs_2CO_3 and strong organic base BTMG furnished moderate yield (entry 1, 8).

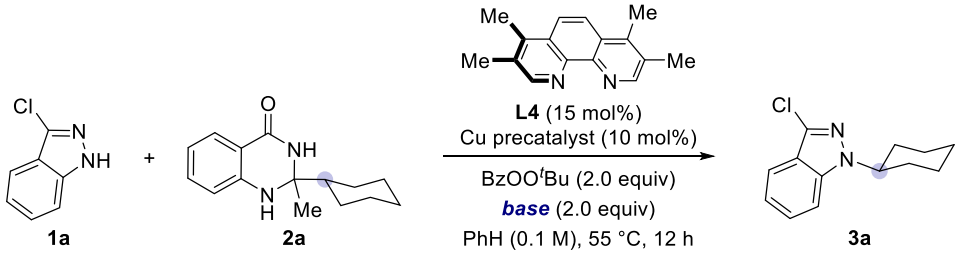

entry	base	**3a** (%)[b]
1	Cs_2CO_3	48
2	K_3PO_4	89
3	^{t}BuOLi	35
4	^{t}BuONa	44
5	^{t}BuOK	48
6	NaH	37
7	LiHMDS	37
8	BTMG	45

[a] Conditions: **1a** (0.10 mmol), **2a** (0.12 mmol), $Cu(MeCN)_4PF_6$ (10 mol%), **L4** (15 mol%), BzOO^{t}Bu (2.0 equiv), base (0.20 mmol) in benzene (0.10 M) at 55 °C for 12 h. [b] GC yield and conversion using dodecane as internal standard.

Table 3.4 Screening of bases.

Next, the effect of solvents on the reaction outcome was studied (Table 3.5). After screening a number of solvents, inferior results were found with polar aprotic solvents such as MeCN (entry 1), EA (entry 3), DMF (entry 8) and DMSO (entry 9). Among less polar solvents tested, arene-containing solvents tended to give better performance (entry 5–7), with benzene providing the best result (entry 5). Another, satisfactory results were obtained with protic ^{t}BuOH (entry 10), halogen-containing DCE (entry 4) and dioxane (entry 2).

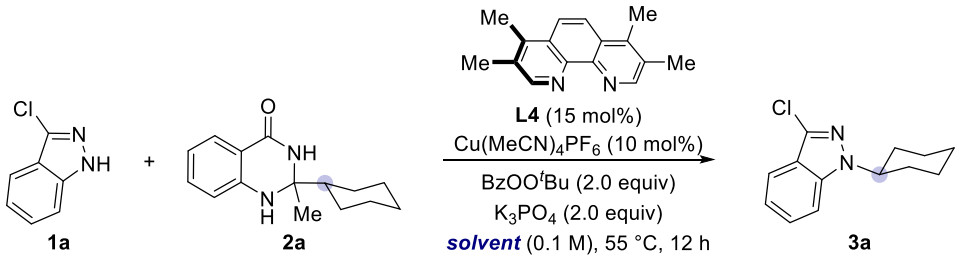

entry	solvent	**3a** (%)[b]
1	MeCN	37
2	dioxane	59
3	EA	53
4	DCE	81
5	PhH	89
6	PhCl	84
7	$PhCF_3$	76
8	DMF	30
9	DMSO	30
10	^{t}BuOH	69

[a] Conditions: **1a** (0.10 mmol), **2a** (0.12 mmol), $Cu(MeCN)_4PF_6$ (10 mol%), **L4** (15 mol%), BzOO^{t}Bu (2.0 equiv), K_3PO_4 (0.20 mmol) in solvent (0.10 M) at 55 °C for 12 h. [b] GC yield and conversion using dodecane as internal standard.

Table 3.5 Screening of solvents.

Finally, control experiments were carried out to ensure all the reaction parameters were essential for the deacylative amination to get high efficiency. Indeed, as shown in Table 3.6, no product was formed in the absence of copper precatalyst (entry 2) or oxidant (entries 5). Lower yield was obtained without ligand (entry 3), might due to the lower stability of copper intermediate. Poor reaction performance was also observed without using a base (entry 4), which might be attributed to the lack of base facilitation for copper(I)-amido complex generation. The best outcome was found when conducting the reaction at 55 °C, obtaining C(sp^3)–N coupling product in 83% isolated yield. Lowering the temperature to 45 °C or increasing to 65 °C resulted in lower product yields (entries 6 and 7).

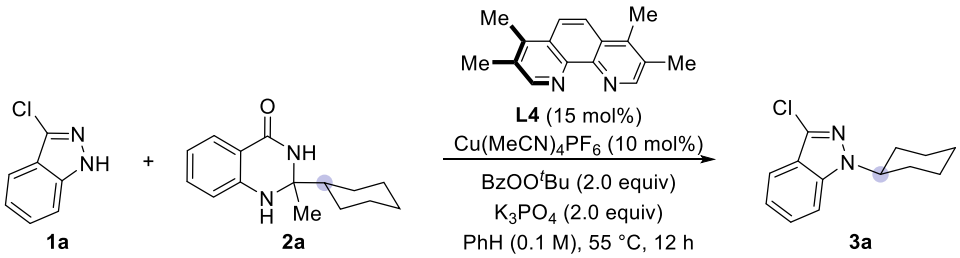

1a + **2a** → **3a**

entry	deviation standard conditions	**3a** (%)[b]
1	none	89 (83)[c]
2	no Cu	<1
3	no ligand	42
4	no base	30
5	no oxidant	<1
6	45 °C	41
7	65 °C	84

[a] Conditions: **1a** (0.10 mmol), **2a** (0.12 mmol), $Cu(MeCN)_4PF_6$ (10 mol%), **L4** (15 mol%), $BzOO^tBu$ (2.0 equiv), K_3PO_4 (0.20 mmol) in benzene (0.10 M) at 55 °C for 12 h. [b] GC yield and conversion using dodecane as internal standard. [c] isolated yield.

Table 3.6 Control experiments.

3.4 Substrate Scope

3.4.1 Scope of Ketone Derived Dihydroquinazolinones

Utilizing the established reaction conditions shown in Table 3.6 (entry 1), the generality of the amination protocol of dihydroquinazolinones via C–C bond cleavage was investigated. As shown in Scheme 3.18, the site-selectivity of the C–C bond scission could be modulated by judicious selection of the substituent on the dihydroquinazolinone core. Specifically, secondary alkyl congeners were transferred preferentially over methyl and primary alkyl residues, allowing dihydroquinazolinones derived from acetyl and propionyl groups to be used (**3a**). Cyclic alkyl moieties possessing different ring sizes and heteroatom back-bones participated well in delivering the targeted C–N coupled products (**3b**–**3e**). Notably, our protocol was extended to acyclic secondary alkyl units (**3f**) in good yield including unsymmetrical examples (**3g**, **3h**). As shown for **3i** and **3j**, aminated trans-1,4-cyclohexanes containing trifluoromethyl or *p*-chlorophenyl substituents were prepared in good diastereomeric ratios. Illustrated by Scheme 3.18 (*bottom*), primary alkyl fragments could be transferred with dihydroquinazolinones bearing methyl (**3k**–**3m**) or aromatic residues (**3k**, **3n**-**s**). It is worth noting this preference for alkyl bond scission over C(sp^3)–C(sp^2) bond cleavage provides an alternative selectivity to the Beckmann rearrangement and

transition-metal-catalyzed C–C activations of ketones.[255,256] Consequently, primary C(sp^3) centers could be transferred when using substrates containing heteroatoms (**3l**, **3m**), proximal *β*-substituents (**3n**), azide (**3o**) or pendant aromatic primary alkyl centers possessing esters (**3q**), silyl ethers (**3r**) and alkyl chlorides (**3s**). The latter observations are noteworthy, as weak C–H bonds may be susceptible to hydrogen-atom transfer with *tert*-butoxy radical formed by Cu-catalyzed decomposition of BzOO^{t}Bu.[257]

[255] (a) Kaur, K.; Srivastava, S. Beckmann Rearrangement Catalysis: A Review of Recent Advances. *New J. Chem*. **2020**, *44*, 18530–18572. (b) Tang, L.; Wang, Z.-L.; Wan, H.-L.; He, Y.-H.; Guan, Z. Visible-Light-Induced Beckmann Rearrangement by Organic Photoredox Catalysis. *Org. Lett*. **2020**, *22*, 6182–6186. (c) Zhang, X.; Rovis, T. Photocatalyzed Triplet Sensitization of Oximes Using Visible Light Provides a Route to Nonclassical Beckmann Rearrangement Products. *J. Am. Chem. Soc*. **2021**, *143*, 21211–21217.

[256] (a) Jun, C. -H. Transition Metal-Catalyzed Carbon–Carbon Bond Activation. *Chem. Soc. Rev*. **2004**, *33*, 610–618. (b) Deng, L.; Dong, G. Carbon–Carbon Bond Activation of Ketones. *Trends Chem*. **2020**, *2*, 183–198.

[257] Punniyamurthy, T.; Rout, L. Recent Advances in Copper-Catalyzed Oxidation of Organic Compounds. *Coord. Chem. Rev*. **2008**, *252*, 134–154.

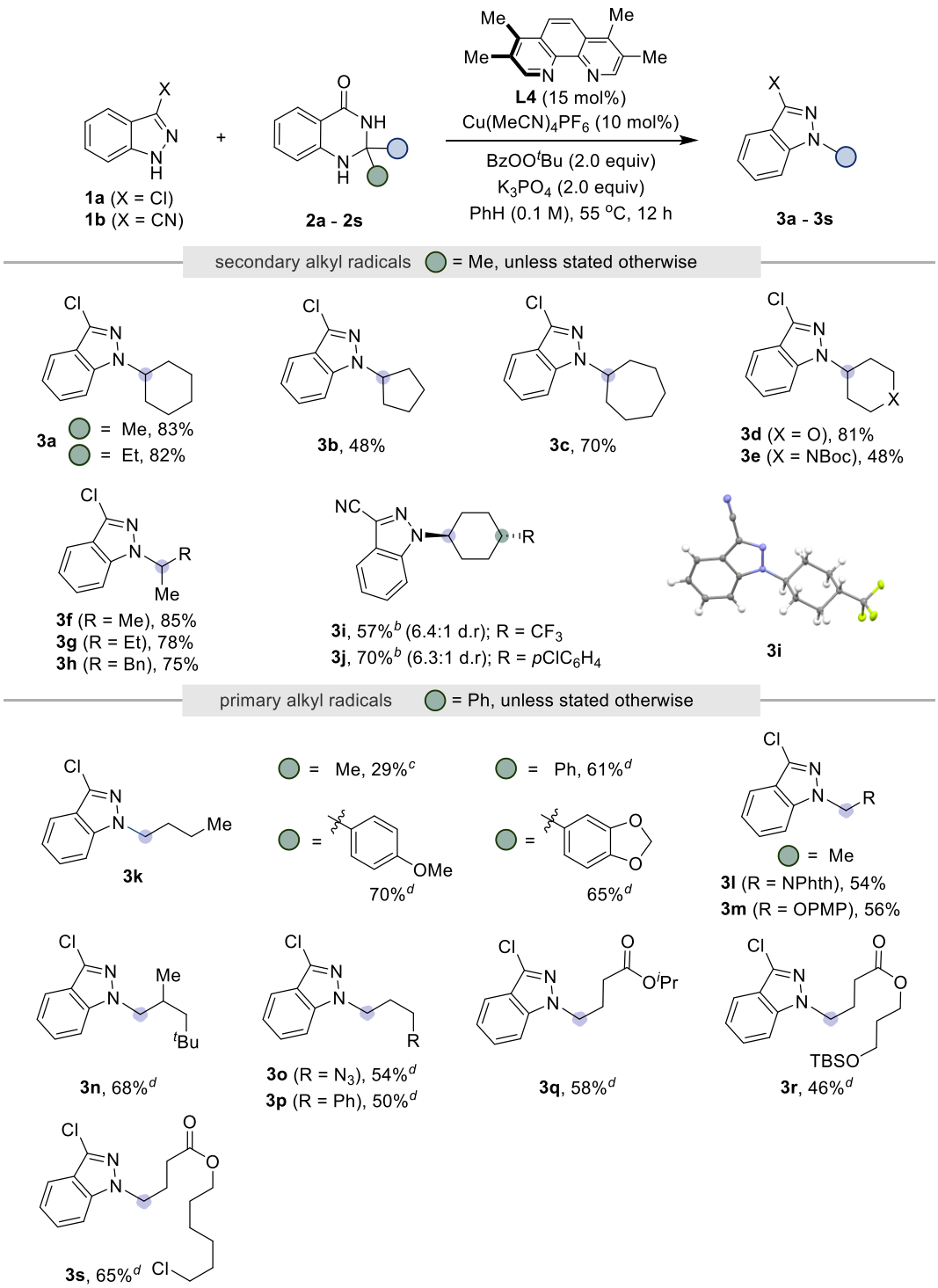

[a] Conditions: **1a** (0.20 mmol), **2a** (0.24 mmol), $Cu(MeCN)_4PF_6$ (10 mol%), **L4** (15 mol%), $BzOO^tBu$ (2.0 equiv), K_3PO_4 (2.0 equiv) in benzene (0.10 M) at 55 °C for 12 h; yields of isolated product, average of two independent runs. [b] Using $Cu(MeCN)_4PF_6$ (20 mol%) and **L4** (30 mol%) at 65 °C; yields of isolated major isomer; d.r. determined by ^1H NMR of crude material. [c] GC yields using dodecane as internal standard (0.1 mmol). [d] Using ^{t}BuOK (2.0 equiv) in place of K_3PO_4.

Scheme 3.18 Scope of dihydroquinazolinones.

3.4.2 Scope of Nitrogen Nucleophiles

Next, we turned our attention to identifying *N*-nucleophiles that might participate

in our Cu-catalyzed amination (Scheme 3.19). The *N*-alkylation of indazoles was successful with substrates containing ester (**5a**), halide (**5b**–**5d**), nitrile (**5e**) and methoxy groups (**5f**). Notably, the reaction could be extended beyond indazoles, as indoles (**5g**, **5h**), pyrazoles (**5i**–**5m**), azaindazoles (**5n**, **5o**) and azaindoles (**5p**) could all be employed. In addition, the use of sulfonamides (**5q**–**5s**) and amides (**5t**) resulted in only monosubstituted products. Also, phthalimide (**5u**) proved to be amenable to alkylation. For the coupling of anilines, sulfoximines or imines provided traces, a brief optimization was required and revealed that the use of [Cu(II)(hfac)$_2$] enabled the desire transformations in good yields (**5v**–**5y**).[258] Use of ^{t}BuOH as co-solvent was found to be beneficial in obtaining **5t** and **5x**, presumably by improving the solubility of the *N*-nucleophile.

[258] Shafir, A.; Lichtor, P. A.; Buchwald, S. L. N- versus O-Arylation of Aminoalcohols: Orthogonal Selectivity in Copper-Based Catalysts. *J. Am. Chem. Soc*. **2007**, *129*, 3490–3491.

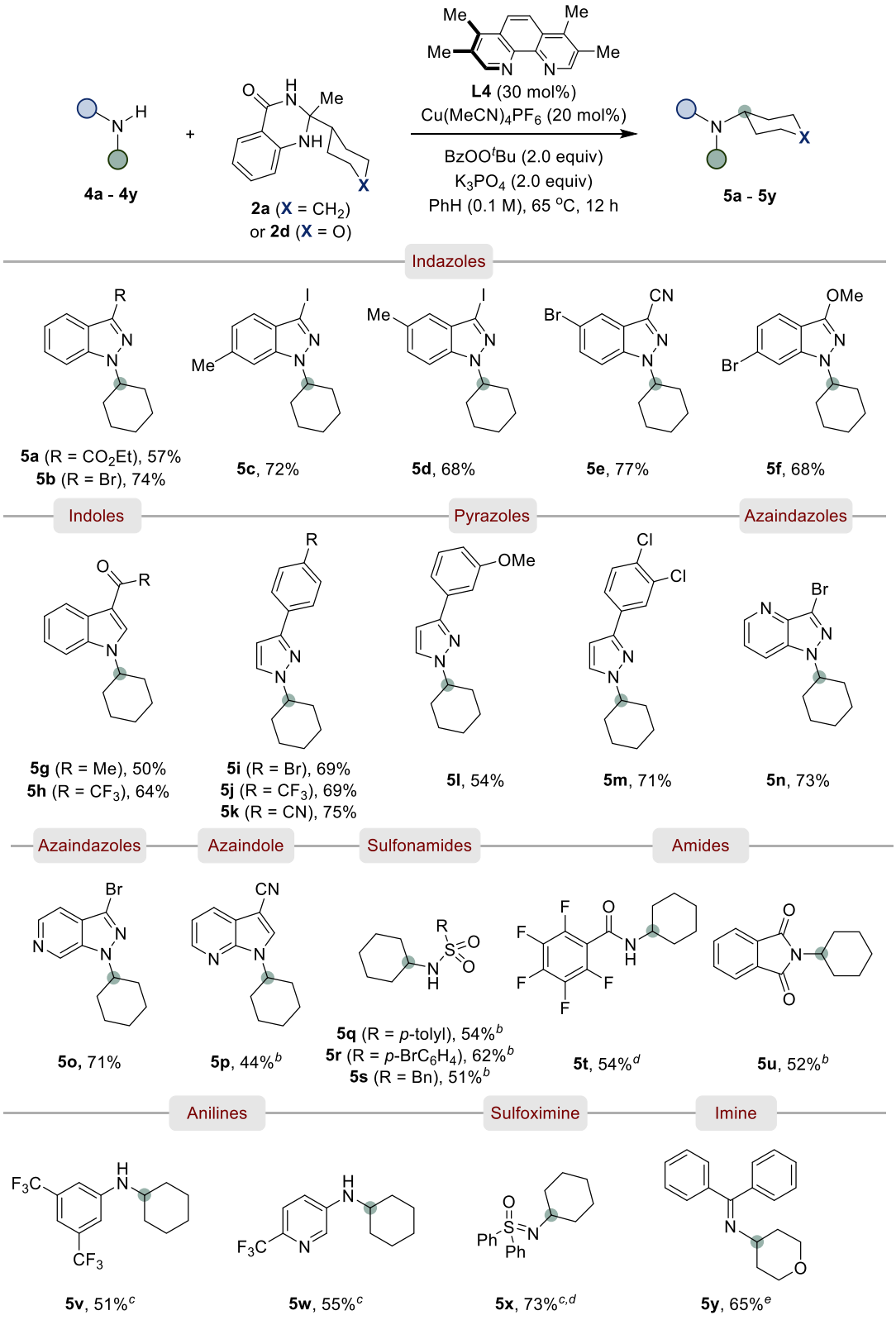

[a] Conditions: **1a** (0.20 mmol), **2a** (0.24 mmol), $Cu(MeCN)_4PF_6$ (20 mol%), **L4** (30 mol%), $BzOO^tBu$ (2.0 equiv), K_3PO_4 (2.0 equiv) in benzene (0.10 M) at 65 °C for 12 h; yields of isolated product, average of two independent runs. [b] Using $PhCF_3$ (0.1 M). [c] Using $[Cu(II)(hfac)_2]$ (20 mol%). [d] Using $PhCF_3$:^{t}BuOH = 9:1 (0.1 M). [e] Using $[Cu(II)(hfac)_2]$ (10 mol%).

Scheme 3.19 Scope of *N*-nucleophiles.

While exploring the substrate scope of this method, certain *N*-nucleophiles were

found to exhibit poor reactivity. Electron-rich heterocycles, sulfonamides and amides tended to provide low conversion, might due to the higher pKa value of the corresponding N–H bond. Besides, this Cu/Phen catalytic system could be sensitive to steric hindrance, given that the utilization of secondary sulfonamides resulted in low conversion.

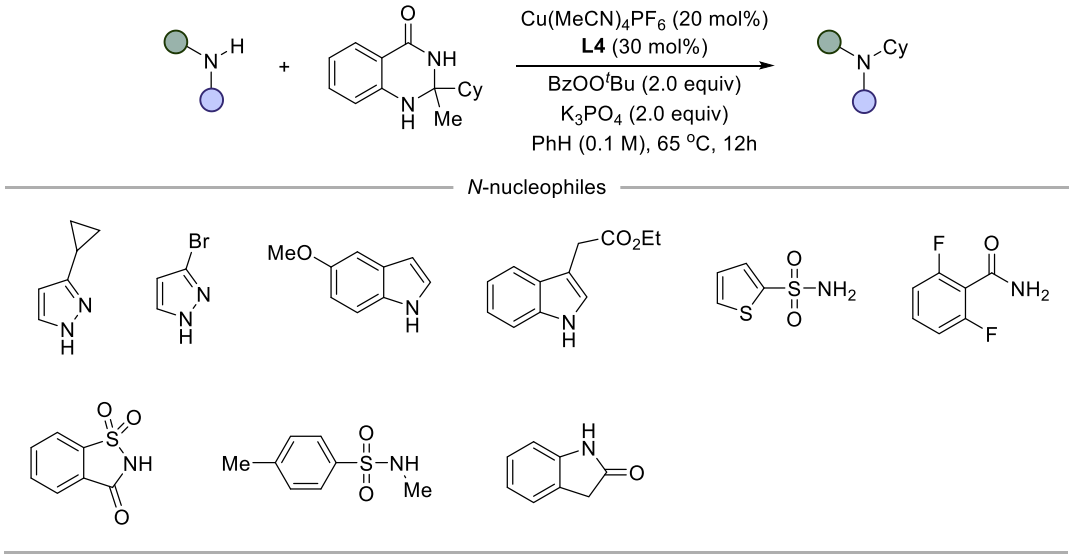

Scheme 3.20 Unsuccessful substrates.

3.4.3 Synthetic Applications

Promoted by the generality of the deacylative amination protocol, we anticipated that our protocol might streamline the derivatization of some advanced intermediates. Gratifyingly, several advanced compounds could be successfully alkylated under our optimized conditions, including zonisamide (**6a**), celecoxib (**6b**), deracoxib (**6c**), phenyltoin (**6d**) and riluzole (**6e**) (Scheme 3.21). Furthermore, dihydroquinazolinone derivatives of a bile acid component (**6f**) and febuxostat (**6g**) could successfully be aminated with indazole **1a**.

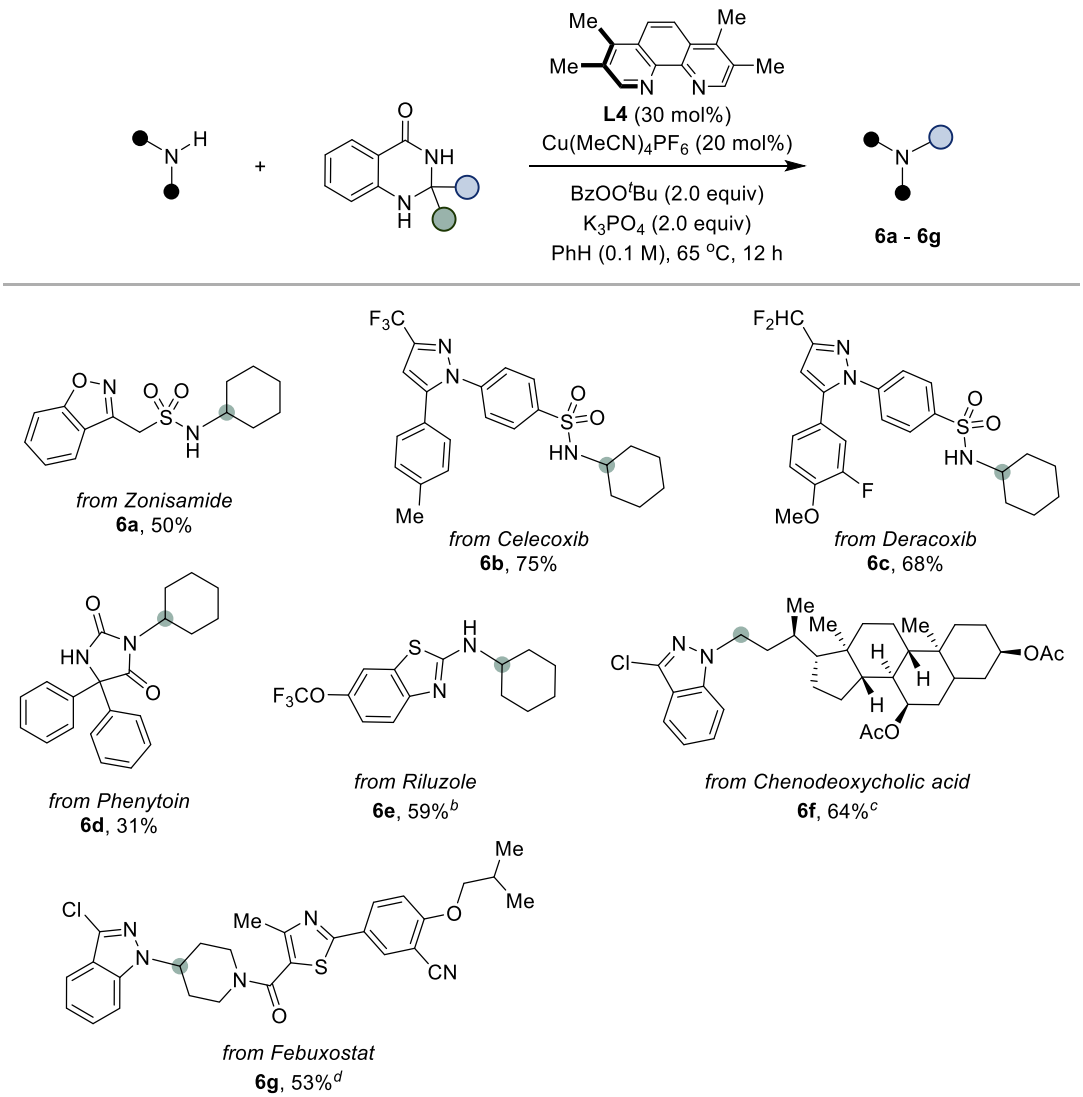

[a] Conditions: **4** (0.20 mmol), **2** (0.24 mmol), $Cu(MeCN)_4PF_6$ (20 mol%), **L4** (30 mol%), K_3PO_4 (2.0 equiv) and BzO^tBu (2.0 equiv) in $PhCF_3$:^{t}BuOH = 9:1 (0.1 M) at 65 °C for 12 h; yields of isolated product, average of two independent runs. [b] Using $[Cu(II)(hfac)_2]$ (20 mol%). [c] Using ^{t}BuOK (2.0 equiv) in place of K_3PO_4 in $PhCF_3$:^{t}BuOH = 9:1 (0.067 M). [d] Using $PhCF_3$:^{t}BuOH = 9:1 (0.05 M).

Scheme 3.21 C(sp^3)-amination of advanced synthetic intermediates.

In the interest of providing a practical approach to utilize this method, we wondered whether we could telescope the formation of dihydroquinazolinones from the corresponding ketones. This turned out to be the case with cross-coupling products **8a** and **8b** being obtained in synthetically useful yields without the need for isolating dihydroquinazolinones **2a** and **2d** derived from their respective ketones **7a** and **7b** (Scheme 3.22).

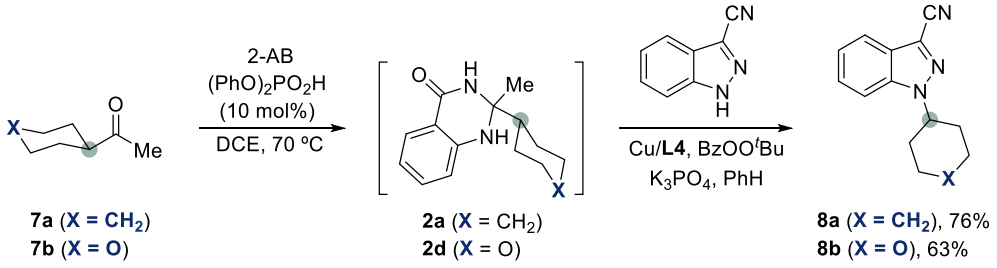

Scheme 3.22 One-pot *N*-alkylation without isolation of dehydroquinazolones.

3.5 Mechanistic Experiments

The mechanistic aspect of Cu-catalyzed amination of dihydroquinazolinones was investigated afterwards. First, alkylation of indazole **1b** with dihydroquinazolinone **9** containing a cyclopropane resulted in ring opening *N*-alkylation (**10**) (Scheme 3.23, a), as well as quinazolin-4-one by-product. In addition, significant product inhibition en route to **8a** was observed in the presence of TEMPO; indeed, **11** could be isolated in a 32% yield. These results indicate the involvement of alkyl radicals arising from oxidation of the dihydroquinazolinone core.

To get more insights into the potential copper catalyst intermediate, phenanthroline Cu(I)-amido complex (**Cu-I**) was synthesized according to literature reports.[259] **Cu-I** was found to be catalytically competent in the alkylation of **4u** with **2a** (Scheme 3.23, b). In line with this notion, the stoichiometric reaction of **2a** and **Cu-I** afforded **5u** in 40% yield. This result suggests **Cu-I** or similar copper complexes can capture alkyl radical under the established reaction conditions to provide C(sp^3)–N bond coupling product, thus indicating the **Cu-I** might be the potential reaction intermediate.

Since the activation of dihydroquinazolinone is the missing piece of the puzzle, we synthesize the *N*-methylated dihydroquinazolinone **2a"**, which led to starting material **2a"** largely recovery, indicating the N–H structure in dihydroquinazolinone core is essential for success (Scheme 3.23, c).

[259] Tye, J. W.; Weng, Z.; Johns, A. M.; Incarvito, C. D.; Hartwig, J. F. Copper Complexes of Anionic Nitrogen Ligands in the Amidation and Imidation of Aryl Halides. *J. Am. Chem. Soc*. **2008**, *130*, 9971–9983.

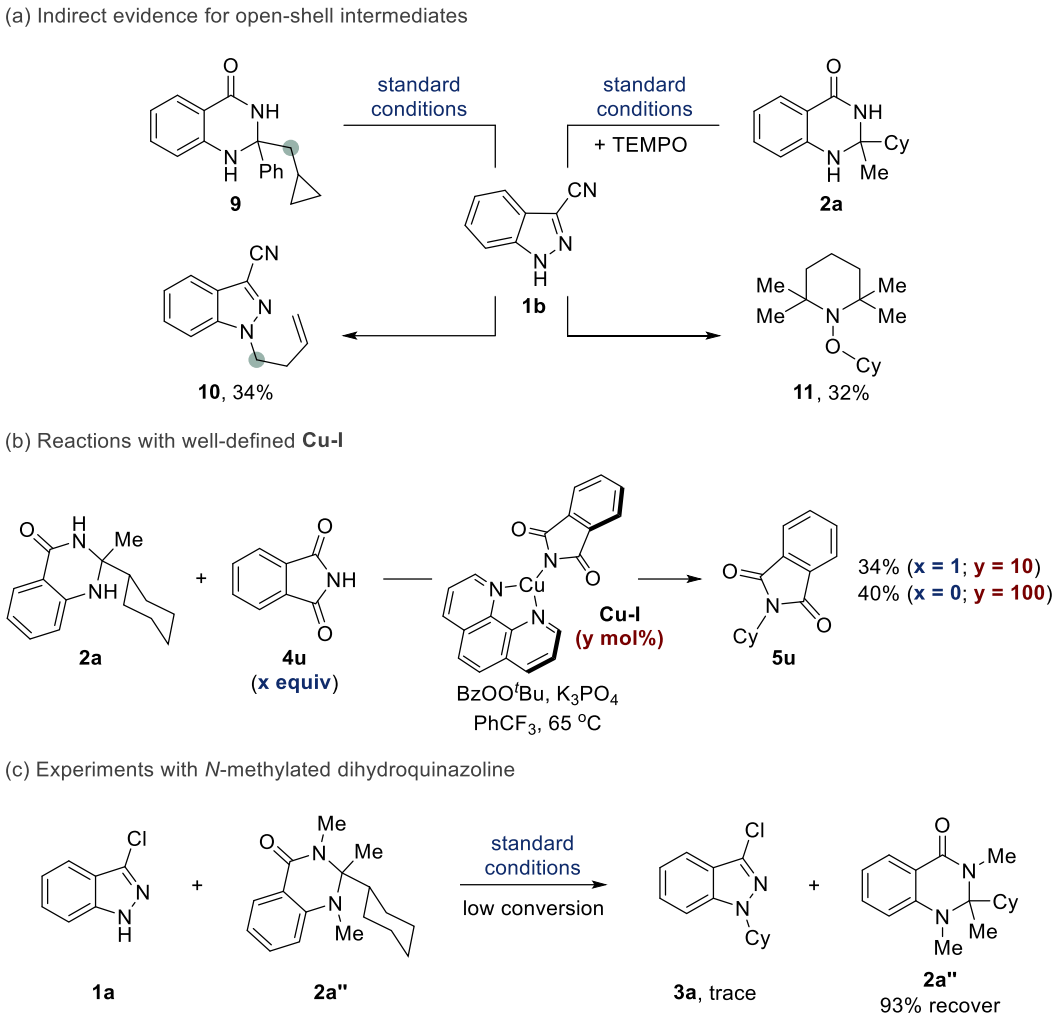

Scheme 3.23 Mechanistic investigations.

UV-Vis. spectroscopy shows the formation of a new wide absorbance band centered at 680 nm when **Cu-I** is exposed to BzOO^{t}Bu, which could be assigned as the oxidation of **Cu-I** according to previous reports.[260] Analogy to the Kharasch-Sosnovsky reaction, where copper sources catalyze the decomposition of BzOO^{t}Bu to generate *tert*-butoxy radical,[261] we currently believe *tert*-butoxy radical is responsible for dihydroquinazolinones activation by HAT pathway.

[260] (a) Górski, B.; Barthelemy, A.-L.; Douglas, J. J.; Juliá, F.; Leonori, D. Copper-Catalysed Amination of Alkyl Iodides Enabled by Halogen-Atom Transfer. *Nat. Catal.* **2021**, *4*, 623–630. (b) Wiese, S.; Badiei, Y. M.; Gephart, R. T.; Mossin, S.; Varonka, M. S.; Melzer, M. M.; Meyer, K.; Cundari, T. R.; Warren, T. H. Catalytic C–H Amination with Unactivated Amines through Copper(II) Amides. *Angew. Chem. Int. Ed.* **2010**, *49*, 8850–8855. (c) Myun Ahn, J.; Ratani, T. S.; Hannoun, K. I.; Fu, G. C.; Peters, J. C. Photoinduced, Copper-Catalyzed Alkylation of Amines: A Mechanistic Study of the Cross-Coupling of Carbazole with Alkyl Bromides. *J. Am. Chem. Soc.* **2017**, *139*, 12716–12723.

[261] (a) Eames, J.; Watkinson, M. Catalytic Allylic Oxidation of Alkenes Using an Asymmetric Kharasch–Sosnovsky Reaction. *Angew. Chem. Int. Ed.* **2001**, *40*, 3567–3571. (b) Punniyamurthy, T.; Rout, L. Recent Advances in Copper-Catalyzed Oxidation of Organic Compounds. *Coord. Chem. Rev.* **2008**, *252*, 134–154.

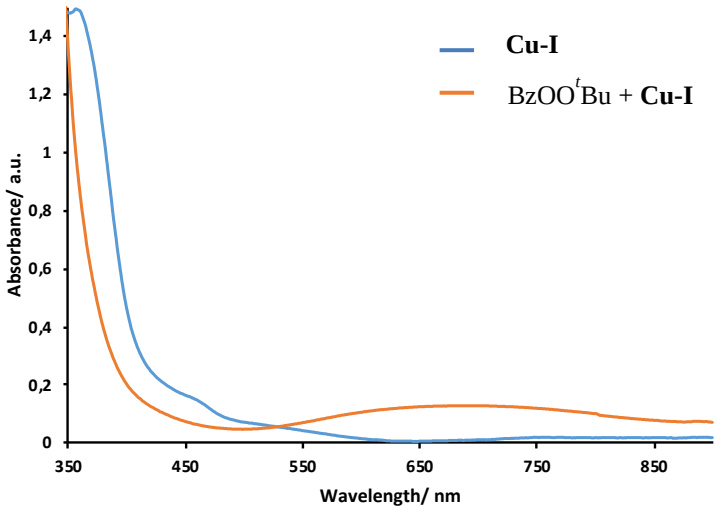

Figure 3.1 Overlaid UV/Vis absorption analysis of 2 mL of a 1.7 mM solution of **Cu-I** in $PhCF_3$ before (blue) and after (orange) being exposed to BzOO^{t}Bu (2.8 mg, 4 equiv, 15 mmol).

Taken together, a plausible mechanism of the present reaction is depicted in Scheme 3.24. Initial oxidation of the *in situ* generated Cu(I)-amido intermediate **3.24a** by BzOO^{t}Bu leads to a Cu(II) species **3.24b** and *tert*-butoxy radical. *Tert*-butoxy radical generated by either thermal decomposition or copper catalysts facilitated decomposition of BzOO^{t}Bu would activate dihydroquinazolinone and lead to alkyl radical **3.24e** formation. Next, Cu(II) species **3.24b** are intercepted by alkyl radical **3.24e** forming an alkyl bounded Cu(III)-amido entity **3.24c**. Reductive elimination of Cu(III) intermediate **3.24c** results in the desired C(sp^3)–N architecture while recovering back the propagating Cu(I)-amido intermediate upon coordination with an appropriate *N*-nucleophilic entity.

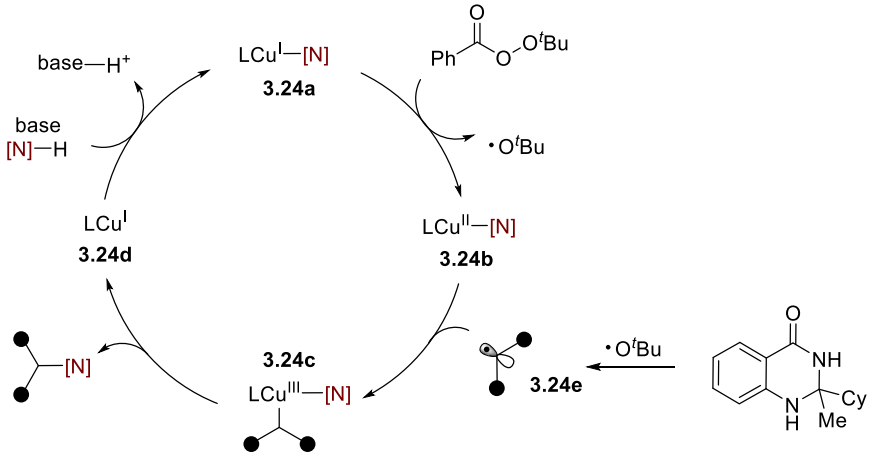

Scheme 3.24 Proposed mechanism.

3.6 Conclusions

This chapter summarizes efforts towards the development of a formally Cu-catalyzed deacylative amination protocol of a verity of *N*-nucleophiles including nitrogen containing heterocycles, amides, sulfonamides and anilines. The reaction was mediated by alkyl radical species arising from homolytic C–C bond-cleavage of pro-aromatic dihydroquinazolinone. The combination of alkyl radical species with the ability of Cu catalysis to promote C(sp^3)–N formation makes this methodology come into a reality.

The protocol is characterized by its operational simplicity and generality, including chemical diversification of advanced intermediates. In addition, judicious selection of the starting ketones allows to control the site-selectivity of C–C bond-cleavage. Preliminary mechanistic experiments were carried out, indicating that *tert*-butoxy radical might be responsible for dihydroquinazolinone core activation.

3.7 Experimental Section

3.7.1 General Considerations

Reagents. Commercially available materials were used as received without further purification. $Cu(MeCN)_4PF_6$ (97% purity) was purchased from Aldrich. Copper(II) trifluoroacetylacetonate (97% purity) was purchased from Aldrich. Phen was purchased from fluorochem. 3,4,7,8-Tetramethyl-1,10-phenanthroline (95% purity) was purchased from Manchester Organics. 2-Aminobenzamide (99+% purity) was purchased from Acros. Anhydrous K_3PO_4 (98+% purity) was purchased from Aldrich. ^{t}BuOK (98% purity) was purchased from Aldrich. Tert-butyl peroxybenzoate (>99% purity) was purchased from Aldrich. Anhydrous benzene (99.8% purity), $PhCF_3$ (99+% purity) and ^{t}BuOH (99.5+% purity) were purchased from Aldrich.

Analytical methods. ^{1}H and ^{13}C NMR spectra were recorded on Bruker 400 MHz or 500 MHz at 20 °C. All ^{1}H NMR spectra are reported in parts per million (ppm) downfield of TMS and were calibrated using the residual water peak (3.33 ppm in DMSO-d_6, 1.56 ppm in $CDCl_3$), residual solvent peak of $CHCl_3$ (7.26 ppm) or DSMO (2.50 ppm), unless otherwise indicated. All ^{13}C NMR spectra are reported in ppm relative to TMS, were calibrated using the signal of residual $CHCl_3$ (77.16 ppm) or DMSO (39.52), ^{19}F NMR was obtained with ^{1}H decoupling unless otherwise indicated. Coupling constants, *J* are reported in hertz (Hz). Gas chromatographic analyses were performed on Hewlett-Packard 6890 gas chromatography instrument with FID detector. Melting points were measured using open glass capillaries in a Büchi B540 apparatus, with samples unless otherwise stated recrystalized by slow evaporation of a solution of DCM. Infrared spectra (FT-IR) measurements were carried out on a Bruker Optics FT-IR Alpha spectrometer equipped with a DTGS detector, KBr beamsplitter at 4 cm^{-1} resolution using a one bounce ATR accessory with diamond windows. Cyclic voltammetry was performed using a PARSTAT 2273 potentiometer using a 3-electrode cell configuration at room temperature. A glassy carbon working electrode, a platinum counter electrode and silver wire/silver nitrate reference electrode were used. The reference electrode was made from a 0.01 M solution of silver nitrate in a 0.1 M solution of NEt_3PF_6 in $PhCF_3$:MeCN (20:1). UV/Vis absorption spectra were recorded using an Shimadzu UV-2401PC UV/Vis spectrophotometer with a silt length of 1.0 nm using quartz cuvettes with a path length of 1.0 cm. Mass spectra were recorded on a Waters LCT Premier spectrometer or in a MicroTOF Focus, Bruker Daltonics spectrometer. Flash chromatography was performed with EM Science silica gel 60 (230-400 mesh). Thin layer chromatography was used to monitor reaction progress and analysed

fractions from column chromatography. To this purpose TLC Silica gel 60 F_{254} aluminium sheets from Merck were used and visualization was achieved using UV irradiation and/or staining with potassium permanganate or cerium molybdate solution. Room temperature was 25 °C.

3.7.2 Synthesis of Starting Materials

General procedure 1 (GP1): Derivatization of aryl ketones by ester coupling.

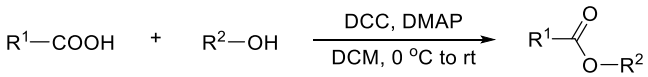

To a stirring solution of carboxylic acid (1.2 equiv.) and alcohol (1.0 equiv.) in DCM (0.5 M) was added DMAP (0.8 equiv) and DCC (1.5 equiv) at 0 °C. The reaction mixture was allowed to stir at 20 °C for 20 hours. The reaction mixture was filtered through a plug of silica and washed through with DCM. The received crude material was concentrated under reduced pressure and purified by silica gel chromatography to yield the desired product.

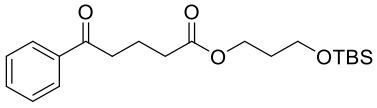

3-((*tert*-Butyldimethylsilyl)oxy)propyl 5-oxo-5-phenylpentanoate (S1). Following GP1, using 5-oxo-5-phenylpentanoic acid (3.46 g, 18.0 mmol) and 3-((*tert*-butyldimethylsilyl)oxy)propan-1-ol (4.10 g, 21.6 mmol) afforded the title compound as a colourless liquid (6.52g, 99%), by using hexane/EtOAc (20:1) as chromatography eluent. **IR (neat, cm^{-1}):** 2929, 2118, 1733, 1686, 1449, 1253, 1100, 834, 775, 690. **^{1}H NMR (400 MHz, $CDCl_3$)** δ 7.99 – 7.93 (m, 2H), 7.59 – 7.53 (m, 1H), 7.49 – 7.42 (m, 2H), 4.18 (t, *J* = 6.4 Hz, 2H), 3.68 (t, *J* = 6.1 Hz, 2H), 3.05 (t, *J* = 7.2 Hz, 2H), 2.44 (t, *J* = 7.2 Hz, 2H), 2.12 – 2.02 (m, 2H), 1.87 – 1.78 (m, 2H), 0.88 (s, 9H), 0.03 (s, 6H) ppm. **^{13}C NMR (101 MHz, $CDCl_3$)** δ 199.6, 173.4, 137.0, 133.2, 128.8, 128.2, 61.6, 59.6, 37.6, 33.5, 31.9, 26.0, 19.5, 18.4, -5.3 ppm. **HRMS** [ESI^+] *calcd*. for ($C_{20}H_{33}O_4Si$) $[M+H]^+$: 365.2143, *found*: 365.2143.

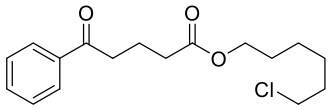

6-Chlorohexyl 5-oxo-5-phenylpentanoate (S2). Following GP1, using 5-oxo-5-phenylpentanoic acid (3.46 g, 18.0 mmol) and 6-chlorohexan-1-ol (2.96 g, 21.6 mmol) afforded the title compound as a colourless liquid (5.40 g, 96%), by using hexane/EtOAc (20:1) as chromatography eluent. **IR (neat, cm^{-1}):** 2937, 1729, 1684, 1448, 1204, 690. **^{1}H NMR (400 MHz, $CDCl_3$)** δ 7.99 – 7.93 (m, 2H), 7.59 – 7.53 (m, 1H), 7.50 – 7.42 (m, 2H), 4.08 (t, *J* = 6.7 Hz, 2H), 3.52 (t, *J* = 6.7 Hz, 2H), 3.06 (t, *J* =

7.1 Hz, 2H), 2.44 (t, *J* = 7.2 Hz, 2H), 2.13 – 2.02 (m, 2H), 1.82 – 1.72 (m, 2H), 1.69 – 1.59 (m, 2H), 1.51 – 1.34 (m, 4H) ppm. **^{13}C NMR (101 MHz, $CDCl_3$)** δ 199.6, 173.5, 137.0, 133.2, 128.8, 128.2, 64.5, 45.1, 37.6, 33.6, 32.6, 28.6, 26.7, 25.4, 19.6 ppm. **HRMS** [ESI$^+$] *calcd*. for ($C_{17}H_{23}ClNaO_3$) [M+Na]$^+$: 333.1228, *found*: 333.1232.

General procedure 2 (GP2): Synthesis of 2,2-disubstituted dihydroquinazolinones

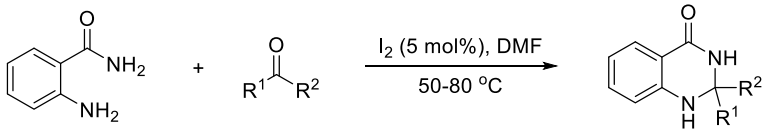

A 100 mL flask containing a stirring bar was charged with 2-aminobenzamide (1.0 equiv), ketone (1.05 equiv), iodine (5 mol%) and DMF. The reaction mixture was stirred at 80 °C for 24 hours. The reaction was cooled to 20 °C and water (50 mL) was added to the reaction generating precipitate that was collected as crude product by suction filtration. The crude material was washed with water and purified by recrystallization (EtOH) to give desired product.

General procedure 3 (GP3): Alternative synthesis of 2,2-disubstituted dihydroquinazolinones

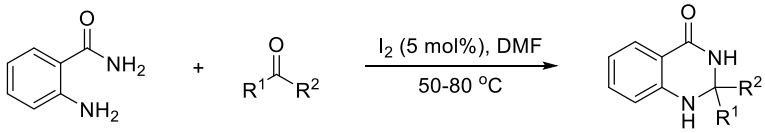

A 100 mL flask containing a stirring bar was charged with 2-aminobenzamide (1.0 equiv), ketone (1.05 equiv), iodine (5 mol%) and DMF. The reaction mixture was stirred at 50-80 °C for 24 hours. The reaction was cooled to 20 °C, quenched with 10% $Na_2S_2O_3$(aq.) (50 mL) and extracted with EtOAc (2 x 50 mL). The combined organic extracts were dried (Na_2SO_4) and concentrated under reduced pressure affording crude material, which was purified by silica gel chromatography yielding the desired product.

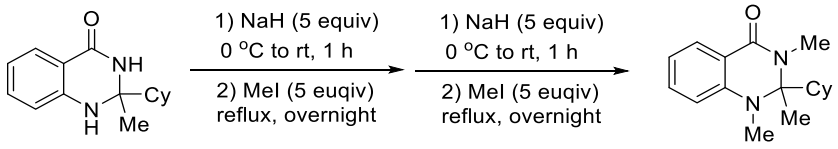

2-cyclohexyl-1,2,3-trimethyl-2,3-dihydroquinazolin-4(1*H*)-one (2a''). A 100 mL oven-dried flask containing a stirring bar was charged with 2-Cyclohexyl-2-methyl-2,3-dihydroquinazolin-4(1*H*)-one (732 mg, 3 mmol) and THF (30 mL). NaH (360 mg, 15 mmol) was added slowly to the solution at 0 °C. The reaction mixture was stirred at 25 °C for 1 h before MeI (2.13 g, 15 mmol) was added and the mixture was heated to reflux overnight. After cooling to rt, water was added to quench the reaction. The mixture was extracted using EtOAc (3 x 30 mL). The combined organic extracts were

dried (Mg_2SO_4) and concentrated under reduced pressure affording crude material. The crude material was subjected to the same conditions again to afford to crude product, which was purified by silica gel chromatography by using hexane/EtOAc (2:1) as eluent, to afford the product as a white solid (336 mg, 41%). **M.p.** 117 °C. **IR (film, cm^{-1}) ν_{max}** = 2930, 2852, 1631, 1601, 1491, 1416, 1391, 1308, 1214, 1148, 1026, 929, 748, 701. **^{1}H NMR (500 MHz, DMSO-*d*$_6$)** δ 7.71 (dd, J = 7.6, 1.6 Hz, 1H), 7.38 (ddd, J = 8.3, 7.2, 1.7 Hz, 1H), 6.85 (d, J = 8.1 Hz, 1H), 6.80 (td, J = 7.6, 0.9 Hz, 1H), 3.05 (s, 3H), 2.98 (s, 3H), 1.95 (tt, J = 12.0, 3.0 Hz, 1H), 1.67 (s, 3H), 1.62 – 1.36 (m, 4H), 1.15 – 1.05 (m, 1H), 1.03 – 0.92 (m, 3H), 0.85 – 0.75 (m, 1H) ppm. **^{13}C NMR (126 MHz, DMSO-*d*$_6$)** δ 162.2, 146.9, 133.1, 127.2, 118.7, 117.7, 114.6, 78.7, 47.0, 35.0, 30.1, 27.4, 27.1, 26.0, 25.9, 25.7, 18.5 ppm. **HRMS** [ESI$^+$] *calcd*. for ($C_{17}H_{25}N_2O$) [M+H]$^+$: 273.1961, *found*: 273.1970.

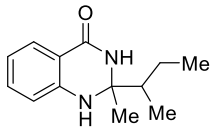

2-(*sec*-Butyl)-2-methyl-2,3-dihydroquinazolin-4(1*H*)-one (2g). Following GP2, using 2-aminobenzamide (1.36 g, 10.0 mmol), 3-methylpentan-2-one (1.05 g, 10.5 mmol) and iodine (0.13 g, 0.5 mmol) in DMF (15 mL) for 24 hours. The product was obtained as a white solid (0.58 g, 27%). **M.p.** 170 °C. **IR (neat, cm^{-1}):** 3311, 2967, 1630, 1507, 754. **^{1}H NMR (400 MHz, DMSO-*d*$_6$, mixture of diastereomers A and B, 1.25:1)** δ 7.97 (br. s, 0.57H, A), 7.92 (br. s, 0.44H, B), 7.53 (d, *J* = 7.7 Hz, 1H, A + B), 7.22 – 7.15 (m, 1H, A + B), 6.67 (dd, *J* = 8.1, 2.2 Hz, 1H, A + B), 6.64 (s, 1H, A + B), 6.60 – 6.52 (m, 1H, A + B), 1.74 – 1.56 (m, 2H, A + B), 1.28 (s, 1.32H, B), 1.27 (s, 1.65H, A), 1.04 – 0.91 (m, 1H, A + B), 0.91 – 0.76 (m, 6H, A + B) ppm. **^{13}C NMR (101 MHz, DMSO-*d*$_6$, mixture of diastereomers A and B)** δ 162.9 (B), 162.8 (A), 146.9 (A), 146.9 (B), 133.2 (B), 133.1 (A), 127.0 (A), 127.0 (B), 115.9 (A), 115.8 (B), 113.9 (B), 113.8 (A), 113.7 (A), 113.7 (B), 71.6 (B), 71.5 (A), 44.2 (B), 44.1 (A), 24.1 (B), 23.6 (A), 23.2 (B), 22.8 (A), 13.3 (A), 12.9 (B), 12.6 (A), 12.4 (B) ppm. **HRMS** [ESI$^+$] *calcd*. for ($C_{13}H_{18}N_2NaO$) [M+Na]$^+$: 241.1311, *found*: 241.1318.

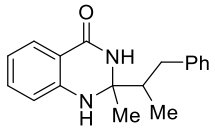

2-Methyl-2-(1-phenylpropan-2-yl)-2,3-dihydroquinazolin-4(1*H*)-one (2h). Following GP2, using 2-aminobenzamide (1.36 g, 10.0 mmol), 3-methyl-4-phenylbutan-2-one (1.70 g, 10.5 mmol) and iodine (0.13 g, 0.5 mmol) in DMF (15 mL) for 24 hours. The product was obtained as a white solid (1.94 g, 69%). **M.p.** 158 °C. **IR (neat, cm^{-1}):** 3300, 1632, 1515, 1151, 752, 700. **^{1}H NMR (400 MHz, DMSO-*d*$_6$, mixture of diastereomers A and B, 1.18:1)** δ 8.17 (br. s, 0.53H, A), 8.12 (br. s, 0.47H, B), 7.59 (t, *J* = 8.5 Hz 1H, A + B), 7.28 – 7.18 (m, 3H, A + B), 7.18 – 7.10 (m, 1H, A +

B), 7.09 (d, *J* = 7.7 Hz, 1H, A + B), 7.06 (d, *J* = 7.7 Hz 1H, A + B), 6.82 – 6.76 (m, 1.47H, A + 2B), 6.71 (d, *J* = 8.0 Hz 0.56H, A), 6.62 (d, *J* = 7.7 Hz, 0.52H, A), 6.59 (d, *J* = 7.7 Hz, 0.49H, B), 3.04 (t, *J* = 11.7 Hz, 1H, A + B), 2.19 – 2.07 (m, 1H, A + B), 2.04 – 1.92 (m, 1H, A + B), 1.39 (s, 3H, A + B), 0.78 (d, *J* = 6.8 Hz, 1.42H, B), 0.78 (d, *J* = 6.8 Hz, 1.67H, A) ppm. **^{13}C NMR (101 MHz, DMSO-*d*$_6$, mixture of diastereomers A and B)** δ 163.0 (A + B), 146.9 (A), 146.9 (B), 141.4 (A), 141.3 (B), 133.3 (A + B), 128.8 (B), 128.8 (A), 128.3 (A), 128.2 (B), 127.1 (A), 127.0 (B), 125.7 (A), 125.7 (B), 116.2 (B), 116.1 (A), 114.0 (B), 113.9 (B), 113.9 (A), 113.8 (A), 71.5 (B), 71.4 (A), 44.9 (A), 44.7 (B), 37.2 (B), 36.6 (A), 24.3 (B), 23.8 (A), 13.3 (A), 12.9 (B) ppm. **HRMS** [ESI$^+$] *calcd*. for ($C_{18}H_{20}N_2NaO$) [M+Na]$^+$: 303.1468, *found*: 303.1476.

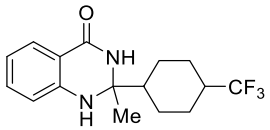

2-Methyl-2-(4-(trifluoromethyl)cyclohexyl)-2,3-dihydroquinazolin-4(1*H*)-one (2i). Following GP2, using 2-aminobenzamide (1.36 g, 10.0 mmol), 1-(4-(trifluoromethyl)cyclohexyl)ethan-1-one (2.04 g, 10.5 mmol) and iodine (0.13 g, 0.5 mmol) in DMF (15 mL) for 24 hours. The product was obtained as a white solid (1.25 g, 40%). **M.p.**: 230 °C. **IR (neat, cm^{-1}):** 3314, 2951, 1629, 1515, 1392, 1340, 1270, 1123, 1086, 758. **^{1}H NMR (400 MHz, DMSO-*d*$_6$, mixture of diastereomers A and B)** δ 7.94 (br. s, 0.23H, B), 7.92 (br. s, 0.73H, A), 7.53 (d, *J* = 7.7 Hz, 1H, A + B), 7.18 (t, *J* = 7.7 Hz, 1H, A + B), 6.70 – 6.61 (m, 2H, A + B), 6.56 (t, *J* = 7.5 Hz, 1H, A + B), 2.46 – 2.32 (m, 0.22H, B), 2.20 – 2.07 (m, 0.88H, A), 2.00 – 1.78 (m, 4H, A + B), 1.69 – 1.40 (m, 2H, A + B), 1.33 – 1.29 (m, 3H, A + B), 1.26 – 1.03 (m, 4H, A + B) ppm. **^{19}F decoupled ^{13}C NMR (126 MHz, DMSO-*d*$_6$ mixture of diastereomers A and B)** δ 162.9 (A+B), 147.0 (B), 147.0 (A), 133.3 (A+B), 129.1 (B), 128.1 (A), 127.1 (A), 127.0 (B), 115.9 (A), 115.9 (B), 113.8 (A+B), 113.6 (B), 113.5 (A), 71.1 (B), 71.0 (A), 46.9 (A), 46.6 (B), 40.5 (A), 35.2 (B), 24.9 (A+B), 24.8 (B), 24.8 (A), 24.5 (A), 24.4 (A), 24.4 (A), 23.2 (B), 23.2 (B), 21.8 (B), 21.5 (B) ppm. **^{1}H decoupled ^{19}F NMR (376 MHz, DMSO-*d*$_6$, mixture of diastereomers A and B, 4.7:1)** δ -65.5 (0.18F, B), -72.4 (0.82F, A) ppm. **HRMS** [ESI$^+$] *calcd*. for ($C_{16}H_{20}F_3N_2O$) [M+H]$^+$: 313.1522, *found*: 313.1523.

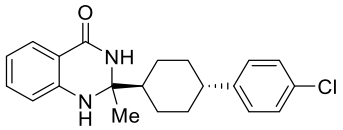

2-(4-(4-Chlorophenyl)cyclohexyl)-2-methyl-2,3-dihydroquinazolin-4(1*H*)-one (2j). Following GP2, using 2-aminobenzamide (1.36 g, 10.0 mmol), 1-(4-(4-chlorophenyl)cyclohexyl)ethan-1-one (2.49 g, 10.5 mmol) and iodine (0.13 g, 0.5 mmol) in DMF (15 mL) for 24 hours. The product was obtained as a white solid (2.03 g, 57%).

M.p.: 223 °C. **IR (neat, cm^{-1}):** 2944, 1633, 1518, 1486, 1089, 1008, 819, 752. **^{1}H NMR (500 MHz, DMSO-*d*$_6$)** δ 7.67 (s, 1H), 7.49 (dd, *J* = 7.7, 1.5 Hz, 1H), 7.13 (ddd, *J* = 8.6, 7.2, 1.6 Hz, 1H), 6.64 (d, *J* = 8.2 Hz, 1H), 6.48 (td, *J* = 7.4, 1.0 Hz, 1H), 6.43 (s, 1H), 1.77 – 1.67 (m, 4H), 1.58 (q, *J* = 7.3, 2H), 1.54 – 1.47 (m, 1H), 1.19 – 0.97 (m, 6H), 0.87 (t, *J* = 7.2 Hz, 3H) ppm. **^{13}C NMR (101 MHz, DMSO)** δ 162.8, 147.0, 146.0, 133.2, 130.3, 128.6, 128.1, 127.0, 115.8, 113.6, 113.5, 71.1, 47.2, 42.9, 33.4, 33.4, 26.7, 26.4, 24.9 ppm. **HRMS** [ESI$^+$] *calcd*. for ($C_{21}H_{23}ClN_2NaO$) [M+Na]$^+$: 377.1391, *found*: 377.1391.

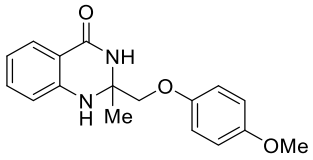

2-((4-Methoxyphenoxy)methyl)-2-methyl-2,3-dihydroquinazolin-4(1*H*)-one (2m). Following GP3, using 2-aminobenzamide (1.36 g, 10.0 mmol), 1-(4-methoxyphenoxy)propan-2-one (1.89 g, 10.5 mmol) and iodine (0.13 g, 0.5 mmol) in DMF (15 mL) for 24 hours. The crude material was purified by silica gel chromatography by using hexane/EtOAc (1:1) as eluent, to afford the product as a white solid (2.44 g, 82%). **M.p.**: 58 °C. **IR (neat, cm^{-1}):** 3272, 1650, 1505, 1227, 1031, 752. **^{1}H NMR (400 MHz, DMSO-*d*$_6$)** δ 8.06 (s, 1H), 7.57 (dd, *J* = 7.7, 1.5 Hz, 1H), 7.24 – 7.15 (m, 1H), 6.86 (s, 1H), 6.82 – 6.74 (m, 4H), 6.70 – 6.64 (m, 1H), 6.64 – 6.57 (m, 1H), 3.88 (d, *J* = 9.3 Hz, 1H), 3.75 (d, *J* = 9.4 Hz, 1H), 3.65 (s, 3H), 1.47 (s, 3H) ppm. **^{13}C NMR (101 MHz, DMSO-*d*$_6$)** δ 163.1, 153.6, 152.6, 146.9, 133.3, 127.1, 116.5, 115.8, 114.5, 114.0, 113.8, 73.9, 68.2, 55.3, 24.8 ppm. **HRMS** [ESI$^+$] *calcd*. for ($C_{17}H_{18}N_2NaO_3$) [M+Na]$^+$: 321.1210, *found*: 321.1207.

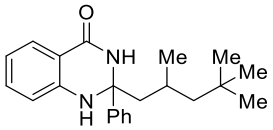

2-Phenyl-2-(2,4,4-trimethylpentyl)-2,3-dihydroquinazolin-4(1*H*)-one (2n). Following GP3, using 2-aminobenzamide (1.36 g, 10.0 mmol), 3,5,5-trimethyl-1-phenylhexan-1-one (2.29 g, 10.5 mmol) and iodine (0.13 g, 0.5 mmol) in DMF (15 mL) at 80 °C for 24 hours. The crude material was purified by silica gel chromatography by using hexane/EtOAc (1:1) as eluent, to afford the product as a white solid (1.57 g, 47%). **M.p.**: 66 °C. **IR (neat, cm^{-1}):** 2948, 1650, 1484, 750, 697. **^{1}H NMR (400 MHz, DMSO-*d*$_6$, mixture of diastereomers A and B, 1.14:1)** δ 8.63 (s, 1H, A + B), 7.53 – 7.47 (m, 2H, A + B), 7.46 (dt, *J* = 7.8, 1.6 Hz, 1H, A + B), 7.40 (s, 0.47H, B), 7.35 (s, 0.53, A), 7.27 (t, *J* = 7.8 Hz, A + B), 7.21 – 7.12 (m, 2H, A + B), 6.86 (d, *J* = 8.1 Hz, 0.52H, A), 6.83 (d, *J* = 8.1 Hz 1H, B), 6.57 – 6.48 (m, 1H, A + B), 2.19 – 2.03 (m, 1H, A + B), 1.83 – 1.57 (m, 2H, A + B), 1.49 (br. d, *J* = 2.0 Hz, 0.46H, B), 1.46 (br. d, *J* = 1.8 Hz, 0.54H, A), 1.05 – 0.93 (m, 4H, A + B), 0.86 (s, 4.24H, B), 0.83 (s, 4.67H, A)

ppm. **^{13}C NMR (101 MHz, DMSO-*d*$_6$, mixture of diastereomers A and B)** δ 164.1 (B), 163.9 (A), 148.6 (B), 148.5 (A), 147.5 (A), 147.4 (B), 133.2 (A + B), 127.8 (A + B), 127.1 (B), 127.1 (A), 126.9 (A + B), 125.3 (A + B), 116.5 (A), 116.4 (B), 114.4 (A + B), 114.3 (A + B), 73.4 (A + B), 51.7 (A), 51.6 (B), 51.4 (B), 51.2 (A), 31.1 (B), 31.0 (A), 30.1 (B), 30.1 (A), 25.3 (A + B), 24.0 (B), 23.9 (A) ppm. **HRMS** [ESI$^+$] *calcd*. for ($C_{22}H_{29}N_2O$) [M+H]$^+$: 337.2274, *found*: 337.2274.

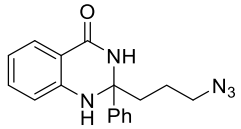

2-(3-Azidopropyl)-2-phenyl-2,3-dihydroquinazolin-4(1*H*)-one (2o). Following GP3, using 2-aminobenzamide (2.12 g, 15.6 mmol), 4-azido-1-phenylbutan-1-one (0.735 g, 3.9 mmol) and iodine (99 mg, 0.39 mmol) in DMF (15 mL) at 80 ºC for 24 hours. The product was obtained as a white solid (222 mg, 19%), by using DCM/acetone (1:0 to 19:1) as chromatography eluent. **M.p.**: 137 °C. **IR (neat, cm^{-1}):** 3325, 2098, 1648, 1611, 1484, 1256, 756, 700. **^{1}H NMR (400 MHz, DMSO-*d*$_6$)** δ 8.74 (s, 1H), 7.54 (s, 1H), 7.51 – 7.44 (m, 3H), 7.34 – 7.25 (m, 2H), 7.25 – 7.15 (m, 2H), 6.83 (d, *J* = 8.1 Hz, 1H), 6.57 (t, *J* = 7.4 Hz, 1H), 3.41 – 3.28 (m, 2H), 1.92 – 1.70 (m, 4H) ppm. **^{13}C NMR (101 MHz, DMSO-*d*$_6$)** δ 164.1, 147.4, 147.4, 133.3, 128.0, 127.2, 127.1, 125.3, 116.8, 114.7, 114.5, 72.7, 50.8, 23.7 ppm. **HRMS** [ESI$^+$] *calcd*. for ($C_{17}H_{18}N_5O$) [M+H]$^+$: 308.1506, *found*: 308.1509.

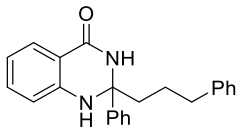

2-Phenyl-2-(3-phenylpropyl)-2,3-dihydroquinazolin-4(1*H*)-one (2p). Following GP3, using 2-aminobenzamide (1.36 g, 10.0 mmol), 1,4-diphenylbutan-1-one (2.35 g, 10.5 mmol) and iodine (0.13 g, 0.5 mmol) in DMF (15 mL) for 24 hours. The crude material was purified by silica gel chromatography by using hexane/EtOAc (1:1) as eluent, to afford the product as a white solid (2.94 g, 86%). **M.p.**: 160 °C. **IR (neat, cm^{-1}):** 3202, 1635, 1480, 698. **^{1}H NMR (400 MHz, DMSO-*d*$_6$)** δ 8.70 (s, 1H), 7.50 – 7.38 (m, 4H), 7.29 – 7.20 (m, 4H), 7.20 – 7.08 (m, 5H), 6.80 (d, *J* = 8.0 Hz, 1H), 6.53 (t, *J* = 7.1 Hz, 1H), 2.62 – 2.50 (m, 2H), 1.91 – 1.67 (m, 4H) ppm. **^{13}C NMR (101 MHz, DMSO-*d*$_6$)** δ 164.0, 147.6, 147.5, 141.9, 133.2, 128.3, 128.2, 127.9, 127.1, 127.0, 125.7, 125.4, 116.6, 114.8, 114.4, 72.9, 42.1, 35.1, 25.7 ppm. **HRMS** [ESI$^+$] *calcd*. for ($C_{23}H_{22}N_2NaO$) [M+Na]$^+$: 365.1624, *found*: 365.1635.

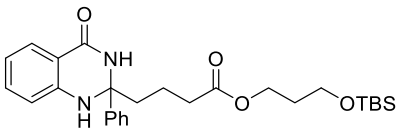

3-((*tert*-Butyldimethylsilyl)oxy)propyl 4-(4-oxo-2-phenyl-1,2,3,4-tetrahydroquinazolin-2-yl)butanoate (2r). Following GP3, using 2-aminobenzamide

(2.72 g, 20.0 mmol), 3-((*tert*-butyldimethylsilyl)oxy)propyl 5-oxo-5-phenylpentanoate (3.65 g, 10.0 mmol) and iodine (0.13 g, 0.5 mmol) in DMF (15 mL) at 80 ºC for 24 hours. The crude material was purified by silica gel chromatography by using hexane/EtOAc (2:1) as eluent, to afford the product as a white solid (0.79 g, 16%). **M.p.**: 148 °C. **IR (neat, cm^{-1}):** 3325, 2928, 1717, 1643, 1487, 1192, 835, 755, 698. **^{1}H NMR (400 MHz, DMSO-*d*$_6$)** δ 8.68 (s, 1H), 7.49 (s, 1H), 7.48 – 7.42 (m, 3H), 7.31 – 7.24 (m, 2H), 7.22 – 7.13 (m, 2H), 6.82 (d, *J* = 8.1 Hz, 1H), 6.55 (t, *J* = 7.4 Hz, 1H), 4.05 (t, *J* = 6.4 Hz, 2H), 3.61 (t, *J* = 6.1 Hz, 2H), 2.33 – 2.24 (m, 2H), 1.84 – 1.68 (m, 6H), 0.82 (s, 9H), -0.01 (s, 6H) ppm. **^{13}C NMR (101 MHz, DMSO-*d*$_6$)** δ 172.7, 164.0, 147.6, 147.4, 133.2, 127.9, 127.1, 127.0, 125.3, 116.6, 114.7, 114.4, 72.8, 60.7, 58.9, 41.4, 33.5, 31.2, 25.7, 19.8, 17.9, -5.5 ppm. **HRMS** [ESI$^+$] *calcd*. for ($C_{27}H_{38}N_2NaO_4Si$) [M+Na]$^+$: 505.2493, *found*: 505.2491.

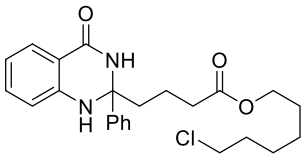

6-Chlorohexyl 4-(4-oxo-2-phenyl-1,2,3,4-tetrahydroquinazolin-2-yl)butanoate (2s). Following GP3, using 2-aminobenzamide (2.72 g, 20.0 mmol), 6-chlorohexyl 5-oxo-5-phenylpentanoate (3.11 g, 10.0 mmol) and iodine (0.13 g, 0.5 mmol) in DMF (15 mL) at 80 ºC for 24 hours. The crude material was purified by silica gel chromatography by using hexane/EtOAc (2:1) as eluent, to afford the product as a white solid (1.44 g, 33%). **M.p.**: 149 °C. **IR (neat, cm^{-1}):** 3320, 2935, 1712, 1643, 1483, 1284, 1196, 761, 702. **^{1}H NMR (400 MHz, DMSO-*d*$_6$)** δ 8.69 (s, 1H), 7.50 (s, 1H), 7.48 – 7.41 (m, 3H), 7.31 – 7.23 (m, 2H), 7.22 – 7.13 (m, 2H), 6.82 (d, *J* = 8.1 Hz, 1H), 6.55 (t, *J* = 7.4 Hz, 1H), 3.98 (t, *J* = 6.6 Hz, 2H), 3.59 (t, *J* = 6.6 Hz, 2H), 2.34 – 2.23 (m, 2H), 1.87 – 1.72 (m, 4H), 1.72 – 1.61 (m, 2H), 1.59 – 1.49 (m, 2H), 1.42 – 1.22 (m, 4H) ppm. **^{13}C NMR (101 MHz, DMSO-*d*$_6$)** δ 172.8, 164.0, 147.5, 147.4, 133.2, 127.9, 127.1, 127.0, 125.3, 116.7, 114.7, 114.4, 72.8, 63.7, 45.3, 41.4, 33.5, 31.9, 28.0, 25.9, 24.6, 19.8 ppm. **HRMS** [ESI$^+$] *calcd*. for ($C_{24}H_{29}ClN_2NaO_3$) [M+Na]$^+$: 451.1759, *found*: 451.1761.

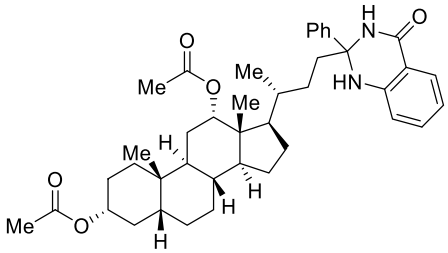

(3*R*,7*R*,8*R*,9*S*,10*S*,13*R*,14*S*,17*R*)-10,13-dimethyl-17-((2*R*)-4-(4-oxo-2-phenyl-1,2,3,4-tetrahydroquinazolin-2-yl)butan-2-yl)hexadecahydro-1H-cyclopenta[*a*]phenanthrene-3,7-diyl diacetate (S3). Following GP3, using 2-aminobenzamide (302 mg, 2.22 mmol), (3*R*,5*R*,8*R*,9*S*,10*S*,12*S*,13*R*,14*S*,17*R*)-10,13-dimethyl-17-((*R*)-5-oxo-5-phenylpentan-2-yl)hexadecahydro-1*H*-

cyclopenta[*a*]phenanthrene-3,12-diyl diacetate (598 mg, 1.1 mmol) and iodine (28 mg, 0.11 mmol) in DMF (4.0 mL) for 24 hours. The product was obtained as a white solid (420 mg, 58%), by using hexane/ethyl acetate (3:1) as chromatography eluent. **M.p.**: 163 °C. **IR (neat, cm^{-1}):** 3307, 2935, 1731, 1655, 1613, 1486, 1363, 1233, 1141, 1023, 753, 699. **^{1}H NMR (500 MHz, DMSO-*d*$_6$, undiscernible mixture of diastereomers A:B)** δ 8.65 (d, *J* = 10.9 Hz, 1H), 7.49 – 7.43 (m, 3H), 7.39 (d, *J* = 7.8 Hz, 1H), 7.27 (t, *J* = 7.7 Hz, 2H), 7.21 – 7.14 (m, 2H), 6.82 (t, *J* = 8.0 Hz, 1H), 6.54 (t, *J* = 7.4 Hz, 1H), 4.75 (br. t, *J* = 3.2 Hz, 1H), 4.45 (td, *J* = 11.0, 5.5 Hz, 1H), 1.97 – 1.95 (m, 6H), 1.94 – 1.69 (m, 6H), 1.69 – 1.54 (m, 4H), 1.50 (br. d, *J* = 12.6 Hz, 1H), 1.46 – 1.39 (m, 3H), 1.39 – 1.07 (m, 10H), 1.07 – 0.98 (m, 2H), 0.91– 0.86 (m, 6H), 0.60 (d, *J* = 4.7 Hz, 3H) ppm. **^{13}C NMR (126 MHz, DMSO-*d*$_6$, undiscernible mixture of diastereomers A:B)** δ 169.8 (A + B), 169.7 (A + B), 164.1(B), 164.1(A), 148.0 (A), 147.8 (B), 147.6 (A), 147.6 (B), 133.2 (A + B), 127.9 (A + B), 127.1 (A + B), 126.9 (A + B), 125.4 (B), 125.4 (A), 116.5 (A + B), 114.7 (A), 114.7 (B), 114.4 (A), 114.4 (B), 73.4 (A + B), 73.1 (A + B), 70.6 (A + B), 55.4 (A), 55.3 (B) 50.0 (A), 50.0 (B) 42.2 (A), 42.2 (B), 40.2 (A + B), 39.8 (A + B), 39.4 (A + B), 37.1 (A + B), 35.1 (B), 35.0 (A), 34.4 (A + B), 34.3 (A + B), 34.3 (A + B), 33.7 (A + B), 30.9 (A + B), 29.7 (B), 29.5 (A), 27.6 (B), 27.6 (A), 26.4 (A + B), 23.0 (A + B), 22.3 (A + B), 21.3 (A + B), 21.1 (A + B), 20.2 (A + B), 18.7 (A + B), 11.6 (A) 11.5 (B) ppm. **HRMS** [ESI$^+$] *calcd*. for ($C_{41}H_{55}N_2O_5$) [M+H]$^+$: 655.4105, *found*: 655.4102.

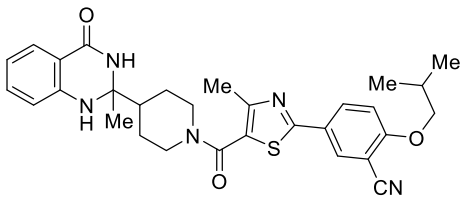

2-Isobutoxy-5-(4-methyl-5-(4-(2-methyl-4-oxo-1,2,3,4-tetrahydroquinazolin-2-yl)piperidine-1-carbonyl)thiazol-2-yl)benzonitrile (S4). Following GP3, using 2-aminobenzamide (441 mg, 3.2 mmol), 5-(5-(4-acetylpiperidine-1-carbonyl)-4-methylthiazol-2-yl)-2-isobutoxybenzonitrile (692 mg, 1.6 mmol) and iodine (40 mg, 0.16 mmol) in DMF (5.0 mL) for 24 hours. The product was obtained as a white solid (873 mg, 99%), by using hexane/acetone (7:3 to 11:9) as chromatography eluent. **M.p.**: 169 °C. **^{1}H NMR (400 MHz, DMSO-*d*$_6$)** δ 8.20 (d, *J* = 2.3 Hz, 1H), 8.14 (dd, *J* = 8.9, 2.3 Hz, 1H), 7.98 (s, 1H), 7.55 (dd, *J* = 7.7, 1.4 Hz, 1H), 7.33 (d, *J* = 9.0 Hz, 1H), 7.19 (td, *J* = 7.9, 7.3, 1.6 Hz, 1H), 6.70 – 6.65 (d, *J* = 7.8 Hz, 2H), 6.57 (t, *J* = 7.5, 1H), 4.12 (br. s, 2H) 3.97 (d, *J* = 6.5 Hz, 2H), 2.86 (br. s, 2H), 2.35 (s, 3H), 2.15 – 2.00 (m, 1H), 1.93 – 1.70 (m, 3H), 1.41 – 1.24 (m, 5H), 1.01 (d, *J* = 6.7 Hz, 6H) ppm. **^{13}C NMR (101 MHz, DMSO-*d*$_6$)** δ 163.9, 162.9, 161. 7, 160.8, 151.6, 146.9, 133.3, 132.7, 131.2, 127.1, 125.5, 125.2, 116.1, 115.5, 113.9, 113.8, 113.4, 101.5, 75.1, 70.7, 46.2, 27.6, 26.3, 25.1, 18.7, 16.2 ppm. Signal for the carbons *α* to the nitrogen of the piperidine invisible due

to broadening caused by restricted rotation. **HRMS** [ESI$^+$] *calcd*. for ($C_{30}H_{33}N_5NaO_3S$) [M+Na]$^+$: 566.2196, *found*: 566.2205.

3.7.3 Synthesis of Product

General procedure 4 (GP4): Copper-catalysed amination of 2,2-disubstituted dihydroquinazolinones

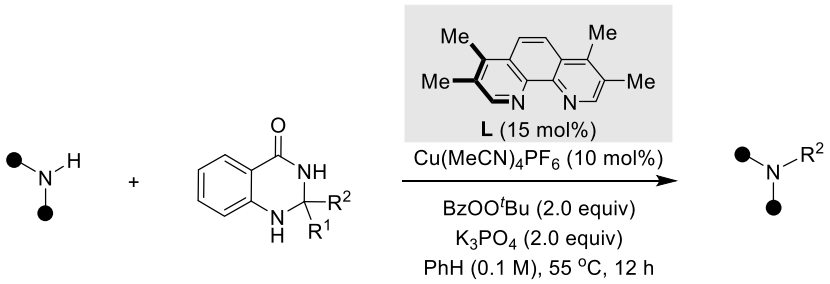

An oven-dried 8 mL screw-cap test tube containing a stirring bar was charged with *N*-nucleophile (1.0 equiv, 0.2 mmol) and dihydroquinazolinone (1.2 equiv), $Cu(MeCN)_4PF_6$ (7.5 mg, 10 mol%) and 3,4,7,8-tetramethyl-1,10-phenantroline (7.1 mg, 15 mol%). The test tube was taken into a nitrogen-filled glovebox where K_3PO_4 (84.8 mg, 2.0 equiv) was added. The reaction vessel was sealed with a screw cap septum and removed from the glovebox. Afterwards, benzene (2.0 mL, 0.1 M) was added by syringe. The reaction mixture was stirred at rt for 5 min, then BzOO^{t}Bu (77.6 mg, 2.0 equiv) was added slowly under vigorous stirring. Parafilm was used to reseal the septum. The reaction mixture was stirred at 55 °C for 12 hours. Afterwards, the reaction mixture was concentrated under reduced pressure and purified by silica gel chromatography to afford the desired product.

General procedure 5 (GP5): Copper-catalysed amination of 2,2-disubstituted dihydroquinazolinones

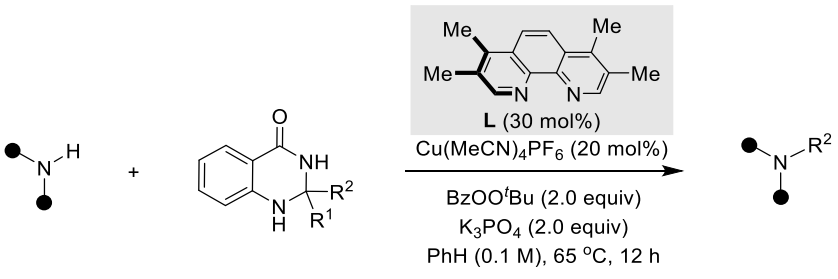

An oven-dried 8 mL screw-cap test tube containing a stirring bar was charged with *N*-nucleophile (1.0 equiv., 0.2 mmol) and dihydroquinazolinone (1.2 equiv),

$Cu(MeCN)_4PF_6$ (14.9 mg, 20 mol%) and 3,4,7,8-tetramethyl-1,10-phenantroline (14.2 mg, 30 mol%). The test tube was taken into a nitrogen-filled glovebox where K_3PO_4 (84.8 mg, 2.0 equiv) was added. The reaction vessel was sealed with a screw cap septum and removed from the glovebox. Afterwards, benzene (2.0 mL, 0.1 M) was added by syringe. The reaction mixture was stirred at rt for 5 min, then BzOO^{t}Bu (77.6 mg, 2.0 equiv) was added slowly under vigorous stirring. Parafilm was used to reseal the septum. The reaction mixture was stirred at 65 °C for 12 hours. Afterwards, the reaction mixture was concentrated under reduced pressure and purified by silica gel chromatography to afford the desired product.

General procedure 6 (GP6): Copper-catalysed amination of 2,2-disubstituted dihydroquinazolinones

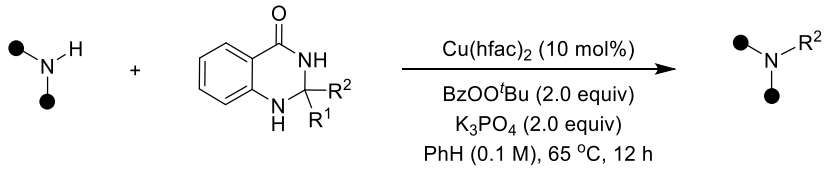

An oven-dried 8 mL screw-cap test tube containing a stirring bar was charged with *N*-nucleophile (1.0 equiv., 0.2 mmol) and dihydroquinazolinone (1.2 equiv), [Cu(II)(hfac)$_2$] (7.4 mg, 10 mol%). The test tube was taken into a nitrogen-filled glovebox where K_3PO_4 (84.8 mg, 2.0 equiv) was added. The reaction vessel was sealed with a screw cap septum and removed from the glovebox. Afterwards, benzene (2.0 mL, 0.1 M) was added by syringe. The reaction mixture was stirred at rt for 5 min, then BzOO^{t}Bu (77.6 mg, 2.0 equiv) was added slowly under vigorous stirring. Parafilm was used to reseal the septum. The reaction mixture was stirred at 65 °C for 12 hours. Afterwards, the reaction mixture was concentrated under reduced pressure and purified by silica gel chromatography to afford the desired product.

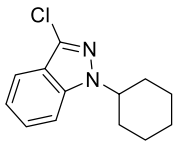

3-Chloro-1-cyclohexyl-1*H*-indazole (3a). Following GP4, using 3-chloro-1*H*-indazole (30.6 mg, 0.20 mmol) and 2-cyclohexyl-2-methyl-2,3-dihydroquinazolin-4(1*H*)-one (58.6 mg, 0.24 mmol), afforded the title product as a colourless liquid (39.9 mg, 85%) after purification by silica gel chromatography (hexane/EtOAc 100:1). In a second independent experiment, 37.4 mg (80%) were obtained, giving an average yield of 83%. **^{1}H NMR (400 MHz, CDCl$_3$)** δ 7.66 (dt, *J* = 8.2, 0.9 Hz, 1H), 7.46 – 7.35 (m,

2H), 7.21 – 7.14 (m, 1H), 4.41 – 4.29 (m, 1H), 2.09 – 1.99 (m, 4H), 1.99 – 1.90 (m, 2H), 1.81 – 1.72 (m, 1H), 1.54 – 1.40 (m, 2H), 1.39 – 1.26 (m, 1H) ppm. **^{13}C NMR (101 MHz, CDCl$_3$)** δ 140.1, 132.3, 127.1, 121.1, 121.1, 119.9, 109.5, 58.6, 32.6, 25.9, 25.4 ppm. Spectral data was in agreement with the literature.[87]

Following GP4, using 3-chloro-1*H*-indazole (30.6 mg, 0.20 mmol) and 2-cyclohexyl-2-ethyl-2,3-dihydroquinazolin-4(1*H*)-one (61.9 mg, 0.24 mmol), afforded the title product as a colourless liquid (37.3mg, 79%) after purification by silica gel chromatography (hexane/EtOAc 100:1). In a second independent experiment, 39.4 mg (84%) were obtained, giving an average yield of 82%. **^{1}H NMR (400 MHz, CDCl$_3$)** δ 7.66 (dt, *J* = 8.2, 1.0 Hz, 1H), 7.46 – 7.35 (m, 2H), 7.22 – 7.13 (m, 1H), 4.41 – 4.29 (m, 1H), 2.10 – 1.99 (m, 4H), 1.99 – 1.91 (m, 2H), 1.81 – 1.72 (m, 1H), 1.54 – 1.40 (m, 2H), 1.39 – 1.27 (m, 1H) ppm. **^{13}C NMR (101 MHz, CDCl$_3$)** δ 140.1, 132.3, 127.1, 121.1, 121.1, 119.9, 109.5, 58.6, 32.6, 25.9, 25.4 ppm.

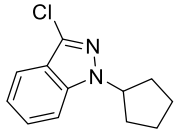

3-Chloro-1-cyclopentyl-1*H*-indazole (3b). Following GP4, using 3-chloro-1*H*-indazole (30.6 mg, 0.20 mmol) and 2-cyclopentyl-2-methyl-2,3-dihydroquinazolin-4(1*H*)-one (55.2 mg, 0.24 mmol), afforded the title product as a colourless liquid (21.7 mg, 49%) after purification by silica gel chromatography (hexane/EtOAc 100:1). In a second independent experiment, 20.7 mg (47%) were obtained, giving an average yield of 48%. **^{1}H NMR (400 MHz, CDCl$_3$)** δ 7.66 (dt, *J* = 8.2, 1.0 Hz, 1H), 7.46 – 7.36 (m, 2H), 7.21 – 7.14 (m, 1H), 4.93 (quin., *J* = 7.4 Hz, 1H), 2.24 – 2.09 (m, 4H), 2.04 – 1.91 (m, 2H), 1.79 – 1.66 (m, 2H) ppm. **^{13}C NMR (101 MHz, CDCl$_3$)** δ 140.7, 132.2, 127.1, 121.3, 121.1, 119.9, 109.7, 60.0, 32.4, 24.7 ppm. Spectral data was in agreement with the literature.[87]

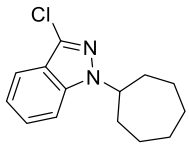

3-Chloro-1-cycloheptyl-7,7a-dihydro-1*H*-indazole (3c). Following GP4, using 3-chloro-1*H*-indazole (30.6 mg, 0.20 mmol) and 2-cycloheptyl-2-methyl-2,3-dihydroquinazolin-4(1*H*)-one (61.9 mg, 0.24 mmol), afforded the title product as a colourless liquid (35.0 mg, 70%) after purification by silica gel chromatography (hexane/EtOAc 100:1). In a second independent experiment, 34.9 mg (70%) were obtained, giving an average yield of 70%. **^{1}H NMR (400 MHz, CDCl$_3$)** δ 7.66 (dt, *J* = 8.2, 0.9 Hz, 1H), 7.44 – 7.35 (m, 2H), 7.22 – 7.13 (m, 1H), 4.56 (ddd, *J* = 14.5, 10.0, 4.5 Hz, 1H), 2.26 – 2.14 (m, 2H), 2.12 – 2.03 (m, 2H), 1.93 – 1.82 (m, 2H), 1.76 – 1.64 (m, 4H), 1.63 – 1.52 (m, 2H) ppm. **^{13}C NMR (101 MHz, CDCl$_3$)** δ 139.9, 132.2, 127.1,

121.1, 121.1, 119.9, 109.7, 61.0, 34.7, 28.0, 25.0 ppm. Spectral data was in agreement with the literature.[87]

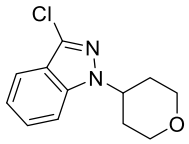

3-Chloro-1-(tetrahydro-2H-pyran-4-yl)-1*H*-indazole (3d). Following GP4, using 3-chloro-1*H*-indazole (30.6 mg, 0.20 mmol) and 2-methyl-2-(tetrahydro-2*H*-pyran-4-yl)-2,3-dihydroquinazolin-4(1*H*)-one (59.0 mg, 0.24 mmol), afforded the title product as a white solid (37.6 mg, 80%) after purification by silica gel chromatography (hexane/EtOAc 10:1). In a second independent experiment, 38.8 mg (82%) were obtained, giving an average yield of 81%. **^{1}H NMR (400 MHz, $CDCl_3$)** δ 7.68 (dt, *J* = 8.2, 0.9 Hz, 1H), 7.46 – 7.39 (m, 2H), 7.23 – 7.18 (m, 1H), 4.59 (tt, *J* = 11.5, 4.2 Hz, 1H), 4.16 (dd, *J* = 11.5, 4.6 Hz, 2H), 3.60 (td, *J* = 12.0, 2.1 Hz, 2H), 2.47 – 2.32 (m, 2H), 2.01 – 1.92 (m, 2H) ppm. **^{13}C NMR (101 MHz, $CDCl_3$)** δ 140.1, 132.9, 127.4, 121.4, 121.4, 120.1, 109.3, 67.3, 55.8, 32.5 ppm. Spectral data was in agreement with the literature.[87]

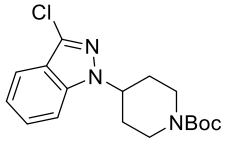

***tert*-Butyl 4-(3-chloro-1*H*-indazol-1-yl)piperidine-1-carboxylate (3e).** Following GP4, using 3-chloro-1*H*-indazole (30.6 mg, 0.20 mmol) and *tert*-butyl 4-(2-methyl-4-oxo-1,2,3,4-tetrahydroquinazolin-2-yl)piperidine-1-carboxylate (82.8 mg, 0.24 mmol), afforded the title product as a colourless liquid (31.7 mg, 46%) after purification by silica gel chromatography (hexane/EtOAc 10:1). In an independent experiment, 33.7 mg (50%) were obtained, giving an average yield of 48%. **^{1}H NMR (500 MHz, $CDCl_3$)** δ 7.67 (dt, *J* = 8.2, 0.9 Hz, 1H), 7.47 – 7.38 (m, 2H), 7.23 – 7.17 (m, 1H), 4.50 (tt, *J* = 11.5, 4.1 Hz, 1H), 4.44 – 4.18 (m, 2H), 3.05 – 2.81 (m, 2H), 2.29 – 2.15 (m, 2H), 2.03 – 1.94 (m, 2H), 1.48 (s, 9H) ppm. **^{13}C NMR (126 MHz, $CDCl_3$)** δ 154.7, 140.2, 133.0, 127.5, 121.5, 121.4, 120.1, 109.3, 80.0, 56.7, 43.5, 31.6, 28.6 ppm. Spectral data was in agreement with the literature.[87]

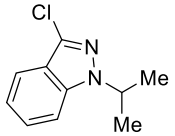

3-Chloro-1-isopropyl-1*H*-indazole (3f). Following GP4, using 3-chloro-1*H*-indazole (30.6 mg, 0.20 mmol) and 2-isopropyl-2-methyl-2,3-dihydroquinazolin-4(1*H*)-one (49.0 mg, 0.24 mmol), afforded the title product as a colourless oil (32.4 mg, 83%) after purification by silica gel chromatography (hexane/EtOAc 100:1). In a second independent experiment, 33.7 mg (86%) were obtained, giving an average yield of 85%.

^{1}H NMR (400 MHz, $CDCl_3$) δ 7.67 (dt, *J* = 8.2, 1.0 Hz, 1H), 7.43 – 7.37 (m, 2H), 7.22 – 7.14 (m, 1H), 4.79 (hept., *J* = 6.7 Hz, 1H), 1.58 (d, *J* = 6.7 Hz, 6H) ppm. **^{13}C NMR (101 MHz, $CDCl_3$)** δ 140.1, 132.4, 127.2, 121.2, 121.2, 119.9, 109.5, 51.0, 22.2 ppm. Spectral data was in agreement with the literature.[87]

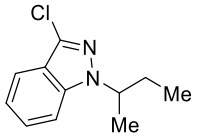

1-(*sec*-Butyl)-3-chloro-1*H*-indazole (3g). Following GP4, using 3-chloro-1*H*-indazole (30.6 mg, 0.20 mmol) and 2-(*sec*-butyl)-2-methyl-2,3-dihydroquinazolin-4(1*H*)-one (52.3 mg, 0.24 mmol), afforded the title product as a colourless oil (32.2 mg, 77%) after purification by silica gel chromatography (hexane/EtOAc 100:1). In a second independent experiment, 33.1 mg (79%) were obtained, giving an average yield of 78%. **IR (neat, cm^{-1}):** 2970, 1616, 1493, 1463, 1336, 1201, 1128, 1005, 767, 739. **^{1}H NMR (400 MHz, $CDCl_3$)** δ 7.67 (d, *J* = 8.2 Hz, 1H), 7.43 – 7.35 (m, 2H), 7.22 – 7.13 (m, 1H), 4.55 – 4.44 (m, 1H), 2.16 – 2.02 (m, 1H), 1.94 – 1.81 (m, 1H), 1.56 (d, *J* = 6.7 Hz, 3H), 0.79 (t, *J* = 7.4 Hz, 3H) ppm. **^{13}C NMR (101 MHz, $CDCl_3$)** δ 140.9, 132.6, 127.2, 121.1, 121.0, 119.9, 109.5, 57.0, 29.7, 20.6, 11.2 ppm. **HRMS** [ESI$^+$] *calcd*. for ($C_{11}H_{14}ClN_2$) [M+H]$^+$: 209.0840, *found*: 209.0838.

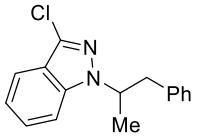

3-Chloro-1-(1-phenylpropan-2-yl)-1*H*-indazole (3h). Following GP4, using 3-chloro-1*H*-indazole (30.6 mg, 0.20 mmol) and 2-methyl-2-(1-phenylpropan-2-yl)-2,3-dihydroquinazolin-4(1*H*)-one (67.2 mg, 0.24 mmol), afforded the title product as a colourless liquid (39.5 mg, 73%) after purification by silica gel chromatography (hexane/EtOAc 100:1). In a second independent experiment, 42.0 mg (77%) were obtained, giving an average yield of 75%. **IR (neat, cm^{-1}):**2979, 1616, 1493, 1463, 1336, 1179, 972, 738, 698. **^{1}H NMR (400 MHz, $CDCl_3$)** δ 7.57 – 7.50 (m, 1H), 7.22 – 7.15 (m, 1H), 7.10 – 6.99 (m, 5H), 6.95 – 6.89 (m, 2H), 4.74 – 4.62 (m, 1H), 3.21 (dd, *J* = 13.6, 8.0 Hz, 1H), 3.03 (dd, *J* = 13.6, 6.5 Hz, 1H), 1.54 (d, *J* = 6.7 Hz, 3H) ppm. **^{13}C NMR (101 MHz, $CDCl_3$)** δ 140.9, 138.4, 132.8, 129.1, 128.5, 127.1, 126.6, 121.1, 120.8, 119.7, 109.2, 57.0, 43.2, 20.4 ppm. **HRMS** [ESI$^+$] *calcd*. for ($C_{16}H_{16}ClN_2$) [M+H]$^+$: 271.0997, *found*: 271.1000.

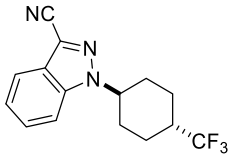

1-((1*r*,4*r*)-4-(Trifluoromethyl)cyclohexyl)-1*H*-indazole-3-carbonitrile (3i). Following GP5, using 1*H*-indazole-3-carbonitrile (28.6 mg, 0.20 mmol) and 2-methyl-

2-(4-(trifluoromethyl)cyclohexyl)-2,3-dihydroquinazolin-4(1*H*)-one (74.9 mg, 0.24 mmol), afforded the title product as a white solid (33.7 mg, 58%) after purification by silica gel chromatography (hexane/EtOAc 25:1). Analysis of the crude post-workup material by ^{1}H NMR showed product was formed in a 6.4:1 diastereomeric ratio. In an independent experiment, 33.6 mg (57%) were obtained, giving an average yield of 57%. **M.p.**: 123 °C. **IR (neat, cm^{-1}):** 2946, 2233, 1466, 1392, 1339, 1274, 1210, 1176, 1147, 1123, 1077, 971, 906, 746. **^{1}H NMR (400 MHz, CDCl$_3$)** δ 7.85 (dt, *J* = 8.2, 0.9 Hz, 1H), 7.58 – 7.47 (m, 2H), 7.40 – 7.32 (m, 1H), 4.52 (tt, *J* = 11.6, 3.8 Hz, 1H), 2.31 – 2.06 (m, 7H), 1.69 – 1.54 (m, 2H) ppm. **^{13}C NMR (101 MHz, CDCl$_3$)** δ 139.1, 127.8, 127.5 (q, $J_{C,F}$ = 279.1 Hz), 125.6, 123.8, 120.0, 117.9, 113.9, 110.0, 58.0, 41.0 (q, $J_{C,F}$ = 27.1 Hz), 30.7, 24.3 (q, $J_{C,F}$ = 2.7 Hz) ppm. **^{19}F NMR** (376 MHz, $CDCl_3$) δ -73.6 ppm. **HRMS** [ESI$^+$] *calcd*. for ($C_{15}H_{15}F_3N_3$) [M+H]$^+$: 294.1213, *found*: 294.1211.

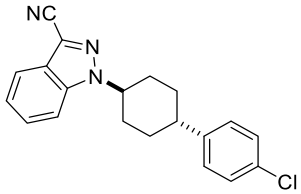

1-((1,4)-4-(4-Chlorophenyl)cyclohexyl)-1*H*-indazole-3-carbonitrile (3j). Following GP5, using 1*H*-indazole-3-carbonitrile (28.6 mg, 0.20 mmol) and 2-(4-(4-chlorophenyl)cyclohexyl)-2-methyl-2,3-dihydroquinazolin-4(1*H*)-one (85.2 mg, 0.24 mmol), afforded the title product as a white solid (44.9 mg, 67%) after purification by silica gel chromatography (hexane/EtOAc 25:1). Analysis of the crude post-workup material by ^{1}H NMR showed product was formed in a 6.3:1 diastereomeric ratio. In an independent experiment, 48.6 mg (72%) were obtained, giving an average yield of 70%. **M.p.**: 108 °C. **IR (neat, cm^{-1}):** 2935, 2858, 2228, 1615, 1491, 1466, 1350, 1213, 1088, 1012, 817, 747, 525. **^{1}H NMR (400 MHz, CDCl$_3$)** δ 7.85 (dt, *J* = 8.2, 0.9 Hz, 1H), 7.60 (d, *J* = 8.6 Hz, 1H), 7.54 – 7.47 (m, 1H), 7.39 – 7.33 (m, 1H), 7.33 – 7.28 (m, 2H), 7.23 – 7.18 (m, 2H), 4.61 (tt, *J* = 10.9, 5.0 Hz, 1H), 2.72 (tt, *J* = 12.2, 3.4 Hz, 1H), 2.34 – 2.19 (m, 4H), 2.18 – 2.09 (m, 2H), 1.80 – 1.65 (m, 2H) ppm. **^{13}C NMR (101 MHz, CDCl$_3$)** δ 144.5, 139.1, 132.1, 128.8, 128.2, 127.6, 125.6, 123.7, 119.9, 117.6, 114.0, 110.2, 58.9, 42.7, 33.2, 32.5 ppm. **HRMS** [ESI$^+$] *calcd*. for ($C_{20}H_{19}ClN_3$) [M+H]$^+$: 336.1262, *found*: 336.1260.

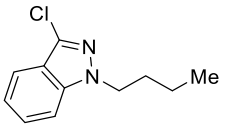

1-Butyl-3-chloro-1*H*-indazole (3k). Following GP4, using 3-chloro-1*H*-indazole (30.6 mg, 0.20 mmol) and 2-butyl-2-phenyl-2,3-dihydroquinazolin-4(1*H*)-one (67.2 mg, 0.24 mmol), afforded the title product as a colourless liquid (26.8 mg, 64%) after purification by silica gel chromatography (hexane/EtOAc 100:1). In a second

independent experiment, 23.8 mg (57%) were obtained, giving an average yield of 61%. **IR (neat, cm^{-1}):** 2959, 2873, 1617, 1495, 1466, 1336, 1239, 1189, 1126, 1056, 1006, 739. **^{1}H NMR (400 MHz, CDCl$_3$)** δ 7.67 (dt, *J* = 8.2, 1.0 Hz, 1H), 7.45 – 7.34 (m, 2H), 7.22 – 7.15 (m, 1H), 4.32 (t, *J* = 7.1 Hz, 2H), 1.95 – 1.85 (m, 2H), 1.40 – 1.28 (m, 2H), 0.94 (t, *J* = 7.4 Hz, 3H) ppm. **^{13}C NMR (101 MHz, CDCl$_3$)** δ 141.0, 132.5, 127.4, 121.2, 121.1, 120.0, 109.5, 49.2, 32.0, 20.2, 13.8 ppm. **HRMS** [ESI$^+$] *calcd*. for ($C_{11}H_{14}ClN_2$) [M+H]$^+$: 209.0840, *found*: 209.0842.

Following GP4, using 3-chloro-1*H*-indazole (30.6 mg, 0.20 mmol) and 2-butyl-2-(4-methoxyphenyl)-2,3-dihydroquinazolin-4(1*H*)-one (74.4 mg, 0.24 mmol), afforded the title product as a colourless liquid (29.2 mg, 70%) after purification by silica gel chromatography (hexane/EtOAc 100:1). In a second independent experiment, 29.7 mg (71%) were obtained, giving an average yield of 70%.

Following GP4, using 3-chloro-1*H*-indazole (30.6 mg, 0.20 mmol) and 2-(benzo[d][1,3]dioxol-5-yl)-2-butyl-2,3-dihydroquinazolin-4(1*H*)-one (77.8 mg, 0.24 mmol), afforded the title product as a colourless liquid (27.5 mg, 66%) after purification by silica gel chromatography (hexane/EtOAc 100:1). In a second independent experiment, 26.6 mg (64%) were obtained, giving an average yield of 65%.

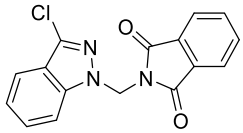

2-((3-Chloro-1*H*-indazol-1-yl)methyl)isoindoline-1,3-dione (3l). Following GP4, using 1*H*-indazole-3-carbonitrile (28.6 mg, 0.20 mmol) and 2-((2-methyl-4-oxo-1,2,3,4-tetrahydroquinazolin-2-yl)methyl)isoindoline-1,3-dione (77.1 mg, 0.24 mmol), afforded the title product as a white solid (32.6 mg, 52%) after purification by silica gel chromatography (hexane/EtOAc 5:1). In a second independent experiment, 35.4 mg (57%) were obtained, giving an average yield of 54%. **M.p.**: 158 °C. **IR (neat, cm^{-1}):** 1775, 1716, 1466, 1309, 1214, 1062, 943, 722, 603, 523. **^{1}H NMR (400 MHz, CDCl$_3$)** δ 7.91 (dt, *J* = 8.6, 0.8 Hz, 1H), 7.90 – 7.85 (m, 2H), 7.76 – 7.70 (m, 2H), 7.63 (dt, *J* = 8.2, 0.9 Hz, 1H), 7.54 – 7.48 (m, 1H), 7.26 – 7.21 (m, 1H), 6.17 (s, 2H) ppm. **^{13}C NMR (101 MHz, CDCl$_3$)** δ 167.3, 141.1, 135.4, 134.7, 131.8, 128.4, 124.0, 122.2, 121.8, 119.8, 110.6, 49.6 ppm. **HRMS** [ESI$^+$] *calcd*. for ($C_{16}H_{11}ClN_3O_2$) [M+H]$^+$: 312.0534, *found*: 312.0535.

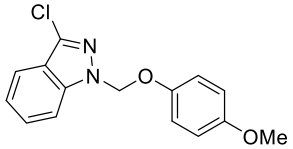

3-Chloro-1-((4-methoxyphenoxy)methyl)-1*H*-indazole (3m). Following GP4, using 3-chloro-1*H*-indazole (30.6 mg, 0.20 mmol) and 2-((4-methoxyphenoxy)methyl)-2-methyl-2,3-dihydroquinazolin-4(1*H*)-one (71.5 mg, 0.24 mmol), afforded the title

product as a white solid (31.4 mg, 54%) after purification by silica gel chromatography (hexane/EtOAc 10:1). In a second independent experiment, 32.8 mg (57%) were obtained, giving an average yield of 56%. **M.p.**: 66 °C. **IR (neat, cm^{-1}):** 3017, 1618, 1510, 1468, 1398, 1332, 1246, 1218, 1005, 858, 820, 741, 522. **^{1}H NMR (400 MHz, $CDCl_3$)** δ 7.68 (dt, *J* = 8.2, 0.9 Hz, 1H), 7.53 – 7.42 (m, 2H), 7.29 – 7.22 (m, 1H), 6.98 – 6.91 (m, 2H), 6.81 – 6.76 (m, 2H), 6.14 (s, 2H), 3.74 (s, 3H) ppm. **^{13}C NMR (101 MHz, $CDCl_3$)** δ 155.5, 150.8, 141.3, 135.2, 128.4, 122.4, 122.3, 120.0, 118.4, 114.9, 110.2, 77.9, 55.8 ppm. **HRMS** [ESI$^+$] *calcd*. for ($C_{15}H_{13}ClN_2NaO_2$) [M+Na]$^+$: 311.0558, *found*: 311.0561.

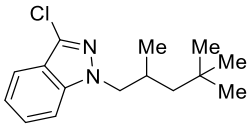

3-Chloro-1-(2,4,4-trimethylpentyl)-1*H*-indazole (3n). Following GP4, using 3-chloro-1*H*-indazole (30.6 mg, 0.20 mmol) and 2-phenyl-2-(2,4,4-trimethylpentyl)-2,3-dihydroquinazolin-4(1*H*)-one (80.6 mg, 0.24 mmol), afforded the title product as a colourless liquid (35.0 mg, 66%) after purification by silica gel chromatography (hexane/EtOAc 100:1). In a second independent experiment, 37.1 mg (70%) were obtained, giving an average yield of 68%. **IR (neat, cm^{-1}):** 2955, 1617, 1495, 1467, 1336, 1254, 1174, 1127, 985, 765, 739. **^{1}H NMR (400 MHz, $CDCl_3$)** δ 7.66 (dt, *J* = 8.2, 0.9 Hz, 1H), 7.46 – 7.33 (m, 2H), 7.22 – 7.15 (m, 1H), 4.18 (dd, *J* = 13.9, 6.6 Hz, 1H), 4.01 (dd, *J* = 13.9, 8.6 Hz, 1H), 2.34 – 2.19 (m, 1H), 1.31 (dd, *J* = 14.0, 3.4 Hz, 1H), 1.16 (dd, *J* = 14.0, 6.5 Hz, 1H), 0.89 (d, *J* = 6.7 Hz, 3H), 0.86 (s, 9H) ppm. **^{13}C NMR (101 MHz, $CDCl_3$)** δ 141.4, 132.5, 127.4, 121.1, 121.0, 119.9, 109.6, 56.8, 48.3, 31.2, 30.9, 29.9, 20.7 ppm. **HRMS** [ESI$^+$] *calcd*. for ($C_{15}H_{22}ClN_2$) [M+H]$^+$: 265.1466, *found*: 265.1469.

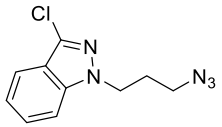

1-(3-Azidopropyl)-3-chloro-1*H*-indazole (3o). Following GP4, using 3-chloro-1*H*-indazole (30.6 mg, 0.20 mmol) and 2-(3-azidopropyl)-2-phenyl-2,3-dihydroquinazolin-4(1*H*)-one (73.7 mg, 0.24 mmol), afforded the title product as a colourless liquid (25.4 mg, 54%) after purification by silica gel chromatography (hexane/EtOAc 20:1). In a second independent experiment, 25.6 mg (54%) were obtained, giving an average yield of 54%. **IR (neat, cm^{-1}):** 2938, 2093, 1616, 1495, 1466, 1336, 1174, 1128, 740. **^{1}H NMR (400 MHz, $CDCl_3$)** δ 7.68 (dt, *J* = 8.2, 0.9 Hz, 1H), 7.49 – 7.39 (m, 2H), 7.24 – 7.18 (m, 1H), 4.41 (t, *J* = 6.5 Hz, 2H), 3.30 (t, *J* = 6.4 Hz, 2H), 2.19 (quin., *J* = 6.4 Hz, 2H) ppm. **^{13}C NMR (101 MHz, $CDCl_3$)** δ 141.3, 133.4, 127.9, 121.5, 121.2, 120.0, 109.3, 48.5, 45.8, 29.1 ppm. **HRMS** [APCI$^+$] *calcd*. for ($C_{10}H_{11}ClN_5$) [M+H]$^+$: 236.0697, *found*: 236.0694.

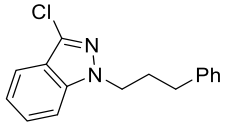

3-Chloro-1-(3-phenylpropyl)-1*H*-indazole (3p). Following GP4, using 3-chloro-1*H*-indazole (30.6 mg, 0.20 mmol) and 2-phenyl-2-(3-phenylpropyl)-2,3-dihydroquinazolin-4(1*H*)-one (82.1 mg, 0.24 mmol), afforded the title product as a colourless liquid (26.3 mg, 49%) after purification by silica gel chromatography (hexane/EtOAc 100:1). In a second independent experiment, 27.7 mg (51%) were obtained, giving an average yield of 50%. **IR (neat, cm^{-1}):** 3026, 2929, 1616, 1495, 1466, 1336, 1170, 1127, 739, 697. **^{1}H NMR (400 MHz, CDCl$_3$)** δ 7.71 – 7.65 (m, 1H), 7.44 – 7.37 (m, 1H), 7.33 – 7.25 (m, 3H), 7.24 – 7.14 (m, 4H), 4.33 (t, *J* = 7.0 Hz, 2H), 2.70 – 2.62 (m, 2H), 2.34 – 2.22 (m, 2H) ppm. **^{13}C NMR (101 MHz, CDCl$_3$)** δ 141.0, 140.9, 132.8, 128.6, 128.6, 127.5, 126.3, 121.3, 121.2, 120.0, 109.5, 48.5, 32.9, 31.1 ppm. **HRMS** [ESI$^+$] *calcd*. for ($C_{16}H_{16}ClN_2$) [M+H]$^+$: 271.0997, *found*: 271.1003.

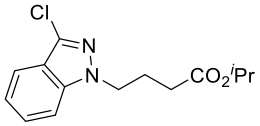

Isopropyl 4-(3-chloro-1*H*-indazol-1-yl)butanoate (3q). Following GP4, using 3-chloro-1*H*-indazole (30.6 mg, 0.20 mmol) and isopropyl 4-(4-oxo-2-phenyl-1,2,3,4-tetrahydroquinazolin-2-yl)butanoate (84.5 mg, 0.24 mmol), afforded the title product as a colourless liquid (30.9 mg, 55%) after purification by silica gel chromatography (hexane/EtOAc 20:1). In a second independent experiment, 34.7 mg (62%) were obtained, giving an average yield of 58%. **IR (neat, cm^{-1}):** 2980, 1724, 1617, 1495, 1467, 1374, 1337, 1171, 1106, 741. **^{1}H NMR (400 MHz, CDCl$_3$)** δ 7.66 (dt, *J* = 8.2, 0.9 Hz, 1H), 7.45 – 7.37 (m, 2H), 7.22 – 7.16 (m, 1H), 5.00 (hept., *J* = 6.3 Hz, 1H), 4.40 (t, *J* = 6.5 Hz, 2H), 2.31 – 2.17 (m, 4H), 1.21 (d, *J* = 6.3 Hz, 6H) ppm. **^{13}C NMR (101 MHz, CDCl$_3$)** δ 172.4, 141.1, 133.0, 127.6, 121.4, 121.2, 119.9, 109.4, 68.1, 48.2, 31.3, 25.1, 22.0 ppm. **HRMS** [ESI$^+$] *calcd*. for ($C_{14}H_{18}ClN_2O_2$) [M+H]$^+$: 281.1051, *found*: 281.1053.

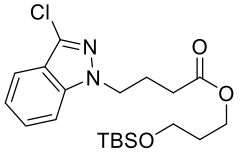

3-((*tert*-Butyldimethylsilyl)oxy)propyl 4-(3-chloro-1*H*-indazol-1-yl)butanoate (3r). Following GP4, using 3-chloro-1*H*-indazole (30.6 mg, 0.20 mmol) and 3-((*tert*-butyldimethylsilyl)oxy)propyl 4-(4-oxo-2-phenyl-1,2,3,4-tetrahydroquinazolin-2-yl)butanoate (115.9 mg, 0.24 mmol), afforded the title product as a colourless liquid (37.6 mg, 46%) after purification by silica gel chromatography (hexane/EtOAc 20:1). In a second independent experiment, 37.5 mg (46%) were obtained, giving an average

yield of 46%. **IR (neat, cm^{-1}):** 3411, 2954, 1730, 1617, 1496, 1467, 1338, 1253, 1171, 1096, 834, 743. **^{1}H NMR (400 MHz, CDCl$_3$)** δ 7.67 (dt, *J* = 8.2, 0.9 Hz, 1H), 7.46 – 7.36 (m, 2H), 7.23 – 7.15 (m, 1H), 4.40 (t, *J* = 6.6 Hz, 2H), 4.16 (t, *J* = 6.4 Hz, 2H), 3.66 (t, *J* = 6.1 Hz, 2H), 2.36 – 2.27 (m, 2H), 2.27 – 2.18 (m, 2H), 1.80 (quin., *J* = 6.3 Hz, 2H), 0.87 (s, 9H), 0.03 (s, 6H) ppm. **^{13}C NMR (101 MHz, CDCl$_3$)** δ 172. 9, 141.1, 133.0, 127.7, 121.4, 121.2, 120.0, 109.4, 61.8, 59.5, 48.1, 31.8, 31.0, 26.0, 25.0, 18.4, -5.3 ppm. **HRMS** [ESI$^+$] *calcd*. for ($C_{20}H_{31}ClN_2NaO_3Si$) [M+Na]$^+$: 433.1685, *found*: 433.1688.

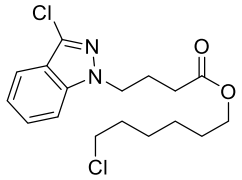

6-Chlorohexyl 4-(3-chloro-1*H*-indazol-1-yl)butanoate (3s). Following GP4, using 3-chloro-1*H*-indazole (30.6 mg, 0.20 mmol) and 6-chlorohexyl 4-(4-oxo-2-phenyl-1,2,3,4-tetrahydroquinazolin-2-yl)butanoate (103.0 mg, 0.24 mmol), afforded the title product as a colourless liquid (44.3 mg, 62%) after purification by silica gel chromatography (hexane/EtOAc 20:1). In a second independent experiment, 48.6 mg (68%) were obtained, giving an average yield of 65%. **IR (neat, cm^{-1}):** 2938, 1728, 1617, 1495, 1467, 1337, 1169, 742. **^{1}H NMR (400 MHz, CDCl$_3$)** δ 7.67 (dt, *J* = 8.2, 0.9 Hz, 1H), 7.47 – 7.35 (m, 2H), 7.23 – 7.16 (m, 1H), 4.40 (t, *J* = 6.6 Hz, 2H), 4.05 (t, *J* = 6.7 Hz, 2H), 3.52 (t, *J* = 6.7 Hz, 2H), 2.36 – 2.29 (m, 2H), 2.28 – 2.19 (m, 2H), 1.82 – 1.71 (m, 2H), 1.67 – 1.56 (m, 2H), 1.51 – 1.40 (m, 2H), 1.40 – 1.30 (m, 2H) ppm. **^{13}C NMR (101 MHz, CDCl$_3$)** δ 172.9, 141.1, 133.0, 127.7, 121.4, 121.2, 120.0, 109.4, 64.6, 48.1, 45.1, 32.5, 31.0, 28.6, 26.6, 25.4, 25.0 ppm. **HRMS** [ESI$^+$] *calcd*. for ($C_{17}H_{22}Cl_2N_2NaO_2$) [M+Na]$^+$: 379.0951, *found*: 379.0951.

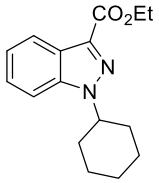

Ethyl 1-cyclohexyl-1*H*-indazole-3-carboxylate (5a). Following GP5, using ethyl 1*H*-indazole-3-carboxylate (38.0 mg, 0.20 mmol) and 2-cyclohexyl-2-methyl-2,3-dihydroquinazolin-4(1*H*)-one (58.6 mg, 0.24 mmol), afforded the title product as a colourless liquid (31.8 mg, 58%) after purification by silica gel chromatography (hexane/EtOAc 20:1). In a second independent experiment, 29.8 mg (55%) were obtained, giving an average yield of 57%. **IR (neat, cm^{-1}):** 2932, 2857, 1704, 1474, 1236, 1167, 1121, 750. **^{1}H NMR (400 MHz, CDCl$_3$)** δ 8.21 (dt, *J* = 8.2, 1.0 Hz, 1H), 7.53 (d, *J* = 8.5 Hz, 1H), 7.40 (ddd, *J* = 8.4, 6.9, 1.1 Hz, 1H), 7.29 (ddd, *J* = 7.8, 6.9, 0.8 Hz, 1H), 4.58 – 4.47 (m, 3H), 2.22 – 2.05 (m, 4H), 2.02 – 1.92 (m, 2H), 1.82 – 1.73 (m, 1H), 1.55 – 1.42 (m, 5H), 1.42 – 1.32 (m, 1H) ppm. **^{13}C NMR (101 MHz, CDCl$_3$)**

δ 163.1, 139.9, 134.7, 126.4, 124.0, 123.0, 122.5, 110.1, 61.0, 59.7, 32.4, 25.9, 25.3, 14.7 ppm. **HRMS** [ESI$^+$] *calcd.* for ($C_{16}H_{20}N_2NaO_2$) [M+Na]$^+$: 295.1417, *found*: 295.1426.

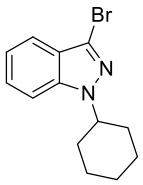

3-Bromo-1-cyclohexyl-1*H*-indazole (5b). Following GP5, using 3-bromo-1*H*-indazole (39.4 mg, 0.20 mmol) and 2-cyclohexyl-2-methyl-2,3-dihydroquinazolin-4(1*H*)-one (58.6 mg, 0.24 mmol), afforded the title product as a colourless liquid (41.4 mg, 74%) after purification by silica gel chromatography (hexane/EtOAc 100:1). In a second independent experiment, 41.2 mg (74%) were obtained, giving an average yield of 74%. **^{1}H NMR (400 MHz, $CDCl_3$)** δ 7.60 (dt, *J* = 8.2, 1.0 Hz, 1H), 7.45 – 7.37 (m, 2H), 7.22 – 7.16 (m, 1H), 4.43 – 4.30 (m, 1H), 2.12 – 2.00 (m, 4H), 2.00 – 1.90 (m, 2H), 1.81 – 1.72 (m, 1H), 1.54 – 1.40 (m, 2H), 1.39 – 1.26 (m, 1H) ppm. **^{13}C NMR (101 MHz, $CDCl_3$)** δ 140.0, 127.1, 123.7, 121.3, 120.6, 119.9, 109.5, 58.8, 32.7, 25.9, 25.4 ppm. Spectral data was in agreement with the literature.[87]

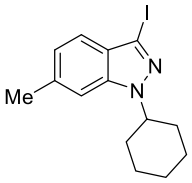

1-Cyclohexyl-3-iodo-6-methyl-1*H*-indazole (5c). Following GP5, using 3-iodo-6-methyl-1*H*-indazole (51.6 mg, 0.20 mmol) and 2-cyclohexyl-2-methyl-2,3-dihydroquinazolin-4(1*H*)-one (58.6 mg, 0.24 mmol), afforded the title product as a colourless oil (49.5 mg, 73%) after purification by silica gel chromatography (hexane/EtOAc 100:1). In a second independent experiment, 47.9 mg (70%) were obtained, giving an average yield of 72%. **IR (neat, cm^{-1}):** 2929, 2854, 1620, 1462, 1323, 1200, 1166, 1131, 965, 796. **^{1}H NMR (400 MHz, $CDCl_3$)** δ 7.33 (d, *J* = 8.3 Hz, 1H), 7.20 – 7.17 (m, 1H), 7.03 – 6.98 (m, 1H), 4.40 – 4.29 (m, 1H), 2.51 (s, 3H), 2.12 – 1.90 (m, 6H), 1.80 – 1.71 (m, 1H), 1.53 – 1.39 (m, 2H), 1.39 – 1.30 (m, 1H) ppm. **^{13}C NMR (101 MHz, $CDCl_3$)** δ 140.0, 137.4, 126.7, 123.6, 121.3, 108.8, 90.4, 58.9, 32.7, 26.0, 25.4, 22.2 ppm. **HRMS** [ESI$^+$] *calcd.* for ($C_{14}H_{18}IN_2$) [M+H]$^+$: 341.0509, *found*: 341.0511.

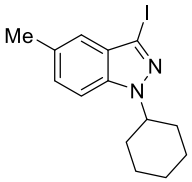

1-Cyclohexyl-3-iodo-5-methyl-1*H*-indazole (5d). Following GP5, using 3-iodo-5-

methyl-1*H*-indazole (51.6 mg, 0.20 mmol) and 2-cyclohexyl-2-methyl-2,3-dihydroquinazolin-4(1*H*)-one (58.6 mg, 0.24 mmol), afforded the title product as a colourless oil (45.0 mg, 66%) after purification by silica gel chromatography (hexane/EtOAc 100:1). In a second independent experiment, 47.9 mg (70%) were obtained, giving an average yield of 68%. **IR (neat, cm^{-1}):** 2930, 2854, 1495, 1447, 1290, 1183, 790. **^{1}H NMR (400 MHz, CDCl$_3$)** δ 7.34 – 7.29 (m, 1H), 7.28 – 7.21 (m, 2H), 4.42 – 4.30 (m, 1H), 2.47 (s, 3H), 2.12 – 2.00 (m, 4H), 2.00 – 1.90 (m, 2H), 1.80 – 1.71 (m, 1H), 1.53 – 1.39 (m, 2H), 1.39 – 1.29 (m, 1H) ppm. **^{13}C NMR (101 MHz, CDCl$_3$)** δ 138.2, 130.9, 129.1, 128.6, 120.7, 109.2, 89.8, 59.2, 32.7, 26.0, 25.4, 21.4 ppm. **HRMS** [ESI$^+$] *calcd*. for ($C_{14}H_{18}IN_2$) [M+H]$^+$: 341.0509, *found*: 341.0509.

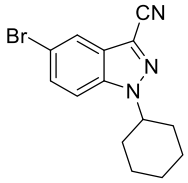

5-Bromo-1-cyclohexyl-1*H*-indazole-3-carbonitrile (5e). Following GP5, using 5-bromo-1*H*-indazole-3-carbonitrile (44.4 mg, 0.20 mmol) and 2-cyclohexyl-2-methyl-2,3-dihydroquinazolin-4(1*H*)-one (58.6 mg, 0.24 mmol), afforded the title product as a white solid (46.3 mg, 76%) after purification by silica gel chromatography (hexane/EtOAc 10:1). In a second independent experiment, 47.8 mg (79%) were obtained, giving an average yield of 77%. **M.p.**: 111 °C. **IR (neat, cm^{-1}):** 2928, 2856, 2233, 1474, 1302, 1271, 1209, 798, 591. **^{1}H NMR (500 MHz, CDCl$_3$)** δ 7.99 (dd, *J* = 1.7, 0.6 Hz, 1H), 7.55 (dd, *J* = 9.0, 1.7 Hz, 1H), 7.45 (d, *J* = 9.0 Hz, 1H), 4.45 (tt, *J* = 10.9, 4.3 Hz, 1H), 2.10 – 1.94 (m, 6H), 1.83 – 1.75 (m, 1H), 1.54 – 1.43 (m, 2H), 1.40 – 1.31 (m, 1H) ppm. **^{13}C NMR (126 MHz, CDCl$_3$)** δ 137.7, 130.8, 126.9, 122.4, 117.2, 116.7, 113.5, 111.7, 59.9, 32.6, 25.6, 25.2 ppm. **HRMS** [ESI$^+$] *calcd*. for ($C_{14}H_{14}BrN_3Na$) [M+Na]$^+$: 326.0263, *found*: 326.0256.

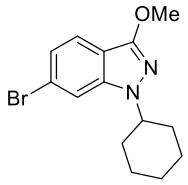

6-Bromo-1-cyclohexyl-3-methoxy-1*H*-indazole (5f). Following GP5, using 6-bromo-3-methoxy-1*H*-indazole (45.4 mg, 0.20 mmol) and 2-cyclohexyl-2-methyl-2,3-dihydroquinazolin-4(1*H*)-one (58.6 mg, 0.24 mmol), afforded the title product as a colourless oil (40.6 mg, 66%) after purification by silica gel chromatography (hexane/EtOAc 20:1). In a second independent experiment, 43.2 mg (70%) were obtained, giving an average yield of 68%. **IR (neat, cm^{-1}):** 2932, 2855, 1611, 1532, 1401, 1209, 1156, 1100, 1048, 798, 706. **^{1}H NMR (400 MHz, CDCl$_3$)** δ 7.50 – 7.43 (m, 2H), 7.09 (dd, *J* = 8.5, 1.5 Hz, 1H), 4.18 – 4.07 (m, 1H), 4.06 (s, 3H), 2.03 – 1.87

(m, 6H), 1.80 – 1.69 (m, 1H), 1.51 – 1.37 (m, 2H), 1.37 – 1.27 (m, 1H) ppm. **^{13}C NMR (101 MHz, $CDCl_3$)** δ 156.0, 141.2, 122.3, 121.4, 121.3, 111.7, 111.4, 58.0, 56.3, 32.2, 25.9, 25.5 ppm. **HRMS** [ESI$^+$] *calcd*. for ($C_{14}H_{18}BrN_2O$) $[M+H]^+$: 309.0597, *found*: 309.0597.

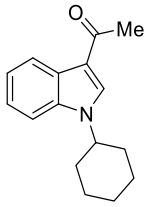

1-(1-Cyclohexyl-1*H*-indol-3-yl)ethan-1-one (5g). Following GP5, using 1-(1*H*-indol-3-yl)ethan-1-one (31.8 mg, 0.20 mmol) and 2-cyclohexyl-2-methyl-2,3-dihydroquinazolin-4(1*H*)-one (58.6 mg, 0.24 mmol), afforded the title product as a white solid (24.9 mg, 52%) after purification by silica gel chromatography (hexane/EtOAc 20:1). In a second independent experiment, 23.7 mg (49%) were obtained, giving an average yield of 50%. **^{1}H NMR (400 MHz, $CDCl_3$)** δ 8.41 – 8.35 (m, 1H), 7.86 (s, 1H), 7.43 – 7.38 (m, 1H), 7.32 – 7.26 (m, 2H), 4.25 (tt, *J* = 11.9, 3.7 Hz, 1H), 2.54 (s, 3H), 2.25 – 2.17 (m, 2H), 2.03 – 1.95 (m, 2H), 1.88 – 1.80 (m, 1H), 1.80 – 1.68 (m, 2H), 1.61 – 1.46 (m, 2H), 1.39 – 1.29 (m, 1H) ppm. **^{13}C NMR (101 MHz, $CDCl_3$)** δ 193.1, 136.7, 131.4, 126.5, 123.1, 122.8, 122.7, 117.3, 110.0, 55.8, 33.6, 27.8, 25.9, 25.6 ppm. Spectral data was in agreement with the literature.[87]

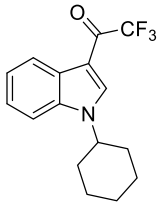

1-(1-Cyclohexyl-1*H*-indol-3-yl)-2,2,2-trifluoroethan-1-one (5h). Following GP5, using 2,2,2-trifluoro-1-(1*H*-indol-3-yl)ethan-1-one (42.6 mg, 0.20 mmol) and 2-cyclohexyl-2-methyl-2,3-dihydroquinazolin-4(1*H*)-one (58.6 mg, 0.24 mmol), afforded the title product as a white solid (39.6 mg, 67%) after purification by silica gel chromatography (hexane/EtOAc 20:1). In a second independent experiment, 35.8 mg (61%) were obtained, giving an average yield of 64%. **M.p.**: 104 °C. **IR (neat, cm^{-1}):** 2937, 2855, 1659, 1520, 1413, 1281, 1181, 1130, 1056, 875, 748, 728. **^{1}H NMR (400 MHz, $CDCl_3$)** δ 8.45 – 8.39 (m, 1H), 8.04 – 7.99 (m, 1H), 7.49 – 7.43 (m, 1H), 7.40 – 7.34 (m, 2H), 4.30 (tt, *J* = 11.9, 3.6 Hz, 1H), 2.30 – 2.19 (m, 2H), 2.06 – 1.96 (m, 2H), 1.90 – 1.82 (m, 1H), 1.76 (qd, *J* = 12.4, 3.4 Hz, 2H), 1.55 (qt, *J* = 13.3, 3.4 Hz, 2H), 1.42 – 1.31 (m, 1H) ppm. **^{13}C NMR (101 MHz, $CDCl_3$)** δ 174.8 (q, $J_{C,F}$ = 34.8 Hz), 136.6, 134.2 (q, $J_{C,F}$ = 5.0 Hz), 127.3, 124.4, 124.1, 122.9, 117.3 (q, $J_{C,F}$ = 290.6 Hz), 110.6, 109.8, 56.6, 33.4, 25.8, 25.4 ppm. **^{19}F NMR (376 MHz, $CDCl_3$)** δ -72.1 ppm. **HRMS** [ESI$^+$] *calcd*. for ($C_{16}H_{17}F_3NO$) $[M+H]^+$: 296.1257, *found*: 296.1255.

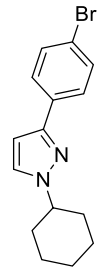

3-(4-Bromophenyl)-1-cyclohexyl-1*H*-pyrazole (5i). Following GP5, using 3-(4-bromophenyl)-1*H*-pyrazole (44.6 mg, 0.20 mmol) and 2-cyclohexyl-2-methyl-2,3-dihydroquinazolin-4(1*H*)-one (58.6 mg, 0.24 mmol), afforded the title product as a white solid (45.1 mg, 74%) after purification by silica gel chromatography (hexane/EtOAc 100:1). In a second independent experiment, 39.6 mg (65%) were obtained, giving an average yield of 69%. **^{1}H NMR (400 MHz, $CDCl_3$)** δ 7.70 – 7.64 (m, 2H), 7.52 – 7.47 (m, 2H), 7.43 (d, *J* = 2.3 Hz, 1H), 6.50 (d, *J* = 2.3 Hz, 1H), 4.15 (tt, *J* = 11.8, 3.8 Hz, 1H), 2.26 – 2.16 (m, 2H), 1.96 – 1.86 (m, 2H), 1.80 – 1.66 (m, 3H), 1.51 – 1.38 (m, 2H), 1.34 – 1.20 (m, 1H) ppm. **^{13}C NMR (101 MHz, $CDCl_3$)** δ 149.6, 133.1, 131.8, 127.9, 127.3, 121.3, 102.3, 61.6, 33.8, 25.5, 25.5 ppm. Spectral data was in agreement with the literature.[87]

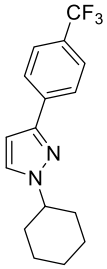

1-Cyclohexyl-3-(4-(trifluoromethyl)phenyl)-1*H*-pyrazole (5j). Following GP5, using 3-(4-(trifluoromethyl)phenyl)-1*H*-pyrazole (42.4 mg, 0.20 mmol) and 2-cyclohexyl-2-methyl-2,3-dihydroquinazolin-4(1*H*)-one (58.6 mg, 0.24 mmol), afforded the title product as a colourless oil (42.4 mg, 72%) after purification by silica gel chromatography (hexane/EtOAc 100:1). In a second independent experiment, 38.8 mg (66%) were obtained, giving an average yield of 69%. **IR (neat, cm^{-1}):** 2935, 2858, 1619, 1320, 1611, 1107, 1063, 848, 758. **^{1}H NMR (400 MHz, $CDCl_3$)** δ 7.94 – 7.86 (m, 2H), 7.66 – 7.59 (m, 2H), 7.47 (d, *J* = 2.4 Hz, 1H), 6.58 (d, *J* = 2.4 Hz, 1H), 4.17 (tt, *J* = 11.8, 3.8 Hz, 1H), 2.26 – 2.18 (m, 2H), 1.98 – 1.87 (m, 2H), 1.82 – 1.68 (m, 3H), 1.46 (qt, *J* = 13.1, 3.4 Hz, 2H), 1.36 – 1.25 (m, 1H) ppm. **^{13}C NMR (101 MHz, $CDCl_3$)** δ 149.2, 137.5, 129.2 (q, $J_{C,F}$ = 32.2 Hz), 128.0, 125.7, 125.6 (q, $J_{C,F}$ = 3.8 Hz), 124.5 (q, $J_{C,F}$ = 272.5 Hz), 102.83, 61.7, 33.8, 25.5, 25.5 ppm. **^{19}F NMR (376 MHz, $CDCl_3$)** δ -62.5 ppm. **HRMS** [ESI$^+$] *calcd.* for ($C_{16}H_{18}F_3N_2$) $[M+H]^+$: 295.1417, *found*: 295.1411.

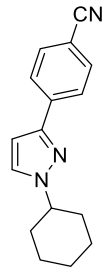

4-(1-Cyclohexyl-1*H*-pyrazol-3-yl)benzonitrile (5k). Following GP5, using 4-(1*H*-pyrazol-3-yl)benzonitrile (33.8 mg, 0.20 mmol) and 2-cyclohexyl-2-methyl-2,3-dihydroquinazolin-4(1*H*)-one (58.6 mg, 0.24 mmol), afforded the title product as a white solid (37.7 mg, 75%) after purification by silica gel chromatography (hexane/EtOAc 10:1). In a second independent experiment, 37.4 mg (75%) were obtained, giving an average yield of 75%. **M.p.**: 118 °C. **IR (neat, cm^{-1}):** 2922, 2854, 2221, 1609, 1494, 1453, 1218, 1053, 840, 754, 551. **^{1}H NMR (400 MHz, $CDCl_3$)** δ 7.92 – 7.87 (m, 2H), 7.68 – 7.61 (m, 2H), 7.47 (d, *J* = 2.4 Hz, 1H), 6.58 (d, *J* = 2.4 Hz, 1H), 4.16 (tt, *J* = 11.7, 3.8 Hz, 1H), 2.25 – 2.15 (m, 2H), 1.97 – 1.87 (m, 2H), 1.81 – 1.68 (m, 3H), 1.45 (qt, *J* = 13.1, 3.4 Hz, 2H), 1.34 – 1.21 (m, 1H) ppm. **^{13}C NMR (101 MHz, $CDCl_3$)** δ 148.7, 138.4, 132.6, 128.3, 126.0, 119.4, 110.6, 103.1, 61.8, 33.7, 25.5, 25.5 ppm. **HRMS** [ESI$^+$] *calcd*. for ($C_{16}H_{17}N_3Na$) [M+Na]$^+$: 274.1315, *found*: 274.1309.

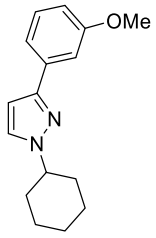

1-Cyclohexyl-3-(3-methoxyphenyl)-1*H*-pyrazole (5l). Following GP5, using 3-(3-methoxyphenyl)-1H-pyrazole (34.8 mg, 0.20 mmol) and 2-cyclohexyl-2-methyl-2,3-dihydroquinazolin-4(1*H*)-one (58.6 mg, 0.24 mmol), afforded the title product as a colourless oil (27.4 mg, 54%) after purification by silica gel chromatography (hexane/EtOAc 20:1). In a second independent experiment, 27.4 mg (54%) were obtained, giving an average yield of 54%. **IR (neat, cm^{-1}):** 2932, 2855, 1604, 1469, 1246, 1204, 1042, 838, 750, 690. **^{1}H NMR (400 MHz, $CDCl_3$)** δ 7.43 (d, *J* = 2.3 Hz, 1H), 7.41 – 7.35 (m, 2H), 7.33 – 7.26 (m, 1H), 6.86 – 6.81 (m, 1H), 6.52 (d, *J* = 2.3 Hz, 1H), 4.16 (tt, *J* = 11.8, 3.8 Hz, 1H), 3.86 (s, 3H), 2.26 – 2.18 (m, 2H), 1.96 – 1.86 (m, 2H), 1.80 – 1.62 (m, 3H), 1.52 – 1.38 (m, 2H), 1.34 – 1.24 (m, 1H) ppm. **^{13}C NMR (101 MHz, $CDCl_3$)** δ 160.0, 150.5, 135.5, 129.7, 127.6, 118.4, 113.4, 110.9, 102.5, 61.5, 55.4, 33.8, 25.6 ppm. **HRMS** [ESI$^+$] *calcd*. for ($C_{16}H_{21}N_2O$) [M+H]$^+$: 257.1648, *found*: 257.1647.

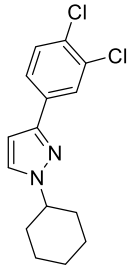

1-Cyclohexyl-3-(3,4-dichlorophenyl)-1*H*-pyrazole (5m). Following GP4, using 3-(3,4-dichlorophenyl)-1*H*-pyrazole (42.6 mg, 0.20 mmol) and 2-cyclohexyl-2-methyl-2,3-dihydroquinazolin-4(1*H*)-one (58.6 mg, 0.24 mmol), afforded the title product as a colourless oil (43.6 mg, 74%) after purification by silica gel chromatography (hexane/EtOAc 100:1). In a second independent experiment, 40.3 mg (68%) were obtained, giving an average yield of 71%. **IR (neat, cm^{-1}):** 2932, 2856, 1489, 1445, 1218, 1134, 1028, 893, 820, 749, 675. **^{1}H NMR (400 MHz, CDCl$_3$)** δ 7.90 (d, *J* = 2.0 Hz, 1H), 7.61 (dd, *J* = 8.4, 2.0 Hz, 1H), 7.46 – 7.41 (m, 2H), 6.50 (d, *J* = 2.4 Hz, 1H), 4.14 (tt, *J* = 11.8, 3.8 Hz, 1H), 2.26 – 2.16 (m, 2H), 1.97 – 1.86 (m, 2H), 1.80 – 1.66 (m, 3H), 1.45 (qt, *J* = 14.4, 3.3 Hz, 2H), 1.35 – 1.21 (m, 1H) ppm. **^{13}C NMR (101 MHz, CDCl$_3$)** δ 148.4, 134.2, 132.8, 131.1, 130.6, 128.1, 127.4, 124.9, 102.6, 61.7, 33.8, 25.5, 25.5 ppm. **HRMS** [ESI$^+$] *calcd*. for ($C_{15}H_{17}Cl_2N_2$) [M+H]$^+$: 295.0763, *found*: 295.0759.

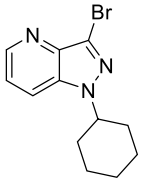

3-Bromo-1-cyclohexyl-1*H*-pyrazolo[4,3-*b*]pyridine (5n). Following GP5, using 3-bromo-1*H*-pyrazolo[4,3-*b*]pyridine (39.6 mg, 0.20 mmol) and 2-cyclohexyl-2-methyl-2,3-dihydroquinazolin-4(1*H*)-one (58.6 mg, 0.24 mmol), afforded the title product as a colourless oil (39.7 mg, 71% yield) after purification by silica gel chromatography (hexane/EtOAc 10:1). In a second independent experiment, 41.5 mg (74%) were obtained, giving an average yield of 73%. **IR (neat, cm^{-1}):** 2932, 2855, 1433, 1346, 1174, 1060, 970, 892, 758, 729, 568. **^{1}H NMR (400 MHz, CDCl$_3$)** δ 8.61 (dd, *J* = 4.3, 1.3 Hz, 1H), 7.80 (dd, *J* = 8.6, 1.3 Hz, 1H), 7.32 (dd, *J* = 8.6, 4.3 Hz, 1H), 4.43 – 4.30 (m, 1H), 2.12 – 2.00 (m, 4H), 2.00 – 1.91 (m, 2H), 1.81 – 1.72 (m, 1H), 1.53 – 1.39 (m, 2H), 1.38 – 1.26 (m, 1H) ppm. **^{13}C NMR (101 MHz, CDCl$_3$)** δ 146.3, 139.4, 132.9, 121.5, 121.4, 117.7, 59.6, 32.7, 25.8, 25.3 ppm. **HRMS** [ESI$^+$] *calcd*. for ($C_{12}H_{15}BrN_3$) [M+H]$^+$: 280.0444, *found*: 280.0439.

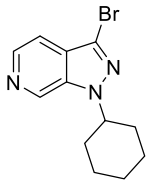

3-Bromo-1-cyclohexyl-1*H*-pyrazolo[3,4-*c*]pyridine (5o). Following GP5, using 3-

bromo-1*H*-pyrazolo[3,4-*c*]pyridine (39.6 mg, 0.20 mmol) and 2-cyclohexyl-2-methyl-2,3-dihydroquinazolin-4(1*H*)-one (58.6 mg, 0.24 mmol), afforded the title product as a colourless oil (39.4 mg, 70% yield) after purification by silica gel chromatography (hexane/EtOAc 5:1). In a second independent experiment, 40.2 mg (72%) were obtained, giving an average yield of 71%. **IR (neat, cm^{-1}):** 2932, 1855, 1455, 1337, 1163, 1030, 893, 809, 769, 599. **^{1}H NMR (400 MHz, CDCl$_3$)** δ 9.01 (s, 1H), 8.35 (d, *J* = 5.6 Hz, 1H), 7.50 (dd, *J* = 5.6, 1.0 Hz, 1H), 4.50 (tt, *J* = 10.2, 5.0 Hz, 1H), 2.14 – 2.02 (m, 4H), 2.02 – 1.93 (m, 2H), 1.83 – 1.74 (m, 1H), 1.57 – 1.43 (m, 2H), 1.40 – 1.27 (m, 1H) ppm. **^{13}C NMR (101 MHz, CDCl$_3$)** δ 139.4, 136.8, 134.2, 127.7, 119.4, 113.9, 60.1, 32.9, 25.8, 25.3 ppm. **HRMS** [ESI$^+$] *calcd*. for ($C_{12}H_{15}BrN_3$) [M+H]$^+$: 280.0444, *found*: 280.0449.

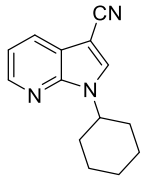

1-Cyclohexyl-1*H*-pyrrolo[2,3-*b*]pyridine-3-carbonitrile (5p). Following GP5, using 1*H*-pyrrolo[2,3-*b*]pyridine-3-carbonitrile (28.6 mg, 0.20 mmol) and 2-cyclohexyl-2-methyl-2,3-dihydroquinazolin-4(1*H*)-one (58.6 mg, 0.24 mmol), afforded the title product as a white solid (20.9 mg, 46% yield) after purification by silica gel chromatography (hexane/EtOAc 5:1). In a second independent experiment, 18.9 mg (42%) were obtained, giving an average yield of 44%. **M.p.**: 114 °C. **IR (neat, cm^{-1}):** 3112, 2935, 2851, 2219, 1599, 1572, 1525, 1431, 1284, 1203, 773, 614. **^{1}H NMR (400 MHz, CDCl$_3$)** δ 8.43 (dd, *J* = 4.7, 1.5 Hz, 1H), 8.06 (dd, *J* = 7.9, 1.6 Hz, 1H), 7.83 (s, 1H), 7.27 – 7.22 (m, 1H), 4.83 (tt, *J* = 11.9, 3.8 Hz, 1H), 2.21 – 2.11 (m, 2H), 2.01 – 1.90 (m, 2H), 1.86 – 1.77 (m, 1H), 1.75 – 1.63 (m, 2H), 1.63 – 1.49 (m, 2H), 1.38 – 1.23 (m, 1H) ppm. **^{13}C NMR (101 MHz, CDCl$_3$)** δ 146.3, 145.0, 132.5, 128.3, 120.4, 118.3, 115.6, 84.3, 54.3, 33.7, 25.8, 25.5 ppm. **HRMS** [ESI$^+$] *calcd*. for ($C_{14}H_{16}N_3$) [M+H]$^+$: 226.1339, *found*: 226.1342.

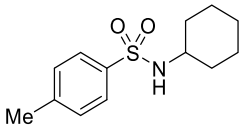

***N*-Cyclohexyl-4-methylbenzenesulfonamide (5q).** Following GP5, using 4-methylbenzenesulfonamide (34.2 mg, 0.20 mmol) and 2-cyclohexyl-2-methyl-2,3-dihydroquinazolin-4(1*H*)-one (58.6 mg, 0.24 mmol), afforded the title product as a white solid (24.8 mg, 49%) after purification by silica gel chromatography (hexane/EtOAc 5:1). In a second independent experiment, 30.1 mg (59%) were obtained, giving an average yield of 54%. **^{1}H NMR (400 MHz, CDCl$_3$)** δ 7.80 – 7.73 (m, 2H), 7.32 – 7.27 (m, 2H), 4.57 (d, *J* = 7.5 Hz, 1H), 3.18 – 3.06 (m, 1H), 2.42 (s, 3H), 1.78 – 1.70 (m, 2H), 1.67 – 1.58 (m, 2H), 1.54 – 1.46 (m, 1H), 1.29 – 1.07 (m, 5H)

ppm. **^{13}C NMR (101 MHz, $CDCl_3$)** δ 143.2, 138.6, 129.8, 127.1, 52.7, 34.1, 25.3, 24.8, 21.7 ppm. Spectral data was in agreement with the literature.[87]

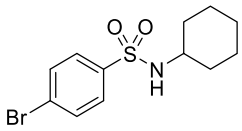

4-Bromo-*N*-cyclohexylbenzenesulfonamide (5r). Following GP5, using 4-bromobenzenesulfonamide (47.2 mg, 0.20 mmol) and 2-cyclohexyl-2-methyl-2,3-dihydroquinazolin-4(1*H*)-one (58.6 mg, 0.24 mmol), afforded the title product as a white solid (39.4 mg, 62%) after purification by silica gel chromatography (hexane/EtOAc 5:1). In a second independent experiment, 39.2 mg (62%) were obtained, giving an average yield of 62%. **^{1}H NMR (400 MHz, $CDCl_3$)** δ 7.79 – 7.71 (m, 2H), 7.68 – 7.60 (m, 2H), 4.66 (d, *J* = 7.6 Hz, 1H), 3.21 – 3.07 (m, 1H), 1.80 – 1.71 (m, 2H), 1.69 – 1.59 (m, 2H), 1.56 – 1.46 (m, 1H), 1.31 – 1.03 (m, 5H) ppm. **^{13}C NMR (101 MHz, $CDCl_3$)** δ 140.8, 132.5, 128.6, 127.4, 52.9, 34.1, 25.2, 24.7 ppm. Spectral data was in agreement with the literature.[87]

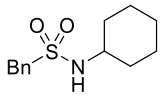

***N*-Cyclohexyl-1-phenylmethanesulfonamide (5s).** Following GP5, using phenylmethanesulfonamide (34.2 mg, 0.20 mmol) and 2-cyclohexyl-2-methyl-2,3-dihydroquinazolin-4(1*H*)-one (58.6 mg, 0.24 mmol), afforded the title product as a white solid (25.9 mg, 51%) after purification by silica gel chromatography (hexane/EtOAc 5:1). In a second independent experiment, 25.8 mg (51%) were obtained, giving an average yield of 51%. **^{1}H NMR (400 MHz, $CDCl_3$)** δ 7.44 – 7.33 (m, 5H), 4.23 (s, 2H), 4.05 (d, *J* = 7.5 Hz, 1H), 3.18 – 3.05 (m, 1H), 1.96 – 1.86 (m, 2H), 1.74 – 1.63 (m, 2H), 1.60 – 1.51 (m, 1H), 1.34 – 1.05 (m, 5H) ppm. **^{13}C NMR (101 MHz, $CDCl_3$)** δ 130.9, 129.7, 128.8, 128.8, 60.2, 53.5, 34.7, 25.3, 24.9 ppm. Spectral data was in agreement with the literature.[87]

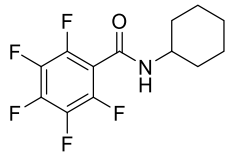

***N*-Cyclohexyl-2,3,4,5,6-pentafluorobenzamide (5t).** Following GP5, using 2,3,4,5,6-pentafluorobenzamide (42.2 mg, 0.20 mmol) and 2-cyclohexyl-2-methyl-2,3-dihydroquinazolin-4(1*H*)-one (58.6 mg, 0.24 mmol), afforded the title product as a white solid (32.4 mg, 55%) after purification by silica gel chromatography (hexane/EtOAc 20:1). In a second independent experiment, 31.3 mg (53%) were obtained, giving an average yield of 54%. **M.p.**: 126 °C. **IR (neat, cm^{-1}):** 3231, 3073, 2939, 2860, 1651, 1489, 1340, 1260, 1078, 989, 739. **^{1}H NMR (500 MHz, $CDCl_3$)** δ 5.96 (brs, 1H), 4.01 – 3.89 (m, 1H), 2.06 – 1.96 (m, 2H), 1.79 – 1.70 (m, 2H), 1.69 –

1.59 (m, 1H), 1.47 – 1.35 (m, 2H), 1.30 – 1.15 (m, 3H) ppm. **^{13}C NMR (126 MHz, $CDCl_3$)** δ 156.5, 144.2 (dm, $J_{C,F}$ = 249.4 Hz), 143.2 (tm, $J_{C,F}$ = 243.3 Hz), 137.6 (dm, $J_{C,F}$ = 254.4 Hz), 112.1 (m), 49.6, 32.9, 25.5, 24.8 ppm. **^{19}F NMR (376 MHz, $CDCl_3$)** δ -141.0 (m), -151.5 (m), -160.4 (m) ppm. **HRMS** [APCI$^+$] *calcd*. for ($C_{13}H_{13}F_5NO$) [M+H]$^+$: 294.0912, *found*: 294.0910.

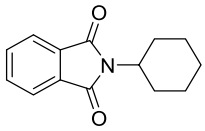

2-Cyclohexylisoindoline-1,3-dione (5u). Following GP5, using isoindoline-1,3-dione (29.4 mg, 0.20 mmol) and 2-cyclohexyl-2-methyl-2,3-dihydroquinazolin-4(1*H*)-one (58.6 mg, 0.24 mmol), afforded the title product as a white solid (22.2 mg, 48%) after purification by silica gel chromatography (hexane/EtOAc 20:1). In a second independent experiment, 25.2 mg (55%) were obtained, giving an average yield of 52%. **^{1}H NMR (400 MHz, $CDCl_3$)** δ 7.84 – 7.78 (m, 2H), 7.72 – 7.65 (m, 2H), 4.11 (tt, *J* = 12.3, 3.9 Hz, 1H), 2.21 (qd, *J* = 12.5, 3.2 Hz, 2H), 1.92 – 1.82 (m, 2H), 1.78 – 1.65 (m, 3H), 1.44 – 1.21 (m, 3H) ppm. **^{13}C NMR (101 MHz, $CDCl_3$)** δ 168.6, 133.9, 132.2, 123.1, 51.0, 30.0, 26.2, 25.3 ppm. Spectral data was in agreement with the literature.[87]

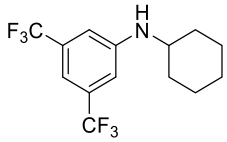

***N*-Cyclohexyl-3,5-bis(trifluoromethyl)aniline (5v).** Following GP6, using 3,5-bis(trifluoromethyl)aniline (45.8 mg, 0.20 mmol) and 2-cyclohexyl-2-methyl-2,3-dihydroquinazolin-4(1*H*)-one (58.6 mg, 0.24 mmol), afforded the title product as a colourless oil (29.5 mg, 47%) after purification by silica gel chromatography (hexane/EtOAc 100:1). In a second independent experiment, 34.0 mg (55%) were obtained, giving an average yield of 51%. **^{1}H NMR (400 MHz, $CDCl_3$)** δ 7.08 (s, 1H), 6.88 (s, 2H), 4.05 – 3.94 (m, 1H), 3.36 – 3.25 (m, 1H), 2.09 – 2.00 (m, 2H), 1.84 – 1.74 (m, 2H), 1.73 – 1.63 (m, 1H), 1.48 – 1.35 (m, 2H), 1.31 – 1.13 (m, 3H) ppm. **^{13}C NMR (101 MHz, $CDCl_3$)** δ 148.0, 132.6 (q, $J_{C,F}$ = 32.6 Hz), 123.8 (q, $J_{C,F}$ = 273.3 Hz), 112.0, 109.6 (quin., $J_{C,F}$ = 3.9 Hz), 51.6, 33.1, 25.8, 24.9 ppm. **^{19}F NMR (376 MHz, $CDCl_3$)** δ -63.3 ppm. Spectral data was in agreement with the literature.[87]

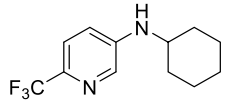

***N*-Cyclohexyl-6-(trifluoromethyl)pyridin-3-amine (5w).** Following GP6, using 6-(trifluoromethyl)pyridin-3-amine (32.4 mg, 0.20 mmol) and 2-cyclohexyl-2-methyl-2,3-dihydroquinazolin-4(1*H*)-one (58.6 mg, 0.24 mmol), afforded the title product as a white solid (26.3 mg, 54%) after purification by silica gel chromatography (hexane/EtOAc 10:1). In a second independent experiment, 27.3 mg (56%) were

obtained, giving an average yield of 55%. **M.p.**: 111 °C. **IR (neat, cm^{-1}):** 3291, 2933, 2858, 1588, 1522, 1327, 1168, 1109, 1082, 837, 634. **^{1}H NMR (400 MHz, CDCl$_3$)** δ 8.00 (d, *J* = 2.8 Hz, 1H), 7.41 (d, *J* = 8.6 Hz, 1H), 6.84 (dd, *J* = 8.6, 2.8 Hz, 1H), 4.00 (d, *J* = 6.4 Hz, 1H), 3.36 – 3.22 (m, 1H), 2.09 – 1.98 (m, 2H), 1.83 – 1.73 (m, 2H), 1.72 – 1.62 (m, 1H), 1.46 – 1.32 (m, 2H), 1.31 – 1.14 (m, 3H) ppm. **^{13}C NMR (101 MHz, CDCl$_3$)** δ 145.3, 136.1, 135.8 (q, $J_{C,F}$ = 34.9 Hz), 122.5 (q, $J_{C,F}$ = 271.9 Hz), 121.3 (q, $J_{C,F}$ = 2.9 Hz), 117.3, 51.4, 33.0, 25.8, 24.8 ppm. **^{19}F NMR (376 MHz, CDCl$_3$)** δ -66.4 ppm. **HRMS** [APCI$^+$] *calcd.* for ($C_{12}H_{16}F_3N_2$) $[M+H]^+$: 245.1260, *found*: 245.1258.

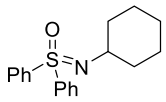

(Cyclohexylimino)diphenyl-λ^6-sulfanone (5x). Following GP6, using iminodiphenyl-λ^6-sulfanone (43.4 mg, 0.20 mmol) and 2-cyclohexyl-2-methyl-2,3-dihydroquinazolin-4(1*H*)-one (58.6 mg, 0.24 mmol), afforded the title product as a white solid (44.0 mg, 74%) after purification by silica gel chromatography (hexane/EtOAc 5:1). In a second independent experiment, 43.5 mg (73%) were obtained, giving an average yield of 73%. **^{1}H NMR (400 MHz, CDCl$_3$)** δ 8.02 – 7.94 (m, 4H), 7.53 – 7.40 (m, 6H), 3.03 (tt, *J* = 10.3, 4.0 Hz, 1H), 1.96 – 1.85 (m, 2H), 1.77 – 1.66 (m, 2H), 1.59 – 1.44 (m, 3H), 1.27 – 1.11 (m, 3H) ppm. **^{13}C NMR (101 MHz, CDCl$_3$)** δ 141.8, 132.3, 129.1, 128.7, 54.2, 37.2, 25.8, 25.4 ppm. Spectral data was in agreement with the literature.[262]

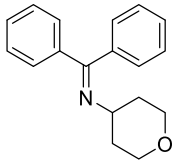

1,1-Diphenyl-*N*-(tetrahydro-2*H*-pyran-4-yl)methanimine (5y). Following GP6, using diphenylmethanimine (36.2 mg, 0.20 mmol) and 2-methyl-2-(tetrahydro-2*H*-pyran-4-yl)-2,3-dihydroquinazolin-4(1*H*)-one (59.0 mg, 0.24 mmol), afforded the title product as a white solid (34.6 mg, 65%) after purification by silica gel chromatography (hexane/EtOAc 10:1). In a second independent experiment, 34.6 mg (65%) were obtained, giving an average yield of 65%. **^{1}H NMR (400 MHz, CDCl$_3$)** δ 7.67 – 7.60 (m, 2H), 7.52 – 7.45 (m, 3H), 7.42 – 7.32 (m, 3H), 7.21 – 7.15 (m, 2H), 4.03 (dt, *J* = 11.6, 3.9 Hz, 2H), 3.51 (tt, *J* = 9.4, 4.3 Hz, 1H), 3.39 (td, *J* = 11.3, 2.4 Hz, 2H), 1.99 – 1.87 (m, 2H), 1.64 – 1.55 (m, 2H) ppm. **^{13}C NMR (101 MHz, CDCl$_3$)** δ 166.7, 140.1, 137.2, 130.0, 128.7, 128.5, 128.4, 128.2, 127.7, 66.1, 58.0, 33.9 ppm. Spectral data was in agreement with the literature.[263]

---

[262] Teng, F.; Sun, S.; Jiang, Y.; Yu, J.-T.; Cheng, J. Copper-Catalyzed Oxidative C(*sp*^{3})–H/N–H Coupling of Sulfoximines and Amides with Simple Alkanes via a Radical Process. *Chem. Commun.* **2015**, *51*, 5902–5905.

[263] Patra, T.; Bellotti, P.; Strieth-Kalthoff, F.; Glorius, F. Photosensitized Intermolecular Carboimination of Alkenes through the Persistent Radical Effect. *Angew. Chem. Int. Ed.* **2020**, *59*, 3172–3177.

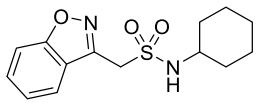

1-(Benzo[*d*]isoxazol-3-yl)-*N*-cyclohexylmethanesulfonamide (6a). Following GP5, using benzo[*d*]isoxazol-3-ylmethanesulfonamide (42.4 mg, 0.20 mmol) and 2-cyclohexyl-2-methyl-2,3-dihydroquinazolin-4(1*H*)-one (58.6 mg, 0.24 mmol), afforded the title product as a white solid (30.0 mg, 51%) after purification by silica gel chromatography (hexane/EtOAc 5:1). In a second independent experiment, 28.9 mg (49%) were obtained, giving an average yield of 50%. **M.p.**: 176 °C. **IR (neat, cm^{-1}):** 3163, 2922, 2852, 1610, 1519, 1469, 1386, 1322, 1159, 1142, 1080, 999, 923, 884, 754, 571, 510. **^{1}H NMR (400 MHz, CDCl$_3$)** δ 7.91 (dt, *J* = 8.0, 1.0 Hz, 1H), 7.63 – 7.55 (m, 2H), 7.41 – 7.33 (m, 1H), 4.67 (s, 2H), 4.40 (d, *J* = 7.5 Hz, 1H), 3.31 – 3.18 (m, 1H), 2.06 – 1.94 (m, 2H), 1.76 – 1.63 (m, 2H), 1.62 – 1.51 (m, 1H), 1.35 – 1.07 (m, 5H) ppm. **^{13}C NMR (101 MHz, CDCl$_3$)** δ 163.8, 150.2, 130.6, 124.4, 122.7, 121.0, 110.0, 53.8, 50.1, 34.4, 25.2, 24.9 ppm. **HRMS** [ESI$^+$] *calcd*. for ($C_{14}H_{18}N_2NaO_3S$) [M+Na]$^+$: 317.0930, *found*: 317.0942.

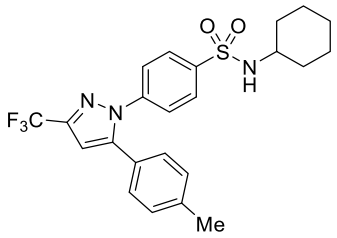

***N*-Cyclohexyl-4-(5-(*p*-tolyl)-3-(trifluoromethyl)-1*H*-pyrazol-1-yl)benzenesulfonamide (6b).** Following GP5, using 4-(5-(*p*-tolyl)-3-(trifluoromethyl)-1*H*-pyrazol-1-yl)benzenesulfonamide (76.2 mg, 0.20 mmol) and 2-cyclohexyl-2-methyl-2,3-dihydroquinazolin-4(1*H*)-one (58.6 mg, 0.24 mmol), afforded the title product as a colourless oil (69.7 mg, 75%) after purification by silica gel chromatography (hexane/EtOAc 10:1). In a second independent experiment, 68.8 mg (74%) were obtained, giving an average yield of 75%. **^{1}H NMR (400 MHz, CDCl$_3$)** δ 7.91 – 7.83 (m, 2H), 7.49 – 7.42 (m, 2H), 7.19 – 7.12 (m, 2H), 7.12 – 7.05 (m, 2H), 6.74 (s, 1H), 4.62 (d, *J* = 7.7 Hz, 1H), 3.20 – 3.07 (m, 1H), 2.37 (s, 3H), 1.83 – 1.70 (m, 2H), 1.69 – 1.58 (m, 2H), 1.57 – 1.48 (m, 1H), 1.30 – 1.07 (m, 5H) ppm. **^{13}C NMR (101 MHz, CDCl$_3$)** δ 145.4, 144.2 (q, $J_{C,F}$ = 38.5 Hz), 142.4, 141.2, 139.9, 129.8, 128.9, 128.1, 125.8, 125.7, 121.21 (q, $J_{C,F}$ = 269.2 Hz), 106.3, 53.0, 34.1, 25.2, 24.8, 21.4 ppm. **^{19}F NMR (376 MHz, CDCl$_3$)** δ -62.5 ppm. Spectral data was in agreement with the literature.[87]

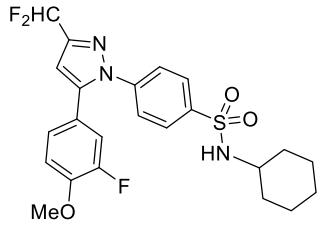

***N*-Cyclohexyl-4-(3-(difluoromethyl)-5-(3-fluoro-4-methoxyphenyl)-1*H*-pyrazol-1-yl)benzenesulfonamide (6c).** Following GP5, using 4-(3-(difluoromethyl)-5-(3-fluoro-4-methoxyphenyl)-1H-pyrazol-1-yl)benzenesulfonamide (79.4 mg, 0.20 mmol) and 2-cyclohexyl-2-methyl-2,3-dihydroquinazolin-4(1*H*)-one (58.6 mg, 0.24 mmol), afforded the title product as a white solid (64.1 mg, 67%) after purification by silica gel chromatography (hexane/EtOAc 4:1). In a second independent experiment, 65.5 mg (68%) were obtained, giving an average yield of 68%. **M.p.**: 153 °C. **IR (neat, cm^{-1}):** 3253, 2929, 2852, 1596, 1444, 1375, 1274, 1156, 1080, 1022, 877, 753, 563. **^{1}H NMR (400 MHz, $CDCl_3$)** δ 7.89 (d, J = 8.5 Hz, 2H), 7.44 (d, J = 8.5 Hz, 2H), 6.99 – 6.87 (m, 3H), 6.76 (t, J = 54.7 Hz, 1H), 6.70 (s, 1H), 4.66 (d, J = 7.5 Hz, 1H), 3.91 (s, 3H), 3.22 – 3.08 (m, 1H), 1.79 – 1.69 (m, 2H), 1.69 – 1.58 (m, 2H), 1.58 – 1.48 (m, 1H), 1.35 – 1.04 (m, 5H) ppm. **^{13}C NMR (101 MHz, $CDCl_3$)** δ 152.2 (d, $J_{C,F}$ = 249.0 Hz), 148.7 (d, $J_{C,F}$ = 10.6 Hz), 148.4 (t, $J_{C,F}$ = 29.9 Hz), 143.9, 142.4, 141.1, 128.2, 125.5, 125.3 (d, $J_{C,F}$ = 3.6 Hz), 121.8 (d, $J_{C,F}$ = 7.0 Hz), 116.7 (d, $J_{C,F}$ = 20.1 Hz), 113.7 (d, $J_{C,F}$ = 2.3 Hz), 111.1 (t, $J_{C,F}$ = 235.3 Hz), 105.8, 56.4, 53.0, 34.1, 25.2, 24.7 ppm. **^{19}F NMR (376 MHz, $CDCl_3$)** δ -112.4, -133.4 ppm. **HRMS** [ESI$^+$] *calcd*. for ($C_{23}H_{25}F_3N_3O_3S$) [M+H]$^+$: 480.1563, *found*: 480.1566.

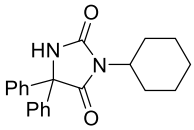

3-Cyclohexyl-5,5-diphenylimidazolidine-2,4-dione (6d). Following GP5, using 5,5-diphenylimidazolidine-2,4-dione (50.4 mg, 0.20 mmol) and 2-cyclohexyl-2-methyl-2,3-dihydroquinazolin-4(1*H*)-one (58.6 mg, 0.24 mmol), afforded the title product as a white solid (20.5 mg, 31%) after purification by silica gel chromatography (hexane/EtOAc 10:1). In a second independent experiment, 21.5 mg (32%) were obtained, giving an average yield of 31%. **^{1}H NMR (400 MHz, $CDCl_3$)** δ 7.40 – 7.31 (m, 10H), 6.45 (s, 1H), 3.96 (tt, J = 12.3, 3.8 Hz, 1H), 2.24 – 2.09 (m, 2H), 1.89 – 1.77 (m, 2H), 1.74 – 1.55 (m, 3H), 1.39 – 1.14 (m, 3H) ppm. **^{13}C NMR (101 MHz, $CDCl_3$)** δ 173.4, 156.8, 139.6, 128.9, 128.6, 127.0, 69.3, 52.1, 29.5, 26.0, 25.2 ppm. Spectral data was in agreement with the literature.[264]

[264] Muccioli, G. G.; Poupaert, J. H.; Wouters, J.; Norberg, B.; Poppitz, W.; Scriba, G. K. E.; Lambert, D. M. A Rapid and Efficient Microwave-Assisted Synthesis of Hydantoins and Thiohydantoins. *Tetrahedron* **2003**, *59*, 1301–1307.

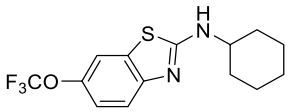

***N*-Cyclohexyl-6-(trifluoromethoxy)benzo[*d*]thiazol-2-amine (6e).** Following GP6, using 6-(trifluoromethoxy)benzo[*d*]thiazol-2-amine (46.8 mg, 0.20 mmol) and 2-cyclohexyl-2-methyl-2,3-dihydroquinazolin-4(1*H*)-one (58.6 mg, 0.24 mmol), afforded the title product as a white solid (34.8 mg, 55%) after purification by silica gel chromatography (hexane/EtOAc 10:1). In a second independent experiment, 39.8 mg (63%) were obtained, giving an average yield of 59%. **^{1}H NMR (400 MHz, $CDCl_3$)** δ 7.50 – 7.42 (m, 2H), 7.17 – 7.11 (m, 1H), 5.49 (s, 1H), 3.62 – 3.51 (m, 1H), 2.17 – 2.07 (m, 2H), 1.83 – 1.73 (m, 2H), 1.70 – 1.60 (m, 1H), 1.50 – 1.37 (m, 2H), 1.36 – 1.17 (m, 3H) ppm. **^{13}C NMR (126 MHz, $CDCl_3$)** δ 167.3, 150.9, 143.6, 130.8, 120.8 (q, $J_{C,F}$ = 256.5 Hz), 119.8, 118.9, 114.2, 54.9, 33.3, 25.5, 24.8 ppm. **^{19}F NMR (376 MHz, $CDCl_3$)** δ -58.4 ppm. Spectral data was in agreement with the literature.[87]

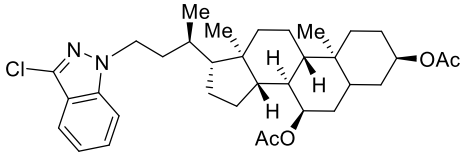

(3*R*,5*R*,8*R*,9*S*,10*S*,12*S*,13*R*,14*S*,17*R*)-17-((*R*)-4-(3-chloro-1*H*-indazol-1-yl)butan-2-yl)-10,13-dimethylhexadecahydro-1*H*-cyclopenta[*a*]phenanthrene-3,12-diyl diacetate (6f). Following GP5, using 3-chloro-1*H*-indazole (30.6 mg, 0.20 mmol) and (3*R*,7*R*,8*R*,9*S*,10*S*,13*R*,14*S*,17*R*)-10,13-dimethyl-17-((2*R*)-4-(4-oxo-2-phenyl-1,2,3,4-tetrahydroquinazolin-2-yl)butan-2-yl)hexadecahydro-1*H*-cyclopenta[*a*]phenanthrene-3,7-diyl diacetate (157.2 mg, 0.24 mmol), afforded the title product as a white solid (78.8 mg, 68%) after purification by silica gel chromatography (hexane/EtOAc 10:1). In a second independent experiment, 71.5 mg (61%) were obtained, giving an average yield of 64%. **M.p.**: 157 °C. **IR (neat, cm^{-1}):** 2938, 2875, 1732, 1468, 1378, 1247, 1233, 1021, 734. **^{1}H NMR (400 MHz, $CDCl_3$)** δ 7.66 (d, *J* = 8.2 Hz, 1H), 7.45 – 7.38 (m, 1H), 7.38 – 7.32 (m, 1H), 7.21 – 7.15 (m, 1H), 4.91 – 4.82 (m, 1H), 4.58 (tt, *J* = 11.3, 4.3 Hz, 1H), 4.42 – 4.32 (m, 1H), 4.32 – 4.22 (m, 1H), 2.11 – 0.96 (m, 33H), 0.92 (s, 3H), 0.61 (s, 3H) ppm. **^{13}C NMR (101 MHz, $CDCl_3$)** δ 170.8, 170.5, 140.7, 132.4, 127.4, 121.2, 121.2, 120.0, 109.4, 74.3, 71.3, 55.9, 50.5, 47.2, 42.9, 41.1, 39.6, 38.0, 35.9, 35.0, 34.9, 34.8, 34.2, 33.9, 31.4, 28.3, 26.9, 23.7, 22.8, 21.7, 21.6, 20.8, 19.0, 11.8 ppm. **HRMS** [ESI$^+$] *calcd*. for ($C_{34}H_{47}ClN_2NaO_4$) [M+Na]$^+$: 605.3117, *found*: 605.3120.

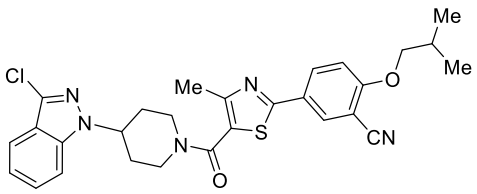

5-(5-(4-(3-Chloro-1*H*-indazol-1-yl)piperidine-1-carbonyl)-4-methylthiazol-2-yl)-2-isobutoxybenzonitrile (6g). Following GP5, using 3-chloro-1*H*-indazole (30.6 mg, 0.20 mmol) and 2-isobutoxy-5-(4-methyl-5-(4-(2-methyl-4-oxo-1,2,3,4-tetrahydroquinazolin-2-yl)piperidine-1-carbonyl)thiazol-2-yl)benzonitrile (130.6 mg, 0.24 mmol), afforded the title product as a white solid (59.3 mg, 56%) after purification by silica gel chromatography (hexane/EtOAc/DCM 3:1:0 to 20:20:1). In a second independent experiment, 53.2 mg (50%) were obtained, giving an average yield of 53%. **M.p.**: 169 °C. **IR (neat, cm^{-1}):** 2960, 2927, 2223, 1620, 1437, 1328, 1197, 1002, 822, 738. **^{1}H NMR (400 MHz, CDCl$_3$)** δ 8.14 (d, *J* = 2.3 Hz, 1H), 8.04 (dd, *J* = 8.8, 2.3 Hz, 1H), 7.69 (dt, *J* = 8.2, 0.9 Hz, 1H), 7.48 – 7.39 (m, 2H), 7.22 (ddd, *J* = 7.9, 6.1, 1.5 Hz, 1H), 7.01 (d, *J* = 8.9 Hz, 1H), 4.65 (tt, *J* = 10.8, 4.1 Hz, 1H), 4.45 (brs, 2H), 3.89 (d, *J* = 6.5 Hz, 2H), 3.25 (t, *J* = 11.9 Hz, 2H), 2.53 (s, 3H), 2.39 – 2.07 (m, 5H), 1.08 (d, *J* = 6.7 Hz, 6H) ppm. **^{13}C NMR (101 MHz, CDCl$_3$)** δ 165.4, 162.4, 162.4, 153.0, 140.3, 133.4, 132.6, 132.0, 127.7, 125.9, 124.5, 121.7, 121.4, 120.2, 115.6, 112.8, 109.1, 103.1, 75.8, 55.8, 44.5, 31.8, 28.3, 19.2, 16.7 ppm. **HRMS** [ESI$^+$] *calcd*. for ($C_{28}H_{28}ClN_5NaO_2S$) [M+Na]$^+$: 556.1544, *found*: 556.1545.

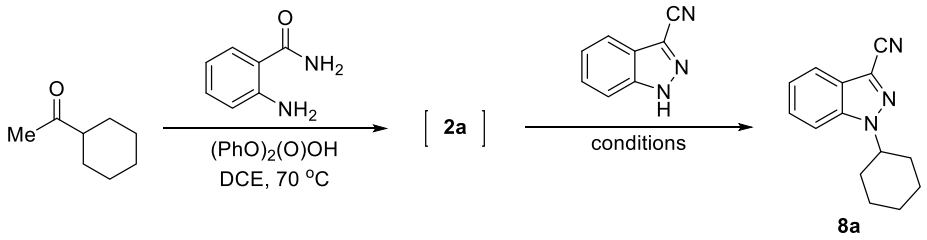

1-Cyclohexyl-1*H*-indazole-3-carbonitrile (8a). An oven-dried 8 mL screw-cap test tube was charged with a stirrer bar, 2-aminobenzamide (81.6 mg, 0.6 mmol), methyl cyclohexyl ketone (79.4 mg, 0.63 mmol), diphenyl phosphate (15.0 mg, 0.06 mmol) and DCE (1.2 mL). The reaction mixture was stirred at 70 °C for 24 hours. The solvent was removed under reduced pressure, then 1*H*-indazole-3-carbonitrile (28.6 mg, 0.2 mmol), $Cu(MeCN)_4PF_6$ (14.9 mg, 20 mol%) and 3,4,7,8-tetramethyl-1,10-phenantroline (14.2 mg, 30 mol%) were added. The test tube was taken into a nitrogen-filled glovebox where K_3PO_4 (84.8 mg, 2.0 equiv) was added. The reaction vessel was sealed with a screw cap and removed from the glovebox. Afterwards, benzene (3.0 mL, 0.067 M) was added by syringe. The reaction mixture was stirred at rt for 5 min, then BzOO^{t}Bu (77.6 mg, 2.0 equiv) was added slowly under vigorous stirring. Parafilm was used to reseal the pierced cap. The reaction mixture was stirred at 65 °C for 12 hours. Afterwards, the reaction mixture was concentrated under reduced pressure and purified by silica gel chromatography (hexane/EtOAc = 20:1), affording **8a** (34.2 mg, 76%) as a white solid. **^{1}H NMR (400 MHz, CDCl$_3$)** δ 7.83 (dt, *J* = 8.2, 1.0 Hz, 1H), 7.60 – 7.54 (m, 1H), 7.51 – 7.43 (m, 1H), 7.37 – 7.29 (m, 1H), 4.49 (tt, *J* = 10.4, 4.7 Hz, 1H), 2.14 – 1.94 (m, 6H), 1.84 – 1.75 (m, 1H), 1.57 – 1.43 (m, 2H), 1.42 – 1.31 (m, 1H) ppm. **^{13}C**

NMR (101 MHz, $CDCl_3$) δ 138.9, 127.4, 125.6, 123.6, 119.8, 117.3, 114.1, 110.3, 59.5, 32.6, 25.7, 25.3 ppm. Spectral data was in agreement with the literature.[87]

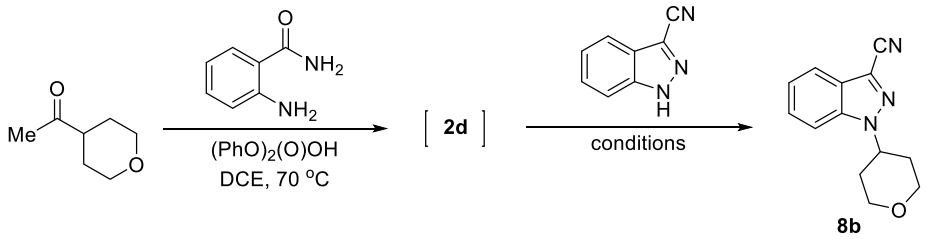

1-(Tetrahydro-2*H*-pyran-4-yl)-1*H*-indazole-3-carbonitrile (8b). An oven-dried 8 mL screw-cap test tube was charged with a stirrer bar, 2-aminobenzamide (81.6 mg, 0.6 mmol), 1-(tetrahydro-2*H*-pyran-4-yl)ethan-1-one (80.6 mg, 0.63 mmol), diphenyl phosphate (15.0 mg, 0.06 mmol) and DCE (1.2 mL). The reaction mixture was stirred at 70 °C for 24 hours. The solvent was removed under reduced pressure, then 1*H*-indazole-3-carbonitrile (28.6 mg, 0.2 mmol), $Cu(MeCN)_4PF_6$ (14.9 mg, 20 mol%) and 3,4,7,8-tetramethyl-1,10-phenantroline (14.2 mg, 30 mol%) were added. The test tube was introduced in a nitrogen-filled glovebox where K_3PO_4 (84.8 mg, 2.0 equiv) was added. The reaction vessel was sealed with a screw cap and removed from the glovebox. Afterwards, benzene (3.0 mL, 0.067 M) was added by syringe. The reaction mixture was stirred at rt for 5 min, then BzOO^{t}Bu (77.6 mg, 2.0 equiv) was added slowly under vigorous stirring. Parafilm was used to reseal the pierced cap. The reaction mixture was stirred at 65 °C for 12 hours. Afterwards, the reaction mixture was concentrated under reduced pressure and purified by silica gel chromatography (hexane/EtOAc 5:1), affording **8b** (28.4 mg, 63%) as a white solid. **M.p.**: 149 °C. **IR (neat, cm^{-1}):** 2967, 2936, 2858, 2226, 1618, 1467, 1352, 1298, 1217, 1143, 1084, 1009, 834, 752, 576, 550. **^{1}H NMR (400 MHz, $CDCl_3$)** δ 7.85 (dt, *J* = 8.2, 0.9 Hz, 1H), 7.62 – 7.56 (m, 1H), 7.54 – 7.47 (m, 1H), 7.40 – 7.33 (m, 1H), 4.75 (tt, *J* = 11.4, 4.2 Hz, 1H), 4.23 – 4.15 (m, 2H), 3.63 (td, *J* = 12.0, 2.1 Hz, 2H), 2.48 – 2.33 (m, 2H), 2.07 – 1.98 (m, 2H) ppm. **^{13}C NMR (101 MHz, $CDCl_3$)** δ 138.9, 127.7, 125.7, 123.8, 120.1, 117.9, 113.9, 110.1, 67.0, 56.6, 32.4 ppm. **HRMS** [ESI$^+$] *calcd*. for ($C_{13}H_{14}N_3O$) $[M+H]^+$: 228.1131, *found*: 228.1137.

3.7.4 Mechanistic Studies

3.7.4.1 Radical Clock Experiments

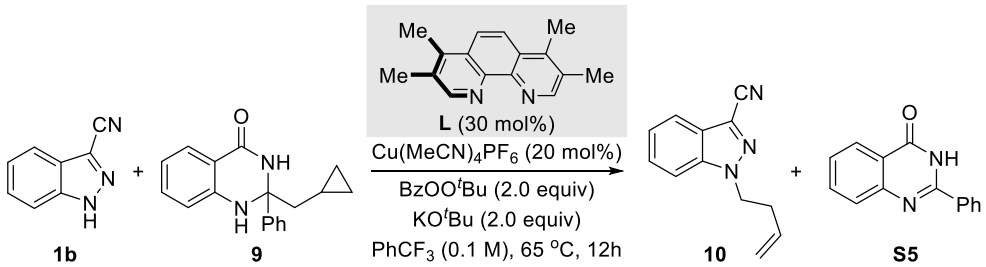

An oven-dried 8 mL screw-cap test tube containing a stirring bar was charged with 1*H*-indazole-3-carbonitrile (28.6 mg, 0.2 mmol) and 2-(cyclopropylmethyl)-2-phenyl-2,3-dihydroquinazolin-4(1*H*)-one (66.7 mg, 1.2 equiv), $Cu(MeCN)_4PF_6$ (14.9 mg, 20 mol%) and 3,4,7,8-tetramethyl-1,10-phenantroline (14.2 mg, 30 mol%). The test tube was introduced in a nitrogen-filled glovebox where KO^{t}Bu (44.8 mg, 2.0 equiv) was added. The reaction vessel was sealed with a screw cap and removed from the glovebox. Afterwards, $PhCF_3$ (2.0 mL, 0.1 M) was added by syringe. The reaction mixture was stirred at rt for 5 min, then BzOO^{t}Bu (77.6 mg, 2.0 equiv) was added slowly under vigorous stirring. Parafilm was used to reseal the pierced cap. The reaction mixture was stirred at 65 °C for 12 hours. Afterwards, the reaction mixture was concentrated under reduced pressure and purified by silica gel chromatography (hexane/EtOAc 20:1 to 4:1), affording **10** (13.2 mg, 34%) as a colourless oil and **S5** (45.6 mg, 86%) as a white solid.
1-(But-3-en-1-yl)-1*H*-indazole-3-carbonitrile (10). IR (neat, cm^{-1}): 2945, 2233, 1617, 1468, 1350, 1197, 993, 921, 743. **^{1}H NMR (400 MHz, $CDCl_3$)** δ 7.83 (dt, *J* = 8.2, 0.9 Hz, 1H), 7.57 – 7.45 (m, 2H), 7.38 – 7.31 (m, 1H), 5.76 (ddt, *J* = 17.1, 10.2, 6.9 Hz, 1H), 5.11 – 4.98 (m, 2H), 4.51 (t, *J* = 7.1 Hz, 2H), 2.77 – 2.66 (m, 2H) ppm. **^{13}C NMR (101 MHz, $CDCl_3$)** δ 139.7, 133.5, 127.8, 125.5, 123.6, 119.8, 118.3, 117.8, 113.8, 110.3, 49. 7, 33.9 ppm. **HRMS** [ESI$^+$] *calcd*. for ($C_{12}H_{12}N_3$) [M+H]$^+$: 198.1026, *found*: 198.1031.
2-Phenylquinazolin-4(3*H*)-one (S5). ^{1}H NMR (400 MHz, DMSO-d_6) δ 8.22 – 8.09 (m, 3H), 7.84 – 7.75 (m, 1H), 7.74 – 7.68 (m, 1H), 7.59 – 7.44 (m, 4H) ppm. NH signal invisible due to deuterium exchange. **^{13}C NMR (101 MHz, DMSO-d_6)** δ 162.3, 152.3, 148.7, 134.6, 132.7, 131.4, 128.6, 127.8, 127.5, 126.5, 125.9, 121.0 ppm. Spectral data was in agreement with the literature.[204]

3.7.4.2 Radical Inhibition Experiments

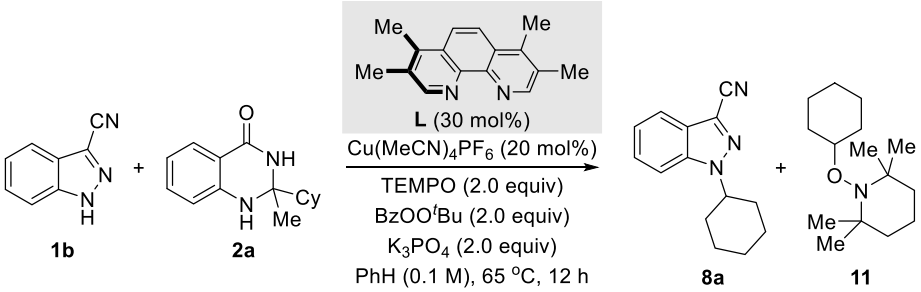

An oven-dried 8 mL screw-cap test tube containing a stirring bar was charged with 1*H*-indazole-3-carbonitrile (28.6 mg, 0.2 mmol) and 2-cyclohexyl-2-methyl-2,3-dihydroquinazolin-4(1*H*)-one (58.6 mg, 1.2 equiv), TEMPO (31.2 mg, 1.0 equiv), $Cu(MeCN)_4PF_6$ (14.9 mg, 20 mol%) and 3,4,7,8-tetramethyl-1,10-phenantroline (14.2

mg, 30 mol%). The test tube was introduced in a nitrogen-filled glovebox where K_3PO_4 (84.8 mg, 2.0 equiv) was added. The reaction vessel was sealed with a screw cap and removed from the glovebox. Afterwards, benzene (2.0 mL, 0.1 M) was added by syringe. The reaction mixture was stirred at rt for 5 min, then BzOO^{t}Bu (77.6 mg, 2.0 equiv.) was added slowly under vigorous stirring. Parafilm was used to reseal the pierced cap. The reaction mixture was stirred at 65 °C for 12 hours. Afterwards, the reaction mixture was concentrated under reduced pressure and purified by silica gel chromatography (hexane/EtOAc 50:1 to 20:1), affording cyclohexyl-TEMPO adduct **11** (15.3 mg, 32%) as a colourless oil and 1-cyclohexyl-1*H*-indazole-3-carbonitrile **8a** (22.7 mg, 50%) as a white solid.

1-(Cyclohexyloxy)-2,2,6,6-tetramethylpiperidine (11). ^{1}H NMR (400 MHz, $CDCl_3$) δ 3.58 (tt, *J* = 9.6, 4.0 Hz, 1H), 2.10 – 1.98 (m, 2H), 1.79 – 1.67 (m, 2H), 1.56 – 1.41 (m, 6H), 1.38 – 1.00 (m, 18H) ppm. **^{13}C NMR (101 MHz, $CDCl_3$)** δ 81.9, 59.8, 40.4, 34.6, 33.1, 26.1, 25.2, 20.4, 17.5 ppm. Spectral data was in agreement with the literature.[265]

3.7.4.3 Control Experiments

Control experiments with Cu(II) salts used in place of BzOO^{t}Bu

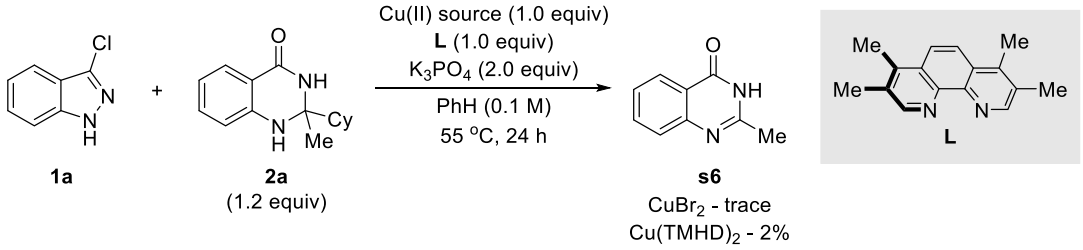

An oven-dried 8 mL screw-cap test tube containing a stirring bar was charged with either $CuBr_2$ (28.0 mg, 0.1 mmol) along with 3,4,7,8-tetramethyl-1,10-phenantroline (23.6 mg, 0.1 mmol) or copper bis(2,2,6,6-tetramethyl-3,5-heptanedionate (22.0 mg, 0.1 mmol), 3-chloro-1*H*-indazole (15.3 mg, 0.1 mmol) and 2-cyclohexyl-2-methyl-2,3-dihydroquinazolin-4(1*H*)-one (24.3 mg, 0.1 mmol). The test tube was introduced in a nitrogen-filled glovebox where K_3PO_4 (42.4 mg, 2.0 equiv) was added. The reaction vessel was sealed with a screw cap and removed from the glovebox. Afterwards, benzene (1.0 mL, 0.1 M) was added by syringe. The reaction mixture was stirred at 55 °C for 24 hours. The reaction mixture was quenched with water (20 mL) and extracted using EtOAc (3 x 15 mL). The combined organic extracts were dried ($MgSO_4$), concentrated under reduced pressure, then analyzed by ^{1}H NMR using 1,3,5-trimethoxybenzene as an internal standard.

[265] Zheng, C.; Wang, Y.; Xu, Y.; Chen, Z.; Chen, G.; Liang, S. H. Ru-Photoredox-Catalyzed Decarboxylative Oxygenation of Aliphatic Carboxylic Acids through N-(acyloxy)phthalimide. *Org. Lett.* **2018**, *20*, 4824–4827.

Control experiment in the absence of copper and ligand

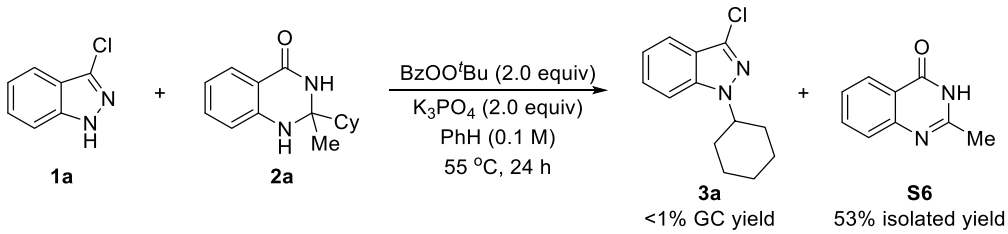

An oven-dried 8 mL screw-cap test tube containing a stirring bar was charged with 3-chloro-1*H*-indazole (15.3 mg, 0.1 mmol) and 2-cyclohexyl-2-methyl-2,3-dihydroquinazolin-4(1*H*)-one (29.3 mg, 1.2 equiv). The test tube was introduced in a nitrogen-filled glovebox where K_3PO_4 (42.4 mg, 2.0 equiv) was added. The reaction vessel was sealed with a screw cap and removed from the glovebox. Afterwards, benzene (1.0 mL, 0.1 M) was added by syringe. The reaction mixture was stirred at rt for 5 min, then BzOO^{t}Bu (38.8 mg, 2.0 equiv) was added slowly under vigorous stirring. Parafilm was used to reseal the pierced cap. The reaction mixture was stirred at 55 °C for 12 hours. After the reaction was completed, the mixture was filtered through celite and analyzed by GC using dodecane (17.0 mg, 0.1 mmol) as internal standard, indicating that no formation of the target coupling product. Afterwards, the reaction mixture was concentrated under reduced pressure and purified by silica gel chromatography (hexane/EtOAc 5:1 to 3:1), affording 2-methylquinazolin-4(3H)-one **S6** (10.1 mg, 53%) as a white solid.

2-Methylquinazolin-4(3*H*)-one (S6). ^{1}H NMR (400 MHz, DMSO-*d*$_6$) δ 8.11 – 7.98 (m, 1H), 7.79 – 7.69 (m, 1H), 7.58 – 7.51 (m, 1H), 7.47 – 7.39 (m, 1H), 5.74 (s, 1H), 2.33 (s, 3H) ppm. **^{13}C NMR (101 MHz, DMSO-*d*$_6$)** δ 161.7, 154.3, 148.9, 134.3, 126.5, 125.8, 125.7, 120.6, 21.4 ppm. Spectral data was in agreement with the literature.[266]

Experiments with *N*-methylated dihydroquinazoline

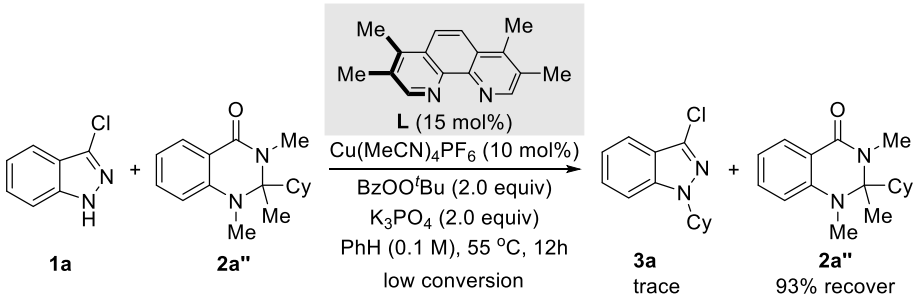

An oven-dried 8 mL screw-cap test tube containing a stirring bar was charged with 3-chloro-1*H*-indazole (15.3 mg, 0.1 mmol) and 2-cyclohexyl-1,2,3-trimethyl-2,3-dihydroquinazolin-4(1*H*)-one (32.6 mg, 1.2 equiv), $Cu(MeCN)_4PF_6$ (3.7 mg, 10 mol%)

[266] Xu, G.; Wang, L.; Li, M.; Tao, M.; Zhang, W. Phosphorous Acid Functionalized Polyacrylonitrile Fibers with a Polarity Tunable Surface Micro-Environment for One-Pot C–C and C–N Bond Formation Reactions. *Green Chem.* **2017**, *19*, 5818–5830.

and 3,4,7,8-tetramethyl-1,10-phenantroline (3.5 mg, 15 mol%). The test tube was introduced in a nitrogen-filled glovebox where K_3PO_4 (42.4 mg, 2.0 equiv) was added. The reaction vessel was sealed with a screw cap and removed from the glovebox. Afterwards, benzene (1.0 mL, 0.1 M) was added by syringe. The reaction mixture was stirred at rt for 5 min, then BzOO^{t}Bu (38.8 mg, 2.0 equiv) was added slowly under vigorous stirring. Parafilm was used to reseal the pierced cap. The reaction mixture was stirred at 55 °C for 12 hours. After the reaction was completed, the mixture was filtered through celite and analyzed by GC using dodecane (17.0 mg, 0.1 mmol) as internal standard, indicating that trace amount of the target coupling product. Afterwards, the reaction mixture was concentrated under reduced pressure and purified by silica gel chromatography (hexane/EtOAc 3:1 to 2:1), recovering 2-cyclohexyl-1,2,3-trimethyl-2,3-dihydroquinazolin-4(1*H*)-one **2a"** (30.4 mg, 93%) as a white solid.

3.7.4.4 Experiments with Copper Complex Cu-I

Preparation of Cu-I

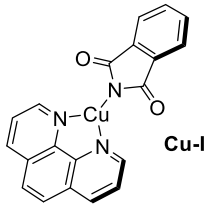

Cu-I

In a nitrogen-filled glovebox, a 20 mL vial was charged sequentially with a magnetic stirrer bar, copper(I) chloride (100 mg, 1.02 mmol) and THF (1.5 mL). A solution of sodium *tert*-butoxide (98 mg, 1.02 mmol) in THF (6 mL) was added to the copper(I) chloride solution while stirring. The reaction mixture was allowed to stir at rt for 1 hour. Afterwards, the reaction mixture was filtered through a fritted funnel and the collected filtrate was transferred to a new 20 mL vial, which was sequentially charged with a magnetic stirrer bar and a solution of 1,10-phenanthroline (551 mg, 3.06 mmol) in THF (3 mL). The resulting dark red reaction mixture was allowed to stir at rt for 15 minutes then isoindoline-1,3-dione (450 mg, 3.06 mmol) was added. The reaction mixture was allowed to stir at rt for 20 minutes, during which a thick orange precipitate formed. The precipitate was collected and dried under reduced pressure. A saturated solution of the precipitate was made from a mixture of DMSO and THF (4:1), which was layered with Et_2O. Over the course of two days, dark red crystals formed which were collected by decantation, washed with a minimal amount of THF and dried under reduced pressure, yielding the desired copper complex as dark red crystals (138 mg, 35%). **^{1}H NMR (500 MHz, DMSO-*d*$_6$)** δ 9.11 (br. s, 2H), 8.84 (d, *J* = 7.8 Hz, 2H), 8.29 (br. s, 2H), 8.08 – 8.02 (m, 2H), 7.64 – 7.60 (m, 4H) ppm. **^{13}C NMR (126 MHz, DMSO-*d*$_6$)** δ 179.4, 149.6, 143.1, 137.5, 136.1, 132.3, 129.0, 127.0, 125.8, 121.1 ppm. Spectral data was in agreement with the literature.[259]

Catalytic competency of Cu-I

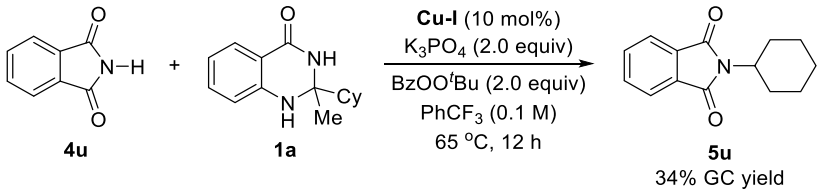

An oven-dried 8 mL screw-cap test tube containing a stirring bar was charged with phthalimide (29.4 mg, 0.2 mmol) and 2-cyclohexyl-2-methyl-2,3-dihydroquinazolin-4(1*H*)-one (58.6 mg, 0.24 mmol). The test tube was taken into a nitrogen-filled glovebox where K_3PO_4 (84.8 mg, 0.4 mmol) and Cu-I (7.8 mg, 0.02 mmol) were added. The reaction vessel was sealed with a screw cap septum and removed from the glovebox. Afterwards, $PhCF_3$ (2.0 mL, 0.1 M) was added by syringe. The reaction mixture was stirred at rt for 5 min, then BzOO^{t}Bu (76 µL, 77.6 mg, 0.4 mmol) was added slowly under vigorous stirring. Parafilm was used to reseal the septum. The reaction mixture was stirred at 55 °C for 12 hours. After which, the reaction mixture was filtered through celite and analyzed by GC using dodecane (34.0 mg, 0.2 mmol) as internal standard, showing that 2-cyclohexylisoindoline-1,3-dione (**5u**) was formed in 34% yield.

Catalytic reaction with 1,10-phenantroline ligand

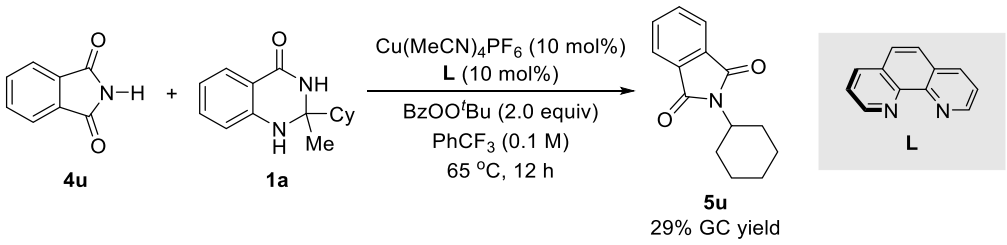

An oven-dried 8 mL screw-cap test tube containing a stirring bar was charged with phthalimide (29.4 mg, 0.2 mmol), 2-cyclohexyl-2-methyl-2,3-dihydroquinazolin-4(1*H*)-one (58.6 mg, 0.24 mmol), $Cu(MeCN)_4PF_6$ (7.5 mg, 10 mol%) and 1,10-phenantroline (3.6 mg, 10 mol%). The test tube was taken into a nitrogen-filled glovebox where K_3PO_4 (84.8 mg, 0.4 mmol) was added. The reaction vessel was sealed with a screw cap septum and removed from the glovebox. Afterwards, $PhCF_3$ (2.0 mL, 0.1 M) was added by syringe. The reaction mixture was stirred at rt for 5 min, then BzOO^{t}Bu (77.6 mg, 0.4 mmol) was added slowly under vigorous stirring. Parafilm was used to reseal the septum. The reaction mixture was stirred at 65 °C for 12 hours. After which, the reaction mixture was filtered through celite and analyzed by GC using dodecane (34.0 mg, 0.2 mmol) as internal standard, showing that 2-cyclohexylisoindoline-1,3-dione (**5u**) was formed in 29% yield.

Stoichiometry experiment with Cu-I

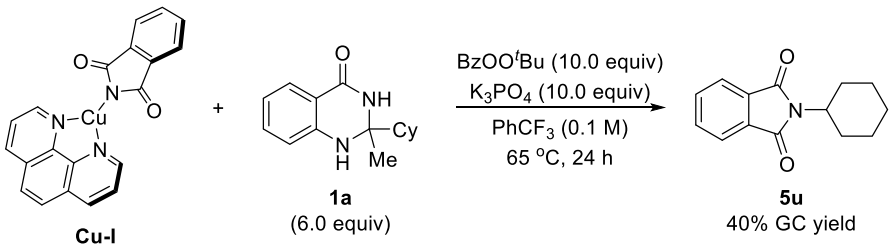

In a nitrogen-filled glove box a 10 mL glass vial was sequentially charged with a magnetic stirrer bar, 2-cyclohexyl-2-methyl-2,3-dihydroquinazolin-4(1*H*)-one (147 mg, 0.6 mmol), tripotassium phosphate (212 mg, 1.0 mmol), Cu-I (39 mg, 0.1 mmol) and $PhCF_3$ (5 mL). The reaction mixture was stirred at 50 °C for 10 minutes forming a dark red mixture, afterward the mixture was allowed to cool to rt and then under vigorous stirring BzOO^{t}Bu (190 µL, 194 mg, 1.0 mmol) was added slowly. The resulting green reaction mixture was capped, removed from the glovebox and stirred at 65 °C for 24 hours. After which, the reaction mixture was filtered through celite and analyzed by GC using dodecane (17.0 mg, 0.1 mmol) as internal standard, showing that 2-cyclohexylisoindoline-1,3-dione (**5u**) was formed in 40% yield.

3.7.4.5 Cyclic Voltammetry Data

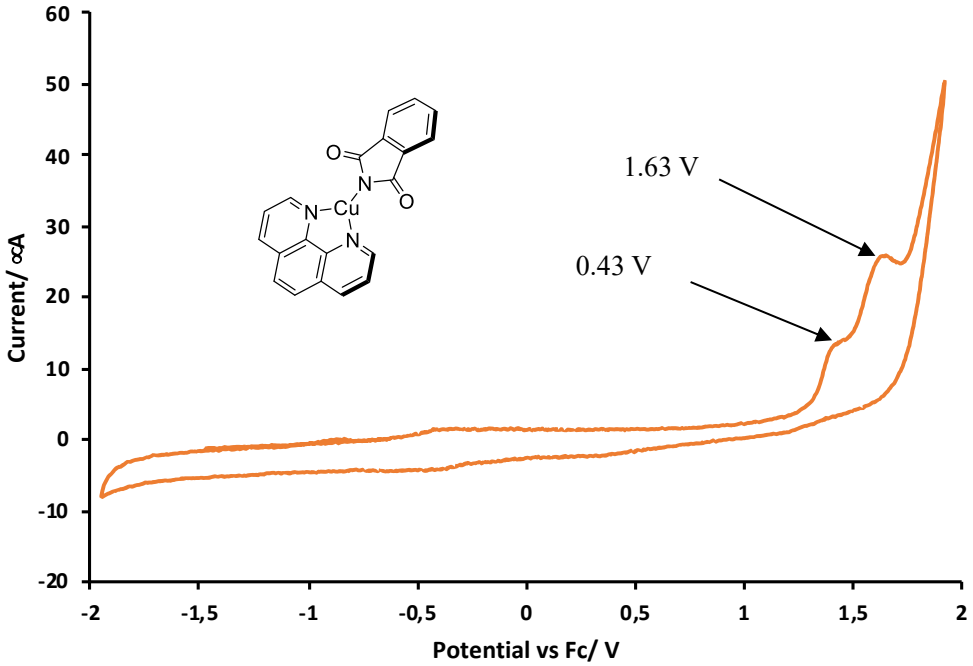

Figure S3.1 Cyclic voltammogram of **Cu-I** (1.9 mg, 5 µmol) in a 0.1 M solution of NBu_4PF_6 in $PhCF_3$:MeCN (5 mL, 25:1) at a scan rate of 100 mV/s.

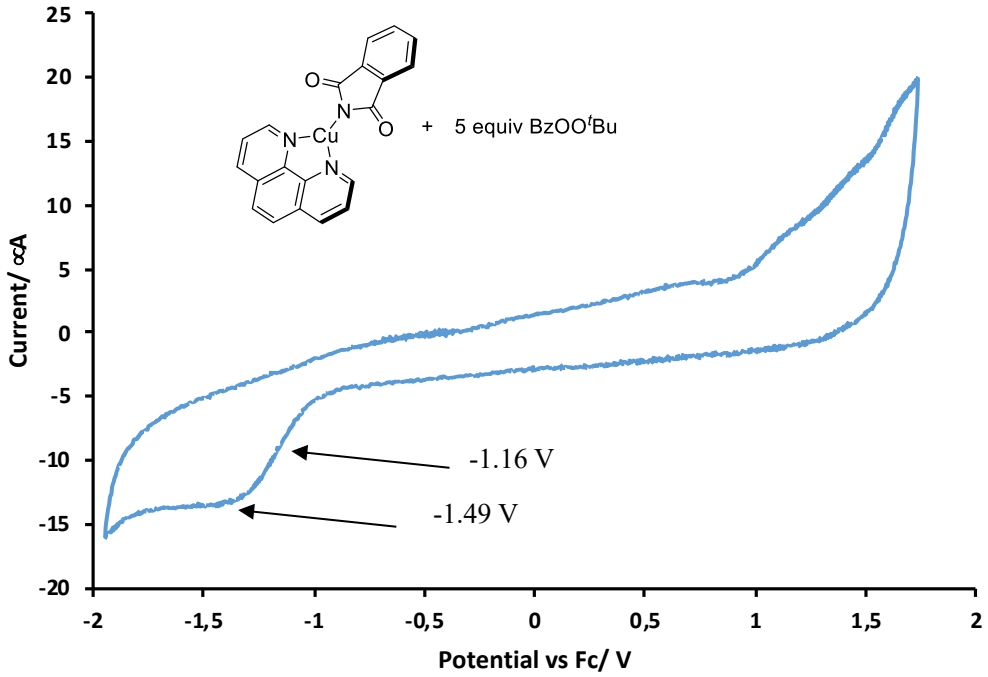

Figure S3.2 Cyclic voltammogram of a mixture of **Cu-I** (1.9 mg, 5 µmol) and BzOO^{t}Bu (4.9 mg, 25 µmol) in a 0.1 M solution of NBu_4PF_6 in $PhCF_3$:MeCN (5 mL, 25:1) at a scan rate of 100 mV/s.

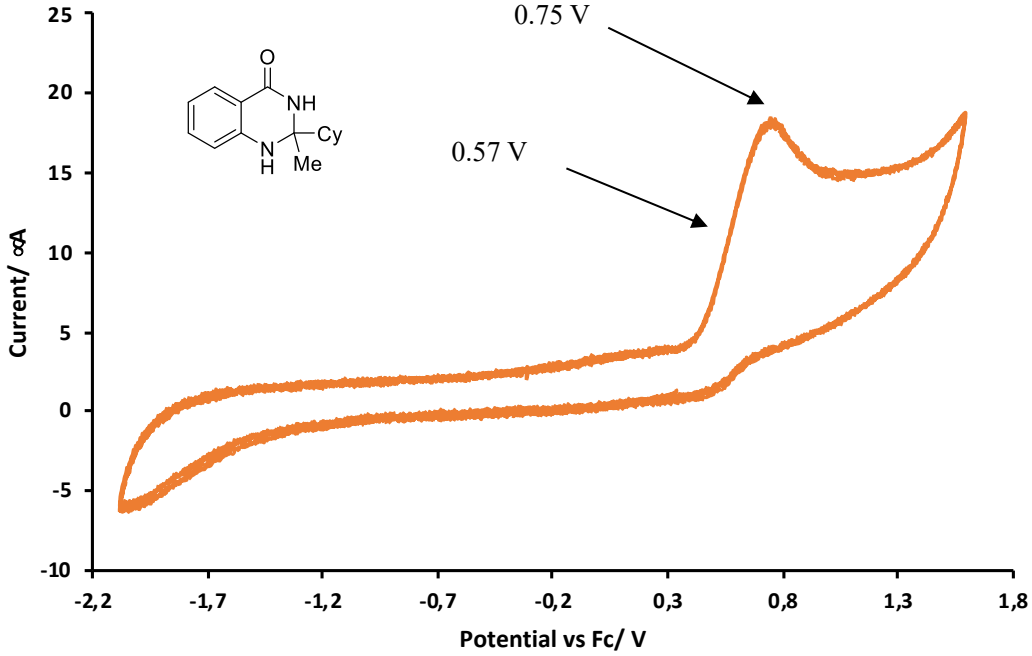

Figure S3.3 Cyclic voltammogram of 2-cyclohexyl-2-methyl-2,3-dihydroquinazolin-4(1*H*)-one (**2a**) (1.2 mg, 5 µmol) in a 0.1 M solution of NBu_4PF_6 in $PhCF_3$:MeCN (5 mL, 25:1) at a scan rate of 100 mV/s.

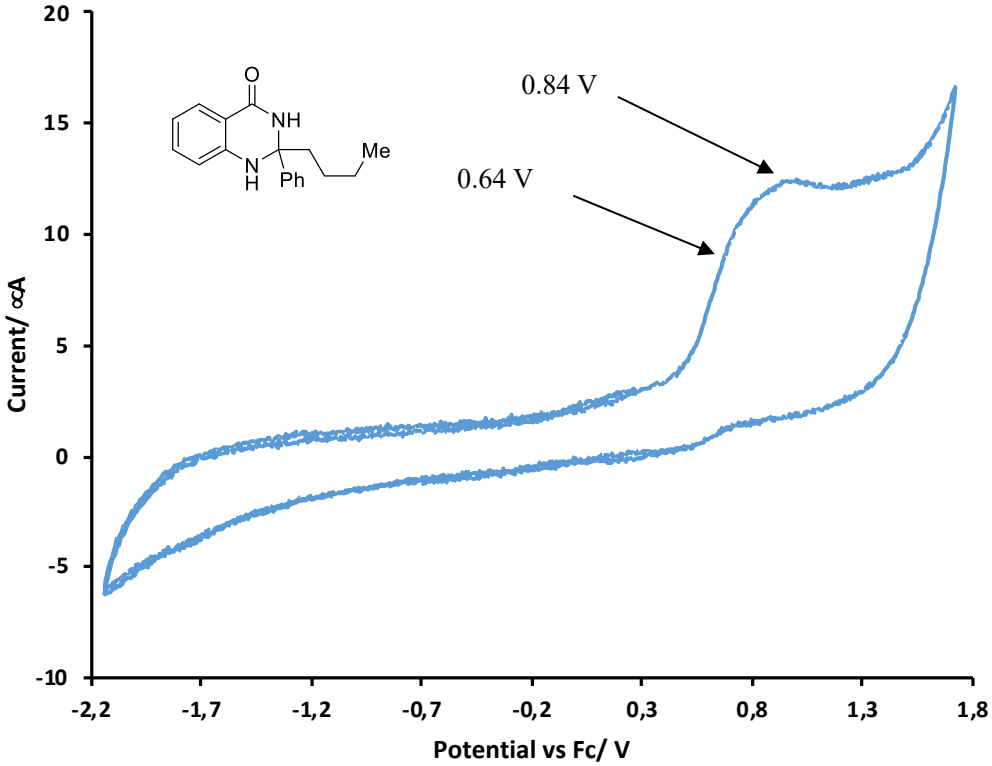

Figure S3.4 Cyclic voltammogram of 2-butyl-2-phenyl-2,3-dihydroquinazolin-4(1*H*)-one (**2k'**) (1.4 mg, 5 µmol) in a 0.1 M solution of NBu_4PF_6 in $PhCF_3$:MeCN (5 mL, 25:1) at a scan rate of 100 mV/s.

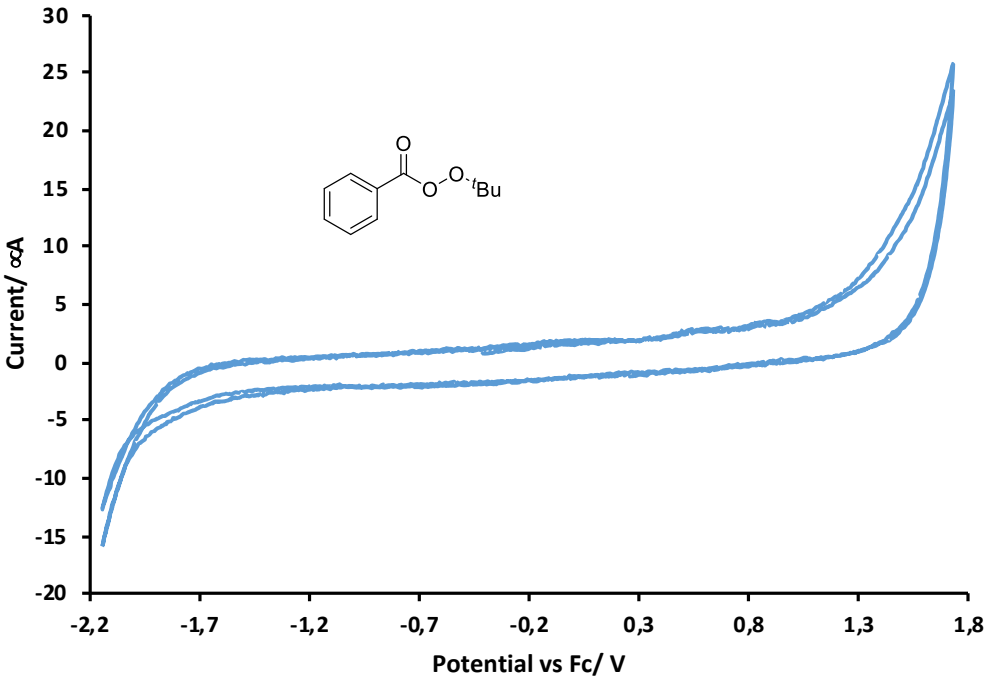

Figure S3.5 Cyclic voltamogram of BzOO^tBu (1.0 mg, 5 µmol) in a 0.1 M solution of NBu_4PF_6 in $PhCF_3$:MeCN (5 mL, 25:1) at a scan rate of 100 mV/s.

3.7.4.6 UV-Vis. Spectroscopy Data

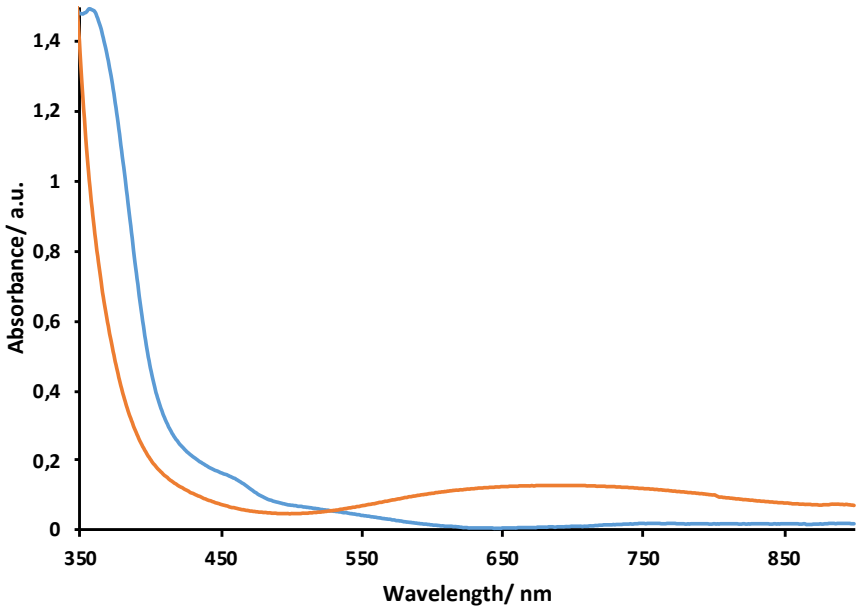

Figure S3.6 Overlaid UV/Vis absorption analysis of 2 mL of a 1.7 mM solution of **Cu-I** in $PhCF_3$ before (blue) and after (orange) being exposed to $BzOO^tBu$ (2.8 mg, 4 equiv, 15 µmol).

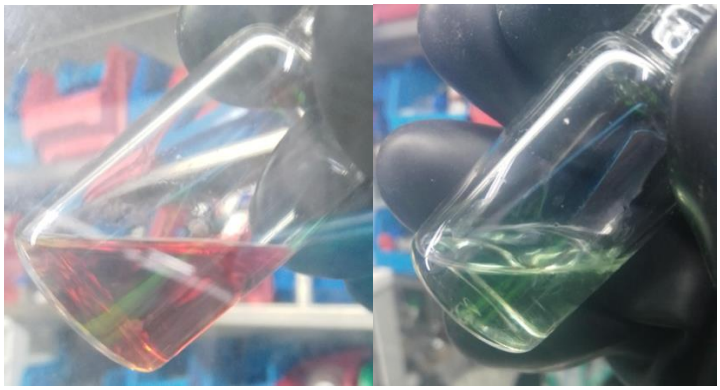

Figure S3.7 Before (left) and after (right) photos of a 1.7 mM solution of **Cu-I** in $PhCF_3$ being exposed to $BzOO^tBu$ (2.8 mg, 4 equiv, 15 µmol).

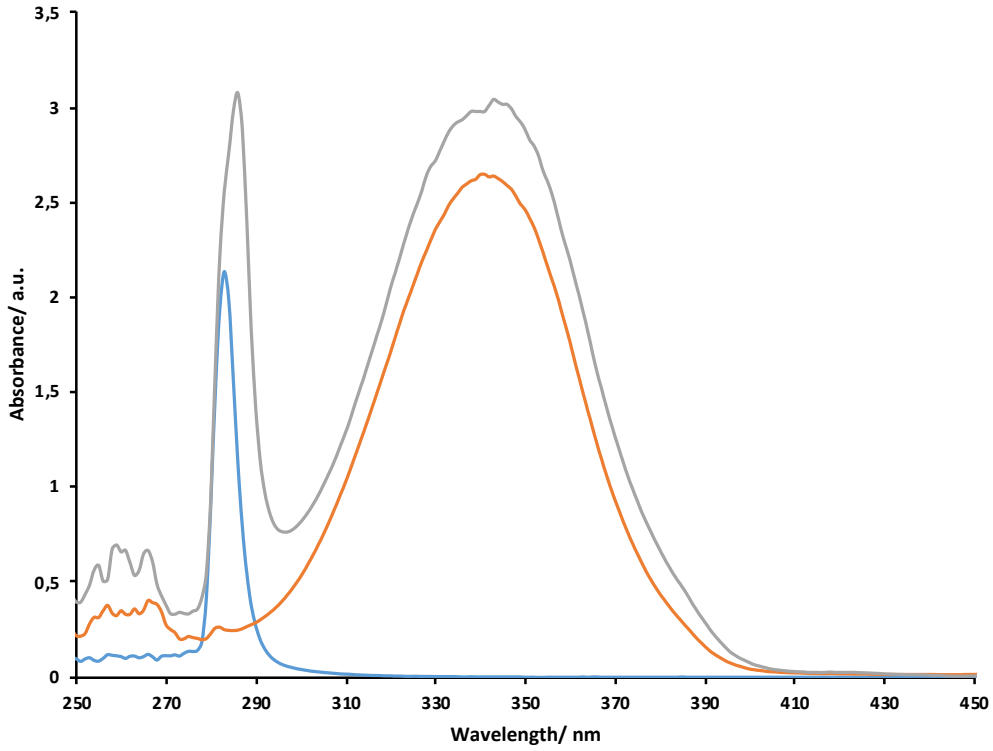

Figure S3.8 Overlaid UV/Vis absorption analysis of BzOO^{t}Bu (3.0 mg, 15 µmol) in 2 mL of $PhCF_3$ (blue), 2-cyclohexyl-2-methyl-2,3-dihydroquinazolin-4(1*H*)-one (**2a**) (2.4 mg, 10 µmol) in 2 mL of $PhCF_3$ (orange), and a mixture of BzOO^{t}Bu (4.1 mg, 21 µmol) and 2-cyclohexyl-2-methyl-2,3-dihydroquinazolin-4(1*H*)-one (**2a**) (2.4 mg, 10 µmol) in 2 mL of $PhCF_3$ (grey).

3.7.4.7 Discussion on How the Dihydroquinazolinone is Activated

Cu-I is a red crystalline material that gives a red solution in $PhCF_3$, upon exposure to BzOO^{t}Bu this solution turns green (Figures S3.7). UV-Vis. spectroscopy shows the formation of a new wide absorbance band centered at 680 nm when **Cu-I** is exposed to BzOO^{t}Bu (Figure S3.6). We believe this indicates the oxidation of **Cu-I** in line with previous reports.[211] However, under our reaction conditions, we currently do not believe Cu(II) is responsible for dihydroquinazolinone activation. Firstly, CV analysis of the green solution formed by exposure of **Cu-I** to BzOO^{t}Bu gave a reduction half-wave at -1.16 V vs Fc (Figure S3.2), meaning outer sphere electron transfer from dihydroquinazolinone (**2a**, $E_{1/2}^{red}$ = +0.57 vs Fc, Figure 3) (**2k´**, $E_{1/2}^{red}$ = +0.64 vs Fc, Figure 4) to oxidized **Cu-I** is unlikely. Although, this does not discount an inner-sphere mechanism. Next, we performed control experiments using stoichiometric amounts of copper(II) salts that were efficient under our catalytic conditions and Tang's conditions

for dihydroquinazolinone aromatization (Section 3.7.4.3).[267] For these only trace amounts of dihydroquinazolinone aromatization product were observed using conditions similar to that of our reaction of interest.

Instead, BzOO^{t}Bu gave a more promising indication of being responsible for dihydroquinazolinone activation, as mixing BzOO^{t}Bu with dihydroquinazolinone in the absence of copper resulted in significant quinazolin-4-one formation (Section 3.7.4.3). We do not believe direct electron transfer from dihydroquinazolinone to BzOO^{t}Bu occurs, as indicated by cyclic voltammetry analysis. We could not observe a reduction wave for BzOO^{t}Bu up to -2.1 V vs Fc (Figure S3.5). We also did not see any new absorption bands or any significant alternation to the absorption bands of **2a** and BzOO^{t}Bu by UV-Vis. spectroscopy when mixed together (Figure S3.8).

In the case of the copper omitted control experiment, we believe BzOO^{t}Bu thermally homolyzes to give oxy radicals. In the case of our copper-catalyzed reaction, in addition to thermal homolysis an analogy to the Kharasch-Sosnovsky reaction can be drawn. Where copper sources catalyze the decomposition of BzOO^{t}Bu to generate *tert*-butoxy radical.[261]

tert-Butoxy radical can undergo β-scission to acetone and methyl radical. Currently, we do not believe methyl radical is the key species for dihydroquinazolinone activation. Firstly, as indicated by Walling and Wagner,[268] the rate of *tert*-butoxy radical β-scission can be accelerated by use of polar solvents (e.g. MeCN) and elevated temperatures. This observation is substantiated upon inspection of copper-catalyzed literature procedures for the methylation of N–H bonds by using peroxides to access methyl radical, which typically require temperatures in excess of 100 °C.[269] In the case of our reaction of interest, we employ lower reaction temperatures in conjunction with apolar solvents (e.g. benzene), which should attenuate β-scission and methyl radical formation. Secondly, during our radical trapping experiments with TEMPO we did not observe the methyl-TEMPO adduct.

Tentatively, this leaves us to currently believe *tert*-butoxy radical is the dihydroquinazolinone activating species, either by EnT or by HAT. Literature cyclic voltammetry analysis of potassium *tert*-butoxide shows an irreversible oxidation wave

[267] Hu, B.-Q.; Wang, L.-X.; Yang, L.; Xiang, J.-F.; Tang, J.-F. Copper-Catalyzed Intramolecular C–C Bond Cleavage To Construct 2-Substituted Quinazolinones. *Eur. J. Org. Chem.* **2015**, 4504–4509.
[268] Walling, C.; Wagner, P. C. Positive Halogen Compounds. X. Solvent Effects in the Reactions of *t*-Butoxy Radicals. *J. Am. Chem. Soc.* **1964**, *86*, 3368–3375.
[269] Teng, F.; Cheng, J.; Yu, J.-T. Copper-Catalyzed *N*-Methylation/Ethylation of Sulfoximines. *Org. Biomol. Chem*. **2015**, *13*, 9934–9937. (b) Xiao, J.; Su, Q.; Dong, W.; Peng, Z.; Zhang, Y.; An, D. Copper-Catalyzed Oxidative Alkylation (Methylation) of Phosphonamides and Phosphinamides Using Dicumyl Peroxide. *J. Org. Chem.* **2017**, *82*, 9497–9504.

at 0.1 V vs SCE.[270] Due to the irreversibility of this wave the reduction potential of the *tert*-butoxy radical is hidden. It could be inferred by how low the oxidation potential of the reverse process is that *tert*-butoxy radical would not be sufficiently oxidizing to oxidize the dihydroquinazolinones we use. However, this does not discount an inner-sphere mechanism.

In support of a HAT mechanism the O–H bond dissociation energy of *tert*-butanol is relatively high (110.6 kcal/mol).[271] By drawing analogy to the N–H bond of methyl aniline (89 kcal/mol) [272] it is conceivable that the aniline N–H BDE of a dihydroquinazolinone is significantly lower than that of the O–H of *tert*-butanol. We synthesized dihydroquinazolinone **2a"** which features N–Me bonds in place of the N–H analogues we used. Using *N*-methylated dihydroquinazolinone derivative **2a"** in our C(sp^3)–N cross-coupling afforded negligible amounts of products cross-coupling product, as well as little conversion of **3a** (Section 3.7.4.3). This result may imply that the N–H bonds of the dihydroquinazolinones we employ are required for C–C bond scission by HAT activation. However, it is worth noting that the pyridium by-product formed after aromatization of **2a"** may be inhibitory to other steps within the reaction.

3.7.4.8 Crystal X-ray Diffraction Data

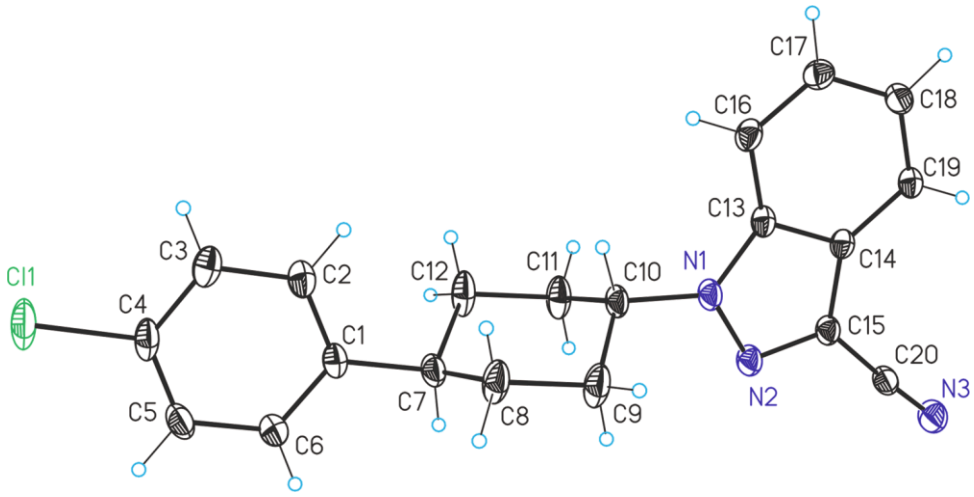

Figure S3.9 ORTEP diagram of **3j**.

Table S3.1 Crystal data and structure refinement for **3j.**

[270] Yi, H.; Jutand, A.; Le, A. Evidence for the Interaction between ^{t}BuOK and 1,10-Phenanthroline to Form the 1,10-Phenanthroline Radical Anion: a Key Step for the Activation of Aryl Bromides by Electron Transfer. *Chem. Commun.* **2015**, *51*, 545–548.
[271] Correia, C. F.; Guedes, R. C.; Borges dos Santos, R. M.; Costa Cabral, B. J.; Martinho Simões, J. A. O–H Bond Dissociation Enthalpies in Hydroxyphenols. A Time-Resolved Photoacoustic Calorimetry and Quantum Chemistry Study. *Phys. Chem. Chem. Phys*. **2004**, *6*, 2109–2118.
[272] Bordwell, F. G.; Zhang, X.-M.; Cheng, J.-P. Bond Dissociation Energies of the Nitrogen-Hydrogen Bonds in Anilines and in the Corresponding Radical Anions. Equilibrium Acidities of Aniline Radical Cations. *J. Org. Chem.* **1993**, *58*, 6410–6416.

Identification code	XLYU-5-74-4
Empirical formula	C20 H18 Cl N3
Formula weight	335.82
Temperature	100(2)K
Wavelength	0.71073 Å
Crystal system	monoclinic
Space group	P 21/n
Unit cell dimensions	a = 10.7323(2)Å a= 90°.
	b = 9.7254(2)Å b = 98.761(2)°.
	c = 16.5551(3)Å g = 90°.
Volume	1707.79(6) Å3
Z	4
Density (calculated)	1.306 Mg/m3
Absorption coefficient	0.229 mm-1
F(000)	704
Crystal size	0.600 x 0.400 x 0.300 mm3
Theta range for data collection	3.581 to 30.784°.
Index ranges	-15<=h<=14,-13<=k<=12,-23<=l<=22
Reflections collected	22692
Independent reflections	4832[R(int) = 0.0218]
Completeness to theta =30.784°	90.4%
Absorption correction	Multi-scan
Max. and min. transmission	1.00 and 0.83
Refinement method	Full-matrix least-squares on F2
Data / restraints / parameters	4832/ 0/ 217
Goodness-of-fit on F2	1.043
Final R indices [I>2sigma(I)]	R1 = 0.0440, wR2 = 0.1136
R indices (all data)	R1 = 0.0510, wR2 = 0.1183
Largest diff. peak and hole	0.846 and -0.711 e.Å-3

Table S3.2 Bond lengths [Å] and angles [°] for **3j**.

Bond lengths----		
Cl1	C4	1.7472(13)
N1	N2	1.3491(14)
N1	C13	1.3704(15)
N1	C10	1.4636(14)
N2	C15	1.3394(15)

N3	C20	1.1471(17)
C1	C6	1.3911(18)
C1	C2	1.3948(18)
C1	C7	1.5173(16)
C2	C3	1.3899(16)
C3	C4	1.381(2)
C4	C5	1.381(2)
C5	C6	1.3943(18)
C7	C12	1.5250(19)
C7	C8	1.532(2)
C8	C9	1.5323(18)
C9	C10	1.5110(19)
C10	C11	1.5147(18)
C11	C12	1.5287(17)
C13	C14	1.4049(15)
C13	C16	1.4070(16)
C14	C19	1.4028(16)
C14	C15	1.4164(16)
C15	C20	1.4318(16)
C16	C17	1.3734(18)
C17	C18	1.4134(16)
C18	C19	1.3749(17)

Angles----------

N2	N1	C13	112.28(9)
N2	N1	C10	121.38(10)
C13	N1	C10	126.21(10)
C15	N2	N1	105.09(10)
C6	C1	C2	118.01(11)
C6	C1	C7	121.27(11)
C2	C1	C7	120.71(11)
C3	C2	C1	121.70(12)
C4	C3	C2	118.60(12)
C5	C4	C3	121.51(12)
C5	C4	Cl1	119.37(11)
C3	C4	Cl1	119.10(11)
C4	C5	C6	118.99(12)
C1	C6	C5	121.18(13)
C1	C7	C12	111.52(11)

C1	C7	C8	110.94(10)
C12	C7	C8	110.48(11)
C7	C8	C9	112.98(11)
C10	C9	C8	108.64(11)
N1	C10	C9	112.58(10)
N1	C10	C11	111.80(10)
C9	C10	C11	110.66(11)
C10	C11	C12	109.91(10)
C7	C12	C11	112.90(11)
N1	C13	C14	106.74(10)
N1	C13	C16	131.31(11)
C14	C13	C16	121.95(11)
C19	C14	C13	120.58(11)
C19	C14	C15	135.79(11)
C13	C14	C15	103.62(10)
N2	C15	C14	112.26(10)
N2	C15	C20	121.37(11)
C14	C15	C20	126.36(11)
C17	C16	C13	116.17(11)
C16	C17	C18	122.53(11)
C19	C18	C17	121.15(11)
C18	C19	C14	117.61(11)
N3	C20	C15	176.88(14)

Table S3.3 Torsion angles [°] for **3j**.

C13	N1	N2	C15	0.66(14)
C10	N1	N2	C15	176.74(11)
C6	C1	C2	C3	-0.75(19)
C7	C1	C2	C3	178.95(12)
C1	C2	C3	C4	0.09(19)
C2	C3	C4	C5	0.6(2)
C2	C3	C4	Cl1	-177.73(10)
C3	C4	C5	C6	-0.6(2)
Cl1	C4	C5	C6	177.73(11)
C2	C1	C6	C5	0.8(2)
C7	C1	C6	C5	-178.94(12)
C4	C5	C6	C1	-0.1(2)
C6	C1	C7	C12	128.86(13)

C2	C1	C7	C12	-50.83(16)
C6	C1	C7	C8	-107.53(14)
C2	C1	C7	C8	72.78(16)
C1	C7	C8	C9	-176.23(12)
C12	C7	C8	C9	-52.02(16)
C7	C8	C9	C10	57.10(17)
N2	N1	C10	C9	54.03(16)
C13	N1	C10	C9	-130.46(14)
N2	N1	C10	C11	-71.27(15)
C13	N1	C10	C11	104.24(14)
C8	C9	C10	N1	173.26(12)
C8	C9	C10	C11	-60.81(16)
N1	C10	C11	C12	-173.35(11)
C9	C10	C11	C12	60.29(15)
C1	C7	C12	C11	174.57(11)
C8	C7	C12	C11	50.71(16)
C10	C11	C12	C7	-55.18(17)
N2	N1	C13	C14	-0.62(14)
C10	N1	C13	C14	-176.47(11)
N2	N1	C13	C16	179.34(13)
C10	N1	C13	C16	3.5(2)
N1	C13	C14	C19	179.72(11)
C16	C13	C14	C19	-0.24(18)
N1	C13	C14	C15	0.31(13)
C16	C13	C14	C15	-179.65(11)
N1	N2	C15	C14	-0.44(14)
N1	N2	C15	C20	-179.29(11)
C19	C14	C15	N2	-179.19(13)
C13	C14	C15	N2	0.08(14)
C19	C14	C15	C20	-0.4(2)
C13	C14	C15	C20	178.86(12)
N1	C13	C16	C17	-179.63(13)
C14	C13	C16	C17	0.32(18)
C13	C16	C17	C18	-0.01(19)
C16	C17	C18	C19	-0.4(2)
C17	C18	C19	C14	0.47(18)
C13	C14	C19	C18	-0.16(17)
C15	C14	C19	C18	179.02(13)

Symmetry operations

1	'x, y, z'
2	'-x+1/2, y+1/2, -z+1/2'
3	'-x, -y, -z'
4	'x-1/2, -y-1/2, z-1/2'

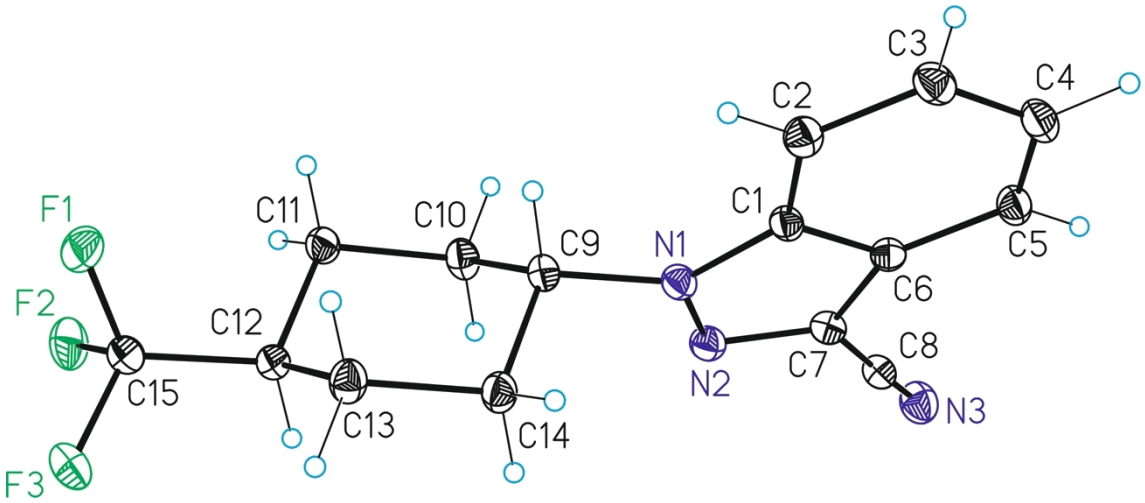

Figure S3.10 ORTEP diagram of **3i**.

Table S3.4 Crystal data and structure refinement for **3i**.

Identification code	xlyu-5-74-1
Empirical formula	C15 H14 F3 N3
Formula weight	293.29
Temperature	100(2)K
Wavelength	0.71073 Å
Crystal system	monoclinic
Space group	P 21
Unit cell dimensions	a = 5.49135(13)Å a= 90°.
	b = 12.1604(2)Å b = 99.903(2)°.
	c = 10.2334(2)Å g = 90°.
Volume	673.18(3) Å3
Z	2
Density (calculated)	1.447 Mg/m3
Absorption coefficient	0.117 mm-1
F(000)	304
Crystal size	0.300 x 0.200 x 0.150 mm3

Theta range for data collection 3.767 to 29.680°.
Index ranges -7<=h<=6,-16<=k<=16,-14<=l<=13
Reflections collected 16282
Independent reflections 3399[R(int) = 0.0207]
Completeness to theta =29.680° 93.0%
Absorption correction Multi-scan
Max. and min. transmission 1.00 and 0.48
Refinement method Full-matrix least-squares on F2
Data / restraints / parameters 3399/ 1/ 190
Goodness-of-fit on F2 1.063
Final R indices [I>2sigma(I)] R1 = 0.0249, wR2 = 0.0683
R indices (all data) R1 = 0.0255, wR2 = 0.0686
Flack parameter x =-0.15(11)
Largest diff. peak and hole 0.252 and -0.201 e.Å-3

Table S3.5 Bond lengths [Å] and angles [°] for **3i**.

Bond lengths----		
F1	C15	1.3510(17)
F2	C15	1.3416(17)
F3	C15	1.3542(16)
N1	N2	1.3480(17)
N1	C1	1.3742(17)
N1	C9	1.4689(18)
N2	C7	1.3348(19)
N3	C8	1.146(2)
C1	C2	1.401(2)
C1	C6	1.407(2)
C2	C3	1.382(2)
C2	H2	0.9500
C3	C4	1.417(2)
C3	H3	0.9500
C4	C5	1.381(2)
C4	H4	0.9500
C5	C6	1.4118(19)
C5	H5	0.9500
C6	C7	1.423(2)
C7	C8	1.435(2)
C9	C10	1.5250(19)

C9	C14	1.5289(18)
C9	H9	1.0000
C10	C11	1.5300(19)
C10	H10A	0.9900
C10	H10B	0.9900
C11	C12	1.5302(18)
C11	H11A	0.9900
C11	H11B	0.9900
C12	C15	1.5038(19)
C12	C13	1.5348(19)
C12	H12	1.0000
C13	C14	1.5321(19)
C13	H13A	0.9900
C13	H13B	0.9900
C14	H14A	0.9900
C14	H14B	0.9900

Angles----------

N2	N1	C1	111.96(12)
N2	N1	C9	120.56(11)
C1	N1	C9	127.35(13)
C7	N2	N1	105.61(12)
N1	C1	C2	130.89(13)
N1	C1	C6	106.85(12)
C2	C1	C6	122.21(12)
C3	C2	C1	116.58(14)
C3	C2	H2	121.7
C1	C2	H2	121.7
C2	C3	C4	121.98(14)
C2	C3	H3	119.0
C4	C3	H3	119.0
C5	C4	C3	121.40(14)
C5	C4	H4	119.3
C3	C4	H4	119.3
C4	C5	C6	117.39(14)
C4	C5	H5	121.3
C6	C5	H5	121.3
C1	C6	C5	120.44(13)
C1	C6	C7	103.45(12)

C5	C6	C7	136.06(14)
N2	C7	C6	112.12(12)
N2	C7	C8	119.68(13)
C6	C7	C8	128.06(13)
N3	C8	C7	178.37(16)
N1	C9	C10	110.33(11)
N1	C9	C14	111.77(11)
C10	C9	C14	111.30(11)
N1	C9	H9	107.8
C10	C9	H9	107.8
C14	C9	H9	107.8
C9	C10	C11	110.71(11)
C9	C10	H10A	109.5
C11	C10	H10A	109.5
C9	C10	H10B	109.5
C11	C10	H10B	109.5
H10A	C10	H10B	108.1
C10	C11	C12	109.84(11)
C10	C11	H11A	109.7
C12	C11	H11A	109.7
C10	C11	H11B	109.7
C12	C11	H11B	109.7
H11A	C11	H11B	108.2
C15	C12	C11	110.69(11)
C15	C12	C13	111.92(11)
C11	C12	C13	110.79(11)
C15	C12	H12	107.8
C11	C12	H12	107.8
C13	C12	H12	107.8
C14	C13	C12	110.38(11)
C14	C13	H13A	109.6
C12	C13	H13A	109.6
C14	C13	H13B	109.6
C12	C13	H13B	109.6
H13A	C13	H13B	108.1
C9	C14	C13	110.64(11)
C9	C14	H14A	109.5
C13	C14	H14A	109.5
C9	C14	H14B	109.5

C13	C14	H14B	109.5
H14A	C14	H14B	108.1
F2	C15	F1	106.31(11)
F2	C15	F3	106.05(12)
F1	C15	F3	105.64(11)
F2	C15	C12	112.60(11)
F1	C15	C12	113.21(12)
F3	C15	C12	112.44(11)

Table S3.6 Torsion angles [°] for **3i**.

C1	N1	N2	C7	0.27(14)
C9	N1	N2	C7	176.42(11)
N2	N1	C1	C2	177.00(13)
C9	N1	C1	C2	1.2(2)
N2	N1	C1	C6	-0.49(15)
C9	N1	C1	C6	-176.32(11)
N1	C1	C2	C3	-176.99(14)
C6	C1	C2	C3	0.16(19)
C1	C2	C3	C4	-0.9(2)
C2	C3	C4	C5	0.9(2)
C3	C4	C5	C6	-0.1(2)
N1	C1	C6	C5	178.36(12)
C2	C1	C6	C5	0.6(2)
N1	C1	C6	C7	0.48(14)
C2	C1	C6	C7	-177.28(12)
C4	C5	C6	C1	-0.6(2)
C4	C5	C6	C7	176.39(14)
N1	N2	C7	C6	0.06(14)
N1	N2	C7	C8	-176.00(12)
C1	C6	C7	N2	-0.34(15)
C5	C6	C7	N2	-177.72(15)
C1	C6	C7	C8	175.31(13)
C5	C6	C7	C8	-2.1(3)
N2	N1	C9	C10	-37.18(16)
C1	N1	C9	C10	138.33(14)
N2	N1	C9	C14	87.22(15)
C1	N1	C9	C14	-97.27(15)

N1	C9	C10	C11	-178.33(11)
C14	C9	C10	C11	56.99(15)
C9	C10	C11	C12	-57.61(15)
C10	C11	C12	C15	-177.08(12)
C10	C11	C12	C13	58.15(15)
C15	C12	C13	C14	178.33(12)
C11	C12	C13	C14	-57.60(15)
N1	C9	C14	C13	-179.96(11)
C10	C9	C14	C13	-56.10(15)
C12	C13	C14	C9	56.06(15)
C11	C12	C15	F2	57.85(15)
C13	C12	C15	F2	-178.03(11)
C11	C12	C15	F1	-62.79(15)
C13	C12	C15	F1	61.34(15)
C11	C12	C15	F3	177.58(11)
C13	C12	C15	F3	-58.30(15)

Symmetry operations

---

1 'x, y, z'

2 '-x, y+1/2, -z'

3.7.6 Representative NMR Spectra

^{1}H NMR of S1

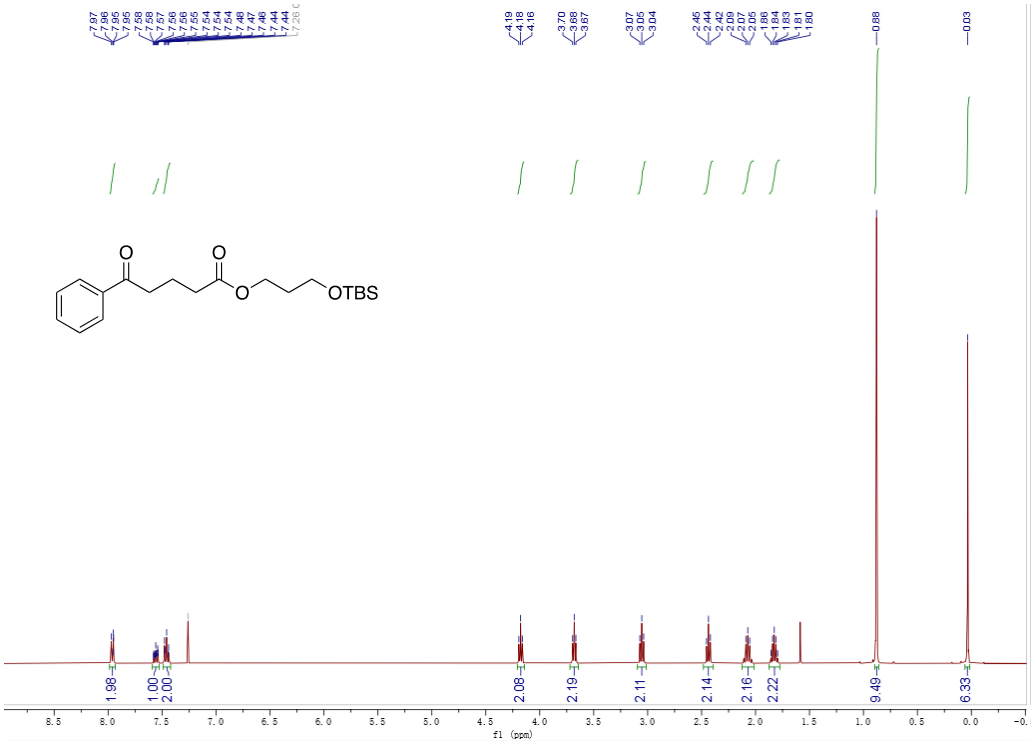

^{13}C NMR of S1

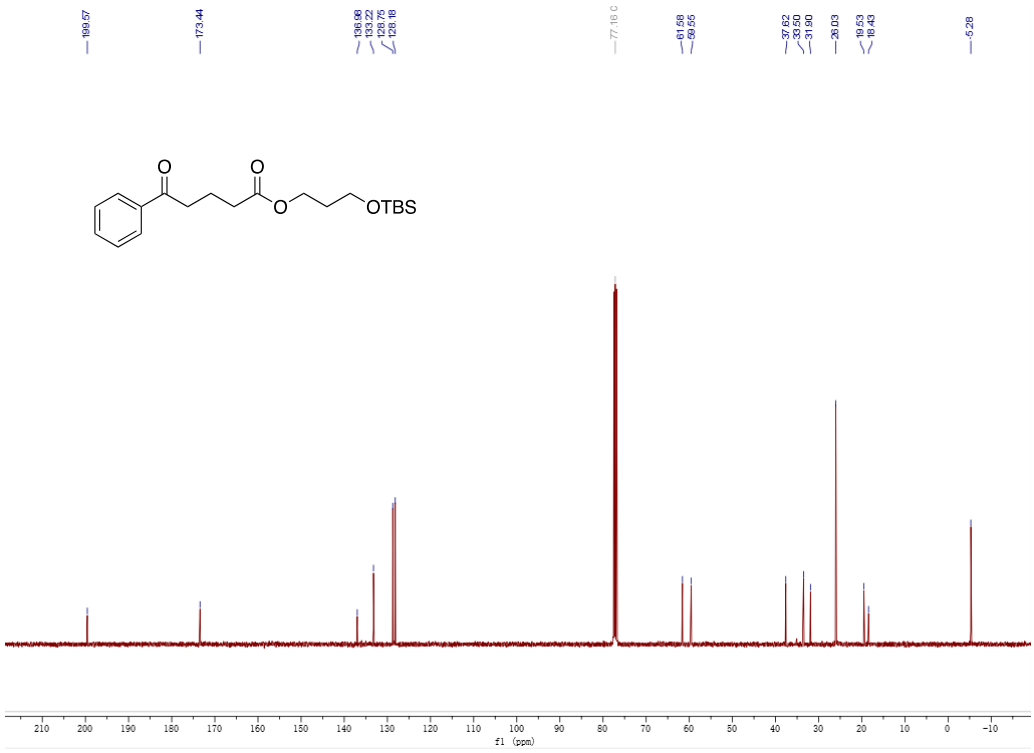

^{1}H NMR of **2a"**

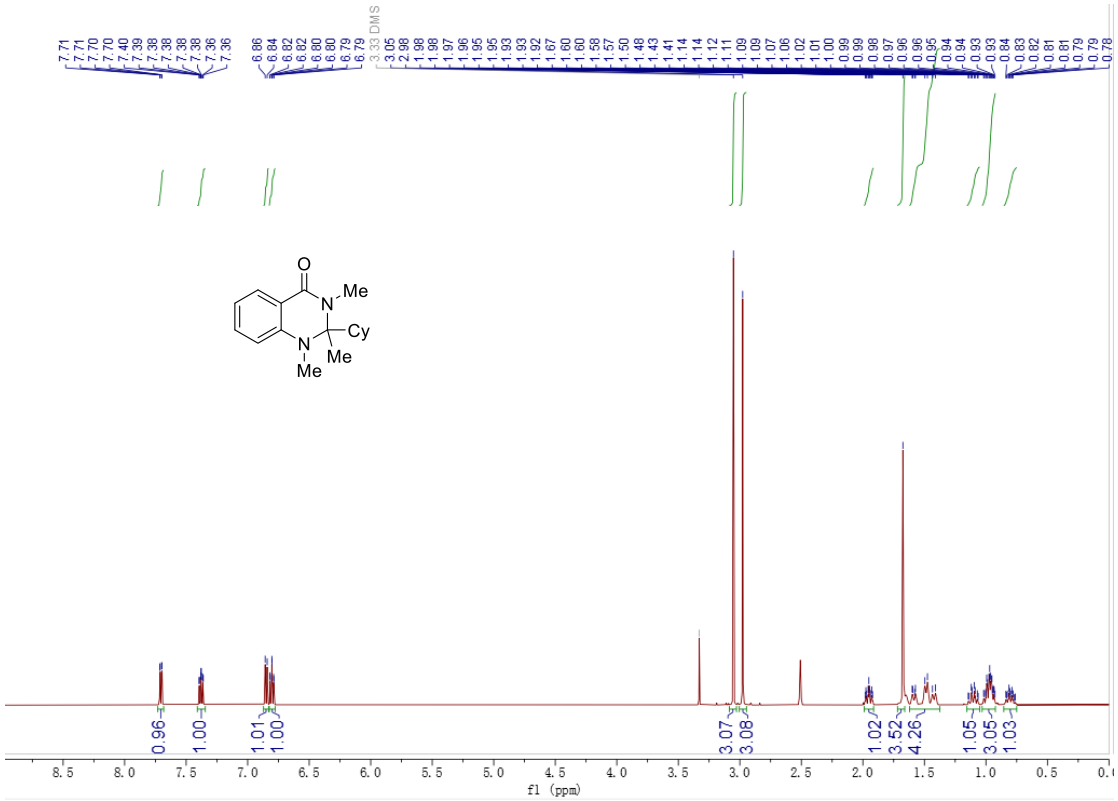

^{13}C NMR of **2a"**

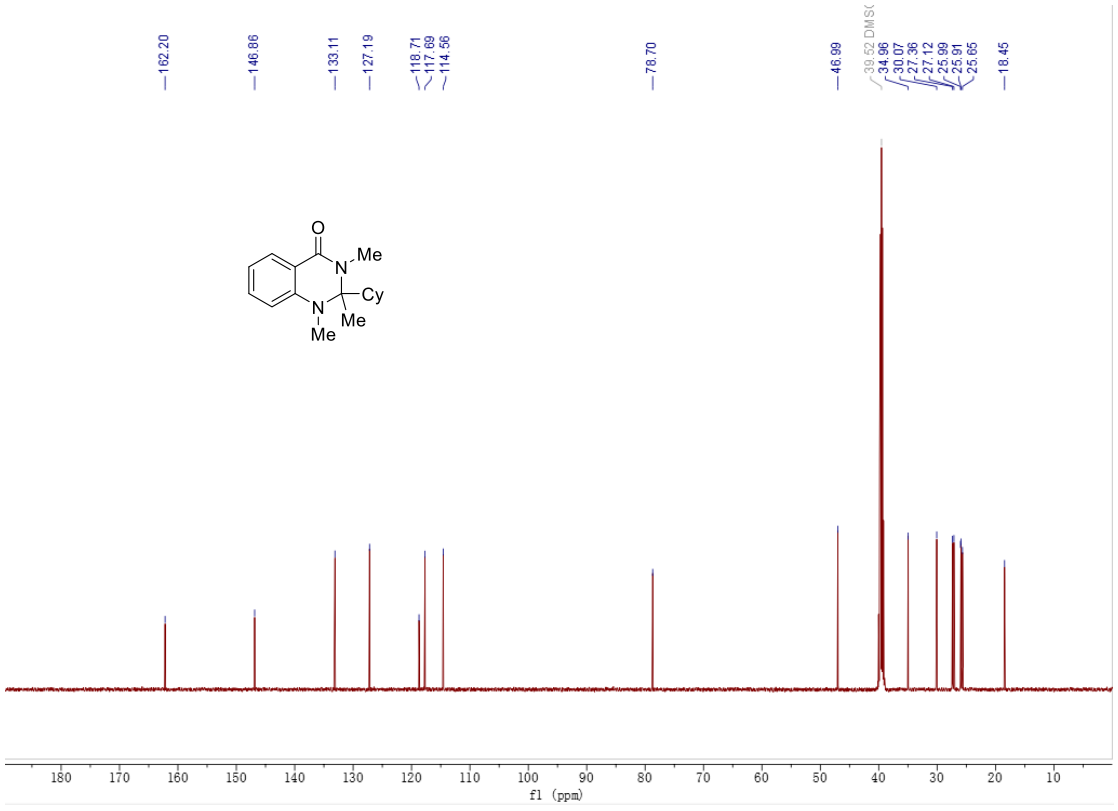

^{1}H NMR of **2s**

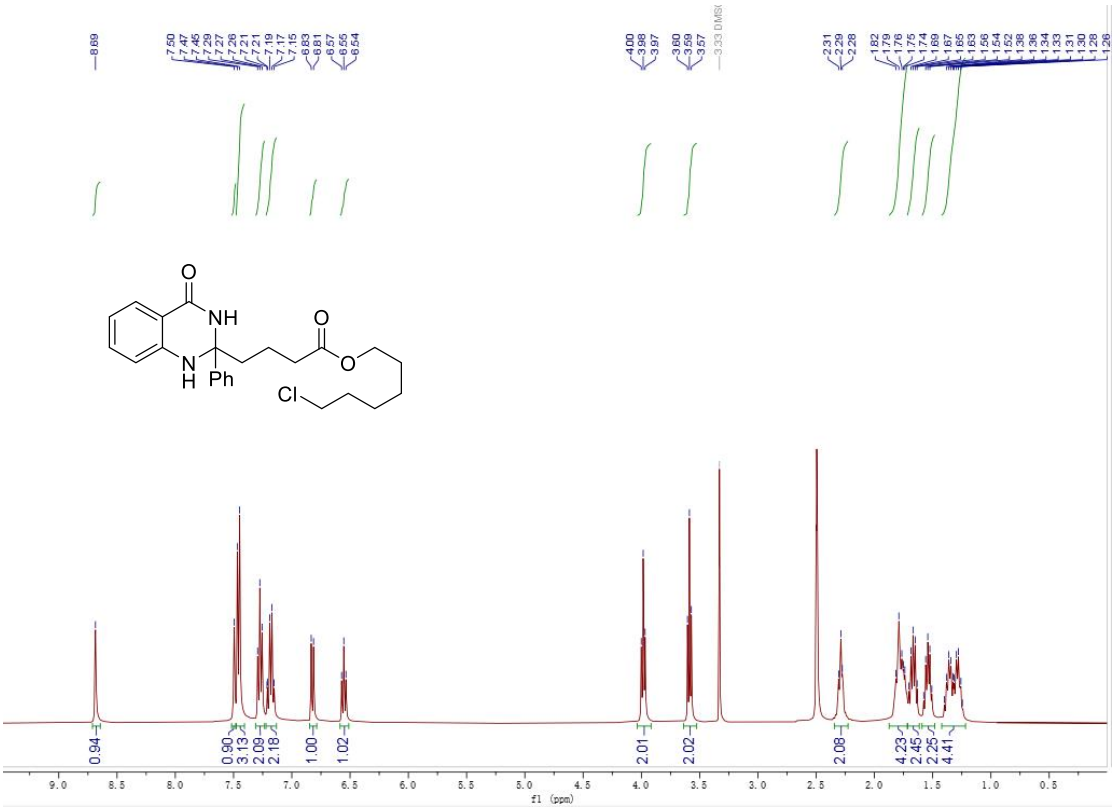

^{13}C NMR of **2s**

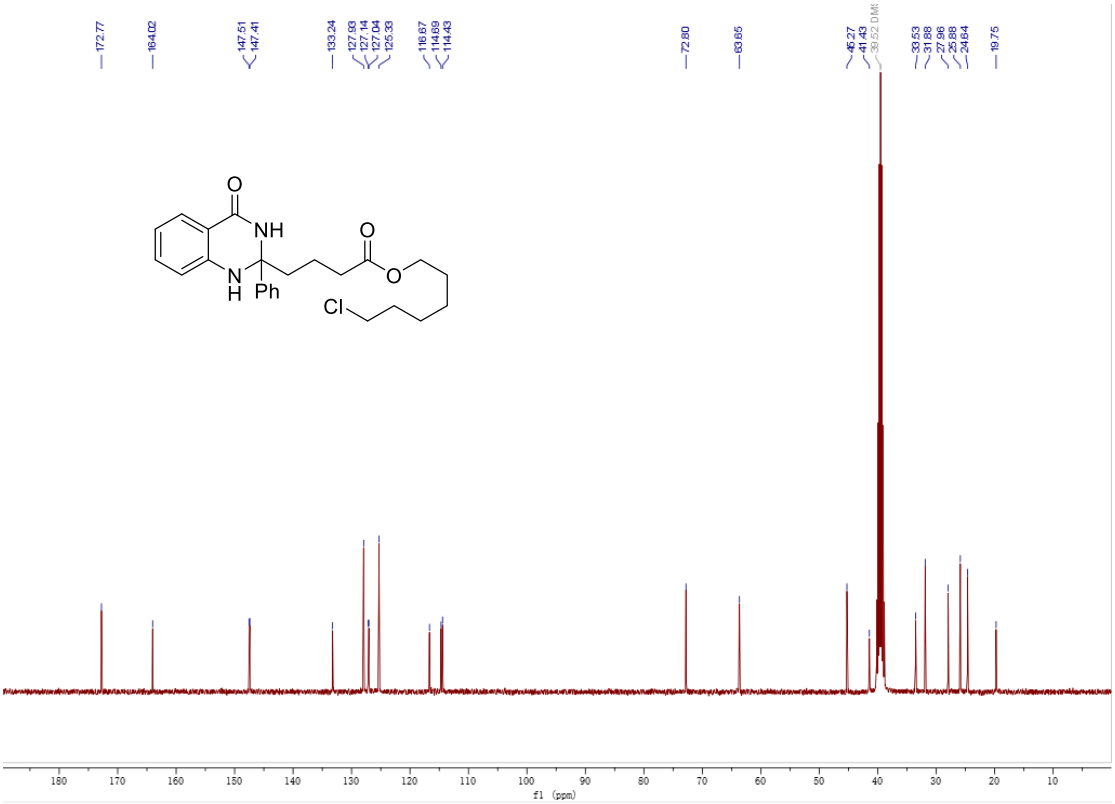

^{1}H NMR of **3i**

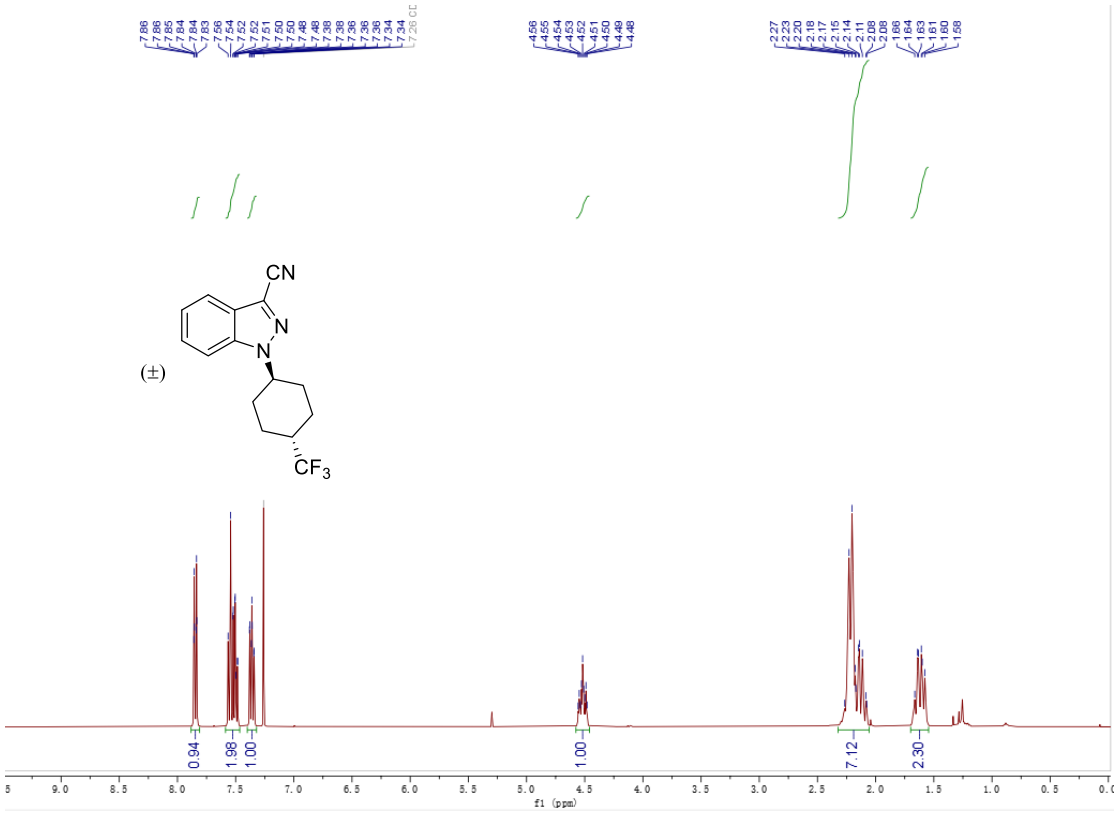

^{13}C NMR of **3i**

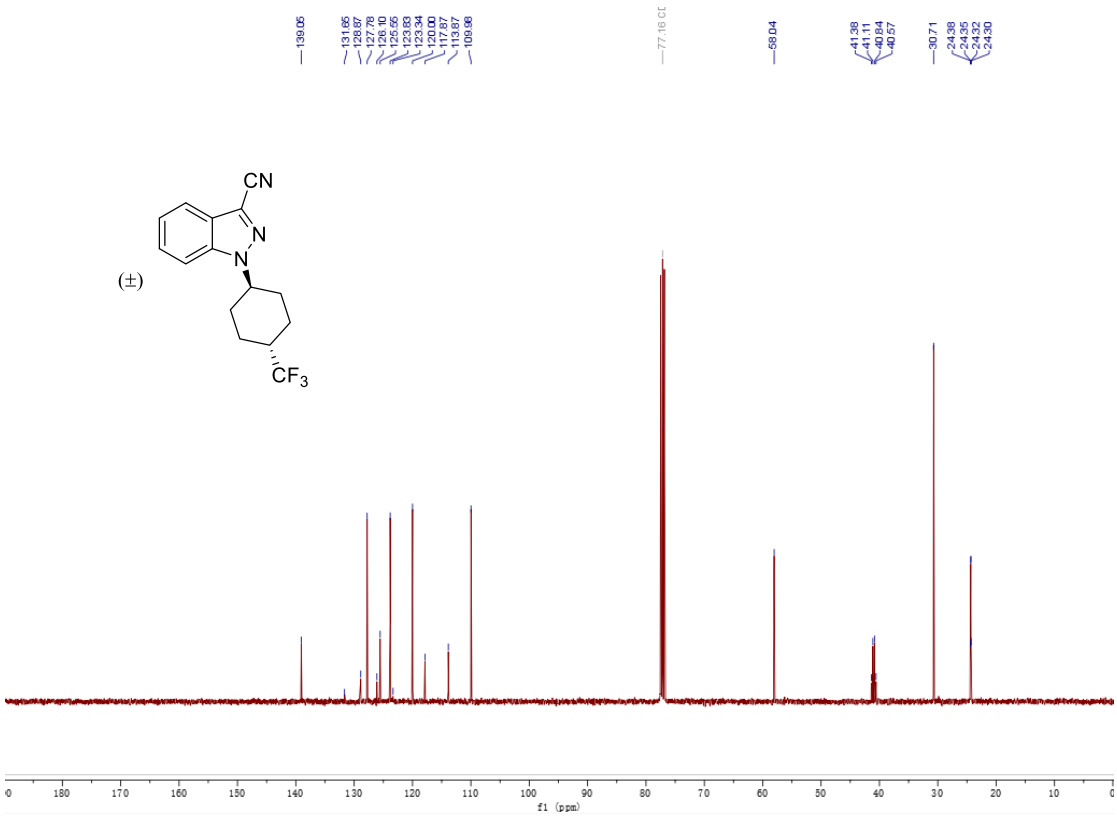

^{19}F NMR of **3i**

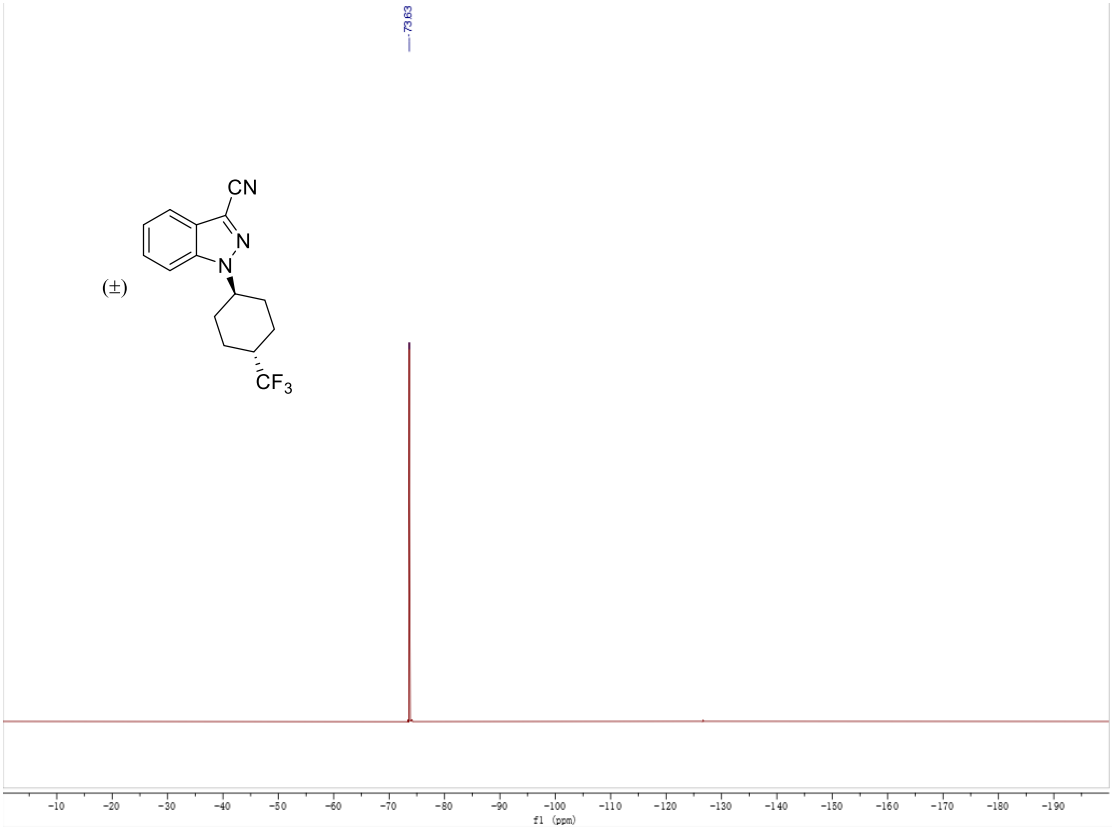
-73.63
CN
N
N
(±)
CF3
-10
-20
-30
-40
-50
-60
-70
-80
-90
-100
-110
-120
-130
-140
-150
-160
-170
-180
-190
f1 (ppm)

^{1}H NMR of **6f**

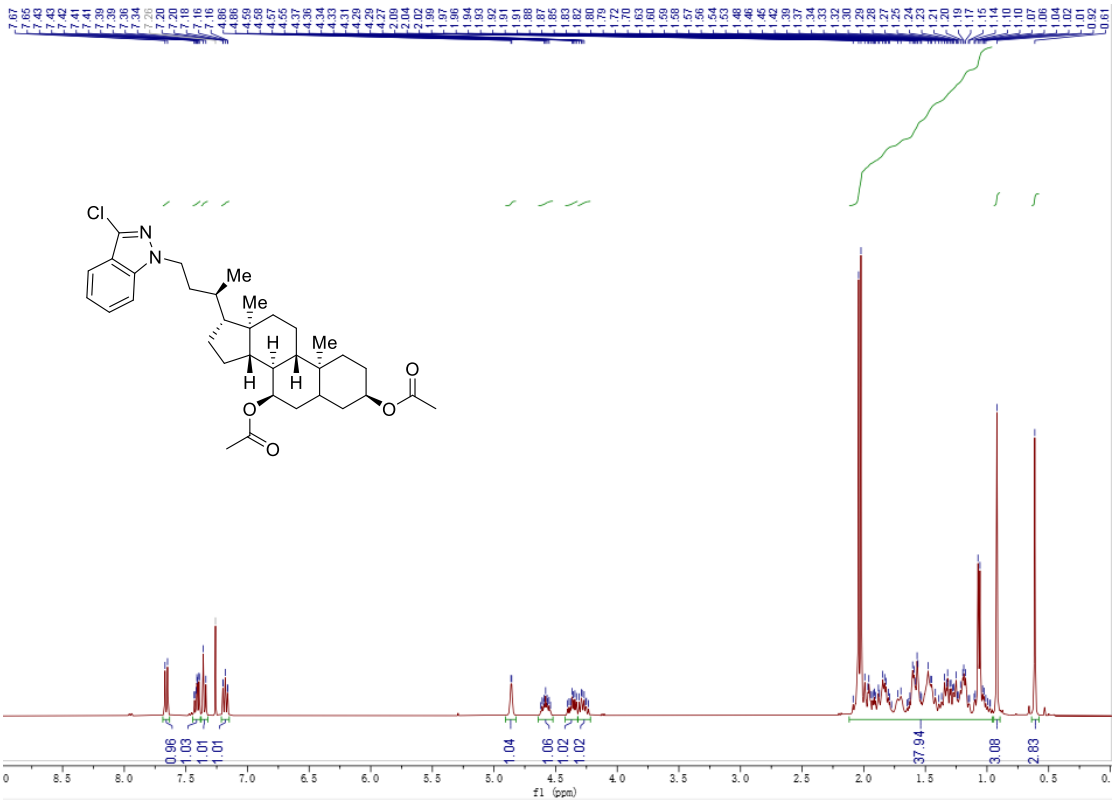

^{13}C NMR of **6f**

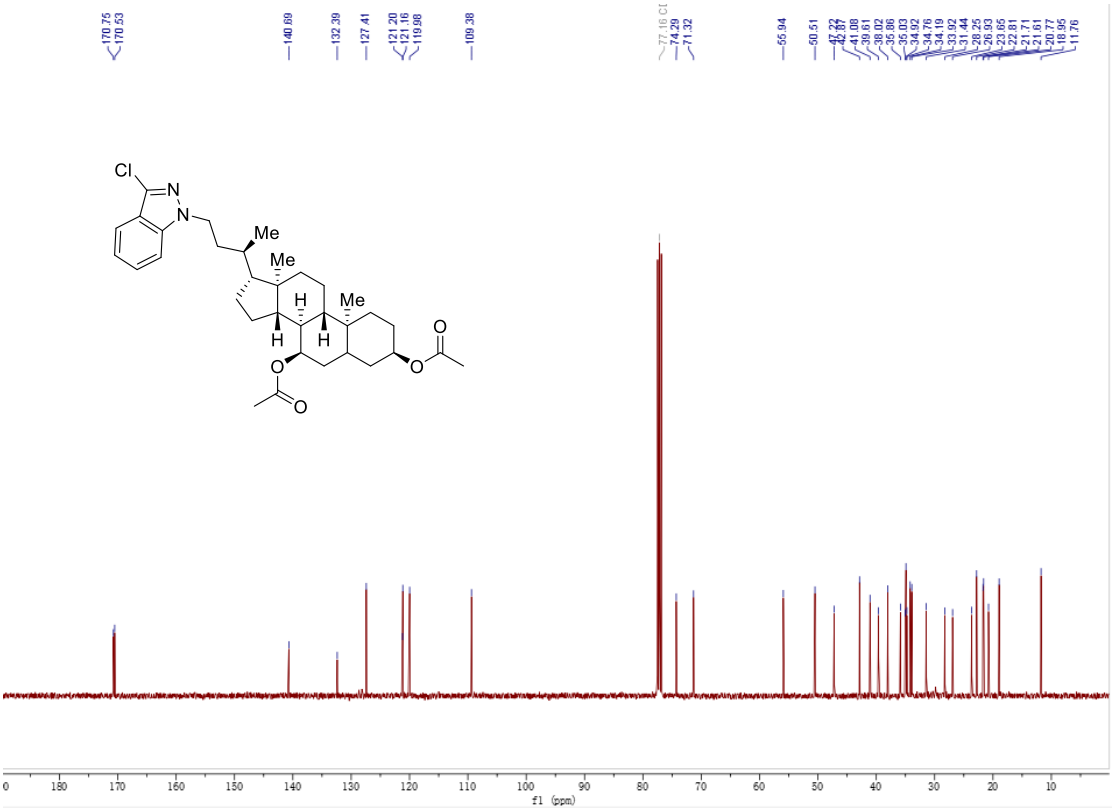

^{1}H NMR of **6g**

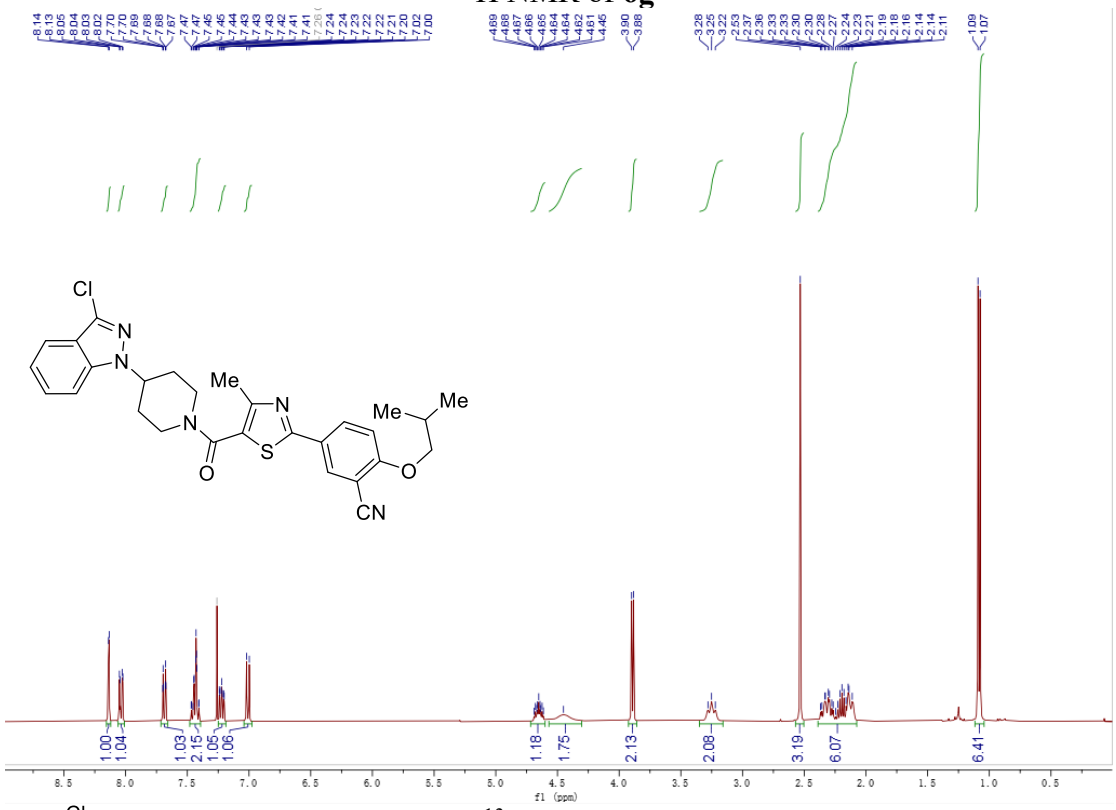

^{13}C NMR of **6g**

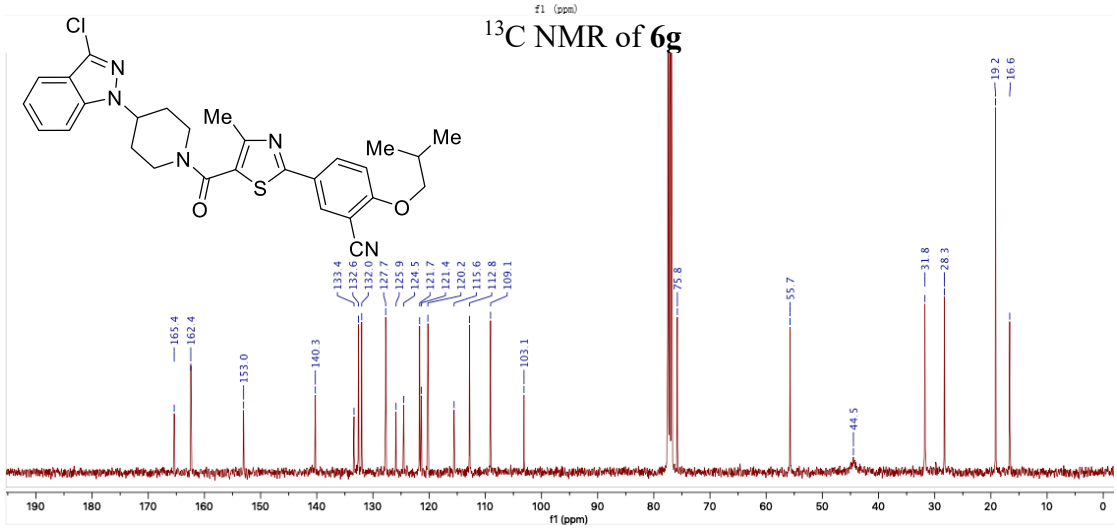

Chapter 4

Cu-Catalyzed C(sp^3) Amination of Unactivated Secondary Alkyl Iodides Promoted by Diaryliodonium Salts

4.1 Introduction

Nitrogen containing organic compounds such as aliphatic amines, amides, heterocyclic amines are pervasive in nature and pharmaceuticals (Scheme 4.1).[273] A large fraction of these molecules contains bonds between nitrogenated residues and saturated carbons, making the development of methods for sp^3 C–N bond construction desirable to both academia and industry.

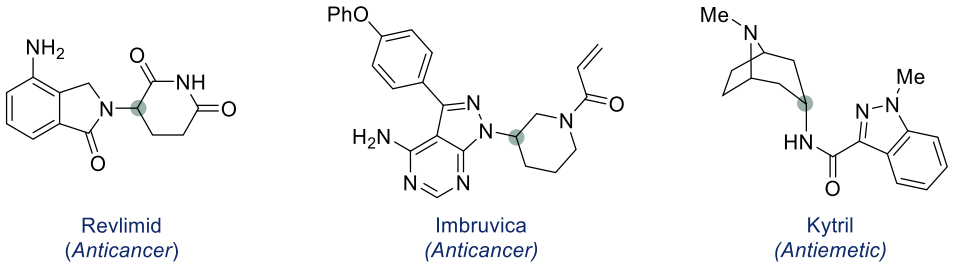

Scheme 4.1 Prevalence of C(sp^3)–N architectures.

Unlike the maturity acquired by Ullmann-type techniques, Chan-Lam couplings, and/or Buchwald-Hartwig amination reactions (Scheme 4.2, *left*), the means to enable metal-catalyzed sp^3 C–N bond formations is not as commonly practiced as one might initially anticipate (Scheme 4.2, *right*), with only limited presented examples.[274] Indeed, the synthesis of sp^3 C–N linkages currently relies on non-catalytic Curtius rearrangements, Mitsunobu reactions, and, in particular, reductive aminations or S_N2 reactions with alkyl (pseudo)halides. While the utilization of secondary alkyl halides is particularly problematic in the latter due to the competing E_2-type elimination,[275] the incorporation of heterocycles or amides is beyond reach in reductive aminations, thus reinforcing the need for new catalytic sp^3 C–N bond-forming strategies.

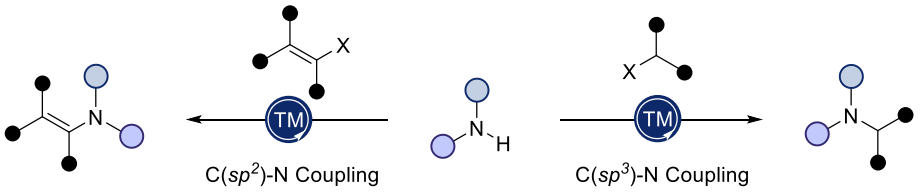

Scheme 4.2 Transition metal-catalyzed C–N bond cross-coupling reactions.

In this chapter, the development of a copper-catalyzed C(sp^3) amination of

[273] Ebenezer, O.; Jordaan, M. A.; Carena, G.; Bono, T.; Shapi, M.; Tuszynski, J. A. An Overview of the Biological Evaluation of Selected Nitrogen-Containing Heterocycle Medicinal Chemistry Compounds. *Int. J. Mol. Sci.* **2022**, *23*, 8117−8159.
[274] Peacock, D. M.; Roos, C. B.; Hartwig, J. F. Palladium-Catalyzed Cross Coupling of Secondary and Tertiary Alkyl Bromides with a Nitrogen Nucleophile. *ACS Cent. Sci.* **2016**, *2*, 647−652.
[275] March, J. *Advanced Organic Chemistry: Reactions, Mechanisms, and Structure;* Wiley: Hoboken, NJ, 1985.

unactivated secondary alkyl iodides methodology and the foundations on which this technique was building will be discussed.

4.1.1 Radical Philicity and Atom Transfer

4.1.1.1 Radical Stability and Radical Philicity

The thermodynamic stability of carbon-centered radicals may be defined in quantitative terms using the hydrogen transfer reaction shown in Scheme 4.3 (a).[276] The reaction enthalpy of this process is commonly referred to as the radical stabilization energy (RSE) of the newly formed radical relative to the unsubstituted methyl radical. Taking isopropyl radical as example (Scheme, *bottom*), a RSE value of -26.8 kJ/mol is derived in this way. It should be noted here that this reaction energy is exactly identical to the difference between the C–H bond dissociation energy in methyl of BDE (CH_3–H) = 439.3 kJ/mol, and that of the central C–H bond in propane with BDE [$(CH_3)_2CH$–H] = 412.5 kJ/mol. Similarly, the stabilities of heteroatom-centered radicals are similarly defined as expressed for carbon-centered radicals in Scheme 4.3 (a), and defining equations for oxygen-, sulfur-, and nitrogen-centered radicals are given in Scheme 4.3 (b). (c) and (d).

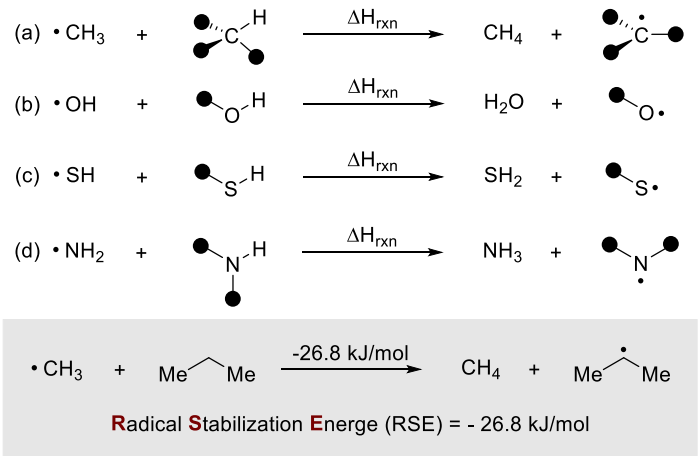

Scheme 4.3 Definition of radical stabilization energy.

Some RSE values of oxygen-, nitrogen-, carbon-, and sulfur- centered radicals are illustrated in Scheme 4.4, which leads to the key factors that affect radical stability: (1) radicals are stabilized by hyperconjugation. (2) radicals are stabilized by resonance. (3) adjacent atoms with lone pairs or empty orbitals increase the stability. (4) across the periodic table, the more electronegativity the less stability of the free radical; down the

[276] (a) Hioe, J.; Zipse, H.; Radical Stability and Its Role in Synthesis and Catalysis. *Org. Biomol. Chem*. **2010**, *8*, 3609–3617 (b) Hioe, J.; Šakić, D.; Vrček, V.; Zipse, H. The Stability of Nitrogen-Centered Radicals. *Org. Biomol. Chem*. **2015**, *13*, 157–169.

periodic table, the largest atom the more free radical stability. (5) the stability of the free radical decreases as the orbital is held closer to the nucleus.

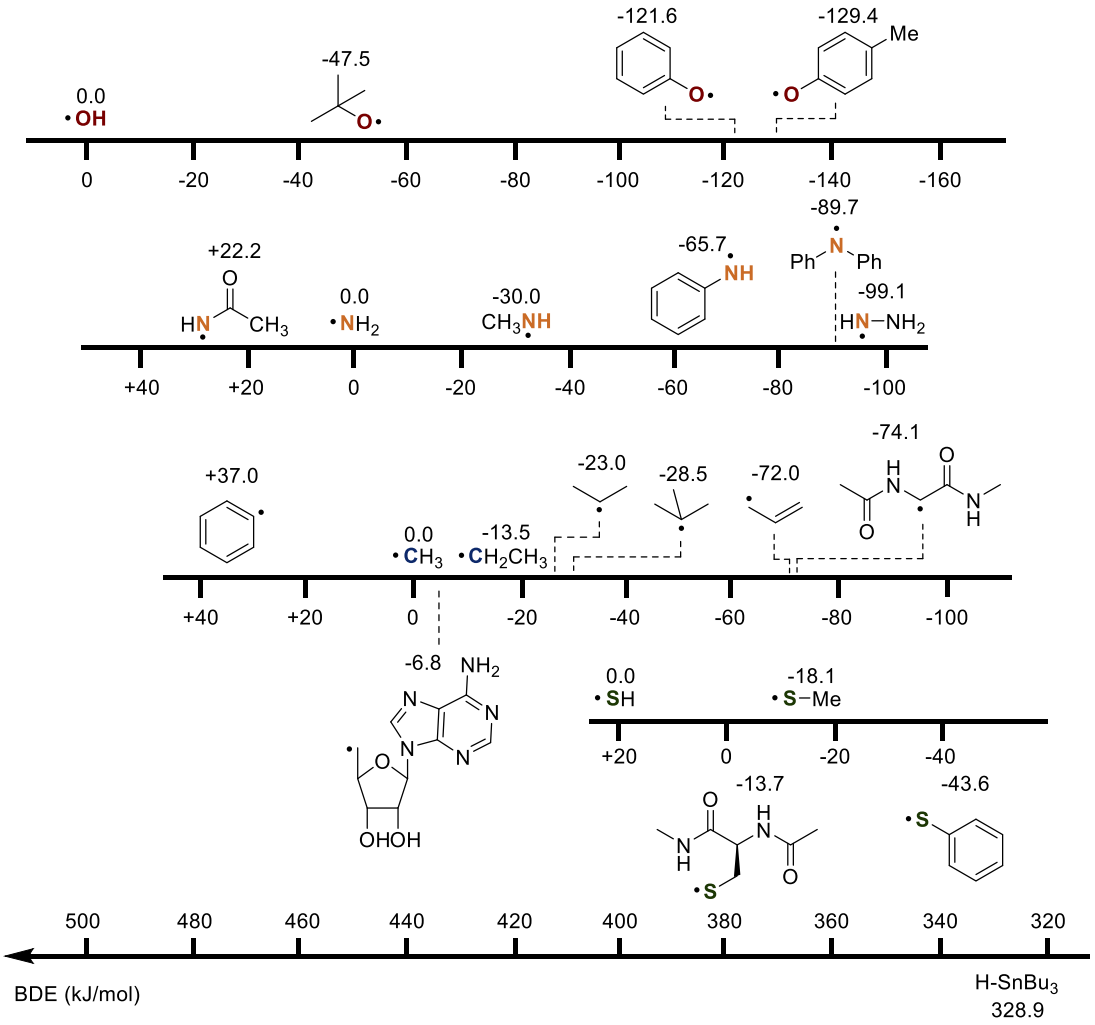

Scheme 4.4 RSE data for selected O-, N-, C-, and S-centered radicals together with BDE data for hydrogen donors $HSnBu_3$.

Some radical species such as galvinoxyl(2,6-di-tert-butyl-a-(3,5-di-tert-butyl-4-oxo-2,5-cyclohexadiene-1-ylidene)-p-tolyloxy) and TEMPO (2,2,6,6-tetramethylpiperidine-1-oxyl) have rather long lifetimes, which are considered as persistent radicals (Scheme 4.5). While most radical species have a lifetime of less than 10^{-3} s due to the high self-reaction rate, they behave in analogy to the methyl radical and belong to transient species. If the two radicals feature significantly different self-reaction rate constants, high cross-coupling selectivity can be achieved — a kinetic phenomenon known as persistent radical effect (PRE).[277] On the other hand, transition-metal complex can be viewed as persistent radicals and therefore, they are able to

[277] Leifert, D.; Studer, A. The Persistent Radical Effect in Organic Synthesis. *Angew. Chem. Int. Ed.* **2020**, *59*, 74–108.

selectively react with transient radicals, obeying the principle of the persistent radical effect. Additionally, the trapping of the transient radical can occur at the ligand or the metal center of the longer-lived transition-metal complex (Scheme 4.6). It is noteworthy to mention it is not necessary for one of the two radicals involved to be a persistent species in order to achieve high cross-coupling selectivity.

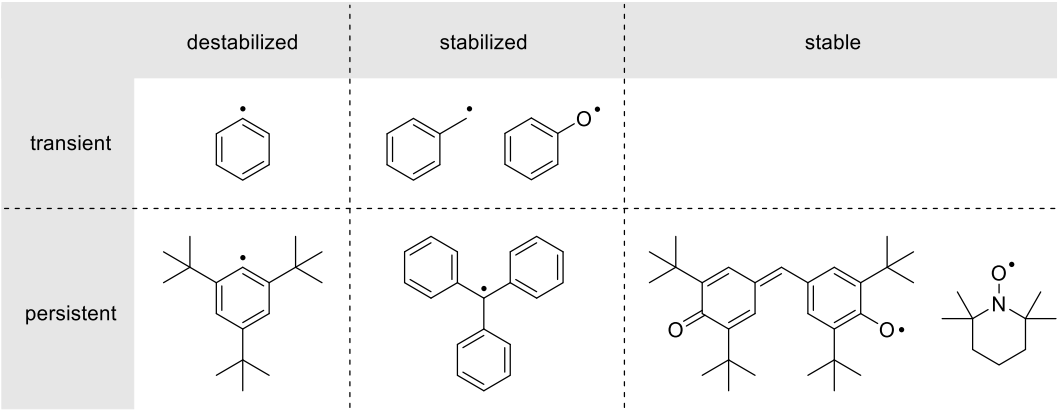

Scheme 4.5 Selected radicals and thermodynamic and kinetic categorization based on the definitions of Griller and Ingold.[278]

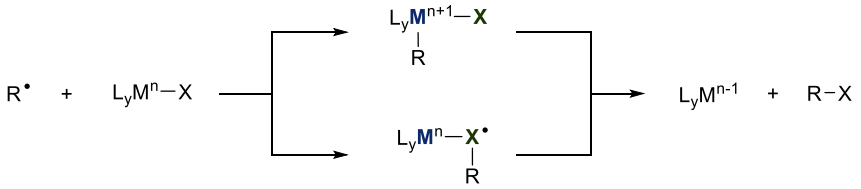

Scheme 4.6 Two modes of radical-metal crossover reactions.

Although they should technically be considered inorganic in nature, heteroatom-centered radicals have an important role in many organic transformations. The philicity of a heteroatom centered radical can be predicted by comparing the electronegativity of the heteroatom to that of carbon (Scheme 4.7, *bottom right*).

Among all the radical species, carbon-centered radicals are the most common type of radical intermediates in organic synthesis. Alkyl radicals are stabilized by hyperconjugative donation of additional alkyl groups, the more appended alkyl groups the greater stability and better nucleophilicity of the carbon-centered radicals. Carbon-centered radicals adjacent to heteroatoms that possess a nonbonding electron pair, such as oxygen in the hydroxymethyl radical (Scheme 4.7, *left*), are stabilized through resonance donation from the lone pair on the heteroatom, resulting in a raised SOMO with enhanced nucleophilicity. Alternatively, carbon-centered radicals adjacent to groups with π^* orbitals or empty *p* orbitals, such as boron in boryl methyl radical, are stabilized through unpaired electron resonance delocalization to vacant orbitals, thus

[278] Griller, D.; Ingold, K. U. Persistent Carbon-Centered Radicals. *Acc. Chem. Res.* **1976**, *9*, 13–19.

resulting in SOMO lowering process but with a loss of nucleophilicity.

Hybrid orbitals with a greater amount of *s* character form stronger bonds than those with less *s* character, and the energetic cost to break a bond to an *sp*-hybridized or sp^2-hybridized carbon atom is higher than it would be for the corresponding sp^3 carbon. Radicals in which the SOMO is an sp^n hybrid orbital are generally higher in energy and less stable than alkyl radicals (for which the SOMO is an unhybridized *p* orbital). Aryl radicals possess a SOMO that lies perpendicular to the π system that makes up the aromatic ring (Scheme 4.7, *top right*). The 90° dihedral angle between the SOMO and the π system results in minimal interaction between the two, and, thus, substitution on the aromatic ring often has little effect on the philicity of the resulting radical. Taken together, sp^n hybridized radicals are more likely to show a mixture of nucleophilic and electrophilic behavior.[279]

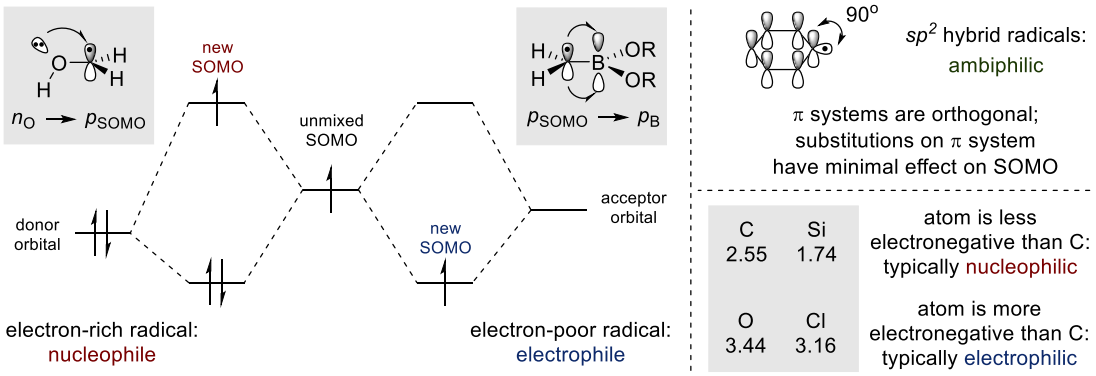

Scheme 4.7 Radical philicity.

4.1.1.2 Hydrogen Atom Transfer (HAT)

Hydrogen atom transfer (HAT) is defined as the concerted transfer of a proton and an electron from one group to another in a single kinetic step (Scheme 4.8, *top*).[280] Since R–H bonds are ubiquitous in organic substrates, the direct activation of R–H bonds via HAT would offer an array of new approaches to enable straightforward functionalization of R–H bonds without the need for pre-functionalization or installation of a directing group. It is well known that electrophilic alkoxy radicals will abstract hydrogen from electron-rich C–H bonds faster than from electron-deficient substrates with comparable C–H bond energies. Indeed, catalysts of a particular philicity can be used to enable site selective HAT, a concept known as polarity reversal

[279] Parsaee, F.; Senarathna, M. C.; Kannangara, P. B.; Alexander, S. N.; E. Arche P. D.; Welin, E. R. Radical Philicity and its Role in Selective Organic Transformation. *Nat. Rev. Chem.* **2021**, *5*, 486–499.
[280] Darcy, J. W.; Koronkiewicz, B.; Parada, G. A.; Mayer, J. M. A Continuum of Proton-Coupled Electron Transfer Reactivity. *Acc. Chem. Res.* **2018**, *51*, 2391–2399.

catalysis (PRC), as described by Roberts and co-workers.[281]

A recent example for PRC catalysis involving combinations of different H-atom donors from Studer and co-workers is shown in Scheme 4.8.[282] The transformation involves the reaction of cyclohexadiene **4.8b** acting not only as an organic H-atom donor, but also as a source of aminyl radicals. The reaction is initiated by 0.5 equivalent of DTBP in benzene solution, but proceeds significantly better in the presence of 20 mol% of thiophenol (HSPh, **4.8e**). While the direct HAT from **4.8b** by intermediate **4.8i** is typically sluggish, nucleophilic radical **4.8i** could be terminated by thiophenol to generate an electrophilic radial **4.8j**, which could further react with **4.8b** to release nucleophilic radical **4.8g**. The art in designing and optimizing PRC reactions is thus connected to finding a thiol whose BDE (S–H) is located in-between the C–H bond cleavage and that of the new C–H bond being made. Noted that except bond dissociation energy and radical philicity, other factors such as steric effect and medium effect could also make a difference in HAT process,[283] which will not be explained in detail due to the less relevant to this thesis.

[281] (a) Paul, V.; Roberts, B. P. Polarity Reversal Catalysis of Hydrogen Atom Abstraction Reactions. *J. Chem. Soc. Chem. Commun*. **1987**, *1987*, 1322–1324. (b) Roberts, B. P. Polarity-Reversal Catalysis of Hydrogen-Atom Abstraction Reactions: Concepts and Applications in Organic Chemistry. *Chem. Soc. Rev*. **1999**, *28*, 25–35.

[282] Guin, J.; Mück-Lichtenfeld, C.; Grimme, S.; Studer, A. Radical Transfer Hydroamination with Aminated Cyclohexadienes Using Polarity Reversal Catalysis: Scope and Limitations. *J. Am. Chem. Soc*. **2007**, *129*, 4498–4503.

[283] (a) Sarkar, S.; Cheung, K. P. S.; Gevorgyan, V. C–H Functionalization Reactions Enabled by Hydrogen Atom Transfer to Carbon-Centered Radicals. *Chem. Sci*. **2020**, *11*, 12974–12993. (b) Capaldo, L.; Ravelli, D. Hydrogen Atom Transfer (HAT): A Versatile Strategy for Substrate Activation in Photocatalyzed Organic Synthesis. *Eur. J. Org. Chem*. **2017**, 2056–2071.

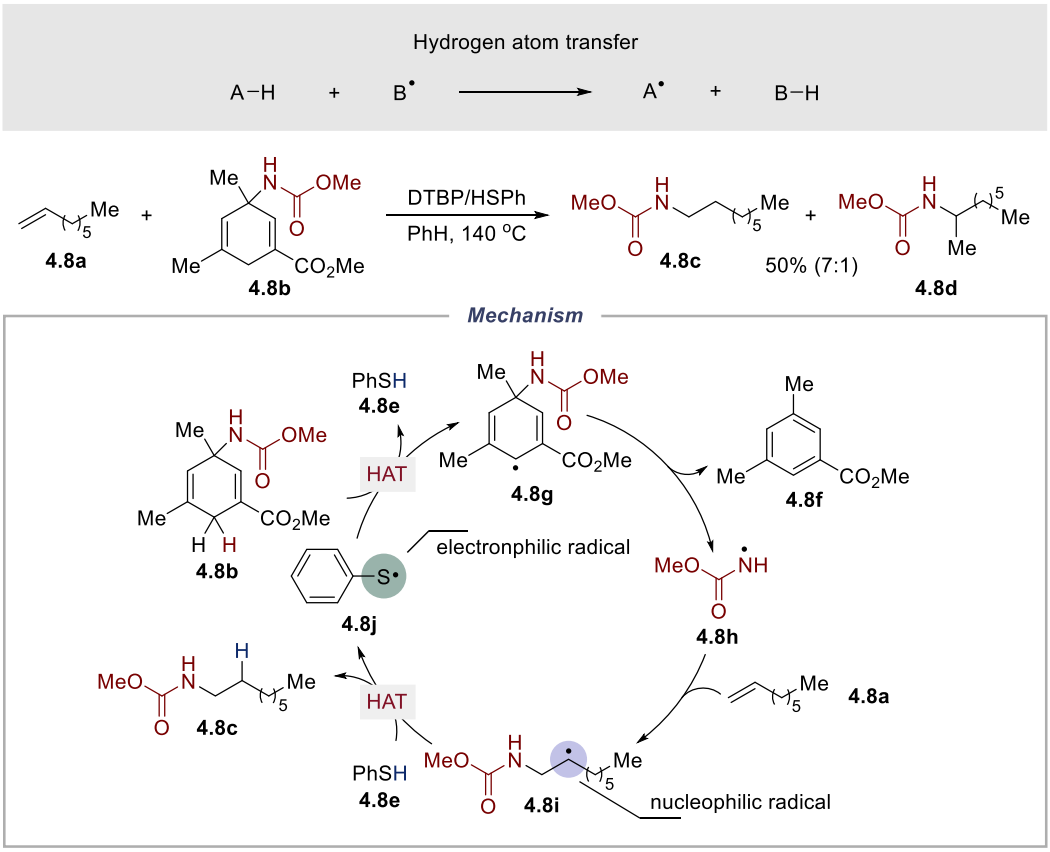

Scheme 4.8 Hydrogen atom transfer.

4.1.1.3 Halogen Atom Transfer (XAT)

Halogen atom transfer belongs to the class of "atom transfer" reactions, involving the direct homolytic abstraction of the halogen atom by an appropriate radical "abstractor", such as the archetypical tin/silicon species.[284] As shown in Scheme 4.9, several factors were found to affect the outcome of the XAT process. For these processes to be exergonic, the Y–halogen bond needs to be stronger than the C–halogen bond in the starting materials (i.e., BDEX–Y > BDER–X). This means that the relative rates for halogen abstractions follow the strength of the C–halogen bonds, with the general trend being iodides > bromides > chlorides. The stability of the ensuing carbon-centered radical is also important in facilitating XAT and this results in the general trend benzylic > tertiary > secondary > primary > phenyl. Noted that although in the case of systems where the product's Y–halogen bond has a similar strength with the substrate's R–halogen bond, the abstraction could still occur if there is a subsequent fast and irreversible reaction taking place.

Contrary to HAT processes where strongly electrophilic radicals (e.g., ^{t}BuO•) are

[284] Juliá, F.; Constantin, T.; Leonori, D. Applications of Halogen-Atom Transfer (XAT) for the Generation of Carbon Radicals in Synthetic Photochemistry and Photocatalysis. *Chem. Rev*. **2022**, *122*, 2292−2352.

usually employed, XAT reactions requires the nucleophilicity of Y•, due to the partial positive charge accumulation on the halogen-abstracting atom Y. On the other hand, electronic properties of the halogen-atom donor I are also important for the modulation of XAT reactivity with electrophilic R increasing the process. As evidence of how inductive effects accurate the XAT reaction, pioneering work from Danen's on XAT reactions promoted by phenyl radical has shown an electron withdrawing carboxylic acid group accelerated the process (Scheme 4.10).[285]

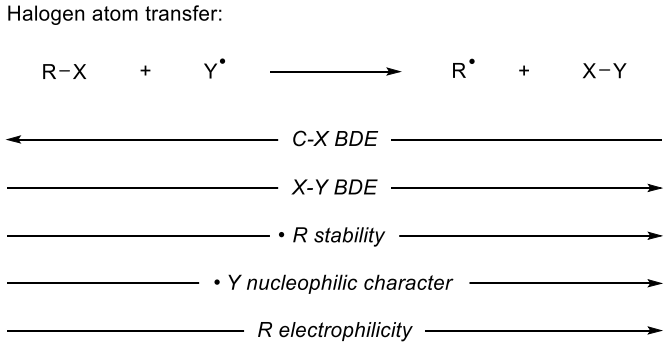

Scheme 4.9 Halogen atom transfer.

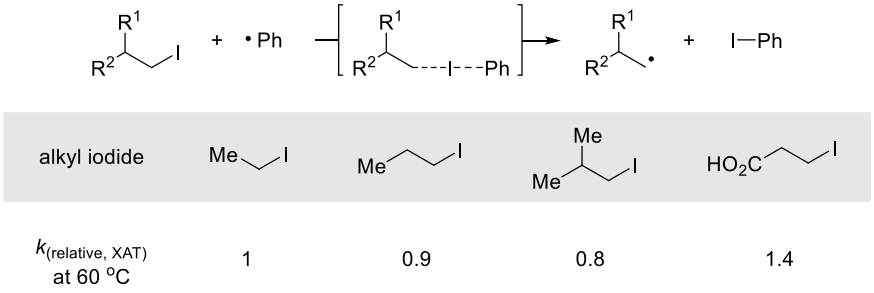

Scheme 4.10 Modulation of XAT by inductive and steric effects.

The used of organotin reagents for the conversion of alkyl/aryl halides into corresponding radicals has a deep impact in synthetic radical chemistry since Menapae's introduction in 1963.[286] The majority of tin radical chemistry is performed using tin hydrides through the thermal decomposition of AIBN as the radical chain initiation step. The relative weak Sn–H bond (BED ≈ 64 kcal/mol) compared to the Sn–Cl (BDE ≈ 97 kcal/mol) provides additional thermodynamic driving force for the entire transformation. As an example showcasing the utility of these processes is the total synthesis of (±)-hirsutene by Curran (Scheme 4.11), where a Bu_3SnH-mediated radical

[285] Danen, W. C.; Winter, R. L. Halogen Abstraction Studies. II. Free-Radical Abstraction of Iodine from Aliphatic Oodides. Evidence to Support Anchimeric Assistance by Neighboring Halogen in Homolytic Reactions. *J. Am. Chem. Soc*. **1971**, *93*, 716−720.
[286] Kuivila, H. G.; Menapace, L. W. Reduction of Alkyl Halides by Organotin Hydrides. *J. Org. Chem*. **1963**, *28*, 2165−2167.

cascade was used to convert **4.11a** to **4.11b**.[287] The reaction is initiated by the thermal decomposition of AIBN releasing alkyl radical **4.11e**, followed by a HAT process with Bu_3SnH to generate the Bu_3Sn•. Termination is realized by a HAT step between a vinyl radical **4.11d** and the Bu_3SnH, which is a mechanistic requirement to regenerate the chain carrier Bu_3Sn•.

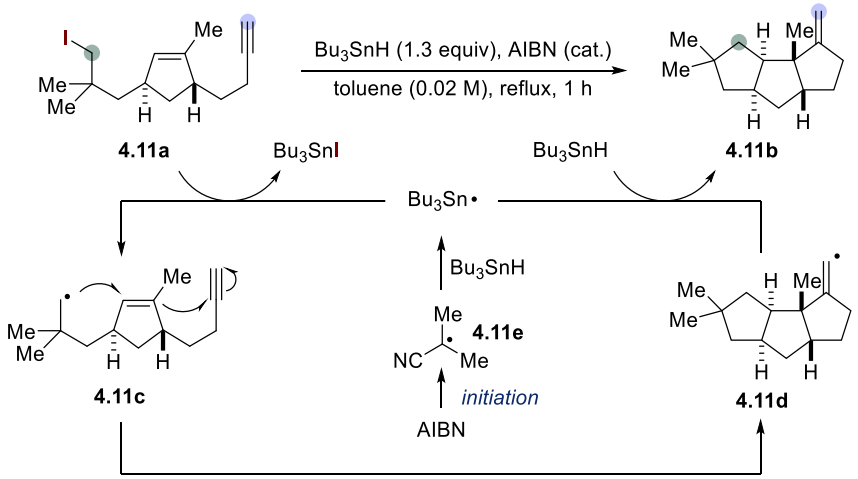

Scheme 4.11 Tin-mediated thermal reductive cascade in curran's total synthesis of (±)-hirsutene.

Despite being powerful and versatile XAT mediators, organotin species suffer from severe drawbacks associated with their toxicity and difficulty of disposal. In this regard, silicon-centered radicals especially supersilane (TTMSS) derived radical have been established as potent XAT mediators. Mechanistically, it is important to note that the superior XAT reactivity of silicon radicals does not always translate into superior synthetic versatility. As an example, trialkyl silanes are poor reductants in radical chemistry because, despite their corresponding silicon radicals (e.g., Et_3Si•) being the most powerful XAT promoters, their Si–H bonds are too strong to sustain radical-chain propagation (Scheme 4.12).

silane	X−H BDE (kcal/mol)	silane	X−H BDE (kcal/mol)
H_3Si—H	91.7	Me_3Si—H	94.7
Et_3Si—H	94.6	$(Me_3Si)_3Si$—H	83.7
$(MeS)_3Si$—H	87.0	Bu_3Sn—H	78.0

Scheme 4.12 BDEs of various Si−H and Sn−H bond.

Gaunt and co-workers recently employed the direct irradiation of TTMSS with

[287] (a) Curran, D. P.; Rakiewicz, D. M. Tandem Radical Approach to Linear Condensed Cyclopentanoids. Total Synthesis of (±)-Hirsutene. *J. Am. Chem. Soc.* **1985**, *107*, 1448−1449. (b) Curranl, D. P.; Rakiewicz, D. M. Radical-Initiated Polyolefinic Cyclizations in Linear Triquinane Synthesis. Model Studies and Total Synthesis of (±)-Hirsutene. *Tetrahedron* **1985**, *41*, 3943−3958.

blue LEDs to achieve the three-component coupling between alkyl iodides, aldehydes, and secondary amines (Scheme 4.13).[288] This reaction is initiated by the generation of silicon-centered radical **4.13e**, followed by a XAT step with alkyl iodide **4.13a** to provide the corresponding alkyl radical **4.13f**. In the meanwhile, aldehyde **4.13b** and amine **4.13c** undergo condensation to the iminium ion **4.13h**, which would be attacked by carbon-centered radical **4.13f** to furnish aminium radical **4.13i**. The radical addition might be reversible, but the subsequent fast and irreversible HAT between **4.13i** and TTMSS process would drive the product formation and chain propagation forwards.

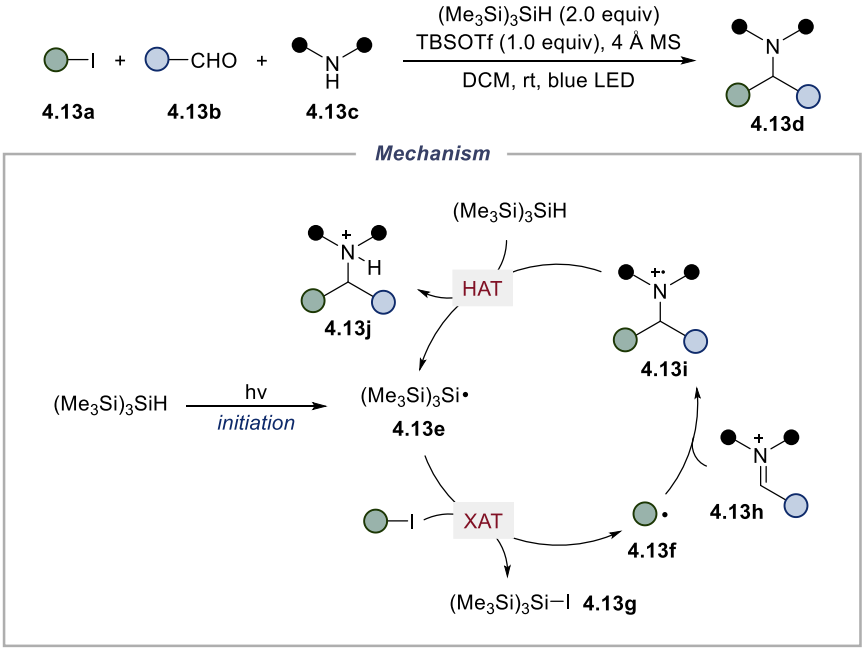

Scheme 4.13 Visible light-mediated three-component reactions of alkyl iodides for the synthesis of tertiary amines.

The conversion of amines into the corresponding *α*-aminoalkyl radicals has been widely investigated to accomplish *α*-*N* C(sp^3)–H functionalization in photochemistry and photoredox catalysis (Scheme 4.14, *top*).[289] Recently, Leonori and co-workers have demonstrated *α*-aminoalkyl radicals to be competent XAT reagents, and the reversible halogen abstraction is driven by the irreversible collapse of the *α*-haloamine into the corresponding iminium ion (Scheme 4.14, *bottom*).[290] Radicals derived from Et_3N (generated by HAT using the *tert*-butoxy radical) undergoes fast XAT with Cy–I

[288] Kumar, R.; Flodén, N. J.; Whitehurst, W.G.; Gaunt, M. J. A General Carbonyl Alkylative Amination for Tertiary Amine Synthesis. *Nature* **2020**, *581*, 415–420.
[289] Beatty, J. W.; Stephenson, C. R. Amine Functionalization via Oxidative Photoredox Catalysis: Methodology Development and Complex Molecule Synthesis. *Acc. Chem. Res.* **2015**, *48*, 1474–1484.
[290] Constantin, T.; Zanini, M.; Regni, A.; Shikh, N. S.; Julia, F. Leonori, D. Aminoalkyl Radicals as Halogen-Atom Transfer Agents for Activation of Alkyl and Aryl Halides. *Science* **2020**, *367*, 1021–1026.

with $k_{XAT} = 10^8\ M^{-1}s^{-1}$ at room temperature, holding promise to accomplish a wide variety of XAT-based processes using both alkyl and aryl halides.

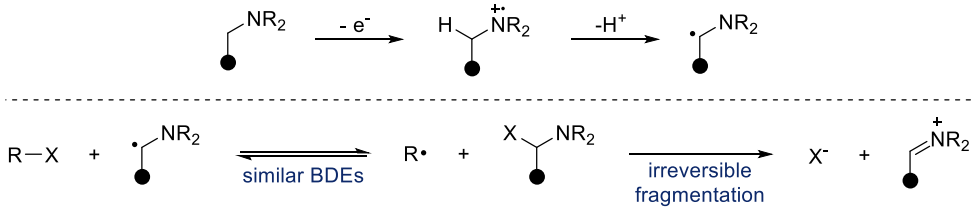

Scheme 4.14 Generation of *α*-aminoalkyl radicals and its utilization in XAT chemistry.

For instance, they recently employed *α*-aminoalkyl radicals to enable the efficient conversion of the iodides into the corresponding alkyl radical by halogen-atom transfer, to achieve the copper catalyzed sp^3 C–N bonds formation without light irradiation (Scheme 4.15).[291] A detailed description of the mechanism is provided in Scheme 4.15 bottom. Oxidation of *in situ* generated Cu(I)-amido **4.15g** with peroxide **4.15d** provides simultaneously Cu(II)-amido intermediate **4.15h** and an oxygen-centered radical **4.15j**. This species would have the appropriate philicity to undergo HAT selectively at the *α*-N position of alkyl amine **4.15e**,[292] leading to the key *α*-aminoalkyl radical **4.15k**, which would further abstract iodine from **4.15a**. At this point, fast capture of radical **4.15m** by **4.15h** would provide the high-valent alkyl-Cu(III)-amido species **4.15i**, from which reductive elimination would release the targeted sp^3 C–N bond coupling product and regenerate the Cu(I) catalyst **4.15f**.

[291] Gorski, B.; Barthelemy, A.-L.; Douglas, J. J.; Julia, F.; Leonori, D. Copper-Catalysed Amination of Alkyl Iodides Enabled by Halogen-Atom Transfer. *Nat. Catal.* **2021**, *4*, 623–630.
[292] Wayner, D. D. M.; Dannenberg, J. J.; Griller, D. Oxidation Potentials of α-Aminoalkyl Radicals: Bond Dissociation Energies for Related Radical Cations. *Chem. Phys. Lett.* **1986**, *131*, 189–191.

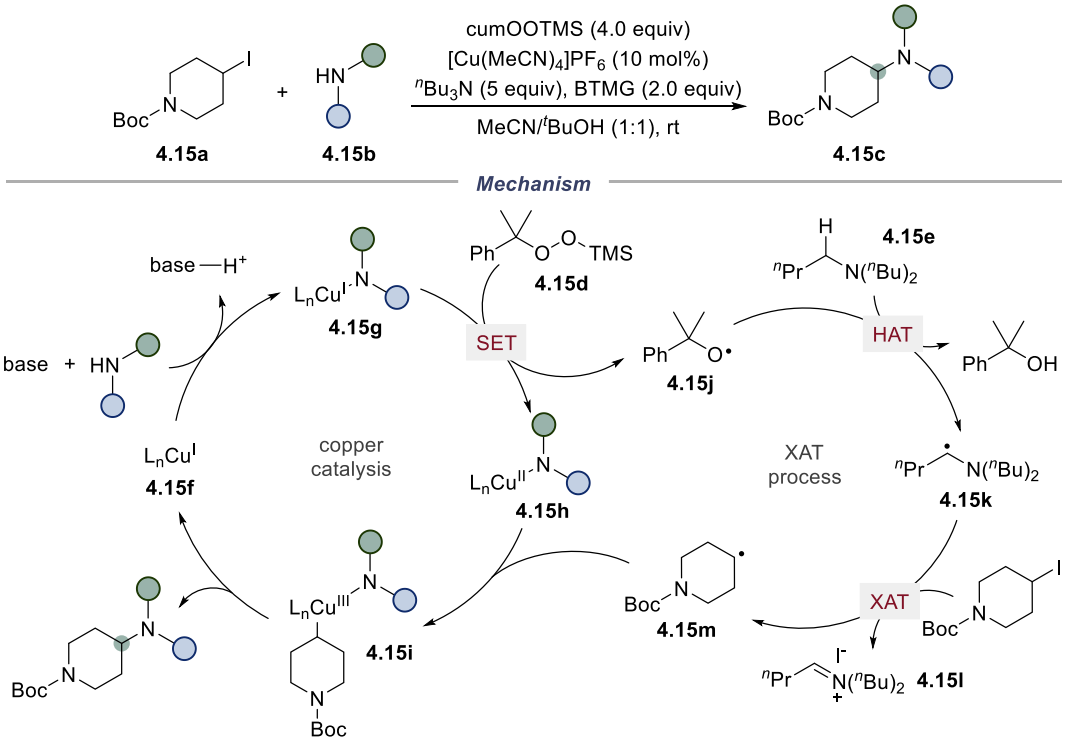

Scheme 4.15 Copper-catalyzed amination of alkyl iodides enabled by *α*-aminoalkyl radical mediated XAT.

Except *α*-aminoalkyl radical, analogous nucleophilic carbon-centered radicals (e.g., acyl,[293] methyl,[294] aryl[295]) have been confirmed to trigger halogen abstraction. For instance, Gevorgyan and co-workers disclosed a remote amination reaction of alcohols initiated by aryl radical meditated XAT process (Scheme 4.16).[296] Iodine atom abstraction from the silyl methyl iodide moiety of a tethered alcohol by an aryl radical, formed from the diazonium salt in the presence of base, leads to silyl methyl radical species **4.16c**. This electrophilic radical undergoes a selective 1,6-HAT process to produce a nucleophilic radical species **4.16d** at the remote C(sp^3)−H site of the alcohol. The latter would be ultimately trapped by excess diazonium salt to furnish **4.16b**.

[293] Kreimerman, S.; Ryu, L.; Minakata, S.; Komatsu, M. Lactone Synthesis Based on Atom Transfer Carbonylation. *Org. Lett*. **2000**, *2*, 389–391.
[294] Wang, Z.; Dong, J.; Hao, Y.; Li, Y.; Liu, Y.; Song, H.; Wang, Q. Photoredox-Mediated Minisci C-H Alkylation Reactions between N-Heteroarenes and Alkyl Iodides with Peroxyacetate as a Radical Relay Initiator. *J. Org. Chem*. **2019**, *84*, 16245−16253.
[295] Hara, R.; Khiar, C.; Dange, N.S.; Bouillac, P.; Robert, F.; Landais, Y. Boronic Acid Mediated Carbocyanation of Olefins and Vinylation of Alkyl Iodides. *Eur. J. Org. Chem*. **2018**, 4058–4063.
[296] Kurandina, D.; Yadagiri, D.; Rivas, M.; Kavun, A.; Chuentragool, P.; Hayama, K.; Gevorgyan, V. Transition-Metal- and Light-Free Directed Amination of Remote Unactivated C(sp^3)−H Bonds of Alcohols. *J. Am. Chem. Soc*. **2019**, *141*, 8104−8109.

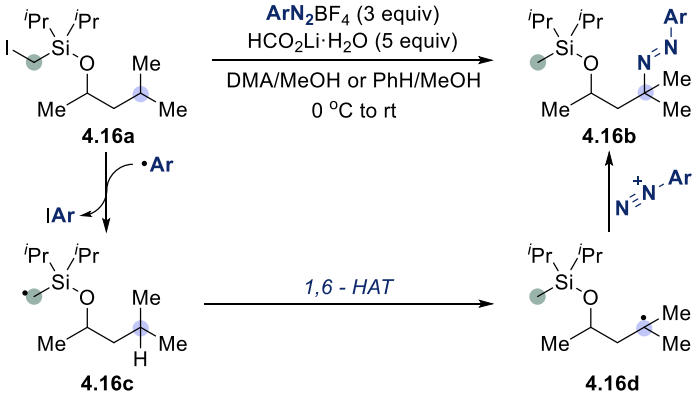

Scheme 4.16 Amination of remote unactivated C(sp^3)−H bonds enabled by aryl radical mediated XAT.

It is important to note that boron radicals,[297] phosphorus radicals[298] as well as some metal complex[299] are known for initiate XAT procedure. These examples will not be discussed in detail considering their less relevance to this thesis.

4.1.2 Transition Metal-Catalyzed Cross-Coupling Reactions Mediated by Aryl Radicals

Aryl radicals can be generated from various sources, among which two most commonly used precursors for this purpose are aryl halides and arenediazonium salts. Due to their high reactivity, aryl radical can be involved in many different reactions with some shown in Scheme 4.17. As an ambiphilic radical species, they could undergo hydrogen atom abstraction from activated positions or halogen atom abstraction from weak carbon halogen bond. The comparatively fast iodine exchange process allows the suppression of most undesired side reactions, turning the corresponding elementary reaction into catalytic useful technique. Aryl radical addition to non-activated olefins proceeds with a lower rate constant of $k \approx 10^7$ $M^{-1}s^{-1}$ compared to activated olefins ($k \approx 10^8$ $M^{-1}s^{-1}$), and biaryl couplings ($k \approx 10^6$ $M^{-1}s^{-1}$) often have to be performed using the aromatic substrate as solvent. The fast and effective transfer of ligands from copper ions to aryl radicals ($k \approx 10^8$ $M^{-1}s^{-1}$) builds the foundation of the Sandmeyer reactions.

[297] Ueng, S. H.; Fensterbank, L.; Lacote, E.; Malacria, M.; Curran, D. P. Radical Reductions of Alkyl Halides Bearing Electron Withdrawing Groups with N-Heterocyclic Carbene Boranes. *Org. Biomol. Chem*. **2011**, *9*, 3415−3420.
[298] Barton, D. H. R.; Ok Jang, D.; Jaszberenyi, J. C. Hypophosphorous acid and its Salts: New Reagents for Radical Chain Deoxygenation, Dehalogenation and Deamination. *Tetrahedron Lett*. **1992**, *33*, 5709−5712.
[299] (a) Tang, T.; Friede, N. C.; Minteer, S. D.; Sigman, M. S. Comparing Halogen Atom Abstraction Kinetics for Mn(I), Fe(I), Co(I), and Ni(I) Complexes by Combining Electroanalytical and Statistical Modeling. *Eur. J. Org. Chem*. **2022**, e202200064. (b) Meyer, T. J.; Caspar, J. V. Photochemistry of Metal-Metal Bonds. *Chem. Rev*. **1985**, *85*, 187−218.

Aryl radical addition to iminium ions and sulfur dioxide are operative according to literature precedents.[300]

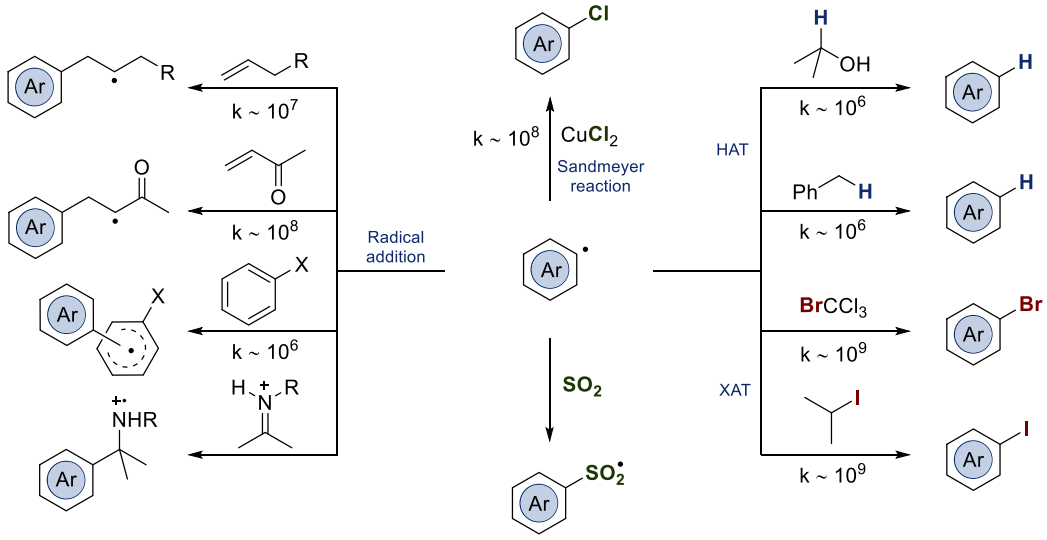

Scheme 4.17 Aryl radical reactions and related rate constants (k in $M^{-1}s^{-1}$).

In 2021, Liu and co-workers disclosed a copper-catalyzed difluoromethylation protocol of alkyl iodides mediated by aryl radical (Scheme 4.18).[301] According to the proposed mechanism, decomposition of diazonium salts **4.18c** facilitated by the presence of Cu(I) species **4.18e** would release aryl radical **4.18h** and Cu(II) complex **4.18f**. The fast and irreversible iodine abstraction should out compete other unwanted pathways of the aryl radicals, leading to the alkyl radical **4.18i** generation. Radical recombination of alkyl radical **4.18i** with Cu(II) **4.18f** gives rise to Cu(III) entity **4.18g** thus setting the basis for difluoromethylation via reductive elimination.

[300] Heinrich, M. R. Intermolecular Olefin Functionalisation Involving Aryl Radicals Generated from Arenediazonium Salts. *Chem. Eur. J.* **2009**, *15*, 820–833.
[301] Cai, A.; Yan, W.; Wang, C.; Liu, W. Copper-Catalyzed Difluoromethylation of Alkyl Iodides Enabled by Aryl Radical Activation of Carbon–Iodine Bonds. *Angew. Chem. Int. Ed*. **2021**, *60*, 27070–27077.

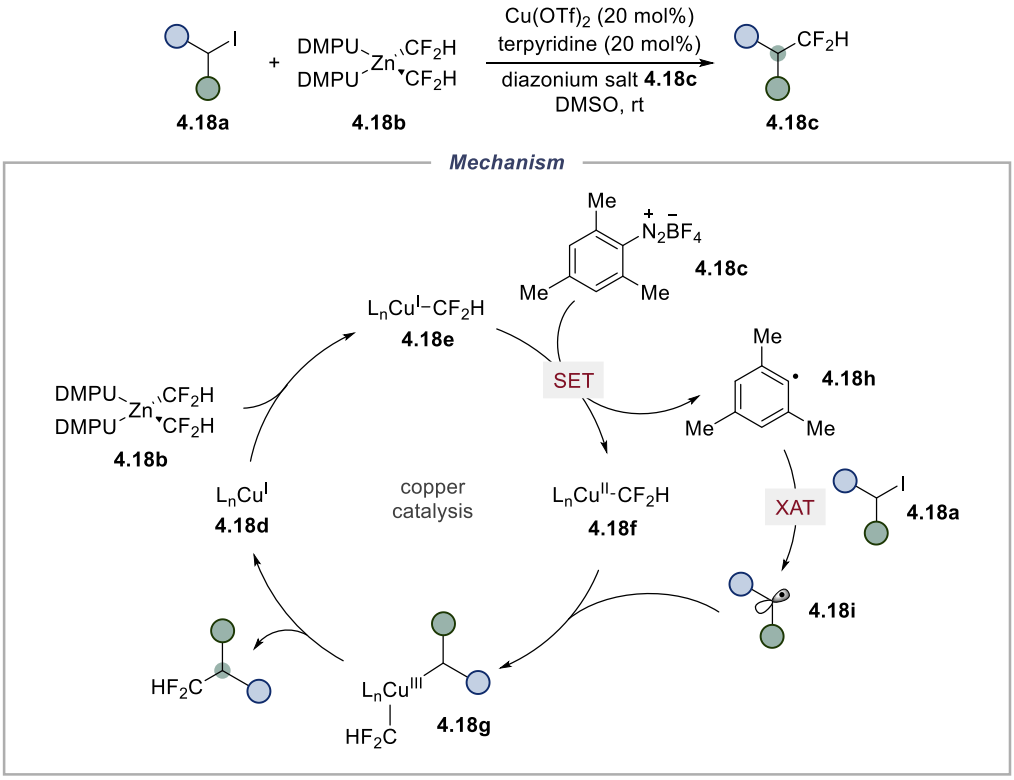

Scheme 4.18 Copper-catalyzed difluoromethylation of alkyl iodides enabled by aryl radical mediated XAT.

Along with their research interest of aryl radical activation, Liu and co-workers realized a deoxygenative difluoromethylation reaction in the same year (Scheme 4.19).[302] Similarly, they harnessed diazonium salts for aryl radical generation, which would sequentially get involve in Barton-McCombie type deoxygenation process,[303] leading to the generation of alkyl radical **4.19g**.

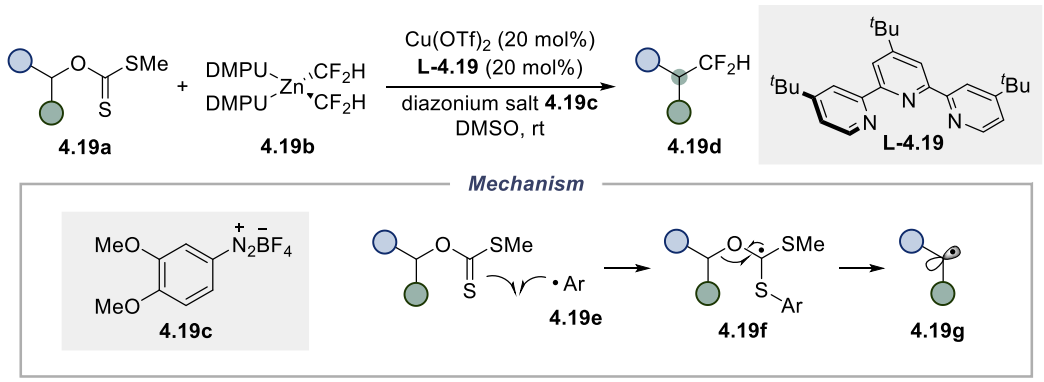

Scheme 4.19 Copper catalyzed deoxygenative difluoromethylation mediated by aryl

[302] Cai, A.; Yan, W.; Liu, W. Aryl Radical Activation of C–O Bonds: Copper-Catalyzed Deoxygenative Difluoromethylation of Alcohols. *J. Am. Chem. Soc.* **2021**, *143*, 9952−9960.
[303] (a) Barton, D. H. R.; McCombie, S. W. A New Method for the Deoxygenation of Secondary Alcohols. *J. Chem. Soc., Perkin Trans.* **1975**, 16, 1574−1585. (b) Crich, D.; Quintero, L. Radical Chemistry Associated with the Thiocarbonyl Group. *Chem. Rev.* **1989**, *89*, 1413−1432.

radical.

Gevorgyan and co-workers recently employed the aryl radical triggered HAT with palladium-catalyzed allylic amination to achieve the direct C–H amination of alkenes with aliphatic amines (Scheme 4.20).[304] The reaction is initiated by photoinduced single electron transfer from Pd(0) species **4.20e** to aryl bromides **4.20c** (or oxidative addition, photoinduced aryl radical release sequence), leading to aryl radical **4.20i** injection into reaction mixture. HAT process with alkene **4.20a** provides an allylic radical **4.20j**, combined with Pd(I) species **4.20g** to furnish a classical, closed-shell allylic Pd(II) complex **4.20h**. The latter could then be intercepted by aliphatic amine **4.20b** to afford the desired C–H amination product, in the meanwhile returning to Pd(0) species **4.20e** to close the cycle.

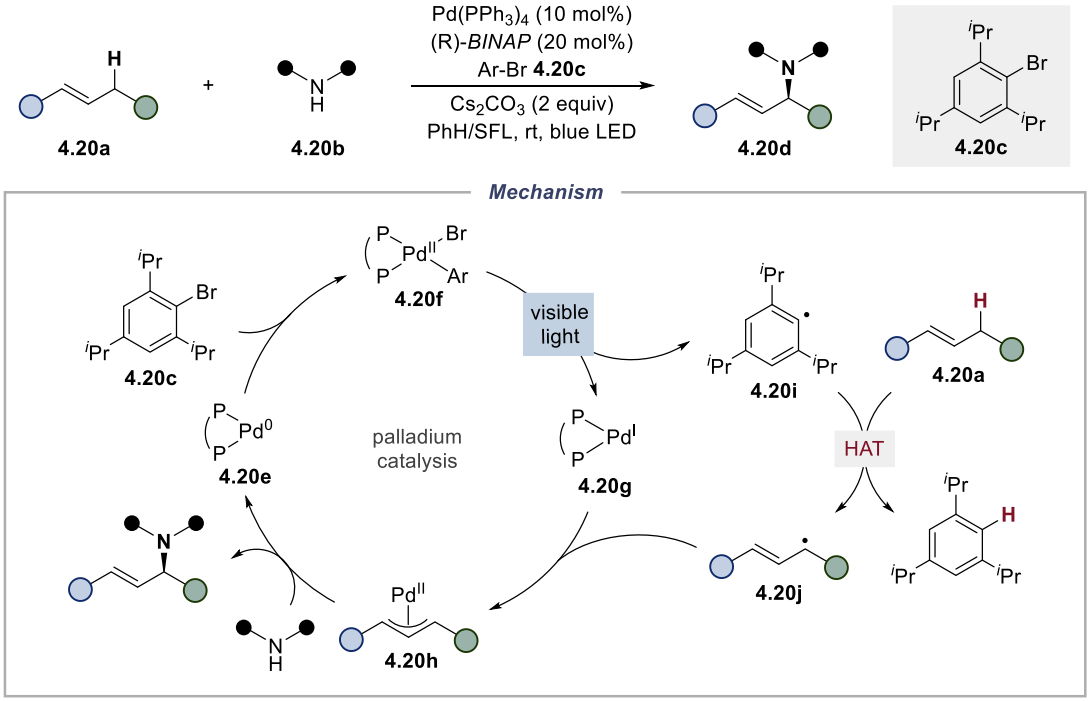

Scheme 4.20 Palladium catalyzed asymmetric allylic C–H amination of alkenes enabled by aryl radical mediated HAT.

Leonori and co-workers recently developed a copper-catalyzed cross-coupling platform, harnessing unactivated secondary alkyl iodides with various nucleophiles (Scheme 4.21).[305] The strategy makes use of the ability of photoredox-generated phenyl radicals to mediate XAT and the ability of copper catalysis for C−N/O/C bond

[304] Cheung, K. P. S.; Fang, J.; Mukherjee, K.; Mihranyan, A.; Gevorgyan, V. Asymmetric Intermolecular Allylic C–H Amination of Alkenes with Aliphatic Amines. *Science* **2022**, *378*, 1207–1213.
[305] Caiger, L.; Zhao, H.; Constantin, T.; Douglas, J. J.; Leonori, D. The Merger of Aryl Radical-Mediated Halogen-Atom Transfer (XAT) and Copper Catalysis for the Modular Cross-Coupling-Type Functionalization of Alkyl Iodides. *ACS Catal*. **2023**, *13*, 4985−4991.

construction. The latter could be demonstrated by the broad substrate scope, including employment of a variety of anilines, boronic acids, phenols, indazoles, sulfonamides, carbamates and TMS−CN in the alkylation events.

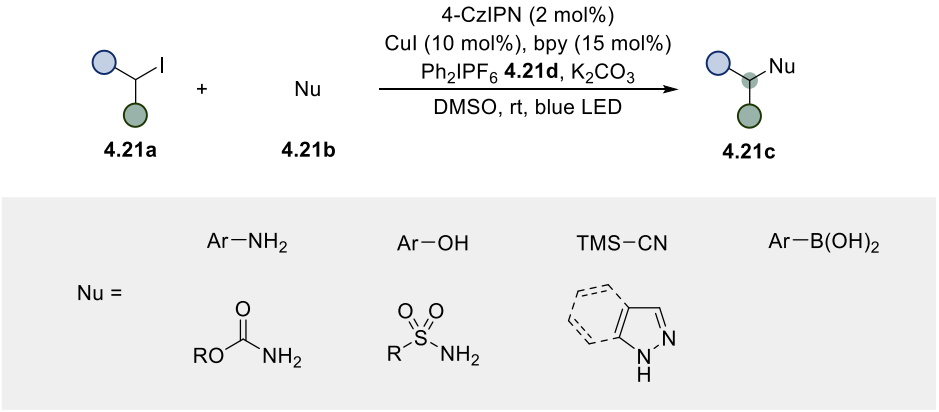

Scheme 4.21 Copper-catalyzed functionalization of alkyl iodides enabled by aryl radical mediated XAT.

4.2 General Aim of the Project

Despite the huge synthetic value C(sp^3)–N bond construction has, at the outset of our investigation, a general and practical cross-coupling protocol which is operated under mild conditions with broad applicability is still needed. As the present copper-catalyzed C(sp^3)–N bond coupling reactions typically require light irradiation, the difficulty associated with such processes could be partially attributed to the sluggish two-electron oxidative addition of copper(I) complexes. In addition, the low reduction potential of unactivated alkyl halides (E_{red} < -2V vs. SCE) hinders the direct single electron transfer (SET) from Cu(I) catalysts at the ground state. By contrast, the capture of alkyl radicals by Cu(II) species and the ensuing reductive elimination of the organocopper(III) complexes can proceed efficiently (Scheme 4.22, *top*).

Motivated by the superior iodine abstraction behavior of aryl radical, we envisioned that the employment of a suitable aryl-radical-generating oxidant to trigger an oxidative coupling protocol might be suitable for this aim even with the absence of photo excitation (Scheme 4.22, *bottom*). The following part of this chapter will focus on accomplishing the concepts by means of establishing reaction conditions and exploring the synthetic potential this reaction may hold.

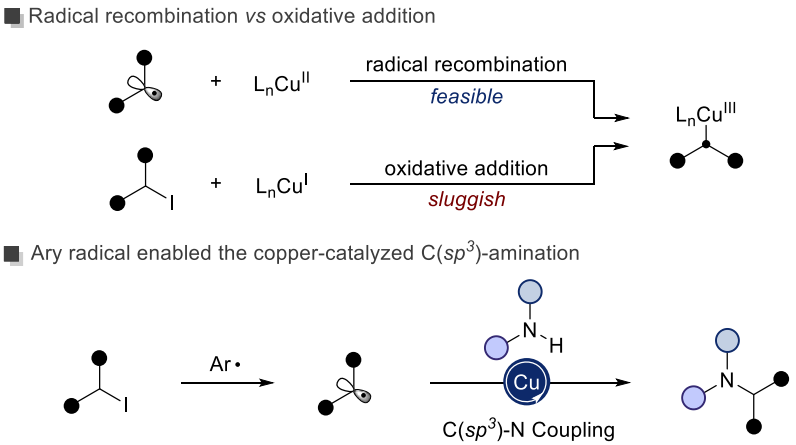

Scheme 4.22 Copper catalyzed C(sp^3) amination of unactivated secondary alkyl iodides promoted by diaryliodonium salts.

4.3 Optimization

A detailed description of our proposal for copper-catalyzed C(sp^3) amination of alkyl iodides is outlined in Scheme 4.23. We anticipated that oxidation of the *in situ* generated Cu(I)-amido complex **4.23a** by diaryliodonium salt provides Cu(II)-amido species **4.23b** and aryl radical **4.23e**, which would further undergo iodine abstraction with alkyl iodide to furnish alkyl radical **4.23f**. Radical recombination of alkyl radical **4.23f** with Cu(II) gives rise to Cu(III) entity **4.23c**, thus setting the basis for C(sp^3)–N formation via reductive elimination.

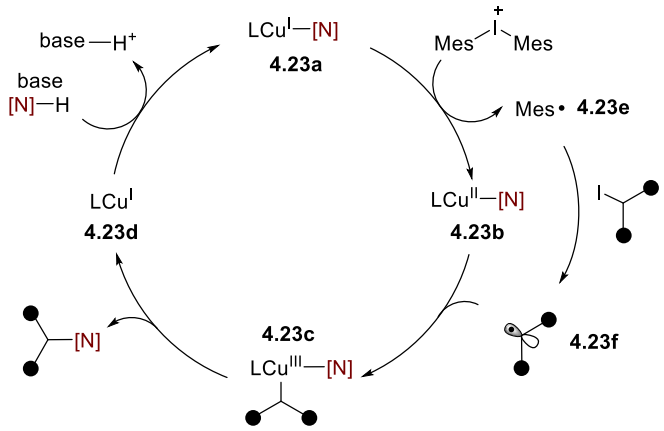

Scheme 4.23 Copper catalyzed C(sp^3) amination of unactivated secondary alkyl iodides promoted by diaryliodonium salts: reaction proposal.

We started our investigations by studying the reaction of indazole **1a** and cyclohexyl iodide **2a** as the standard substrates. Considering the crucial role ligands play in modulating the properties of the copper catalyst, the initial optimization studies were focused on screening a variety of ligands. Redox non-innocent nitrogen ligands were preferentially evaluated since the reaction was proposed to operative in a Cu (0/I/II) cycle. As shown in Table 4.1, a series of bidentate nitrogen ligands were tested in the reactions (**L1**–**L10**), resulting in the product formation in good yields. In the phenanthroline series (**L3**–**L10**), inferior results were obtained for ligands having electro-withdrawing group on the phenanthroline backbone or with substituents adjacent to the coordinating nitrogen. Among all the phenanthroline ligands series, tetramethyl substituted **L8** provided the best result, affording the cross-coupling product **3a** in 89% yield. Inferior results were found with tridentate nitrogen ligand (**L11**).

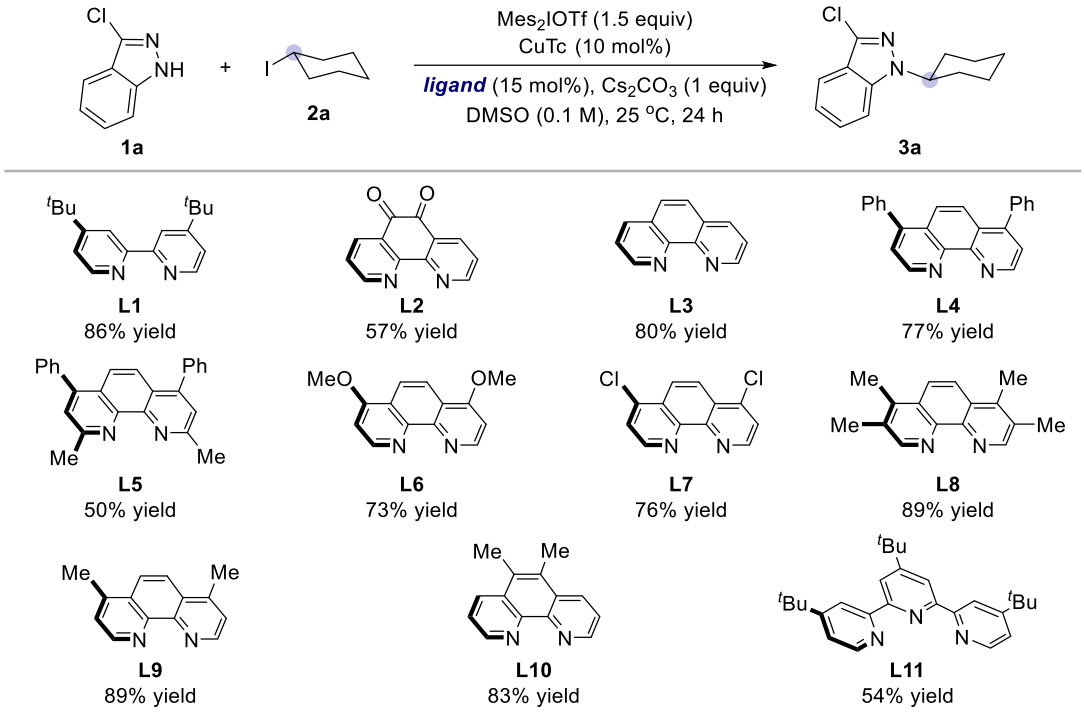

[a] Conditions: **1a** (0.10 mmol), **2a** (0.15 mmol), CuTc (10 mol%), ligand (15 mol%), Mes_2IOTf (1.5 equiv), Cs_2CO_3 (0.10 mmol) in DMSO (0.10 M) at 25 °C for 24 h. [b] GC yield and conversion using dodecane as internal standard.

Table 4.1 Screening of ligands.

With **L8** found as the optimal ligand, the effect of solvents was next investigated. As shown in Table 4.2, the employment of polar aprotic solvents including NMP, DMF, DMSO or MeCN (entries 1–4) gave good product yields, with DMSO yielding the best results, probably owing to the superior dissolving capacity. Interestingly, halogenated solvents such as $PhCF_3$ and DCE gave inferior results (entries 5 and 6). Ether-based solvent, ester-based solvent, alcohol-based solvent and acetone provided satisfactory results (entry 7–10), albeit with lower yields compared to DMSO.

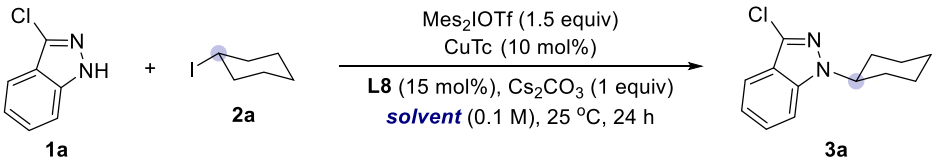

entry	solvent	**3a** (%)[b]
1	NMP	46
2	DMF	56
3	DMSO	89
4	MeCN	61
5	$PhCF_3$	36
6	DCE	10
7	Dioxane	55
8	EA	70
9	Acetone	67
10	^tBuOH	61

[a] Conditions: **1a** (0.10 mmol), **2a** (0.15 mmol), CuTc (10 mol%), **L8** (15 mol%), Mes_2IOTf (1.5 equiv), Cs_2CO_3 (0.10 mmol) in solvent (0.10 M) at 25 °C for 24 h. [b] GC yield and conversion using dodecane as internal standard.

Table 4.2 Screening of solvents.

With these results in hand, we then focused our attention on studying the effect of the copper precatalyst. As show in Table 4.3, a series of copper(I) and copper (II) precatalysts could provide **3a** in good yields (85%). The best result was found when utilizing CuTc as copper precatalyst. $Cu(TMHD)_2$ failed to provide satisfactory yield somehow (entry 10), might due to its poor solubility. The in situ generated Cu(III) entity by oxidation underwent reductive elimination to furnish Cu(I) complex, making sure effectiveness brought by Cu(II) precatalyst.

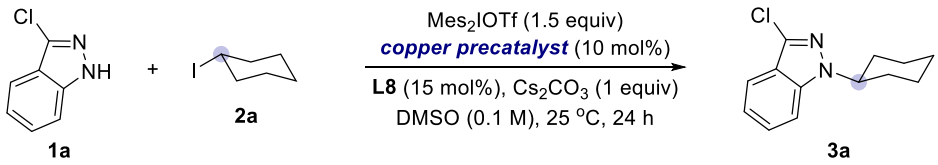

entry	Ni precatalyst	**3a** (%)[b]
1	$Cu(MeCN)_4PF_6$	93
2	$Cu(MeCN)_4BF_4$	96
3	CuTc	99
4	CuCl	92
5	CuBr	94
6	CuI	96
7	$CuCl_2$	95
8	$CuBr_2$	85
9	$Cu(OAc)_2$	94
10	$Cu(TMHD)_2$	19
11	$Cu(hfac)_2$	95
12	$Cu(OTf)_2$	93

[a] Conditions: **1a** (0.10 mmol), **2a** (0.15 mmol), copper precatalyst (10 mol%), **L8** (15 mol%), Mes_2IOTf (1.5 equiv), Cs_2CO_3 (0.10 mmol) in solvent (0.10 M) at 25 °C for 24 h. [b] GC yield and conversion using dodecane as internal standard.

Table 4.3 Screening of copper precatalysts.

Using CuTc as the optimal precatalyst, the effect of base was investigated afterwards. As shown in Table 4.3, carbonate bases performed excellent in cross-coupling reactions (entry 1–3), with cesium carbonate giving the best yield. Cesium bicarbonate and cesium pivalate were found to have a deleterious effect on reactivity (entry 4 and 5). Other bases such as potassium phosphate, strong potassium *tert*-butoxide and organic TMG and BTMG couldn't promote the reaction effectively (entry 6–9).

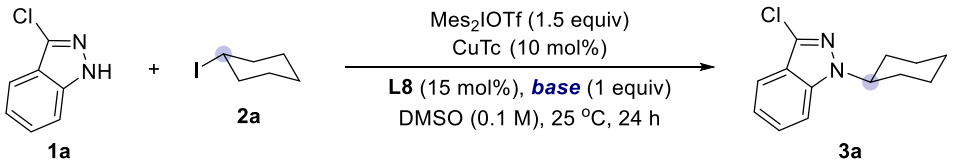

entry	base	**3a** (%)[b]
1	Na_2CO_3	63
2	K_2CO_3	92
3	Cs_2CO_3	94
4	$CsHCO_3$	69
5	CsOPiv	35
6	K_3PO_4	41
7	^{t}BuOK	36
8	TMG	74
9	BTMG	73

[a] Conditions: **1a** (0.10 mmol), **2a** (0.15 mmol), CuTc (10 mol%), **L8** (15 mol%), Mes_2IOTf (1.5 equiv), base (0.10 mmol) in DMSO (0.10 M) at 25 °C for 24 h. [b] GC yield and conversion using dodecane as internal standard.

Table 4.4 Screening of bases.

In the end, control experiment were conducted to ensure that all the reaction parameters were necessary for obtaining high yield. Indeed, as indicated in Table 4.5, no targeted product was formed in the absence of ligand and copper precatalyst, iodonium salt or base (entries 2–5), thus arguing against the intervention of S_N2-type pathways. Comparable yields were found with commercial available diaryliodonium salts other than Mes_2IOTf (entry 6). Unfortunately, <5% yield was found with cyclohexyl bromide as the counterpart.

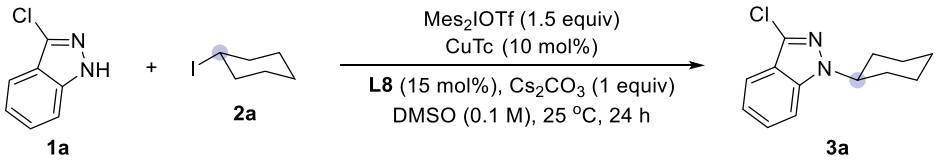

entry	deviation standard conditions	**3a** (%)[b]
1	none	97 (94)[c]
2	no **L8**	<5
3	no Cu	<5
4	no Mes_2IOTf	<5
5	no base	<5
6	Ph_2IOTf, PhI_2Cl instead of Mes_2IOTf	91, 86

[a] Conditions: **1a** (0.10 mmol), **2a** (0.15 mmol), CuTc (10 mol%), **L8** (15 mol%), Mes_2IOTf (1.5 equiv), Cs_2CO_3 (0.10 mmol) in DMSO (0.10 M) at 25 °C for 24 h. [b] GC yield and conversion using dodecane as internal standard. [c] isolated yield.

Table 4.5 Control experiments.

4.4 Substrate Scope

4.5.1 Scope of Alkyl Iodides

With the established reaction conditions in hand, we next explored the generality of our Cu-catalyzed sp^3 amination event. As shown in Scheme 4.24, cyclic alkyl iodides possessing different ring sizes (**3a**−**3c**) and heteroatom backbones participated well in our amination reaction (**3d** and **3e**). As shown for compounds **3f** and **3g**, substrates containing carbonyl groups or acetals did not interfere with productive sp^3 C−N bond formation. Likewise, strained cyclobutyl rings could be incorporated with exceptional ease (**3h**−**3j**). Particularly noteworthy was the ability to extend these conceptions to acyclic secondary alkyl fragments, thus illustrating the potential that this technique might have beyond cyclic structures (**3k**−**3n**). Notably, spyrocyclic motifs (**3o**), bridged bicyclic frameworks (**3p** and **3q**), or substrates containing medicinally relevant piperidinopyridazine (**3r**)[306] were all competent for our Cu-catalyzed sp^3 amination endeavor. With respect to the limitation of this reaction, cyclopropyl iodide and tertiary iodide couldn't be applied in this reaction, providing only traces of the amination products.

[306] Watson, K. G.; Brown, R. N.; Cameron, R.; Chalmers, D. K.; Hamilton, S.; Jin, B.; Krippner, G. Y.; Luttick, A.; McConnell, D. B.; Reece, P. A.; Ryan, J.; Stanislawski, P. C.; Tucker, S. P.; Wu, W.-Y.; Barnard, D. L.; Sidwell, R. W. An Orally Bioavailable Oxime Ether Capsid Binder with Potent Activity against Human Rhinovirus. *J. Med. Chem*. **2003**, *46*, 3181−3184.

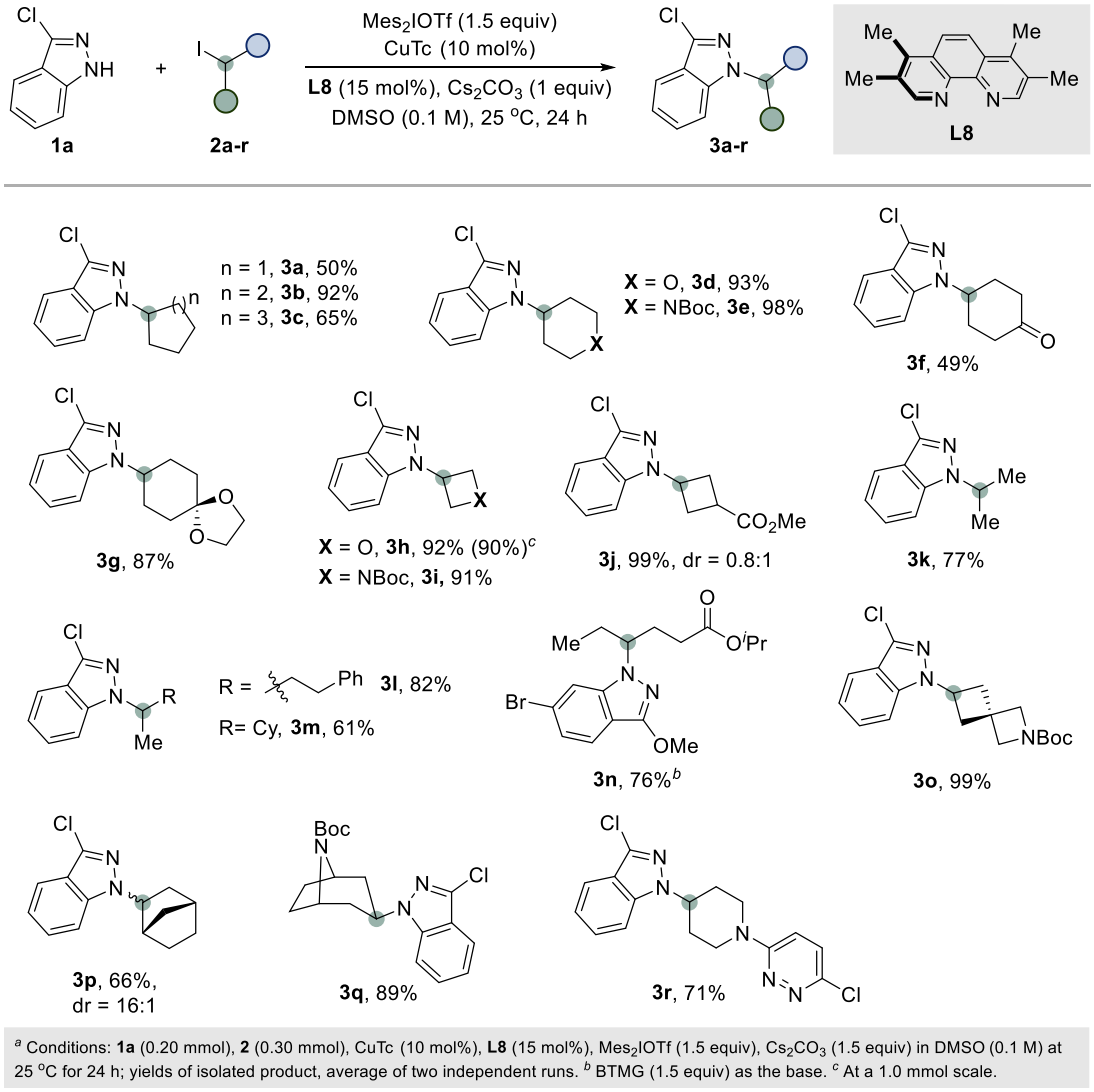

[a] Conditions: **1a** (0.20 mmol), **2** (0.30 mmol), CuTc (10 mol%), **L8** (15 mol%), Mes_2IOTf (1.5 equiv), Cs_2CO_3 (1.5 equiv) in DMSO (0.1 M) at 25 °C for 24 h; yields of isolated product, average of two independent runs. [b] BTMG (1.5 equiv) as the base. [c] At a 1.0 mmol scale.

Scheme 4.24 Scope with alkyl iodides

4.5.2 Scope of Nucleophiles

Next, we turned our attention to the scope of nitrogen nucleophiles that might participate in our amination protocol. As shown, a variety of substituted indazoles (**5a**–**5c**), indoles (**5d**–**5f**), azaindazoles (**5g** and **5h**), azaindole (**5i**), and pyrazoles (**5j** and **5k**) were all suited as coupling counterparts. Even the presence of nitroles (**5b**) or aryl bromides (**5c** and **5h**) could be accommodated, thus leaving ample room for further derivatization via conventional cross-coupling reactions. In addition, quantitative yields were obtained regardless of whether electron-rich or electron-poor sulfonamides were utilized as nucleophilie entities, resulting in all cases in exclusive monoalkylation events (**5l**–**5o**); although tentative, the result might be interpreted on the difficulty of copper catalysts to enable bond formation at relatively congested sites.

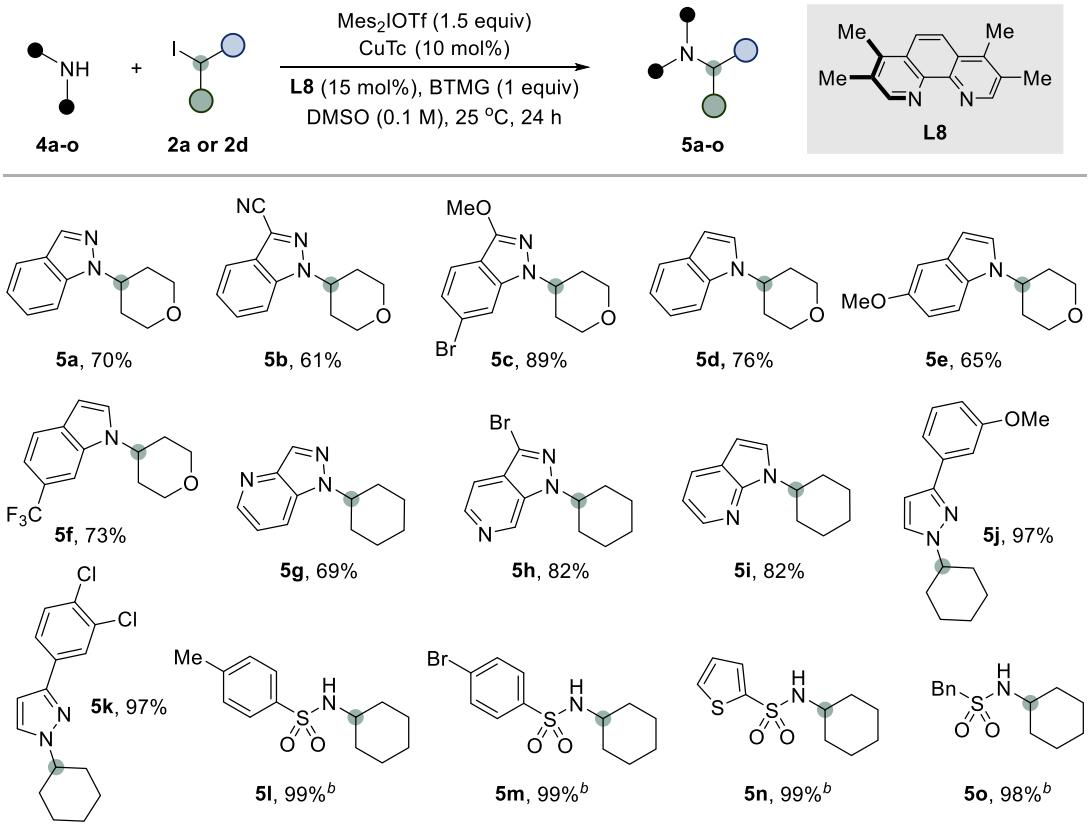

[a] Conditions: **4** (0.20 mmol), **2a** or **2d** (0.30 mmol), CuTc (10 mol%), **L8** (15 mol%), Mes_2IOTf (1.5 equiv), BTMG (1.5 equiv) in DMSO (0.1 M) at 25 °C for 24 h; yields of isolated product, average of two independent runs. [b] ^{t}BuOH (0.1 M) as the solvent.

Scheme 4.25 Scope with nucleophiles.

4.5 Mechanistic Studies

To support our initial hypothesis that a radical fragmentation was generated during the reaction process, TEMPO inhabitation experiment was conducted. Compound **6** was obtained in a 59% yield by exposure of indazole **1a** and alkyl iodide **2a** to (2,2,6,6-tetramethylpiperidin-1-yl)oxyl (TEMPO) under our optimized conditions, thus strongly suggesting the intervention of radical species (Scheme 4.26, *top*). This observation was further corroborated by observing dimerization of compound **2g** in the absence of nitrogen-containing nucleophiles (Scheme 4.26, *middle*).

In addition, >2 equiv of mesityl iodide was isolated in analytically pure form when attempting the reaction of compound **3h** at a 1.0 mmol scale (Scheme 4.26, *bottom*), thus suggesting that XAT-type processes come into play. Taken together, these experiments suggest a mechanistic pathway which was shown in Scheme 4.23.

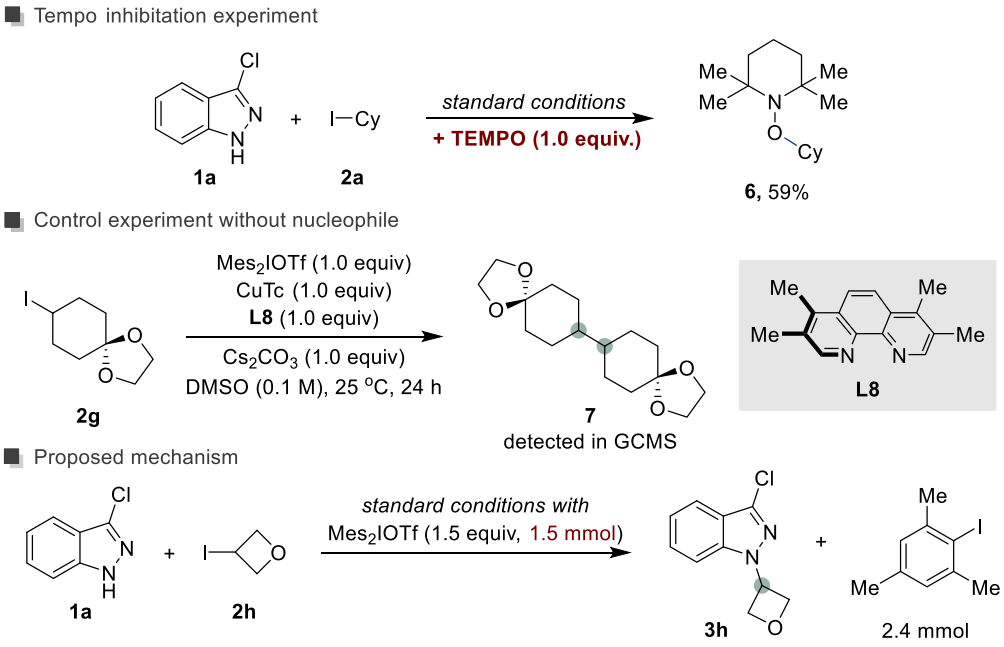

Scheme 4.26 Mechanistic studies.

4.6 Conclusions

This chapter summarizes the efforts towards the development of a Cu-catalyzed C(sp^3) amination of secondary alkyl iodides mediated by diaryliodonium salts. This reaction was conducted under mild reaction conditions and the protocol could be applied to a variety of *N*-nucleophiles and unactivated alkyl iodides with excellent chemo- and regio-selectivity.

Preliminary mechanistic experiments were carried out, indicating that the involvement of alkyl radicals derived from aryl radical enabled halogen atom abstraction.

4.7 Experimental Section

4.7.1 General Considerations

Reagents. Commercially available materials were used as received without further purification. CuTc was purchased from Aldrich. 3,4,7,8-Tetramethyl-1,10-phenanthroline (95% purity) was purchased from Manchester Organics. Anhydrous Cs_2CO_3 (99.9% purity) was purchased from Alfa Aesar. BTMG (97%+ purity) was purchased from Aldrich. Mesitylene (98% purity) was purchased from Aldrich. 2,4,6-Trimethyliodobenzene (98%+ purity) was purchased from TCI. 3-Chloroperoxybenzoic acid (≤ 77%) was purchased from Aldrich. Anhydrous DMSO (99.9+% purity) and ^{t}BuOH (99.5+% purity) were purchased from Aldrich. Starting materials (**1a** or **4a** - **4o**) are commercial available and bought for direct use without further purification.

Analytical methods. ^{1}H and ^{13}C NMR spectra were recorded on Bruker 400 MHz or 500 MHz at 20 °C. All ^{1}H NMR spectra are reported in parts per million (ppm) downfield of TMS and were calibrated using the residual water peak (1.56 ppm in $CDCl_3$), residual solvent peak of $CHCl_3$ (7.26 ppm), unless otherwise indicated. All ^{13}C NMR spectra are reported in ppm relative to TMS, were calibrated using the signal of residual $CHCl_3$ (77.16 ppm). ^{19}F NMR was obtained with ^{1}H decoupling unless otherwise indicated. Coupling constants, *J* are reported in hertz (Hz). Gas chromatographic analyses were performed on Hewlett-Packard 6890 gas chromatography instrument with FID detector. Melting points were measured using open glass capillaries in a Büchi B540 apparatus, with samples unless otherwise stated recrystalized by slow evaporation of a solution of DCM. Infrared spectra (FT-IR) measurements were carried out on a Bruker Optics FT-IR Alpha spectrometer equipped with a DTGS detector, KBr beamsplitter at 4 cm^{-1} resolution using a one bounce ATR accessory with diamond windows. Mass spectra were recorded on a Waters LCT Premier spectrometer or in a MicroTOF Focus, Bruker Daltonics spectrometer. Flash chromatography was performed with EM Science silica gel 60 (230-400 mesh). Thin layer chromatography was used to monitor reaction progress and analysed fractions from column chromatography. To this purpose TLC Silica gel 60 F_{254} aluminium sheets from Merck were used and visualization was achieved using UV irradiation and/or staining with potassium permanganate or cerium molybdate solution. Room temperature was 25 ºC.

4.7.2 Synthesis of Starting Materials

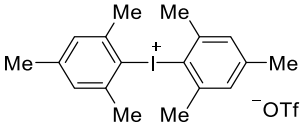

Dimesityliodonium triflate (S1). Mesitylene (2.2 mL, 16 mmol) and *m*-CPBA 77% (3.60 g, 16 mmol) were added sequentially to a stirred solution of mesityl iodide (3.60 g, 14.6 mmol, 1.0 equiv) in CH_2Cl_2 (56 mL). TfOH (2.6 mL, 29.2 mmol, 2 equiv) was introduced dropwise via syringe at 0 ºC, causing the reaction mixture to turn dark red. After the mixture was stirred at 0 ºC for 30 min, the cooling bath was removed and stirring was continued at room temperature for 2.5 h before concentrating to dryness by rotary evaporation. The crude material was triturated with diethyl ether and placed in freezer at -20 ºC overnight. Isolation by filtration and multiple washes with diethyl ether yielded the dimesityliodonium triflate (4.53 g, 60%). **^{1}H NMR (400 MHz, $CDCl_3$)** δ 7.05 (s, 4H), 2.51 (s, 12H), 2.33 (s, 6H) ppm. **^{13}C NMR (101 MHz, $CDCl_3$)** δ 144.0, 142.4, 131.1, 117.4, 26.3, 21.1 ppm. Spectral data was in agreement with the literature.[307]

General procedure 1 (GP1): Preparation of alkyl iodides.

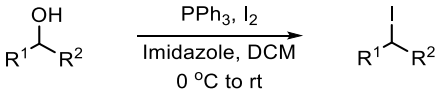

An oven-dried round-bottom flask equipped with a stirring bar was charged with an aliphatic alcohol (1.0 equiv), PPh_3 (1.2 equiv) and imidazole (1.2 equiv). The flask was evacuated and refilled with Ar, followed by the addition of dry DCM (0.1 M). The reaction was cooled to 0 ºC with an ice-water bath. I_2 (1.2 equiv) was added portion-wise and the cooling bath was removed. The reaction mixture was allowed to stir at room temperature overnight and was quenched with $Na_2S_2O_3$ (saturated, aq.). The layers were separated and the aqueous layer was extracted with CH_2Cl_2 (x 3). The combined organic layers were washed with brine, dried ($MgSO_4$), filtered and concentrated under reduced pressure. The received crude material was purified by silica gel chromatography to afford the desired product.

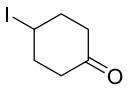

4-Iodocyclohexan-1-one (2f). Following GP1, using 4-hydroxycyclohexan-1-one (456 mg, 4.0 mmol) afforded the title compound as a white solid (623 mg, 70%), by using hexane/EtOAc (20:1) as chromatography eluent. **^{1}H NMR (400 MHz, $CDCl_3$)** δ 4.71 (tt, *J* = 7.0, 3.2 Hz, 1H), 2.70 – 2.56 (m, 2H), 2.43 – 2.26 (m, 4H), 2.23 – 2.12 (m, 2H) ppm. **^{13}C NMR (101 MHz, $CDCl_3$)** δ 208.6, 40.9, 38.2, 27.7 ppm. Spectral data was in

[307] Lucchetti, N.; Scalone, M.; Fantasia, S.; Muñiz, K. Sterically Congested 2,6-Disubstituted Anilines from Direct C−N Bond Formation at an Iodine(III) Center. *Angew. Chem. Int. Ed*. **2016**, *55*, 13335–13339.

agreement with the literature.[308]

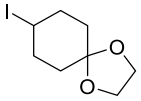

8-Iodo-1,4-dioxaspiro[4.5]decane (2g). Following GP1, using 1,4-dioxaspiro[4.5]decan-8-ol (316 mg, 2.0 mmol) afforded the title compound as a colourless oil (370 mg, 69%), by using hexane/EtOAc (20:1) as chromatography eluent. **^{1}H NMR (400 MHz, $CDCl_3$)** δ 4.48 – 4.36 (m, 1H), 4.00 – 3.88 (m, 4H), 2.22 – 2.02 (m, 4H), 1.87 – 1.76 (m, 2H), 1.67 – 1.55 (m, 2H) ppm. **^{13}C NMR (101 MHz, $CDCl_3$)** δ 107.6, 64.51, 64.45, 36.4, 34.9 ppm. Spectral data was in agreement with the literature.[307]

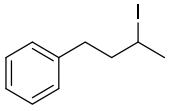

(3-Iodobutyl)benzene (2l). Following GP1, using 4-phenylbutan-2-ol (609 mg, 4.0 mmol) afforded the title compound as a colourless oil (1034 mg, 99%), by using hexane as chromatography eluent. **^{1}H NMR (400 MHz, $CDCl_3$)** δ 7.33 – 7.28 (m, 2H), 7.25 – 7.19 (m, 3H), 4.19 – 4.07 (m, 1H), 2.91 – 2.81 (m, 1H), 2.77 – 2.65 (m, 1H), 2.23 – 2.11 (m, 1H), 1.96 (d, J = 6.8 Hz, 3H), 1.94 – 1.84 (m, 1H) ppm. **^{13}C NMR (101 MHz, $CDCl_3$)** δ 140.9, 128.7, 128.6, 126.3, 44.5, 36.0, 29.7, 29.1 ppm. Spectral data was in agreement with the literature.[291]

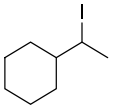

(1-Iodoethyl)cyclohexane (2m). Following GP1, using 1-cyclohexylethan-1-ol (640 mg, 5.0 mmol) afforded the title compound as a colourless oil (639 mg, 54%), by using hexane as chromatography eluent. **^{1}H NMR (400 MHz, $CDCl_3$)** δ 4.22 (qd, J = 7.0, 4.0 Hz, 1H), 1.90 (d, J = 7.0 Hz, 3H), 1.87 – 1.81 (m, 1H), 1.81 – 1.72 (m, 3H), 1.71 – 1.61 (m, 1H), 1.38 – 1.22 (m, 2H), 1.20 – 0.97 (m, 4H) ppm. **^{13}C NMR (101 MHz, $CDCl_3$)** δ 46.7, 40.4, 32.1, 31.6, 26.5, 26.2, 26.0 ppm. Spectral data was in agreement with the literature.[309]

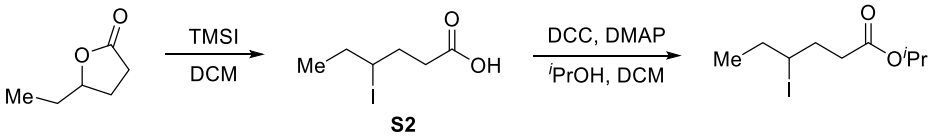

S2

4-iodohexanoic acid (s2). An oven-dried round-bottom flask equipped with a stirring

[308] Zhang, Z.; Górski, B.; Leonori, D. Merging Halogen-Atom Transfer (XAT) and Copper Catalysis for the Modular Suzuki–Miyaura-Type Cross-Coupling of Alkyl Iodides and Organoborons. *J. Am. Chem. Soc*. **2022**, *144*, 1986–1992.
[309] Matier, C. D.; Schwaben, J.; Peters, J. C.; Fu, G. C. Copper-Catalyzed Alkylation of Aliphatic Amines Induced by Visible Light. *J. Am. Chem. Soc.* **2017**, *139*, 17707–17710.

bar was evacuated and refilled with Ar, followed by the addition of 4-hexanolide (2.28g, 20 mmol) and dry CH_2Cl_2 (80 mL). TMSI (16.0 g, 4.0 equiv., 80 mmol) was added drop-wise and the reaction was stirred at room temperature overnight. Then the reaction was poured into ice-water and was stirred for 30 mins. The layers were separated and the aqueous layer was extracted with CH_2Cl_2 (30 mL x 3). The combined organic phase was sequentially washed with $Na_2S_2O_3$ (saturated, aq) and brine, dried over $MgSO_4$, filtered and concentrated under reduced pressure. The received crude material was purified by silica gel chromatography (hexane/ethyl acetate = 1:1) to afford the 4-iodohexanoic acid (**S2**) as a colourless oil (4.84 g, 99% yield). **^{1}H NMR (400 MHz, $CDCl_3$)** δ 4.10 (tt, *J* = 8.9, 4.5 Hz, 1H), 2.71 – 2.61 (m, 1H), 2.60 – 2.49 (m, 1H), 2.19 – 2.00 (m, 2H), 1.95 – 1.72 (m, 2H), 1.05 (t, *J* = 7.2 Hz, 3H) ppm. **^{13}C NMR (101 MHz, $CDCl_3$)** δ 177.5, 40.0, 35.0, 34.1, 34.0, 14.2 ppm. Spectral data was in agreement with the literature.[310]

Isopropyl 4-iodohexanoate (2n). To a stirring solution of 4-iodohexanoic acid (2.42 g, 10 mmol) and isopropanol (1.8 g, 3.0 equiv., 30 mmol) in CH_2Cl_2 (40 mL) was added DMAP (244 mg, 0.2 equiv., 2 mmol) and DCC (2.27 g, 1.1 equiv., 11 mmol) at 0 ºC. The reaction mixture was allowed to stir at 25 °C overnight. The reaction mixture was filtered through a plug of silica and washed through with DCM. The received crude material was concentrated under reduced pressure and purified by silica gel chromatography (hexane/ethyl acetate = 40:1) to yield the isopropyl 4-iodohexanoate as a colourless oil (2.24 g, 79%). **IR (neat, cm^{-1}):** 2976, 2935, 1726, 1455, 1374, 1254, 1180, 1143, 1105. **^{1}H NMR (400 MHz, $CDCl_3$)** δ 5.00 (hept, *J* = 6.3 Hz, 1H), 4.08 (tt, *J* = 9.0, 4.7 Hz, 1H), 2.59 – 2.48 (m, 1H), 2.47 – 2.36 (m, 1H), 2.15 – 1.97 (m, 2H), 1.93 – 1.72 (m, 2H), 1.23 (dd, *J* = 6.3, 1.2 Hz, 6H), 1.03 (t, *J* = 7.2 Hz, 3H) ppm. **^{13}C NMR (101 MHz, $CDCl_3$)** δ 172.3, 68.0, 40.5, 35.3, 34.9, 34.0, 21.98, 21.96, 14.2 ppm. **HRMS** [ESI$^+$] *calcd*. for ($C_9H_{17}IN_aO_2$) [M+Na]$^+$: 307.0165, *found*: 307.0155.

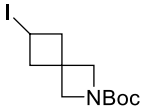

***Tert*-butyl 6-iodo-2-azaspiro[3.3]heptane-2-carboxylate (2o).** Following GP1, using *tert*-butyl 6-hydroxy-2-azaspiro[3.3]heptane-2-carboxylate (852 mg, 4.0 mmol) afforded the title compound as a white solid (246 mg, 19%), by using hexane/EtOAc (20:1) as eluent. **^{1}H NMR (500 MHz, $CDCl_3$)** δ 4.33 – 4.25 (m, 1H), 3.94 (d, *J* = 15.5 Hz, 4H), 2.96 – 2.88 (m, 2H), 2.74 – 2.66 (m, 2H), 1.42 (s, 9H) ppm. **^{13}C NMR (126 MHz, $CDCl_3$)** δ 156.2, 79.7, 61.5, 60.7, 47.2, 38.6, 28.5, 7.6 ppm. Spectral data was in agreement with the literature.[291]

[310] Narayana, C.; Reddy, N. K.; Kabalka, G. W. An Efficient Cleavage of Lactones with Boron Triiodide-N,N-Diethylaniline Complex. *Tetrahedron Lett.* **1991**, *32*, 6855–6856.

(1*S*,4*R*)-2-Iodobicyclo[2.2.1]heptane (2p). Following GP1, using *exo*-Norborneol (448 mg, 4.0 mmol) afforded the title compound as a colourless oil (488 mg, 55%), by using hexane as eluent. **^{1}H NMR (400 MHz, $CDCl_3$, 4:1 dr ratio)** δ 4.29 – 4.22 (m, 0.2H), 4.02 – 3.94 (m, 0.8H), 2.65 – 2.56 (m, 0.8H), 2.44 – 2.37 (m, 0.2H), 2.33 – 2.19 (m, 2H), 2.14 – 2.04 (m, 1H), 1.96 – 1.81 (m, 1H), 1.69 – 1.46 (m, 2H), 1.44 – 1.33 (m, 1H), 1.32 – 1.05 (m, 2H) ppm. **^{13}C NMR (101 MHz, $CDCl_3$, 4:1 dr ratio)** δ 48.2, 45.4, 44.9, 43.5, 38.2, 37.1, 36.5, 36.4, 32.6, 30.5, 29.7, 28.9, 28.63, 28.58 ppm. Spectral data was in agreement with the literature.[311]

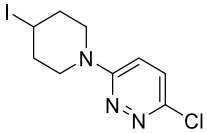

3-Chloro-6-(4-iodopiperidin-1-yl)pyridazine (2r). Following GP1, using 1-(6-chloropyridazin-3-yl)piperidin-4-ol (856 mg, 4.0 mmol) afforded the title compound as a white solid (1.16 g, 90%), by using hexane/EtOAc (3:1 to 2:1) as chromatography eluent. **M.p.**: 123 – 125 °C. **IR (neat, cm^{-1}):** 2980, 2958, 2851, 1582, 1524, 1440, 1158, 993, 825, 763, 647, 472. **^{1}H NMR (500 MHz, $CDCl_3$)** δ 7.20 (d, *J* = 9.5 Hz, 1H), 6.91 (d, *J* = 9.6 Hz, 1H), 4.60 – 4.51 (m, 1H), 3.87 – 3.80 (m, 2H), 3.59 – 3.52 (m, 2H), 2.19 – 2.12 (m, 4H) ppm. **^{13}C NMR (126 MHz, $CDCl_3$)** δ 158.9, 147.0, 129.0, 115.4, 45.6, 36.8, 27.2 ppm. **HRMS** [ESI$^+$] *calcd*. for ($C_9H_{12}ClIN_3$) $[M+H]^+$: 323.9759, *found*: 323.9756.

4.8.3 Synthesis of Product

General procedure 2 (GP2): Copper-catalyzed amination of alkyl iodides.

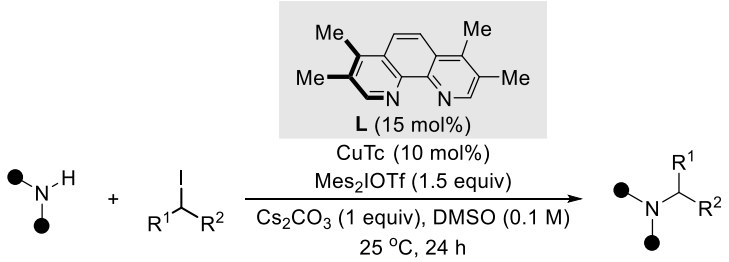

An oven-dried 8 mL screw-cap test tube containing a stirring bar was charged with *N*-nucleophile (1.0 equiv, 0.2 mmol), alkyl iodide (if solid, 1.5 equiv, 0.3 mmol), CuTc (3.8 mg, 10 mol%), 3,4,7,8-tetramethyl-1,10-phenantroline (7.1 mg, 15 mol%) and

311 Tian, X.; Kaur, J.; Yakubov, S.; Barham, J. P. α-Amino Radical Halogen Atom Transfer Agents for Metallaphotoredox-Catalyzed Cross-Electrophile Couplings of Distinct Organic Halides. *ChemSusChem*. **2022**, *15*, e202200906.

diaryliodonium salt (1.5 equiv, 0.3 mmol). The test tube was taken into a nitrogen-filled glovebox where Cs_2CO_3 (65.2 mg, 1.0 equiv) was added. The reaction vessel was sealed with a screw cap septum and removed from the glovebox. Afterwards, alkyl iodide (if liquid) and DMSO (2.0 mL, 0.1 M) was added by syringe. Parafilm was used to reseal the septum. The reaction mixture was stirred at 25 °C for 24 hours. The reaction mixture was diluted ethyl acetate (20 mL) and washed with H_2O (2 x 10 mL) followed by NaCl (saturated, 10 mL). The organic layer was dried (Na_2SO_4), filtered and concentrated under reduced pressure. The received crude material was purified by silica gel chromatography to afford the desired product.

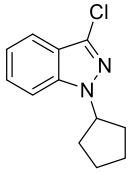

3-Chloro-1-cyclopentyl-1*H*-indazole (3a). Following GP4, using 3-chloro-1*H*-indazole (30.6 mg, 0.20 mmol) and iodocyclopentane (58.8 mg, 0.30 mmol), afforded the title product as a colourless oil (22.7 mg, 51%) after purification by silica gel chromatography (hexane/EtOAc 100:1). In a second independent experiment, 21.8 mg (49%) were obtained, giving an average yield of 50%. **^{1}H NMR (400 MHz, $CDCl_3$)** δ 7.66 (dt, *J* = 8.2, 1.0 Hz, 1H), 7.45 – 7.36 (m, 2H), 7.21 – 7.15 (m, 1H), 4.99 – 4.88 (m, 1H), 2.21 – 2.10 (m, 4H), 2.04 – 1.92 (m, 2H), 1.79 – 1.66 (m, 2H) ppm. **^{13}C NMR (101 MHz, $CDCl_3$)** δ 140.7, 132.2, 127.1, 121.3, 121.1, 119.9, 109.7, 60.0, 32.4, 24.7 ppm. Spectral data was in agreement with the literature.[312]

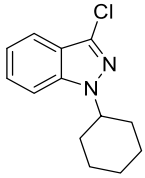

3-Chloro-1-cyclohexyl-1*H*-indazole (3b). Following GP4, using 3-chloro-1*H*-indazole (30.6 mg, 0.20 mmol) and iodocyclohexane (63.0 mg, 0.30 mmol), afforded the title product as a colourless oil (43.1 mg, 92%) after purification by silica gel chromatography (hexane/EtOAc 100:1). In a second independent experiment, 43.4 mg (92%) were obtained, giving an average yield of 92%. **^{1}H NMR (400 MHz, $CDCl_3$)** δ 7.66 (dt, *J* = 8.2, 1.0 Hz, 1H), 7.45 – 7.36 (m, 2H), 7.21 – 7.14 (m, 1H), 4.41 – 4.28 (m, 1H), 2.07 – 1.99 (m, 4H), 1.99 – 1.91 (m, 2H), 1.76 (ddd, *J* = 13.0, 6.4, 3.1 Hz, 1H), 1.53 – 1.39 (m, 2H), 1.38 – 1.26 (m, 1H) ppm. **^{13}C NMR (101 MHz, $CDCl_3$)** δ 140.1, 132.3, 127.1, 121.13, 121.08, 119.9, 109.5, 58.6, 32.6, 25.9, 25.4 ppm. Spectral data

[312] Lv, X.-Y.; Abrams, R.; Martin, R. Copper-Catalyzed C(sp3)-Amination of Ketone-Derived Dihydroquinazolinones by Aromatization-Driven C−C Bond Scission. *Angew. Chem. Int. Ed.* **2023**, *62*, e20221738.

was in agreement with the literature.[312]

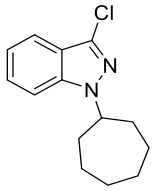

3-Chloro-1-cycloheptyl-7,7a-dihydro-1*H*-indazole (3c). Following GP4, using 3-chloro-1*H*-indazole (30.6 mg, 0.20 mmol) and iodocycloheptane (67.2 mg, 0.30 mmol), afforded the title product as a colourless oil (31.6 mg, 63%) after purification by silica gel chromatography (hexane/EtOAc 100:1). In a second independent experiment, 33.4 mg (67%) were obtained, giving an average yield of 65%. **^{1}H NMR (400 MHz, $CDCl_3$)** δ 7.66 (dt, *J* = 8.2, 0.9 Hz, 1H), 7.44 – 7.36 (m, 2H), 7.22 – 7.12 (m, 1H), 4.62 – 4.50 (m, 1H), 2.26 – 2.13 (m, 2H), 2.13 – 2.02 (m, 2H), 1.94 – 1.82 (m, 2H), 1.77 – 1.51 (m, 6H) ppm. **^{13}C NMR (101 MHz, $CDCl_3$)** δ 139.9, 132.2, 127.1, 121.1, 119.9, 109.7, 61.0, 34.7, 28.0, 25.0 ppm. Spectral data was in agreement with the literature.[312]

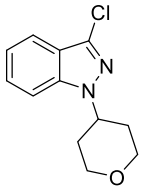

3-Chloro-1-(tetrahydro-2H-pyran-4-yl)-1*H*-indazole (3d). Following GP4, using 3-chloro-1*H*-indazole (30.6 mg, 0.20 mmol) and 4-iodotetrahydro-2*H*-pyran (63.6 mg, 0.30 mmol), afforded the title product as a white solid (44.4 mg, 94%) after purification by silica gel chromatography (hexane/EtOAc 10:1). In a second independent experiment, 44.1 mg (93%) were obtained, giving an average yield of 93%. **^{1}H NMR (400 MHz, $CDCl_3$)** δ 7.72 – 7.63 (m, 1H), 7.49 – 7.37 (m, 2H), 7.24 – 7.15 (m, 1H), 4.59 (tt, J = 11.4, 4.0 Hz, 1H), 4.24 – 4.06 (m, 2H), 3.69 – 3.50 (m, 2H), 2.48 – 2.30 (m, 2H), 2.04 – 1.86 (m, 2H) ppm. **^{13}C NMR (101 MHz, $CDCl_3$)** δ 140.1, 132.9, 127.4, 121.42, 121.37, 120.1, 109.3, 67.3, 55.8, 32.5 ppm. Spectral data was in agreement with the literature.[312]

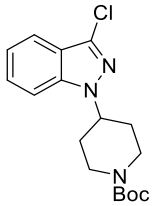

***Tert*-Butyl 4-(3-chloro-1*H*-indazol-1-yl)piperidine-1-carboxylate (3e).** Following GP4, using 3-chloro-1*H*-indazole (30.6 mg, 0.20 mmol) and *tert*-butyl 4-iodopiperidine-1-carboxylate (93.3 mg, 0.30 mmol), afforded the title product as a colourless oil (65.0 mg, 97%) after purification by silica gel chromatography (hexane/EtOAc 10:1). In an independent experiment, 66.8 mg (99%) were obtained,

giving an average yield of 98%.[7] **^{1}H NMR (400 MHz, $CDCl_3$)** δ 7.70 – 7.64 (m, 1H), 7.46 – 7.37 (m, 2H), 7.19 (dt, *J* = 7.8, 3.9 Hz, 1H), 4.50 (tt, *J* = 11.4, 4.1 Hz, 1H), 4.39 – 4.22 (m, 2H), 3.03 – 2.83 (m, 2H), 2.21 (qd, *J* = 12.5, 4.3 Hz, 2H), 2.02 – 1.94 (m, 2H), 1.48 (s, 9H) ppm. **^{13}C NMR (101 MHz, $CDCl_3$)** δ 154.6, 140.2, 132.9, 127.5, 121.5, 121.3, 120.1, 109.3, 80.0, 56.7, 43.1, 31.6, 28.6 ppm. Spectral data was in agreement with the literature.[312]

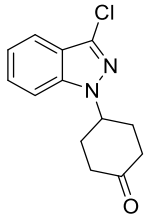

4-(3-Chloro-1*H*-indazol-1-yl)cyclohexan-1-one (3f). Following GP4, using 3-chloro-1*H*-indazole (30.6 mg, 0.20 mmol) and 4-iodocyclohexan-1-one (67.2 mg, 0.30 mmol), afforded the title product as a colourless oil (23.8 mg, 48%) after purification by silica gel chromatography (hexane/EtOAc 10:1 to 5:1). In a second independent experiment, 24.8 mg (50%) were obtained, giving an average yield of 49%. **IR (neat, cm^{-1}):** 2954, 1713, 1615, 1464, 1337, 1172, 950, 741, 634. **^{1}H NMR (400 MHz, $CDCl_3$)** δ 7.72 – 7.65 (m, 1H), 7.48 – 7.41 (m, 2H), 7.22 (dt, *J* = 7.9, 3.9 Hz, 1H), 4.92 – 4.81 (m, 1H), 2.73 – 2.62 (m, 2H), 2.60 – 2.46 (m, 4H), 2.41 – 2.28 (m, 2H) ppm. **^{13}C NMR (101 MHz, $CDCl_3$)** δ 209.0, 140.4, 133.1, 127.6, 121.6, 121.3, 120.1, 109.2, 55.2, 39.3, 31.1 ppm. **HRMS** [ESI$^+$] *calcd*. for ($C_{13}H_{13}ClN_2NaO$) [M+Na]$^+$: 271.0609, *found*: 271.0607.

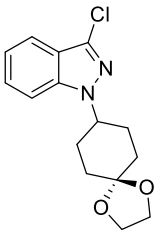

3-Chloro-1-(1,4-dioxaspiro[4.5]decan-8-yl)-1*H*-indazole (3g). Following GP2, using 3-chloro-1*H*-indazole (30.6 mg, 0.20 mmol) and 8-iodo-1,4-dioxaspiro[4.5]decane (80.4 mg, 0.30 mmol), afforded the title product as a white solid (49.9 mg, 85%) after purification by silica gel chromatography (hexane/EtOAc 10:1). In an independent experiment, 51.6 mg (88%) were obtained, giving an average yield of 87%. **^{1}H NMR (400 MHz, $CDCl_3$)** δ 7.69 – 7.62 (m, 1H), 7.47 – 7.35 (m, 2H), 7.21 – 7.14 (m, 1H), 4.45 (tt, *J* = 11.6, 4.0 Hz, 1H), 3.99 (s, 4H), 2.40 (qd, *J* = 13.2, 3.8 Hz, 2H), 2.07 – 1.89 (m, 4H), 1.77 (td, *J* = 13.5, 4.3 Hz, 2H) ppm. **^{13}C NMR (101 MHz, $CDCl_3$)** δ 140.2, 132.4, 127.2, 121.3, 121.2, 119.9, 109.6, 107.7, 64.6, 64.5, 57.4, 33.8, 29.4 ppm. Spectral data was in agreement with the literature.[291]

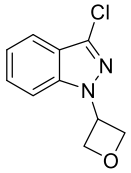

3-Chloro-1-(oxetan-3-yl)-1*H*-indazole (3h). Following GP2, using 3-chloro-1*H*-indazole (30.6 mg, 0.20 mmol) and 3-iodooxetane (55.2 mg, 0.30 mmol), afforded the title product as a white solid (39.3 mg, 95%) after purification by silica gel chromatography (hexane/EtOAc 10:1 to 5:1). In a second independent experiment, 37.9 mg (91%) were obtained, giving an average yield of 92%. **^{1}H NMR (400 MHz, $CDCl_3$)** δ 7.69 (dt, *J* = 8.2, 0.9 Hz, 1H), 7.51 – 7.42 (m, 2H), 7.23 (ddd, *J* = 8.0, 6.1, 1.6 Hz, 1H), 5.73 (tt, *J* = 7.7, 6.4 Hz, 1H), 5.27 (t, *J* = 6.7 Hz, 2H), 5.09 (t, *J* = 7.5 Hz, 2H) ppm. **^{13}C NMR (101 MHz, $CDCl_3$)** δ 140.5, 134.2, 128.0, 121.9, 121.8, 120.2, 109.3, 77.2, 53.0 ppm. Spectral data was in agreement with the literature.[291]

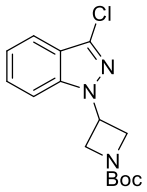

***Tert*-butyl 3-(3-chloro-1*H*-indazol-1-yl)azetidine-1-carboxylate (3i).** Following GP2, using 3-chloro-1*H*-indazole (30.6 mg, 0.20 mmol) and *tert*-butyl 3-iodoazetidine-1-carboxylate (84.9 mg, 0.30 mmol), afforded the title product as a colourless oil (56.4 mg, 92%) after purification by silica gel chromatography (hexane/EtOAc 10:1). In a second independent experiment, 55.4 mg (90%) were obtained, giving an average yield of 91%. **^{1}H NMR (400 MHz, $CDCl_3$)** δ 7.68 (dt, *J* = 8.2, 0.9 Hz, 1H), 7.48 – 7.38 (m, 2H), 7.23 (ddd, *J* = 7.8, 6.5, 1.2 Hz, 1H), 5.32 (tt, *J* = 8.1, 5.7 Hz, 1H), 4.55 – 4.47 (m, 2H), 4.46 – 4.38 (m, 2H), 1.48 (s, 9H) ppm. **^{13}C NMR (101 MHz, $CDCl_3$)** δ 156.2, 140.8, 134.3, 128.1, 122.0, 121.8, 120.3, 109.2, 80.2, 56.1, 47.6, 28.5 ppm. Spectral data was in agreement with the literature.[291]

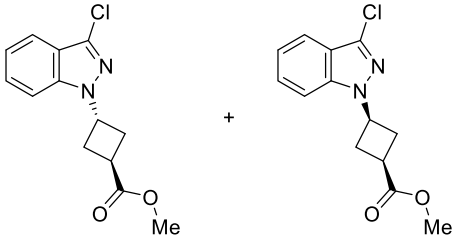

A B

Methyl 3-(3-chloro-1H-indazol-1-yl)cyclobutane-1-carboxylate (3j). Following GP2, using 3-chloro-1*H*-indazole (30.6 mg, 0.20 mmol) and methyl 3-iodocyclobutane-1-carboxylate (72.0 mg, 0.30 mmol), afforded **A** as a colourless oil (23.1 mg, 44%), **B** as a colourless oil (29.9 mg, 56%) after purification by silica gel chromatography (hexane/EtOAc 10:1). In a second independent experiment, 24.3 mg (46%) **A** and 28.7

mg (54%) **B** were obtained, giving an average yield of 99% (**A**+**B**), average ratio: **A**(*trans*)/**B**(*cis*) = 0.8 : 1. **A** (*trans*): **^{1}H NMR (400 MHz, CDCl$_3$)** δ 7.65 (d, *J* = 8.2 Hz, 1H), 7.45 – 7.37 (m, 2H), 7.23 – 7.14 (m, 1H), 5.38 – 5.28 (m, 1H), 3.78 (s, 3H), 3.31 – 3.20 (m, 1H), 3.12 – 3.00 (m, 2H), 2.84 – 2.73 (m, 2H) ppm. **^{13}C NMR (101 MHz, CDCl$_3$)** δ 176.5, 140.6, 133.5, 127.6, 121.6, 121.3, 119.9, 109.4, 52.2, 50.7, 33.1, 32.5 ppm. Spectral data was in agreement with the literature.[240] **B** (*cis*): **IR (neat, cm^{-1}):** 2998, 2952, 1729, 1616, 1466, 1337, 1199, 1167, 995, 741, 633. **^{1}H NMR (400 MHz, CDCl$_3$)** δ 7.65 (d, *J* = 8.2 Hz, 1H), 7.50 – 7.37 (m, 2H), 7.23 – 7.16 (m, 1H), 5.00 – 4.89 (m, 1H), 3.74 (s, 3H), 3.15 – 2.95 (m, 3H), 2.84 – 2.72 (m, 2H) ppm. **^{13}C NMR (101 MHz, CDCl$_3$)** δ 174.3, 140.4, 133.3, 127.5, 121.6, 121.5, 120.0, 109.6, 52.1, 49.2, 33.3, 31.3 ppm. **HRMS** [ESI$^+$] *calcd*. for ($C_{13}H_{13}ClN_2NaO_2$) [M+Na]$^+$: 287.0558, *found*: 287.0561.

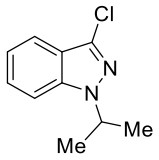

3-Chloro-1-isopropyl-1*H*-indazole (3k). Following GP4, using 3-chloro-1*H*-indazole (30.6 mg, 0.20 mmol) and 2-iodopropane (51.0 mg, 0.30 mmol), afforded the title product as a colourless oil (30.0 mg, 77%) after purification by silica gel chromatography (hexane/EtOAc 100:1). In a second independent experiment, 30.0 mg (77%) were obtained, giving an average yield of 77%. **^{1}H NMR (400 MHz, CDCl$_3$)** δ 7.67 (dt, *J* = 8.2, 1.0 Hz, 1H), 7.44 – 7.37 (m, 2H), 7.23 – 7.14 (m, 1H), 4.79 (hept, *J* = 6.7 Hz, 1H), 1.58 (d, *J* = 6.7 Hz, 6H) ppm. **^{13}C NMR (101 MHz, CDCl$_3$)** δ 140.1, 132.4, 127.2, 121.19, 121.16, 119.9, 109.5, 50.9, 22.2 ppm. Spectral data was in agreement with the literature.[312]

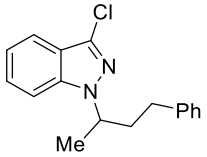

3-Chloro-1-(4-phenylbutan-2-yl)-1*H*-indazole (3l). Following GP4, using 3-chloro-1*H*-indazole (30.6 mg, 0.20 mmol) and (3-iodobutyl)benzene (78.0 mg, 0.30 mmol), afforded the title product as a colourless oil (47.5 mg, 83%) after purification by silica gel chromatography (hexane/EtOAc 100:1). In a second independent experiment, 46.5 mg (82%) were obtained, giving an average yield of 82%. **^{1}H NMR (400 MHz, CDCl$_3$)** δ 7.69 (d, *J* = 8.2 Hz, 1H), 7.40 (ddd, *J* = 8.0, 6.9, 1.0 Hz, 1H), 7.30 – 7.23 (m, 3H), 7.23 – 7.16 (m, 2H), 7.09 – 7.03 (m, 2H), 4.63 – 4.50 (m, 1H), 2.61 – 2.41 (m, 3H), 2.22 – 2.10 (m, 1H), 1.56 (d, *J* = 6.7 Hz, 3H) ppm. **^{13}C NMR (101 MHz, CDCl$_3$)** δ 141.1, 140.8, 132.9, 128.6, 128.5, 127.2, 126.1, 121.2, 121.0, 119.9, 109.5, 54.3, 37.7, 32.6, 21.0 ppm. Spectral data was in agreement with the literature.[291]

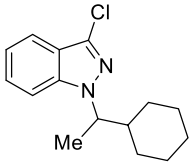

3-Chloro-1-(1-cyclohexylethyl)-1*H*-indazole (3m). Following GP2, using 3-chloro-1*H*-indazole (30.6 mg, 0.20 mmol) and (1-iodoethyl)cyclohexane (71.4 mg, 0.30 mmol), afforded the title product as a colourless oil (31.6 mg, 60%) after purification by silica gel chromatography (hexane/EtOAc 100:1). In a second independent experiment, 32.7 mg (62%) were obtained, giving an average yield of 61%. **IR (neat, cm^{-1}):** 2924, 2851, 1615, 1463, 1337, 1202, 1128, 969, 739. **^{1}H NMR (400 MHz, CDCl$_3$)** δ 7.68 (dt, *J* = 8.2, 1.0 Hz, 1H), 7.45 – 7.38 (m, 2H), 7.23 – 7.15 (m, 1H), 4.34 – 4.23 (m, 1H), 2.04 – 1.90 (m, 2H), 1.84 – 1.75 (m, 1H), 1.70 – 1.55 (m, 5H), 1.36 – 1.23 (m, 1H), 1.22 – 0.98 (m, 4H), 0.93 – 0.78 (m, 1H) ppm. **^{13}C NMR (101 MHz, CDCl$_3$)** δ 141.2 132.4, 127.1, 121.0, 120.7, 119.9, 109.7, 60.4, 43.7, 30.4, 30.2, 26.3, 26.1, 25.9, 18.2 ppm. **HRMS** [ESI$^+$] *calcd.* for ($C_{15}H_{20}ClN_2$) [M+H]$^+$: 263.1310, *found*: 263.1306.

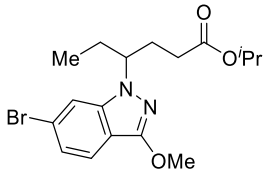

Isopropyl 4-(6-bromo-3-methoxy-1*H*-indazol-1-yl)hexanoate (3n). Following GP2, using 6-bromo-3-methoxy-1*H*-indazole (45.4 mg, 0.20 mmol) and isopropyl 4-iodohexanoate (85.2 mg, 0.30 mmol), afforded the title product as a colourless oil (56.6 mg, 74%) after purification by silica gel chromatography (hexane/EtOAc 40:1). In a second independent experiment, 59.8 mg (78%) were obtained, giving an average yield of 76%. **IR (neat, cm^{-1}):** 2924, 2851, 1615, 1463, 1337, 1202, 1128, 969, 739. **^{1}H NMR (400 MHz, CDCl$_3$)** δ 7.46 (d, *J* = 8.5 Hz, 1H), 7.37 (d, *J* = 1.2 Hz, 1H), 7.09 (dd, *J* = 8.5, 1.5 Hz, 1H), 4.96 (hept, *J* = 6.3 Hz, 1H), 4.25 – 4.13 (m, 1H), 4.05 (s, 3H), 2.32 – 2.19 (m, 1H), 2.17 – 1.90 (m, 4H), 1.87 – 1.74 (m, 1H), 1.17 (dd, *J* = 6.3, 3.5 Hz, 6H), 0.72 (t, *J* = 7.4 Hz, 3H) ppm. **^{13}C NMR (101 MHz, CDCl$_3$)** δ 172.9, 156.6, 143.2, 122.4, 121.8, 121.3, 111.4, 110.9, 67.9, 59.5, 56.4, 31.1, 29.7, 28.2, 22.0, 21.9, 11.2 ppm. **HRMS** [ESI$^+$] *calcd*. for ($C_{17}H_{23}BrN_2NaO_3$) [M+Na]$^+$: 405.0784, *found*: 405.0782.

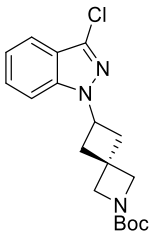

***Tert*-butyl 6-(3-chloro-1*H*-indazol-1-yl)-2-azaspiro[3.3]heptane-2-carboxylate (3o).** Following GP2, using 3-chloro-1*H*-indazole (30.6 mg, 0.20 mmol) and *tert*-butyl 6-

iodo-2-azaspiro[3.3]heptane-2-carboxylate (96.9 mg, 0.30 mmol), afforded the title product as a colourless oil (67.6 mg, 97%) after purification by silica gel chromatography (hexane/EtOAc 10:1). In an independent experiment, 69.6 mg (99%) were obtained, giving an average yield of 99%. **^{1}H NMR (400 MHz, $CDCl_3$)** δ 7.64 (dt, *J* = 8.2, 0.9 Hz, 1H), 7.43 – 7.32 (m, 2H), 7.18 (ddd, *J* = 7.8, 6.7, 1.0 Hz, 1H), 4.94 – 4.83 (m, 1H), 4.08 (s, 2H), 3.98 (s, 2H), 2.98 – 2.88 (m, 2H), 2.78 – 2.68 (m, 2H), 1.44 (s, 9H) ppm. **^{13}C NMR (101 MHz, $CDCl_3$)** δ 156.3, 140.5, 133.3, 127.6, 121.5, 121.4, 120.0, 109.3, 79.6, 61.7, 60.3, 47.8, 40.6, 31.8, 28.5 ppm. Spectral data was in agreement with the literature.[291]

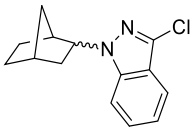

1-((1S,4R)-Bicyclo[2.2.1]heptan-2-yl)-3-chloro-1H-indazole (3p). Following GP2, using 3-chloro-1*H*-indazole (30.6 mg, 0.20 mmol) and (1*S*,4*R*)-2-iodobicyclo[2.2.1]heptane (66.6 mg, 0.30 mmol), afforded the title product as a colourless oil (33.5 mg, 68%) after purification by silica gel chromatography (hexane/EtOAc 100:1). In an independent experiment, 31.7 mg (64%) were obtained, giving an average yield of 66%. **^{1}H NMR (400 MHz, $CDCl_3$, 16:1 dr ratio)** δ 7.70 – 7.62 (m, 1H), 7.45 – 7.36 (m, 2H), 7.24 – 7.14 (m, 1H), 4.85 (dtd, *J* = 11.2, 4.4, 1.9 Hz, 0.06H), 4.46 – 4.37 (m, 0.94H), 2.71 – 2.65 (m, 0.06H), 2.56 – 2.38 (m, 2.94H), 2.15 – 2.05 (m, 0.06 H), 2.05 – 1.95 (m, 0.94H), 1.94 – 1.83 (m, 1H), 1.71 – 1.55 (m, 2H), 1.52 – 1.46 (m, 0.06H), 1.42 – 1.33 (m, 0.94H), 1.33 – 1.20 (m, 2H) ppm. **^{13}C NMR (101 MHz, $CDCl_3$, mixture of diasteromers)** δ 141.4, 140.6, 131.7, 127.04, 127.01, 121.8, 121.5, 121.2, 119.8, 110.0, 109.8, 61.7, 60.8, 43.2, 42.2, 38.9, 37.3, 36.9, 35.99, 35.95, 32.9, 29.3, 28.8, 27.4, 22.4 ppm. Spectral data was in agreement with the literature.[313]

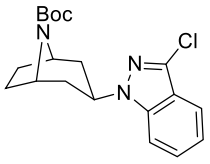

***Tert*-butyl 3-*exo*-(3-Chloro-1*H*-indazol-1-yl)-8-azabicyclo[3.2.1]octane-8-carboxylate (3q).** Following GP2, using 3-chloro-1*H*-indazole (30.6 mg, 0.20 mmol) and 8-azabicyclo[3.2.1]octane-8-carboxylic acid, 3-iodo-, 1,1-dimethylethyl ester (101.1 mg, 0.30 mmol), afforded the title product as a white solid (65.6 mg, 90%) after purification by silica gel chromatography (hexane/EtOAc 10:1). In a second independent experiment, 63.9 mg (88%) were obtained, giving an average yield of 89%. **^{1}H NMR (400 MHz, $CDCl_3$)** δ 7.69 – 7.63 (m, 1H), 7.42 – 7.34 (m, 2H), 7.22 – 7.13

[313] Dow, N. W.; Cabre, A.; MacMillan, D. W. C. A General *N*-Alkylation Platform via Copper Metallaphotoredox and Silyl Radical Activation of Alkyl Halides. *Chem* **2021**, *7*, 1827–1843.

(m, 1H), 4.94 (tt, *J* = 11.8, 5.7 Hz, 1H), 4.40 (brs, 2H), 2.55 – 2.39 (m, 2H), 2.16 – 2.05 (m, 2H), 1.97 – 1.88 (m, 2H), 1.86 – 1.78 (m, 2H), 1.53 (s, 9H) ppm. **^{13}C NMR (101 MHz, CDCl$_3$)** δ 153.5, 139.9, 132.6, 127.3, 121.7, 121.4, 120.2, 109.7, 79.8, 53.4, 52.8, 52.4, 36.6, 36.3, 28.6, 27.9 ppm. Spectral data was in agreement with the literature.[291]

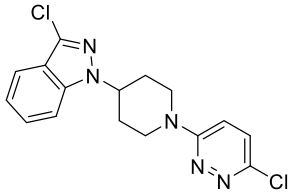

3-Chloro-1-(1-(6-chloropyridazin-3-yl)piperidin-4-yl)-1*H*-indazole (3r). Following GP4, using 3-chloro-1*H*-indazole (30.6 mg, 0.20 mmol) and 3-chloro-6-(4-iodopiperidin-1-yl)pyridazine (97.2 mg, 0.30 mmol), afforded the title product as a white solid (49.7 mg, 71%) after purification by silica gel chromatography (hexane/EtOAc 3:1 to 1:1). In a second independent experiment, 48.8 mg (70%) were obtained, giving an average yield of 71%. **M.p.**: 124 – 125 °C. **IR (neat, cm^{-1}):** 2960, 2896, 1582, 1458, 1333, 1238, 1006, 922, 830, 766, 732, 563. **^{1}H NMR (400 MHz, CDCl$_3$)** δ 7.67 (dt, *J* = 8.2, 0.9 Hz, 1H), 7.47 – 7.39 (m, 2H), 7.25 – 7.16 (m, 2H), 6.98 (d, *J* = 9.6 Hz, 1H), 4.67 (tt, *J* = 11.2, 4.2 Hz, 1H), 4.57 – 4.48 (m, 2H), 3.28 – 3.16 (m, 2H), 2.34 (qd, *J* = 12.6, 12.0, 4.2 Hz, 2H), 2.17 – 2.09 (m, 2H) ppm. **^{13}C NMR (101 MHz, CDCl$_3$)** δ 158.8, 147.0, 140.2, 133.1, 129.0, 127.6, 121.6, 121.3, 120.1, 115.6, 109.2, 56.3, 44.9, 31.0 ppm. **HRMS** [ESI$^+$] *calcd*. for ($C_{16}H_{16}Cl_2N_5$) [M+H]$^+$: 348.0777, *found*: 348.0777.

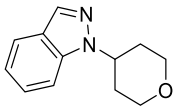

1-(Tetrahydro-2*H*-pyran-4-yl)-1*H*-indazole (5a). Following GP2, using 1*H*-indazole (23.6 mg, 0.20 mmol) and 4-iodotetrahydro-2*H*-pyran (63.6 mg, 0.30 mmol), afforded the title product as a white solid (28.4 mg, 70%) after purification by silica gel chromatography (hexane/EtOAc 10:1). In a second independent experiment, 28.1 mg (70%) were obtained, giving an average yield of 70%. **^{1}H NMR (400 MHz, CDCl$_3$)** δ 8.05 – 7.99 (m, 1H), 7.74 (dt, *J* = 8.1, 1.0 Hz, 1H), 7.47 (dd, *J* = 8.5, 0.8 Hz, 1H), 7.42 – 7.34 (m, 1H), 7.15 (ddd, *J* = 7.8, 6.8, 0.9 Hz, 1H), 4.65 (tt, *J* = 11.5, 4.2 Hz, 1H), 4.22 – 4.13 (m, 2H), 3.63 (td, *J* = 12.0, 2.1 Hz, 2H), 2.50 – 2.35 (m, 2H), 2.03 – 1.94 (m, 2H) ppm. **^{13}C NMR (101 MHz, CDCl$_3$)** δ 138.7, 133.0, 126.1, 124.3, 121.4, 120.7, 109.0, 67.4, 55.3, 32.5 ppm. Spectral data was in agreement with the literature.[314]

[314] Nguyen, V. T.; Nguyen, V. D.; Haug, G. C.; Vuong, N. T. H.; Dang, H. T.; Arman, H. D.; Larionov, O. V. Visible-Light-Enabled Direct Decarboxylative *N*-Alkylation. *Angew. Chem. Int. Ed*. **2020**, *59*, 7921–7927.

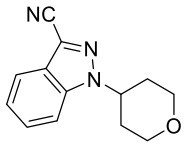

1-(Tetrahydro-2*H*-pyran-4-yl)-1*H*-indazole-3-carbonitrile (5b). Following GP2, using 1*H*-indazole-3-carbonitrile (28.6 mg, 0.20 mmol) and 4-iodotetrahydro-2*H*-pyran (63.6 mg, 0.30 mmol), afforded the title product as a white solid (29.5 mg, 65%) after purification by silica gel chromatography (hexane/EtOAc 5:1 to 3:1). In a second independent experiment, 25.7 mg (57%) were obtained, giving an average yield of 61%. **^{1}H NMR (400 MHz, $CDCl_3$)** δ 7.83 (dt, *J* = 8.2, 0.9 Hz, 1H), 7.63 – 7.57 (m, 1H), 7.53 – 7.47 (m, 1H), 7.35 (ddd, *J* = 7.8, 6.9, 0.8 Hz, 1H), 4.75 (tt, *J* = 11.4, 4.2 Hz, 1H), 4.23 – 4.13 (m, 2H), 3.63 (td, *J* = 12.0, 2.1 Hz, 2H), 2.47 – 2.33 (m, 2H), 2.07 – 1.98 (m, 2H) ppm. **^{13}C NMR (101 MHz, $CDCl_3$)** δ 138.9, 127.7, 125.7, 123.8, 119.9, 117.8, 113.9, 110.1, 67.0, 56.5, 32.3 ppm. Spectral data was in agreement with the literature.[312]

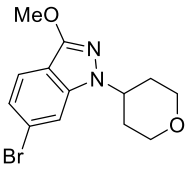

6-Bromo-3-methoxy-1-(tetrahydro-2*H*-pyran-4-yl)-1*H*-indazole (5c). Following GP2, using 6-bromo-3-methoxy-1*H*-indazole (45.4 mg, 0.20 mmol) and 4-iodotetrahydro-2*H*-pyran (63.6 mg, 0.30 mmol), afforded the title product as a white solid (56.9 mg, 91%) after purification by silica gel chromatography (hexane/EtOAc 20:1 to 10:1). In a second independent experiment, 53.2 mg (86%) were obtained, giving an average yield of 89%. **M.p.**: 103 – 105 °C. **IR (neat, cm^{-1}):** 3064, 2959, 2928, 2846, 1613, 1533, 1405, 1351, 1290, 1215, 1143, 885, 791, 590, 552. **^{1}H NMR (400 MHz, $CDCl_3$)** δ 7.51 – 7.45 (m, 2H), 7.14 – 7.09 (m, 1H), 4.36 (tt, *J* = 11.4, 4.2 Hz, 1H), 4.17 – 4.10 (m, 2H), 4.06 (s, 3H), 3.56 (td, *J* = 12.0, 2.1 Hz, 2H), 2.40 – 2.25 (m, 2H), 1.91 – 1.81 (m, 2H) ppm. **^{13}C NMR (101 MHz, $CDCl_3$)** δ 156.3, 141.4, 122.7, 121.7, 121.4, 111.8, 111.5, 67.3, 56.3, 54.9, 32.1 ppm. **HRMS** [ESI$^+$] *calcd*. for ($C_{13}H_{16}BrN_2O_2$) $[M+H]^+$: 311.0390, *found*: 311.0389.

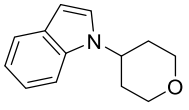

1-(Tetrahydro-2*H*-pyran-4-yl)-1*H*-indole (5d). Following GP2, using 1*H*-indole (23.4 mg, 0.20 mmol) and 4-iodotetrahydro-2*H*-pyran (63.6 mg, 0.30 mmol), afforded the title product as a colourless oil (29.6 mg, 74%) after purification by silica gel chromatography (hexane/EtOAc 20:1 to 10:1). In a second independent experiment, 31.2 mg (78%) were obtained, giving an average yield of 76%.**^{1}H NMR (400 MHz, $CDCl_3$)** δ 7.72 – 7.65 (m, 1H), 7.43 (d, *J* = 8.2 Hz, 1H), 7.29 – 7.22 (m, 2H), 7.19 – 7.12 (m, 1H), 6.58 (d, *J* = 2.9 Hz, 1H), 4.49 (tt, *J* = 11.4, 4.5 Hz, 1H), 4.22 – 4.14 (m,

2H), 3.64 (td, *J* = 11.8, 2.5 Hz, 2H), 2.19 – 2.02 (m, 4H) ppm. **^{13}C NMR (101 MHz, $CDCl_3$)** δ 135.5, 128.7, 123.9, 121.5, 121.3, 119.7, 109.3, 101.8, 67.6, 52.4, 33.5 ppm. Spectral data was in agreement with the literature.[315]

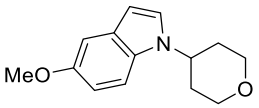

5-Methoxy-1-(tetrahydro-2*H*-pyran-4-yl)-1*H*-indole (5e). Following GP2, using 5-methoxy-1*H*-indole (29.4 mg, 0.20 mmol) and 4-iodotetrahydro-2*H*-pyran (63.6 mg, 0.30 mmol), afforded the title product as a white solid (29.7 mg, 64%) after purification by silica gel chromatography (hexane/EtOAc 10:1 to 6:1). In a second independent experiment, 29.9 mg (65%) were obtained, giving an average yield of 65%. **M.p.**: 137 – 138 °C. **IR (neat, cm^{-1}):** 2956, 2848, 1484, 1451, 1240, 1137, 1084, 1007, 803, 726, 572. **^{1}H NMR (400 MHz, $CDCl_3$)** δ 7.30 (d, *J* = 8.9 Hz, 1H), 7.20 (d, *J* = 3.2 Hz, 1H), 7.12 (d, *J* = 2.4 Hz, 1H), 6.90 (dd, *J* = 8.9, 2.4 Hz, 1H), 6.50 – 6.45 (m, 1H), 4.46 – 4.35 (m, 1H), 4.21 – 4.10 (m, 2H), 3.87 (s, 3H), 3.61 (td, *J* = 11.7, 2.8 Hz, 2H), 2.16 – 1.99 (m, 4H) ppm. **^{13}C NMR (101 MHz, $CDCl_3$)** δ 154.2, 130.9, 129.0, 124.5, 111.9, 110.0, 102.8, 101.3, 67.6, 56.0, 52.6, 33.5 ppm. **HRMS** [ESI$^+$] *calcd*. for ($C_{14}H_{18}NO_2$) [M+H]$^+$: 232.1332, *found*: 232.1322.

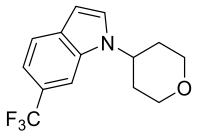

1-(Tetrahydro-2*H*-pyran-4-yl)-6-(trifluoromethyl)-1*H*-indole (5f). Following GP2, using ethyl 6-(trifluoromethyl)-1*H*-indole (37.0 mg, 0.20 mmol) and 4-iodotetrahydro-2*H*-pyran (63.6 mg, 0.30 mmol), afforded the title product as a white solid (39.9 mg, 74%) after purification by silica gel chromatography (hexane/EtOAc 20:1 to 10:1). In a second independent experiment, 38.5 mg (72%) were obtained, giving an average yield of 73%. **M.p.**: 112 – 114 °C. **IR (neat, cm^{-1}):** 2925, 2850, 1462, 1341, 1275, 1219, 1143, 1086, 1056, 913, 815, 662, 508. **^{1}H NMR (400 MHz, $CDCl_3$)** δ 7.72 (d, *J* = 8.3 Hz, 1H), 7.68 (s, 1H), 7.40 – 7.33 (m, 2H), 6.63 – 6.59 (m, 1H), 4.57 – 4.46 (m, 1H), 4.23 – 4.13 (m, 2H), 3.66 (td, *J* = 11.8, 2.6 Hz, 2H), 2.19 – 2.02 (m, 4H) ppm. **^{13}C NMR (101 MHz, $CDCl_3$)** δ 134.5, 131.0, 126.7, 125.5 (q, $J_{C,F}$ = 271.3 Hz), 123.7 (q, $J_{C,F}$ = 31.8 Hz), 121.6, 116.4 (q, $J_{C,F}$ = 3.5 Hz), 106.8 (q, $J_{C,F}$ = 4.4 Hz), 102.3, 67.5, 52.7, 33.6 ppm. **^{19}F NMR (376 MHz, $CDCl_3$)** δ -60.4 ppm. **HRMS** [APCI$^+$] *calcd*. for ($C_{14}H_{15}F_3NO$) [M+H]$^+$: 270.1100, *found*: 270.1096.

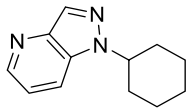

[315] Wang, Z.; Zeng, H.; Li, C.-J. Dearomatization–Rearomatization Strategy for Reductive Cross-Coupling of Indoles with Ketones in Water. *Org. Lett.* **2019**, *21*, 2302–2306.

1-Cyclohexyl-1*H*-pyrazolo[4,3-*b*]pyridine (5g). Following GP2, using 1*H*-pyrazolo[4,3-*b*]pyridine (23.8 mg, 0.20 mmol) and iodocyclohexane (63.0 mg, 0.30 mmol), afforded the title product as a colourless oil (27.3 mg, 68%) after purification by silica gel chromatography (hexane/EtOAc 3:1). In a second independent experiment, 27.9 mg (69%) were obtained, giving an average yield of 69%. **IR (neat, cm-1):** 2931, 2855, 1561, 1427, 1264, 1166, 1020, 913, 892, 832, 787, 755, 562. **^{1}H NMR (400 MHz, $CDCl_3$)** δ 8.56 (d, *J* = 3.5 Hz, 1H), 8.24 (s, 1H), 7.82 (dt, *J* = 8.6, 1.1 Hz, 1H), 7.30 – 7.22 (m, 1H), 4.46 – 4.34 (m, 1H), 2.12 – 2.01 (m, 4H), 2.01 – 1.92 (m, 2H), 1.84 – 1.74 (m, 1H), 1.57 – 1.42 (m, 2H), 1.41 – 1.28 (m, 1H) ppm. **^{13}C NMR (101 MHz, $CDCl_3$)** δ 145.4, 141.9, 133.4, 131.5, 120.2, 117.2, 58.9, 32.6, 25.8, 25.4 ppm. **HRMS** [ESI$^+$] *calcd*. for ($C_{12}H_{16}N_3$) $[M+H]^+$: 202.1339, *found*: 202.1344.

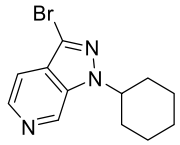

3-Bromo-1-cyclohexyl-1*H*-pyrazolo[3,4-*c*]pyridine (5h). Following GP2, using 3-bromo-1*H*-pyrazolo[3,4-*c*]pyridine (39.6 mg, 0.20 mmol) and iodocyclohexane (63.0 mg, 0.30 mmol), afforded the title product as a white solid (46.2 mg, 83%) after purification by silica gel chromatography (hexane/EtOAc 5:1 to 3:1). In a second independent experiment, 46.0 mg (82%) were obtained, giving an average yield of 82%. **^{1}H NMR (400 MHz, $CDCl_3$)** δ 9.00 (s, 1H), 8.34 (d, *J* = 5.4 Hz, 1H), 7.54 – 7.41 (m, 1H), 4.49 (tt, *J* = 10.1, 5.0 Hz, 1H), 2.13 – 2.01 (m, 4H), 2.00 – 1.91 (m, 2H), 1.83 – 1.71 (m, 1H), 1.57 – 1.39 (m, 2H), 1.38 – 1.25 (m, 1H) ppm. **^{13}C NMR (101 MHz, $CDCl_3$)** δ 139.3, 134.1, 127.6, 119.4, 113.9, 60.0, 32.9, 25.7, 25.3 ppm. Spectral data was in agreement with the literature.[312]

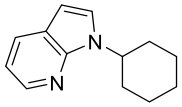

1-Cyclohexyl-1*H*-pyrrolo[2,3-*b*]pyridine (5i). Following GP2, using 1*H*-pyrrolo[2,3-*b*]pyridine (23.6 mg, 0.20 mmol) and iodocyclohexane (63.0 mg, 0.30 mmol), afforded the title product as a colourless oil (33.1 mg, 83%) after purification by silica gel chromatography (hexane/EtOAc 20:1). In a second independent experiment, 32.5 mg (81%) were obtained, giving an average yield of 82%. **IR (neat, cm-1):** 3048, 2929, 2853, 1592, 1505, 1426, 1302, 1278, 1206, 1114, 996, 894, 772, 713, 495. **^{1}H NMR (400 MHz, $CDCl_3$)** δ 8.32 (dd, *J* = 4.7, 1.5 Hz, 1H), 7.89 (dd, *J* = 7.8, 1.6 Hz, 1H), 7.31 (d, *J* = 3.6 Hz, 1H), 7.04 (dd, *J* = 7.8, 4.7 Hz, 1H), 6.45 (d, *J* = 3.6 Hz, 1H), 4.81 (tt, *J* = 11.9, 3.8 Hz, 1H), 2.17 – 2.06 (m, 2H), 1.96 – 1.86 (m, 2H), 1.84 – 1.50 (m, 5H), 1.35 – 1.21 (qt, *J* = 12.9, 3.7 Hz, 1H) ppm. **^{13}C NMR (101 MHz, $CDCl_3$)** δ 147.1, 142.5, 128.8, 124.8, 120.8, 115.7, 99.4, 52.9, 33.8, 25.9, 25.7 ppm. **HRMS** [ESI$^+$] *calcd*. for ($C_{13}H_{17}N_2$) $[M+H]^+$: 201.1386, *found*: 201.1392.

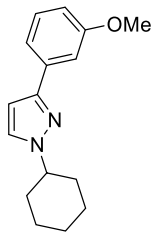

1-Cyclohexyl-3-(3-methoxyphenyl)-1*H*-pyrazole (5j). Following GP2, using 3-(3-methoxyphenyl)-1*H*-pyrazole (34.8 mg, 0.20 mmol) and iodocyclohexane (63.0 mg, 0.30 mmol), afforded the title product as a colourless oil (49.9 mg, 97%) after purification by silica gel chromatography (hexane/EtOAc 20:1). In a second independent experiment, 49.9 mg (97%) were obtained, giving an average yield of 97%. **^{1}H NMR (400 MHz, $CDCl_3$)** δ 7.43 (d, *J* = 2.3 Hz, 1H), 7.41 – 7.37 (m, 2H), 7.33 – 7.27 (m, 1H), 6.86 – 6.81 (m, 1H), 6.52 (d, *J* = 2.3 Hz, 1H), 4.17 (tt, *J* = 11.8, 3.8 Hz, 1H), 3.87 (s, 3H), 2.27 – 2.18 (m, 2H), 1.96 – 1.86 (m, 2H), 1.80 – 1.66 (m, 3H), 1.52 – 1.38 (m, 2H), 1.34 – 1.20 (m, 1H) ppm. **^{13}C NMR (101 MHz, $CDCl_3$)** δ 160.0, 150.5, 135.4, 129.7, 127.6, 118.3, 113.4, 110.9, 102.5, 61.5, 55.4, 33.8, 25.6 ppm. Spectral data was in agreement with the literature.[312]

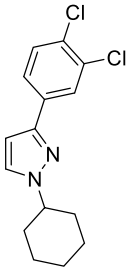

1-Cyclohexyl-3-(3,4-dichlorophenyl)-1*H*-pyrazole (5k). Following GP2, using 3-(3,4-dichlorophenyl)-1*H*-pyrazole (42.6 mg, 0.20 mmol) and iodocyclohexane (63.0 mg, 0.30 mmol), afforded the title product as a colourless oil (59.0 mg, 99%) after purification by silica gel chromatography (hexane/EtOAc 100:1). In a second independent experiment, 56.3 mg (95%) were obtained, giving an average yield of 97%. **^{1}H NMR (400 MHz, $CDCl_3$)** δ 7.90 (d, J = 2.0 Hz, 1H), 7.61 (dd, J = 8.3, 2.0 Hz, 1H), 7.47 – 7.40 (m, 2H), 6.50 (d, J = 2.3 Hz, 1H), 4.14 (tt, J = 11.7, 3.8 Hz, 1H), 2.25 – 2.15 (m, 2H), 1.97 – 1.87 (m, 2H), 1.81 – 1.67 (m, 3H), 1.45 (qt, J = 13.0, 3.3 Hz, 2H), 1.35 – 1.21 (m, 1H) ppm. **^{13}C NMR (101 MHz, $CDCl_3$)** δ 148.4, 134.2, 132.8, 131.1, 130.6, 128.1, 127.4, 124.9, 102.5, 61.7, 33.8, 25.52, 25.50 ppm. Spectral data was in agreement with the literature.[312]

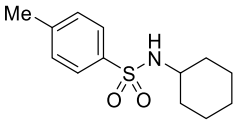

***N*-cyclohexyl-4-methylbenzenesulfonamide (5l).** Following GP2, using 4-methylbenzenesulfonamide (34.2 mg, 0.20 mmol) and iodocyclohexane (63.0 mg, 0.30 mmol), afforded the title product as a white solid (50.6 mg, 99%) after purification by

silica gel chromatography (hexane/EtOAc 10:1 to 5:1). In a second independent experiment, 50.3 mg (99%) were obtained, giving an average yield of 99%. **^{1}H NMR (400 MHz, $CDCl_3$)** δ 7.79 – 7.73 (m, 2H), 7.31 – 7.26 (m, 2H), 4.82 (d, *J* = 7.5 Hz, 1H), 3.16 – 3.04 (m, 1H), 2.41 (s, 3H), 1.80 – 1.67 (m, 2H), 1.65 – 1.54 (m, 2H), 1.53 – 1.43 (m, 1H), 1.29 – 1.02 (m, 5H) ppm. **^{13}C NMR (101 MHz, $CDCl_3$)** δ 143.2, 138.6, 129.7, 127.0, 52.7, 34.0, 25.2, 24.7, 21.6 ppm. Spectral data was in agreement with the literature.[312]

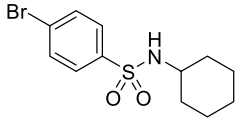

4-Bromo-*N*-cyclohexylbenzenesulfonamide (5m). Following GP2, using 4-bromobenzenesulfonamide (47.2 mg, 0.20 mmol) and iodocyclohexane (63.0 mg, 0.30 mmol), afforded the title product as a white solid (63.6 mg, 99%) after purification by silica gel chromatography (hexane/EtOAc 10:1 to 5:1). In a second independent experiment, 63.6 mg (99%) were obtained, giving an average yield of 99%. **^{1}H NMR (400 MHz, $CDCl_3$)** δ 7.78 – 7.72 (m, 2H), 7.67 – 7.60 (m, 2H), 4.88 (d, *J* = 7.6 Hz, 1H), 3.18 – 3.07 (m, 1H), 1.79 – 1.68 (m, 2H), 1.67 – 1.58 (m, 2H), 1.55 – 1.45 (m, 1H), 1.30 – 1.03 (m, 5H) ppm. **^{13}C NMR (101 MHz, $CDCl_3$)** δ 140.7, 132.4, 128.6, 127.4, 52.9, 34.0, 25.2, 24.7 ppm. Spectral data was in agreement with the literature.[312]

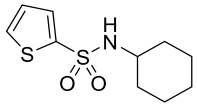

***N*-cyclohexylthiophene-2-sulfonamide (5n).** Following GP2, using thiophene-2-sulfonamide (32.6 mg, 0.20 mmol) and iodocyclohexane (63.0 mg, 0.30 mmol), afforded the title product as a white solid (49.0 mg, 99%) after purification by silica gel chromatography (hexane/EtOAc 10:1 to 5:1). In a second independent experiment, 49.0 mg (99%) were obtained, giving an average yield of 99%. **^{1}H NMR (400 MHz, $CDCl_3$)** δ 7.61 (dd, *J* = 3.7, 1.3 Hz, 1H), 7.56 (dd, *J* = 5.0, 1.3 Hz, 1H), 7.06 (dd, *J* = 5.0, 3.7 Hz, 1H), 4.78 (d, *J* = 7.4 Hz, 1H), 3.28 – 3.17 (m, 1H), 1.85 – 1.74 (m, 2H), 1.71 – 1.60 (m, 2H), 1.57 – 1.47 (m, 1H), 1.34 – 1.06 (m, 5H) ppm. **^{13}C NMR (101 MHz, $CDCl_3$)** δ 142.7, 131.9, 131.6, 127.4, 53.2, 33.9, 25.2, 24.8 ppm. Spectral data was in agreement with the literature.[316]

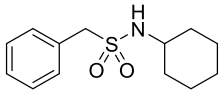

***N*-cyclohexyl-1-phenylmethanesulfonamide (5o).** Following GP2, using phenylmethanesulfonamide (34.2 mg, 0.20 mmol) and iodocyclohexane (63.0 mg, 0.30

[316] Chinn, A. J.; Sedillo, K.; Doyle. A. G. Phosphine/Photoredox Catalyzed Anti-Markovnikov Hydroamination of Olefins with Primary Sulfonamides via *α*-Scission from Phosphoranyl Radicals. *J. Am. Chem. Soc*. **2021**, *143*, 18331–18338.

mmol), afforded the title product as a white solid (49.2 mg, 97%) after purification by silica gel chromatography (hexane/EtOAc 10:1 to 5:1). In a second independent experiment, 49.6 mg (98%) were obtained, giving an average yield of 98%. **^{1}H NMR (400 MHz, $CDCl_3$)** δ 7.43 – 7.34 (m, 5H), 4.27 (d, *J* = 7.6 Hz, 1H), 4.21 (s, 2H), 3.15 – 3.02 (m, 1H), 1.94 – 1.84 (m, 2H), 1.72 – 1.63 (m, 2H), 1.58 – 1.49 (m, 1H), 1.32 – 1.04 (m, 5H) ppm. **^{13}C NMR (101 MHz, $CDCl_3$)** δ 130.8, 129.7, 128.8, 128.7, 60.1, 53.4, 34.6, 25.2, 24.9 ppm. Spectral data was in agreement with the literature.[312]

4.8.4 Enlarge Experiment

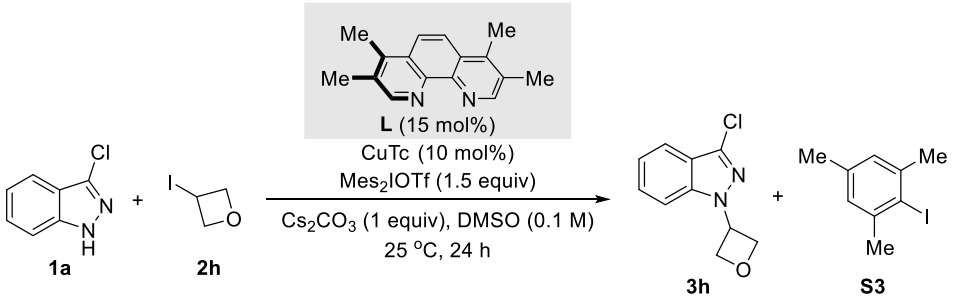

An oven-dried 100 mL round-bottom Schlenk bottle equipped with a stirring bar was charged with indazole **1a** (153 mg, 1.0 mmol), CuTc (19.2 mg, 10 mol%), 3,4,7,8-tetramethyl-1,10-phenantroline (35.4 mg, 15 mol%) and dimesityliodonium triflate (771 mg, 1.5 equiv, 1.5 mmol). The bottle was taken into a nitrogen-filled glovebox where Cs_2CO_3 (326 mg, 1.0 equiv, 1.0 mmol) was added. The reaction bottle was sealed and removed from the glovebox. Afterwards, alkyl iodide **2h** (276 mg, 1.5 equiv, 1.5 mmol) and DMSO (10.0 mL, 0.1 M) was added by syringe. The reaction mixture was stirred at 25 °C for 24 hours. The reaction mixture was stirred at 25 °C for 24 hours. The reaction mixture was diluted ethyl acetate (50 mL) and washed with H_2O (2 x 20 mL) followed by NaCl (saturated, 20 mL). The organic layer was dried (Na_2SO_4), filtered and concentrated under reduced pressure. The received crude material was purified by silica gel chromatography to afford the desired product **3h** as white solid (188 mg, 90% yield) along with mesityl iodide **S3** as colourless oil (582 mg, 2.4 mmol).
3h: **^{1}H NMR (400 MHz, $CDCl_3$)** δ 7.74 – 7.67 (m, 1H), 7.52 – 7.42 (m, 2H), 7.28 – 7.21 (m, 1H), 5.79 – 5.69 (m, 1H), 5.29 (t, *J* = 6.7 Hz, 2H), 5.10 (t, *J* = 7.4 Hz, 2H) ppm. **^{13}C NMR (101 MHz, $CDCl_3$)** δ 140.6, 134.3, 128.1, 122.0, 121.9, 120.3, 109.3, 77.3, 53.1 ppm.
S3: **^{1}H NMR (400 MHz, $CDCl_3$)** δ 6.89 (s, 2H), 2.44 (s, 6H), 2.24 (s, 3H) ppm. **^{13}C NMR (101 MHz, $CDCl_3$)** δ 141.9, 137.5, 128.1, 104.4, 29.6, 20.8 ppm. Spectral data was in agreement with the literature.[317]

[317] Palav, A.; Misal, B.; Chaturbhuj, G. NCBSI/KI: A Reagent System for Iodination of Aromatics through In Situ Generation of I-Cl. *J. Org. Chem.* **2021**, *86*, 12467–12474.

4.8.5 Mechanistic Experiments

4.8.5.1 TEMPO Inhibition Experiment

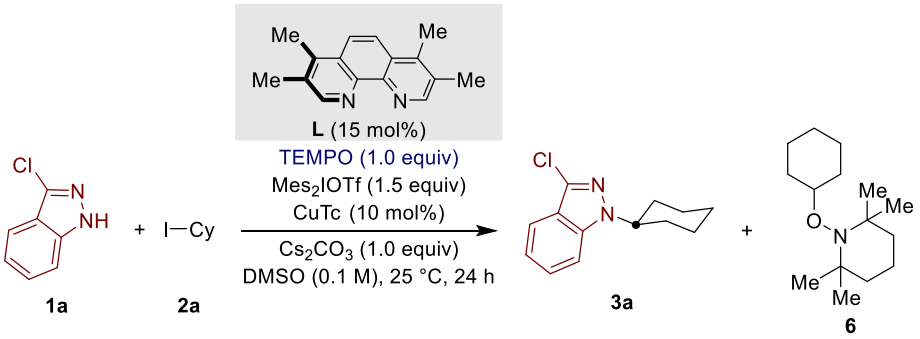

An oven-dried 8 mL screw-cap test tube containing a stirring bar was charged with 3-Chloro-1*H*-indazole (15.3 mg, 1.0 equiv, 0.1 mmol), CuTc (1.9 mg, 10 mol%), 3,4,7,8-tetramethyl-1,10-phenantroline (3.5 mg, 15 mol%) TEMPO (15.6 mg, 1.0 equiv, 0.1 mmol) and dimesityliodonium triflate (77.1 mg, 1.5 equiv, 0.15 mmol). The test tube was taken into a nitrogen-filled glovebox where Cs_2CO_3 (32.6 mg, 1.0 equiv) was added. The reaction vessel was sealed with a screw cap septum and removed from the glovebox. Afterwards, cyclohexyl iodide (31.5 mg, 1.5 equiv, 0.15 mmol) and DMSO (1.0 mL, 0.1 M) was added by syringe. Parafilm was used to reseal the pierced cap. The reaction mixture was stirred at 25 °C for 24 hours. After the reaction was completed, the mixture was filtered through celite and analyzed by GCMS. Then the reaction mixture was quenched with water/brine (10 mL) and extracted with ethyl acetate (3 x 10 mL). The combined organic extracts were dried (Na_2SO_4), filtered and concentrated under reduced pressure. The received crude material was purified by silica gel chromatography (hexane/EtOAc 50:1 to 20:1), affording cyclohexyl-TEMPO adduct **6** (14.0 mg, 59%) as a colourless oil.

1-(Cyclohexyloxy)-2,2,6,6-tetramethylpiperidine (6). ^{1}H NMR (400 MHz, $CDCl_3$) δ 3.58 (tt, *J* = 9.6, 4.0 Hz, 1H), 2.10 – 1.98 (m, 2H), 1.79 – 1.67 (m, 2H), 1.56 – 1.41 (m, 6H), 1.38 – 1.00 (m, 18H) ppm. **^{13}C NMR (101 MHz, $CDCl_3$)** δ 81.9, 59.8, 40.4, 34.6, 33.1, 26.1, 25.2, 20.4, 17.5 ppm. Spectral data was in agreement with the literature.[312]

GCMS data

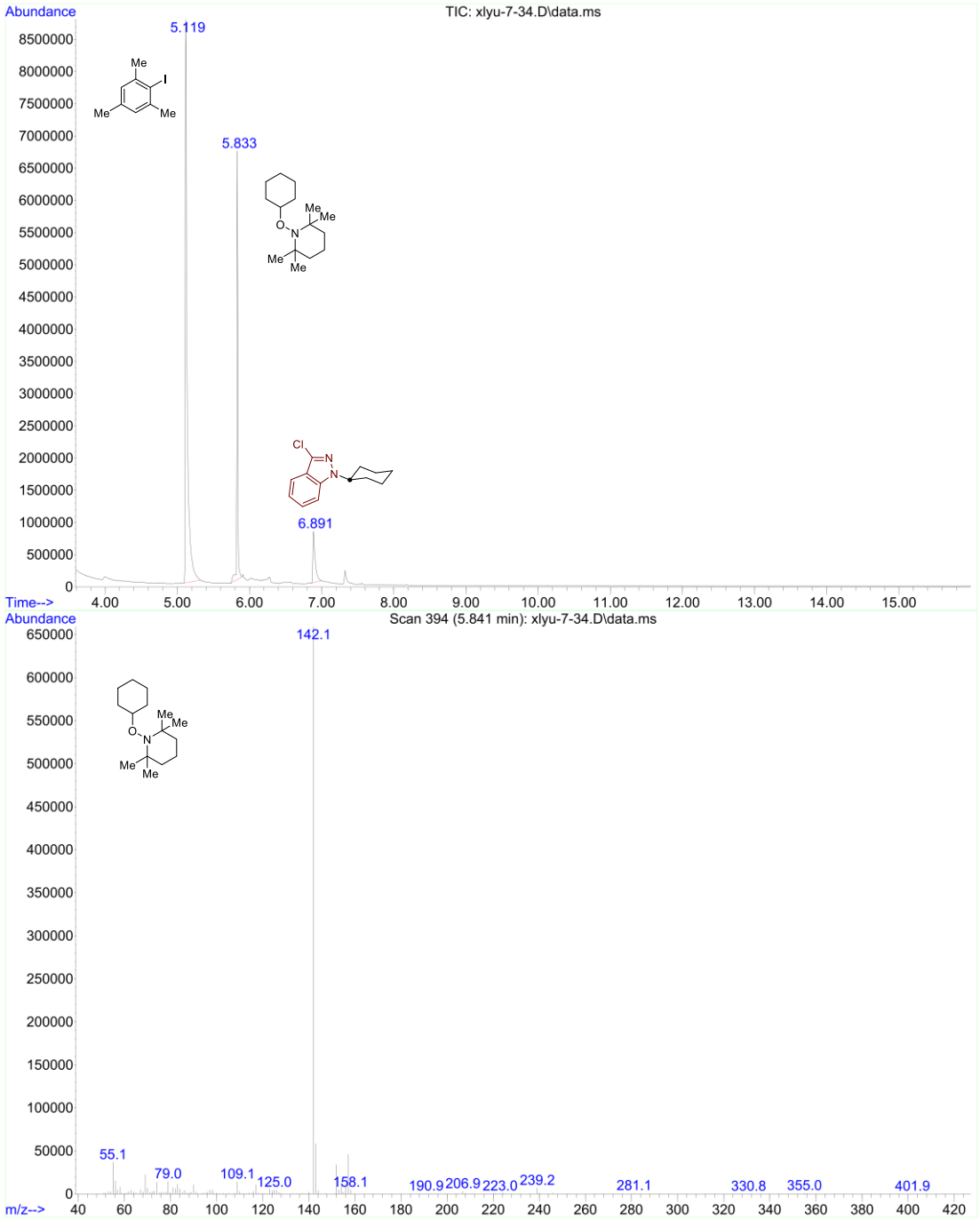

Figure S4.1 GC-MS spectra of radical inhibition reaction mixture.

4.8.5.2 Control Experiments in the Absence of *N*-Nucleophile

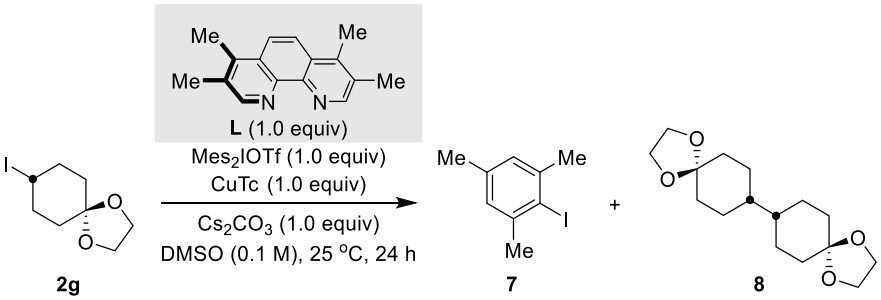

An oven-dried 8 mL screw-cap test tube containing a stirring bar was charged with CuTc (19.2 mg, 1.0 equiv., 0.1 mmol), 3,4,7,8-tetramethyl-1,10-phenantroline (23.6 mg, 1.0 equiv.) and dimesityliodonium triflate (51.4 mg, 1.0 equiv.). The test tube was taken into a nitrogen-filled glovebox where Cs_2CO_3 (32.6 mg, 1.0 equiv.) was added. The reaction vessel was sealed with a screw cap septum and removed from the glovebox. Afterwards, 8-iodo-1,4-dioxaspiro[4.5]decane (26.8 mg, 1.0 equiv.) and DMSO (1.0 mL, 0.1 M) was added by syringe. Parafilm was used to reseal the pierced cap. The reaction mixture was stirred at 25 °C for 24 hours. After the reaction was completed, the mixture was filtered through celite and analyzed by GCMS. **7** and **8** were exclusively observed in the GCMS.

GCMS data:

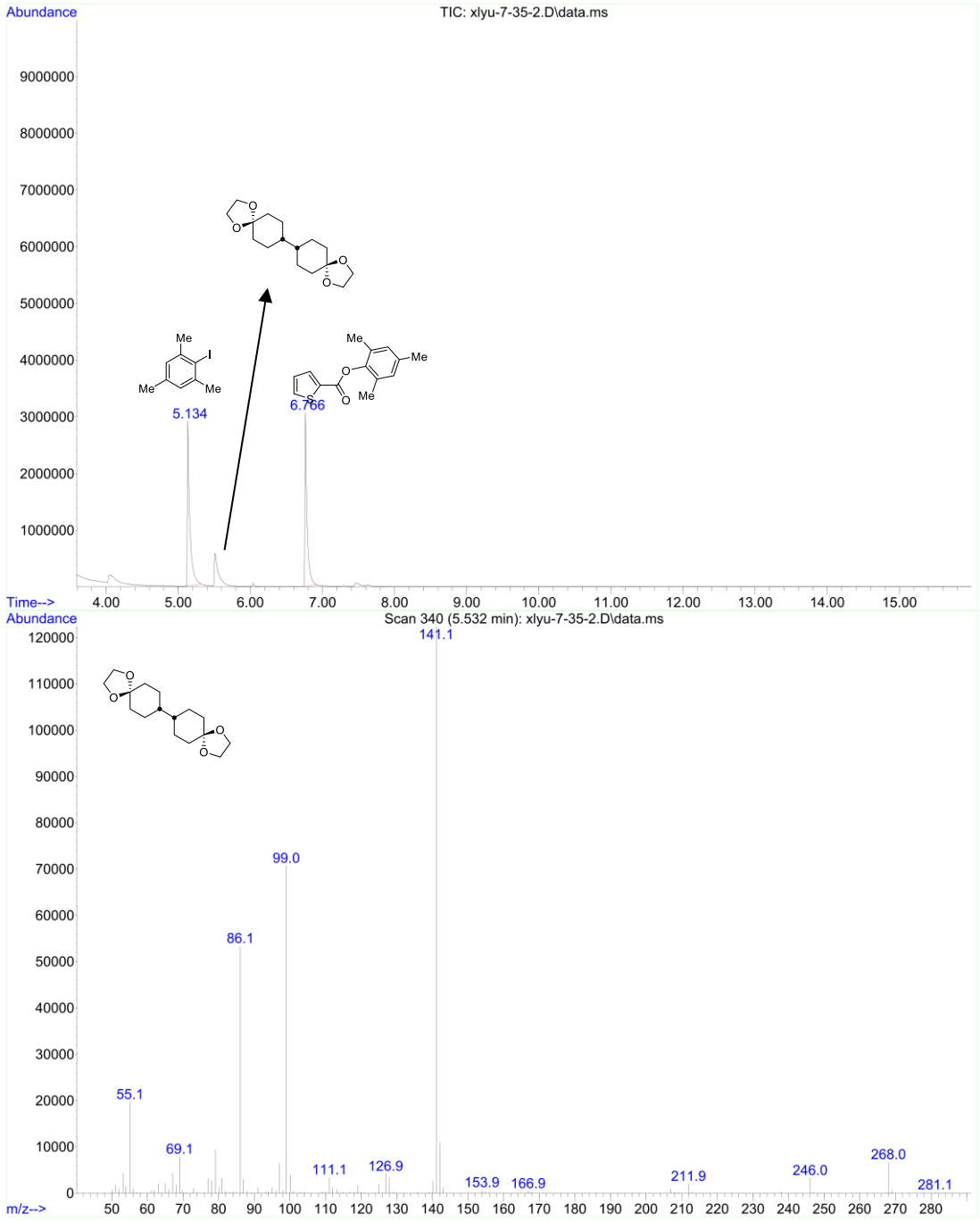

Figure S4.2 GC-MS spectra of control experiment reaction mixture.

4.8.6 Representative NMR Spectra

^{1}H NMR of **S1**

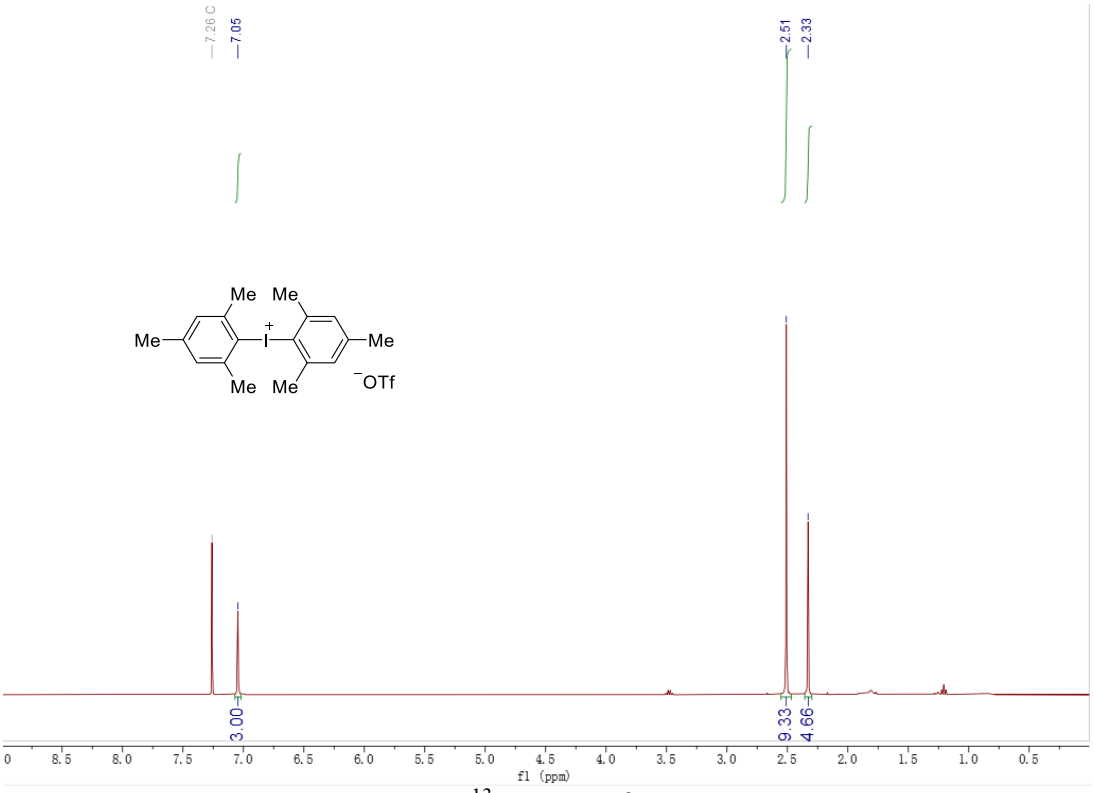

^{13}C NMR of **S1**

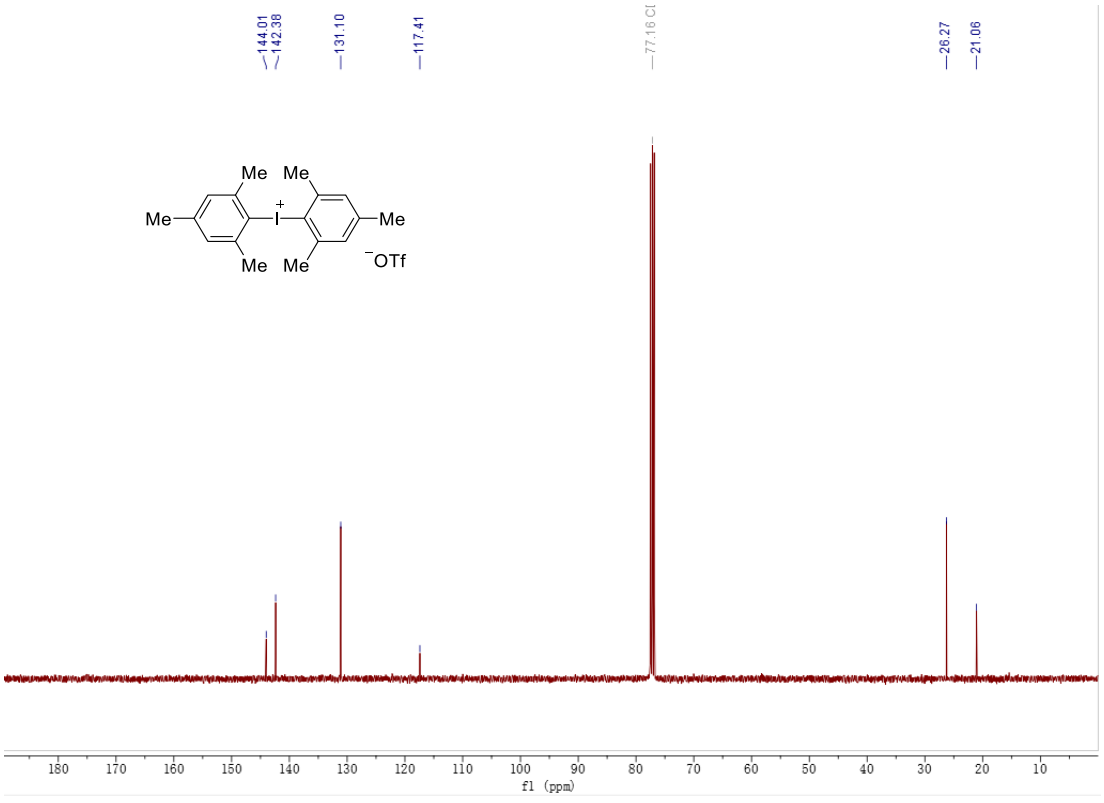

^{1}H NMR of **2n**

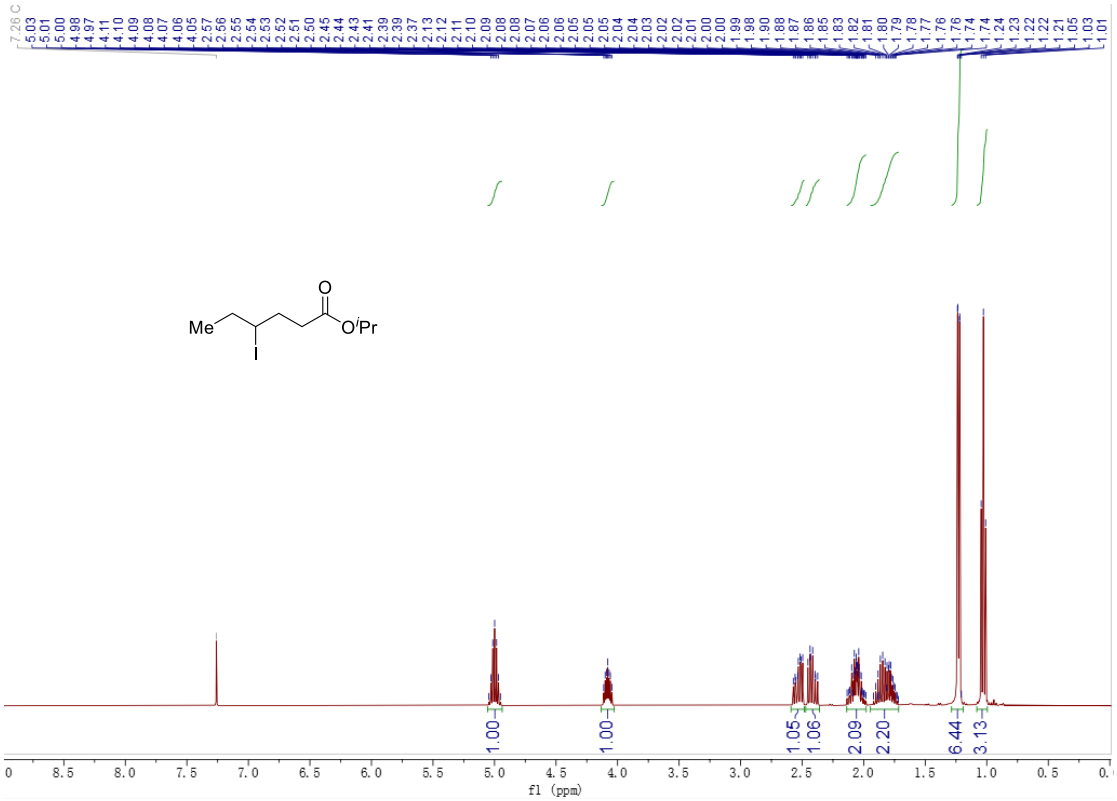

^{13}C NMR of **2n**

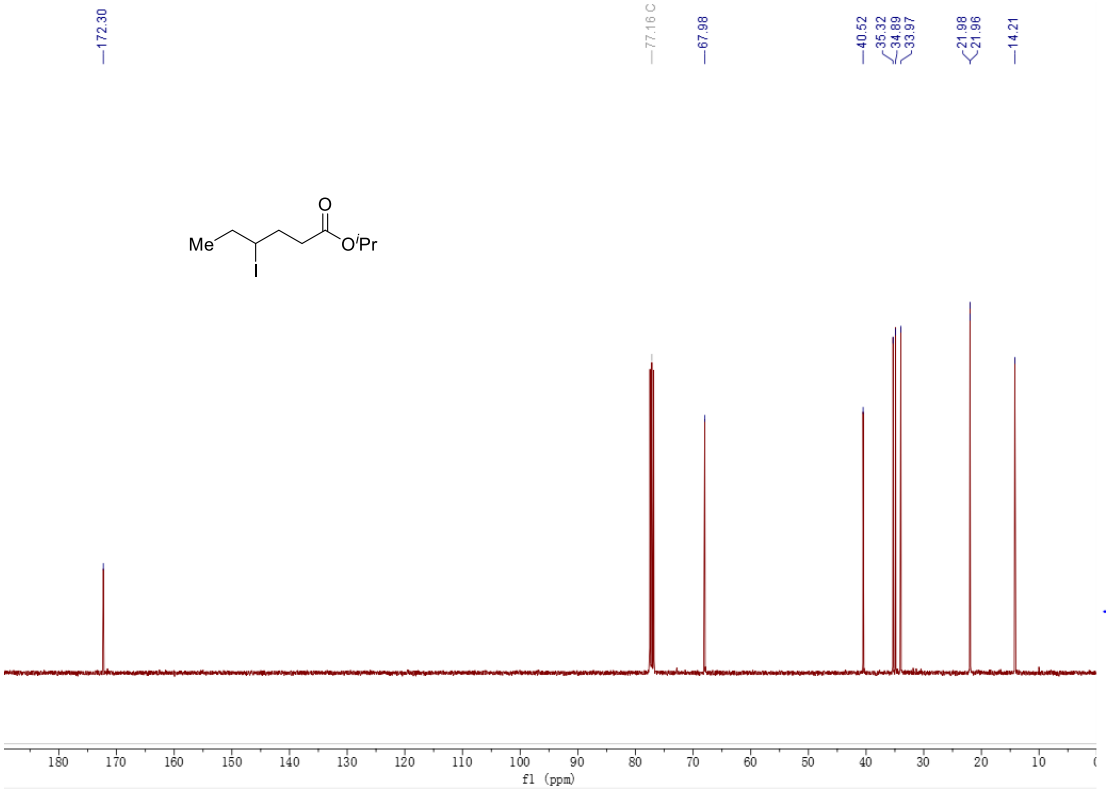

^{1}H NMR of **3r**

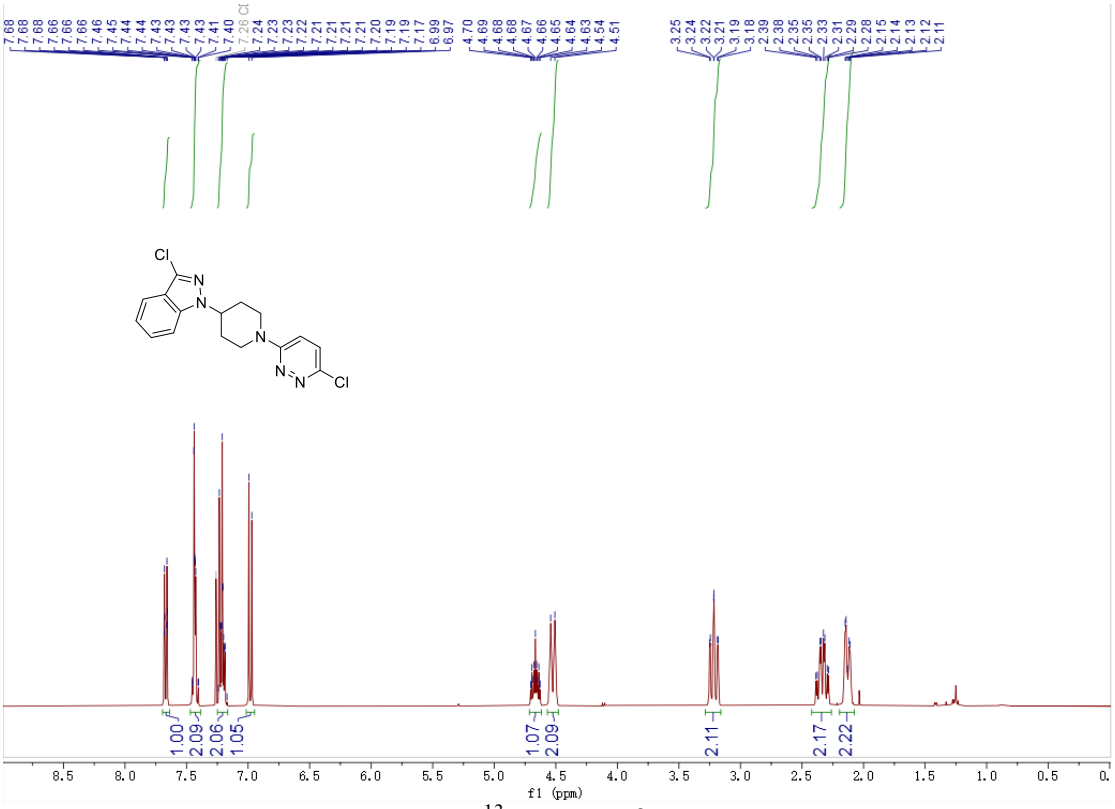

^{13}C NMR of **3r**

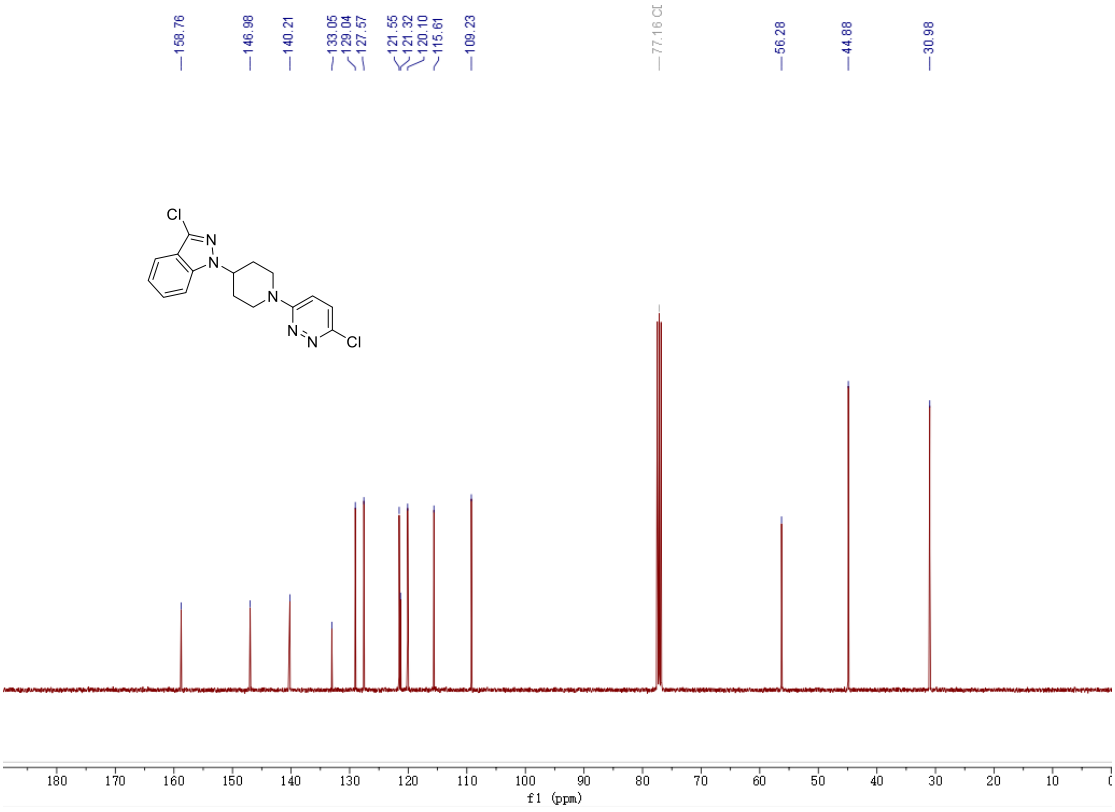

^{1}H NMR of **S3**

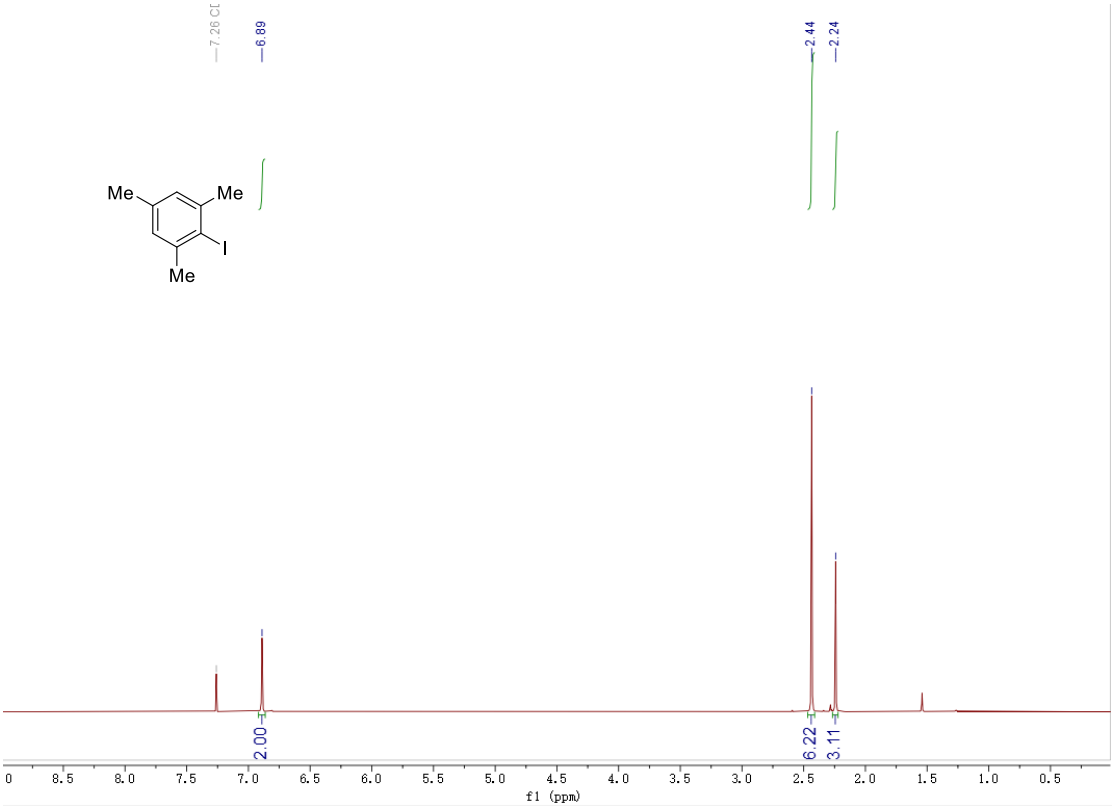

^{13}C NMR of **S3**

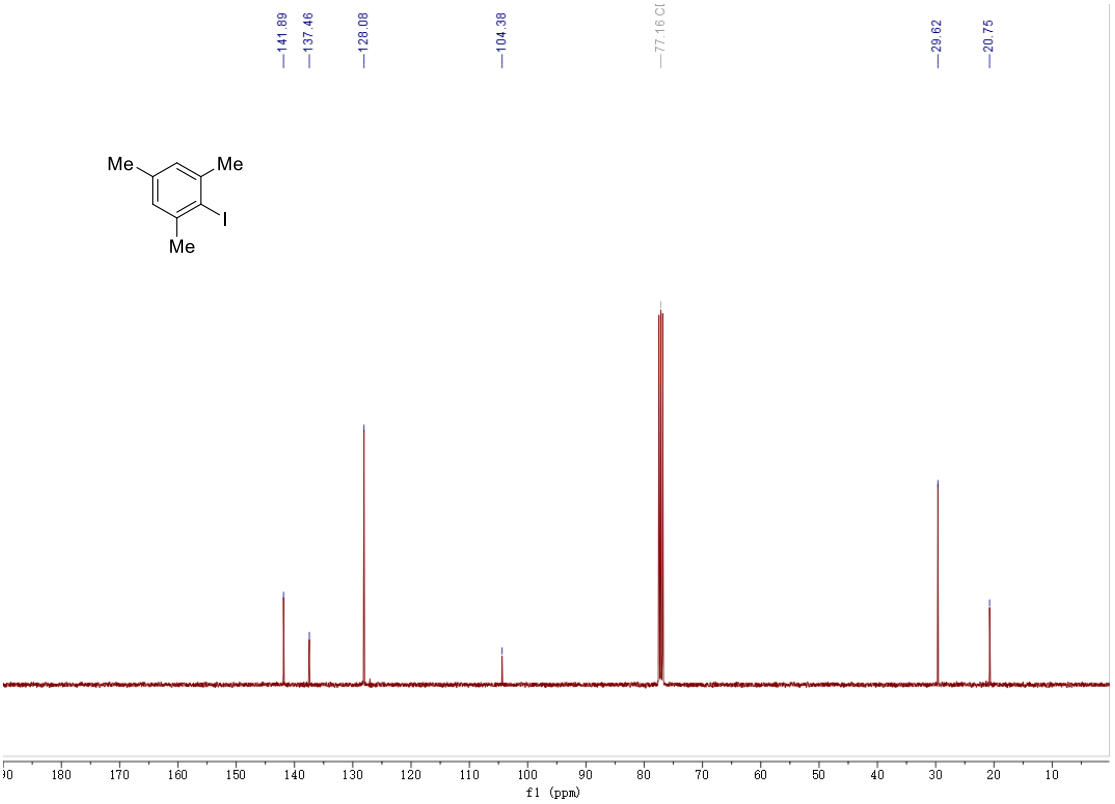

^{1}H NMR of **6**

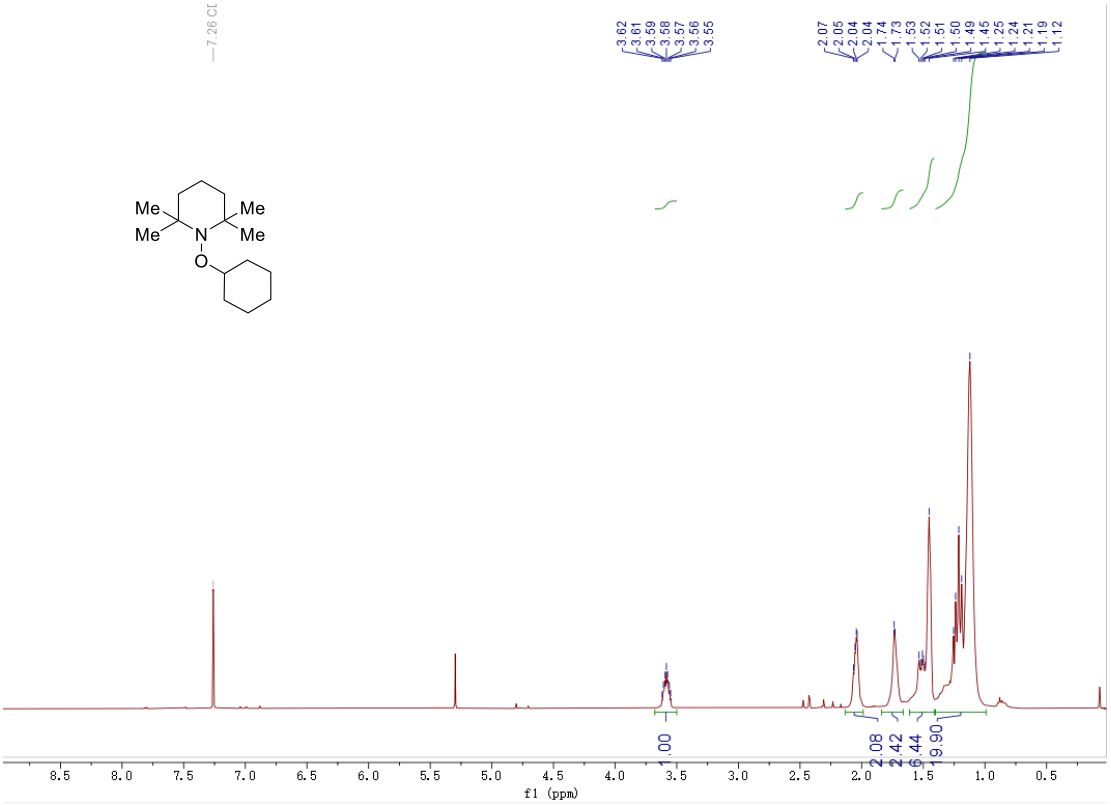

^{13}C NMR of **6**

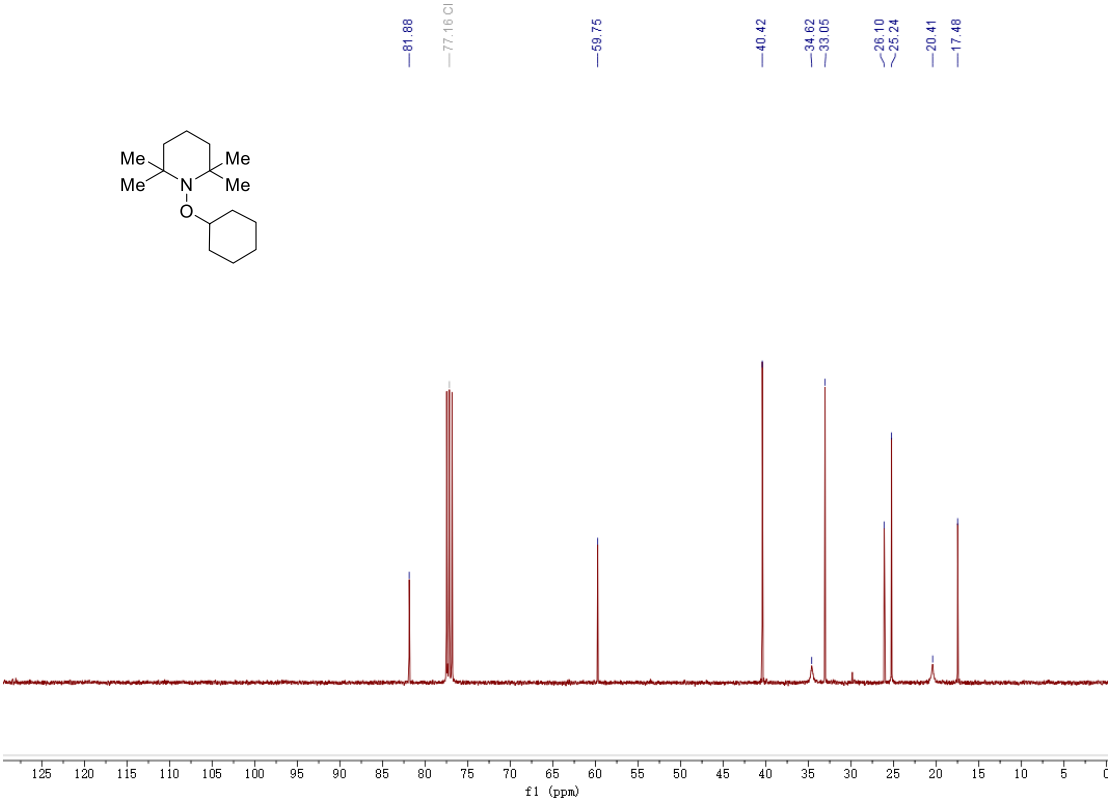

Chapter 5

Conclusion

The synthetic methods developed during this Doctoral Thesis demonstrate the unlimited potential of radical engagement in transition metal-catalyzed cross-coupling reactions. It would be useful to highlight what we have achieved in our initial aims.

Chapter 2:

■ A nickel/photoredox dual catalytic system for forging sp^2–sp^3 and sp^3–sp^3 bonds using ketone derived dihydroquinazolinones has been developed. This method is distinguished by its wide scope and broad application profile — including chemical diversification of advanced intermediates.

■ The protocol shown here demonstrate the feasibility of radical induced C–C bond scission enabled inert ketone α C–C bond cleavage, which otherwise would require harsh conditions for transition metal-catalyzed C–C bond activation.

■ Terpyridine ligated aryl nickel(II) complex was prepared. As a potential organometallic intermediate, the complex was found to be competent for the C–C bond construction process under established reaction conditions.

■ Stern-Volmer fluorescence quenching experiments were conducted, which revealed a reductive quenching photoredox cycle, beginning with oxidative single-electron transfer of dihydroquinazolinone by excited-state photocatalyst.

Chapter 3:

■ A copper-catalyzed C(sp^3)-amination reaction of proaromatic dihydroquinazolinones with a variety of *N*-nucleophiles has been developed. Considering the prevalence of carbonyl compounds, this method might offer a new entry point to access C(sp^3)–N architectures utilizing ketones as traceless synthons.

■ Phenanthroline ligated copper(I)-amido complex was prepared — as a potential reaction intermediate, which was found to be competent in the amination event under established reaction conditions.

■ Preliminary mechanistic experiment revealed that *tert*-butoxy radical generated by either thermal decomposition of BzOO^{t}Bu or copper catalysts might be the key species for dihydroquinazolinone activation, leading to the alkyl radical formation.

Chapter 4:

■ A copper-catalyzed C(sp^3) amination of unactivated secondary alkyl iodides mediated by diaryliodonium salts has been described. The method is characterized by its mild reaction conditions, excellent regioselectivity, and wide substrate scope.

■ The difficulty of low reactivity of Cu(I) species towards alkyl halide was overcome by hypervalent iodine reagents to generate aryl radicals in the presence of amido-Cu(I) complexes, thus setting the basis for enabling a halogen atom transfer with an alkyl halide prior to sp^3 C−N construction.

UNIVERSITAT ROVIRA I VIRGILI
NICKEL/COPPER CATALYZED C-C AND C-N BOND FORMATION REACTIONS TO FORGE SP3 CARBON LINKAGES
Xinyang Lyu

UNIVERSITAT
ROVIRA i VIRGILI